591

TURBULENCE AND TURBULENT COMBUSTION IN SPARK IGNITION ENGINES

By

CHAN NYEIN
B.E(Mech.)., M.Sc., D.I.C.

Thesis Submitted for the Degree of
Doctor of Philosopy
in the Faculty of Engineering of the
University of London

1979

Department of Mechanical Engineering
Imperial College of Science and Technology
London SW7 2BX

To My Parents

A Dedication to My Supervisor

Mr. D. G. Martin

Who has made it possible for me to cross the Mighty Sea of Research in the Small Boat of My Knowledge by providing,

* Map of Guidance to follow the Right Path
* Food for Thought to fill up the Knowledge
* Light of Encouragement to brighten my Spirit against the Fear of Darkness
* Breeze of Support to sail out of the Unexpected Trouble Spots
* Rudder of Help to steer the Boat to Destiny.

ACKNOWLEDGEMENTS

I would like to express my sincere and deepest gratitude to Mr. D. G. Martin, my supervisor, for initiating this research project and for his continuous and very close supervision, guidance and encouragement which I have received throughout the past four years. I am very fortunate to be one of the research students under his supervision which has given me not only the invaluable and advanced knowledge of the subject but also the ability and confidence to tackle difficult problems. I am grateful to him also for his efforts which allowed me to obtain the full financial grant as well as permission to stay in this country for carrying out the research project. I would like to emphasize that it would have been completely impossible for me to have completed this research without my supervisor's very kind help, guidance and encouragement.

My deepest thanks and gratitude are due to The British Council for sponsoring me and to Mr. A. Holland, Section Head of the Technical Cooperative and Training Department, for his kind help, encouragement and for arranging my grant. I am deeply grateful to the Minister Dr. U. Khin Maung Win and the Senior Officials of the Education Ministry, Burma and to Rector U. Khin Aung Kyi and Professor U. Ba Than of Rangoon Institute of Technology for giving me permission to go abroad and carry out this long term research project.

I am also indebted to Mr. J. A. Barnes of the Thermal Power Section for his very valuable advice in designing the modifications to the engine under test, and for his general encouragement. My thanks are due to Dr. A. S. C. Ma of Heat Transfer Section for the loan of the Hot-Wire Anemometry equipment. My gratitude is also due to Mr. R. C. Charge for his valuable advice in the design and construction of hot wire probes and for his general help.

I owe my gratitude to all the academic staff and colleagues of the Thermal Power Section, especially to Mr. S. A. Ali, for their help, advice, encouragement and useful critism on my research work. I am also grateful to Mr. R. D. Bloxham for his effort, valuable advice and help in constructing the necessary electronic units and for his encouragement. My sincere thanks and gratitude are to Mr. C. Buzby, Mr. D. Grant and Mr. C. Hall of I.C. Engine Laboratory for their very kind help and advice

which I have received during the experimental stage of the project and for their general encouragement. A special word of thanks to Mr. H. J. Ramsey, Chief Technician of the Mechanical Engineering Department Work Shop and to Mr. A.J. Dowden, Chief Technician of the Student Work Shop, for their help in making the parts required for the experiment.

I am also thankful to all the staff of the Mechanical Engineering Department Library and the Lyon Playfair Library of Imperial College for their efforts in making available all the literature which were necessary for the research work and to all the staff of the Computer Department for their very efficient service and useful advice.

My gratitude is to the Cultural Attache U.M.M. Soe Tint and the staff of the Burmese Embassy in London for their general help and to all the academic staff of the Mechanical Engineering Department, Rangoon Institute of Technology, Burma for their encouragement.

Finally, my thanks are to Miss J. Miles for efficiently typing my thesis in a very short time.

ABSTRACT

A theoretical and experimental investigation of turbulence and turbulent combustion in a variable compression ratio spark ignition engine cylinder was carried out to establish the nature of the quantitative relationship existing between the turbulent flow field and the subsequent turbulent combustion field. Experimentally measured cold level turbulence parameters were related to the turbulent combustion field by using a specially developed spark ignition engine cycle simulation programme.

The cold level turbulence field within the engine cylinder was measured by using the hot wire anemometry technique. Measurements were made at nine different locations, including positions over the piston crown, by using 3-wire sensor probes. A high speed electronic digital data acquisition system, which was synchronized to the engine cycle was developed based on an existing available digital tape recorder unit. All necessary hot wire probes and the telemetering linkage system, for monitoring the probes which were mounted on piston crown, were also designed, developed and successfully employed throughout the experiment.

The high speed digitally recorded raw turbulence data which included cylinder charge pressure, cylinder charge temperature and anemometer voltage variations were analysed on a digital computer using a specially developed data analysis programme which was written based on the digital filtering principle. This is believed to be the first occasion on which digital filtering has been employed for engine cylinder turbulence data anaylsis. Full details of the filter configuration employed and their performance characteristics together with their filter coefficient values are presented. The interpreted results based on data of measured turbulence parameters are presented in detail.

The measured cold level turbulence parameters were used to calculate the spatial turbulent flame speed and burning velocity via a knowledge of the hypothetical laminar flame speed at the prevailing local conditions. The programme developed for this purpose considers the details of flame front movement, and its location within the chamber at any instant during combustion period is defined by using a three dimensional co-ordinate grid system. Swirl effect causing distortion of flame kernal could also be included. Details of the thermodynamic consideration and of the simulation procedure for the developed model are presented. Its prediction accuracy was confirmed by the results

of a second experiment involving cylinder pressure and flame arrival time measurements. The latter was measured by using ionization probe technique, employing six probes which were attached to the cylinder head surface.

The laminar flame speed data required for this purpose was derived from a new model which seems likely to be of considerable value in Spark Ignition Engine Cycle Simulation where the flame speed predictions have to be made over quite a wide range of initial unburnt conditions. The model predicts laminar flame speed throughout the range of air fuel ratios, from very lean to very rich and for any initial pressure, temperature and oxygen concentration and gives good agreement with experimentally observed values of the others (86,97).

A chemical equilibrium programme was also developed to predict the properties of burnt charge and adiabatic flame temperatures by considering equilibrium condition of 18 components of products. Predicted properties of burnt charge of octane and air mixture and its adiabatic combustion temperatures are presented in details for various conditions which cover the range of spark ignition engine operations.

It was found that engine cylinder cold level turbulence parameters can be used with good accuracy to predict the turbulent flame propagation speed and hence the combustion rate and performance of the spark ignition engine.

CONTENTS Page No.

	A Dedication to my Supervisor	(i)
	Acknowledgement	(ii)
	Abstract	(iv)
	Contents	(vi)
	Nomenclature	(xi)
1.0	Introduction	1
2.0	Turbulent Combustion and Turbulent Flow in Engines	5
2.1	Review of Previous Work on the Description of the Turbulent Combustion Process in the Spark Ignition Engine	5
2.2	The Nature of Turbulent Flow	9
2.2.1	Description of a Flow Field	9
2.2.2	Types of Turbulent Flow Field	9
2.3	Parameters used to Describe a Turbulent Flow Field	11
2.4	Turbulent Flow Field in an Engine Cylinder	16
3.0	Experimental Procedure for Turbulent Investigation within Engine Cylinders	26
3.1.0	Available Experimental Techniques	27
3.1.1	Flow Visualization Technique	27
3.1.2	Vane Anemometry Technique	27
3.1.3	Spark Discharge Technique	28
3.1.4	Vortex Shedding Frequency Technique	28
3.1.5	Hot Wire Anemometry Technique	28
3.1.6	Laser Anemometry Technique	28
3.2.0	Selection of an Experimental Technique	29
3.3.0	Hot Wire Anemometry	29
3.4.0	Hot Wire Sensor Probes for Engine Cylinder Flow Application	33
3.4.1	Description of the Hot Wire Sensor Probe Design	34
3.4.2	The Choice of Sensor Wire Element for the Hot Wire Probes	34
3.4.3	Sensor Wire Size	34
3.5.0	Measuring Positions	35
3.6.0	Lead Wire and Linkage System	35
3.7.0	Data Recording Method	37
3.8.0	Instrumentation for Analogue Signals	47

3.9.0	Modifications to Engine Under Investigation	48
3.10.0	Data Taking Procedure	48
3.11.0	Engine Operating Conditions	48
4.0.0	Experimental Data Analysis	50
4.1.0	The Quasi-Steady State Analysis Method	50
4.2.0	Ensemble Averaging Analysis Method	51
4.3.0	Present Analysis Method	53
4.3.1	Filtering	53
4.4.0	Digital Filtering	54
4.5.0	Steps Involved in Data Analysis	56
4.5.1	Data Retrival from the Recorded Magnetic Tape	56
4.5.2	Calculation of Instantaneous Comvective Heat Transfer Coefficient of the Hot Wire	69
4.5.3	Nusselt Number Calculation	73
4.5.4	Reynold's Number of the Flow Calculation	73
4.5.5	Instantaneous Velocity Calculation	73
4.5.6	Mean Velocity Separation	73
4.5.7	High Frequency Turbulent Component of Velocity Separation	73
4.5.8	Intensity of Turbulence Calculation	73
4.5.9	Power Spectra Estimate	73
4.5.10	Scale of Turbulence	74
5.0.0	Conclusion on Measured Results on Engine Cylinder Turbulence	75
5.1.0	Time History of Turbulence Intensity Fluctuations	75
5.2.0	Turbulence Intensity Variation with Positions in Combustion Chamber.	77
5.3.0	Turbulence Intensity Variation with Directions	77
5.4.0	Turbulence Intensity Variation with Engine Speed	77
5.5.0	Turbulence Intensity Variation with Compression Ratio	77
5.6.0	Turbulence Intensity Variation with Volumetric Efficiency	77
5.7.0	Percentage of Turbulence Intensity Variation	77
5.8.0	Micro-Length and Time Scales	78
5.9.0	General Conclusion	78
5.10.0	Error Analysis	78

6.0.0	Turbulence and Flame Propagation	99
6.1.0	Laminar Flame Propagation	99
6.2.0	Types of Laminar Flame Theories	100
6.2.1	Momentum Theory	101
6.2.2	Diffusion Theory	101
6.2.3	Thermal Theory	101
6.2.4	Other Empherical Forms of Laminar Flame Speed Equations	104
6.3.0	An Alternative Model of Laminar Flame Speed	104
6.4.0	Turbulent Flame Propagation	106
6.4.1	Laminar Transport Model	110
6.4.2	Turbulent Transport Model	112
6.4.3	Other Models	112
6.5.0	Turbulent Flame Speed Model for Spark Ignition Engine Cycle	119
7.0.0	Computer Simulation of the Spark Ignition Engine Cycle	121
7.1.0	Computer Simulation Procedure	121
7.2.0	General Structure of the Prediction Procedure	124
7.3.0	Thermodynamic Considerations	125
7.3.1	Valve Opening Period or Gas Exchange Period	125
7.3.2	Compression and Expansion Period	126
7.3.3	Combustion Period	126
7.4.0	Evaluation Procedure for the Terms Involved	126
7.4.1	Heat Transfer To and From the Surrounding Metal Surfaces	126
7.4.2	Mass Flow Rate Across the Valves	127
7.4.3	Change of Mass of the Cylinder Charge	127
7.4.4	Increase in Enthalpy of Cylinder Charge due to Incoming Charges from Manifolds	127
7.4.5	Change of Enthalpy Content During Valve Opening Period and Change of Internal Energy Content during Compression and Expansion Periods	128
7.4.6	Change of Energy Content during Combustion Period	129
7.4.7	Rate of Heat Released	130
7.4.8	Calculation Steps Involved for the Heat Release	133
7.5.0	Heat Transfer Process	137
7.5.1	Heat Transfer Surfaces Considered	137

7.5.2	Metal Surface Temperature	137
7.5.3	Equivalent Resistance Network	137
7.6.0	Heat Transfer Formulae	138
7.7.0	Flow Through Valves	143
7.8.0	Computer Simulation Program	144
7.8.1	Structure of Computer Program	145
7.8.2	Input to the Program	145
7.8.3	Output from the Program	145
7.8.4	Programme Structure for Valve Opening Period	145
7.8.5	Programme Structure for Compression and Expansion Period	146
7.8.6	Programme Structure for Combustion Period	148
7.9.0	Accuracy of the Engine Cycle Simulation Model with its Associated Turbulent Flame Correlation	153
7.10.0	Conclusion and Recommendation	160
	References	162

CONTENTS Page No.

Appendix (A.1) 174
Combustion Products Properties and Combustion Temperature
Appendix (A.2) 203
Digital Filtering and Design of Digital Filters
Appendix (A.3) 235
Power-Frequency Spectral Determination of a Turbulent Field
Appendix (A.4) 238
Flame Arrival Time Measurement by the Ionization Probe Method
Appendix (A.5) 242
Calibration of Hot Wire Probes.
Appendix (A.6) 246
Viscosity of Octane + Air Combustion Products
Appendix (A.7) 251
Data Recovery from Recorded Magnetic Tape
Appendix (A.8) 253
Indexing System for Recorded Data
Appendix (A.9) 254
Telemetering of Information from Moving Piston
Appendix (A.10) 258
Description of the Engine Test Rig
Appendix (A.11) 259
Compression Ratio Calibration Curve
Appendix (A.12) 260
Detail Drawing of the Auxillary Crank
Appendix (A.13) 266
Flow Diagram of the Computer Programs
Appendix (A.14) 277
Tables of the Predicted Properties of Octane + Air Combustion Products
Appendix (A.15) 287
Tables of the Employed Thermochemical Data

NOMENCLATURE

A: Reactant species concentration in chemical equilibrium calculation

A: Cross-sectional area of hot wire element

a: Constant in Reynold's Analogy for convective heat transfer

B: Product species concentration in chemical equilibrium calculation

b: Constant in Reynold's Analogy for convective heat transfer

C: A constant

C: Specific heat

D: Diameter of hot wire sensing element

d: Engine Cylinder Bore

E: Anemometer output voltage

F: Power in spectral Analysis

f: Frequency

G: Gibb's function

G: Transfer function in frequency domain

g: Transfer function in frequency domain

h: Convective heat transfer coefficient

h: Specific enthalpy

K: Thermal conductivity

k: Reaction rate constant in equilibrium calculation

L: Macro scale of Turbulence

L: Length of connecting rod

L: Length of hot wire element

l: Eddy radius

M: Mass

m: Mass or flow rate

Nu: Nusselt number

n: Power index used in Reynold's Analogy

Q: Heat or heat released rate

R: Hot wire resistance

R: Gas Constant

Re: Reynold's Number

S: Flame Speed

s: Specific entropy

T: Absolute Temperature

T: Sampling Time

U: Mean velocity in X-direction

u: Fluctuating Component of velocity in X-direction

V: Cylinder volume

V: Mean velocity in Y-direction

v: Fluctuating Component of velocity in Y-direction

W: Mean Velocity in Z-direction

w: Fluctuating component of velocity in z-direction

X: A Dummy variable

Z: Z-transformation

Subscripts:-

ave: Average value or at average condition

C: At burnt charge condition

C: Backward reaction in equilibrium composition calculation

Cy: At cylinder charge condition

e: At Exhaust manifold condition (for properties calculation)

e: Coming into or going out of the exhaust manifold in mass flow calculation

eg: At equilibrium condition

F: Fuel

f: Forward reaction in equilibrium composition calculation.

i: At inlet manifold condition in properties calculation

i: Coming into or going out out of the inlet manifold in mass flow calculation

j: Dummy Index

l: At Laminar condition

p: At the temperature and pressure of the combustion product

p: At constant pressure

R: At reactant temperation and pressure

t: Related to time or time scale

t: At turbulent condition

u: At unburnt charge temperature and pressure condition

v: At constant volume condition

wall: At cylinder wall temperature

1.0 INTRODUCTION

With the increasing demands for greater thermal efficiency and low pollutant emissions, there have been considerable efforts to improve the performance of spark ignition engines. The improvement sought can be achieved either by design, manufacture and testing of new engine geometries and observing the resulting performances particularly in respect of emission characteristics or by using analytical techniques and computer simulation models to predict the performance and emission characteristics of a proposed engine geometry. The first approach, that of designing and testing of engines, is not only increasingly expensive but the improvement sought, in this way, are increasingly more difficult to attain without a detailed understanding of the processes involved. On the other hand, the development and advancement in the application of high speed digital computers to perform complex calculations economically has led to the development of computer simulation programmes to study the performance and emission characteristics of the spark ignition engines. The accuracy and reliability of these programmes, however, depends on the degree of knowledge about the associated basic phenomena of the spark ignition engine cycle, especially in its combustion aspect.

In order to predict the engine performance, which depends on the accurate computation of pressure and temperature histories, it is necessary to understand the mechanism of flame propagation in such an engine. The flame propagation rate determines the rate of energy release in the combustion chambers which in turn determines the pressure and temperature histories. However an adequate description of the flame propagation phenomena during the cycle is difficult to achieve and is the major difficulty in developing realistic computer models, as neither the nature of the turbulence, which is the major influencing parameter for turbulent flame propagation, is exactly known, nor is the exact quantitative relationship between the turbulence and the flame propagation rate.

Various attempts have been made to study the nature of turbulence in engine cylinders both by using theoretical modelling techniques (106, 107) and by using experimental techniques (1, 2, 3, 5, 6, 41, 66). The art of theoretical modellingof engine cylinder turbulence is still in its infancy, and thus for the predictions made have been limited to two dimensional systems only, for engines fitted with simplified port shapes and valves (106, 107). The accuracy and reliability of these modeling methods and their results still need to be confirmed before proceeding to the development of advanced more

realistic models. On the other hand, various experimental techniques have been employed in the studies of the flow pattern and turbulence inside engine cylinders (1, 2, 3, 4, 5, 41, 66, 71, 72) and some useful information about the nature of turbulence have been established (1, 2, 3, 5, 6, 41, 66). But the detailed spatial and temporal variations of engine cylinder turbulence were still unknown because of the inherent experimental difficulties, and in default various assumptions had to be made to represent their nature in previous computer simulation studies of spark ignition engines (42, 45, 52). The lack of knowledge of the detailed nature of engine cylinder turbulence made it impossible to test the validity of the turbulence flame propagation models employed which were derived from experimental observations remote from engine cylinder combustion conditions, and used for engine combustion applications.

The aim of the research effort was therefore to reveal the nature of the engine cylinder turbulence and its influence on engine combusiton by:-

(i) Investigating the spatial and temporal variation nature of the turbulence field in a variable compression ratio engine cylinder.

(ii) Establishing the nature of the quantitative influence of the cold level turbulence measured as shown on flame propagation rate and hance on the engine performance by using a computer simulation model to be developed for this purpose.

(iii) Confirmation of accuracy and validity of the above relationship between turbulence and flame propagation and of the computer sumulation model by experimental observations involving measurements on local flame front arrival times and on cylinder pressure.

The first phase of the research effort was accomplished by an experimental investigation into the spatial and temporal nature of turbulence by using hot wire anemometry. The experimental technique employed and the data analysis employed are mentioned in detail and the measured results are discussed.

The second phase of the research effort was accomplished by using a spark ignition engine cycle simulation programme which was specifically developed for this purpose.

The third and final phase of the research effort was accomplished by observing the local flame front arrival times by using ionization probe technique and by measuring the cylinder

pressure.

It is firmly believed that the result of the present research effort provides much needed information on the detailed nature of engine cylinder turbulence and its quantitative influence on flame propagation rate under engine cylinder combustion conditions. The above information plus the modelling technique used in the simulation of the spark ignition cycle is believed to be a valuable step on the way to the development of accurate realistic computer simulation models in the future for fuel economy and pollutant emission studies.

The layout of the report is as follows:-

Section (1) Introduction.

Section (2) Review of previous work on turbulent combustion and on turbulent flow measurement within engine cylinders.

Section (3) Present experimental approach to turbulent measurement within engine cylinder.

Section (4) Data analysis procedure for the above experimentally recorded data.

Section (5) Discussion of the measured results of turbulence parameters.

Section (6) Review of the existing relationships between turbulence and flame propagation.

Section (7) Discussion of the approach to the construction of a computer simulation model for spark ignition engine cycles for checking the validity of a proposed turbulent flame propagation model. Discussion of the predicted results, general conclusions and proposals for future research attempts are also included.

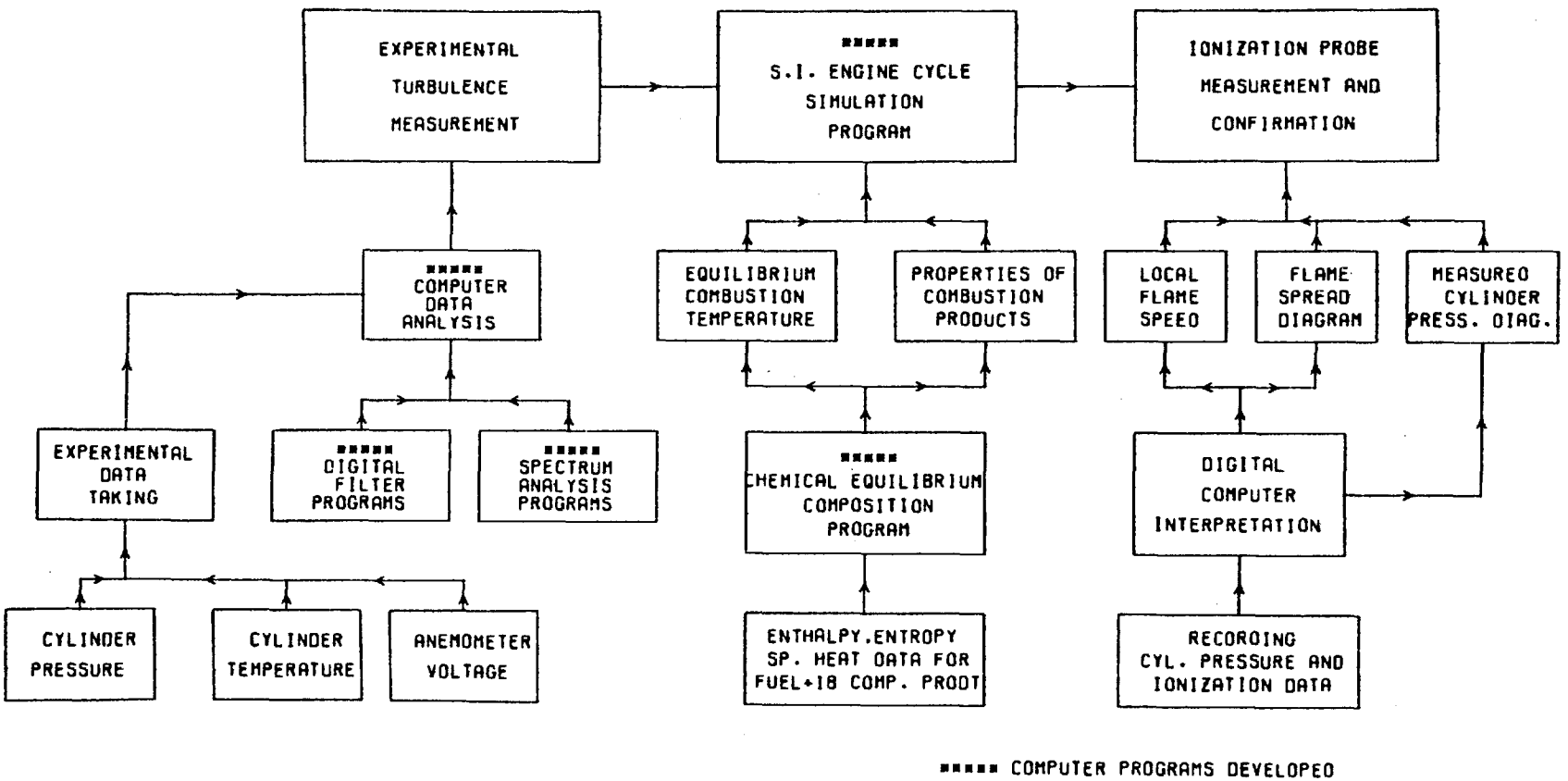


Fig (1.1) PLAN OF THE PROJECT

2. TURBULENT COMBUSTION AND TURBULENT FLOW IN ENGINES

2.1 Review of Previous Work on the Description of the Turbulent Combustion Process in the Spark Ignition Engine:- Combustion in the spark ignition engine is complex, involving, as it does,

(1) the propagation of flame through a transient turbulent flow field and its associated aerodynamic effect

(2) chemical kinetics

(3) pre and post flame reactions

(4) quenching of flame by surrounding metal surfaces and

(5) unsteady nature of heat transfer

Satisfactory computer simulation of the spark ignition engine will involve a description of the combustion process which takes all the above factors into account, but this is not at the moment possible. In this section are reviewed all the major attempts which have been made to achieve an adequate description of the combustion process, so that the limitations of what has this far been done can be seen, and so that the contribution made by the present work can be seen in context.

(i) Arrigoni Et Al (75):- An experimental investigation of the turbulent combustion stage was made by measuring the cylinder pressure and the ionization intensity, which is taken to be the most significant quantity defining turbulent flame structure. From the measured cylinder pressure diagram, the heat release rate was derived by using the method of Eyzat Et Al (47). To estimate the flame speed and hence the burning velocity it was assumed that the flame propagation process was completed after 80% of the charge was burned. The remaining20% of charge was taken to be burnt after the completion of the flame propagation process. (This assumption was made on an arbitrary basis and its validity is not clear. In fact heat release after the flame propagation process is complete can only be estimated by using chemical kinetic consideration).

The gross pattern of the flame propagation was studied by assuming three stages of combustion as used by Taylor (90). The first period, called delay, was defined as the time from the beginning of the spark to the point where appreciable pressure rise occurs relative to the motored cylinder pressure diagram. The second period is taken to be from the end of the first delay period to the time of occurence of the peak cylinder pressure, and the third period is defined as from the peak cylinder pressure occurence time to the end of the combustion

process, as shown by the derived heat released diagram.

The apparent flame propagation speed at any instant was assumed to be proportional to the square root of the heat release.

$$(S_s)_i = G \sqrt{\Delta Q_i}$$

The turbulent flame speed was obtained by dividing the apparent flame speed by a expansion ratio factor which is defined as:-

$$\varepsilon = \rho u / \overline{\rho b}$$

$$Su_t = Ss / \varepsilon$$

The validity of the expression for the apparent flame speed and the expansion ratio factor is not clear.

(ii) Blizard et Al (52):- The first assumption made was that eddies are entrained into the flame front by an eddy entrainment velocity and each eddy is assumed to be burnt with laminar flame speed u_l. Thus if l_e is the eddy radius, eddy burning time is defined as:-

$$\tau = l_e / u_l$$

The second assumption made was the exponential variation of the eddy burning time. Zeleznik (88) showed that Blizard's (52) approach of modelling is exactly equivalent to introducing a relaxation factor in the finite mass burning rate approach and hence there is some trapped mass left to be burned after the apparent flame propagation time. Eddy size was related to valve lift and the entrainment velocity was related to inlet charge velocity. By assuming a spherical flame propagation shape, all the necessary data for evaluation of the derived equations were obtained.

(iii) Lancaster (42):- An attempt was made to find a correlation between the single-position measured cold level turbulence parameter to the turbulent flame propagation speed within a spark ignition engine cylinder. The flame propagation rate was derived from the measured cylinder pressure diagram, involving the following steps:-

(a) The heat released rate was first estimated from the measured cylinder pressure diagram using the method of Krieger Et Al (102).

(b) The surface area A_f of the flame front was found by assuming the flame propagation shape to be spherical.

(c) The turbulent flame speed was then evaluated by using the equation:-

$$V_T = \frac{\dot{m}}{Af \cdot \rho u}$$

This enabled to estimate the ratio of the turbulent flame speed, defined in this way, to the computed laminar flame speed, and the result (V_T/U_l) was related to the measured cold level turbulence parameters. A conclusion was drawn that the flame speed ratio is a linear function of the measured cold level turbulence intensity.

(iv) Babu Et Al (48):- In their approach, turbulence intensity within the engine cylinder during the combustion stage was assumed to be a function of laminar flame speed, and the burnt and unburnt charge densities.

$$u' = \frac{S_l}{\sqrt{3}} \left(\rho u/\rho_b - 1\right)$$

The validity of the above expression is doubtful as the turbulence intensity estimated by using the above expression is independent of engine speed which is observed to be the major influencing factor on engine cylinder turbulence (1, 41, 66). The intensity of turbulence was related to the turbulence flame speed using the following relation:-

$$S_t = S_l + \sqrt{2\, S_l\, u'}$$

An apparent flame propagation speed was calculated by employing an expansion factor which was expressed in terms of burnt and unburnt charges' densities.

$$Vf/St = \rho u/\rho_b - 1$$

(v) Samagu Et Al (49):- In this research, the turbulent flame speed was expressed as a function of the laminar flame speed and Reynolds number based on the mean induction air velocity and bore of the cylinder.

$$V_T = \left(S_l^2 + C_1\, R_e^{C_2}\right)^{\frac{1}{2}}$$

The apparent flame propagation speed was obtained by using a multiplying factor C_T, termed the coefficient of flame transportation. The value of C_T was derived from the measured experimental cylinder pressure diagram.

$$Vapp = C_T \cdot V_T$$

The employment of the term C_T was equivalent to the use of expansion factor by Arrigoni (45) and Babu (48).

(vi) Benson Et Al (99):- In their research on spark ignition engine cycle simulation, the turbulent flame propagation speed was estimated by applying a multiplying factor (ff) to the computed laminar flame speed value. Two possible approaches exist, The first alternative is that of adjusting the value of the flame factor (ff) until the predicted cylinder pressure diagram matches with the experimentally measured one. The second alternative is for cases where no experimental data is available and is to adjust on the value of flame factor (ff) until symmetrical burning time was achieved about the top dead centre (TDC).

The above survey of previous attempts to calculate flame propagation rate and heat release rate show that all the researchers in the spark ignition engine field have noted the importance of the turbulence on flame propagation and the combustion rate, and hence on engine performance, fuel economy and emissions. However scarcity of turbulence flow field data, due to inherent difficulties of measuring and analysing gas velocities within engine cylinders, have resulted in limited understanding of its nature and its influence on flame propagation rate. In these circumstances the only possible approach is that of making and testing a variety of possible assumptions. Thus eddy size was estimated from valve lift by Blizzard (52), intensity of turbulence was estimated from burnt and unburnt charge densities by Babu (45), the effect of turbulence on flame propagation was estimated by using a Reynold's number expression by Samaga (49) and an arbitrary multiplying factor (ff) was used by Benson Et Al (14). Thus it is clear that the lack of the information on turbulence flow field was imposing considerable restriction on the development of more realistic computer simulation models. Clearly in order to construct a more realistic computer simulation model we need to eliminate all arbitrary assumptions about turbulence and its effects on flame propagation by acquiring a knowledge of the quantitative distribution of spatial

and temporal turbulence field within engine cylinder. It was therefore decided to embark on an experimental effort to determine the detailed nature of the engine cylinder turbulence, which is known to be unsteady in nature and is of the form which is difficult to be measured experimentally or modelled theoretically. Before the details of the work which has been done can be described, it is necessary to have a clear understanding of the nature of an unsteady turbulent flow. The following section therefore contains a description of the laminar flow, steady state turbulent flow and unsteady state turbulent flow; followed by an account of previous work which has been done in an attempt to describe the turbulent flow field in engines.

2.2. THE NATURE OF TURBULENT FLOW

2.2.1 Description of a flow field:- Generally a flow field can be classified into two categories, whether the flow is

(i) Laminar or

(ii) Turbulent

In a laminar flow fluid particles travel along parallel paths and there is no transverse component of velocity. Each particle follows the path of the preceeding particle without any deviation.

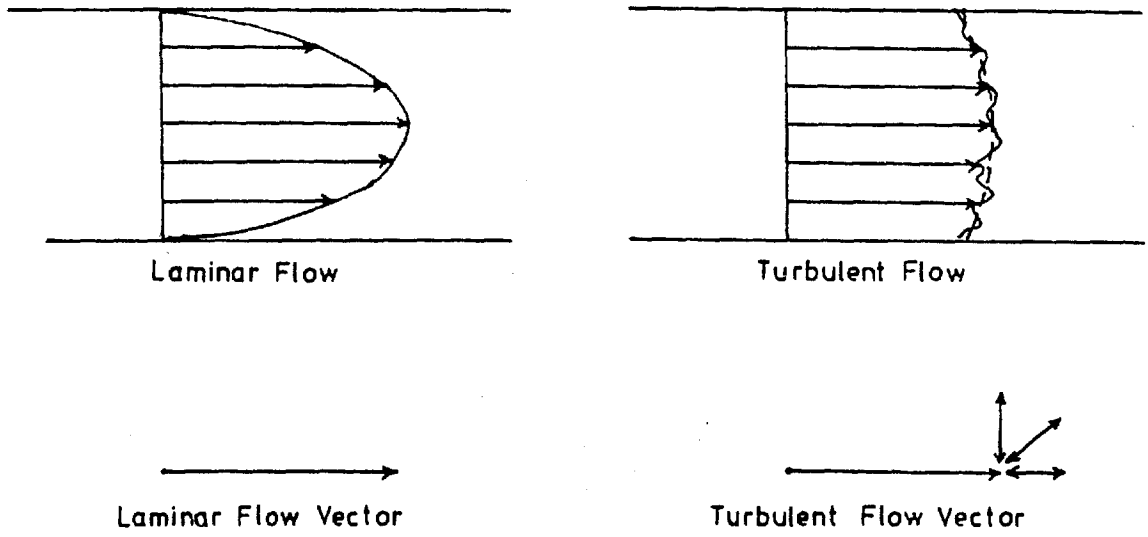
Turbulent flow is characterised by fluctuating pressures, temperatures and particle velocities. Progression of a fluid particle is irregular and with a seemingly haphazard interchange of position. Individual particles are subjected to fluctuating transverse velocities so that the motion is sinuous, called eddying, rather that rectilinear. Formation and decay of multitude of small eddies throughout the flow stream is in a random manner. The resulting intermixing of eddies gives rise to shear stresses. This type of eddy interaction is on a much larger scale than molecular interaction which is associated with laminar flow and hence losses are relatively high. In laminar flow losses are found to be proportioned to the magnitude of the velocity where as in turbulent flow losses are roughly proportional to the square of the mean velocity (94). The difference between laminar and turbulent flow is shown diagramatically in fig. (2.1).

2.2.2. Types of Turbulent Flow Field:- This can be divided into two sub-categories:-

(i) Statistically Stationary turbulent flow field and

(ii) Non-Statistically Stationary turbulent flow field.

In a very strict sense, all turbulent flow fields are unsteady, but by statistically stationary it means that local mean velocity



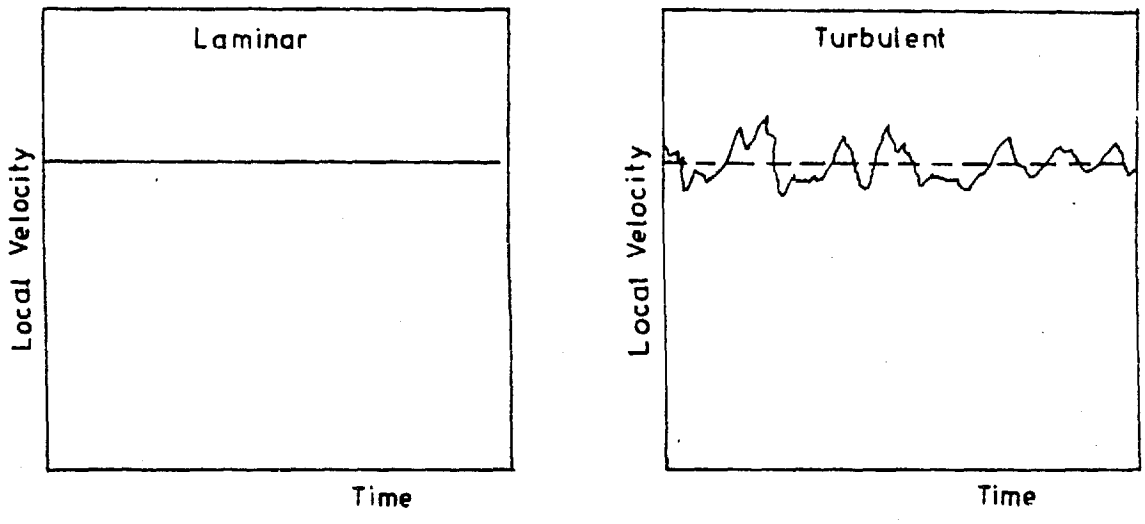


Fig (2.1) GRAPHICAL REPRESENTATION OF LAMINAR AND TURBULENT FLOW

components, local root mean square values of fluctuating components of velocity and other similar properties used to describe a turbulent flow field remain constant with time. An example of which this would be typically true is the turbulent flow field generated by a steady flow turbulent jet. A statistically non-stationary turbulent flow field is one in which all parameters used to describe the flow field are varying with time. Turbulent flow fields inside engine cylinders are of a non-stationary nature of the latter type and are also subjected to very large pressure and temperature variations. The transient nature of the turbulence parameters makes the non-statistically stationary type of turbulent flow field difficult to investigate. To illustrate, comparison can be made between the typical instrumentation set up required for a stationary turbulence flow analysis shown in fig.(2.2) and the data recording and the data analysis procedure used in the present non-stationary engine cylinder turbulence flow analysis shown in fig. (2.3).

2.3 Parameters used to describe a Turbulent Flow Field:- A turbulent flow field is composed of random happenings, and hence it can only be represented by statistical parameters to represent its nature. Some of the important and the most commonly employed parameters are briefly mentioned below.

(i) Mean velocity component of the a Turbulent Flow:- This is the magnitude of the flow velocity around which the fluctuations of velocity takes place. In case of statistically stationary turbulent flow, this value can be found by simple averaging on by the integrated averaging method. The above method does not apply for statistically non-stationary flow, for this case the mean value can only be found out by using the ensemble averaging technique or by using a Quasi-steady approach analysis technique or by using a filtering technique. All the above three methods remove the fluctuating components of velocity from the instantaneous velocity-time record. These three methods for non-stationary turbulence flow analysis are discussed under Section (7.0).

(ii) Intensity of Turbulence:- This is the term which is referred to as the root mean square (RMS) value of fluctuating component of velocity and is an indication of the strength of eddy internal recirculation. Thus intensity of turbulence in the X, Y, Z directions are denoted by $\sqrt{\overline{u'^2}}$, $\sqrt{\overline{v'^2}}$, $\sqrt{\overline{w'^2}}$. This parameter is that most commonly used by investigators seeking to relate the flow field to the subsequent turbulent combustion field.

(iii) The Length Scale of Turbulence:- This parameter is used to

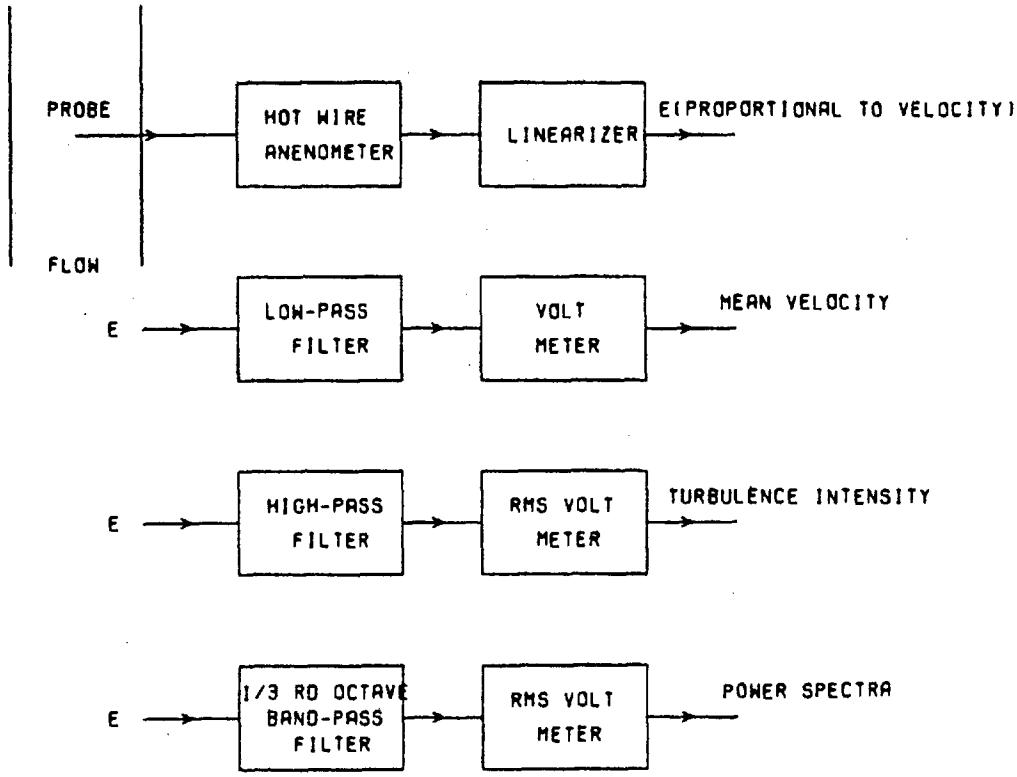


Fig (2.2) TYPICAL FORM OF EQUIPMENT SET UP FOR STEADY STATE TURBULENCE FLOW ANALYSIS

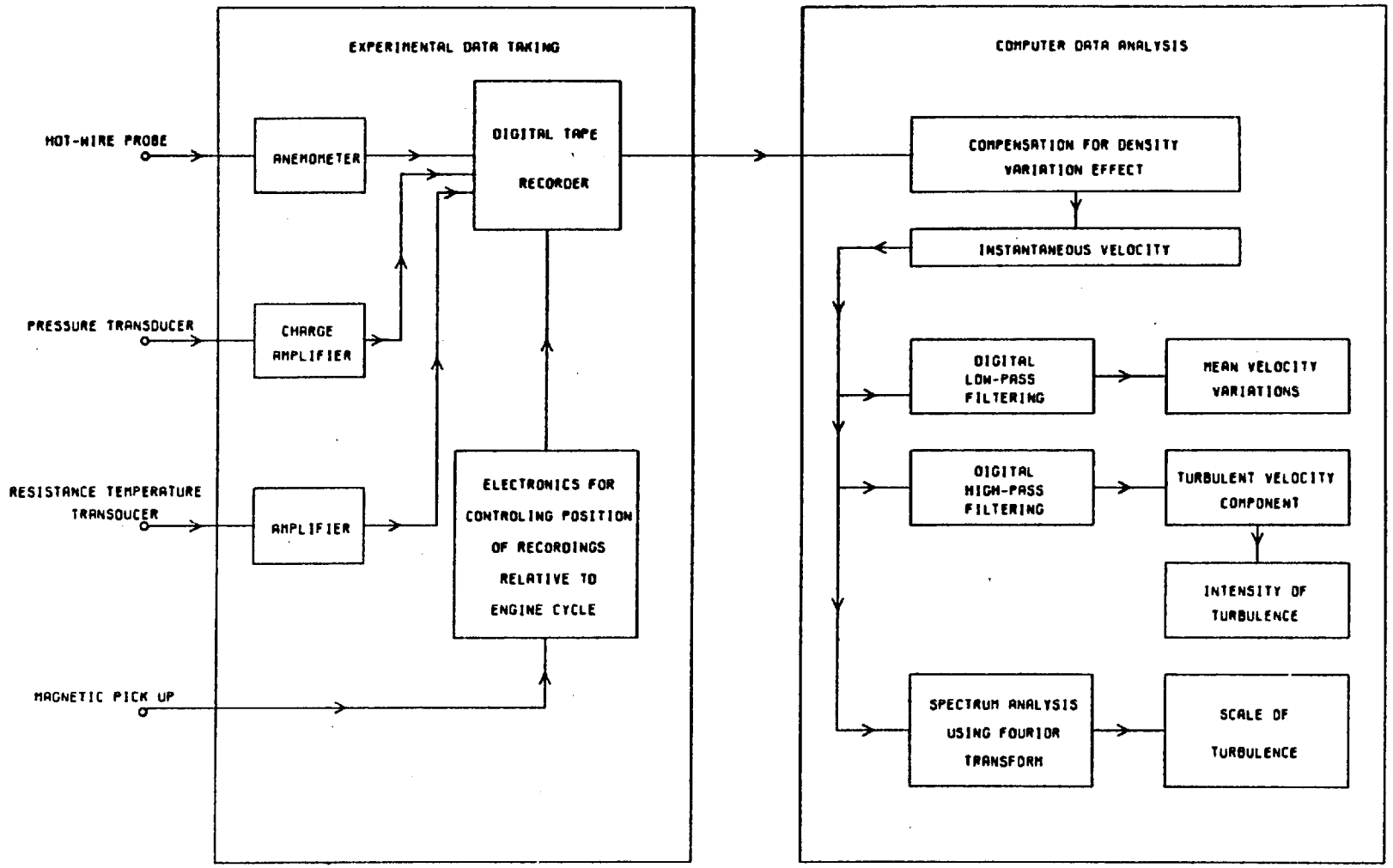


Fig (2.3) STRATEGY FOR UNSTEADY TURBULENCE FLOW ANALYSIS MADE INSIDE A MOTORED ENGINE CYLINDER

indicate the eddy size composition of a turbulent flow field. The macro-length scale of turbulence refers to the average largest size of eddy that can exist in flow field where as micro-length scale of turbulence refers to the average smallest size of eddy that can exist before it is broken up and dissipate into heat. Estimates of macro and micro length scales of turbulence can be made through the use of power spectral analysis or through the use of correlation analysis. Rouse Et Al (94) suggested a way of estimating the average eddy size of turbulent flow field by multiplying the average time interval $\overline{\Delta t}$, between the points at which the velocity variation curve crosses it mean line, by the value of mean velocity $\overline{V}$.

(iv) Time scale or Taylor Scale of Turbulence:- This can be taken as the characteristic life time of an eddy before it decays by mixing with neighbouring eddies or before it decays into heat. Macro-time scale refers to the life time of the largest eddy before it breaks into small eddy sizes where as the micro-time scale refers to the life time of the smallest eddy before it decays into heat. The life time of an eddy can be related to eddy size by knowing the mean value of the velocity of the flow field.

Macro-time scale $\qquad L_t = {}^{L}/_{\overline{U}}$

Micro-time scale $\qquad \lambda_t = {}^{\lambda}/_{\overline{U}}$

(v) Diffusivity of a Turbulent Flow Field:- Turbulent flow field, because of the presence of eddies having high internal recirculation, possess a highly diffusive nature. For an isotropic homogeneous turbulent flow field it can be defined as:-

$$\epsilon = u'^2 \int_o^\infty R(t)\, dt$$

$$\epsilon = u'^2 \, {}^{L}/_{\overline{U}}$$

$$\epsilon = u'^2 L_t$$

(iv) Spectrum of Turbulence:- It is noted that eddies of smaller sizes have higher internal recirculating velocities than that of larger sized eddies. Thus the fluctuations of a local velocity-time record consist of high frequency fluctuations due to smaller sized eddies and low frequency fluctuations due to larger sized

eddies, and hence the information on power content in separate frequency bands, termed spectrum of turbulence, enables the eddy composition of the turbulent flow field to be estimated. The analysis which is made to find the power content in frequency bands is calledspectral analysis and the analysis can be carried out by using a filtering technique involving a set of band pass filters or by using Fourior Transformation Techniques.

(vii) Correlation Function:- A characterization of the eddy size distribution within a turbulent flow can be obtained from the auto-correlation function of the velocity fluctuation at a point. The auto-correlation function in normalized form is defined as:-

$$R(\tau) = \frac{1}{T} \int_0^T \frac{U(t) \cdot U(t+\tau)}{\overline{U}^2} \, dt$$

where t is time, T is the period of the measurement, and τ is the correlation time. This relationship allows the size of the turbulent eddies to be determined from velocity measurements taken at one point in the flow. The macro and micro length scales of turbulence are related to the auto-correlation function as:-

Macro-Length Scale $$L = \overline{U} \int_0^T R(\tau) \, d\tau$$

Micro-Length Scale $$\lambda = \overline{U} \cdot \lim_{\tau \to 0} \left\{ - \frac{d^2 R(\tau)}{d\tau^2} \right\}^{-\frac{1}{2}}$$

(viii) Isotropy of a Turbulence Field:- A turbulent flow field is said to be isotropic when its parameters are independent of the orientation of the co-ordinate axes. Thus the requirement for a turbulent field to be isotropic is(94),

$$\overline{u^2} = \overline{v^2} = \overline{w^2}$$

$$\overline{uv} = \overline{vw} = \overline{wv} = 0$$

(ix) Homogeneous Turbulent Flow Field:- A turbulent flow field is said to be homogeneous, if the local turbulence parameters of each and every point within the flow field is identically the same. Thus for a homogeneous turbulent flow field,

$$\overline{v}_x = \overline{v}_y = \overline{v}_z \quad \& \quad \overline{v_x}^2 = \overline{v_y}^2 = \overline{v_z}^2$$

$$\overline{U}_x = \overline{U}_y = \overline{U}_z \quad \& \quad \overline{u}_x^2 = \overline{u}_y^2 = \overline{u}_z^2$$

$$\overline{W}_x = \overline{W}_y = \overline{W}_z \quad \& \quad \overline{w}_x^2 = \overline{w}_y^2 = \overline{w}_z^2$$

where the subscripts x,y,z denote any separate locations in the flow field.

2.4 Turbulent Flow Field in an Engine Cylinder:- In view of the major influence of the turbulent flow field on subsequent flame propagation and hence its influence on combustion rate, fuel economy, pollutant emissions and cyclic dispersion; several researches have been undertaken to investigate the flow pattern and turbulence in engine cylinders both of an experimental and a theoretical character.

Previous experimental observations involve quantitative study of the flow pattern produced inside cylinders using water flow models (71, 72) and quantitative assessment of swirl rate by using a swirl vane anemometer and hot wire anemometer (2, 3, 5, 41, 66). (Swirl vane anemometers, because of their simplicity in use, are still being employed to indicate swirl rate in diesel engine cylinders (98)). With the development in the application of the hot wire anemometer technique for engine cylinder flow investigation, turbulence parameters inside engine cylinders were successfully measured by various researchers (41, 66). Still later attempts have been made to use the laser anemometer for engine cylinder turbulence measurements (67), but this particular application still needs further development to yield reliable results. A short summary of previous experimental investigations on engine cylinder flow field and turbulence is shown in Table (2.1) to Table (2.3).

On the other hand, the quantitative theoretical prediction of engine cylinder turbulence has not yet reached a reliable stage and since it is not of immediate practical interest, its detail aspects will not be discussed.

The experimental findings (1, 2, 3, 4, 5, 41, 66) may be summarised qualitatively as follows:- The most important source of the turbulence in engine cylinder lies in the induction process. The fresh charge is drawn into the cylinder through the inlet valve opening in the form of an air jet by the action of the moving piston and thus causes the existence of large velocity gradients between the air jet and surrounding cylinder charge as well as within the jet. These local high velocity gradients create eddies and turbulence within the cylinder, figs. (2.4, 2.5). An additional swirl

Worker	Year	Title	Type of Experiment	Method of Calibration used	Remarks
Lee (70)	1938	A study of air flow in engine cylinder	Optical method of flow observation		Qualitative flow pattern observation
Semenov (1)	1958	A device for measureing turbulence in piston engine	Self constructed anemometer with analogue compensation circuit was used for turbulence investigation	Hot wire probes were calibrated using a flow nozzle. Equn. $h=Ckd^{m-1}\left(\frac{\rho V}{\mu}\right)^{m}$ was used	Measurement on mean velocity and turbulence
Kastner Et Al (103)	1966	Velocity and rate of flow measurements in internal combustion engines	Constant current anemometer was used for flow investigation	Calibration of hot wire probes was done in a nozzle flow stream	The aim was set at proving the suitability of hot wire for flow investigation in engine cylinder
Willis et Al (72)	1967	Mapping of air flow patterns in engines with induction swirl	Observation on swirl inside engine cylinder by optical method		Qualitative observation on swirl development

Table (2.1) A Short Summary on Previous Flow Measurement Inside Engine Cylinders

Worker	Year	Title	Type of Experiment	Method of Calibration Used	Remarks
Hovertin Et Al (2)	1969	Measurement of air movements in internal combustion engine cylinder	Constant temperature hot wire anemometer was used for flow investigation	King's Law of the form $Nu=a+b\ Re^{n}$ was used together with heat loss to prongs by assuming parabolic temperature distribution along the sensing wire	Investigation was done on mean velocity variation only
Barton Et Al (110)	1971	An emperical model for correlating cycle-by-cycle gas motion and combustion variations in a spark ignition engine	Constant temperature hot wire anemometer was used to measure air movements near sparking plug location	King's Law was used for calibrating the probes	An attempt was made to find out relation between cycle-by-cycle air motion to cyclic variation of engine cycle
Hassan Et Al (3)	1971	Measurement of air velocity in a motored internal combustion engine using a hot wire anemometer	Constant temperature hot wire anemometer was used to investigate air movement in pre-chamber of a diesel engine	Davies and Fisher relation, $h=C_f \rho V c_v k_w / k_o$ was used for hot wire calibration	Investigation on mean velocity variation

Table (2.2) A Short Summary on Previous Flow Measurements Inside Engine Cylinders

Worker	Year	Title	Type of Experiment	Method of Calibration Used	Remarks
Arnold Et Al (5)	1972	Induction gas velocities in a reciprocating engine	Treversing constant temperature hot wire probe was used to investigate induction gas velocities	Equation of the form, $q=A(T_w - T_g) + B(\rho V)^n$ was used for calibration of the hot wire probes	Magnitude of mean induction gas velocities were found out
Dent Et Al (66)	1975	Turbulence Structure in spark ignition engine	Constant temperature hot wire anemometer was used for investigating turbulence at sparking plug position		The effect of engine speed, throttle position and turbulence promoter on turbulence nature was investigated

Table (2.3) A Short Summary on Previous Flow Measurement Inside Engine Cylinders

component (which is the tangential component of velocity with respect to the cylinder) may be generated by using a guided inlet port or shrouded valve. Thus the nature of these initial swirl and turbulence greatly depends on the port and valve shapes, their sizes, and the angles they make with the axis of the cylinder. However, the time history of the swirl and turbulence after inlet valve closure and during the compression period is largely influenced by the combustion chamber shape. From the results of the previous experimental efforts (1, 41, 66), it was concluded that swirl and turbulence decay with time for an engine having flat disc combustion chamber shape, figs (2.5, 2.6) whereas for and engine having small squish volume or a bowl in the piston, the swirl and turbulence are amplified due to the great reduction in inertia of the cylinder charge as it is compressed into a very small volume while it tries to maintain its initial momentum, fig. (2.7). Thus previous experimental results show the large dependent of swirl and turbulence on port, valve and combustion chamber shape.

It must follow therefore that the results of experimental observations of swirl and turbulences in one engine geometry are not directly applicable to another engine of different design, unless they have identical geometrical shapes, port and valve angles and the results are to be applied for the same engine operating conditions. Most of the previous effort (41, 66) on turbulence measurement were made at a single location, usually at the sparking plug position, which forms the most accessible position for mounting hot wire probes. A very little information exists on the nature of the spatial variation of turbulence (1). But for study of the influence of turbulence on flame propagation rate it is highly desirable to have detailed information on the spatial and temporal variation of turbulence parameters for various engine operating conditions. Thus a decision was taken to make experimental investigation on spatial and temporal variations of turbulence, though it required a very extensive experimental research effort, with the aim of obtaining a detailed picture of the turbulence and hence helping in the study of its influence on flame propagation, combustion rate and in finding a suitable turbulent combustion model for spark ignition engine cycle simulation. The detailed approach to the experimental procedure is discussed under section (3.0).

It is also very encouraging to note from the work of Ohigashi Et Al (124) using a spark discharge probe, that the flow pattern during compression period appears to be almost unaffected by the

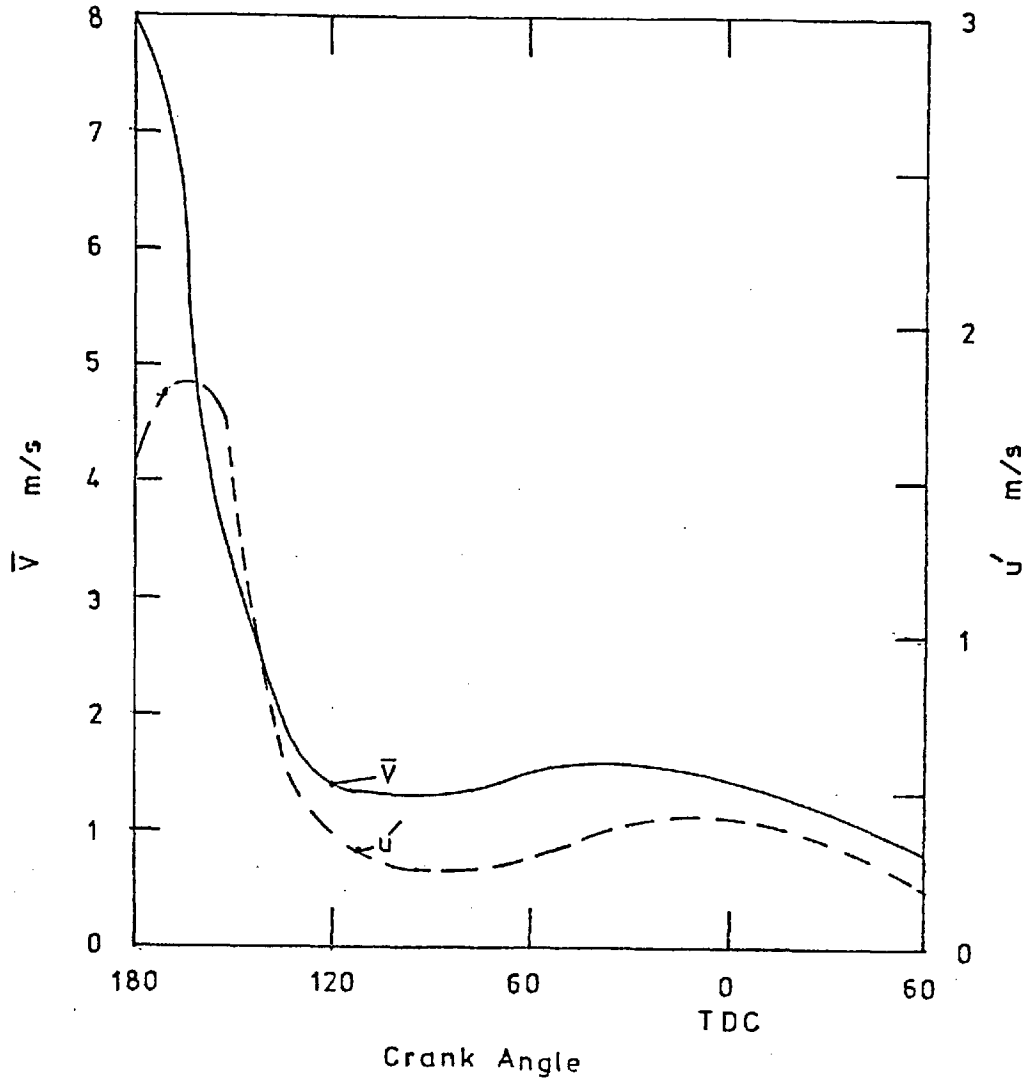


Fig (2.4) Mean Gas Velocity and Intensity of Turbulence against Crank Angle. Semenov (1)

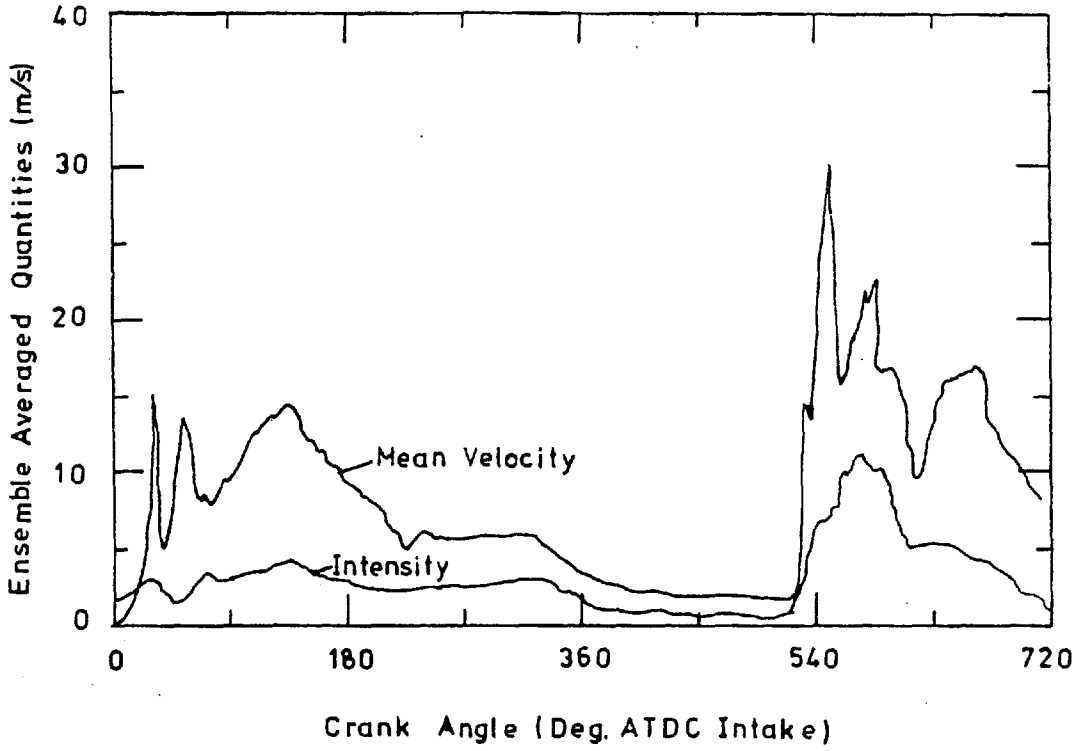


Fig (2.5) Ensemble-Averaged mean velocity and turbulent intensity at base operating condition with non shrouded valve. Lancaster (41).

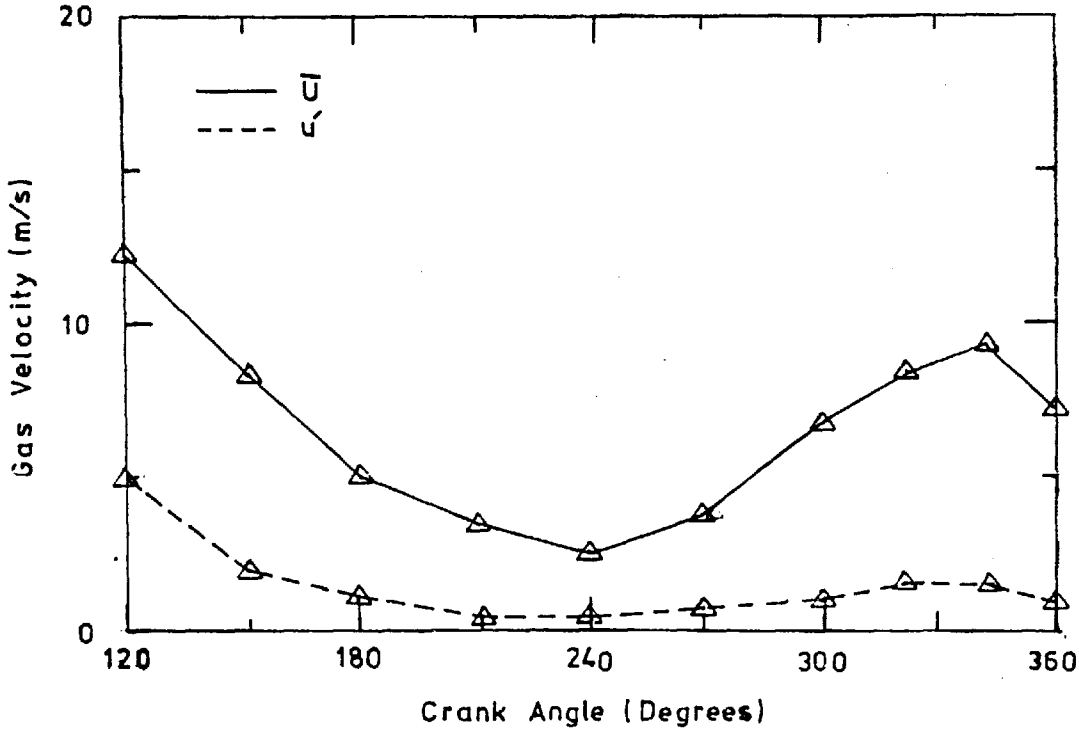


Fig (2.6) Variation of Gas Velocity in a Wedge Chamber (W.O.T.) Dent Et Al (66)

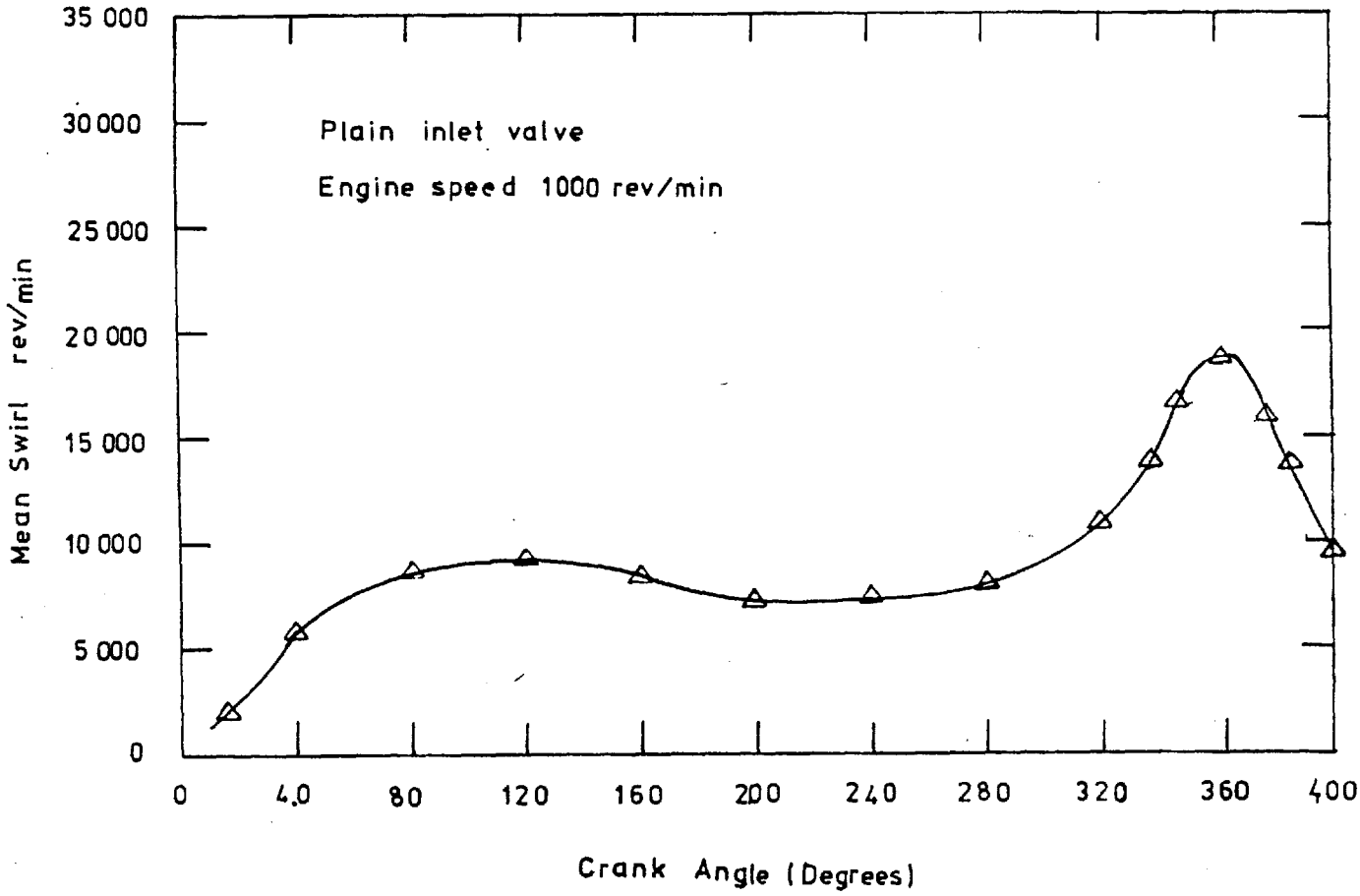
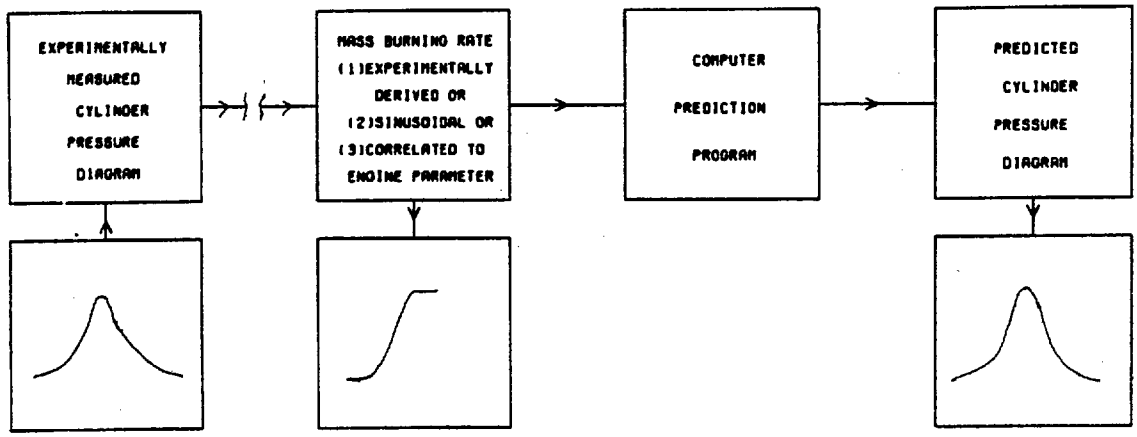


Fig (2.7) Mean Swirl Variation during engine cycle at 1000 rev/min Bowl in Piston Crown. Dent Et Al (66)

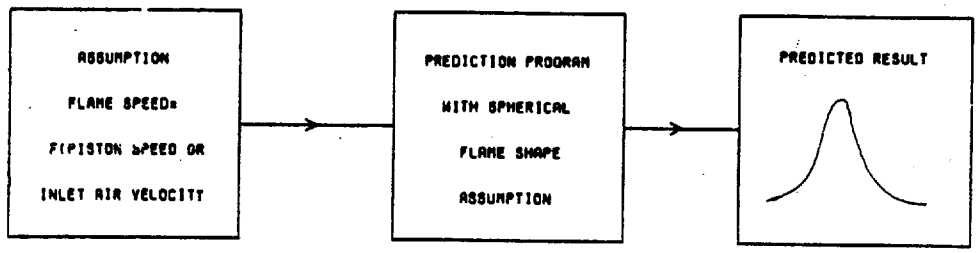
process of combustion in preceding cycles. It may therefore be deduced that the measured cold level flow patterns and turbulence obtained during the compression period in a motored engine will give an acceptable representation of the nature of the flow pattern and turbulence prior to and during the combustion process in the firing case. This is a matter on which the current work bears strongly.

(1) PREVIOUS APPROACHES

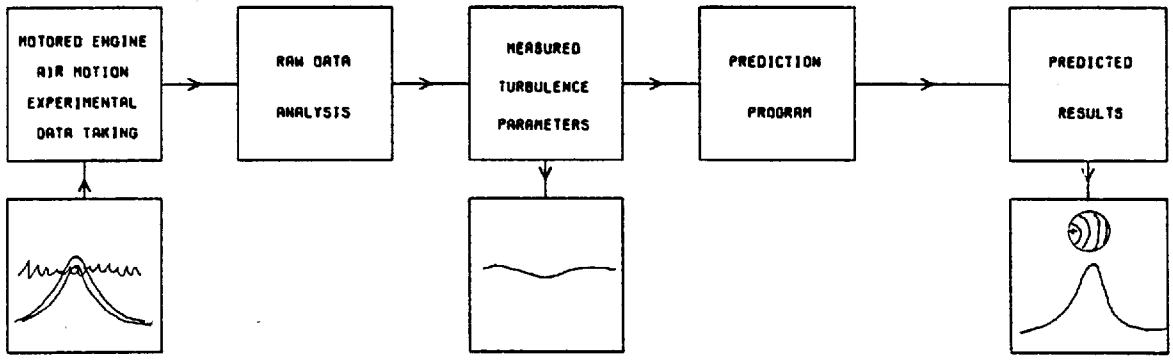
(i) Finite Mass Burning Rate Approach



(ii) Finite Flame Propagation



(2) PRESENT RESEARCH APPROACH



3.0 EXPERIMENTAL PROCEDURES FOR TURBULENCE INVESTIGATION WITHIN ENGINE CYLINDERS.

The nature of the engine cylinder turbulence which controls the turbulent flame propagation speed, combustion rate and hence the fuel economy, pollutant emissions and cyclic dispersion has been under investigation using various experimental techniques (1, 2, 3, 5, 6, 41, 66). The results of these observations generally indicate the flow inside cylinder to be three dimensional. Thus an effort was made to measure the three dimensional variation (spatial and directional) of engine cylinder turbulence. Normal steady state turbulence measurement techniques do not apply for this case. In addition engine vibration and lubricating oil leakage across the piston and down valve guides add further problems in measurements which use fine wire sensor probes or optical windows, which are generally associated with existing turbulent flow measurement techniques. The presence of large variations in pressure and temperature of the fluid medium due to the expansion and compression effect of the moving piston requires some means of compensation for cases where the measuring instrument responds to these fluctuations as well. In order to measure turbulence successfully the following factors have to be taken into account.

(a) Sensor probes or optical windows, which are necessary depending on the choice of experimental techniques, must have sufficient service life before they need to be replaced or cleaned due to lubricating oil leakage or engine vibrations.

(b) Some form of synchronization between the engine cycle and the measuring or recording instruments is necessary so that the results can be referred to the relevant part of the engine cycle.

(c) Compensation for pressure and temperature variations of the fluid medium must be possible if the measuring instrument responds to these fluctuations.

(d) The measuring instrument employed must have a frequency response up to the maximum turbulent frequency of interest.

With the above requirements in mind, the following steps were taken in choosing and using a particular turbulence measurement technique.

(i) A survey of the available existing flow measurement techniques was undertaken as a preliminary to a final decision on

the use of a particular technique.

(ii) A survey of all possible operating modes of the flow measuring instrument which is associated with the selected measurement technique.

(iii) Design of sensor probes and any telemetering system required.

(iv) Design of electronics for interfacing, synchronizing and controlling operations.

(v) Design of any necessary modifications to be made to engine under investigation.

As the decisions to be made in each of the above steps forms an important factor in a successful experiment, the problems associated with each step are reviewed and the decisions taken are briefly mentioned in the following sections (Section 3.1 to 3.12).

3.1.0 Available Experimental Techniques:- The following are the experimental techniques which are available for flow investigation inside engine cylinders.

(i) Flow Visualization Technique
(ii) Vane Anemometer Technique
(iii) Spark Discharge Technique
(iv) Vortex Sheding Frequency Technique
(v) Hot Wire Anemometry Technique
(vi) Laser Anemometry Technique

The selection and use of a particular experimental technique must be based on its ability to satisfy the requirements of the proposed investigation. Each of the above available measurement technique is briefly described and its suitability, adaptability and limitations for turbulence investigation considered.

3.1.1. Flow Visualization Technique:- This is only applicable where the aim is limited to qualitative accessment of the flow pattern produced by a particular engine geometry. A rough estimate of the mean velocity of the flow field can be made by seeding the flow medium and using time synchronized flash photography, but it is difficult to use in unsteady flow.

3.1.2. Vane Anemometry Technique:- This method is employed to indicate the swirl level in engine cylinders where a well organised swirl exists. This method, because of its ease in application, is still being used for swirl indication in diesel engine cylinders (98). However, vane anemometers are insensitive to small turbulence fluctuations and does not permit study of small scale flow patterns, while at all times it has to be oriented correctly to a flow which is

not known at outset. This technique cannot be used for turbulence flow investigation.

3.1.3. Spark Discharge Technique:- The time interval for electrically charged particles to travel from a sparking positon to a sensor probe of known distance can be used to indicate the mean velocity of the flow. The arrival time of the charged particle is sensed as a rise in voltage in the sensor probe. This technique has been employed to measure mean velocity in an engine cylinder during motored and firing state (124) as well as used for measuring mean exhaust gas velocity in an exhaust pipe of an engine (96). But its insensitivity to responding to turbulent fluctuations makes it unsuitable for turbulence flow investigation. It has, in addition, to be correctly oriented in an unknown flow.

3.1.4. Vortex Shedding Frequency Technique:- This method is based on the Karman Vortex Shedding Frequency as a velocity sensor. Though this method of measurement is independent of the properties of the fluid medium, it has difficulties in separating the shedding signal from the turbulence signal, and at high turbulence level it becomes difficult to detect on shedding signal. (4). Thus this technique is only suitable for mean velocity indication where the turbulence level is very low or absent.

3.1.5. Hot Wire Anemometry Technique:- This technique has been successfully applied to measure swirl and turbulence in engine cylinders (1, 2, 3, 5, 41, 66). A high accuracy in measured results can be obtained if the necessary precautions are taken during the experimental data taking stage and in the data interpretation stage of the raw recorded data. The hot wire sensor probe can be designed to produce minimal flow disturbances in the region which is under measurement. Its ability to respond to high frequency turbulent fluctuations plus three alternative operating modes which may be chosen to suit particular applications make it very attractive for engine cylinder turbulence investigations.

3.1.6. Laser Anemometry Technique:- In this flow measurement technique, a laser beam is scattered by seeding particles in the fluid medium and results in a Doppler Shift Effect as the wavelength of the scattered light is altered by the particle motion. This Doppler shift frequency, from which the velocity of the particle can be determined, is detected by using a suitable electronic tracker circuit. The instrument responds to high frequency turbulent fluctuations and its output signal is independent of the fluid medium properties. However, its application to engine cylinder flow measurement has encountered

several difficulties and problems (67). Noises due to flare when the laser beam hits the cylinder wall, engine vibrations and the requirements of a uniform seeding medium are still posing problems for its successful application in engine cylinder turbulence measurement. Also engine combustion chamber geometry normally only permits use of a single optical window and hence a backward scattering technique has to be employed. In this mode of laser operation it requires 100 fold increase in laser power relative to the forward scattering technique (4). However, judging from the rate of progress in this field, this technique may become available for engine use with reliability in the forseeable future.

3.2.0. Selection of an Experimental Technique:- The above brief description on the available flow measuring techniques clearly show that, the flow visulization technique, the vane anemometry technique, the spark discharge technique and the Vortex shedding frequency technique are not applicable for turbulence measurement. Previous efforts to study engine cylinder flow measurements using laser anemometry (67, 68) have shown that this type of laser application still need further developments for successful engine cylinder flow measurement applications, where as hot wire anemometry has been successfully employed for both swirl and turbulence investigations within engine cylinders (1, 2, 3, 5, 41, 66). However, hot wire anemometry also has some limitations, which have to be taken into consideration, when applied to engine cylinder flow measurements and these are shown in Table (3.1) compared with those limitations associated with laser anemometry for the same application. As the aim of the first part of the research is to have a reliable spatial and temporal variations of turbulence data, which can later be applied to check its influence on turbulent flame propagation in engine cylinder using a computer simulation model, hot wire anemometry, which has previously been used and proved to be successful for engine flow applications, was finally chosen for engine cylinder turbulence investigation.

3.3.0. Hot Wire Anemometry:- Hot wire anemometry is a standard technique for measuring local mean velocity and turbulence level in both statistically stationary or non-stationary (transient) turbulent flow. The output voltage of the anemometer is not only a non-linear function of velocity but also is affected by the fluid density change. Thus some form of compensation for these pressure and temperature changes (density changes) has to be provided. The method of compensation for these changes or, in other words,

Limitations of Hot-Wire and Laser Anemometeries when applied to Engine Cylinder Flow Measurement

Hot Wire Anemometry.

(i) Compensation for Fluid Density Change is necessary

(ii) It has Directional Ambiguity

(iii) Frequent Wire Breakage

(iv) Conduction heat loss effect to supports has to be taken into account

(v) Flow disturbances caused by support

Laser Anemometry

(i) The number and size of seeding particles must be optimized

(ii) Reflection from metal sufaces surrounding the measuring position causing flare

(iii) The electrical signal is not a real time analogue but a step function

(iv) Dirt on the window must be avoided

(v) Engine vibrations

(vi) More extensive modification to the combustion chamber is necessary to instal optical window

Table (3.1) Limitations of Hot-Wire and Laser Anemometry Methods when applies to Engine Cylinder Flow Measurement

the calibration method used for the present research effort is mentioned under section (A.5). The hot wire anemometer (the resistance bridge) can be operated in one of three possible operating modes, they are:-

(i) The Constant Current Mode

(ii) The Constant Temperature Mode

(iii) The Temperature Compensated Mode

Each mode of operation will be briefly mentioned.

(i) The Constant Current Mode:- The principle of this mode of operation of the bridge (fig. 3.1) has already been outlined. The hot wire sensor heating current is maintained at a constant value using a constant current source. This current does not change irrespective of the flow velocity changes around the sensor wire. The flow velocity change causes the temperature and hence the resistance of the wire to change and thus gives bridge voltage variation. This type of operating mode limits the attainable value of the maximum frequency response of the bridge, as the hot wire sensor element which has finite thermal inertia is allowed to vary its temperature with flow velocity fluctuations.

(ii) The Constant Temperature Mode:- In this mode of operation the sensor hot wire element is kept at a constant temperature which is determined by the value of the resistance R_i employed in the passive arm of the bridge, (fig 3.2). The bridge is always maintained in balance by heating the sensor wire using current from a very high gain feed back amplifier. Thermal inertia effect of the sensor wire is made less significant by keeping its temperature (resistance) constant irrespective of flow velocity fluctuations by the high gain feed back amplifier. Thus this mode of operation offers a higher maximum frequency response than the other two configurations and is therefore the desired operating mode for turbulence investigations.

(iii) The Temperature Compensated Mode:- In this mode of operation, the temperature difference between the sensor wire and the fluid medium is kept constant by employing a temperature sensing resistor R_T in the passive arm of the bridge, (fig 3.3). The amount of overheat temperature above the fluid medium temperature is determined by the cold resistance ratio of the sensor and the compensating resistor. The value of the maximum frequency response in this case is lower than that of constant temperature operating mode because the temperatures of the sensor wire and the compensating resistor, both having finite thermal inertia, are allowed to vary and follow

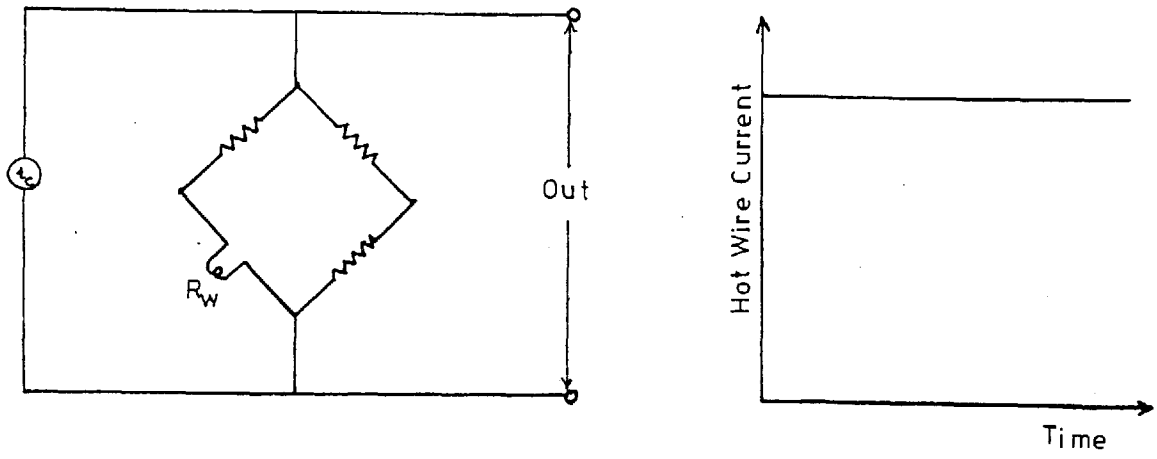


Fig (3.1) Constant Current Mode Operation

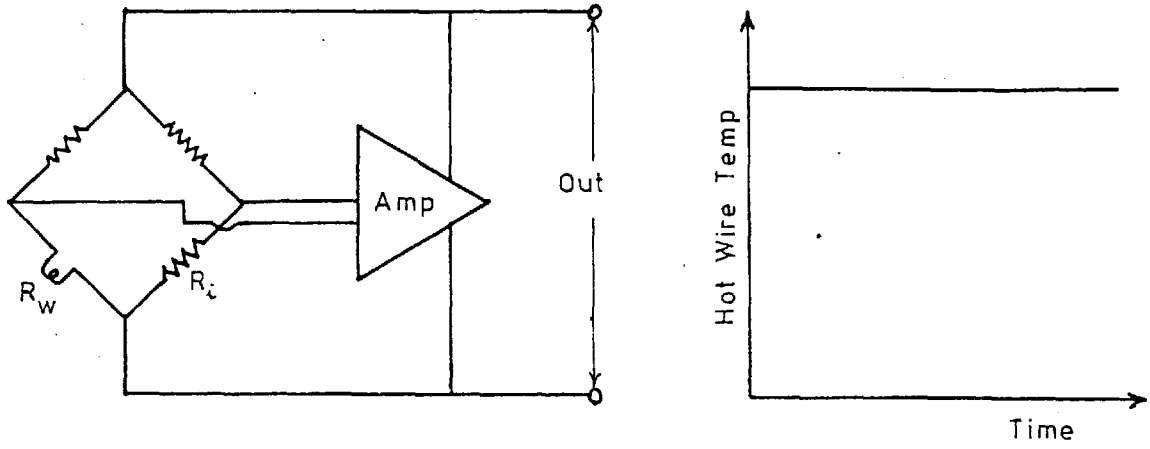


Fig (3.2) Constant Temperature Mode Operation

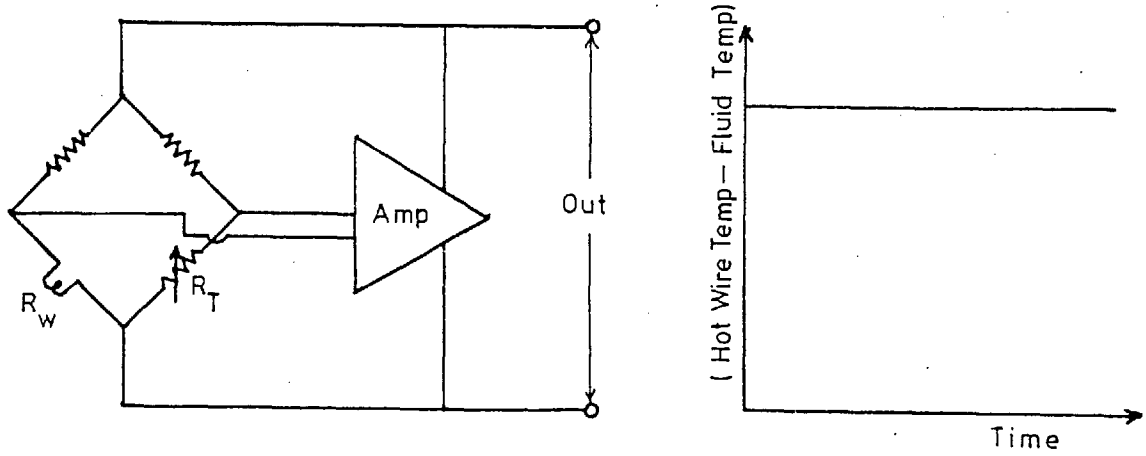


Fig (3.3) Temperature Compensated Mode Operation

the fluid medium temperature variation. This mode of operation is often used for cases, where the fluid medium temperature is subject to fluctuations, because of its automatic temperature compensation effect.

Based on the above considerations, the constant current mode of operation is not desirable because of its poor frequency response together with the increased danger of wire breakage at low flow velocity. The temperature compensated mode, however, may be used for this purpose, but the compensation for the fluctuations of pressure still has to be added. The constant temperature mode of operation, on the other hand, is highly desirable for turbulence investigation because of its higher maximum frequency response than the other alternatives. The arrangements in favour of this mode were reinforced by the fact that it was previously used successfully by others (41, 66) in engine cylinder flow investigations. Hence the constant temperature hot wire operating mode was chosen for the present engine cylinder turbulence investigations.

3.4.0. Hot Wire Sensor Probes for Engine Cylinder Flow Applications:-
The hot wire sensor probes for engine applications are required to withstand and operate in a hostile environment within a small confined engine combustion chamber. All commercial probes, which have a long probe body, are not applicable for engine cylinder flow investigations. The basic requirements of the hot wire probes for engine cylinder flow and turbulence investigation are as follows:-

(i) The probes must have a reasonably small size so that they can be placed in the small combustion chamber without significantly affecting its overall geometry and shape.

(ii) The probes must be of such design so that they can be attached to and detached from either the cylinder head surface or piston crown with relative ease.

(iii) The supporting prongs of the sensor wire element must have enough strength and rigidity to prevent wire breakage via prong vibration but must be small enough to make negligible disturbance in the flow around the prong regions.

(iv) The probes must be of such shape and size they permit the use of the existing hot wire welder and manipulator (DISA Type) to weld the fine sensor wires to the supporting prongs.

(v) The probes must be of such design that they permit the use of a lead wire system that can be used successfully under engine motoring operations.

The above considerations led to the design and development of a hot wire probe system which was successfuly employed for engine turbulence investigation.

3.4.1. Description of the Hot Wire Probe Design:- The probe support has to carry the connection for three hot wires. The support used consists of a small threaded steel tube of 10mm outside diameter with a 7mm diameter centrally drilled hole. A ceramic casting, 7mm diameter, which holds six supporting prongs for the three sensor wires is placed inside the drilled hole and is held in position by epoxy glue. The prong tips are of ground conical shapes spaced 2.1mm apart. 10 micron-diameter Platinum-radium wire was welded across the tips of the prongs to form a three sensor wire probe. This arrangement gives length/diameter (l/d) ratio for the sensor wire element around 210 which is well over the accepted minimum hot wire length of (l/d) ratio of 40 needed to keep the magnitude conduction losses small compared to the total energy loss from the wire. The probe design is shown in fig (3.4). Designed probes together with some probe handling attachments which were designed to be used with the existing welder and manipulator enabled the three sensor wires, two horizontal wires and one vertical wire of the probe to be welded with no difficulties.

3.4.2. The Choice of Sensor Wire Element for the Hot Wire Probes:- Careful selection of the type of sensing wire element is necessary as it is required to operate at a high temperature, which has to be above the maximum engine compression temperature, and at the same time withstand the hostile engine cylinder environment. The major requirements for a sensor wire for flow investigations in engine cylinders are that it should:

(i) have sufficient strength to withstand to engine vibrations while it is operating at high wire temperature.

(ii) to maintain its physical composition and resistive properties during its operating life. (This condition is necessary because hot wire elements operated at a high temperature are subjected to an oxidation effect by the surrounding medium and this can cause large variations in properties of the wire and hence cause error in measured results).

3.4.3. Sensor Wire Size:- The size (diameter) of the sensor wire was selected based on a compromise to between two conflicting requirements, which are:-

(i) the wire must have sufficient mechanical strength and

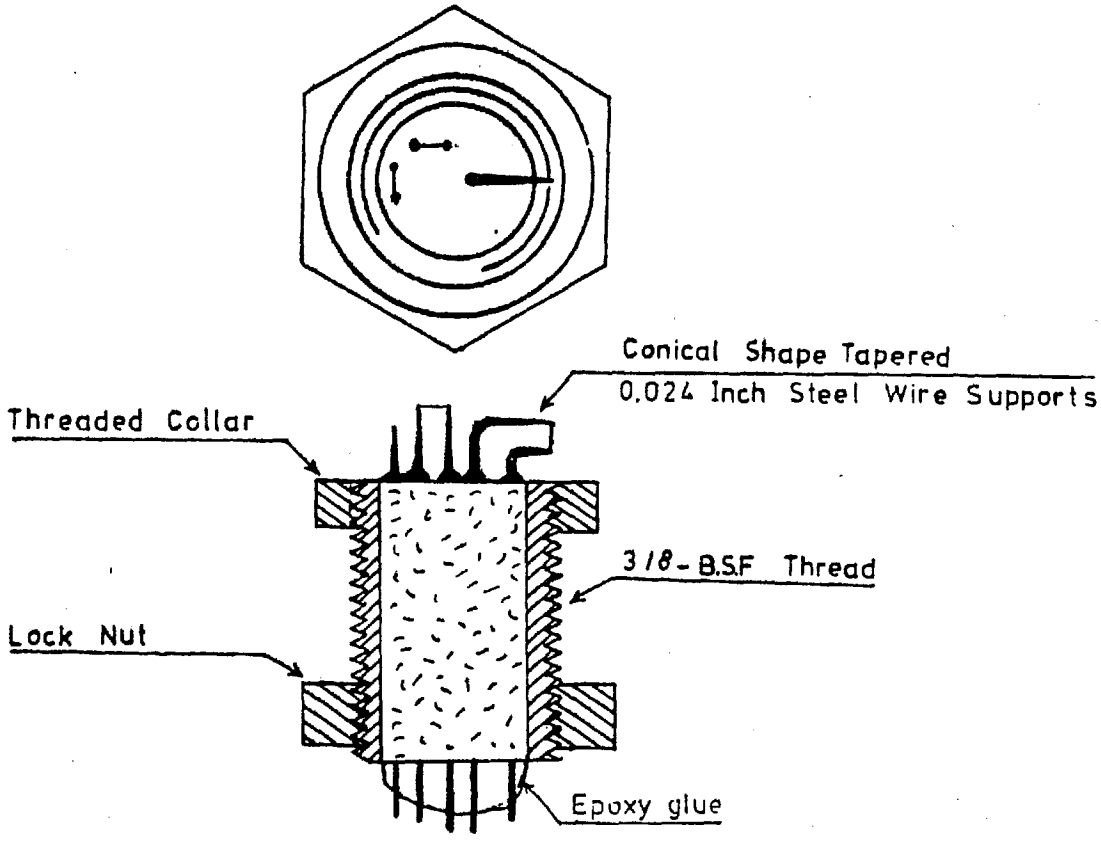
(ii) must have high frequency response.

For mechanical strength it is desirable to have a large diameter wire where as for the maximum frequency response it is desirable to have a very small diameter wire. Initial tests were made using several different diameter wires and found that wire below 10 micron meter diameter did not survive long enough to yield useful experimental results. Based on this experience 10 micron meter diameter wire, which was the minimum size to have a reasonable service life, typically of the order of 20 minutes, was chosen for the experimental investigation.

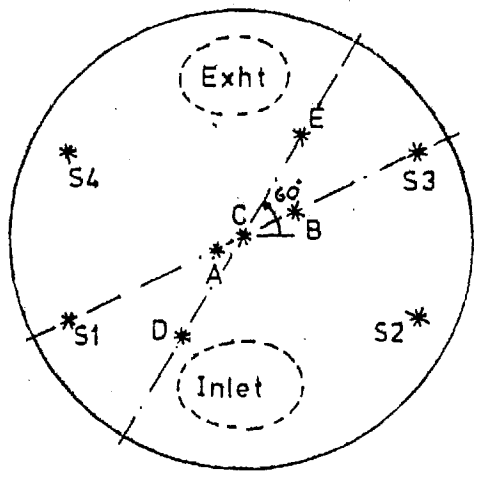
3.5.0 Measuring Positions:- It is necessary to make measurements at some representative locations so that a comprehensive picture of the spacial distribution of turbulence field in the combustion chamber can be drawn from the measured results. But the decision on the choice of measuring positions is largely influenced by the shape of the piston crown, shape of the cylinder head and the locations of the valves and the sparking plug holes. For the employed engine configuration, turbulence characteristics at the circumferential regions of the bore of the cylinder was investigated by using the existing four sparking plug holes which are located in the cylinder head and for those at the inner regions of the bore were investigated by using sensor probes which were mounted at five different locations on the piston crown, which was made detachable, to reduce the amount of work for dismantaling and reassembling the engine when changing the probes. The positions used for measurements are shown in fig. (3.5). Thus turbulence characteristics were investigated at nine different locations and the measured results gave a fairly good detail about spatial and temporal variations of turbulence field in the employed engine cylinder (Section 5).

3.6.0 Lead Wire and Linkage System:- A special lead wire and linkage system became necessary for getting information from probes which were mounted on the piston crown. After an initial survey on previous work involving similar type of telemetering (Appendix A.9), the decision was taken to make use of a continuous type telemetering linkage.

A continuous mechanical two bar linkage was designed and made by the author and was successfully applied throughout the experimental work for telemetering of the probes on the piston crown. The linkage was made from alluminium alloy to have light in weight. Steel tubes were used to serve as bearings at the joints as well as to serve as passages for lead wires while they



Fig(3.4) Designed Hot-Wire Probe



Located on Piston Crown	Radius in CM
A	0.5
B	1.0
C	0.0
D	2.0
E	2.0
Cylinder Head	
S1	3.5
S2	3.5
S3	3.5
S4	3.5

Fig(3.5) Positions Of Measurement

pass from one arm to another. Piston, connecting rod and the linkage assembly used is shown in fig (3.6).

3.7.0 Data Recording Method:- One requirement for a successful turbulence flow investigation within an engine cylinder is acquiring a high speed data recording system whose operation is sychronized to the occurence of the engine cycle. After an initial survey on all possible and available data recording systems, a high speed digital data acquisition system was built based on the availability of a Kennedy Digital Tape Unit. All additional electronics required were designed and built to suit the specific requirements of the present investigation.

The recorded data were cylinder pressure, cylinder temperature and anemometer output voltage. The instrumentations used and their set up is shown schematically in fig (3.7). The high speed digital data acquisition system comprised of:-

(i) An Electronic Pulse Generator and Pulse Synchronizer Unit
(ii) A Batch Control Logic Unit
(iii) A Kennedy Digital Tape Unit consisting of a multiplexer, an analogue to digital coverter (ADC), two high speed storage buffer units and a tape drive.

Tape Unit makes one sequential recording of information from input channels whenever it receives a control pulse from an external device, which is the batch control logic unit in our case. The batch control logic unit is so designed that it releases a predetermined amount of control pulses at a predetermined frequency (2048 pulses at 50KHZ in the present case), starting from a selected crank angle position, so that desired number of digital recordings are made by the tape unit from the input channels at the desired part of the engine cycle. The starting position of recordings can be shifted to a new position after a specified number of repetitions of recording 2048 words have been made. The square wave pulses at an accurate base freqency and the engine revolution marker pulse from the pulse generator and synchronizer unit are used by the batch control logic unit for deriving respectively the recording frequency and the positions of the tape unit control pulses with respect to engine cycle. The available recording pattern by using the present data acquisition system is shown in fig (3.8) relative to engine cylinder pressure diagram.

To clarify the operation of the data acquisition system the following terms are defined:-

A Batch of Data:- This consists of 2048 recorded data words which

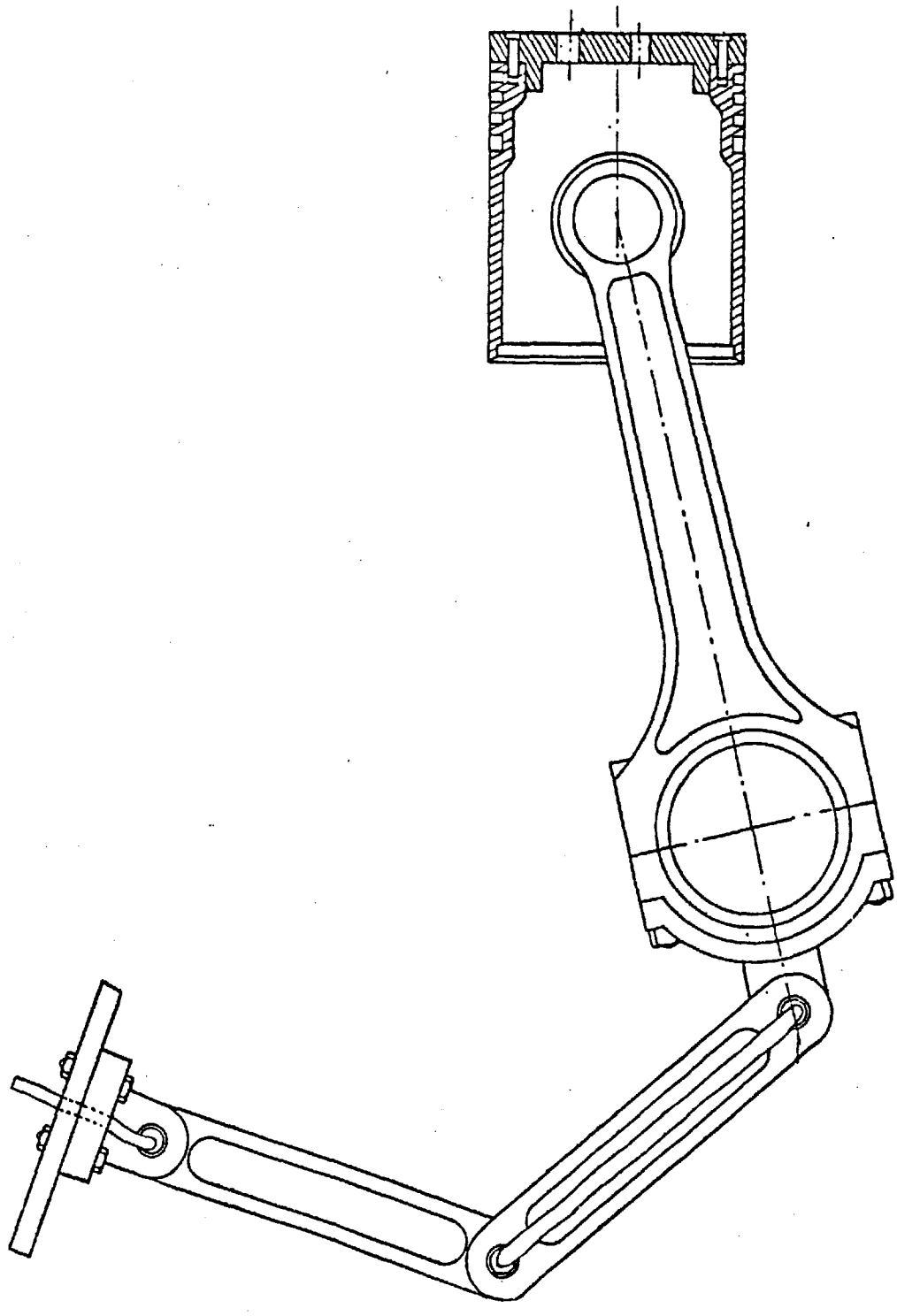


Fig.(3,6) Piston, Connecting Rod And Linkage Assembly

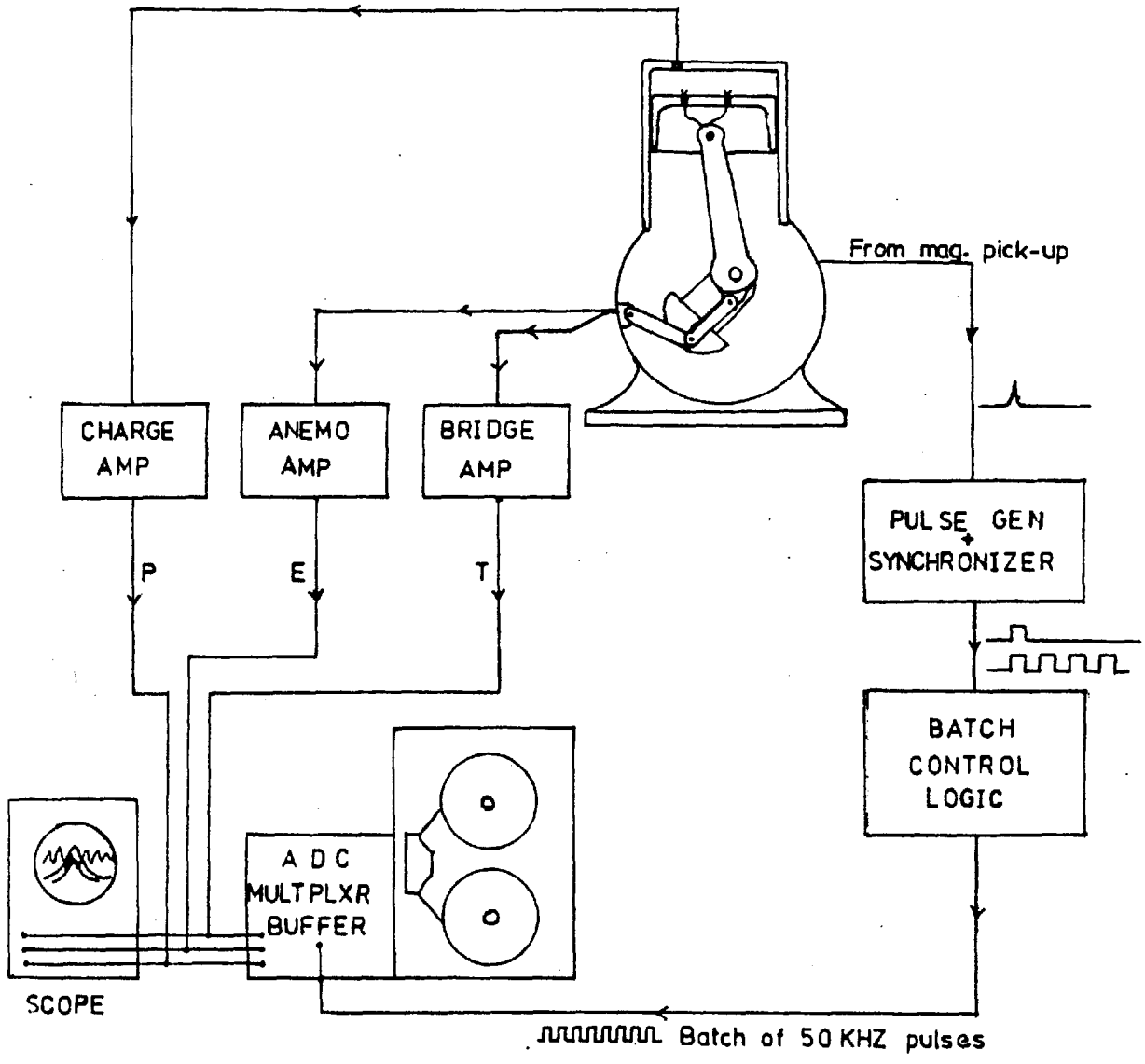


Fig (3.7) Instrumentation Set Up Diagram for Turbulent Measurement

Recorded Signals:- (i) Cylinder Pressure
(ii) Cylinder Temperature
(iii) Anemometer Voltage

Mode of Recording:- Single channel at a time

Recording Frequency:- 50KHZ

Starting Position of Recording:- 60 degrees BTDC (Compression Stroke)

Number of Recording Cycles:- 50 cycles

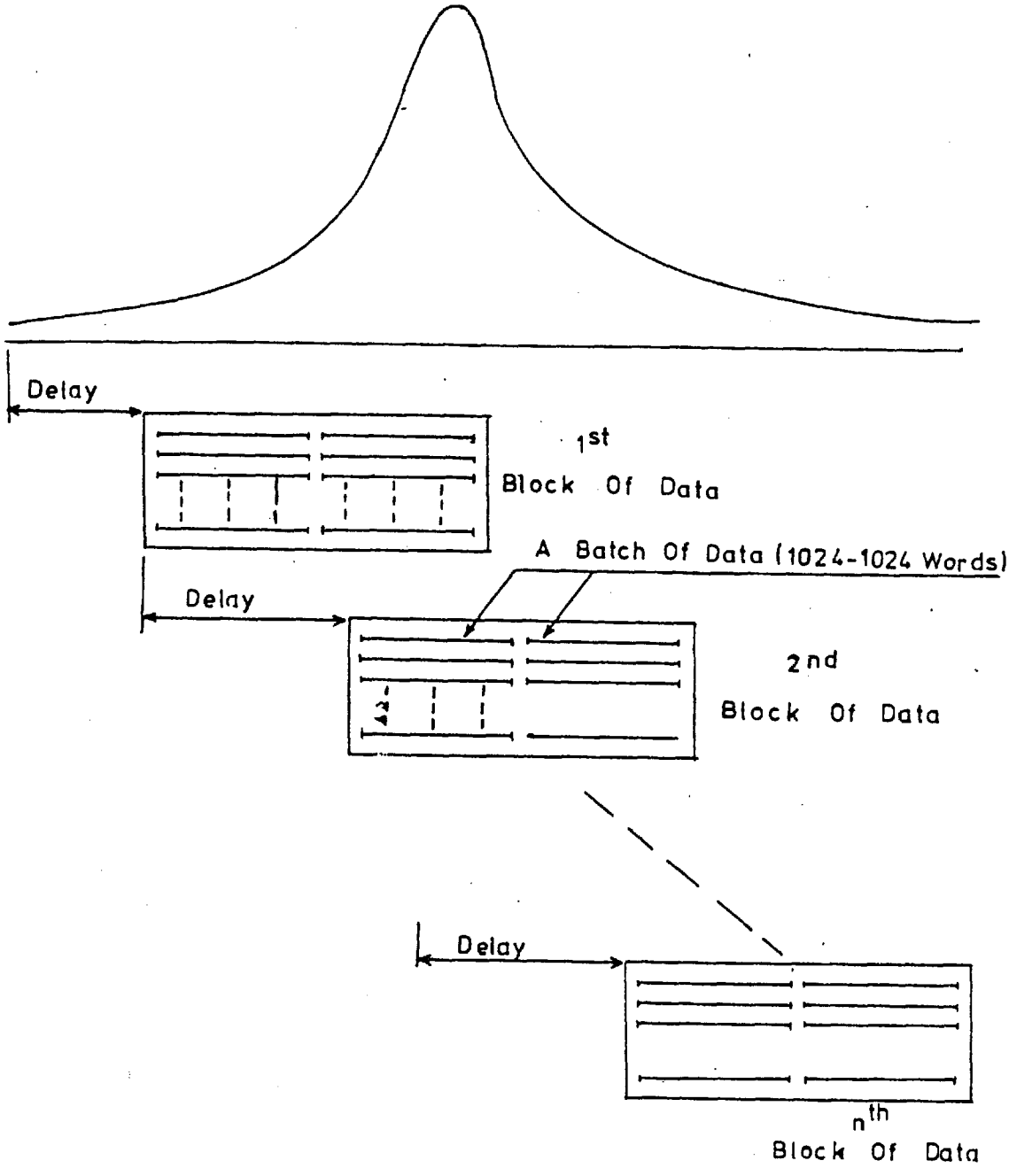


Fig (3.8) A data recording pattern which can be obtained by preprogramming the batch and block formation control unit. (The pattern is shown here relative to motored cylinder pressure diagram).

are obtained by the recording made at the specified part of the engine cycle. (The number 2048 is fixed by the overall size of the two high speed storage buffers within the tape unit).
A Block of Data:- This consists of a specified number of batches of data.
Cycle Skip:- Number of engine cycles to be skipped after recording a batch of data and before next batch of data is recorded. (The cycle skip provides time for transfering data which has been temporarily stored in two high speed buffers to the magnetic tape).
Recording Frequency:- The frequency with which data are recorded by the tape unit.

The following sequences were involved in the operation of the digital data acquisiton system.

(i) Recording a Batch of Data:- Beginning from the specified position in the engine cycle (60 degrees before top dead centre during compression stage for the present case), 2048 data words were recorded at a specified frequency (50 KHZ) to form a batch of data. To satisfy the hard ware limitation of the tape unit the first 1024 words were first recorded, then a pause followed by the recording of the second 1024 words. The pause in the present was 60 micro-seconds.

(ii) Cycle Skip:- After recording of a batch of data, a specified number of engine cycles were skipped before recording the next batch to allow for the time for transferring data from the high speed storage buffers to the magnetic tape.

(iii) Batch Repetition:- After the cycle skip the recording of next batch of data was made (Step 1). Steps 1 and 2 were repeated in the above way until specified number of batches in a data block were recorded.

(iv) Block Repetition:- The recording stopped if no more data were to be recorded, otherwise the recording of next block of data was repeated in the same way at a specified new position. After a total number of specified blocks of data were recorded, the data recording stopped. The whole recording pattern and sequences could be repeated by pressing the manual reset and start key.

For the present investigation, as the interest was on the quantitative nature of turbulence which influences flame propagation and combustion rate, the turbulent flow field data were recorded for that relevant part of the motored engine cycle and the corresponding recording pattern used is shown in fig (3.9). The function of each electronic unit is briefly mentioned below.

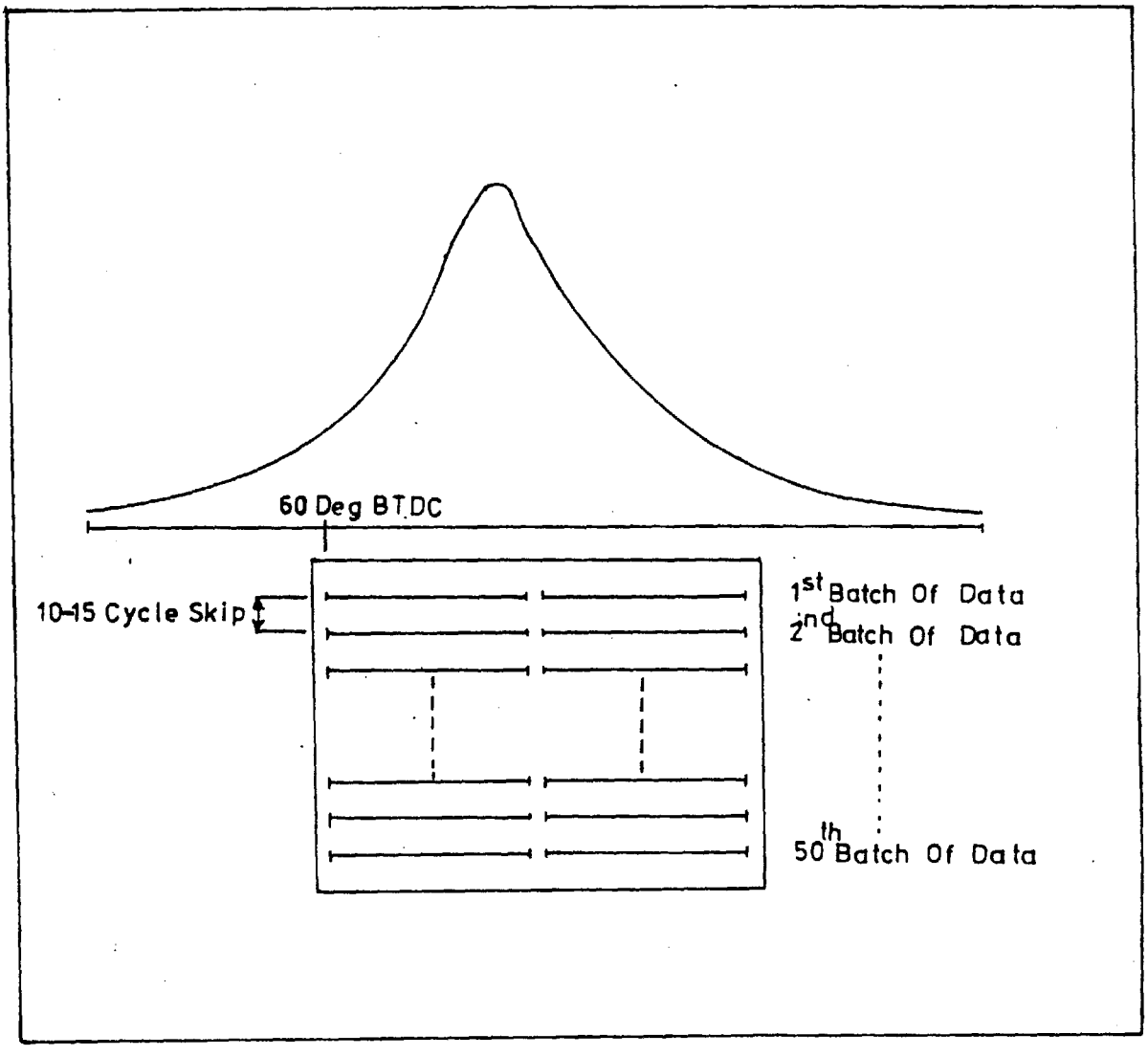


Fig (3.9) Data Recording Pattern Used by the Present Research Effort.

(i) An Electronic Pulse Generator and Pulse Synchronizer Unit:-
The function of this unit is two fold:-

(a) To generate a reference marker pulse of the engine cycle so that the position of a batch recording can be determined relative to this marker pulse position as well as the marker pulse itself can be used for counting engine cycles.

(b) To generate an accurate base frequency from which the recording frequency is to be derived.

The cycle reference marker pulse is derived from the magnetic pick up output which is amplified and wave shaped into a square wave by an amplifier and Schmidtt trigger circuit. The base frequency is generated at 25 KHZ by a square wave generator. The marker pulse (revolution pulse) is then synchronized to the nearest pulse of this base frequency 25KHZ pulse train. The outputs from this unit which consist of the marker revolution pulse and the base frequency pulse train, are used as inputs to the batch control logic unit. The function of this unit is shown schematically in fig (3.10) and this unit was specifically designed and made for the present research purpose by the author.

(ii) Batch Control Logic Unit:- The function of this unit is to control the recording position patterns, which can be pre-programmed by using the decade switches, of the data relative to engine cycle by making the following operations in sequence.

(a) Controlling the recording operation of a batch of data.

(b) Allowing for the necessary cycle skips and delay before next batch of data is recorded.

(c) Checking whether a specified number of batches of data in a block have been recorded.

(d) If more than one block of data is to be recorded, to control their starting positions, as specified, with respect to the engine cycle occurance.

In operation each output pulse from this unit causes a data to be recorded by the tape unit. The function of each individual electronic section in this unit is as follows:- (Referring to fig 3.11).

Pulse Multiplier and Divider Section:- This multiplies or divides the incoming pulse train at the base frequency by an assigned integer number to get a pulse train at the recording frequency.

Batch Released Logic Section:- This section releases a batch of tape unit control signal, 2 x 1024 pulses with a time gap of 60μsec between the first 1024 and the second 1024 pulses, whenever it

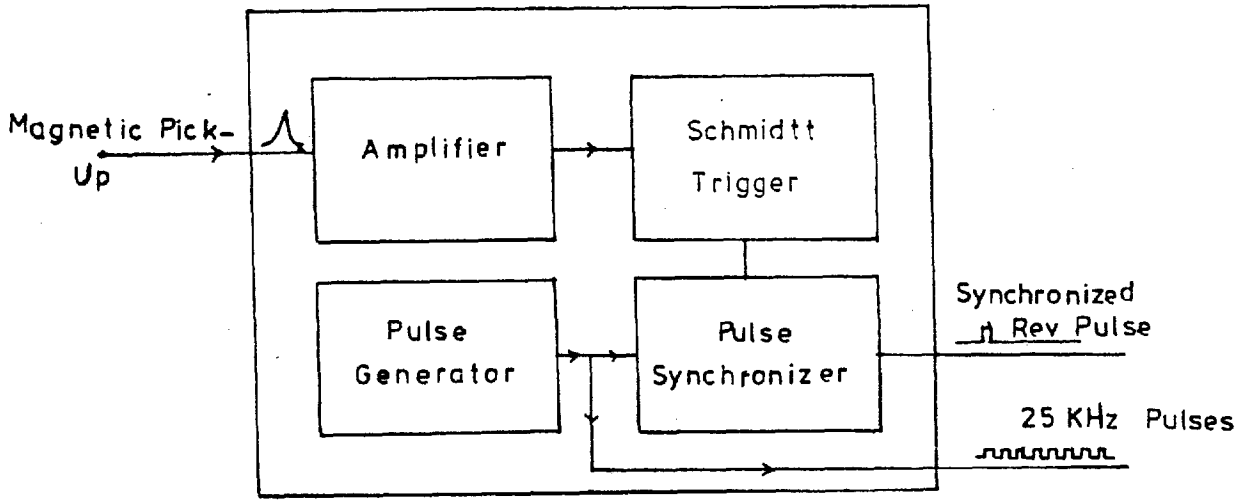


Fig (3.10) Layout Diagram of Pulse Generator and Pulse Synchronizer.

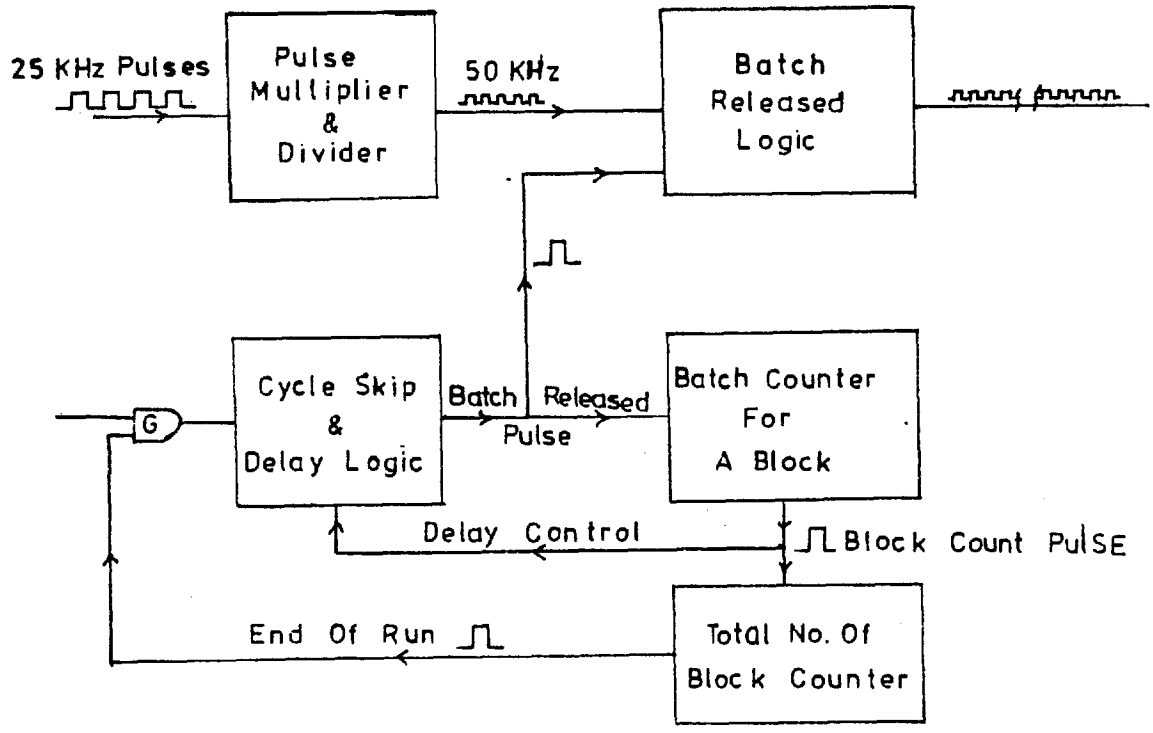


Fig (3.11) Layout Diagram of Batch and Block Formation Control Unit.

receives a command pulse from the cycle skip and delay section. These tape unit control pulses are derived from the pulse multiplier-divider output pulses, and they both have the same frequency.

Cycle Skips and Delay Logic Section:- This section gives out a command pulse to release a batch of control signal to the batch released logic section after every specified number of marker (revolution) pulse counts and delay. The delay is the time, after each specified number of revolution pulse count, which is allowed to pass before the release of the command pulses.

(iii) Multiplexer, Analogue to Digital Converter (ADC), Buffer and Tape Drive Units:- All these units are constructed into a one package. Their function is to make sequential recording from the data input channels whenever it receives control signal pulses from an external control device, which is the above mentioned batch control logic unit in our case.

Upon receiving a control pulse (refering to fig 3.12), the multiplexer scanned the next sequential input data channel and the scanned analogue information is passed on to ADC Unit where it is converted into a digital number and is temporarily stored in one location of the two buffers, as the high speed data cannot be directly written to the magnetic tape. After the two buffers are full, these temporarily stored data are transferred to the magnetic tape at a relatively slow speed. No further recording can be started unless the total transfer of the contents of the two buffers to the magnetic tape is completed. (The cycle skip is thus provided for this purpose by the batch control logic unit).

A brief description of each unit is as follows:-

Multiplexer:- This can be programmed to scan sequentially any number of specified channels from a total maximum of eight input data channels. The sequential scanning operation is cyclically repeated. The output from this multiplexer section is passed on to ADC unit through a sample and hold section.

ADC (Analogue to Digital Converter):- This unit converts the analogue voltage which is held in sample and hold section into a digital value of ten binary bits accuracy. The speed of the ADC unit is 1.5 micro-second per conversion.

Buffers:- Two buffer units of each 1024 words capacity temporarily hold the fast output information from the ADC Unit. The information from ADC is first channelled to the first buffer, then to the second

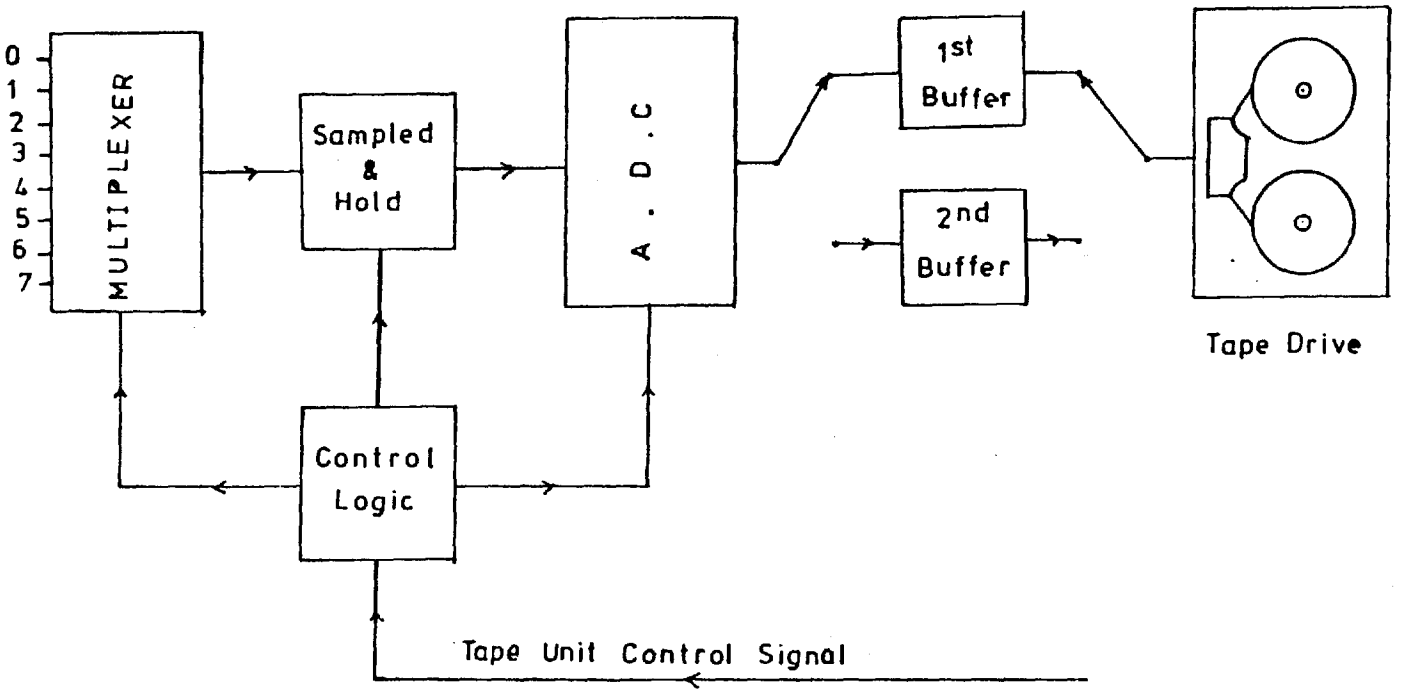


Fig (3.12) Schematic Diagram showing arrangements of Multiplexer, ADC, Buffers and Tape Drive.

buffer after the first buffer becomes full. The switching of the ADC output information from the first to the second buffer takes 40 micro-seconds during which no information can be accepted. Thus a minimum time gap of 40 micro-seconds has to be provided before starting to fill the second buffer. In our case a time gap of 60 micro-seconds is provided for this purpose by the batch and block forming control unit.

Magnetic Tape Unit:- It is used for copying the digital information which are held in the two storage buffers onto the magnetic tape. The transfering of data to the magnetic tape is a relatively slow process and no new data can be recorded until the data transfer process is completed.

By using the above mentioned electronic units, the analogue signals which consist of cylinder charge pressure, cylinder charge temperature and anemometer output voltage variations were recorded one channel at a time, at a frequency 50 KHZ and for a repetition of 50 engine cycles. The data recording was started 60 degress before top dead centre during the compression period. The recorded data on magnetic tape were then processed and analysed using computer analysis programme on college CDC digital computer (Section 4.0).

3.8.0. Instrumentation for Analogue Signals:- For turbulent flow investigations inside engine cylinders by using hot wire anemometry, it is necessary to know the magnitude of pressure and temperature variations, so that necessary compensations can be taken for their effects on the output of the anemometer. Thus the experiment was set up as in fig (3.7) to record cylinder pressure, cylinder temperature and anemometer voltage variations. The instrumentations employed for getting these signals are as follows:-

(i) Cylinder Pressure:- A Kistler pressure transducer and a Kistler charge amplifier were used for measuring cylinder pressure. The combined unit was calibrated by using a dead weight pressure tester unit.

(ii) Cylinder Temperature:- One sensor of the three wire probe was used as a resistance temperature sensor together with a bridge amplifier. Each sensor wire and the amplifier unit before use was calibrated by heating the sensor probe in an electric oven.

(iii) Local Mass Flow Rate:- Constructed hot wire probes, as mentioned under section (3.4) were used together with a DISA (DØ5) model anemometer unit. Calibration of probes were done by using a steady air flow test rig which comprises of an air nozzle

supplied with air from a rotary blower unit through a damper section. Details of the hot wire calibration method used is mentioned under section (A.5).

3.9.0 Modifications to Engine Under Investigation:- The engine was modified to run with a dry sump to reduce oil leakage across the piston rings. An additional crank was installed inside the crank case for telemetering the probes which were mounted on the piston crown. The piston crown was made detachable for reducing the amount of work in dismantaling and re-assembling the engine when changing the probes. (Initial attempts were faced with lubricating oil leakage problem, which was later solved by reboring the cylinder and fitting with a new oversized piston. This attempt plus the dry sump operation with controlled amount of lubricant feed virtually eliminated the oil leakage problem).

3.10.0 Data Taking Procedure:- Before data recording, all electronic units involved were switched on and were warmed up for at least 30 minutes to minimize the temperature drift effect. The engine was then motored by using an electric dynamometer and its speed was controlled by a Ward-Leonard Control Unit. Engine speed was checked by an attached techometer as well as by a frequency counter to count the output pulses from the magnetic pick up unit which gave a pulse at every engine revolution. The engine was run for about 20 minutes and then the hot wire sensor was energized. All the three analogue signals, cylinder pressure, cylinder temperature and anemometer voltage, were monitored by using a four channel oscilloscope. The fourth channel was used for displaying the batches of tape recorder control signal relative to motored cylinder pressure diagram so that the relative positions of recording to engine cycle could be checked. The analogue signals were recorded one channel at a time. For each engine operating condition and each sensor wire location and direction, data were recorded from 50 engine cycles.

3.11.0 Engine Operating Conditions:- To study the effect of various engine operating parameters on spatial and temporal variation of turbulence, experimental data were recorded at eight different set of engine operating conditions. Frequent hot wire sensor wire breakage at higher engine speeds than those employed made it not feasible for investigations. The following are the engine operating conditions which were employed for the present investigation.

Run No.	Speed RPM	Compression Ratio	Throttle Valve Opening Position
1	500	5.53	Full
2	500	5.53	Quarter
3	700	5.53	Full
4	700	5.53	Quarter
5	500	6.01	Full
6	500	6.01	Quarter
7	700	6.01	Full
8	700	6.01	Quarter

4.0 EXPERIMENTAL DATA ANALYSIS

An interpretation of the recorded data or in other words data analysis is required to yield knowledge of the turbulence parameters. Digital data processing was employed using the college CDC computers to determine the characteristics of the engine cylinder turbulence from the experimental digital data record of cylinder pressure, cylinder temperature and anemometer output voltage. The computation of the gas velocity from anemometer output voltage was based on a calibration equation of the Reynolds analogy type and this method is the same as that employed by other workers for engine cylinder flow studies (2,41). The heat conduction effect to the supporting prong was taken into account by considering the energy balance of the wire in which all terms except the convective heat transfer coefficient of the wire are known. Davies and Fisher (7) suggested an itterative method of solution and this was used in previous studies on engine cylinder flow analysis (2). An alternative itterative free method of solution was used in the present work and is described in section (4.5.2.). The computed unsteady instantaneous velocity data were then treated with digital filtering techniques together with some classical statistical analysis to yield the magnitude of instantaneous values of mean velocity, turbulence intensity and its scales. The detailed steps involved are discussed under section (4.5.0.).

The application of the digital filtering in engine cylinder turbulence flow analysis is believed to be the first on which this has been used in this type of application and the method seems to yield much more accurate and reliable results than the previously employed methods, which are:-

(i) Quasi-steady state Analysis Method and

(ii) Ensemble Averaging Analysis Method

4.1.0. The Quasi-steady state Analysis Method:- This is the simplest form of analysing unsteady data. The unsteady velocity data is divided into portions of small time intervals and each interval of data is treated and analysed as in a steady flow analysis. This method of analysis is suitable for cases where the mean velocity fluctuation is small and hence the mean value of velocity which is computed in each interval by this method approaches its actual value with high degree of accuracy. This method was used by Dent Et Al (66) for engine cylinder turbulence analysis. If large gradients of velocity exists with respect to

time, the applicability of this method without serious loss of accuracy is doubtful. The quasi-steady approach to data analysis is shown diagramatically in fig (4.1).

Referring to fig (4.1), by virtue of the quasi-steady assumptions,

$$\overline{X}[T] = \frac{1}{\Delta t} \int_{T - \Delta t/2}^{T + \Delta t/2} x(t)\, dt$$

The interval length is to be decided by a compromise between the conflicting requirements. This interval, on one hand, is desirable to be as short as possible to minimize changes in characteristics of flow velocity, and on the other hand, it is desirable to have longer intervals to have better lower end frequency resolution of the turbulence parameters. Compromise intervals lengths were thus chosen in previous studies, 24C.A. degrees by Semenov (1), 30C.A. degrees by Dent Et Al (66) and 45 C.A. degress by Lancaster (41).

4.2.0 Ensemble Averaging Analysis Method:- This method is usually applied to the analysis of unsteady turbulent flow of a cyclically varying nature, such as turbulent flow in engine cylinders. The mean or average values of the fluctuations at a position in the cycle were found by averaging the non-stationary data from several cycles (fig 4.2). As this approach does not give the cycle to cycle statistical parameters of the non-stationary data, the minimum number of cycles to be taken into account to get true ensemble average value is normally large, and this number depends on the magnitude of superimposed turbulent frequency fluctuations. Lancaster (41) used this approach for engine cylinder turbulence analysis and concluded that 1000 engine cycles data were required to get reliable true average values.

Referring to fig (4.2), by the ensemble averaging method,

$$\overline{X}(t) = \frac{1}{N} \sum_{n=1}^{N} x(nT + t)$$

$$x'(t) = x(nT + t) - \overline{X}(t)$$

Thus to get true representative results by means of either of the above two methods, difficulties are encountered in deciding the optimum interval length in the first case and in deciding the minimum number of cycles to be taken into account to get true representative ensemble average value in the second case. One

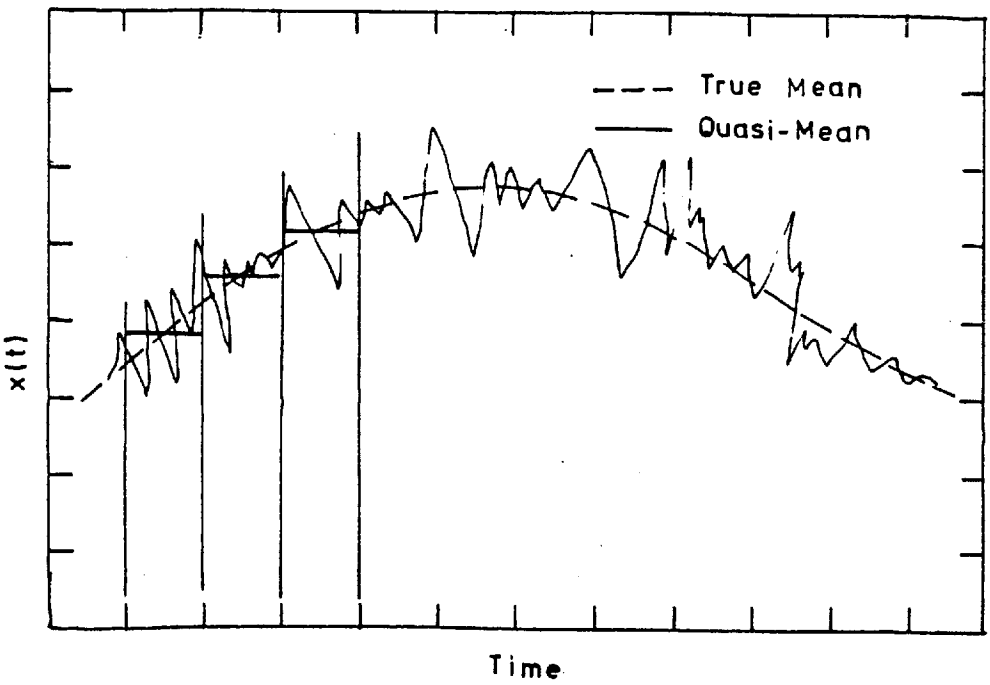


Fig (4.1) Graphical representation of Quasi-steady Approach

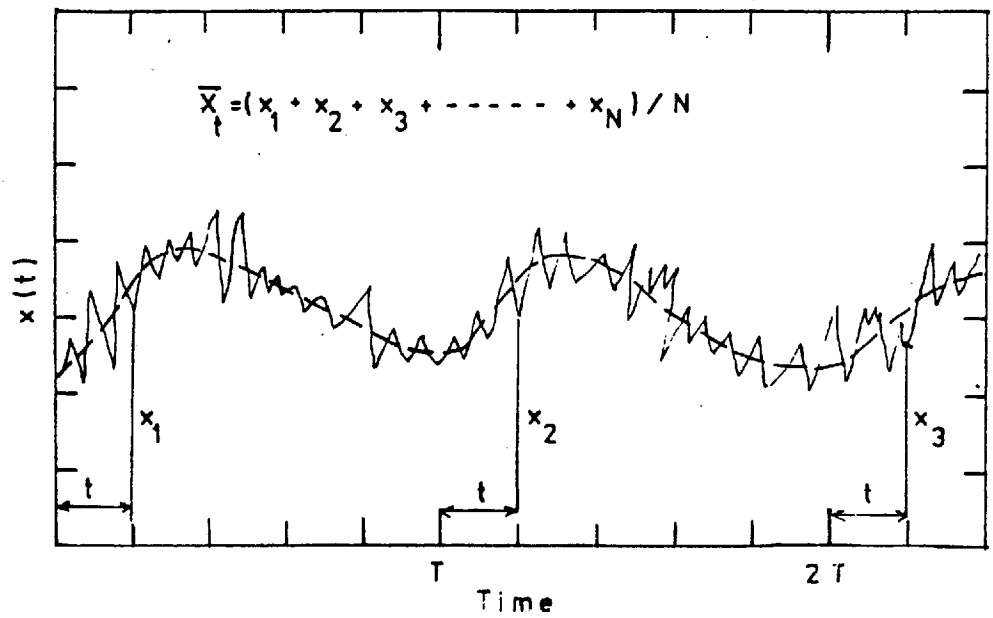


Fig (4.2) Graphical representation of Ensemble Average Approach to Transient data Analysis

alternative method for removing unsteady mean velocity components or the high frequency turbulent component from the unsteady instantaneous time domain data is by using a filtering technique. This consists of transforming the time domain unsteady data into a frequency domain function and this transformed function is then operated on by a transfer function, the operation of which is equivalent to the removal of undesired frequency components from the unsteady data in the time domain. The transformation back to the time domain of the resulting frequency domain function will give the desired mean or high frequency fluctuating component in the time domain. This analysis not only elimates the requirement for deciding optimum interval length as in the quasi-steady state method but also gives cycle to cycle variations of the statistical parameters of the non-stationary data and hence eliminates the need for many engine cycle data as in the ensemble averaging method if truly representative results are to be achieved.

4.3.0. Present Analysis Method:- The present non-stationary data analysis employs a digital filtering technique, where the digital filters employed have characteristics which are not only superior to those of the analogue counterpart but are also approaching those of ideal ones. The statistical parameters obtained by employing digital filters are believed to have higher accuracy and reliability than those obtained by using other methods, as the accuracy of the results in this case is not strongly dependent on the choice of the optimum interval length as in quasi-steady state analysis or on the choice of the minimum number of cycles to be taken into account as in ensemble averaging analysis method.

The principle of filtering is briefly mentioned below and the design procedure of the digital filter employed is explained under section (A2).

4.3.1. Filtering:- Filtering is a process in which signals which lie in a specified frequency range from the given input signals are allowed to pass. Ideal filtering is a process in which there is no phase shift between the input and output signals and there is unity gain throughout the band width. More widely used filtering processes are:-

(i) Low-pass filtering:- Signals with frequencies below a specified limit are allowed to pass.

(ii) High-pass filtering:- Signals with frequencies above a specified limit are allowed to pass.

(iii) Band-pass filtering:- Signals with frequencies which lie between two specified limits are allowed to pass.

The filtering operation can be performed either by using analogue filters or by using digital filters. For digital filtering, the filter configurations can be arranged such that their characteristics approaches those of ideal filters. Typical gain-frequency charateristics of ideal, digital and analogue filters for the low-pass, high-pass and band pass filtering processes are shown in fig (4.3).

For the analysis of the unsteady turbulent flow velocity data, digital filters were used to separate the time varying mean velocity component and the superimposed high frequency fluctuating turbulent components from the input data. The statistical treatment was then applied to the high frequency fluctuating component to find its statistical characteristics which include turbulence intensity and the scales of turbulence. A brief mention is made in the following section about the employed digital filters.

4.4.0 Digital Filtering:- When the input signal is in digital form the filtering process may be performed entirely by digital operations using digital filters. Digital filters may be either hard wired units or soft-ware computer programmes. The digital filtering process basically consists of sets of averaging operations, using sum and difference equations involving the employment of weighting factors called digital filter coefficients. The values of these filter coefficients can be found for a specified filter configuration by knowing its number of poles, cut-off frequency and band width and the sampling time of the input signal. The evaluating procedure for filter coefficients is discussed under section (A.2). The configuration of digital filter stages may be either in parallel or in cascade or in a combination of parallel-cascaded forms. The use of a multi-stage filter configuration is desirable as it reduces the truncation error of the filtering operation below that obtained by using an equivalent single stage filter arrangement (Section A.2). The cascaded form of multi-stage filters gives nearly 1/3rd saving in computing time compared to the equivalent parallel form (Section A.2). Because of these considerations, the multi-stage cascaded form of digital filters was used in the present unsteady turbulent flow data analysis for separating mean and high frequency turbulent components from input signal.

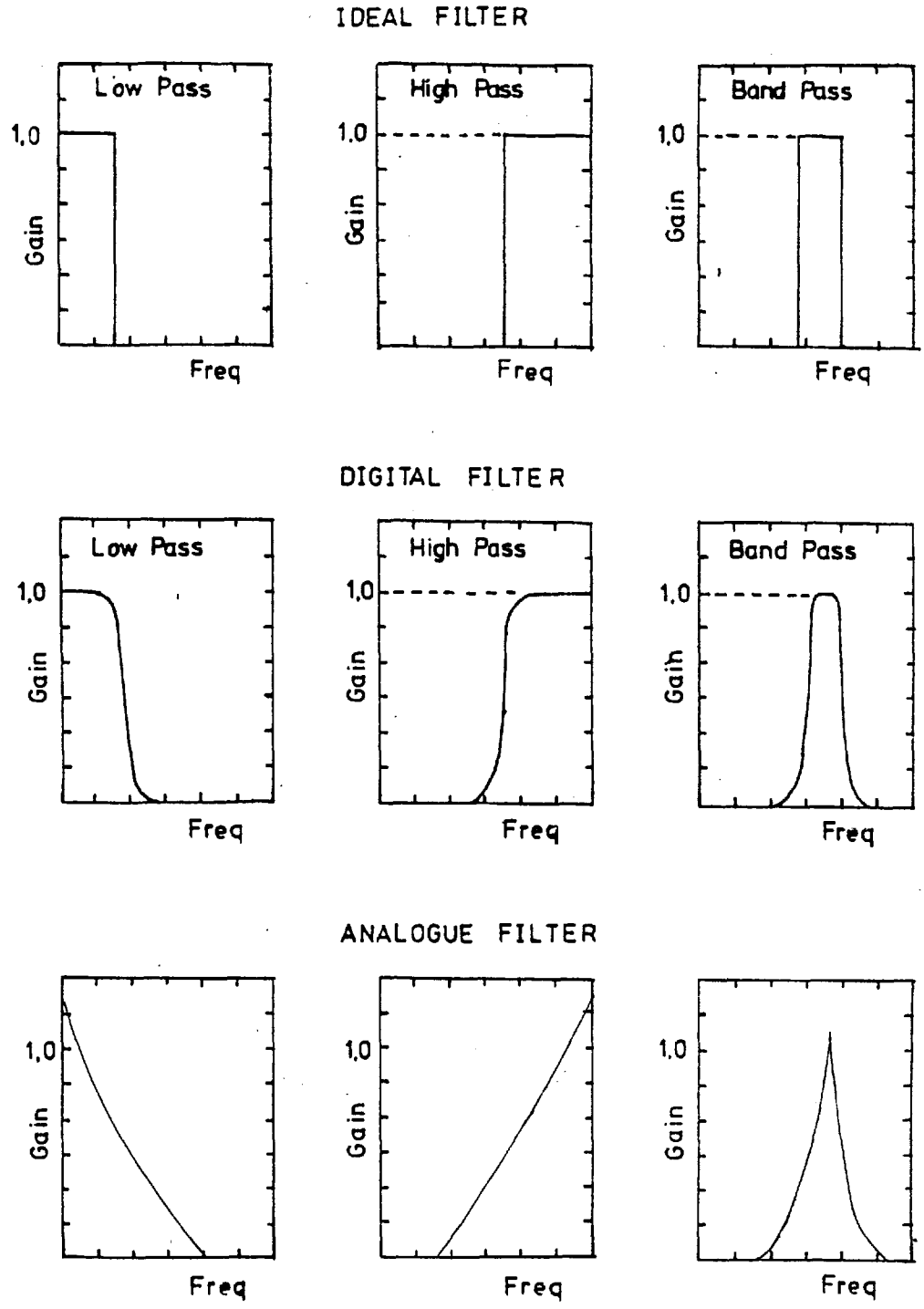


Fig (4.3) Typical Characteristic Form of Ideal, Digital and Analogue Filters

Digital filters may be designed with characteristics approaching those of ideal filters by employing a higher number of poles. As a large number of poles require more filtering operations and hence more computing time, compromise number of poles must be used to suit a particular application. The arrangement of the filter operations for four pole and six pole low pass filters and high pass filters are shown in fig (4.4) to fig (4.7) and the computed filter coefficients are given in Table (4.1) to Table (4.4). The gain-frequency characteristics of some of the designed digital filters are shown in fig (4.8) to fig (4.10) and their test results of their filtering operations on a given sinusoidal input test signal having superimposed high frequency fluctuations are shown in fig (4.11) to fig (4.12).

These test results and the results of data analysis on the recorded unsteady turbulent flow data showed there is no significant improvement in accuracy of the final results by using digital filters with more than four poles. Thus four pole cascaded digital low pass and high pass filters were used respectively for separating the mean and high frequency turbulent component from the computed instantaneous unsteady turbulent velocity signals. The steps involved in the data analysis are briefly mentioned in the following section.

4.5.0 Steps Involved in Data Analysis:- The following steps are involved in the analysis of recorded unsteady engine cylinder turbulent flow field data.

(i) Data retrieval from the recorded magnetic tape.
(ii) Calculation of Instantaneous heat transfer coefficient of wire
(iii) Nusselt Number calcualtion
(iv) Reynold's Number of flow calculation
(v) Instantaneous Velocity Calculation
(vi) Separation of Mean Velocity by low-pass digital filtering
(vii) Separation of High Frequency Turbulent Component Fluctuations by high-pass digital filtering
(viii) Calculation of Intensity of Turbulence
(ix) Estimation on Power Spectra
(x) Estimation on Spatial and temporal Scales of turbulence

These steps are shown in fig (4.13)

4.5.1 Data Retrieval From the Recorded Magnetic Tape:- This step became necessary because of the difference which exists between the data format used by the tape unit and that of the computer

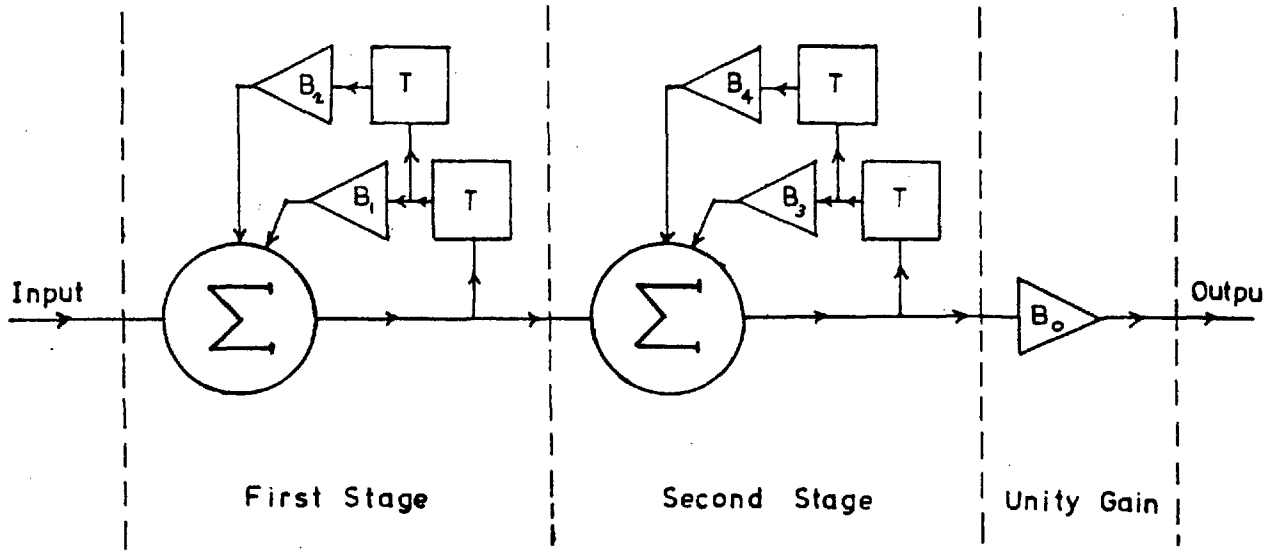


Fig (4.4) Arrangement Form of the Cascaded Four Pole Low Pass Filter used.

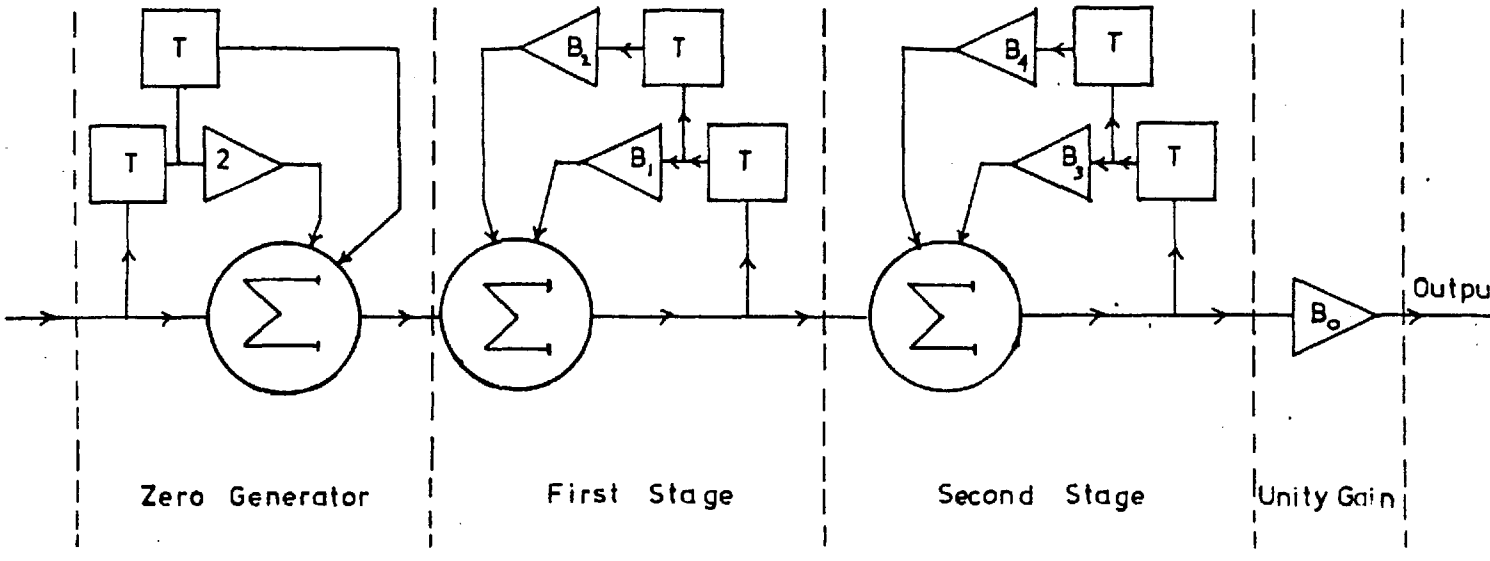


Fig (4.5) Arrangement form of the Cascaded Four Pole High Pass Filter Used.

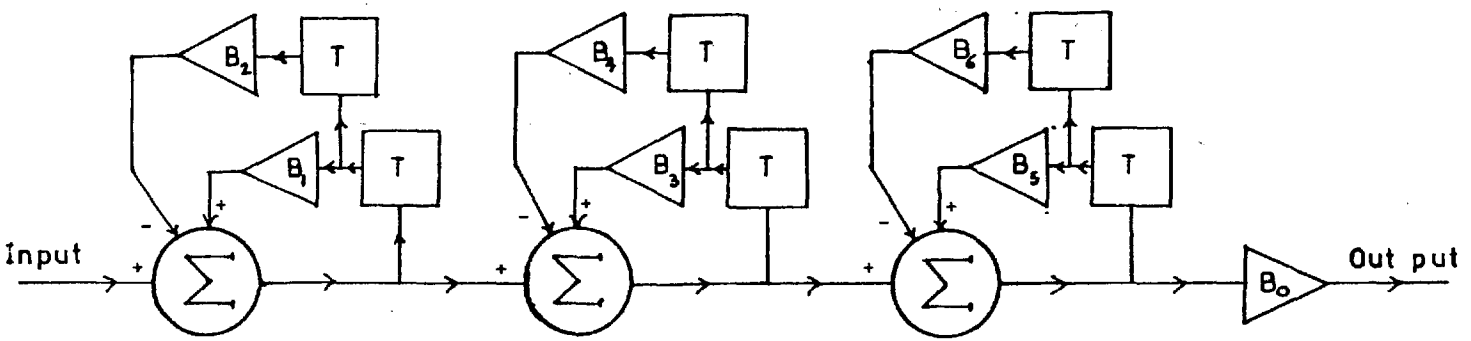


Fig (4.6) Arrangement of a Six Pole Cascaded Low Pass Filter

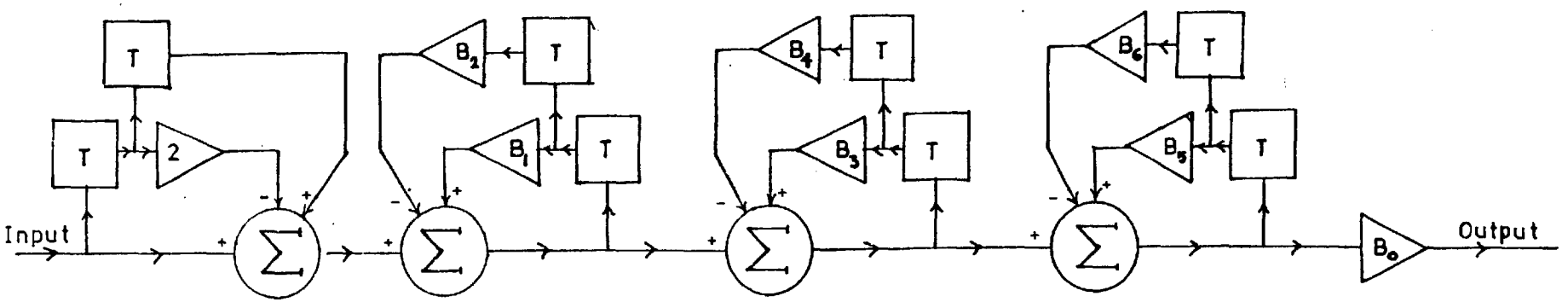


Fig (4.7) Arrangement of a Six Pole High Pass Filter

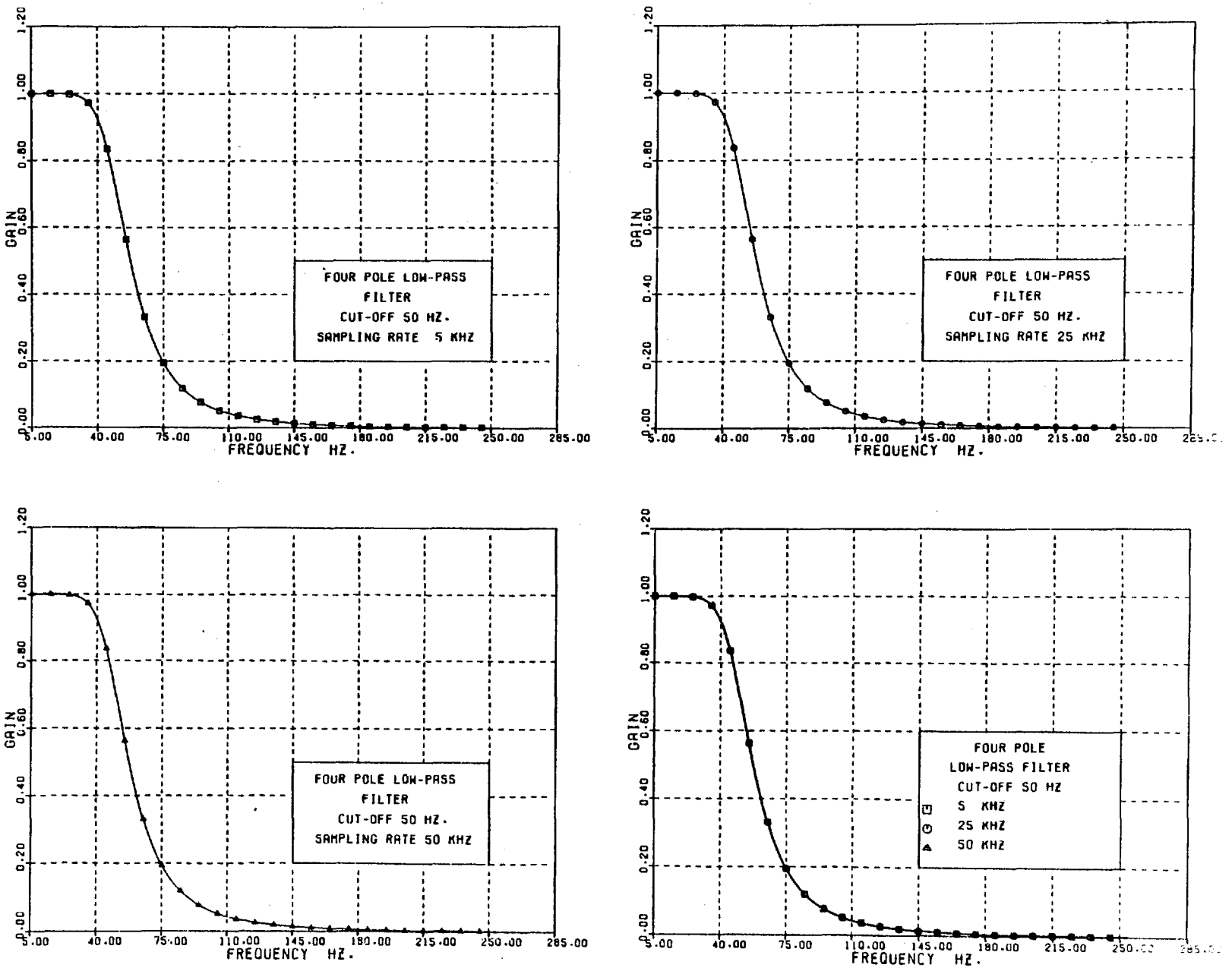


Fig (4.8) Effect of Different Sampling Rate on Low Pass Filter Characteristics

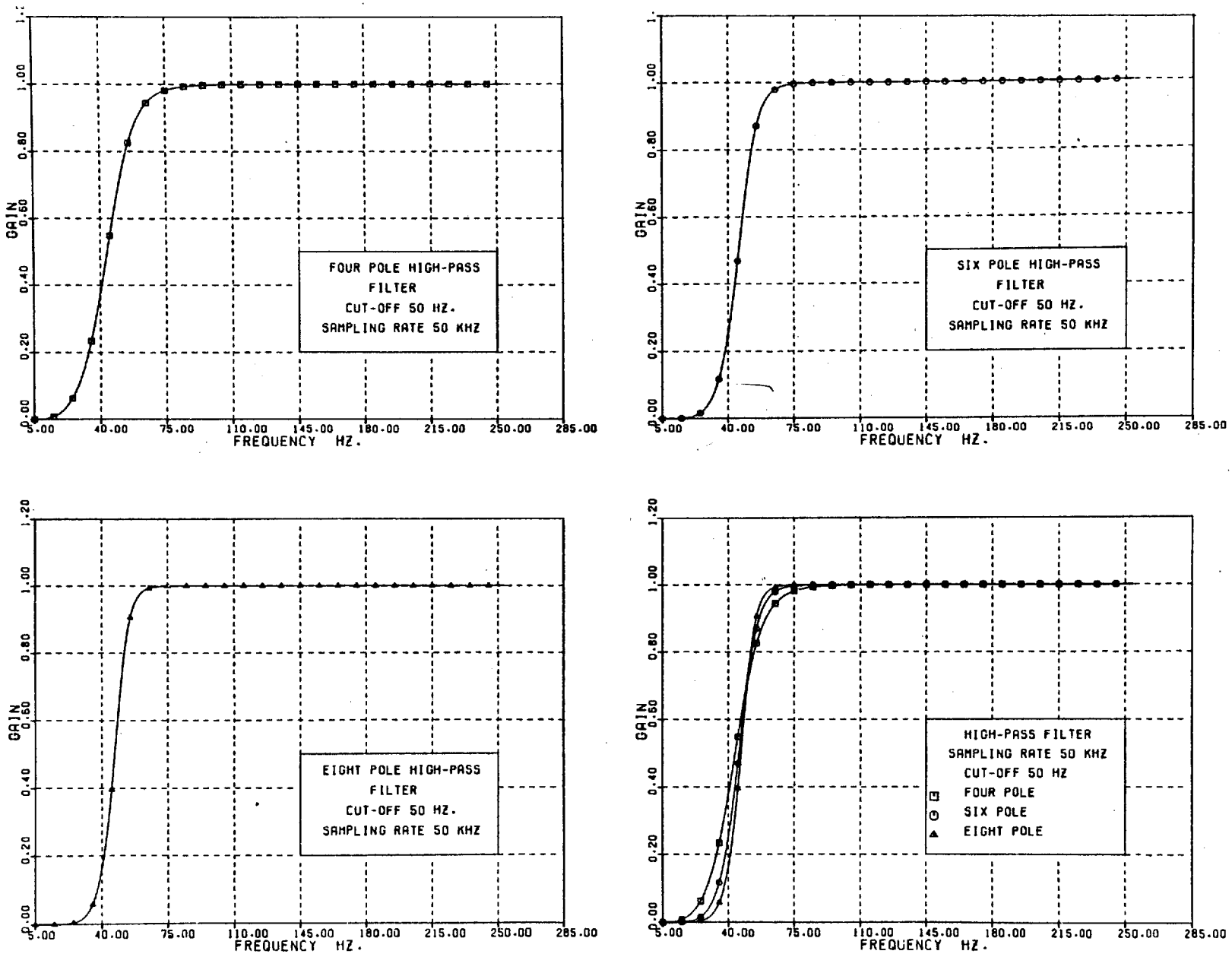


Fig (4.9) Effect of Different Number of Poles on High Pass Filter Characteristics

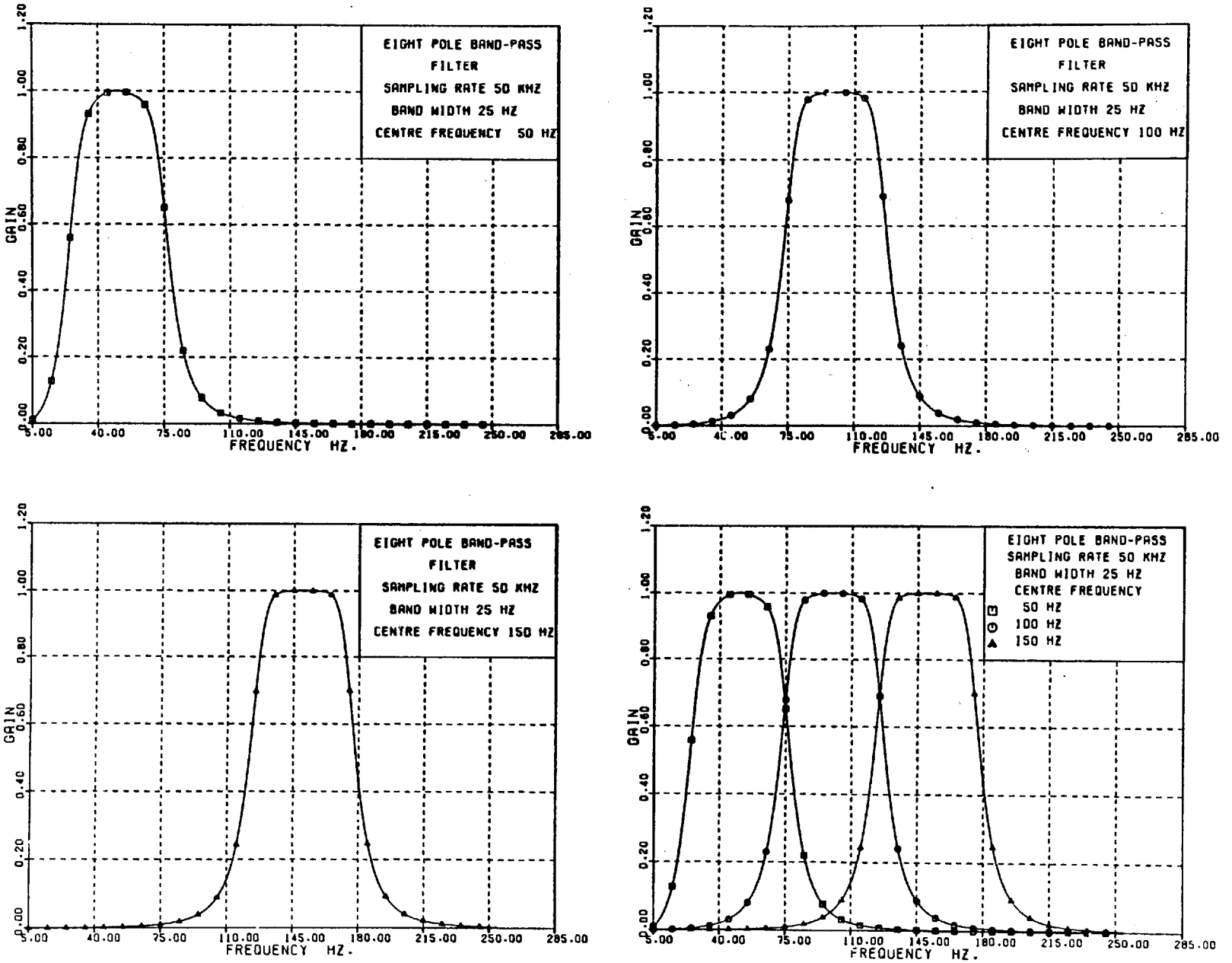


Fig (4.10) Characteristics of Band Pass Filters with Different Centre Frequency

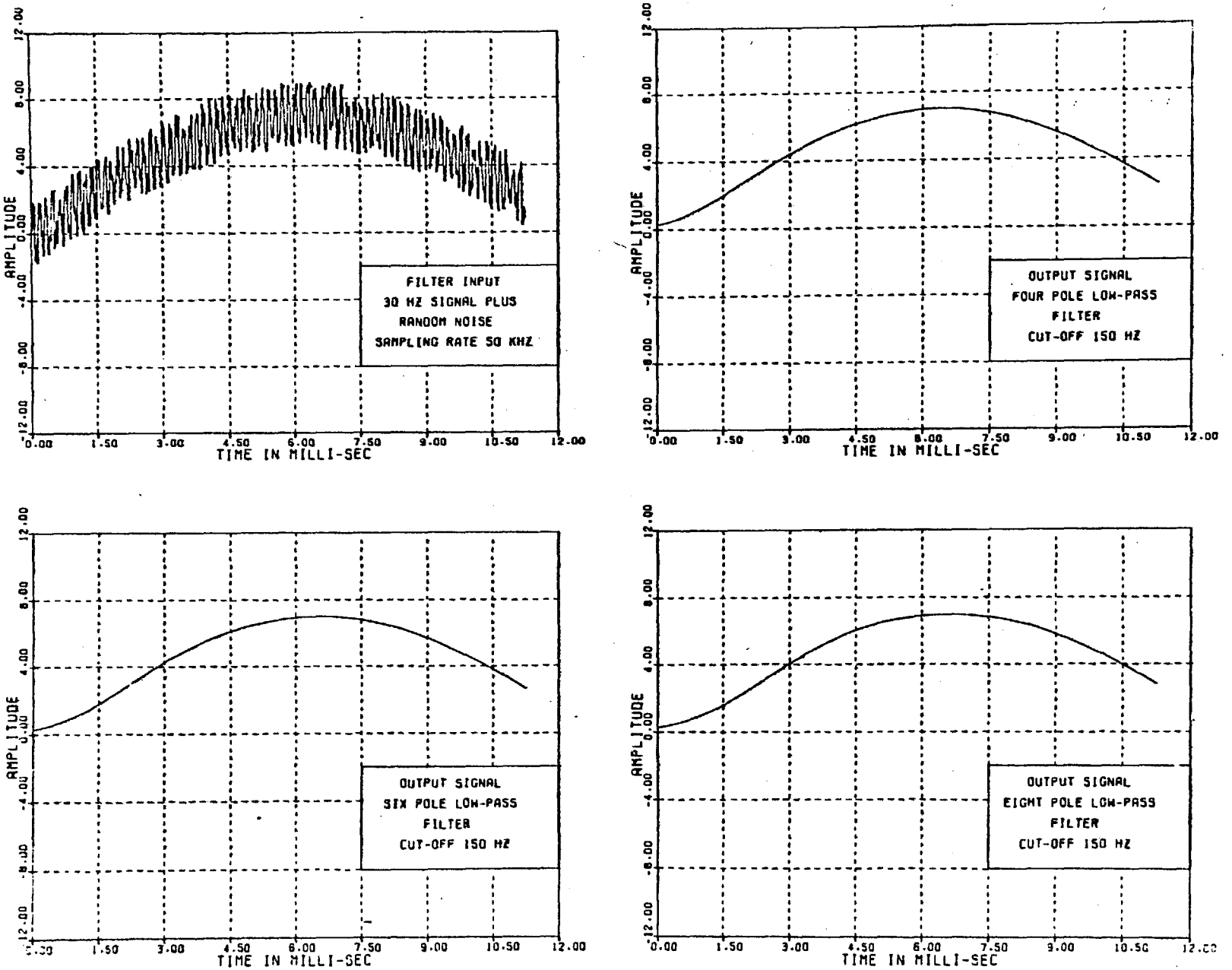


Fig (4.11) Test Results of a Low Pass Digital Filter.

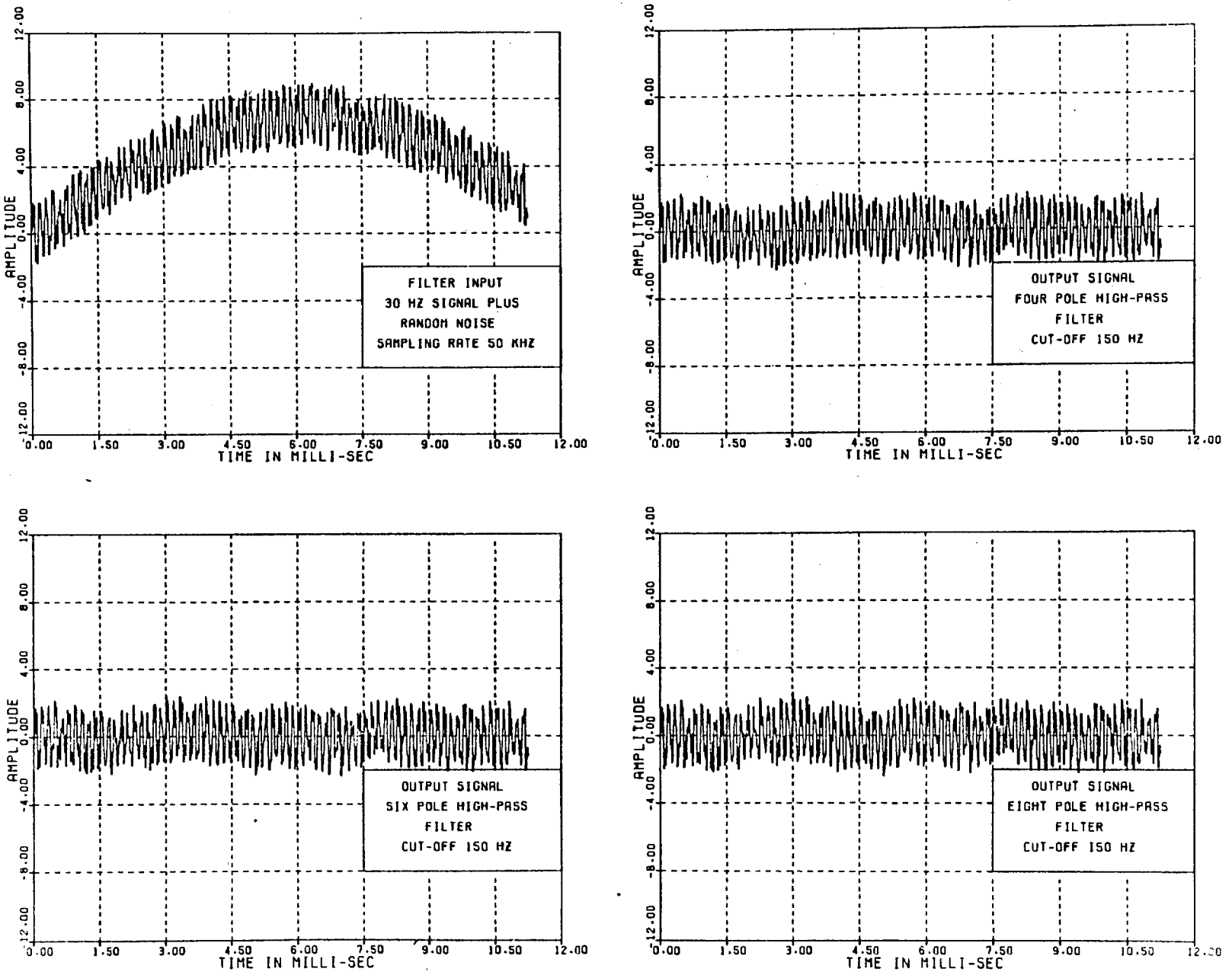


Fig (4.12) Test on High Pass Filters having Different Number of Poles

COMPUTED FILTER COEFFICIENTS
FOUR POLE HIGH-PASS FILTER
SAMPLING RATE 50 KHZ

CUT-OFF HZ	B0	B1	B2	B3	B4
25	.995990372E+00	-1.994202063	.994211904	-1.997588554	.997598422
50	.991824235+00	-1.988418061	.988457311	-1.995163228	.995202612
75	.987761446+00	-1.982647969	.982736026	-1.992724049	.992812556
100	.983715306+00	-1.976891763	.977047855	-1.990271084	.990428239
125	.979686736+00	-1.971149420	.971392609	-1.987804390	.988040648
150	.975672066+00	-1.965420916	.965770096	-1.985324025	.985676770
175	.971676046+00	-1.959706228	.960188176	-1.982830046	.983309591
200	.967695796+00	-1.954005331	.954622512	-1.980322510	.980948097
225	.963731846+00	-1.948318202	.949071066	-1.977801474	.978592273
250	.959784136+00	-1.942644816	.943603601	-1.975266997	.976242103
275	.955852586+00	-1.936985153	.938111934	-1.972719134	.973897527
300	.951937156+00	-1.931339186	.932711879	-1.970157944	.971556396
325	.948037756+00	-1.925706891	.927313253	-1.967583483	.969225422
350	.944154336+00	-1.920088246	.921945875	-1.964995809	.966897752
375	.940286816+00	-1.914483227	.916609564	-1.962394979	.964575672
400	.936435136+00	-1.908891809	.911304141	-1.959781050	.962259168
425	.932599246+00	-1.903313970	.906029425	-1.957154080	.959948228
450	.928779056+00	-1.897749685	.900785240	-1.954514125	.957642837
475	.924974526+00	-1.892198931	.895571409	-1.951861244	.955342984
500	.921185576+00	-1.886661684	.890387757	-1.949195492	.953048653
525	.917412146+00	-1.881137921	.885234107	-1.946516928	.950759833
550	.913654166+00	-1.875627617	.880110298	-1.943825608	.948476509
575	.909911596+00	-1.870130749	.875016125	-1.941121590	.946198669
600	.906184356+00	-1.864647294	.869951448	-1.938404931	.943926299
625	.902472376+00	-1.859177227	.864916086	-1.935675683	.941659387
650	.898775586+00	-1.853720526	.859909859	-1.932933917	.939397919
675	.895093946+00	-1.848277155	.854932529	-1.930179677	.937141881
700	.891427396+00	-1.842847123	.849984107	-1.927413025	.934891262
725	.887775886+00	-1.837430375	.845064407	-1.924634016	.932646048
750	.884139236+00	-1.832026997	.840173094	-1.921842709	.930406226
775	.880517606+00	-1.826636666	.835310092	-1.919039181	.928171783
800	.876910766+00	-1.821259658	.830475237	-1.916223428	.925942707
825	.873318696+00	-1.815895956	.825669367	-1.913395567	.923718083
850	.869741346+00	-1.810545718	.820889320	-1.910555636	.921500500
875	.866178536+00	-1.805207738	.816137934	-1.907703692	.919287545
900	.862630236+00	-1.799883367	.811414049	-1.904839791	.917079804
925	.859096356+00	-1.794572141	.806717507	-1.901963990	.914877356
950	.855577746+00	-1.789273936	.802048149	-1.899076347	.912680217
975	.852073176+00	-1.783988	.797406818	-1.895176918	.910488344
1000	.848582846+00	-1.77871	.792790357	-1.893265760	.908301735

COMPUTED FILTER COEFFICIENTS
FOUR POLE HIGH-PASS FILTER
SAMPLING RATE 25 KHZ

CUT-OFF HZ	B0	B1	B2	B3	B4
25	.991824236+00	-1.988418061	.988457311	-1.995163228	.995202612
50	.983715306+00	-1.976891763	.977047856	-1.990271084	.990428239
75	.975672566+00	-1.965420916	.965770096	-1.985324025	.985676770
100	.967695796+00	-1.954005331	.954622512	-1.980322510	.980948097
125	.959784136+00	-1.942644816	.943603601	-1.975266997	.976242108
150	.951937156+00	-1.931339186	.932711878	-1.970157944	.971558636
175	.944154336+00	-1.920086246	.921945675	-1.964995809	.966897752
200	.936435136+00	-1.908891809	.911304141	-1.959781050	.962259168
225	.928779056+00	-1.897749585	.900785240	-1.954514125	.957642837
250	.921185576+00	-1.886661684	.890387757	-1.949195492	.953048653
275	.913654166+00	-1.875627617	.880110208	-1.943825608	.948476509
300	.906184336+00	-1.864647294	.869951448	-1.938404931	.943926299
325	.898775586+00	-1.853720526	.859909869	-1.932933917	.939397919
350	.891427396+00	-1.842847123	.849984197	-1.927413025	.934891262
375	.884139236+00	-1.832026997	.840173094	-1.921842709	.930406226
400	.876910766+00	-1.821259658	.830475237	-1.916223428	.925942707
425	.869741346+00	-1.810545218	.820889320	-1.910555636	.921500600
450	.862633536+00	-1.799883397	.811414049	-1.904839791	.917079804
475	.855577656+00	-1.789273376	.802048149	-1.899076347	.912680217
500	.848582846+00	-1.778715798	.792790357	-1.893265760	.908301735
525	.841645026+00	-1.768211652	.783539424	-1.887408485	.903944260
550	.834763126+00	-1.757758382	.774394119	-1.881504977	.899607698
575	.827939036+00	-1.747355759	.765653219	-1.875555690	.895291921
600	.821170046+00	-1.737000634	.756815522	-1.869561078	.890996858
625	.814456346+00	-1.726707791	.748079830	-1.863521594	.886722401
650	.807797526+00	-1.716460050	.739444983	-1.857437592	.882468449
675	.801193166+00	-1.706263224	.730909800	-1.851309324	.878234906
700	.794642786+00	-1.696117126	.722473133	-1.845138443	.874021672
725	.788145966+00	-1.686021569	.714133852	-1.838924000	.869828651
750	.781702266+00	-1.675975365	.705890827	-1.832666346	.865655746
775	.775311246+00	-1.665981327	.697742949	-1.826367733	.861502659
800	.768972476+00	-1.656036269	.689689119	-1.820026811	.857359996
825	.762685536+00	-1.646141005	.681729252	-1.813644630	.853256760
850	.756449386+00	-1.636295347	.673859275	-1.807221838	.849163353
875	.750265426+00	-1.626499109	.666091127	-1.800758285	.845089590
900	.744131426+00	-1.616752107	.658392760	-1.794255019	.841035367
925	.738047566+00	-1.607054153	.650793137	-1.787712788	.837000594
950	.732013456+00	-1.597405063	.643281234	-1.781130538	.832985178
975	.726028456+00	-1.587804651	.635858039	-1.774510216	.828989025
1000	.720092636+00	-1.578252732	.628516553	-1.767851767	.825012043

Table (4.1) Computed Filter Coefficients of Four Pole High Pass Filter

COMPUTED FILTER COEFFICIENTS
SIX POLE HIGH-PASS FILTER
SAMPLING RATE 25 KHZ

CUT-OFF HZ	B0	B1	B2	B3	B4	B5	B6
25	.98793519E+00	-1.987895937	.987935177	-1.991114290	.991153594	-1.996713467	.996752881
50	.97601594E+00	-1.975859903	.976015914	-1.982228930	.982385447	-1.993358906	.993516305
75	.96424049E+00	-1.963891549	.964240454	-1.973344264	.973694866	-1.989936671	.990290239
100	.95260711E+00	-1.951990529	.952607063	-1.964460636	.965081166	-1.986447117	.987074649
125	.94111408E+00	-1.940156497	.941114028	-1.955578386	.956543666	-1.982090599	.983869500
150	.92975972E+00	-1.928389109	.929759653	-1.946697851	.948081692	-1.979267476	.980674758
175	.91854234E+00	-1.916688023	.918542267	-1.937819365	.939694576	-1.975578106	.977490390
200	.90746030E+00	-1.905052898	.907460217	-1.929943259	.931381656	-1.971822851	.974316362
225	.89651196E+00	-1.893483396	.896511870	-1.920059860	.923142276	-1.968002071	.971162641
250	.88569571E+00	-1.881979177	.885695613	-1.911189493	.914975705	-1.964116130	.967999193
275	.87500938E+00	-1.870539906	.875009852	-1.902332481	.906881537	-1.960165393	.964855984
300	.86445313E+00	-1.859165249	.864453013	-1.893469141	.898858895	-1.956150226	.961722981
325	.85402367E+00	-1.847854872	.854023540	-1.884603790	.890907224	-1.952070997	.958600152
350	.84372003E+00	-1.836608443	.843719897	-1.875754741	.883025697	-1.947920074	.955487463
375	.83354071E+00	-1.825425632	.833540565	-1.866904303	.875214291	-1.943721828	.952384881
400	.82348419E+00	-1.814306111	.823484046	-1.858058784	.867471790	-1.939452629	.949292374
425	.81354901E+00	-1.803249552	.813548856	-1.849218488	.859797782	-1.935120851	.946209909
450	.80373369E+00	-1.792255629	.803733533	-1.840383716	.852191662	-1.930726868	.943137452
475	.79403680E+00	-1.781324018	.794036630	-1.831554706	.844652828	-1.926271054	.940074972
500	.78445689E+00	-1.770454397	.784456719	-1.822731935	.837180886	-1.921753786	.937022437
525	.77499257E+00	-1.759645444	.774992387	-1.813915514	.829774646	-1.917175442	.933979813
550	.76564243E+00	-1.748899838	.765642241	-1.805105793	.822434122	-1.912536400	.930947069
575	.75640503E+00	-1.738214262	.756404903	-1.796303060	.815158536	-1.907837040	.927924173
600	.74727921E+00	-1.727589398	.747279011	-1.787507593	.807947313	-1.903077744	.924911093
625	.73826342E+00	-1.717024432	.738263222	-1.778719690	.800799883	-1.898258894	.921907796
650	.72935641E+00	-1.706520548	.729356207	-1.769939513	.793715682	-1.893380873	.918914252
675	.72055686E+00	-1.696075934	.720556653	-1.761167643	.786694150	-1.888444065	.915930427
700	.71186348E+00	-1.685690780	.711863264	-1.752404053	.779734734	-1.883448855	.912956292
725	.70327498E+00	-1.675364774	.703274760	-1.743649115	.772836884	-1.878395631	.909991814
750	.69479010E+00	-1.665097608	.694789874	-1.734903094	.766000055	-1.873284780	.907035962
775	.68640758E+00	-1.654888977	.686407357	-1.726166257	.759223708	-1.868116691	.904091705
800	.67812621E+00	-1.644738573	.678125974	-1.717438864	.752507305	-1.862891752	.901156012
825	.66994474E+00	-1.634646093	.669944504	-1.708721177	.745850321	-1.857610355	.898229850
850	.66186198E+00	-1.624611234	.661851742	-1.700013451	.739252226	-1.852272891	.895313191
875	.65387674E+00	-1.614633594	.653876497	-1.691315941	.732712501	-1.846879753	.892406002
900	.64596784E+00	-1.604713174	.645987593	-1.682628897	.726230628	-1.841431333	.889508254
925	.63814411E+00	-1.594849374	.638193966	-1.673952570	.719806097	-1.835928026	.886619914
950	.63040442E+00	-1.585041998	.630494170	-1.665287205	.713438400	-1.830370227	.883740954
975	.62274762E+00	-1.575290750	.622887370	-1.656633045	.707127034	-1.824758333	.880871341
1000	.61517260E+00	-1.565595335	.615372344	-1.647990333	.700871501	-1.819092740	.878011047

Table (4.2) Computed Filter Coefficients of Six Pole High Pass Cascaded Filters

COMPUTED FILTER COEFFICIENTS
SIX POLE HIGH-PASS FILTER
SAMPLING RATE 50 KHZ

CUT-OFF HZ	B0	B1	B2	B3	B4	B5	B6
25	.99394929E+00	-1.993939443	.993949283	-1.995557123	.995566971	-1.998365259	.998375120
50	.987935139E+00	-1.987695937	.987935177	-1.991114290	.991153594	-1.996713467	.996752881
75	.981957438E+00	-1.981869438	.981957460	-1.986671545	.986759781	-1.995044668	.995133277
100	.976015946E+00	-1.975859903	.976015914	-1.982228930	.982385447	-1.993358906	.993516305
125	.970110356E+00	-1.969867289	.970110317	-1.977786488	.978030503	-1.991655226	.991901961
150	.964240429E+00	-1.963891549	.964240454	-1.973344264	.973694866	-1.989936671	.990290239
175	.958406156E+00	-1.957932644	.958405108	-1.968902299	.969378448	-1.988200287	.988681137
200	.952607116E+00	-1.951990529	.952607063	-1.964460636	.965081166	-1.986447117	.987074649
225	.946843166E+00	-1.946065161	.946843107	-1.960019318	.960802933	-1.984677206	.985470771
250	.941114498E+00	-1.940156497	.941114028	-1.955578386	.956543666	-1.982890399	.983869500
275	.935419577E+00	-1.934264494	.935419513	-1.951137884	.952303280	-1.981087341	.982270930
300	.929759072E+00	-1.928389109	.929759053	-1.946697851	.948081692	-1.979267476	.980674758
325	.924134018E+00	-1.922530300	.924133940	-1.942258332	.943870818	-1.977431050	.979081250
350	.918542346+00	-1.916688023	.918542267	-1.937819365	.939694576	-1.975578106	.977490390
375	.912984516+00	-1.910862237	.912984428	-1.933380994	.935528083	-1.973708692	.975902086
400	.907460306+00	-1.905052998	.907460217	-1.928943259	.931361656	-1.971822851	.974316352
425	.901969928+00	-1.899259965	.901969432	-1.924506201	.927252815	-1.969920523	.972733216
450	.896511966+00	-1.893483303	.896511870	-1.920069960	.923142276	-1.968002071	.971152641
475	.891087436+00	-1.887723147	.891087330	-1.915634278	.919049950	-1.966067222	.969574635
500	.885695712+00	-1.881979177	.885695613	-1.911199493	.914975785	-1.964116130	.967999193
525	.880336402+00	-1.876251444	.880336519	-1.906765548	.910919670	-1.962148038	.966426310
550	.875009965+00	-1.870539906	.875009852	-1.902332481	.906881537	-1.960165393	.964855994
575	.869715535+00	-1.864844522	.869715415	-1.897900332	.902861305	-1.958165940	.963288209
600	.864453113+00	-1.859165249	.864453013	-1.893469141	.898858695	-1.956150226	.961722981
625	.859222675+00	-1.853502046	.859222452	-1.889038947	.894874227	-1.954118596	.960160297
650	.854023075+00	-1.847854572	.854023540	-1.884609790	.890907224	-1.952070997	.958600152
675	.848855271E+00	-1.842223685	.848856085	-1.880181708	.886957806	-1.950007474	.957042542
700	.843720088+00	-1.836608443	.843719897	-1.875754741	.883025897	-1.947928074	.955487453
725	.838614902E+00	-1.831009106	.838614786	-1.871328926	.879111417	-1.945832843	.953934911
750	.833540511E+00	-1.825425642	.833540565	-1.866904303	.875214291	-1.943721823	.952384881
775	.828497719E+00	-1.819857981	.828497847	-1.862480909	.871334441	-1.941595074	.950838370
800	.823484419E+00	-1.814306111	.823484046	-1.858058784	.867471790	-1.939452629	.949292374
825	.818501453E+00	-1.808769982	.818501377	-1.853637954	.863626262	-1.937294533	.947749888
850	.813549016+00	-1.803249552	.813548856	-1.849218488	.859797782	-1.935120851	.946209909
875	.808626406+00	-1.797744781	.808626302	-1.844800392	.855986274	-1.932931512	.944672431
900	.803733836+00	-1.792255629	.803733533	-1.840383716	.852191662	-1.930726968	.943137452
925	.798870356+00	-1.786782055	.798870369	-1.835968495	.848413071	-1.928506656	.941604957
950	.794036906+00	-1.781324018	.794036530	-1.831554766	.844652828	-1.926271054	.940074972
975	.789232416+00	-1.775881479	.789232139	-1.827142567	.840908458	-1.924020078	.938547464
1000	.784456716+00	-1.770454397	.784456719	-1.822731935	.837180686	-1.921753705	.937022437

Table (4.3) Computed Filter Coefficients of Six Pole High Pass Cascaded Filter

COMPUTED FILTER COEFFICIENTS
FOUR POLE LOW-PASS FILTER
SAMPLING RATE 50 KHZ

CUT-OFF HZ	B0	B1	B2	B3	B4
25	.97010490E-10	-1.994202063	.994211904	-1.997588564	.997598422
50	.15458097E-08	-1.988418061	.988457311	-1.995163228	.995202612
75	.77936057E-08	-1.982647969	.982736026	-1.992724049	.992812556
100	.24530745E-07	-1.976891763	.977047856	-1.990271084	.990426239
125	.59644189E-07	-1.971149420	.971392609	-1.987804390	.988049548
150	.12317157E-06	-1.965420916	.965770096	-1.985324025	.985676770
175	.22725581E-06	-1.959706228	.960180126	-1.982830046	.983309591
200	.38610030E-06	-1.954005331	.954622512	-1.980322510	.980948097
225	.61592465E-06	-1.948318202	.949097066	-1.977801474	.978592273
250	.93492098E-06	-1.942644818	.943603601	-1.975266997	.976242108
275	.13632107E-05	-1.936985153	.938141934	-1.972719134	.973897587
300	.19228022E-05	-1.931339186	.932711878	-1.970157944	.971558696
325	.26375481E-05	-1.925706891	.927313253	-1.967583483	.969225422
350	.35331044E-05	-1.920088246	.921945875	-1.964995809	.966897752
375	.46368892E-05	-1.914483227	.916609564	-1.962394979	.964575672
400	.59780421E-05	-1.908891809	.911304141	-1.959781050	.962259168
425	.75873843E-05	-1.903313970	.906029425	-1.957154080	.959948228
450	.94973791E-05	-1.897749685	.900785240	-1.954514125	.957642837
475	.11742093E-04	-1.892198931	.895571409	-1.951861244	.955342984
500	.14357157E-04	-1.886661684	.890387757	-1.949195492	.953048653
525	.17379729E-04	-1.881137921	.885234107	-1.946516928	.950759837
550	.20848456E-04	-1.875627617	.880110288	-1.943825608	.948476509
575	.24803438E-04	-1.870130749	.875016125	-1.941121590	.946198669
600	.29286189E-04	-1.864647294	.869951448	-1.938404931	.943926299
625	.34339504E-04	-1.859177227	.864916066	-1.935675688	.941659387
650	.40007922E-04	-1.853720526	.859909869	-1.932933917	.939397919
675	.46336691E-04	-1.848277166	.854932629	-1.930179677	.937141881
700	.53372733E-04	-1.842847123	.849984197	-1.927413025	.934891262
725	.61164111E-04	-1.837430375	.845064407	-1.924634016	.932646040
750	.69760093E-04	-1.832026897	.840173094	-1.921842709	.930406226
775	.79211121E-04	-1.826636666	.835310092	-1.919039161	.928171783
800	.89568779E-04	-1.821259658	.830475237	-1.916223428	.925942707
825	.10086576E-03	-1.815895850	.825668367	-1.913395567	.923718983
850	.11321582E-03	-1.810545218	.820889320	-1.910555636	.921500600
875	.12661378E-03	-1.805207738	.816137934	-1.907703592	.919287545
900	.14113547E-03	-1.799883387	.811414049	-1.904839791	.917079804
925	.15683768E-03	-1.794572141	.806717507	-1.901963990	.914877366
950	.17377819E-03	-1.789273976	.802048149	-1.899076347	.912680217
975	.19201567E-03	-1.783988870	.797405818	-1.896176918	.910488344
1000	.21160969E-03	-1.778716798	.792790357	-1.893265760	.908301735

COMPUTED FILTER COEFFICIENTS
FOUR POLE LOW-PASS FILTER
SAMPLING RATE 25 KHZ

CUT-OFF HZ	B0	B1	B2	B3	B4
25	.15458097E-08	-1.988418061	.988457311	-1.995163228	.995202612
50	.24530745E-07	-1.976891763	.977047856	-1.990271084	.990426239
75	.12317157E-06	-1.965420916	.965770096	-1.985324025	.985676770
100	.38610030E-06	-1.954005331	.954622512	-1.980322510	.980948097
125	.93492098E-06	-1.942644818	.943603601	-1.975266997	.976242108
150	.19228022E-05	-1.931339186	.932711878	-1.970157944	.971558696
175	.35331044E-05	-1.920088246	.921945875	-1.964995809	.966897752
200	.59780421E-05	-1.908891809	.911304141	-1.959781050	.962259168
225	.94973791E-05	-1.897749685	.900785240	-1.954514125	.957642837
250	.14357157E-04	-1.886661684	.890387757	-1.949195492	.953048653
275	.20848456E-04	-1.875627617	.880110288	-1.943825608	.948476509
300	.29286189E-04	-1.864647294	.869951448	-1.938404931	.943926299
325	.40007922E-04	-1.853720526	.859909869	-1.932933917	.939397919
350	.53372733E-04	-1.842847123	.849984197	-1.927413025	.934891262
375	.69760093E-04	-1.832026897	.840173094	-1.921842709	.930406226
400	.89568779E-04	-1.821259658	.830475237	-1.916223428	.925942707
425	.11321582E-03	-1.810545218	.820889320	-1.910555636	.921500600
450	.14113547E-03	-1.799883387	.811414049	-1.904839791	.917079804
475	.17377819E-03	-1.789273976	.802048149	-1.899076347	.912680217
500	.21160969E-03	-1.778716798	.792790357	-1.893265760	.908301735
525	.25510999E-03	-1.768211662	.783639424	-1.887408485	.903944260
550	.30477246E-03	-1.757758382	.774594118	-1.881504977	.899607688
575	.36110297E-03	-1.747356769	.765653219	-1.875555690	.895291921
600	.42461897E-03	-1.737006634	.756815522	-1.869561078	.890995858
625	.49584869E-03	-1.726707791	.748079836	-1.863521594	.886722401
650	.57533029E-03	-1.716460050	.739444983	-1.857437692	.882468449
675	.66361106E-03	-1.706263224	.730909800	-1.851309824	.878234906
700	.76124666E-03	-1.696117126	.722473135	-1.845138443	.874021672
725	.86880033E-03	-1.686021569	.714133852	-1.838924000	.869828651
750	.98684221E-03	-1.675976365	.705890827	-1.832666946	.865655746
775	.11159486E-02	-1.665981327	.697742948	-1.826367733	.861502859
800	.12567012E-02	-1.656036269	.689689119	-1.820026811	.857369995
825	.14096867E-02	-1.646141005	.681728252	-1.813644630	.853256760
850	.15754957E-02	-1.636295347	.673859275	-1.807221638	.849163356
875	.17547225E-02	-1.626499109	.666081127	-1.800758285	.845089590
900	.19479642E-02	-1.616752107	.658392760	-1.794255019	.841035367
925	.21558204E-02	-1.607054153	.650793137	-1.787712288	.837000594
950	.23788923E-02	-1.597405063	.643281234	-1.781130538	.832985178
975	.26177824E-02	-1.587804651	.635856039	-1.774510216	.828989025
1000	.28730937E-02	-1.578252732	.628516550	-1.767851767	.825012043

Table (4.4) Computed Filter Coefficients of Four Pole Low Pass Cascaded Filters

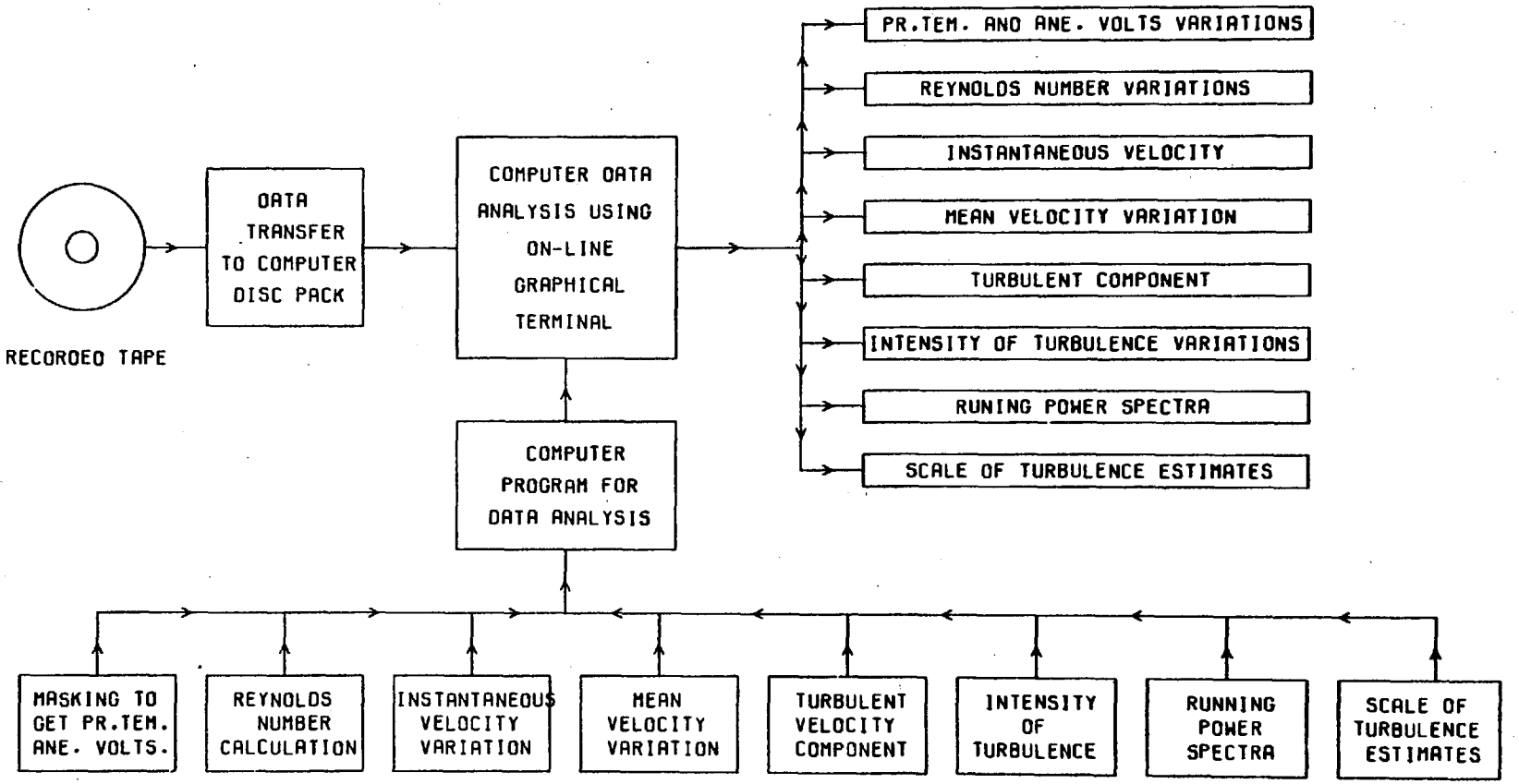
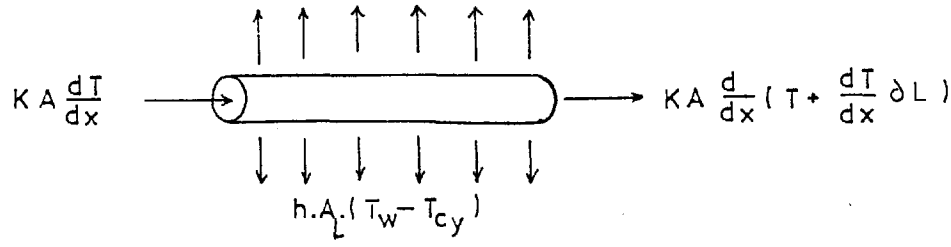


Fig (4.13) Data Processing Procedure

used for data analysis. According to the hard ware arrangement which exists within the tape recorder, all recorded data were written to the magnetic tape with 10 binary bits accuracy but occupying 12 bits space with two leading zeros; where as the computer used for data analysis has 60 binary bits accuracy. Hence each group of five recorded data (each occupying 12 bits space) is seen by computer as a single recorded word or experimental value. The computer word is thus required to be equally subdivided into five divisions of each 12 binary bits to recover all recorded data. This operation was achieved by using the soft ware masking and shifting process mentioned under Section(A.7).

4.5.2 Calculation of Instantaneous Convective Heat Transfer:- Coefficient of the hot wire:- This value is necessary to calculate the Nusselt number and hence the Reynolds number of the flow from the calibration curve. The convective heat transfer coefficient of the hot wire element at any instant was calcualated by considering the energy balance of the wire taking into account of the conduction losses effect to the supporting prongs. By solving the energy equation it is able to estimate the temperature gradient at the ends of the wire and hence the amount of conduction losses. The energy applied to the wire minus the conduction losses gives the convective heat losses (radiation losses are taken to be small and neglected), thus the convective heat transfer coefficient of the wire.

For an elementary hot wire sensor length dL, the energy balance equation can be written as:-



$$\Sigma\text{conduction losses} + \Sigma\text{convection losses} + \Sigma\text{energy applied} = 0$$

$$\{KA\frac{d}{dx}(T + \frac{dT}{dx}dL) - KA\frac{dT}{dx}\} + \{h\pi D\, dL\,(Tw - T_{cy})\} +$$

$$\{-\frac{I^2 Ro}{L}(1 + \alpha\,(t_w - T_{ref}))\times dL\} = 0$$

The assumptions made are:-

(i) There is no variation of temperature in the radial direction.

(ii) The values of conductive and convective heat transfer coefficients remain constant along the length of the wire.

(iii) Radiation losses are negligible compared to conductive and convective heat losses.

By substituting, $T_x = T_w - T_{cy}$ and $I^2 R_o = {}^{E^2}/_{R_o}$

$$\frac{d^2 Tx}{dx^2} + \frac{(h\pi D - {}^{E^2}/RoL \,.\, \alpha)}{KA} Tx - \frac{{}^{E^2}/RoL \,(1 + \alpha\,(T_{cy} - T_{ref})}{KA} = 0$$

$$\frac{d^2 Tx}{dx^2} + C_1 T_x + C_2 = 0$$

The solution of the above type of differential equation is given by Davies and Fisher (7), as

$$Tx = A \,\mathrm{Cosh}\sqrt{C_1}\; x - {}^{C_2}/_{C_1}$$

No direct solution for T_x can be found as the expression for C_1 contains the unknown convective heat transfer coefficient "h". An iterative method of solution was suggested by Davies and Fisher (7), in which an initial guess of the convective heat transfer coefficient "h" is made and the value of T_x, the temperature distribution along the length of the wire is solved. Iteration with new corrected value of "h" is carried out until a value of "h" which satisfies the end boundary conditions of T_x is found. This iterative method of solution is very uneconomical in computing time and the accuracy in value of "h" is dependent on the accuracy level set and the number of iterations.

Thus an alternative method of solution which is free from iteration and maintains high degree of accuracy in computed convective heat transfer coefficient was developed and adopted. The solution procedure is to replace the hyperbolic function in the analytical expression of solution by an equivalent exponential expression such that,

$$T_x = A \,\mathrm{Cosh}\,\sqrt{C_1}\; x - {}^{C_2}/_{C_1}$$

$$T_x = A\left(\frac{e^{\sqrt{C_1}x} + \bar{e}^{\sqrt{C_1}x}}{2}\right) - C_2/C_1$$

Now each exponential term is replaced by its polynonial expansion up to 4th power term and results in,

$$T_x = A\left(1 + C_1\frac{x^2}{2} + \frac{C_1^2 x^4}{24}\right) - C_2/C_1$$

The truncation error involved by neglecting x^6, x^8, ... terms and so on is negligible as the wire length under consideration is very very small.

The known boundary conditions are:-

(i) The known hot wire average temperature (operating temperature) which is expressed mathematically as:-

$$Tave = \frac{1}{L}\int_o^L Tw\ dx$$

$$Tave = \frac{1}{L}\int_o^L (Tx + Tcy)\ dx$$

By substituting the expression for T_x (equation A)

$$Tave = Tcy + A\left\{1 + C_1\frac{L^2}{6} + \frac{C_1^2 L^4}{120}\right\} - \frac{C_2}{C_1} \qquad (1)$$

(ii) At the end of the wire, wire temperature is taken to be equal to prong temperature which is supposed to be at ambient cylinder charge temperature.

Thus at the ends, $Tw = Tprong = Tcyl$

or $Tx = 0$

$$\text{or}\quad 0 = A\left\{1 + C_1\frac{L^2}{2} + \frac{C_1^2 L^4}{24}\right\} - C2/C1 \qquad (2)$$

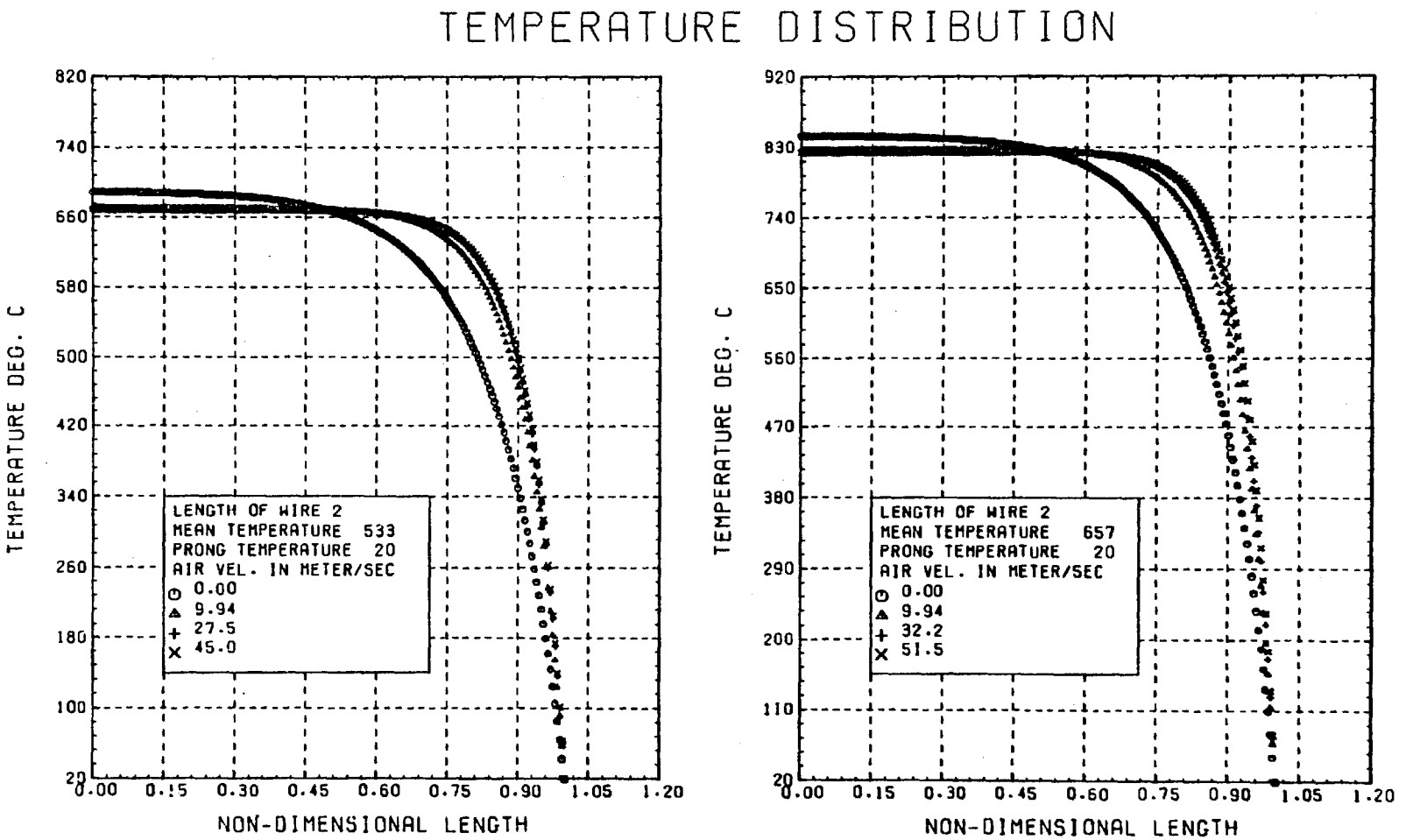


Fig (4.14) Computed Temperature Distribution Along the Length of the Hot Wire Sensor

Equations 1 and 2 can be solved for the two unknown A and C_1, without any iterative procedure and hence the variation of hot wire temperature along its length, the conduction heat loss, convective heat loss and the convective heat transfer coefficient of the hot wire are known.

4.5.3 Nusselt Number Calculation:- The knowledge of the Nusselt number $(\frac{hD}{k})$ is needed for use in the calibration equation which relates the Nusselt number to the Reynolds number of the flow. The Nusselt number is calculated by knowing the value of instantaneous convective heat transfer coefficient from the previous step. The thermal conductivity of the air was taken from Ref (105).

4.5.4 Reynolds Number of the Flow Calculation:- Using the Reynolds Analogy $Nu = a + b\ R_e^{\ n}$, Reynolds number of the flow was calculated by knowing the Nusselt number from the previous step calculation. The values of the constants a, b, and n were established by the hot wire calibration procedure as mentioned under section (A.5).

4.5.5 Instantaneous Velocity Calculation:- The values of the instantaneous Reynold numbers of the flow from the previous step of the calculation enable the evaluation of the instantaneous local velocity as sensed by the hot wire.

$$V_{inst} = R_e \quad {}^{u}/_{(\rho.D)}$$

The density term was evaluated from the measured cylinder pressure and temperature. The instantaneous velocity thus found was later processed to yield it statistical parameters. The viscosity values of air were taken from Ref(105)

4.5.6 Mean Velocity Separation:- Mean velocity component of the flow was separated from its instantaneous velocity values by the digital low pass filtering process. A cascaded four pole low-pass filter arrangement was used.

4.5.7 High Frequency Turbulent Component of Velocity Separation:- This was obtained by the digital high-pass filtering process which applied to the instantaneous values of the computed velocity signal. A cascaded four pole high-pass filter arrangement was used.

4.5.8 Intensity of Turbulence Calculation:- A running root mean square value of the high frequency turbulent component was calculated to obtain the intensity of turbulence.

4.5.9 Power Spectra Estimate:- The power content of the high

frequency turbulent fluctuations in each assigned frequency bands was estimated by using Fourior Transformation Technique. A computer programme subroutine was written to simulate a 1/3rd octave band pass filters system and was used for estimating the power spectra of the high frequency turbulent signals for each 20 degree crank angle interval. Alternative ways of estimating power spectra are mentioned under section (A.3).

4.5.10 Scale of Turbulence:- Length and time scales of the turbulent eddies were estimated from the knowledge of the power-spectral distribution as calculated by the previous step.

The above turbulence parameters were calculated for 25 recorded engine cycles and were then averaged to give the representtative average value for a particular set of engine operating condition. The nature of the measured and analysed results are discussed under the next section.

A data analysis procedure for analysing unsteady turbulent flow data to yield its statistical parameters was thus developed based on the digital filtering principle in combination with classical statistical analysis method. It is the first occasion on which such an analysis procedure has been applied and has proved to be successful and reliable for engine cylinder turbulence analysis. The method has advantages over the previous existing alteratives by giving the statistical parameters on a cycle to cycle basis, which the ensemble averaging method does not, and at the same time does not require quasi-steady assumption on mean velocity calculation as in quasi-steady data analysis method. Thus it seems to be preferable to use this method for general unsteady turbulence data analysis.

5.0.0 CONCULSION ON MEASURED RESULTS ON ENGINE CYLINDER TURBULENCE:-

The quantitative spatial and temporal nature of the engine cylinder turbulence was obtained by analysing the experimentally recorded data of cylinder pressure, cylinder temperature and anemometer output voltage (Sections 3 and 4). Hot wire anemometer readings were taken using three sensor-wire probes at nine different places, including five locations on piston crown, inside the engine cylinder (fig. 5.1). The measured results show that turbulence variations follow the mean velocity profile and in fact turbulence intensity variations can be taken as a small scale diagram of the mean velocity fluctuations, fig. (5.2 to 5.5). Hence a common conclusion will be drawn with respect to the nature of their variations with various engine operating parameters.

5.1.0 Time History of Turbulence Intensity Fluctuations:- The measured results show that turbulence as well as mean velocity are decaying with time during the compression process. It reaches a minimum value at or around the time when piston reaches top dead centre (TDC) position. This can be explained by the fact that though the cylinder charge tries to maintain its initial momentum and turbulence level,which have been generated by the incoming airjet during the induction process, the fluid friction losses and the losses between fluid particles and surrounding walls cause the turbulences and mean velocity to decay with time. On the other hand, the compression effect of the moving piston causes a reduction in the inertia of the cylinder charge and hence promotes increase in the magnitude of local velocity according to conservation of momentum principle. The observed initial small rise in mean velocity and turbulences during the early stage of the compression seems to be due to a reduction in inertia of the cylinder charge while effects due to fluid friction losses are still not significant. During the later part of the compression process however, the effect of losses has increased to such an extent that it causes a reduction in the magnitude of mean velocity and turbulence. On the expansion stroke, the downward accelerating movement of the piston induces a rise in turbulence level. The observations made are in agreement with the results of Semenov (1) and Dent (66). If

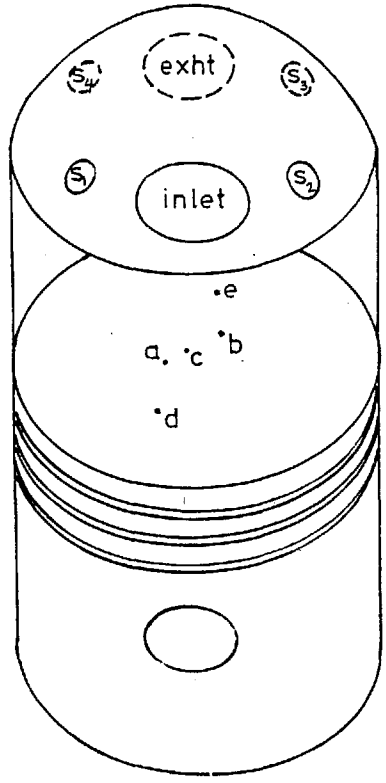


Fig (5.1) Positions Of Measurement in 3 Dimensional Representation.

the combustion chamber has a small squish volume or a bowl in piston, the cylinder charge will be compressed into a small volume and this will reduce its inertia to such an extent that its effect dominates the losses effect, thus it might be expected that swirl and turbulence will increase with compression as observed by Dent Et Al (108) in his observations of swirl in a Diesel Engine Cylinder.

5.2.0 Turbulence Intensity Variation With Positions in Combustion Chamber:- The measured results show that during compression and the early part of the expansion stroke, the variation of turbulence is fairly uniform over the cylinder volume (fig. 5.2) and suggests that flame will propagate spherically in flat topped piston combustion chambers fitted with normal inlet ports and valve shapes. This suggestion has been confirmed by the author's second experiment in which local flame front arrival time at six locations were measured by using ionization probe technique and is also in agreement with Gussak Et Al (112) observations where flame propagation was studied by using Schlieren photography.

5.3.0 Turbulence Intensity Variation with Directions:- The measured results show that directional properties of turbulence are not marked (figs. 5.8, 5.9, 5.10, 5.11) and this seems a logical consequence of the observations that the initial turbulence has largely decayed throughout the compression process. A very weak directional dependence of mean velocity can be seen from figs (5.21, 5.23).

5.4.0 Turbulence Intensity Variation with Engine Speed:- Turbulence intensity is found to increase with increase in engine speed (figs. 5.24 to 5.29). The slopes of measured turbulence intensity against engine speed are found to remain fairly constant over different crank angle positions.

5.5.0 Turbulence Intensity Variation with Compression Ratio:- Turbulence in general is found to increase with increase in compression ratio (figs 30-33) and is in agreement with the observations made by others (113). For the values of the compression ratio (5.53 and 6.01), which are close to one another, the observed effects were not so pronounced.

5.6.0 Turbulence Intensity Variation With Volumetric Efficiency:- The measured results show the general trend of a slight drop in turbulence level with decrease in volumetric efficiency from full to quarter throttle, Figs (5.14, 5.15).

5.7.0 Percentage of Turbulence Intensity Variation:- The

percentage of turbulence intensity to the mean velocity is found to remain fairly constant, around 0.4, for all engine crank angle positions, figs. (5.20, 5.22).

5.8.0 Micro-length and Time Scales:- The micro-length scale of turbulence eddy was found to be around 0.2mm where as its life time or the micro-time scale was found to be around 0.2 milli-seconds for all employed engine operating conditions, figs. (5.34 to 5.39).

5.9.0 General Conclusion:- The measured results show that:-

(i) Turbulence intensity increases with increase in engine speed.

(ii) Turbulence intensity increased with increase in compression ratio.

(iii) Turbulence intensity decreases with decrease in volumetric efficiency.

(iv) The percentage of turbulence is around 0.4 at all crank angles for the employed geometry.

(v) The micro-length scale of turbulence is around 0.2mm and the micro-time scale is around 0.2 milli-seconds.

(vi) The turbulent intensity variation follows the mean velocity profile.

(vii) Turbulence is decaying throughout the compression process and reaches to a stage where its spatial and directional dependence becomes very weak at or around when the piston reaches TDC position.

Because of the observed low dependence of turbulence on spatial and directional properties, an averaged value of the measured temporal variations over the employed measuring locations was used to represent its nature throughout the combustion chamber volume during the combustion period in the computer simulation programme for predicting turbulence flame speed (Section 7) using the correlation as suggested in section 6.5.0.

5.10.0 Error Analysis:- Some inherent errors are associated with the type of employed data recording, calibration and data analysis methods. These will be briefly mentioned.

(i) Error Due to Analogue to Digital Converter (ADC) on Quantization Error:- All analogue to digital converters introduce a type of error known as quantization error or quantization noise. This error is the difference between the input voltage value and its digitally converted rounded value. Ontes and Enochson (109) showed that for a given range of input voltage, the

power spectral density of the quantization noise decreased exponentially with the number of bits, say 10 as in our case, the quantization error tends to be negligible.

(ii) Error due to the conduction heat losses of hot wires:- It is not possible to have an ideal compensation for conduction heat losses of hot wire to the supporting prongs and thus it causes error in computed air velocity values (Radiation losses are accepted to be negligible). Without raking into account the conduction losses effect, Barton Et Al (110) observed 8% difference between the observed air velocities obtained by using two different wire operating temperatures ($700^{\circ}F$ and $800^{\circ}F$) with the same hot wire sensor probe. This type of error was estimated to be very low in our case as the conduction heat losses of the hot wire were estimated and taken into account (Section 4.0).

(iii) Error due to Digital Filtering:- The small non-linear characteristic part of the digital filter may introduce a small amount of distortion in the filtered output if part of the input signal lies in that non-linear range. But this type of error is thought to be negligible as the non-linearity part is very small and its overall characteristic is approaching that of an ideal filter.

With the above inherent errors and allowing for some possible experimental errors on pressure and temperature measurements, the total error in measured air velocity results is estimated to be less than 15%.

In addition to the above error estimate it is to be noted that the resolution of the measured mean air velocity and turbulence intensity is also dependent on the mean velocity being of known direction and much larger in magnitude than that of the turbulence fluctuations (111). The latter two conditions are seldom satisfied in an I.C. engine. There are certain times and locations in an engine where there is imperceptable mean flow, even when the turbulent velocities may be quite large and in such a situation the hot wire's insensitivity to flow direction called directional ambiguity occurs (111). A similar situation was observed in our case and hence no attempt was made to construct a three dimensional flow pattern of the observed mean flow from the measured results.

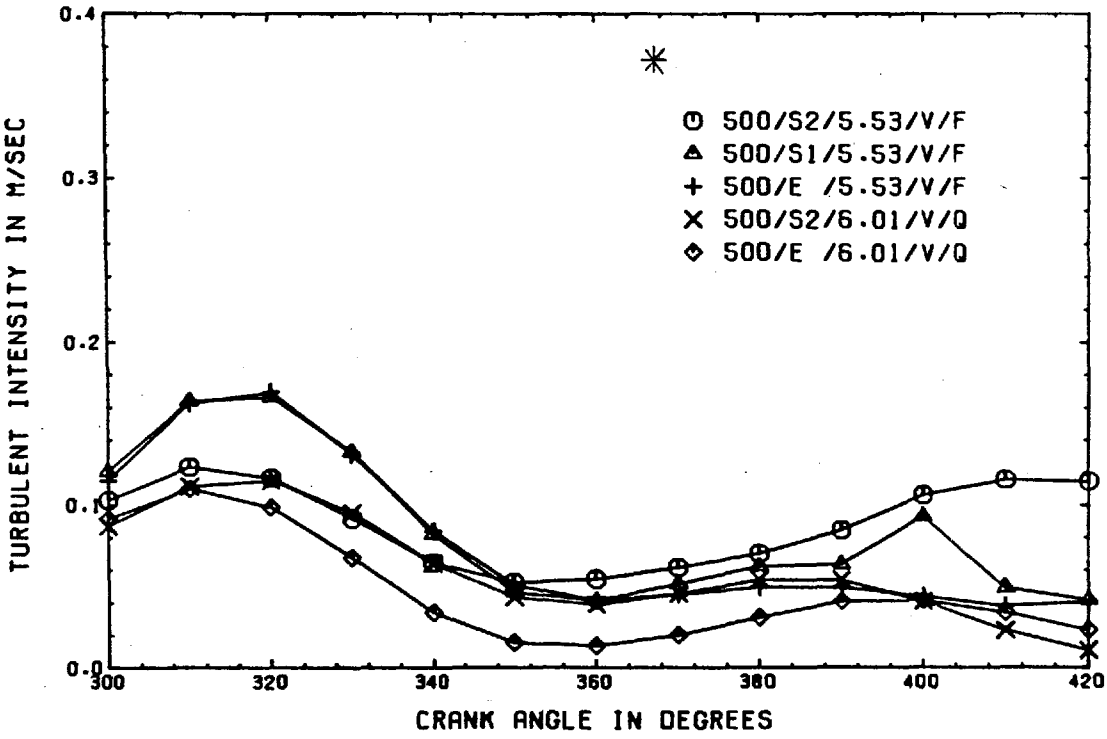


Fig (5.2) Time History of Turbulence Intensity Variation at different Positions in Combustion Chamber.

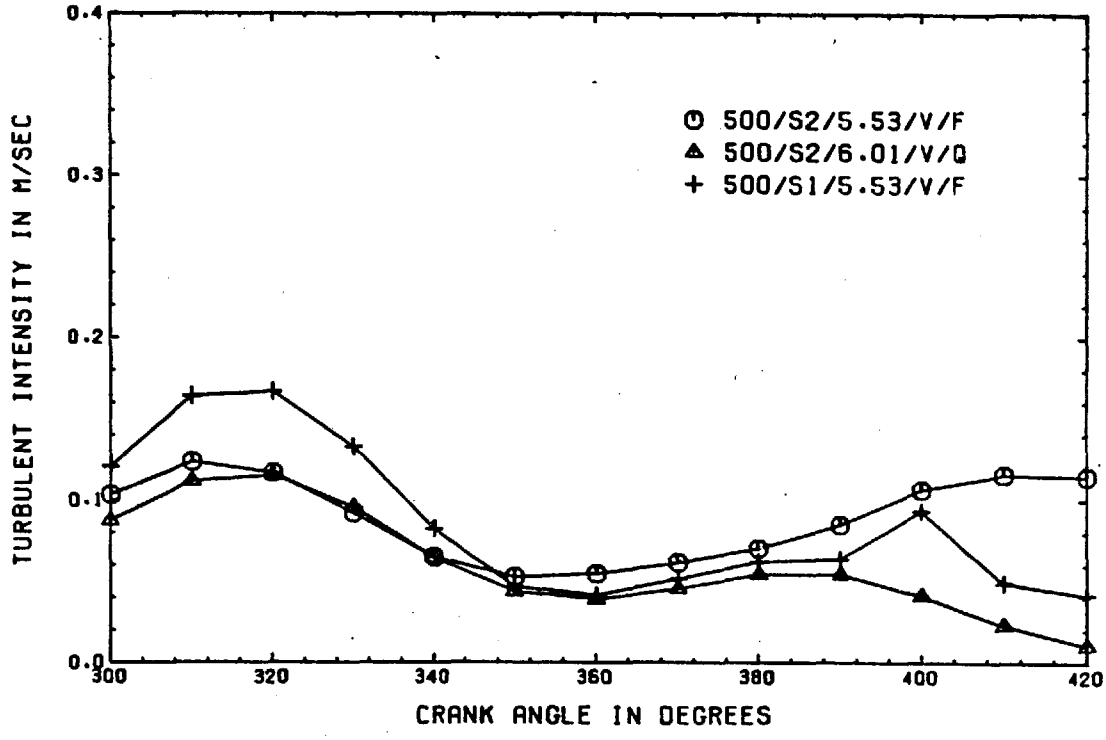


Fig (5.3) Time History of Turbulence Intensity Variation

✳ The Coding Represents

Speed / Position of Measurement / Comp. Ratio / Wire Direction / Throttle Valve Position

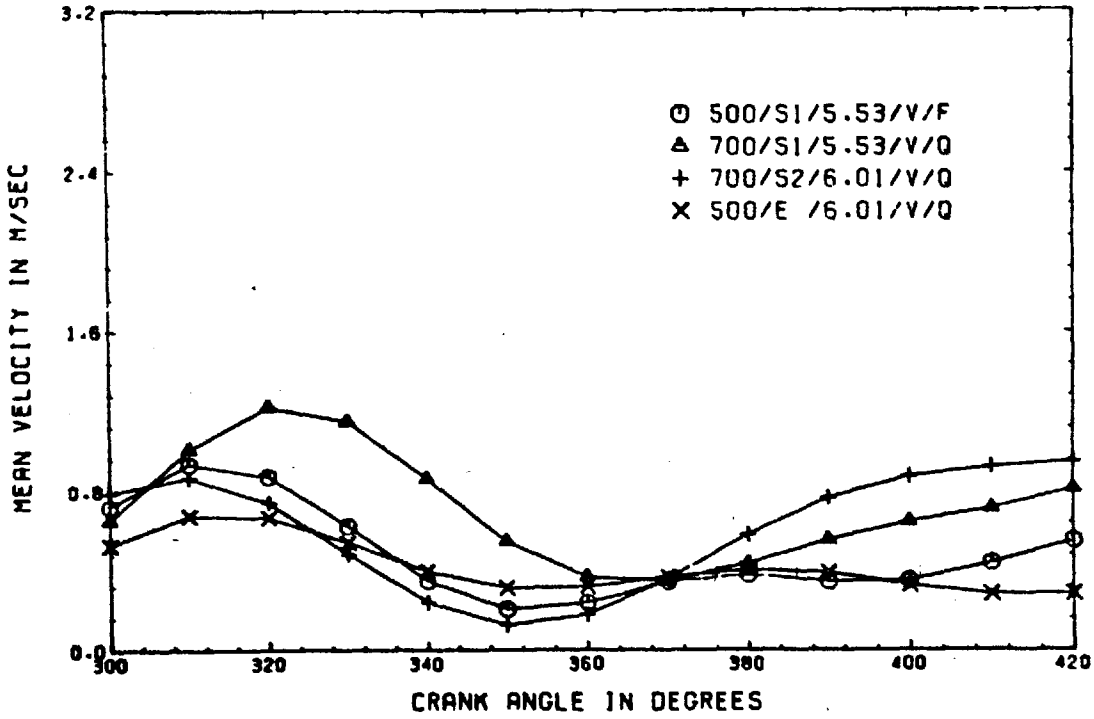


Fig (5.4) Time History of Measured Turbulence Intensity Variations

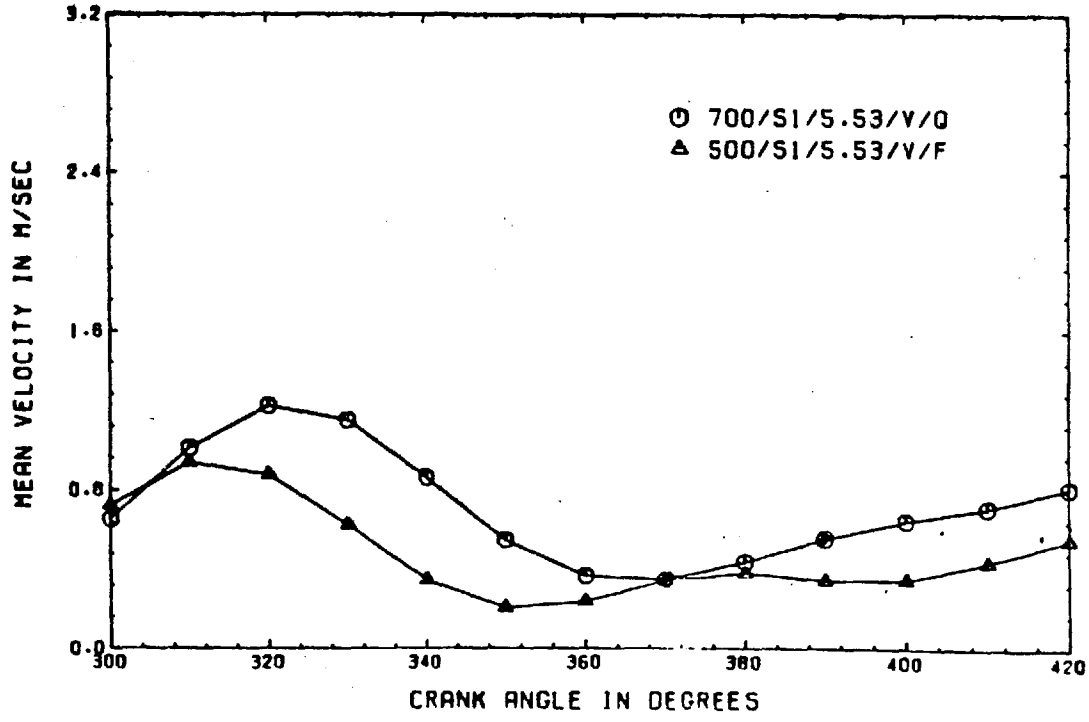


Fig (5.5) Time History of Measured Turbulence Intensity variations

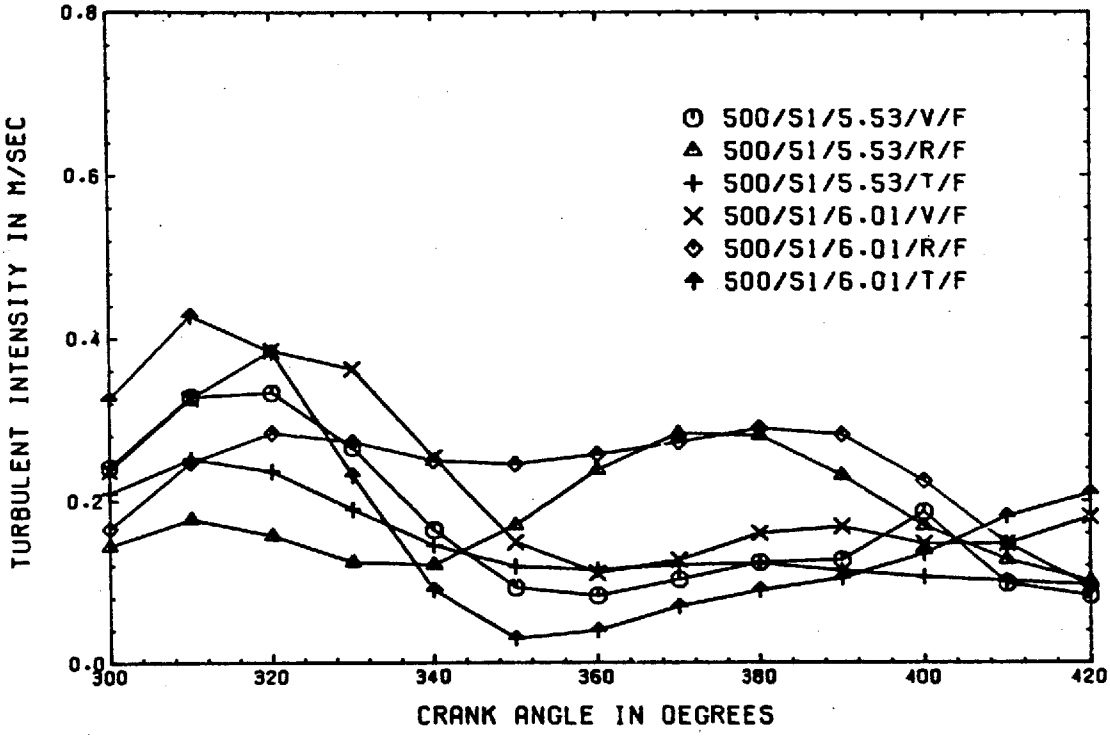


Fig (5.6) Time History of Measured Turbulence Intensity Variations

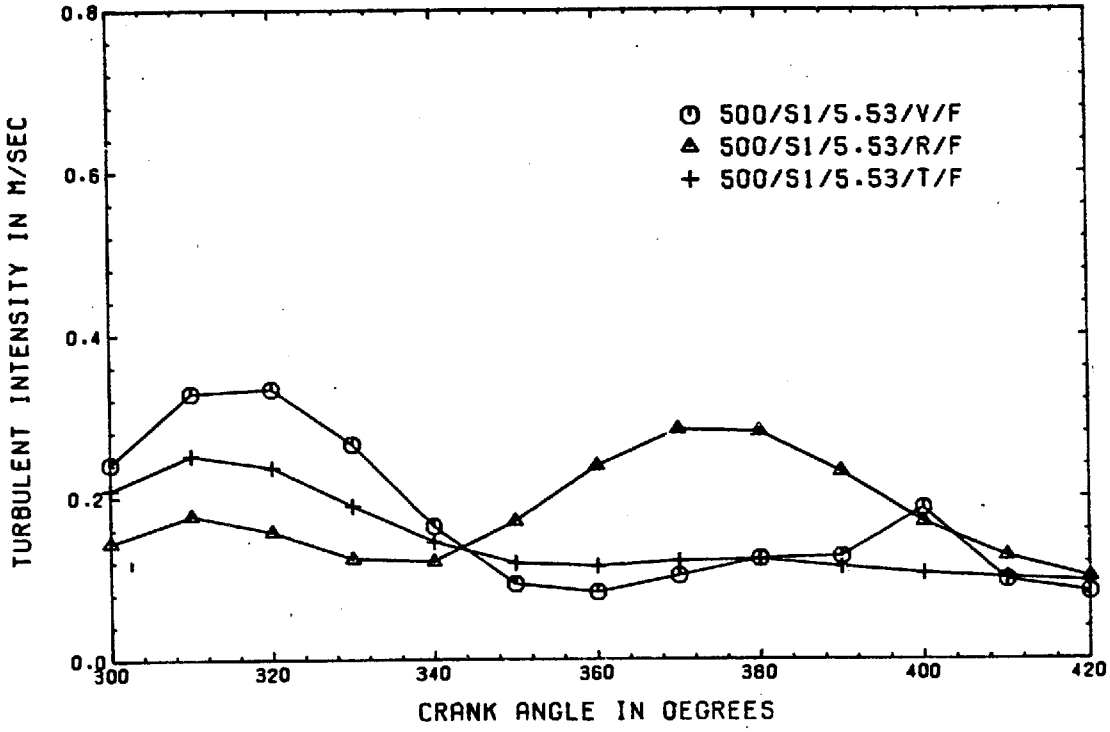


Fig (5.7) Time History of Measured Turbulence Intensity Variation

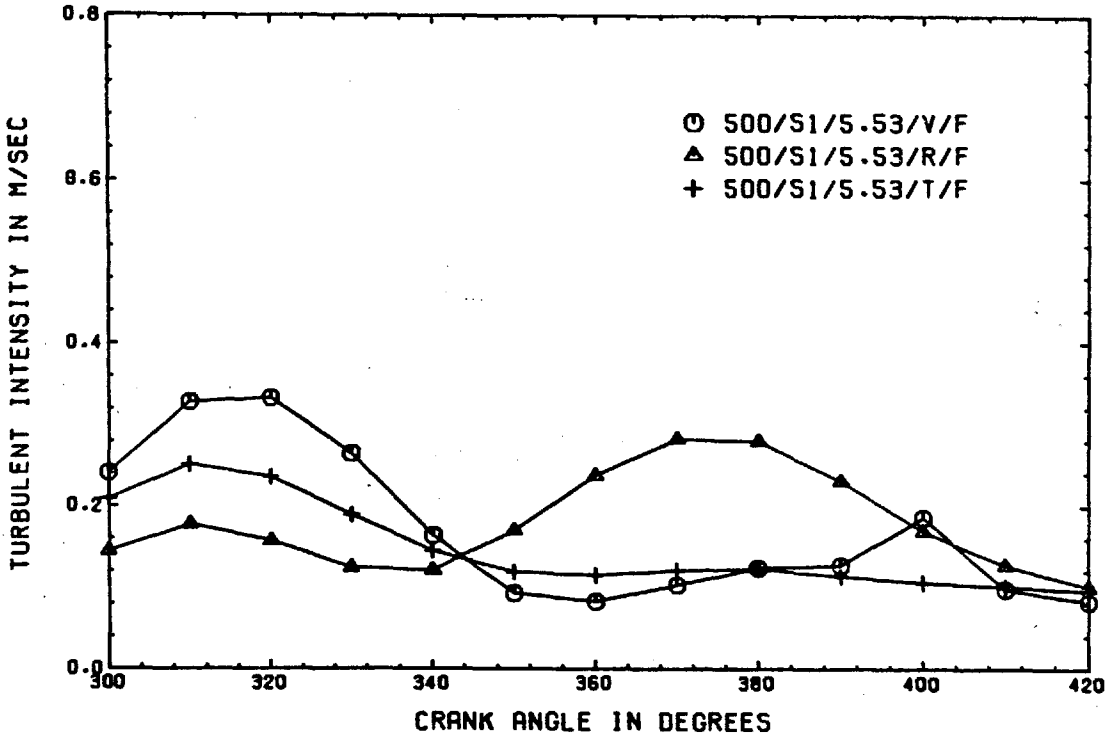


Fig (5.8) Directional Variation of Turbulence Intensity at Measuring Position S1

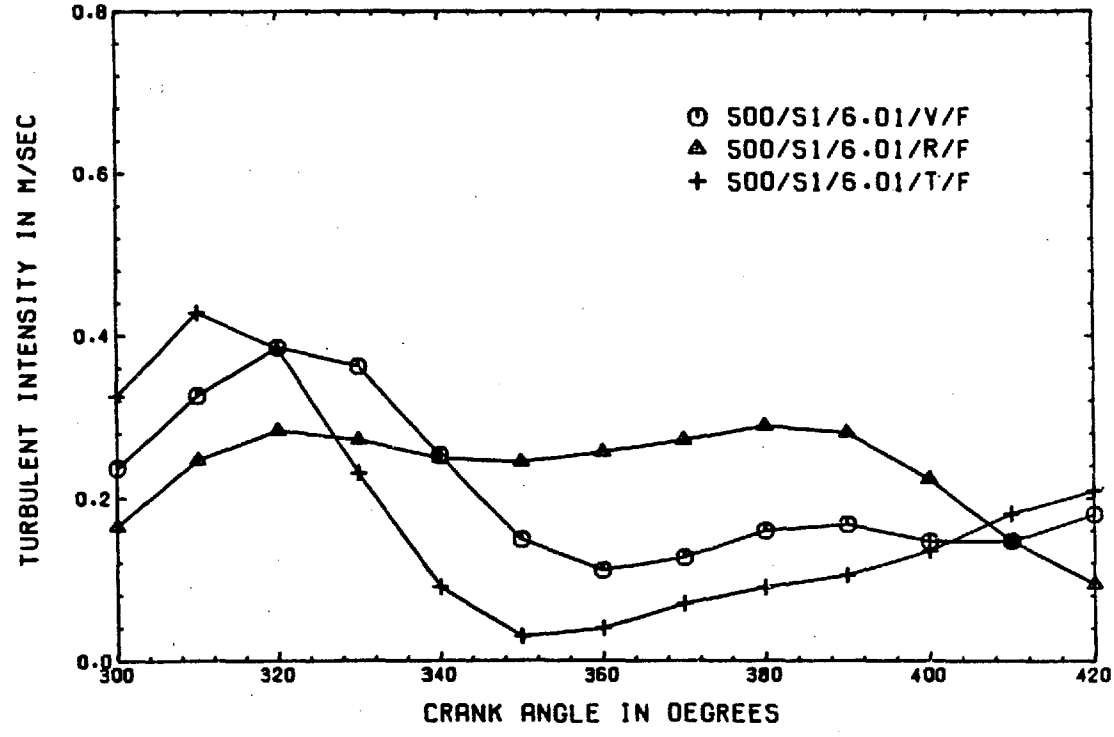


Fig (5.9) Directional Variation of Turbulence Intensity at Measuring Position S1

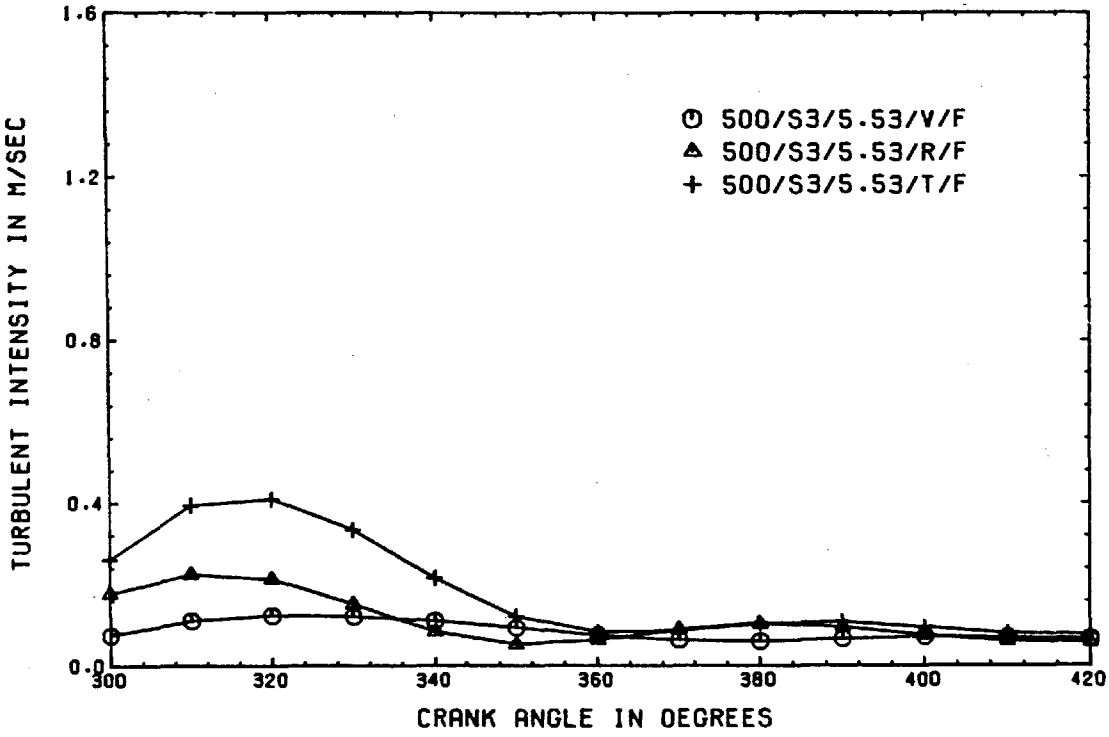


Fig (5.10) Directional Variation of Turbulence Intensity at Measuring Position S3

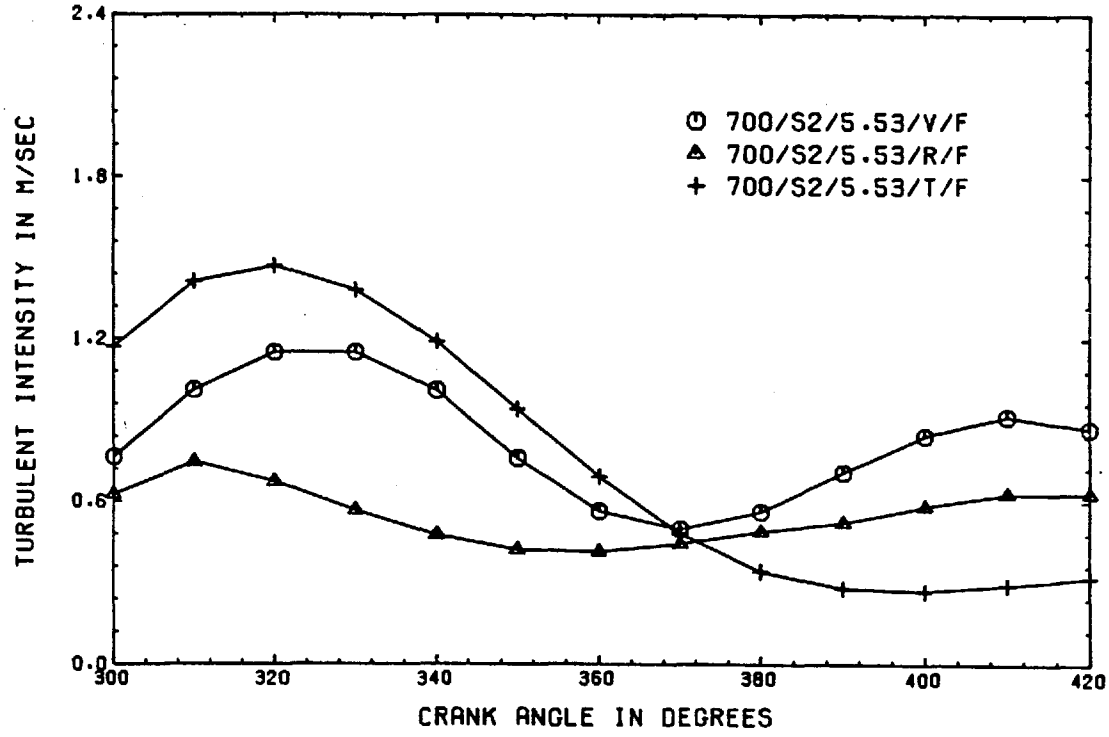


Fig (5.11) Directional Variation of Turbulence Intensity at Measuring Position S2

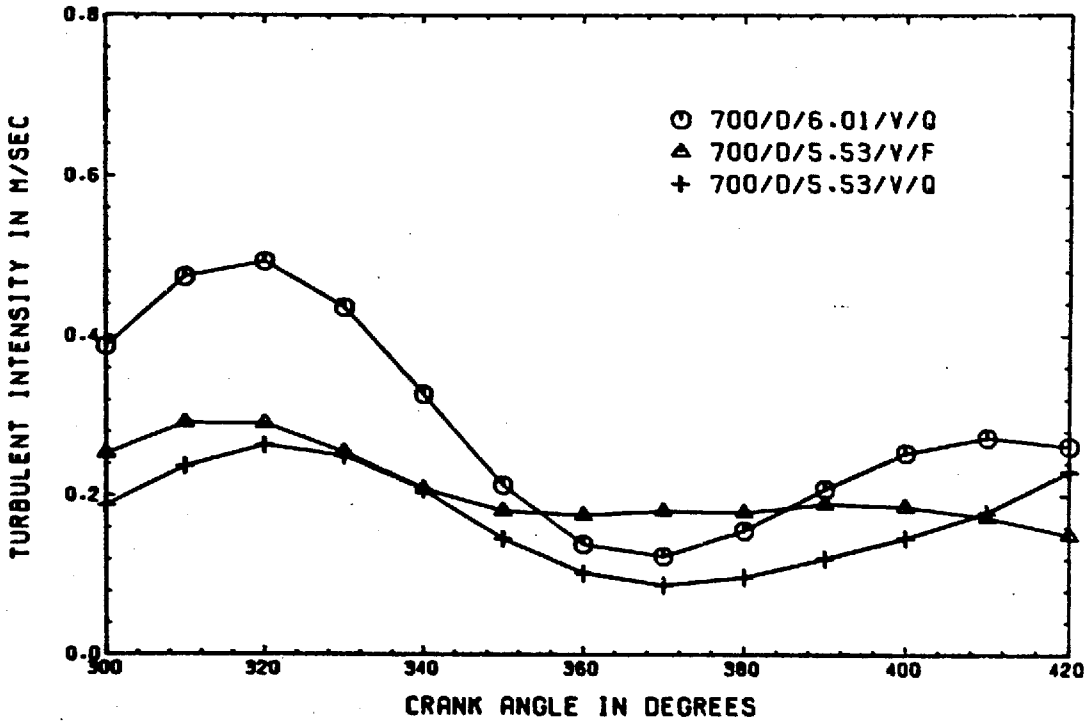


Fig (5.12) Effect of Compression ratio and Throttle Valve Opening Position

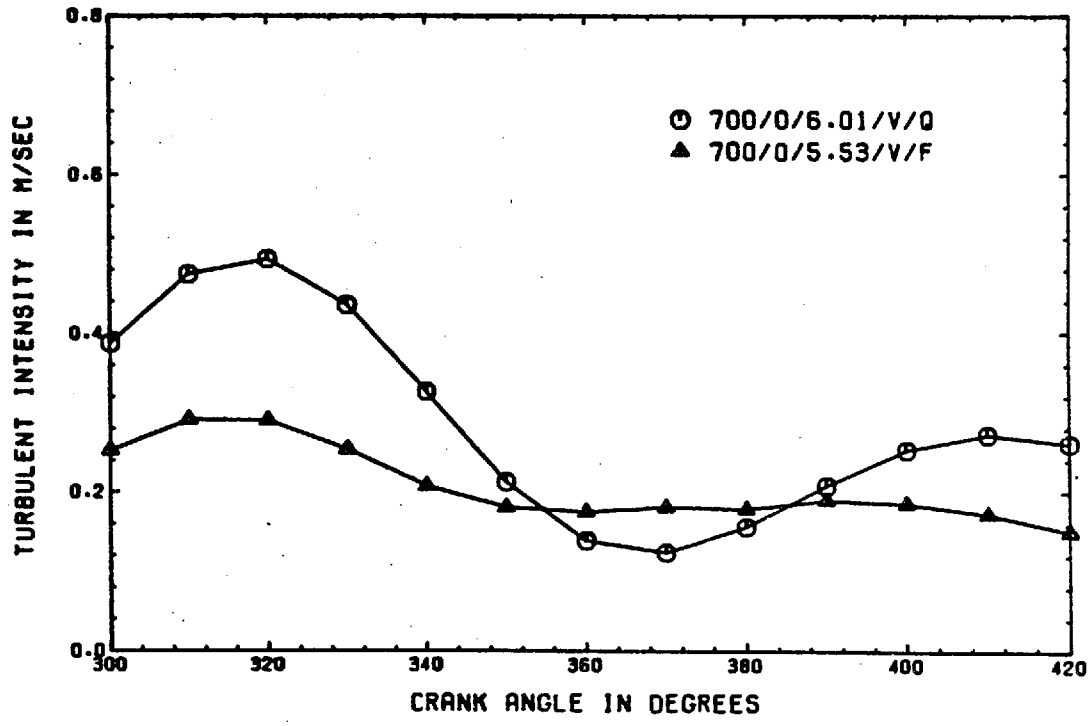


Fig (5.13) Effect of Compression Ratio on Turbulence

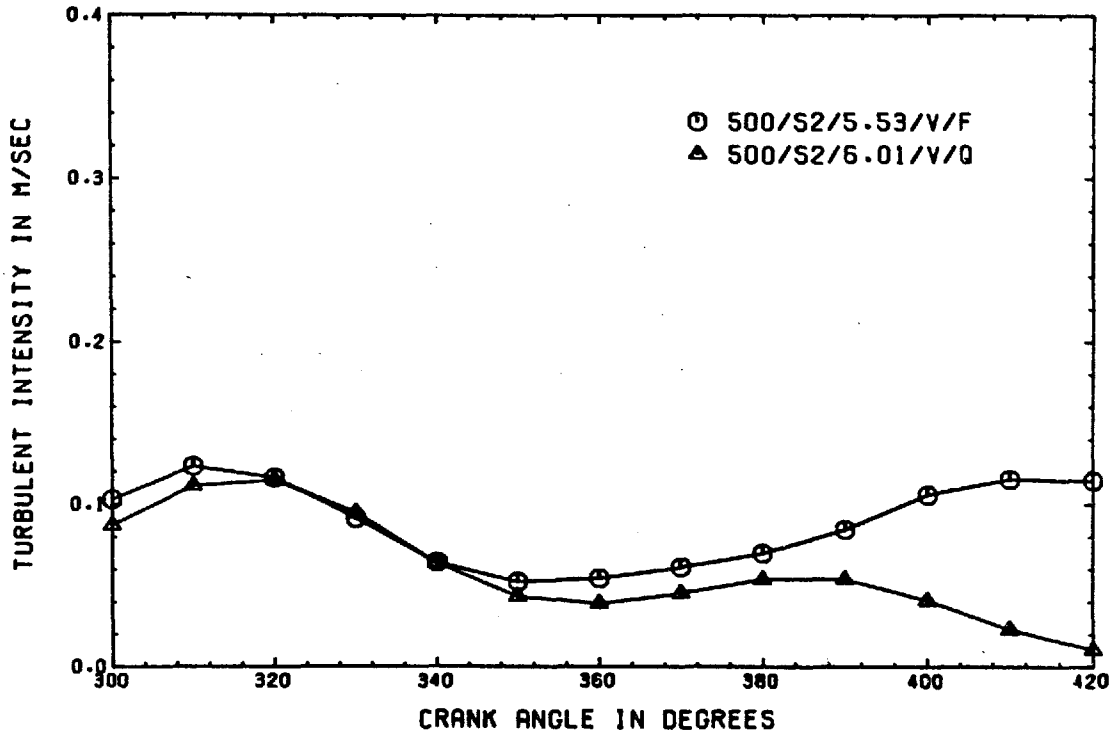


Fig (5.14) Effect of Throttle Valve Opening Position on Turbulence Intensity. Position S2

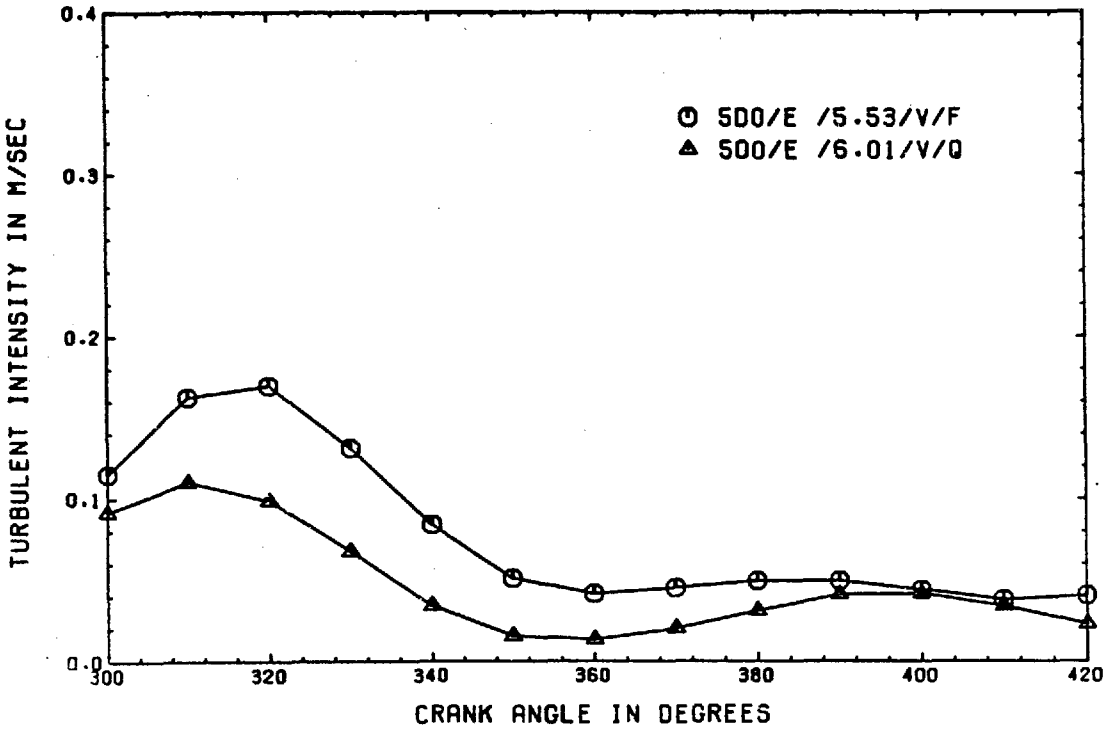


Fig (5.15) Effect of Throttle Valve Opening Position on Turbulence Intensity. Position E

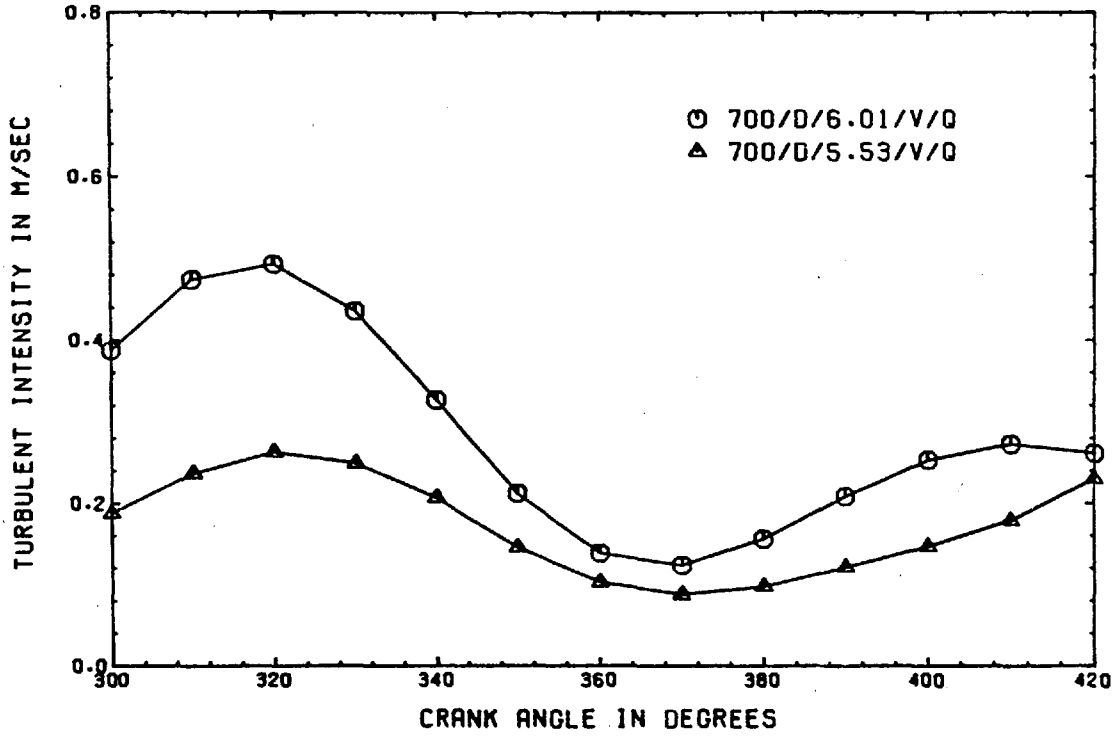


Fig (5.16) Effect of Compression Ratio on Turbulence Intensity

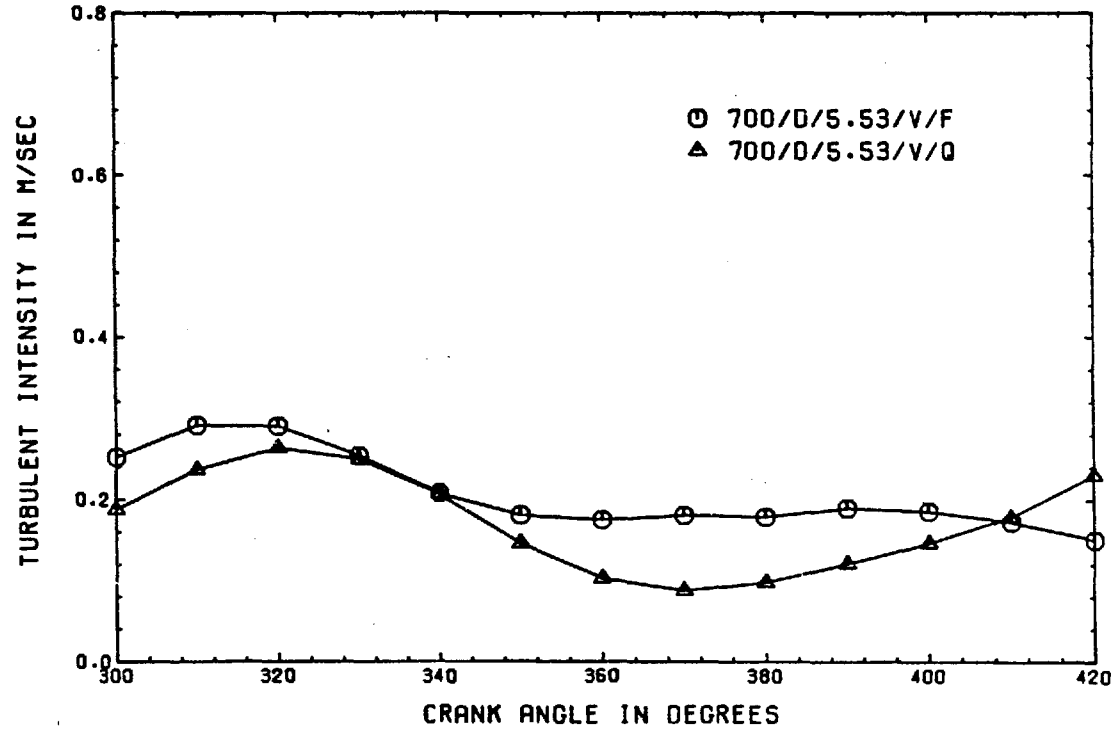


Fig (5.17) Effect of Throttle Valve Opening Position on Turbulence Intensity. Position D

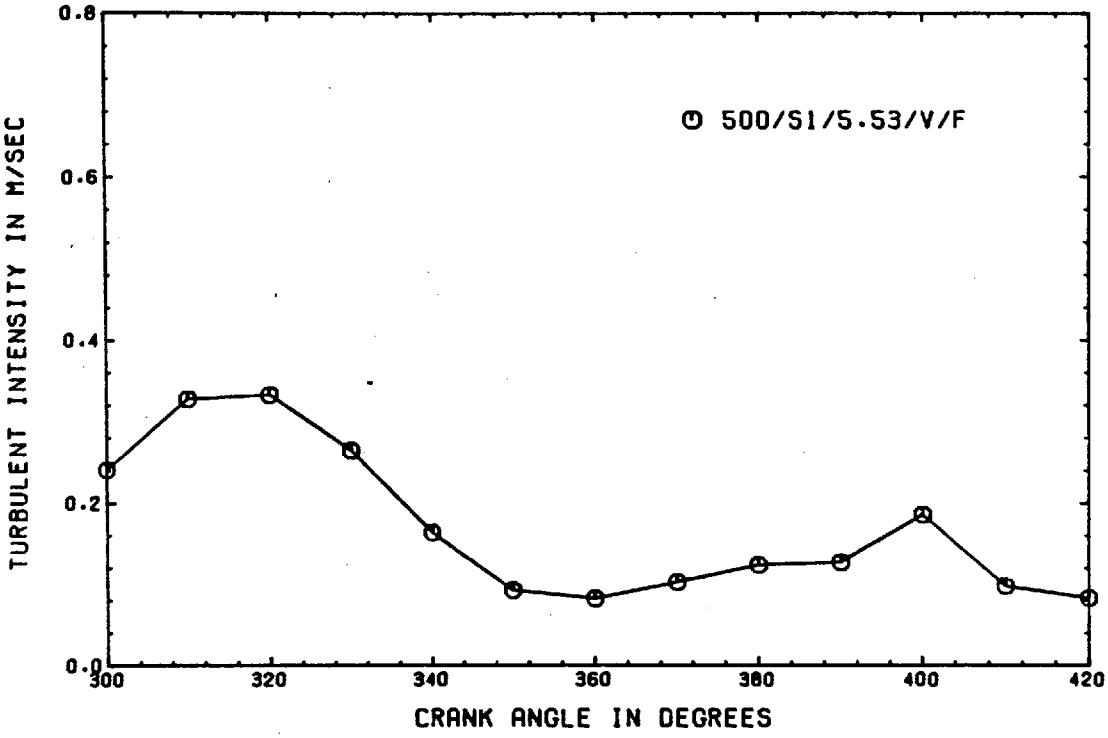


Fig (5.18) Time Variation of Turbulence measured at Position S1

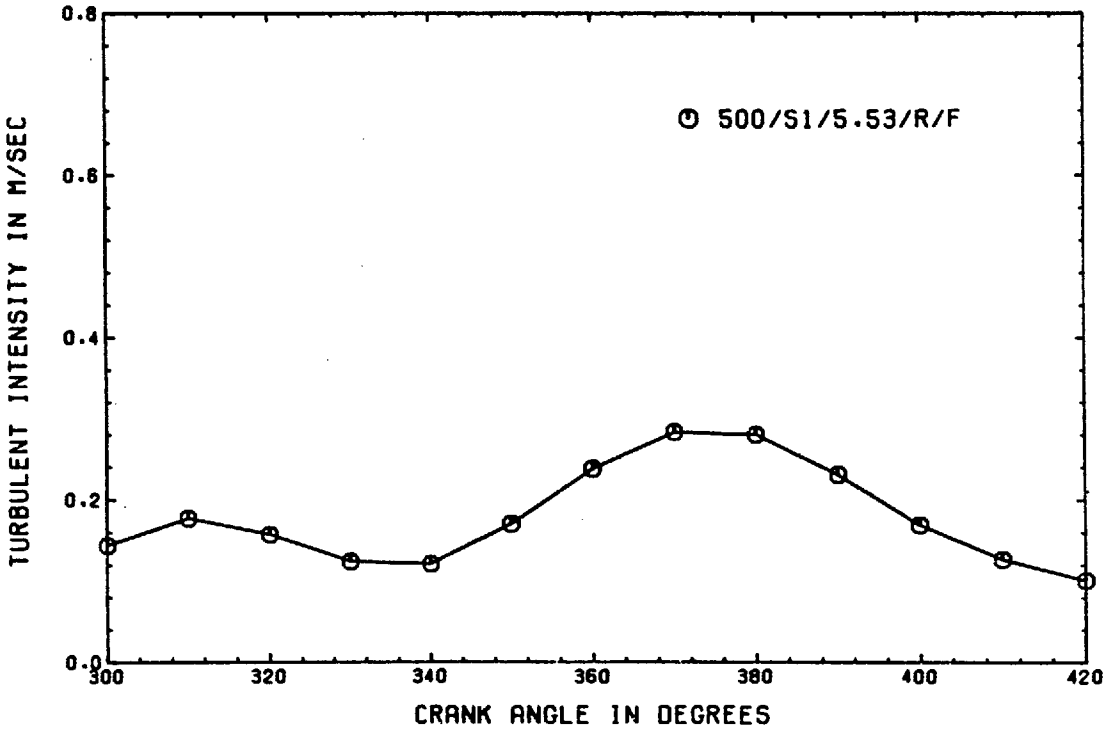


Fig (5.19) Time Variation of Turbulence measured at S1

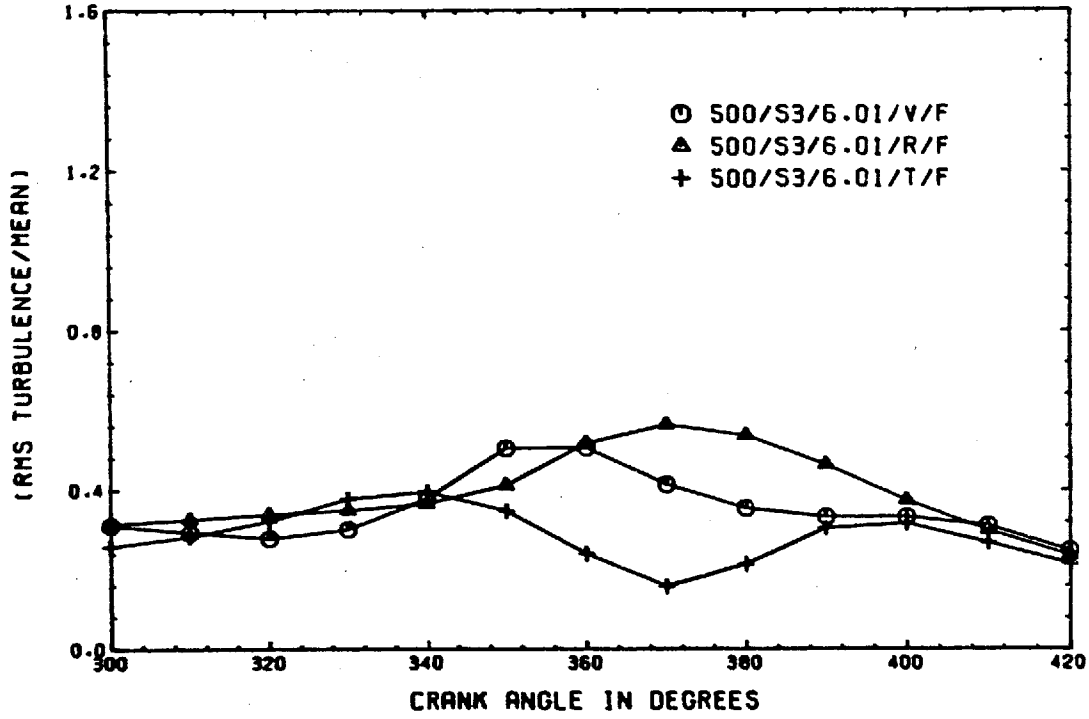


Fig (5.20) Percentage of Turbulence to Mean Velocity measured at Position S3

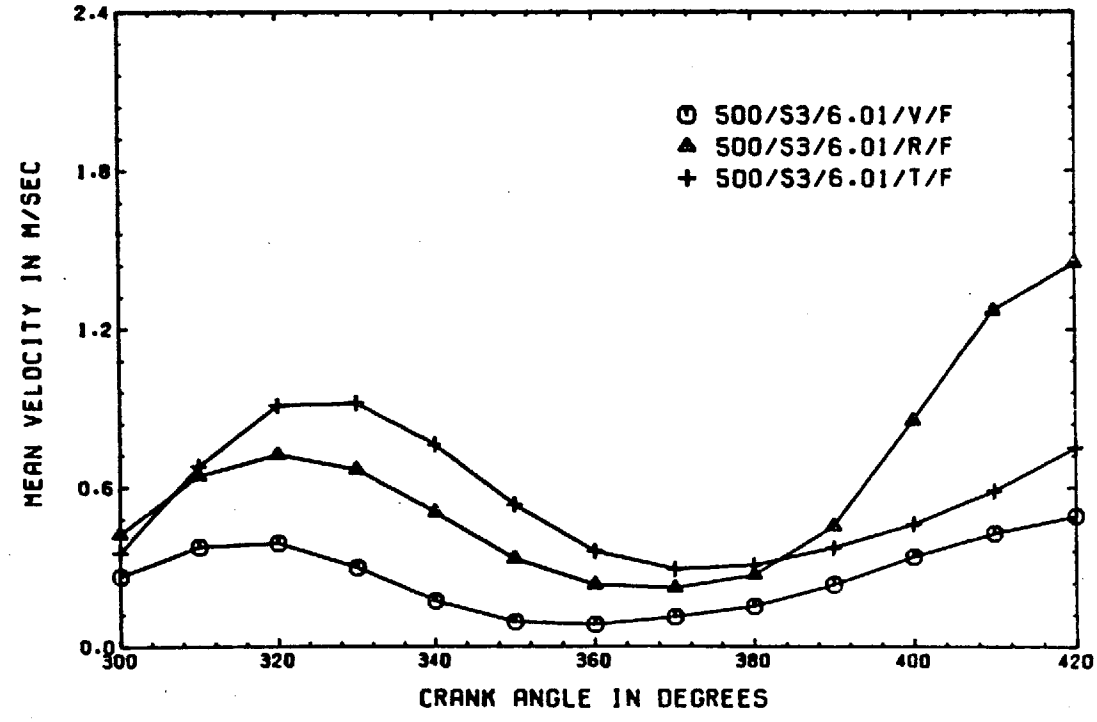


Fig (5.21) Mean Velocity Variation measured at Position S3

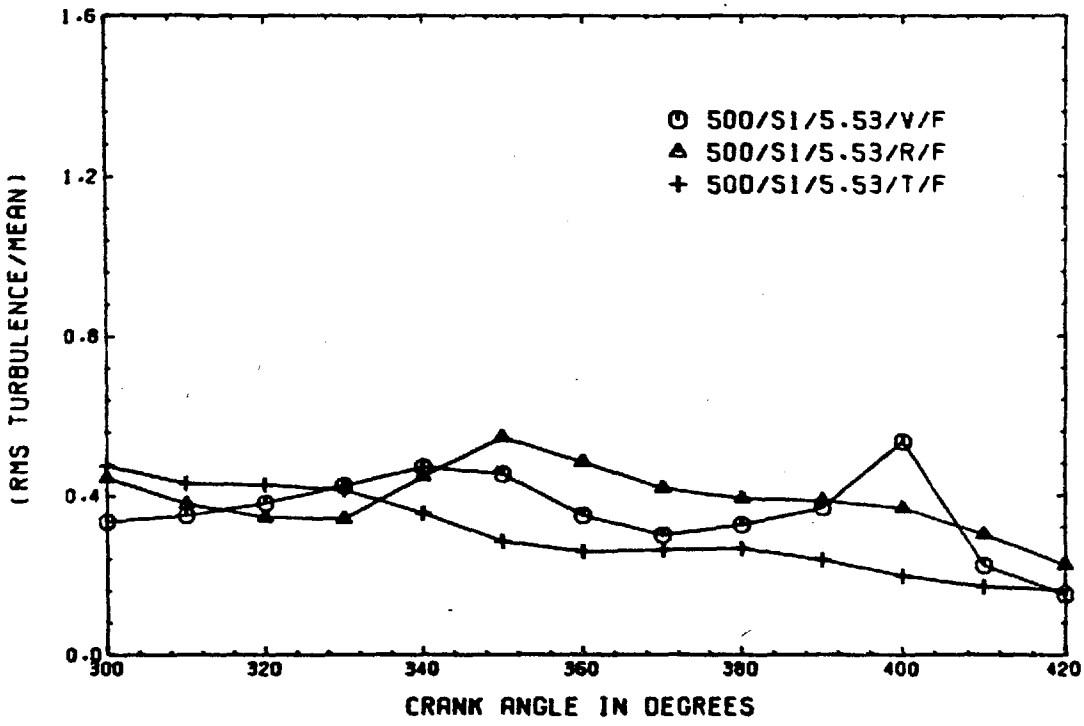


Fig (5.22) Percentage of Turbulence to Mean Velocity measured At Position S1

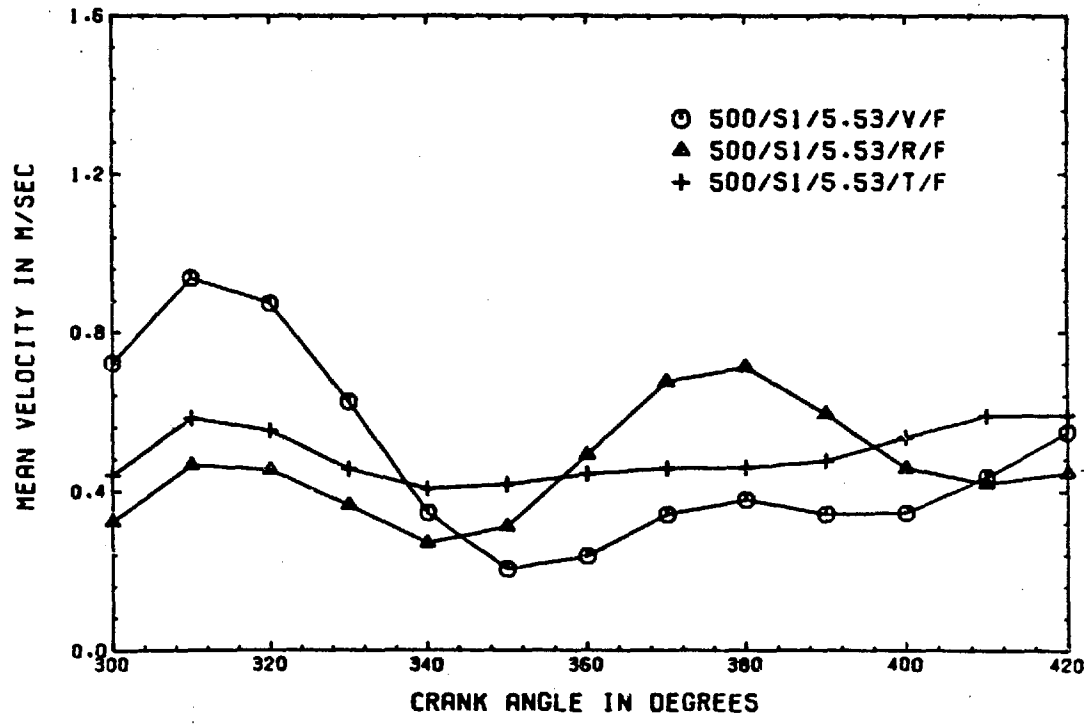


Fig (5.23) Mean Velocity Variation Measured at Position S1

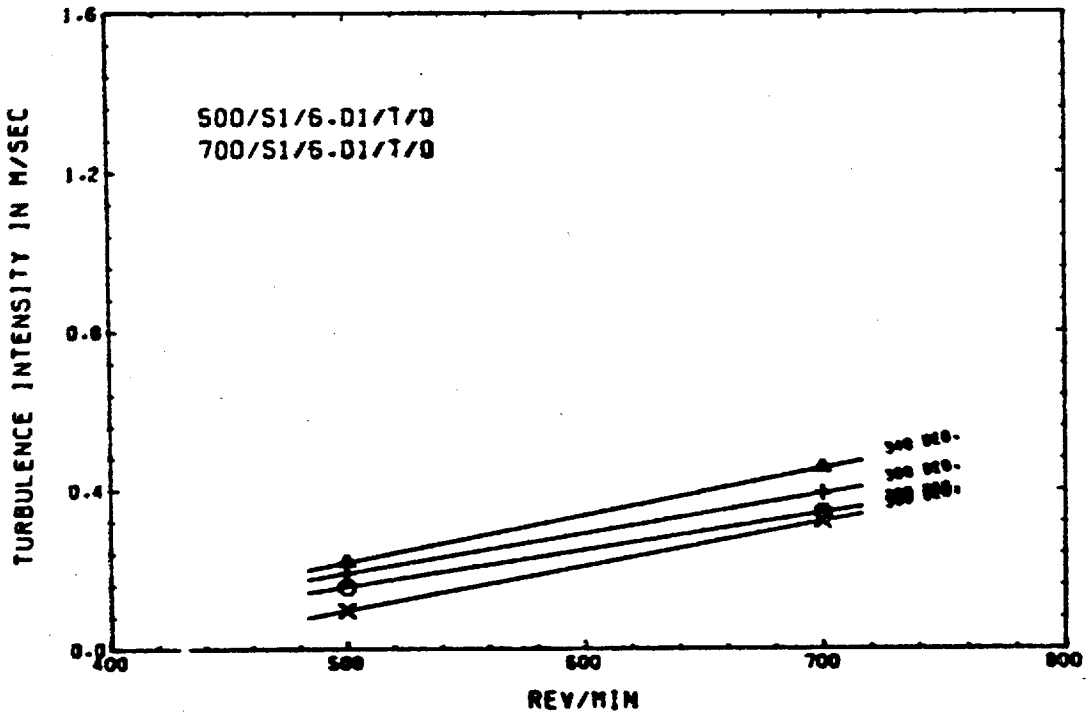


Fig (5.24) Effect of Engine Speed on Turbulence Intensity. Position S1

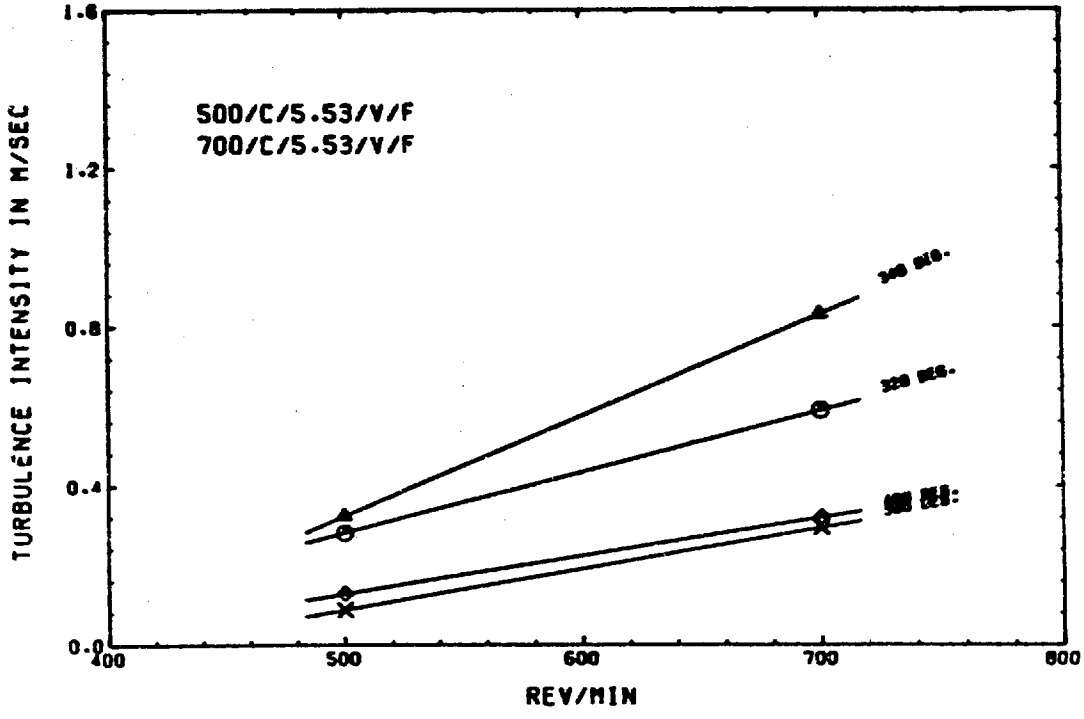


Fig (5.25) Effect of Engine Speed on Turbulence Intensity Position C.

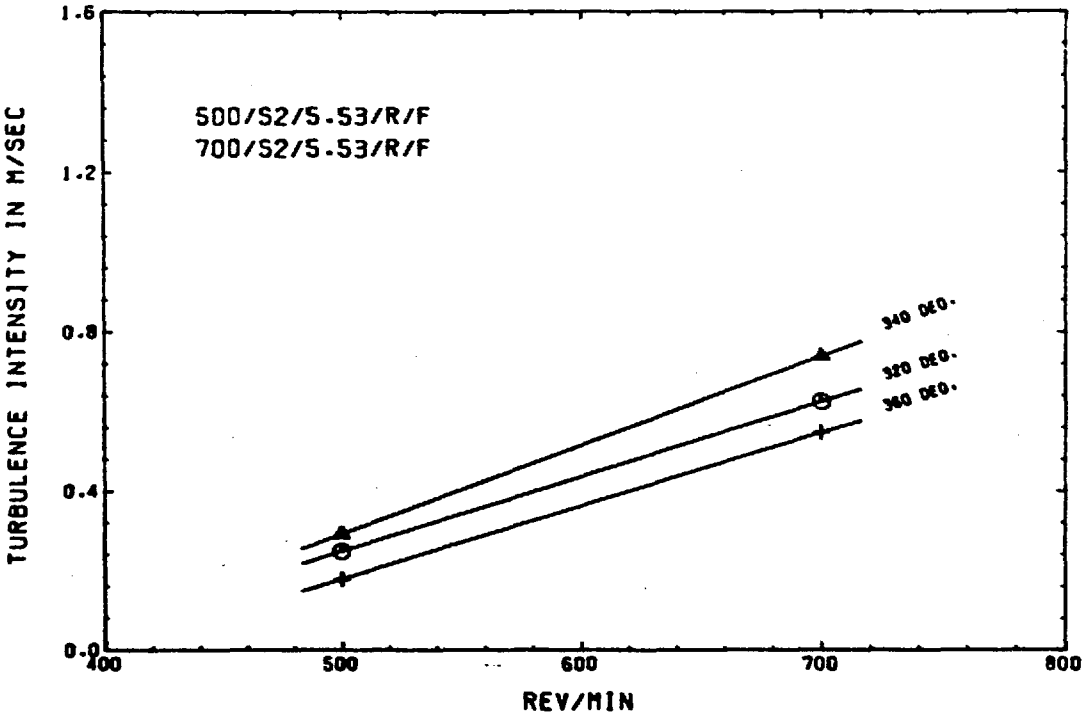


Fig (5.26) Effect of Engine Speed on Turbulence Intensity. Position S2

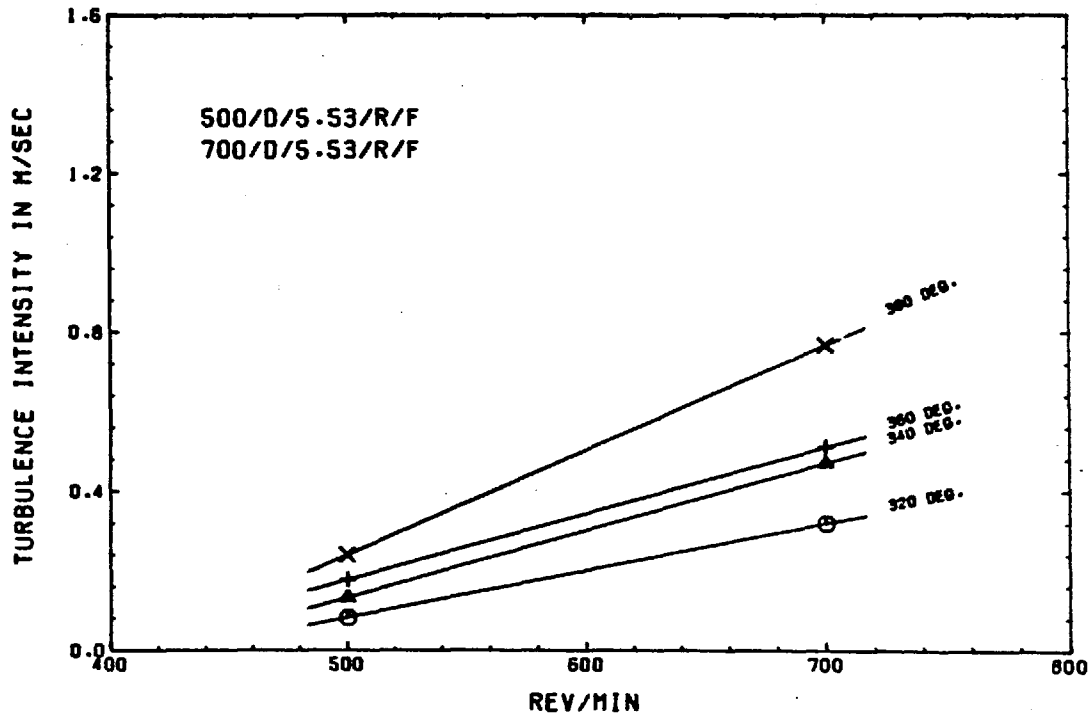


Fig (5.27) Effect of Engine Speed on Turbulence Intensity. Position D

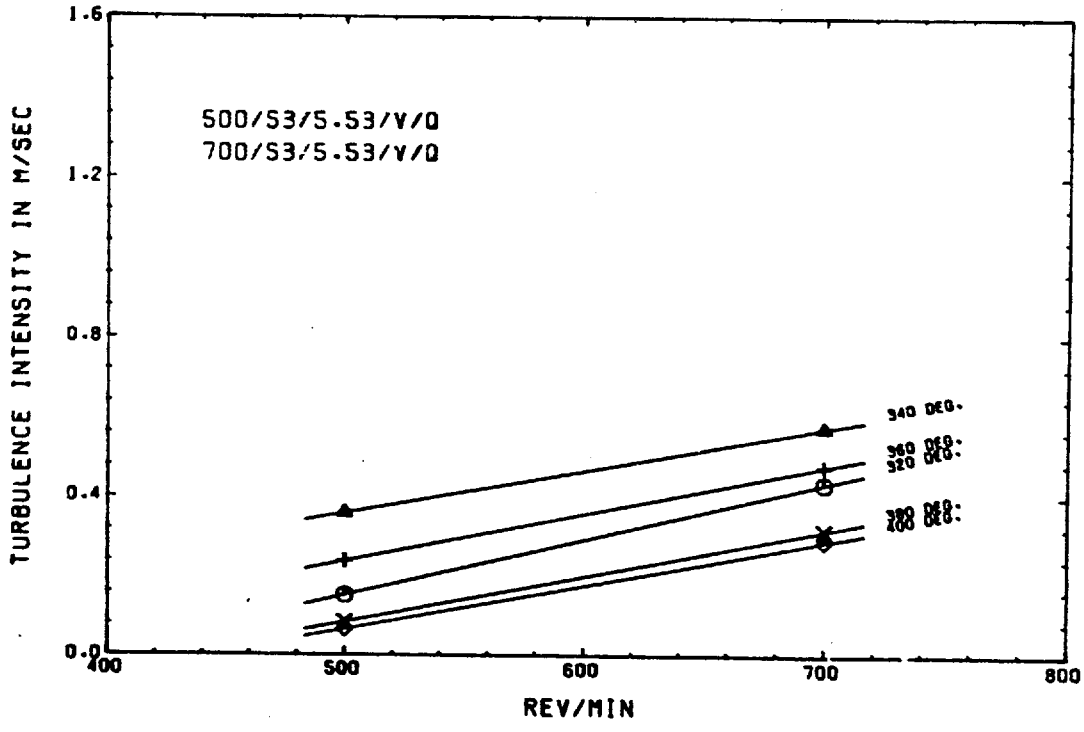


Fig (5.28) Effect of Engine Speed on Turbulence Intensity. Position S3

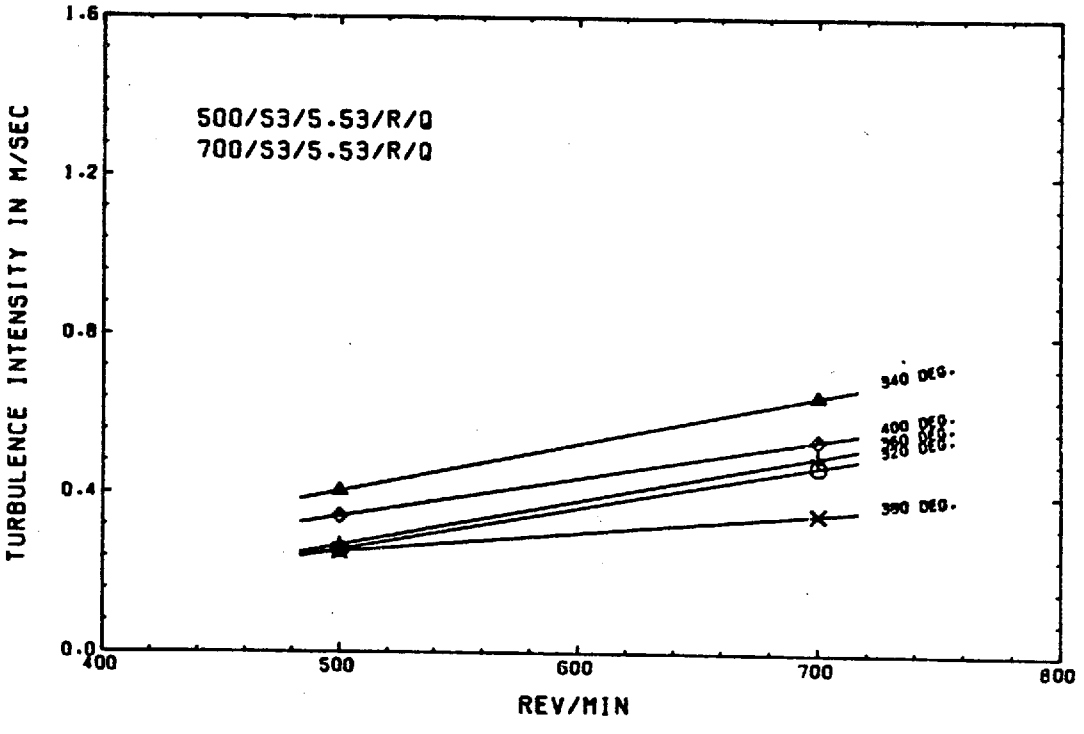


Fig (5.29) Effect of Engine Speed on Turbulence Intensity. Position S3

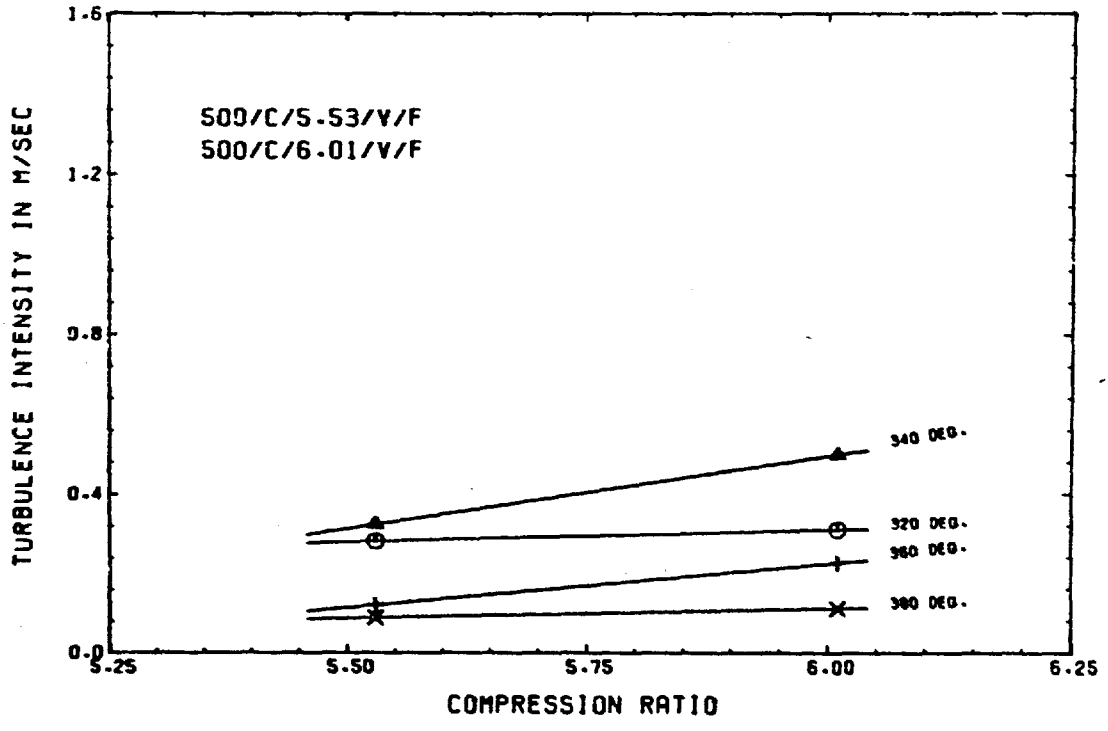


Fig (5.30) Effect of Compression Ratio on Turbulence Intensity. Position C.

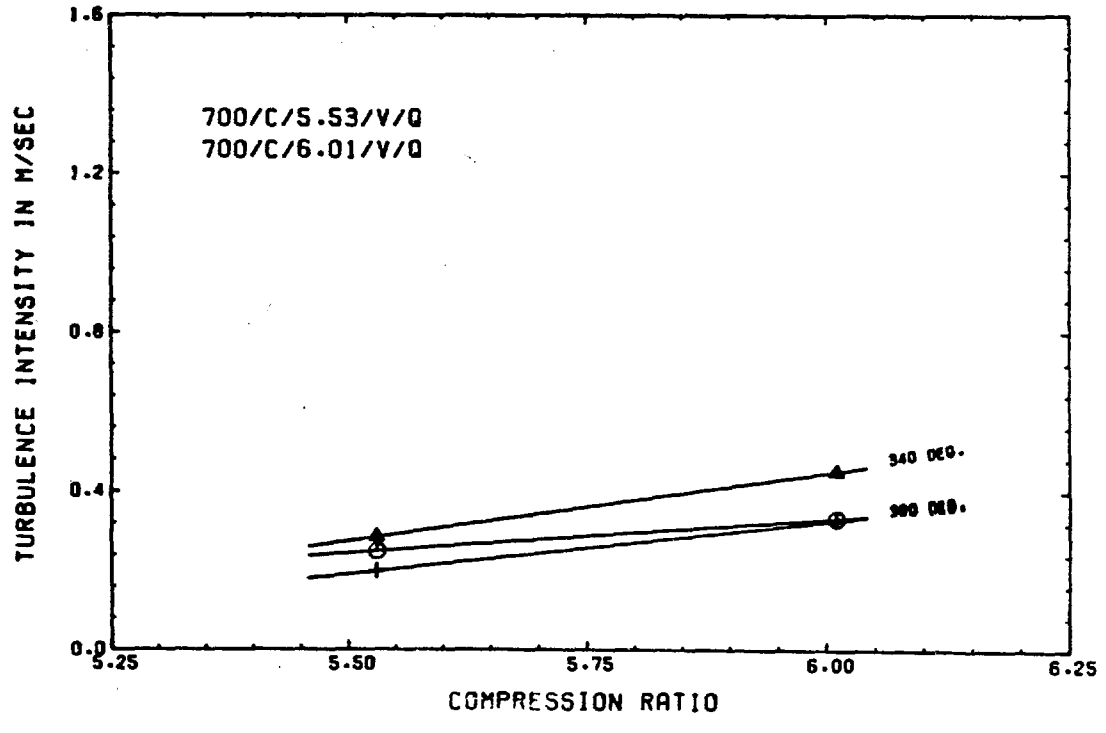


Fig (5.31) Effect of Compression Ratio on Turbulence Intensity. Position C.

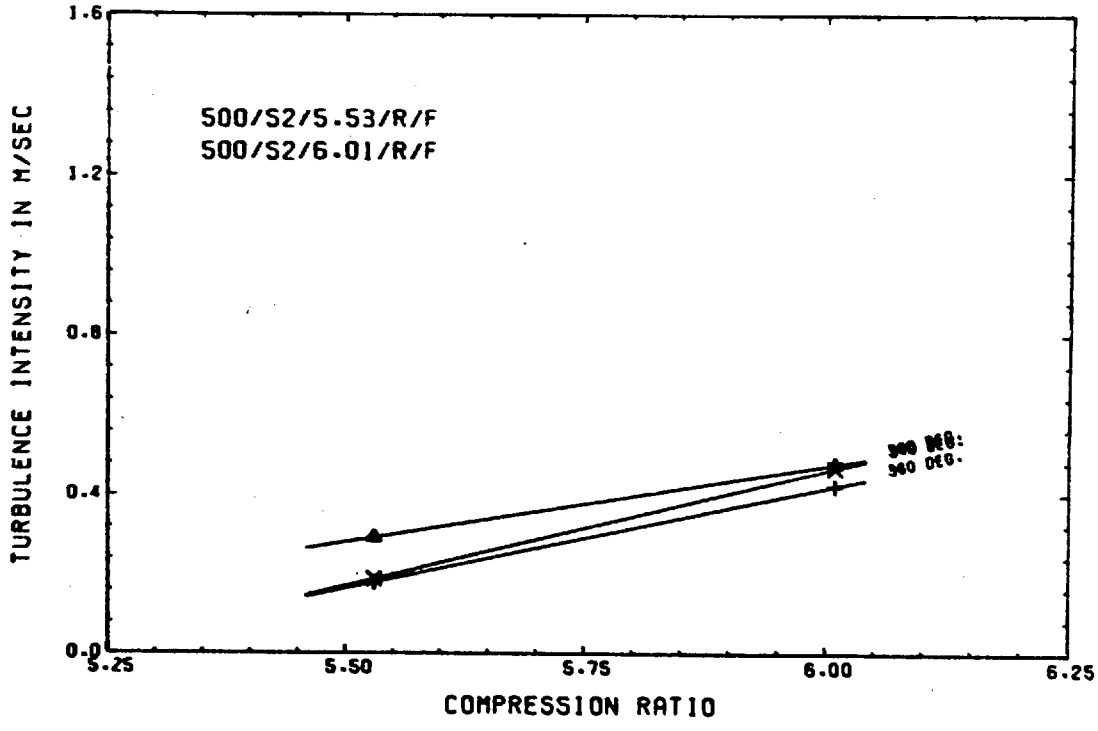


Fig (5.32) Effect of Compression Ratio on Turbulence Intensity. Position S2.

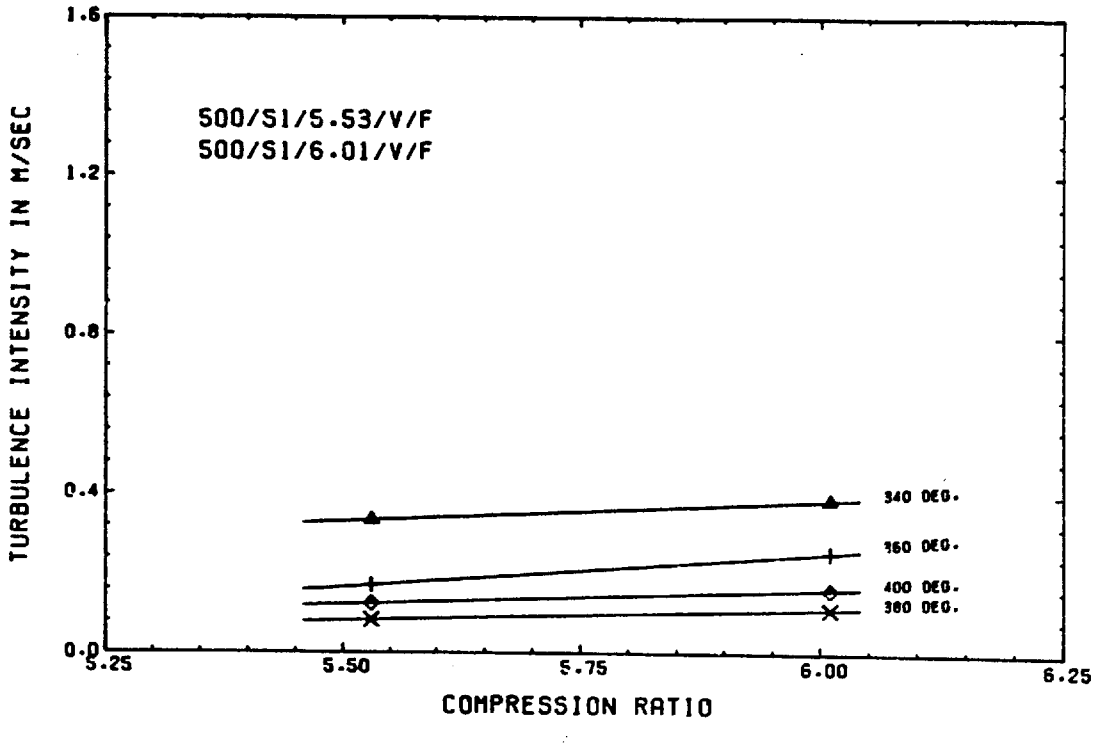


Fig (5.33) Effect of Compression Ratio on Turbulence Intensity. Position S1.

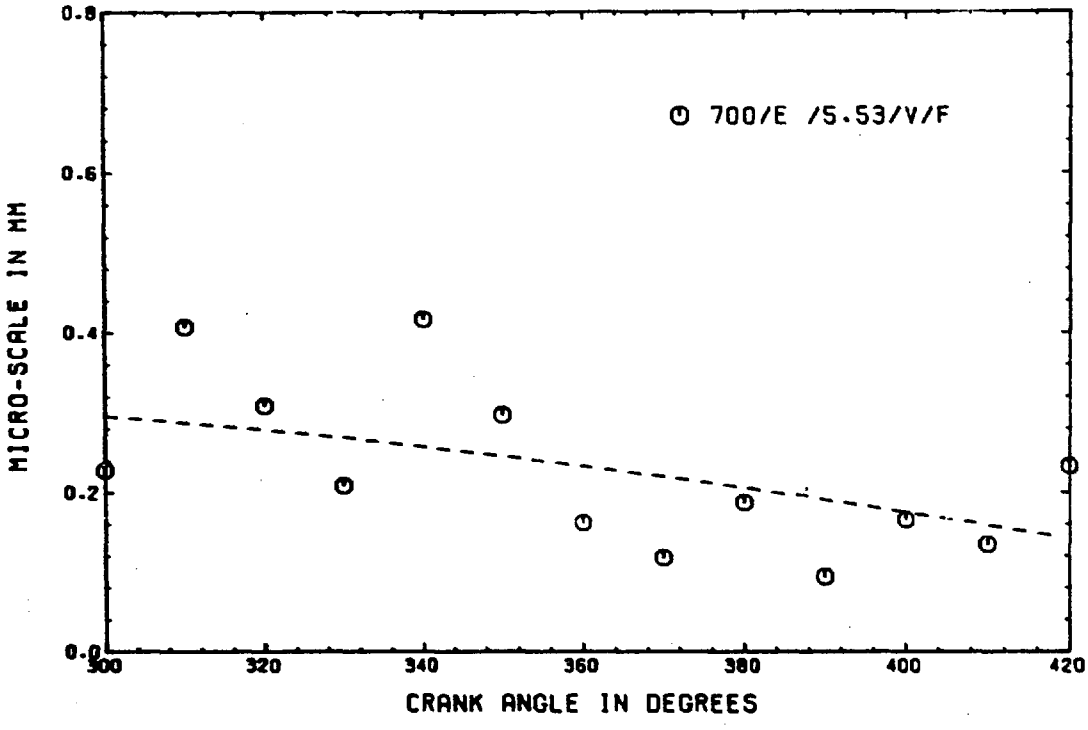


Fig (5.34) Measured Micro-Length Scale of Turbulence. Position E.

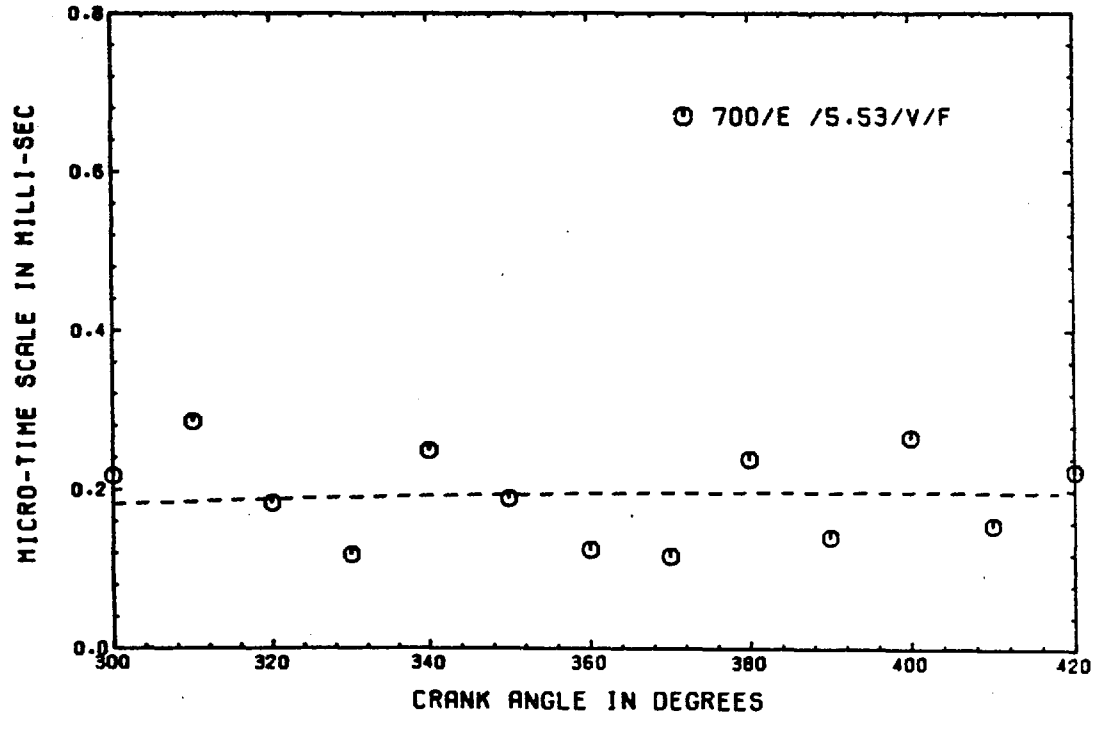


Fig (5.35) Measured Micro-Time Scale of Turbulence. Position E.

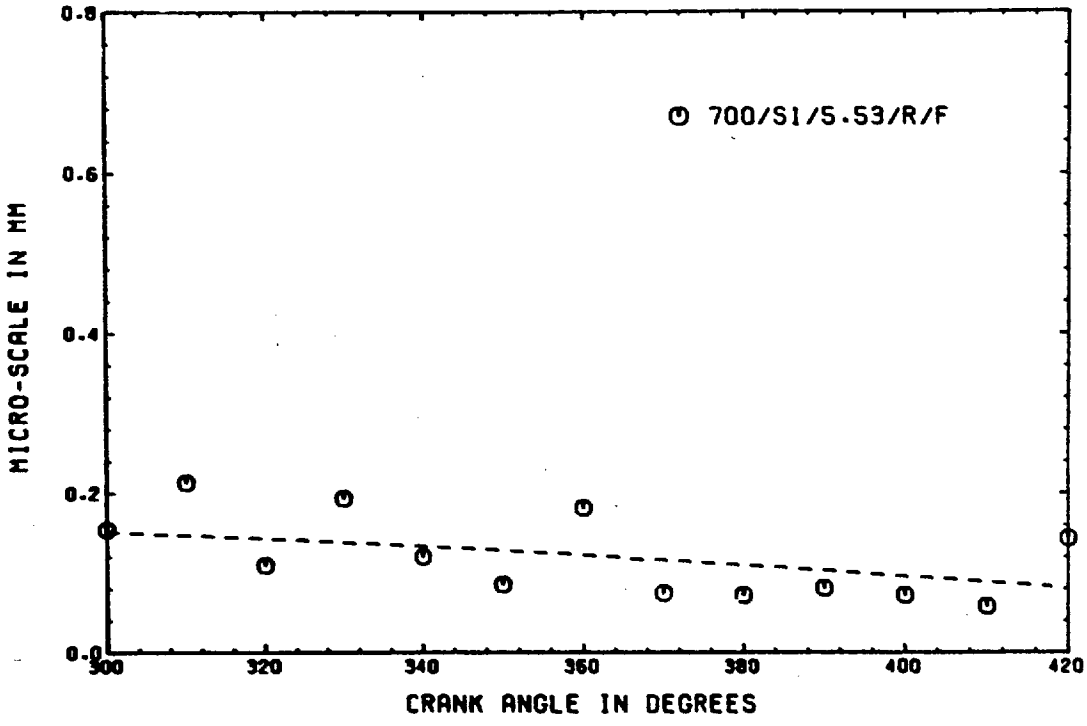


Fig (5.36) Measured Micro-Length Scale of Turbulence. Position S1.

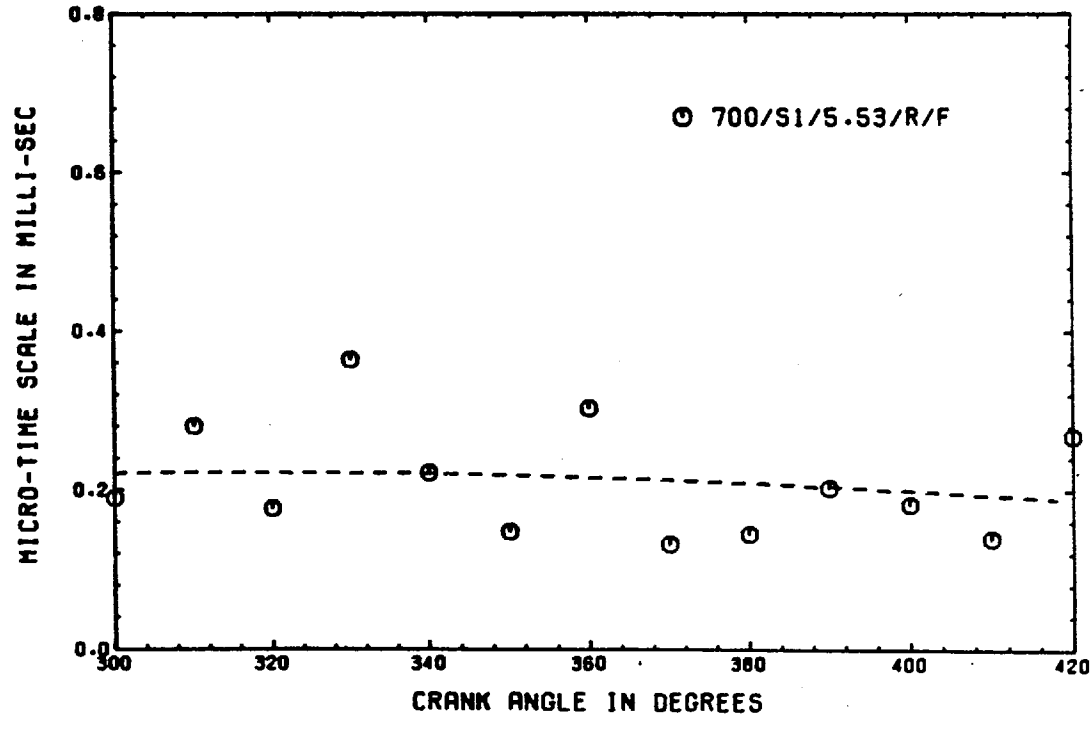


Fig (5.37) Measured Micro-Time Scale of Turbulence. Position S1.

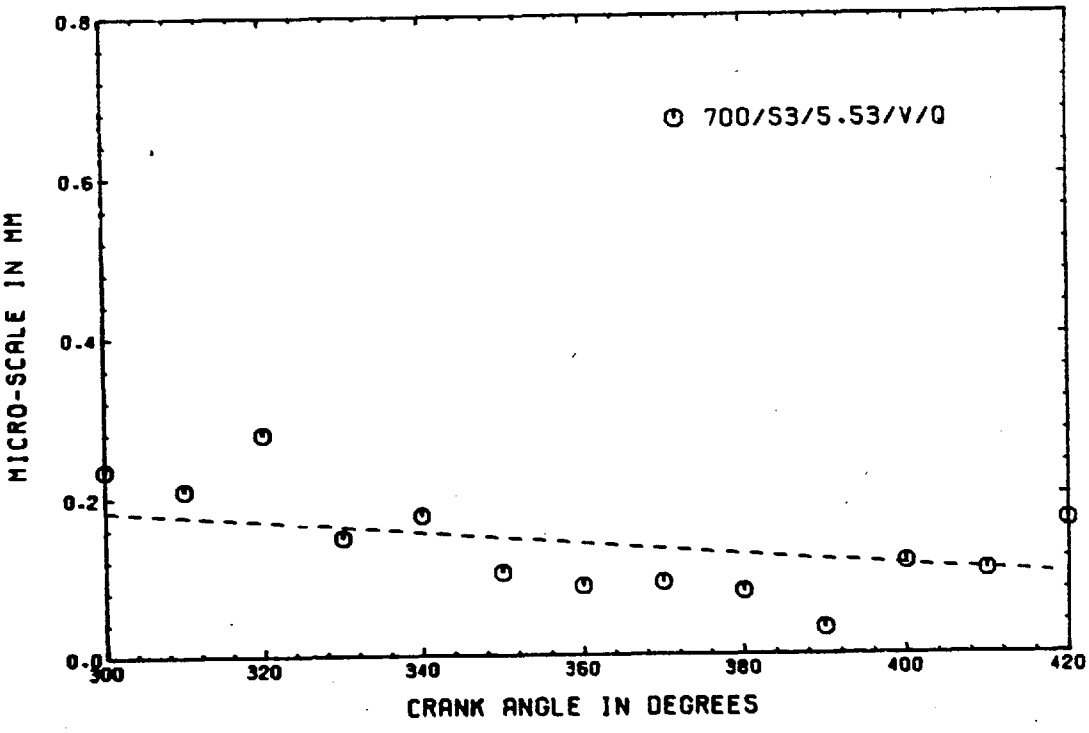


Fig (5.38) Measured Micro-length Scale of Turbulence. Position S1.

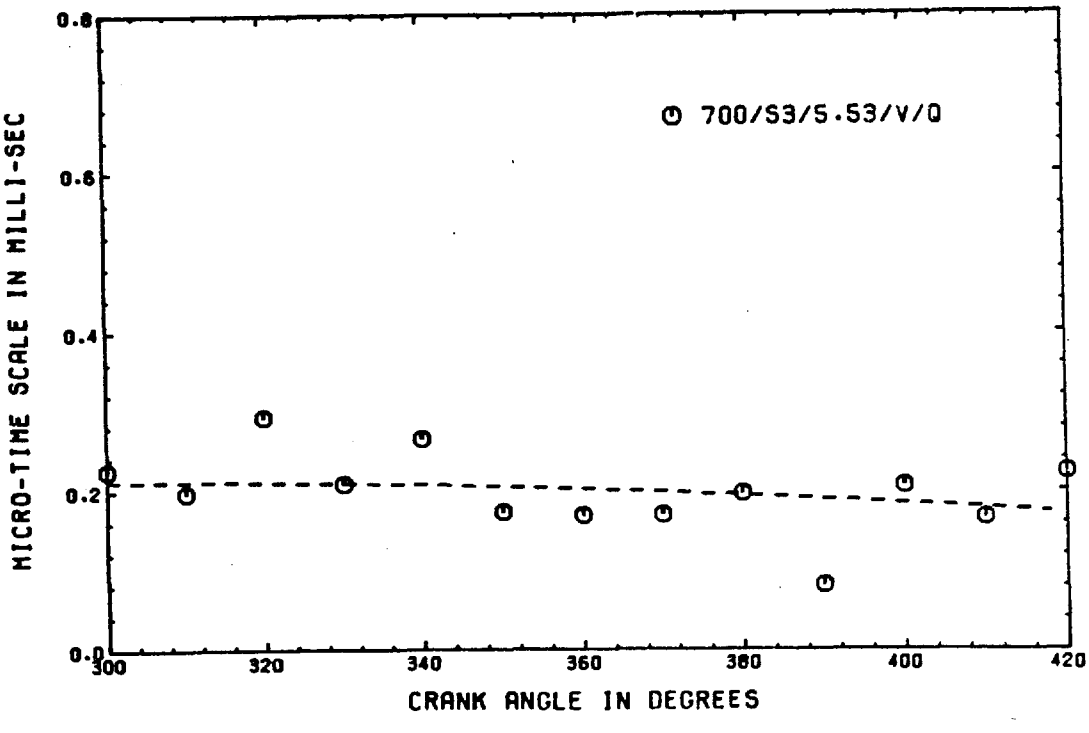


Fig (5.39) Measured Micro-Time Scale of Turbulence. Position S3.

6.0.0. TURBULENCE AND FLAME PROPAGATION

In order to determine the pressure and temperature histories of the gas in a spark ignition engine, it is necessary to understand the influence of turbulence on the mechanism of flame propagation. In a non-turbulent mixture flame propagation is laminar, and the flame has a smooth surface and a relatively thin reaction zone. The flame speed or the speed with which the chemical reaction zone moves relative to the unburnt mixture is determined by the chemical and thermodynamic properties of the mixture. When turbulence is present, as, for example, inside an engine cylinder, the flame front is no longer smooth and the reaction zone is thicker than in the laminar case. In addition the flame speed when turbulence is present is several times the laminar value, depending on the intensity of turbulence.

The usual approach used in the study of turbulent flame propagation is to isolate the effects of turbulence from those of mixture composition and temperature by correlating the ratio of turbulent flame to laminar flame speed with intensity of turbulence. To study the applicability of this approach to engine cylinder combustion, it would be most useful to have a simple laminar flame speed model or equation which predicts laminar flame speed with acceptably good accuracy over a wide range of air-fuel ratios, dilutent conditions, initial pressures and temperatures that would normally encounter in spark ignition engine cylinders.

6.1.0 Laminar Flame Propagation:- For a simple case of steady state, one dimensional laminar flame propagation, the following equations are formulated in reference (109),

ρV = Constant

The conservation of energy requires,

$$\frac{d}{dx}\left(\lambda\frac{dt}{dx}\right) - \frac{d}{dx}\left(C_p T \rho V\right) + Q.U = 0$$

For the conservation of the number of atoms,

$$\frac{d}{dx}\left(D_j \frac{dn_j}{dx}\right) - \frac{d}{dx}\left(n_j V\right) - \gamma_j.U = 0$$

Where $\lambda\frac{dt}{dx}$ is the heat current

$C_p T \rho V$ is the heat carried away by the flow

$Q.U$ is the heat released by the chemical reaction

$D\frac{dnj}{dx}$ is the diffusion current of species j

$n_j V$ is the number of moles of j carried by the flow

$\gamma_j U$ is the number of moles of species j removed by the chemical reaction

The boundary conditions are,

$T = T_u$ at $x = -\infty$

$T = T_b$ at $x = +\infty$

Even for the above simple steady state one dimensional model, an accurate expresson for the rate of reaction and hence the flame speed is a difficult matter. The values of λ and C_p vary with temperature in a way which is supposed to be known but is not (40). With some approximations, the laminar flame speed equations may be solved by using either numerical integration or by using approximate analytical solution methods. There are several semi-theoretical models which have been developed to estimate the value of laminar flame speed. These semi-theoretical models are of practical use for spark ignition engine cycle simulation purposes as the interest is in the flame propagation speed rather than in information about the detailed structure of the flame front or reaction zone. Thus these models or theories will be mentioned briefly.

6.2.0 Types of Laminar Flame Theory:- There are three types of laminar flame theory,

(a) The Momentum Pressure Drop Theory by Manson (quoted 87).

(b) The Diffusion Theory by Tanford and Pease (85).

(c) The Thermal Theory by Semenov (84).

The Semenov (84) model is essentially a thermal model which supposes a bimolecular reaction between fuel and oxidant molecules. The Tanford and Pease (85) model is based on the diffusion of chain carriers in the oxidation reaction and Manson (quoted 87) used a modification of the pressure drop equation which does not include reaction Kinetics. There are other semi-empherical equations which may give better predictions for a particular set of conditions, but the above three types will be discussed because they view the problem from different points

of view.

6.2.1 Momentum Theory (quoted 87):- The momentum relation between the burning velocity and the pressure drop across a plane steady-state flame front may be expressed in the following form:-

$$U = \left(\rho_f / \rho_o \cdot \frac{\Delta P}{P_o - P_f} \right)^{\frac{1}{2}}$$

Manson's suggestion (quoted 87) was that a small pressure drop could be caused by the projection of hydrogen ions into the unburnt gas and thus deduced that,

$$\Delta P = \tfrac{1}{2} P_H . \, T_o / T_f$$

6.2.2 Diffusion Theory (85):- This theory equates the amount of product formed at the flame front by the conversion of the fresh charge to the amount of product formed in the combustion zone by a second order reaction between fuel molecules and hydrogen atoms. An approximate solution for burning velocity from this equation is :-

$$U = \left(\frac{\rho_m \, Q\acute{m}}{Qm^2} \; \Sigma \; \frac{Ki \; Pi \; Dim}{Bi} \right)^{\frac{1}{2}}$$

6.2.3 Thermal Theory (84):- From heat conduction and fuel concentration change across the flame front, an approximate solution for the rate of flame propagation is obtained.

$$U = \left[\frac{2\lambda \int_o^{T_f} w dt}{a_o \rho_o \bar{C}_p (T_f - T_o)} \left(\frac{n_1}{n_2} \right)^{\gamma} \left(\frac{\lambda}{D \, C_p \, \rho} \right)_f^{\gamma} \right]^{\frac{1}{2}}$$

For a bimolecular reaction between unlike molecules:-

$$\int_o^{T_f} w dt = \int_o^{T_f} k.a.b.dT$$

$$\approx a_{eff} \cdot b_{eff} \cdot PZ \cdot \frac{RT_f^2}{E} \; e^{-E/RT_f}$$

The effective fuel and oxydent concentrations are then

approximated as follows:-

For lean mixture $\phi < 1$

$$a_{eff} = a_o \cdot \frac{T_o}{T_f} \cdot \frac{R T_f^2/E}{Tf - T_o}$$

$$b_{eff} = b_o \cdot \frac{T_o}{T_f} \cdot \left[1 - \phi \left(1 - \frac{R T_f^2/E}{T_f - T_o}\right) \right]$$

For rich mixture $\phi > 1$

$$a_{eff} = a_o \cdot \frac{T_o}{T_f} \left[1 - \frac{1}{\phi} \left(1 - \frac{R T_f^2/E}{T_f - T_o}\right) \right]$$

$$b_{eff} = b_o \cdot \frac{T_o}{T_f} \cdot \frac{R T_f^2/E}{T_f - T_o}$$

From these three approaches, the Momentum Theory by Menson (quoted 87) and the Diffusion Theory by Tanford and Pease (85) can be regarded approximately as empirical models because of their lack of consideration of basic reaction Kinetics. The Thermal theory by Semenov (84) considers the chemical Kinetics of reaction based on a single step bimolecular reaction of fuel and oxident molecules. Semenov thus approximated the reaction rate by using equations involving terms called effective fuel and oxygen concentractions. Semenov's (84) model gives poor agreement with experimental observations of flame speeds around stoichiometric mixture, but otherwise gives satisfactory agreement with experimental results throughout the range of air fuel ratios from very lean to very rich as can be seen in fig (6.1). The weakness of Semenov (84) equation around stoichiometric region may be cured by the added complexity of incorporating a suitable interpolating formula for calculation of flame speeds in the critical region (92).

A different form of laminar flame speed equation which was derived by considering the bimolecular reaction between fuel and oxident (104) is,

$$U_L = K T_m^{\frac{1}{2}} \sqrt{A_o^a B_o^b} \quad \text{Exp} \left(- E/RT_m\right)$$

In this approach, the laminar flame speed is expressed as a function of mean reaction zone temperature T_m, initial fuel concentration A_o and initial oxident concentration B_o. This

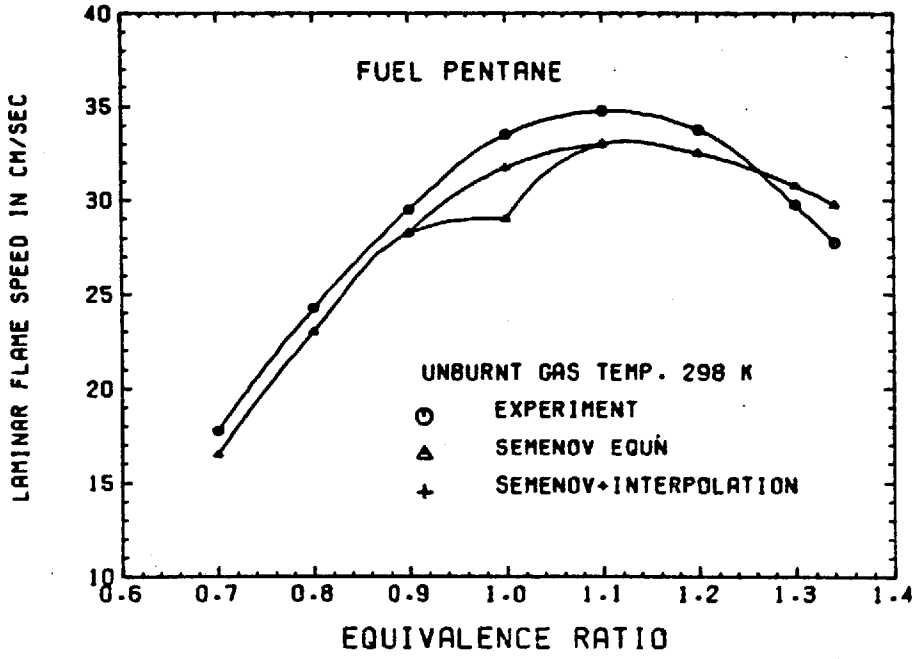


Fig (6.1) Predicted Value of Laminar Flame Speed by Using Semenov's Equation. Ref (92).

is the expression used by Lancaster (42) for his computer simulation model of the spark ignition engine cycle. As the value of K varies with air-fuel ratio used, Lancaster (42) avoided the use of the coefficient K by using the reference state of flame speeds. For a given air-fuel ratio, the laminar flame speed at a required condition was evaluated by knowing the reference flame speed,

$$\frac{U_l}{U_{l\ ref}} = \left(\frac{T}{T_{ref}}\right)^{0.5} \times \text{Exp}\left\{\frac{E}{R} \cdot \left(\frac{1}{T_{ref}} - \frac{1}{T}\right)\right\}$$

To apply this approach for predicting laminar flame speed of octane-air mixture, established reference flame speeds throughout the range of air-fuel ratio are needed but not available.

6.2.4 Other Empirical Forms of the Laminar Flame Speed Equations:- The type of equation which is suitable and may be used in spark ignition engine cycle simulation cycle procedure is,

$U_l = 13.3\ \text{Ln}\left(\frac{X_{o2}}{X_f}\right) + 14.9$ for Methane-Oxygen-Nitrogen flame at 2000K and $0.3 < \frac{X_{o2}}{X_f} < 0.7$ (quoted 54).

$U_l = 7650\ X_f^2\ X_{O_2} + 54$ for Hydrogen-Oxygen-Nitrogen flame at 2000K and $0.8 < \frac{X_{O_2}}{X_f} < 8$ (quoted 54).

The above equations were derived from experimental observations to find the effect of fuel-oxidant ratio on laminar flame.

6.3.0 An Alternative Model of Laminar Flame Speed:- All of the above equations are subjected to the critism that they lack the ability to predict laminar flame speed with an acceptable accuracy throughout the usable range of air-fuel ratios for various initial conditions as encounter in spark ignition engines. An empirical model of laminar flame speed was derived using an approximation for the complex reaction steps by employing a gross bimolecular reaction rate expression between fuel and oxident molecules. The derived laminar flame speed equation is affected by air-fuel ratio, oxygen and diluent concentrations, initial unburnt temperature and pressure. The basic considerations involved are as follows.

For a chemical reaction involving reactant A and B, and the products C and D, its stoichiometric equation is

$$a\,A + b\,B \underset{K_b}{\overset{K_f}{\rightleftharpoons}} c\,C + d\,D$$

The forward reaction rate is given by $R_f = K_f A^a B^b$

and the backward reaction rate is given by $R_b = K_b C^c D^d$.

In general, the reaction rate constants K_f and K_b have the form,

$$K = \text{Const } T^M \text{ Exp } (^{-E}/_{RT})$$

Thus the forward reaction rate is, $R_f = \text{Const. } T^M A^a B^b \text{ Exp } (^{-E}/_{RT})$

Clearly the reaction rate is an exponential function of temperature, Exp $(^{-E}/_{RT})$, and is also affected by the initial fuel and oxidant concentra tions. If the above expression holds true for various initial conditions, and if it can be used to approximate the overall effect of various complex reaction steps which occur in the reaction zone of fuel molecule A and oxidant molecule B, then the above expression can be used to predict laminar flame speeds. From the result of the work of various attempts on laminar flame speed (116, 117, 118), it has been clearly established that the laminar flame speed can be taken to be proportional to the square root of the reaction rate with a very good degree of approximation.

Thus,

$$U_L \propto R_f^{\frac{1}{2}}$$

$$U_L \propto [\text{ Const } T^M A^a B^b \text{ Exp } (^{-E}/_{RT})]^{\frac{1}{2}}$$

$$U_L = \text{Const } T^{M'} A^{a'} B^{b'} \text{ Exp } (^{-E}/_{2RT}) \rightarrow \text{(A)}$$

For the temperature term T, Semenov (84) employed the adiabetic reaction zone temperature T_f, where as Tanford and Pease (85) employed the mean reaction zone temperature T_m. In this work T has been chosen to equal T_m, which causes equation (A) to become similar to the form of equation used by Lancaster (42),

$$U_L = K T_m^{\frac{1}{2}} \sqrt{A^a B^b} \text{ Exp } (^{-E}/_{2RT_m})$$

It can be said that equation (A) is a more general form

of the above equation. The values of the unknown constants in equation (A) were found by using a least square curve fitting technique in the logrithemic domain using the experimental data of laminar flame speeds for Octane and Air flame by Dugger Et Al (86). For Octane and Air flame the equation is,

$$U_L = 5.1 \times 10^{-8} T_m^{2.08} A_o^{-1.9} B_o^{1.9} \text{Exp} \left(-\frac{E}{2RT_m}\right) \text{ cm/sec.}$$

OR

$$U_L = 5.1 \times 10^{-8} T_m^{2.08} \left(\frac{Bo}{Ao}\right)^{1.9} \text{Exp} \left(-\frac{E}{2RT_m}\right) \text{ cm/sec.}$$

where $T_m = 0.7 (T_B + T_u)$ in deg. K.

Ao = Initial fuel concentration in moles /cm^3

Bo = Initial oxygen concentration in moles /cm^3

The above model is free from the weakness in prediction around stoichiometric region as in Semenov's model (84) and does not need to employ reference flame speeds to predict flame speeds at different air-fuel ratios as in the model used by Lancaster (42). The predicted results are shown in fig (6.2) to fig (6.7). The model gives very good agreement between predicted results and all available experimental flame speed data on octane + air flame (86,114) employing various air-fuel ratios, oxygen and dilluent concentrations, initial pressures and temperatures: and it is therefore believed that this model will form a very useful aid in predicting laminar flame speeds under various initial conditions and hence be of value the study of the applicability of the existing turbulent flame speed models, which generally relate the ratio of turbulent to laminar flame speed to turbulence intensity, for computer spark ignition engine cycle simulation.

6.4.0 Turbulent Flame Propagation:- The turbulent flame propagation rate determines the rate of combustion of unburnt charge in a spark ignition engine cylinder (assuming the reaction goes to completion) and hence the rate of pressure development, engine performance, fuel economy and pollutant emission. It is therefore highly desirable to have an acceptably accurate procedure for predicting the turbulent flame propagation rate to be used in the computer simulation study of the spark

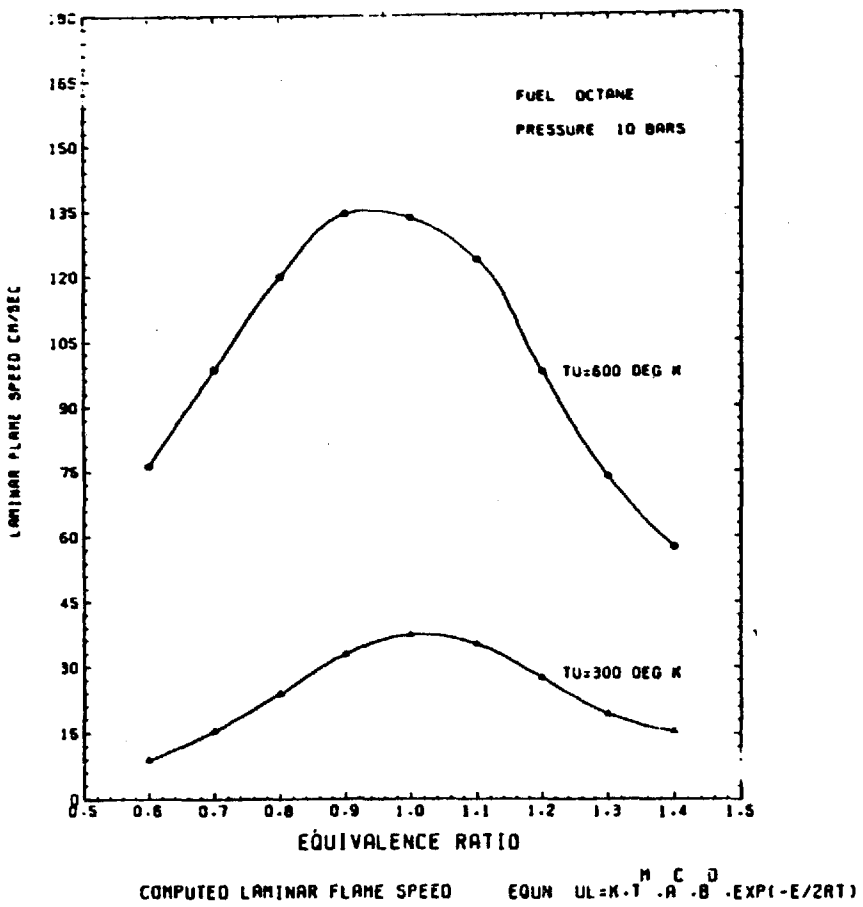
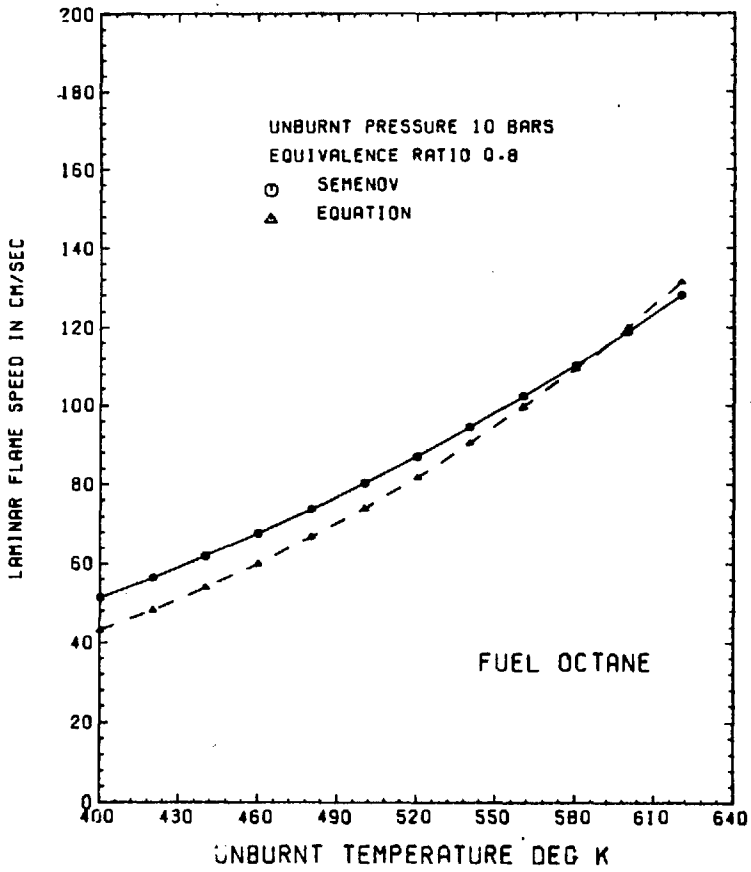


Fig (6.2) Predicted Value of Laminar Flame Speed. Equation (A).



Fig(6.3) Comparison of Predicted Lamianr Flame Speeds by Using Equation (A) and Semenov's Equation.

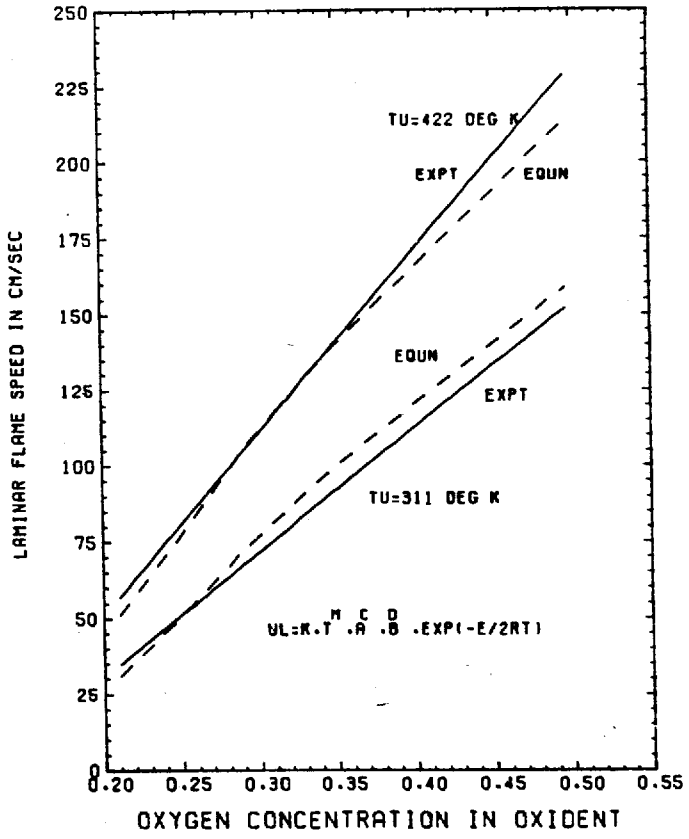


Fig (6.4) Comparison of Equation (A) with the Experimental Results of (86). Fuel (Octane + Air).

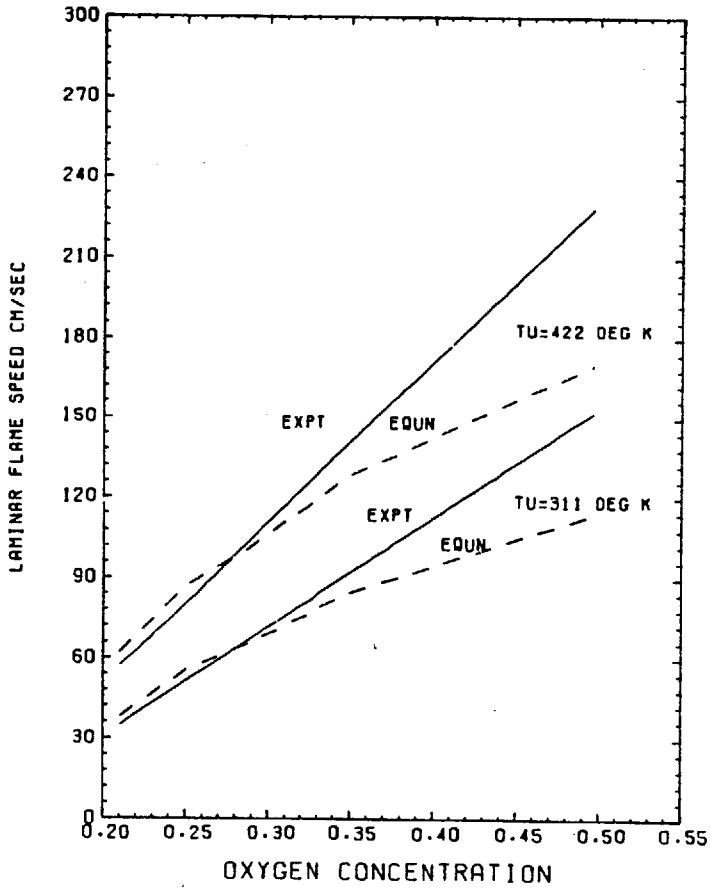


Fig (6.5) Comparison of Semenov's Equation with the Experimental Results of (86). Fuel (Octane + Air).

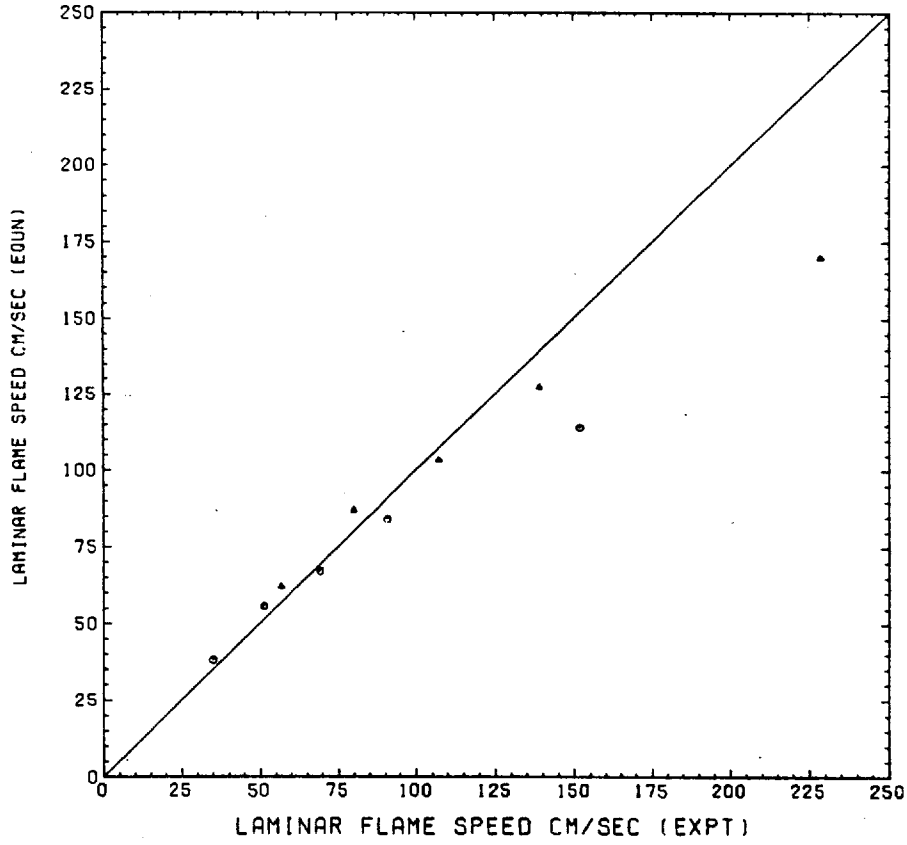


Fig (6.6) Comparison of Predicted Values of Laminar Flame Speeds using Semenov's Equation to the Measured Values of Ref (86). Fuel (Octane + Air).

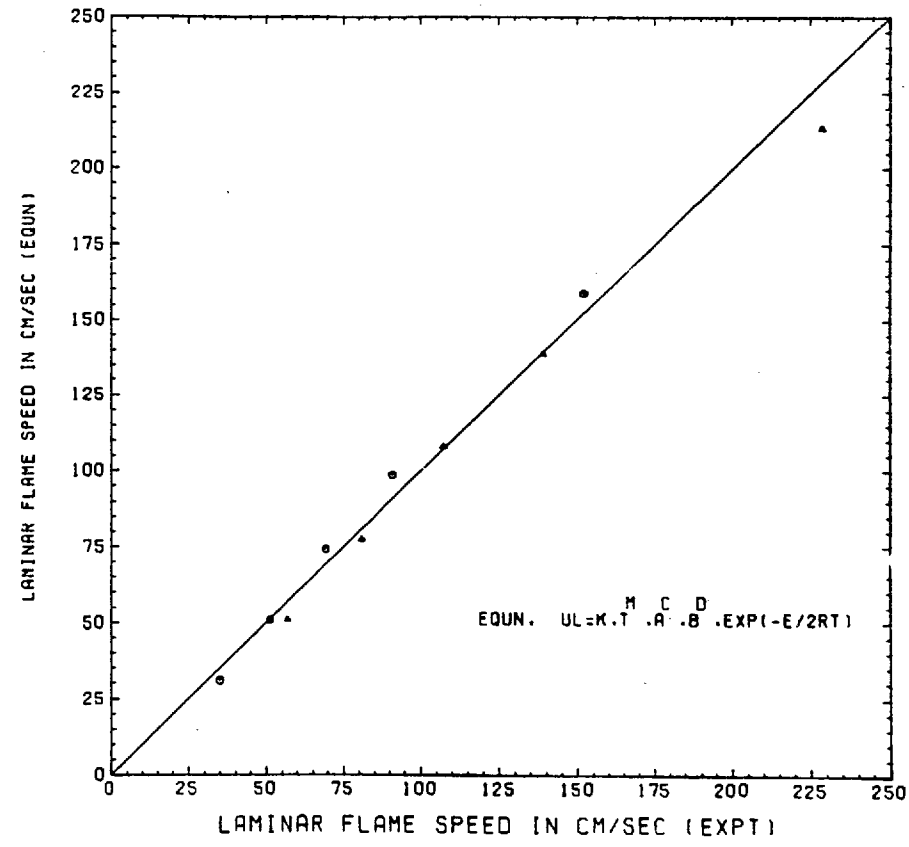


Fig (6.7) Comparison of Predicted Values of Laminar Flame Speeds using Equation (A) to the measured values of Ref (86). Fuel (Octane + Air).

ignition engine cycles. Unfortunately the lack of basic information on the complex physical and chemical processes involved in the turbulent flame in association with statistical nature of the fluctuating flow properties make it impossible to develop a pure theoretical approach to predict the nature of various types of turbulent flame propagation. For the turbulent flame, if the equations of the laminar case were allowed to include terms of all the fluctuating quantities, they would result in various double and triple correlations and thus make it impossible to solve. This arises from making various arbitrary assumptions (75, 76, 77, 78, 80, 81, 82, 83) in developing correlation type equations. These correlation type equations, being derived from a particular type of experimental observation, tend to have a device dependent nature.

These correlations or models can be grouped into three major catagories depending on the basic ideas employed.

(i) Laminar or Molecular Transport Model.

(ii) Turbulent Transport Model, and

(iii) Others which compromise between the above two.

6.4.1 Laminar Transport Model:- Several correlations were developed (80, 81, 82, 83) from experimental observations of turbulent flame speed using the molecular transport concept. The increase in flame speed is attributed to the increase in flame front area or reaction zone area while the laminar transport effect remains as a predominating factor in the turbulent combustion process. Damkohler (75) was the first to introduce this concept. The flame front was supposed to consist of a pattern of Kernals each connical shape thus enabling an estimate of the increase reaction zone surface area to be made. Eddy size was related to turbulent intensity. Thus it became possible to construct a relationship between turbulence flame propagation speed and intensity of turbulence which is one of the most easily measurable parameters in a turbulent flow.

The increment in flame surface or reaction zone area by the distortion of the plane flame front by a single large eddy as it passes the flame zone is shown diagramatically in fig (6.8). The flame propagation models (80, 81, 82, 83) based on the laminar concept relate the flame speed to intensity of turbulence in various ways, the exact relationship used being influenced by the results of experimental observations made

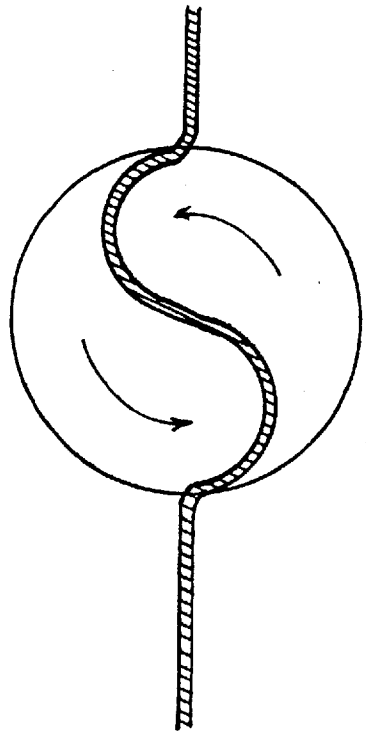


Fig (6.8) Distortion of a Plane Flame Front by a Passing Eddy.

using a particular type of device or apparatus. These models usually employ a normalized form of turbulence flame speed and intensity of turbulence formed by dividing them by the laminar flame speed value at the existing conditions, so as to isolate the influence of chemical Kinetics in their relations. The results of the various models are plotted in fig (6.9) to fig (6.11), and show that the observed magnitude of the influence of turbulence intesity on turbulent flame propagation rate differs from one observer to another and hence clearly show the device dependent nature of these derived correlations. Some of the laminar transport model equations are listed in Table (6.1).

From the basic assumption made, it can be argued that the validity of these models are for cases where there is significant distortion of the flame front by the presence of the large sized eddies. If eddy sizes are small compared to the reaction zone thickness or flame front thickness, there will be no appreciable distortion of the flame front. Experimental observations show that flame speed increases in any type of turbulent flow field, thus some (75, 76, 77, 79, 19) argued that turbulent flame propagation mechanism is free from laminar transport effect and is largely influenced by the turbulent transport properties.

6.4.2 Turbulent Transport Models:- Generally these models were derived by replacing the laminar transport properties which were employed in laminar flame speed correlations by the corresponding turbulent parameters or by other turbulent parameters which were taken to be of important factors in determining the flame speed. The turbulent flow parameters employed by various workers are shown in Table (6.2). Using these parameters and making various assumptions, turbulent flame speed models or equations were formulated and are shown in Table (6.3). Because of the diversity of parameters employed no reliable direct comparison between these models can be made.

6.4.3 Other Models:- Attempts (50, 63) to construct models or equations to predict turbulent flame speed using alternative approaches have been made. These will be briefly mentioned.

(a) The Spectral Theory of Turbulent Flame Propagation (50):- In this approach, it was argued that the turbulent flame propagation speed was entirely controlled by neither the molec-

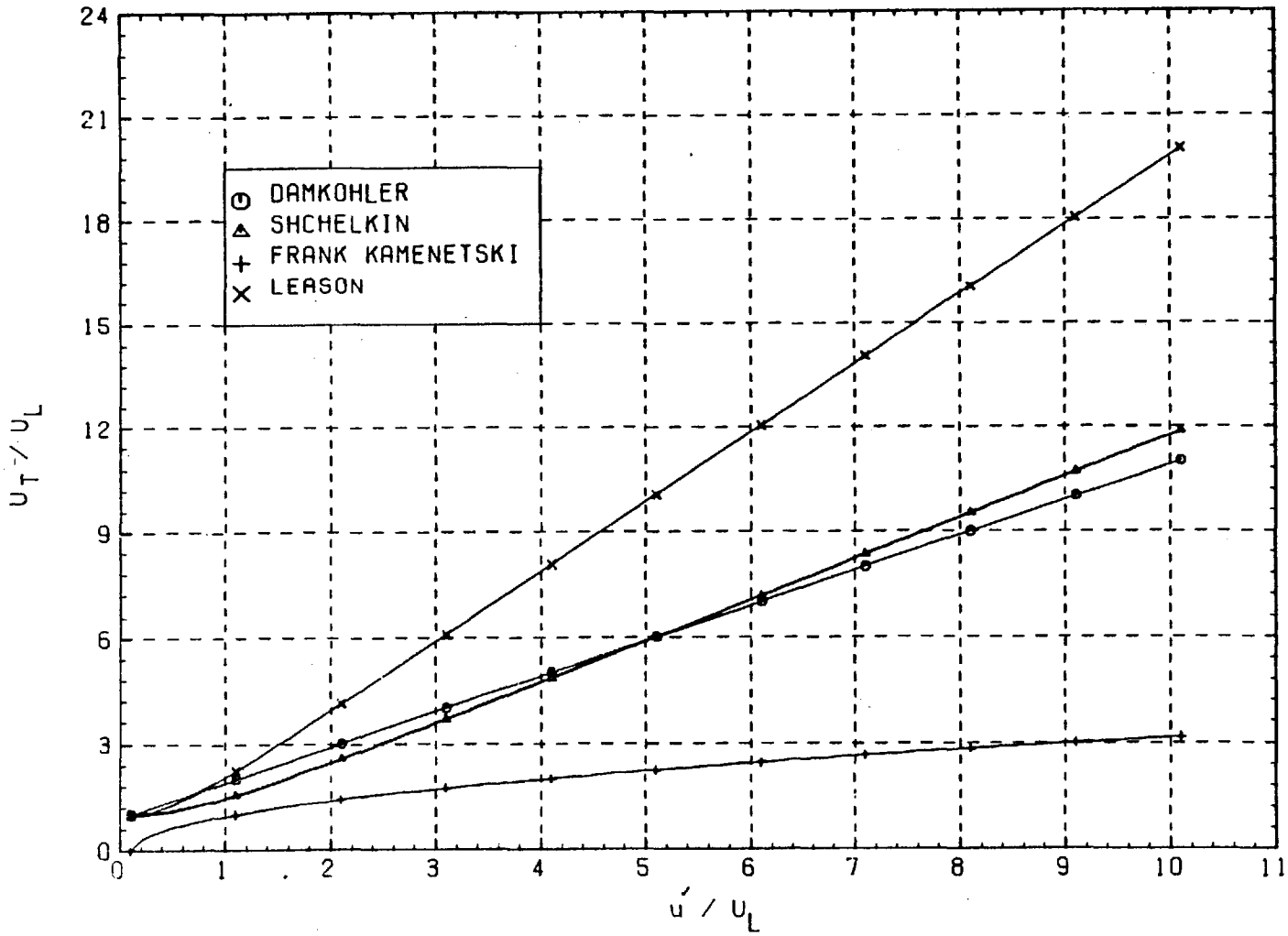


Fig (6.9) Turbulence Flame Speed Equations Proposed by Various Workers.

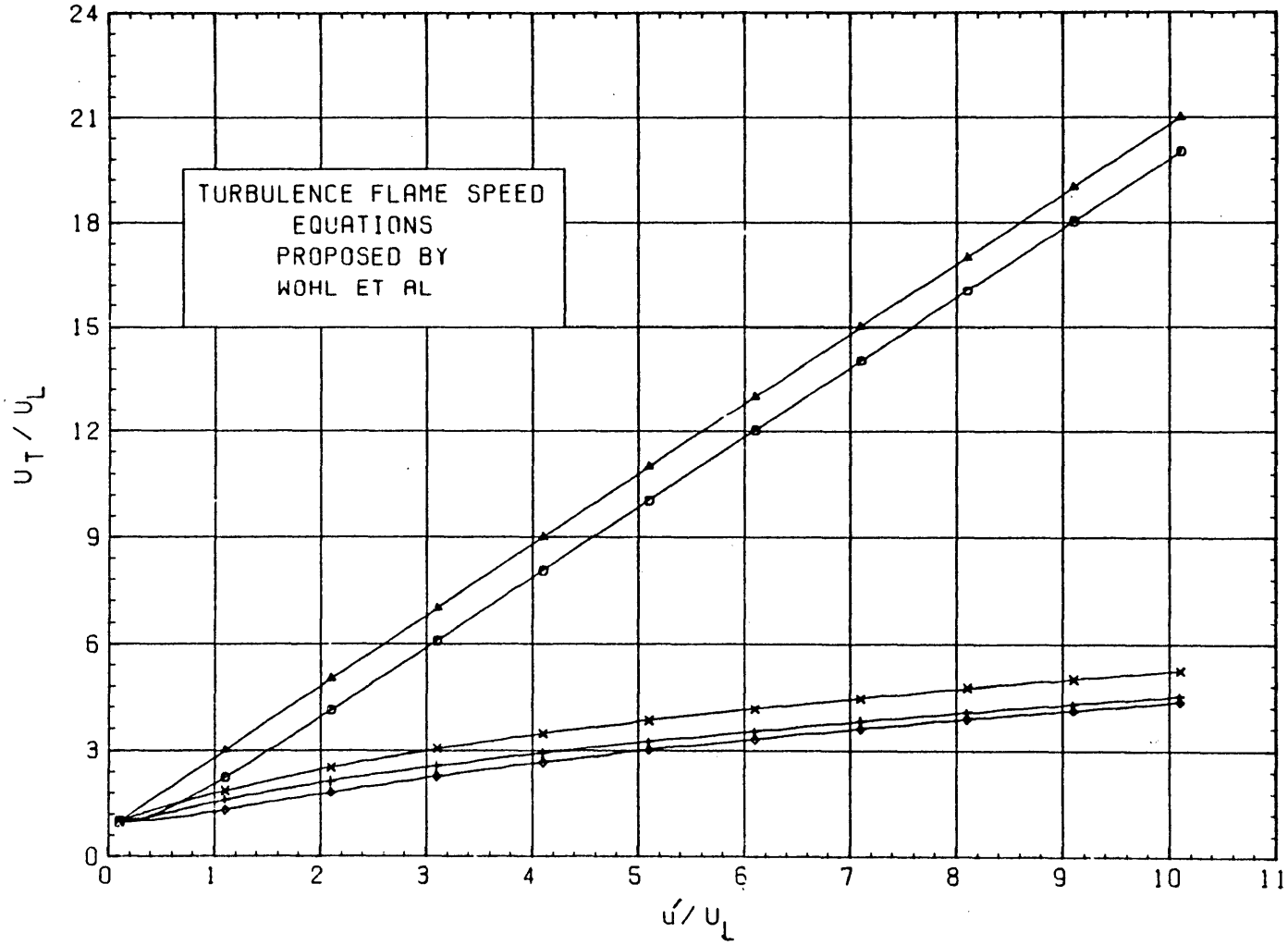


Fig (6.10) Turbulence Flame Speed Equations Proposed by Wohl Et Al (80, 81).

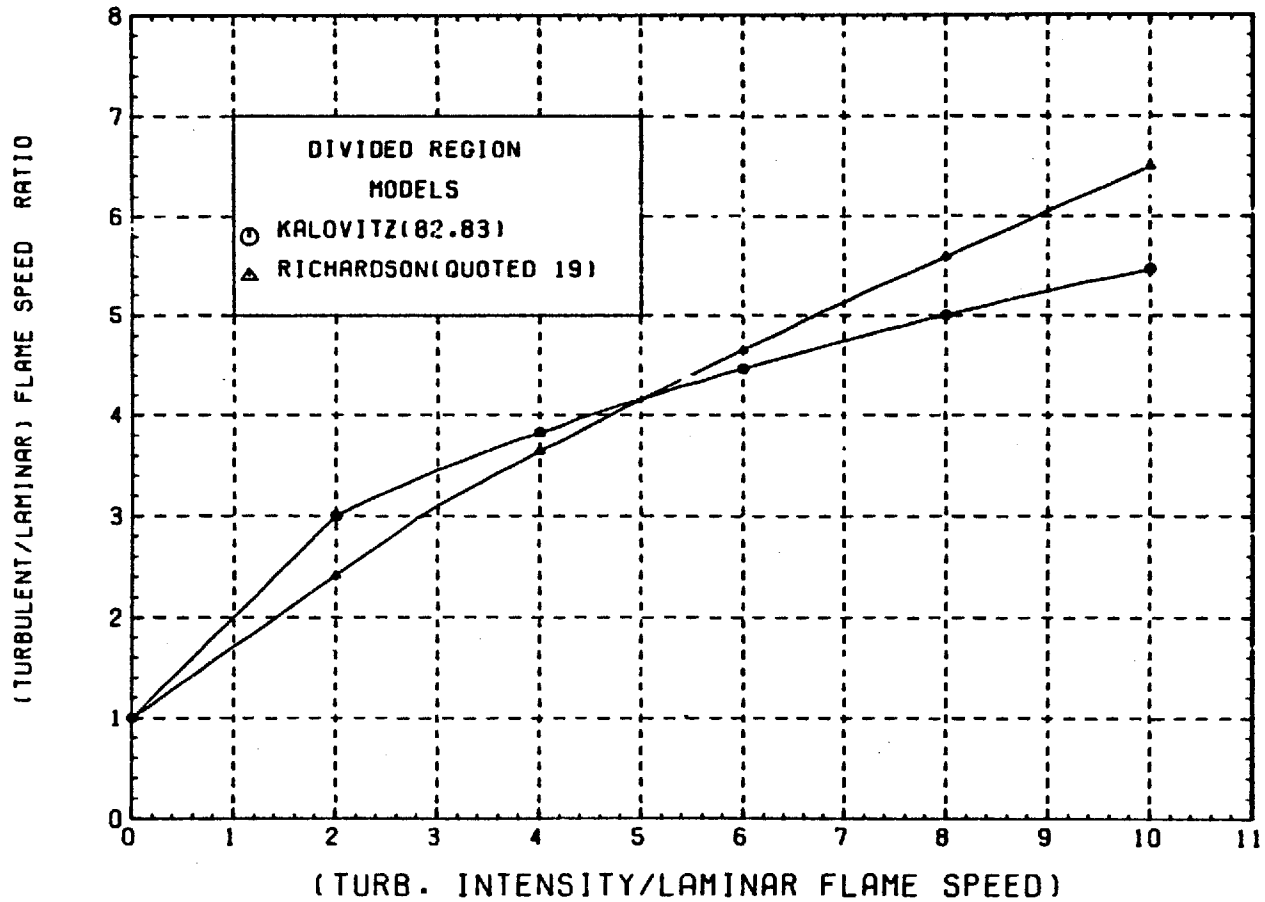


Fig (6.11) Turbulence Flame Speed Equations Proposed by Kalovitz (82,83) and Richardson (quoted 19).

Turbulent Flame Propagation Models Based on Laminar Transport Concept

Worker		Type of Equation
Damkohler		$\frac{U_T}{U_L} = 1 + {u'}/{U_L}$ for $u' >> U_L$, $U_T = u'$
Shchelkin (76)		$\frac{U_T}{U_L} = \left[1 + \left(k \frac{u'}{U_L} \right)^2 \right]^{\frac{1}{2}}$
Frank Kamenetoki (quoted 19)		$\frac{U_T}{U_L} = \left(\frac{u'}{U_L}\right)^{\frac{1}{2}}$
Leason (115)		${U_T}/{U_L} = \left[1 + \left(\frac{2u'}{U_L}\right)^2 \right]^{\frac{1}{2}}$
Wohl Et Al (80)	(i)	$\frac{U_T}{U_L} = \left[1 + \left(\frac{2u'}{U_L}\right)^2 \right]^{\frac{1}{2}}$
	(ii)	$\frac{U_T}{U_L} = 1 + 2\ {u'}/{U_L}$
	(iii)	$\frac{U_T}{U_L} = \left[\frac{1}{2} \left\{ 1 + \left(1 + \left(\frac{4u'}{U_L}\right)^2 \right) \right\} \right]^{\frac{1}{2}}$
	(iv)	$\frac{U_T}{U_L} = 1 + \left[2 \left\{ \frac{u'}{U_L} - 1 + \mathrm{Exp}\left(-\frac{u'}{U_L}\right) \right\} \right]^{\frac{1}{2}}$
	(v)	$\frac{U_T}{U_L} = \left[2 \left\{ \frac{u'}{U_L} - \frac{1}{2} + \mathrm{Exp}\left(-\frac{u'}{U_L}\right) \right\} \right]^{\frac{1}{2}}$
Kalovity (82,83)		$\frac{U_T}{U_L} = 1 + \frac{u'}{U_L}$ when $u' << U_L$
		$\frac{U_T}{U_L} = 1 + \left(\frac{2u'}{U_L}\right)^{\frac{1}{2}}$ when $u' >> U_L$
Richardson (quoted 19)		$\frac{U_T}{U_L} = 1 + \frac{1}{\sqrt{2}} \frac{u'}{U_L}$ when $u' << U_L$
		$\frac{U_T}{U_L} = 1 + \frac{1}{2^{1/5}} \left(\frac{u'}{U_L}\right)^{4/5}$ when $u' >> U_L$

TABLE (6.1) Laminar Concept of Turbulent flame Propagation Models

Employed Paratmeters in Turbulent Flame Propagation Models Based on Turbulent Transport Concept.

Worker	Employed Parameter
Damkohler (75)	Turbulent diffusivity ϵ and kinematic viscosity ν.
Shchelkin (76)	λ_t $(= C_p \rho \epsilon)$
Summerfield (77, 78)	Turbulence Diffusivity and the ratio of turbulent to laminar flame thickness.
Bahduri (79)	λ_t
Andrews Et Al (19)	Re_λ $(= \frac{u' \lambda}{\nu})$ where λ is the micro-length scale.

TABLE (6.2) Employed Turbulence Parameters by Various Workers

Turbulent Flame Propagation Models Based on Turbulent Transport Concept.

Worker	Assumption	Equation
Damkohler (75)	$U_L \propto \left(\frac{K}{C_p \rho_o}\right)^{\frac{1}{2}}$	$\frac{U_T}{U_L} = \left(\frac{\epsilon}{\nu}\right)^{\frac{1}{2}}$
Shchelkin (76)	$U_L \propto \left(\frac{K}{e^{-E/RT}}\right)$	$\frac{U_T}{U_L} = \left(1 + \frac{\lambda t}{K}\right)$
Summerfield (77, 78)		$\frac{U_T}{U_L} = \frac{\epsilon}{\nu} \cdot \frac{\partial l}{\partial t}$
Bhaduri (77)		$\frac{U_T}{U_L} = \frac{U_t}{U} \cdot \frac{K}{\lambda t}$ U = Approach flow velcity
Andrews Et Al (19)		$\frac{U_T}{U_L} = f(Re_\lambda)$

TABLE (6.3) Turbulent Transport Concept of Turbulent Flame Propagation Models.

ular transport phenomenon nor the turbulent transport phenomenon. Thus by employing weighting factors it was possible to predict turbulent flame speeds which included both turbulent and laminar transport effect. The laminar weighting factor is attributed due to the presence of the large sized eddies while the turbulent weighting factor is attributed due to the presence of smaller sized eddies. Thus it is possible to estimate the values of the weighting factors by knowing the power spectral distribution of the turbulent flow field.

(b) ESCIMO model by Spalding (63):- In this approach it is assumed that turbulent combustion is composed of the following phenomena.

(i) Engulfment
(ii) Stretching
(iii) Coherence
(iv) Inter-Diffusion

Basically this model is Kin to the laminar transport concept and the chemical Kinetic and the aerodynamic effects are virtually isolated by using a Moving Observer System. The modelling method is still under development and it is of a more theoretical nature.

6.5.0 Turbulent Flame Speed Model for Spark Ignition Engine Cycle:- In the light of the above brief discussion, it is seen that there exists no theoretical or empirical formula which will predict the turbulent flame speed under different types of combustion conditions with reliable accurary. Theoretical modelling is undergoing active development (63) and is still far away from a condition in which it can be used practically whereas empirical models have proved to be applicable for cases which have similar or identical conditions as those under which these models were derived. All these correlations, however, were derived from observations made under steady state turbulent combustion and their validity under unsteady state turbulence condition, such as in the engine cylinder, remains to be confirmed. All the existing models give a common trend in which turbulent flame propagation speed increases with increase in turbulence, but the assumptions made about the relative importance of turbulence on flame propagation differ from one another. This shows the dependence of the response of the flame front not only to the approach stream turbulence but also on the type of combustion system. In this situation the

Shchelkin equation (76), which allows room for a different response of the flame front in different situations, seems to be most suitable for application in spark ignition engine cylinder simulation.

$$\frac{U_T}{U_L} = \left[1 + \left(k \frac{u'}{U_L} \right)^2 \right]^{1/2} \qquad \text{Shchelkin (76)}$$

Based on the above considerations, Shchelkin's equation was applied in the developed engine cycle simulation programme and the degree of response of the flame front to the measured cold level engine cylinder turbulence was adjusted by varying the value of the coefficient "k", until an acceptable agreement between the predicted and the experimentally observed cylinder pressure and local flame front arrival times was achieved (Section 7.0).

The value of the constant "k" thus determined is expected to hold true to predict the response of the flame front to cold level engine cylinder turbulence under all spark ignition engine combustion conditions and hence it seems to be very useful for future spark ignition engine cycle simulation purposes.

7.0.0 COMPUTER SIMULATION OF THE SPARK IGNITION ENGINE CYCLE

Better methods of modelling the processes in the spark ignition engine cycles are needed due to increasing demands for improvement in thermal efficiency and lower pollutant emissions. Consequently various improved analytical, numerical, computer modelling and experimental techniques are being developed and their development has reached a stage at which further noticeable improvement in neither the theoretical predicition methods nor the improvements in engine design by experimental technique can be achieved without an improved understanding of the combustion process. The main obstacle is the lack of understanding of the quantitative influence of engine cylinder turbulence on flame propagation rate and hence on the combustion rate within engine cylinder. The aim of this part of the research effort was thus directed to finding a quantitative relationship between mixture turbulence and engine cylinder flame propagation.

A computer simulation program for spark ignition engine cycle was specifically developed for this purpose. The effect of the spatial variation of turbulence on the flame propagation was taken into account by employing a three dimensional co-ordinate system within the engine cylinder boundary to locate the position of the flame kernal which was under the influence of local swirl and turbulence parameters.

The developed computer program together with the information on the measured cold level engine cylinder turbulence parameters (Section 5) enables a study of the effect of turbulence on flame propagation and hence on engine performance to be made by embodying a particular flame propagation model. The accuracy of such a turbulent flame propagation model requires confirmation by comparing the predicted results on cylinder pressure development and local flame arrival times with the experimentally observed ones.

This section discusses the approach which was used in constructing the computer simulation model for the above mentioned purpose.

7.1.0 The Computer Simulation Procedure:- The simulation procedure was constructed based on quasi-steady assumptions. Properties during a step length, which is a time interval of one degree of engine crank angle rotation for the present calculation, were assumed to remain constant. The change of

the cylinder charge conditions for the next time step were predicted by using a Predictor-Corrector method. The variables which were required for calculation in a time step were computed as follows:-

(i) Enclosed Cylinder Volume:- This was calculated by knowing bore, stroke, clearance volume and connecting rod length of the engine. To save computing time in calculating the cylinder volumes in successive iterative engine cycle calculations, the values of the enclosed cylinder volumes for all 720 degress of rotation of the engine crank of an engine cycle were computed and stored in a dimensional array before starting the main cycle calculation.

$$Vcyl = \frac{\pi}{4} d^2 \left[L + \frac{S}{2} (1 - \cos\theta) - \sqrt{L^2 - \frac{S^2}{4} \sin^2\theta} \right] + V_{cl}$$

(ii) Valve Lift Data:- Valve lift data were calculated from cam profile data which were measured at every 5 degrees engine crank angle interval. The cam profile diagrams for inlet and exhuast valves are shown in fig (8.1).

(iii) Geometric Flow area across Valve:- From a knowledge of the valve lift, valve geometry and port shape, the geometric flow area was calculated.

(iv) Discharge Coefficient of Valve:- This value was estimated using the method of Kastner Et Al (60) by knowing the up stream and down stream conditions of the valve, engine speed and valve lift (Section 7.7).

(v) Convective Heat Transfer Coefficient on the Gas Side:- This value was estimated by using a Reynold's Analogy of the type suggested by Annand (16). A brief discussion of the various available formulae for estimating heat transfer is made under section (7.6.0).

(vi) Properties of Unburnt Charge:- The unburnt charge was assumed to be of dry air and octane vapour. Properties of octane was taken from data of (121) and that of dry air from ref (105).

(vii) Properties of Burnt Charges:- The burnt gases as well as the gases in the wake of the flame were assumed to be in chemical equilibrium. Thus the properties of these gases were calculated by knowing its equilibrium composition (Section A.1). A total of 18 components of the products were considered and the assumed equilibrium reactions were same as those used by Kopa

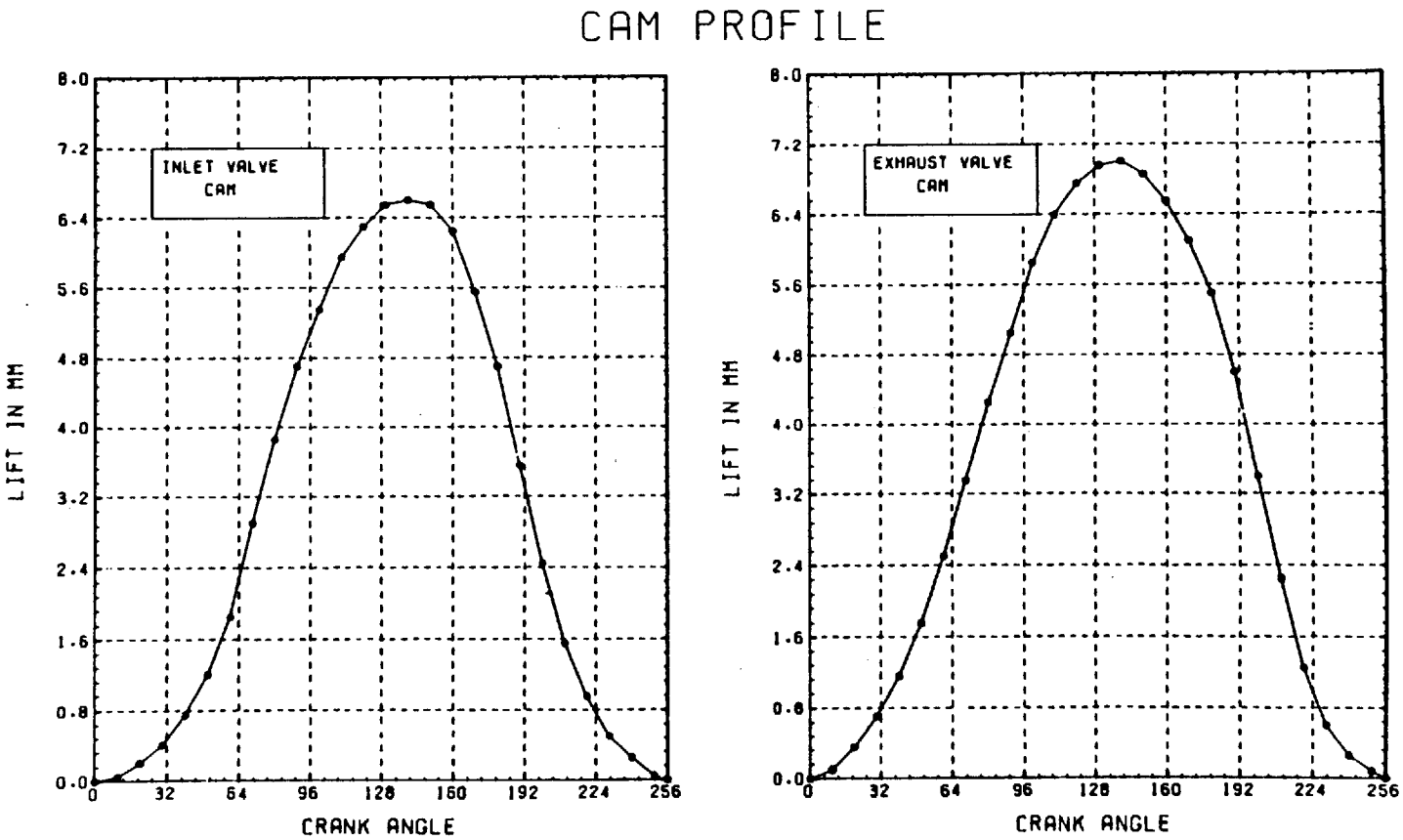


Fig (7.1) Cam Lift Diagrams for Inlet of Exhaust Valves

Et Al (121).

(viii) Adiabetic Flame Temperature:- This value was calculated by extending the chemical equilibrium composition prediction program to include the conservation of enthalpy (for constant pressure combustion) and the conservation of internal energy (for constant volume combustion) between the reactants and the products. To save computing time during engine cycle calculations, computed flame temperatures were fitted into polynomical expressions as a function of unburnt charge temperature for various initial unburnt pressure and equivalence ratios, and the polymonials were used to estimate the combustion temperature for a given initial condition.

(ix) Metal Surface Temperatures on Gas Side:- These values were initially assumed and were corrected at the end of each iterative engine cycle of calculation by using a resistance network analogy to heat transfer (Section 7.5.3).

(x) Flame Propagation:- Turbulent flame propagation was calculated by using the turbulent flame propagation model (Section 6.5) and the knowledge of measured spatial and temporal variation of cold level turbulence parameters (Section 5.0).

7.2.0 General Structure of the Prediction Procedure:- The prediction procedure is divided and constructed to do necessary calculations for the three distinct phases or periods of an engine cycle.

(i) Valve Opening Peridd:- To calculate the change in cylinder mass and properties when inlet valve or exhaust valve or both are open. In other words, to calculate the mass of cylinder charge and properties changes during induction, scavenging and exhaust periods.

(ii) Compression and Expansion Period:- To calculate the change in cylinder pressure, temperature and properties during compression and expansion processes when all the valves are closed and there is no combustion.

(iii) Combustion Period:- During this period the cylinder charge is divided into two regions, burnt and unburnt regions by the propagating flame front. This step calculates the mass burning rate and hence the change in cylinder pressure and temperature in both burnt and unburnt regions of the charge. The flame kernal is assumed to propagate radially outwards and its propagation rate or turbulent flame speed was taken to

be influenced by the measured cold level turbulence parameter (intensity of turbulence).

The major steps which were involved in calculations for the combustion period, during a time -step, are

(a) the flame front is allowed to propagate into the unburnt region and this causes the combustion of the newly trapped unburnt cylinder charge. The combustion of the newly trapped charge is assumed to take place in a const volume process and is first allowed to expand into the already burnt region: and this causes pressure rise in the burnt portion of the cylinder charge.

(b) The mixed burnt region is then allowed to expand into unburnt region until pressure equilibrium is established between the burnt and unburnt regions of the cylinder charge. (After this step the program allows for the effect of organised gas flow (swirl) on the distortion of flame shape. For our case experimental observations show there is no swirling flow inside the engine cylinder. So the input value of the magnitude for swirl is equated to zero and hence there is no effect of swirl on predicted flame shape in the present case).

(c) Heat transfer is allowed to take place from both regions to the surrounding metal surfaces and the two regions are then subjected to piston movement effect. Any disturbances in pressure equilibrium thus produced is allowed to equilibrate again between the two regions.

(d) The new position of the flame kernal is located before beginning the next time step calculation.

The detailed calculation procedure involved during this combustion period is discussed under section (7.4.8).

7.3.0 Thermodynamic Consideration:- Equations were derived based on conservation of mass and conservation of energy principles. These equations together with the equation of state for perfect gases were used to solve for the unknown variables.

7.3.1 Valve Opening Period (or Gas Exchange Period).

Energy Equation

$$-\frac{dQ_{loss}}{dt} + \frac{dW_{cy}}{dt} + \frac{d(m_{cy}\,u_{cy})}{dt} + \frac{d(m_e\,h_e)}{dt} + \frac{d(m_i\,h_i)}{dt} = 0$$

Continuity Equation

$$\frac{dm_{cy}}{dt} + \frac{dm_e}{dt} + \frac{dm_i}{dt} = 0$$

7.3.2 Compression and Expansion Period

Energy Equation

$$\frac{dQ_{loss}}{dt} + \frac{dW_{cy}}{dt} + \frac{d(m_{cy}\, u_{cy})}{dt} = 0$$

Continuity Equation

$$\frac{d\, m_{cy}}{dt} = 0$$

7.3.3 Combustion Period

Energy Equation

$$\frac{dQ_{loss}}{dt} + \frac{dQ_{fuel}}{dt} + \frac{dW_{cy}}{dt} + \frac{d(m_{cy}\, u_{cy})}{dt} = 0$$

Continuity Equation

$$\frac{dm_{cy}}{dt} = \frac{dm_b}{dt} + \frac{dm_u}{dt} = 0$$

The above equations were solved with the known boundary conditions. The cycle calculation was started when the piston was at the top dead centre position during the induction stroke. Initial pressure and temperature at the beginning of the cycle calculation were assumed. After each iterative cycle of calculation, the assumed pressure and temperature were compared with the computed values and were corrected for the next cycle of iteration. The iteration process was stopped when the desired accuracy in the values of cylinder pressure and temperature at the beginning of the cycle was obtained.

7.4.0 Evaluation Procedure for the Terms Involved:- The following evaluation procedures were used for estimating the values of the terms in the previously mentioned differential equations describing the conservation of energy and mass.

7.4.1 Heat Transfer to and from the Surrounding Metal Surfaces

$\left(\frac{dQ_{loss}}{dt}\right)$:-

This term was evaluated by knowing the exposed metal surface area, convective heat transfer coefficient, metal wall and cylinder gas temperature. For a chosen metal surface,

$$\frac{dQ_{loss}}{dt} = hA\ (T_{cy} - T_{wall})$$

A total of five heat transfer surfaces were considered and the evaluated values of heat losses were added to give the overall or total heat transfer rate. During combustion period each surface considered was exposed to both burnt and unburnt regions of the cylinder charge. The area under each region of each metal surface was estimated by knowing the flame kernal shape and distance from the sparking plug position. The gas side metal surface temperatures were the last corrected values which were obtained by solving the resistance network analogy of heat transfer (Section 7.5.3) at the end of each iterative cycle. The cylinder gas temperature was the existing step temperature of the burnt or unburnt charge.

7.4.2 Mass Flow Rate Across the Valves $\left(\frac{\dot{dm}_i}{dt}\right.$ and $\left.\frac{\dot{dm}_e}{dt}\right)$

These terms were evaluated by knowing the effective flow area across the valve and isentropic flow rate per unit area. The former was calculated by knowing the geometric flow area and the discharge coefficient which was estimated by using the method of Kastner Et Al (60). The isentropic flow rate was calculated from a knowledge of existing cylinder and manifold conditions.

$$\frac{dm}{dt} = A_{eff} \cdot m_{isen}$$

$$\frac{dm}{dt} = C_D \cdot A_{geo} \cdot m_{isen}$$

7.4.3 Change of Mass of the Cylinder Charge $\left(\frac{dm_{cy}}{dt}\right)$

By knowing the mass flow through valves, change in cylinder mass was calculated by using conservation of mass equation.

7.4.4 Increase in Enthalpy of Cylinder Charge due to Incoming

Charges from Manifolds $\frac{d(h_i\ m_i)}{dt}$, $\frac{d(h_e\ m_e)}{dt}$

These terms can be expressed as,

$$\frac{d(h_i\ m_i)}{dt} = h_i \frac{dm_i}{dt} + m_i \frac{dh_i}{dt}$$

$$\frac{d(h_e\ m_e)}{dt} = h_e \frac{dm_e}{dt} + m_e \frac{dh_e}{dt}$$

The conditions in the inlet and exhaust manifolds are assumed to remain constant, thus the term $\frac{dh_i}{dt}$ or $\frac{dh_e}{dt}$ is equal to zero. Thus the knowledge of the mass flow across the valve into the cylinder from the manifolds($\frac{dm_i}{dt}$) and ($\frac{dm_e}{dt}$) enable the evaluation of the above terms. The term $\frac{d(h_i\ m_i)}{dt}$ is considered under normal inlet valve flow and the term $\frac{d(h_e\ m_e)}{dt}$ is considered under reverse exhaust flow, ~~otherwise these terms are neglected~~.

7.4.5 Change of Enthalpy Content $(\frac{dm_{cy}\ h_{cy}}{dt})$ during the valve opening period and change of internal energy content $(\frac{dm_{cy}\ u_{cy}}{dt})$ during compression and expansion periods.

The above terms can be expanded as follows.

$$\frac{d\,m_{cy}\ h_{cy}}{dt} = h_{cy} \frac{d\,m_{cy}}{dt} + m_{cy} \frac{d\,h_{cy}}{dt}$$

$$= h_{cy} \frac{d\,m_{cy}}{dt} + m_{cy}\ C_p \frac{dT}{dt}$$

$$\frac{d\,m_{cy}\ u_{cy}}{dt} = u_{cy} \frac{d\,m_{cy}}{dt} + m_{cy} \frac{du_{cy}}{dt}$$

$$= u_{cy} \frac{d\,m_{cy}}{dt} + m_{cy}\ C_v \frac{dT}{dt}$$

Thus the value of $\frac{dT}{dt}$, during valve opening or compression and expansion periods, can be solved from energy equations since all other variables are known. By applying the equation of state, dP/dt can be calculated.

7.4.6 Change of Energy Content during the Combustion Period $\left(\frac{d m_{cy} u_{cy}}{dt}\right)$

During this period the cylinder charge is divided into two regions, one that of the burnt and the other, that of the unburnt charge. Thus the above term can be expanded as follows.

$$\frac{d m_{cy} u_{cy}}{dt} = \left(\frac{d m_{cy} u_{cy}}{dt}\right)_{burnt} + \left(\frac{d m_{cy} u_{cy}}{dt}\right)_{unburnt}$$

$$= \frac{d m_b u_b}{dt} + \frac{d m_u u_u}{dt}$$

$$= m_b \frac{du_b}{dt} + u_b \frac{dm_b}{dt} + m_u \frac{du_u}{dt} + u_u \frac{dm_u}{dt}$$

$$= m_b C_{V_b} \frac{dT_b}{dt} + u_b \frac{dm_b}{dt} + m_u C_{V_u} \frac{dT_u}{dt} + u_u \frac{dm_u}{dt} \quad ----(1)$$

The mass burning rate as determined by the flame propagation rate (Section 7.4.7) determines the value of the term $\frac{dm_b}{dt}$ and $\frac{dm_u}{dt}$. The above term still contans two unknowns $\frac{dT_b}{dt}$ (burnt region temperature rise) and $\frac{dT_u}{dt}$ (burnt region temperature rise) to be solved. Thus to have another known condition, it is assumed that the pressure and temperature rise in the unburnt region is caused by the expansion of the burnt charge into unburnt region and thus causing adiabatic compression of the unburnt charge.

For unburnt charge aidabatic compression PV^r = Const,

$$dP_{u/Pu} + r_u \, dV_{u/V_u} = 0$$

Equation of state PV = mRT for unburnt charge gives,

$$dP_{u/Pu} + dV_{u/Vu} = dm_{u/m_u} + dT_{u/T_u}$$

Eliminated the term $\frac{dP}{p}$ from the above two equations,

$$(1 - r_u)\ \frac{dV_u}{V_u} = \frac{dm_u}{m_u} + \frac{d\,T_u}{T_u}$$

Differentiating with respect to 'dt' and rearranging

$$\frac{d\,T_u}{dt} = T_u \left(-\frac{1}{m_u}\ \frac{dm_u}{dt} + \frac{(1-r_u)}{V_u}\ \frac{d\,V_u}{dt} \right) \text{-----(2)}$$

Equations 1 and 2 can be used to solve for $\frac{dT_u}{dt}$ and $\frac{dT_b}{dt}$ together with the energy equation for combustion period. But direct solution is not possible as the unknown term $\frac{d\,V_u}{dt}$ is present in equation 2. One possible solution is to guess a value of $\frac{d\,V_u}{dt}$ (the volume which is compressed into the unburnt charge region) thus enabling the estimation of $\frac{dT_u}{dt}$ from equation 2 and hence the value of $\frac{dP_u}{dt}$ (unburnt region pressure rise). By using the computed $\frac{dT_u}{dt}$, equation 1 and the energy equation will allow evaluation of $\frac{dP_b}{dt}$ (burnt region pressure rise). If the values of dP_u/dt and dP_b/dt computed in this way are not equal, readjustment on the value of $\frac{dV_u}{dt}$ is made, by moving the flame kernal, until pressures in burnt and unburnt regions are in equilibrium. To facilitate the computing process, it is assumed that the unburnt region is at first not disturbed by combustion, that is combustion of the fresh charge causes a pressure rise in the burnt region only, after which the burnt region is allowed to expand gradually into unburnt region till pressure equilibrium is established in burnt and unburnt regions. This enables the evaluation of the temperature and pressure rise in both regions by the combustion of the newly trapped charge.

7.4.7 Rate of Heat Released $\left(\frac{dQ_{fuel}}{dt}\right)$

The rate of heat released was evaluated by knowing the turbulent flame propagation speed and hence the rate of combustion of the fresh unburnt charge during the quasi-time step. A three dimensional flame propagation pattern was considered. The assumptions made are,

(i) The flame is radially propagated outwards starting from the sparking plug position.

(ii) Reaction zone thickness or flame front thickness is too small to take into account.

(iii) Flame propagation speed is taken to be influenced by the measured local turbulence intensities, Section (6.0).

(iv) Combustion of the trapped fresh charge in the wake of the flame occurs at constant volume.

(v) Complete mixing condition exists in both burnt and unburnt portion of the charge.

(vi) Flame quenching effect is neglected.

With the above assumptions, the heat released during a quasi-time step was calculated as follows:-

If dM_b is the mass fresh charge which is trapped and burned during a time step, the heat released due to this is,

$$dQ_{fuel} = dM_b \cdot \Delta u$$

Where Δu is the specific internal energy increased due to combustion at constant volume.

Thus,

$$dQ_{fuel} = dM_b \cdot C_v \Delta t$$

or

$$\frac{dQ_{fuel}}{dt} = C_v \Delta t \cdot \frac{dM_b}{dt}$$

Where Δt is the adiabatic combustion temperature rise due to constant volume combustion, estimated by using the polymonials for adiabatic flame temperatures (Section A.1), which were predicted from the equilibrium composition program.

The term for the rate of fresh charge burning rate $\frac{dM_b}{dt}$ is calculated by considering three dimensional flame movement as follows.

If dm_b is the elemental mass of fresh charge, trapped by the flame front during the time step 'dt', at a location (x, y, z) on the reation zone surface inside the cylinder, the total mass of newly trapped charge dM_b over the whole reaction zone surface within the cylinder volume is, (Referring to fig 7.2).

$$dM_b = \iiint_{Vcyl} d\,m_b = \iiint \rho_u \, dV$$

$$dM_b = \iiint \rho_u \, V_f \, dA. \, dt. \, n$$

Where n is a unit normal vector to the elemental flame

surface.

Thus,

$$\frac{dM_b}{dt} = \iint n.\ \rho_u\ V_f\ dA$$

By the assumption of radially outwards propagation of the flame front, n is always equal to 1.

$$\frac{dM_b}{dt} = \iint \rho_u\ V_f\ dA \quad \text{----------(A)}$$

The integral shows that rate of newly trapped mass of charge is equal to sum of the locally trapped fresh charge per unit time over the whole reaction zone surface. The right hand side of the equation was numerically integrated over the whole flame front area which is subjected to the physical cylinder boundary conditions. Analytical integration would be difficult for this case because of the type of physical boundary conditions involved and the fact that each reaction zone element is subjected to local swirl and turbulence which are generally varying with time. Numerical integration was done by employing a suitable three dimensional co-ordinate system which was used for defining the flame front position. The particular co-ordinate system employed was chosen based on the considerations which were given to several possible alternatives which are mentioned briefly below.

Rectangular X-Y-Z Co-ordinate System:- The cylindrical shape of the physical cylinder geometry plus radially outwards propagation nature of the flame make it unsuitable for employment of rectangular co-ordinate system for locating flame front position.

Cylindrical R,Θ,Z Co-ordinate System:- Though this co-ordinate system is quite adaptable for defining physical cylinder boundary, it is a difficult task to define the radially outwards propagating flame using this co-ordinate system.

Spherical R,Θ,Ø Co-ordinate System:- This system is the most suitable one for defining the flame front position because of its radially outwards propagation nature, but also it can be adopted in defining the physical cylinder boundary conditions with relative ease compared to the rectangular co-ordinate system.

The above considerations show that spherical co-ordinate system is the most suitable system among the above three possible

alternatives to locate the flame kernal position whose movement is influenced by local swirl and turbulence level and is also subjected to the engine physical geometry boundary conditions. Thus a spherical co-ordinate system was chosen for the present case and its origin was taken at the sparking plug position. To save computing time, preselected and fixed (θ, ϕ) values or directions, which form a total of 60 radial directions, were used for locating and defining the flame front position. The basic idea employed in using the co-ordinate system is as follows.

At each time-interval of calculation, the magnitude of the flame front movements in each of 60 chosen radial directions were computed and a surface was fitted over these points or flame kernal locations to define the flame front position (fig 7.3). To facilitate the numerical computing procedure, surface fitting was replaced by horizontal sections. Over each section, a spline curve was fitted passing over the computed positions of the flame front location while the spline curve, which represents flame front, was subjected to physical boundary conditions (fig 7.4). A total of six equally spaced horizontal sections were considered and the computed enclosed areas on these sections enable to estimate the volume of the burnt gases enclosed by the flame front. The distance between the horizontal sections was varied with the flame front movement in such a way that there were six equally spaced cutting sections across the flame envelope. The difference in values of the enclosed volumes of burnt gases before and after the flame propagation gave the volume of the newly trapped charge, and this value multiplied by the unburnt charge density gave the value of the integral $\int\int \rho_u \, V_f \, dA \, dt$, which is the mass of newly trapped charge during the quasi-time step 'dt'.

By using preselected values of θ and ϕ, and the horizontal cutting sections, a considerable reduction incomputing time was obtained in evaluating the integral while the accuracy of the result was maintained.

7.4.8 Calculation Steps Involved for the Heat Release

The steps which are involved in calculation of heat release are mentioned below.

(i) The flame front is allowed to propagate from the existing position (the position of the flame front at the beginning of the time -step) to a new position. The amount moved in each direction is influenced by the measured cold level turbulence intensities and is subjected to the physical boundary conditions as well

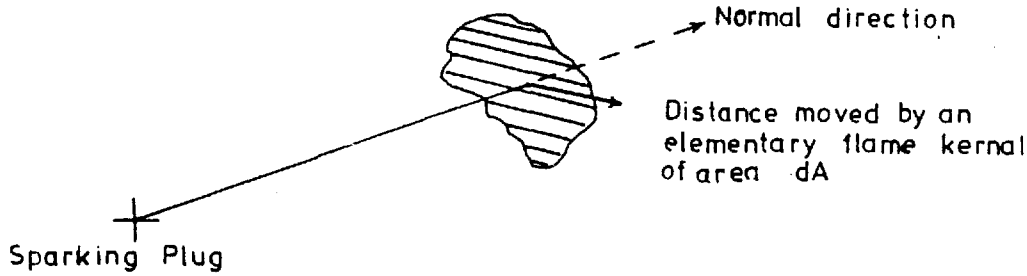


Fig (7.2) Movement of an Elementary Flame Kernal of Area dA



Fig (7.3) Spherical Co-ordinate System Employed to Locate the Flame Front Position



Fig (7.4) Flame Front as Seen on a Horizontal and a Vertical Section

(ii) A cubic spline curve is fitted over the new flame front position on each horizontal section and this enables the positions at which the flame front touches the cylinder boundary to be estimated.

(iii) A new enclosed volume for burnt gases is then computed and hence the values of the volume and mass of the fresh charge trapped by the flame front.

(iv) Combustion of the newly trapped charge is assumed to occur at constant volume process and then the new combustion products thus formed are taken to mix thoroughly with the previously formed combustion charge. This causes the pressure rise in burnt region.

(v) The burnt region is allowed to expand into unburnt region in such a way that the flame front moves radially outwards until pressure equilibrium is established between the burnt and unburnt regions.

(vi) If swirl is present it is allowed to distort the flame kernal.

(vii) Both burnt and unburnt regions are then subjected to heat transfer and piston movement.

(viii) Any disturbance in pressure equilibrium due to the previous step is allowed to equilibrate again by adjustment of the flame kernal position by radial movements.

(ix) Check for the completion of combustion. It is assumed that combustion is completed after 99% of cylinder charge has been burned or 99% of the total cylinder volume has been occupied by the burnt gases, which ever occur first.

The major steps involved are diagrammatically illustrated from fig (7.5) to fig (7.7).

The simulation procedure shows that heat release in a spark ignition engine can be realistically modelled, including the effect of swirl and turbulences on the movement of the flame front. The modelling technique forms the first attempt in the engine cycle simulation field where flame envelope shape could be predicted provided information about spatial and temporal variations of turbulences and mean velocities are known. The model is not only able to fullfil its main purpose which is studying the quantitative influence of the measured cold level turbulence on flame propagation and hence on the validity of a particular turbulent flame model, but also it forms a very useful tool for the study of the effect of various swirl and turbulence

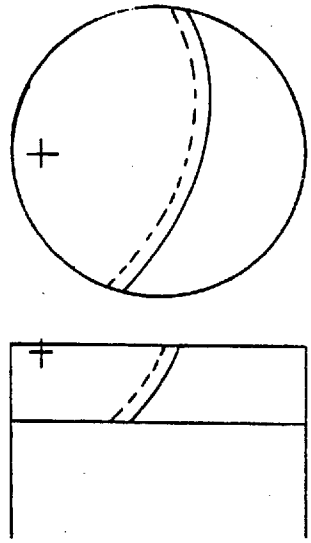


Fig (7.5) Movement of Flame Kernal Due to Combustion

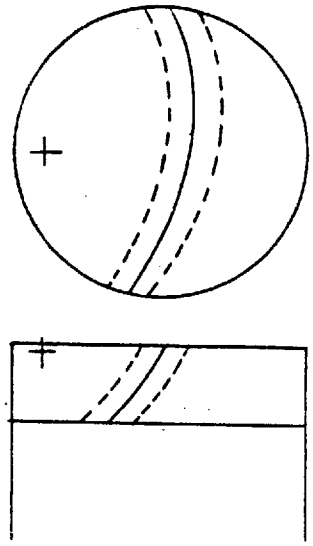


Fig (7.6) Expansion of Burnt Charge inot Unburnt Region

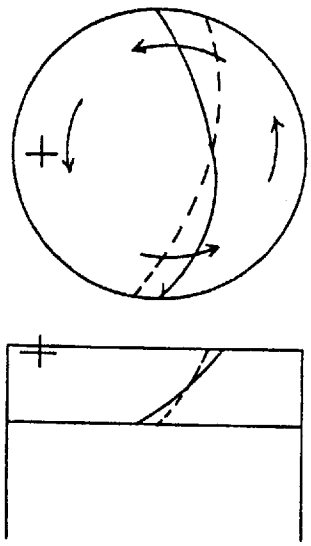


Fig (7.7) Distortion of Flame Kernal by Swirl

flow fields on engine performance and fuel economy.

7.5.0 Heat Transfer Process

As the heat transfer process presents the amount of energy losses from the cylinder charge system under consideration to its surroundings, it seems to be very valuable to examine briefly the modelling technique to be used and the existing available heat transfer formulae. Experimental observations (64,100) showed that metal temperature differences exist in metal surfaces in a running engine. An attempt was thus made to take into account the effect of the metal surface temperature differences on the rate of heat transfer.

7.5.1 Heat Transfer Surfaces Considered

A total of five heat transfer surfaces, which are listed below together with their heat transfer paths, were considered for evaluating the heat losses.

(i) Cylinder Head:- This exchanges heat with cylinder gases, cooling water, exhaust valve, inlet valve and cylinder liner.

(ii) Cylinder Liner:- This exchanges heat with cylinder gases, cooling water, cylinder head and piston.

(iii) Piston:- This exchanges heat with cylinder gases, lubricating oil and cylinder liner.

(iv) Exhaust Valve:- This exchanges heat with cylinder gases, exhaust manifold gases and the cylinder head.

(v) Inlet Valve:- This exchanges heat with cylinder gases, inlet manifold gases and cylinder head.

The heat transfer from each of the above metal surfaces was calculated by knowing the metal and gas temperatures, and then were added together to give the total amount of heat transfer from cylinder gases.

7.5.2. Metal Surface Temperature

Previous experimental measurements (65,100) on metal temperatures showed that the fluctuating component of the metal temperature is small compared to the mean metal temperature, due to the high thermal inertia of the metal walls and surfaces involved. Thus without effecting the accuracy, metal surface temperatures were taken to remain constant. The metal surface temperatures were initially assumed and were corrected at the end of each iterative engine cycle calculation by using an equivalent resistance network analogy on heat transfer.

7.5.3 Equivalent Resistance Network

With the considerations of five chosen heat transfer

surfaces and their associated conductive and convective media, it is now possible to construct an equivalent resistance network to represent the heat transfer process. Equivalent resistance values of the network is calculated as follows:-

For a convective heat transfer surface, $R_{conv} = \frac{1}{hA}$

For a conductive heat transfer medium, $R_{cond} = \frac{\Delta x}{K.A}$

The effective resistance of a heat transfer path consisting of n_v convective surfaces and n_d conductive media is,

$$R_{eff} = \sum_{i=1}^{n_d} R_{cond_i} + \sum_{i=1}^{n_v} R_{conv_i}$$

The thermal conductivity values of cast iron liner, cast iron cylinder head and aluminium alloy piston were taken from (122) and the water side convective heat transfer coefficient was estimated by the method of Shroff Et Al (101). For the gas sideconvective heat transfer coefficient, A Reynold's Analogy equation of the type suggested by Annand (16) was used. The Annand's type formula (16) was chosen because of its dimensional homogeneity and the criticisms which exist for other existing formulae (16).

The equivalent resistance network employed and the knowledge provided of the amount of heat transfer from each gas side metal surface during a cycle enables the gas side metal temperature to be corrected after each iterative engine cycle calculation.

7.6.0 Heat Transfer Formulae

Although it was decided to use the Annand correlation (16) for reason of accuracy, it would be appropriate to consider briefly the alternatives which are available for predicting the heat transfer of cylinder gases. These different formulae, which are listed in Table (7.1), exist due to uncertainty about the gas side convective heat transfer coefficient, which are essential for engine cycle calculations to estimate the heat transfer to and from the walls. The estimated heat transfer values by using these formulae are compared in fig (7.9) which is taken from Ref (17). The formulae by Nusselt (quoted 16), Eichelberg (15) and Pflaum (85) are not dimensionally correct, the constants have dimensions (16). The choice of the form of

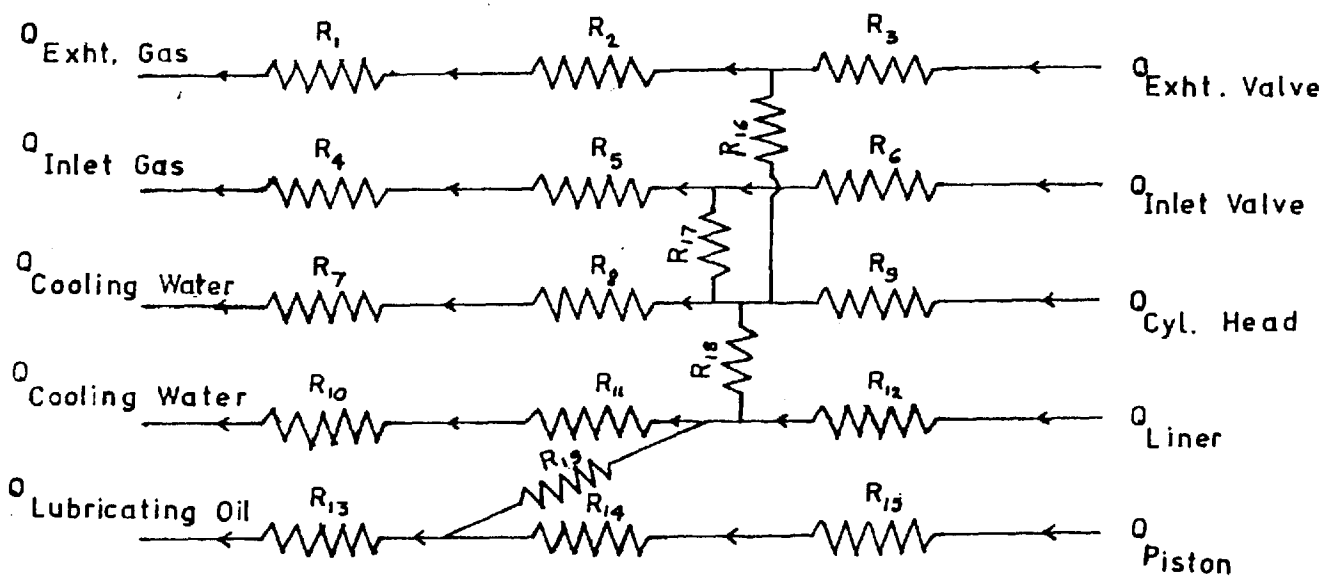


Fig (7.8) Equivalent Network Resistance Used for Calculating Heat Transfer and in Estimating Gas Side Metal Temperatures

Heat Transfer Formulae

Worker	Type of Equation	Remarks
Nusselt (quoted 16)	$q/_A = C_1 (1 + 0.38V_p) (P^2T)^{1/3} (T - T_w) + C_2(T^4 - T_w^4)$	Convective heat transfer coefficient is effected by engine Reynold's number through the use of the term V_p and $(P^2T)^{1/3}$. Radiation term is also included. The equation was derived from the results of a test using a cylindrical bomb.
Eichelberg (15)	$q/_A = CV_p^{1/3} (PT)^{\frac{1}{2}} (T - T_w)$	Convective heat ransfer term is effected by the engine Reynold's number through the use of the term $V_p^{1/3}$ and $(PT)^{\frac{1}{2}}$. Radiative component is neglected.
Annand (16)	$q/_A = a.\frac{k}{d} R_e^b (T - T_w) + c(T^4 - T_w^4)$	Convective heat transfer coefficient is calculated by using Reynold's analogy. Radiative term is also included.

Table (7.1.a) Heat Transfer Formulae by Various Workers

Heat Transfer Formulae

Worker	Type of Equation	Remarks
Woschni (17)	$q/_A = c\, d^{m-1}\, P^m\, W^m .\ T^{0.75 - 1.62m}\ (T - T_w)$	The equation was derived based on Reynold's Analogy and was manipulated to reach to its final established form. No radiative term.
Le Feuvre (64)	$q/_A = \frac{ak}{r}\ R_e^{0.8}\ Pr^{0.33}\ (T - T_w)$	Convective heat transfer term was calculated by using Reynold's Analogy including Prandtl number variation effect. No radiative term.
Pflaum (85)	$q/_A = K\ \ 3.0 \pm 2.57\ (1 \pm \text{Exp}\ (1.5 - 0.416\ V_p))\ .\ (PT)^{\frac{1}{2}}\ .\ (T - T_w)$	The equation was derived from the results of measurement made on diesel engines with and without pressure charging. Use of a correction factor K, which is function of boast pressure, was also suggested.

Table (7.1.b) Heat Transfer Formulae by Various Workers

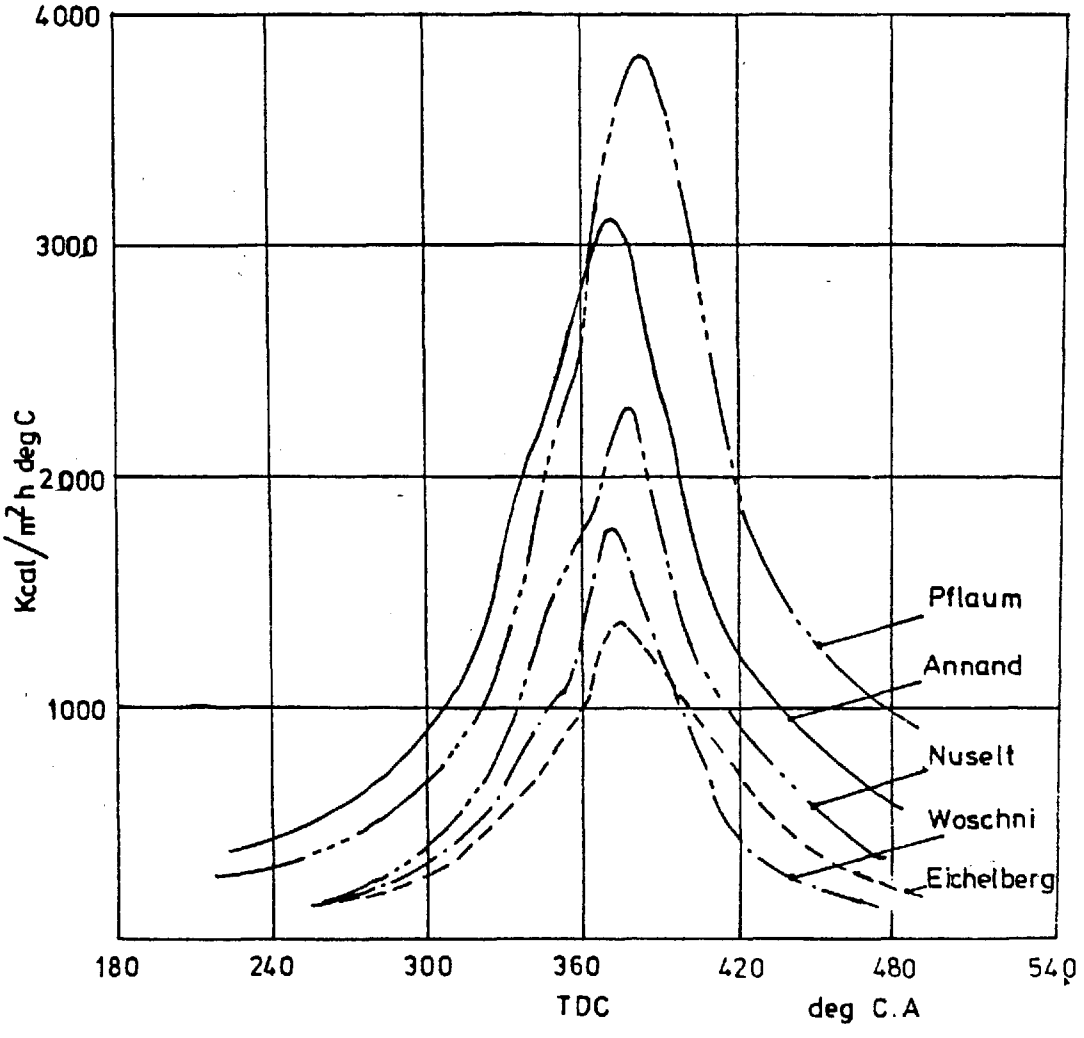


Fig (7.9) Predicted Heat Transfer by Using Various Formulae (Ref. 17)

'pT' group in the Eichelberg equation (15) was a very arbritrary step (16). The formulae of Annand (16), Woschni (17) and Le Feuvre(64) for convective heat transfer are based on the Nusselt-Reynold Relationship and hence incorporate the same basic concept of the Reynold's Number as the major parameter affecting convection.

Radiation effect can only be included in a much over simplified form which is based on a black body radiation formula (16). In fact the gases are very far from black, for they absorb and emit radiations almost exclusively in certain wave length bands which are characteristics of the material (16). A shape factor is required to be applied to cover the fact that the angle of incidence of radiation in general varies over any actual surface (16). In addition to the above difficulties, controversy exists (16, 17, 19) over the importance of the radiant heat transfer component. According to Henein (quoted 119) radiation has a negligible effect in the process of heat transfer inside an engine, because of the very short length of the radiating beam and the low partial pressures of the radiating gases, which consist mainly of water and carbondioxide. In general it is accepted that radiation effect in a spark ignition engine is much smaller than that in a diesel engine (16). Thus radiant part of the heat transfer is neglected for the present case. For the convective term, Annand's formula (16) which gives a fairly good agreement with experimentally measured values of Le Feuvre (64) was chosen to be used in the computer simulation model of the spark ignition engine.

7.7.0 Flow Through Valves.

The boundary curves for inlet and exhaust processes, that is the mass flow through valves, were investigated and successfully established by various previous experimental observations (18, 60, 61, 62). These boundary curves may be expressed using one of the three following methods.

(i) Employing Mass Flow Rate Parameters:- The boundary curves are expressed using a non-dimensional mass flow rate parameter $\frac{\dot{M}\sqrt{T}}{A\,p}$ which in turn may be expressed as a function of non-dimensional valve lift (L/D) and pressure ratio across the valve.

(ii) Employing the Effective Flow Area:- The boundary curves are expressed using the effective flow area which in turn is expressed as a function of non-dimensional valve lift (L/D) and

pressure ratio across the valve. The effective flow area together with the knowledge of isentropic flow rate enables the evaluation of the mass flow rate across the valve.

(iii) Employing a Discharge Coefficient:- The boundary curves are expressed using a discharge coefficient which in turn is expressed as a function of non-dimensional valve lift (L/D), pressure drop across the valve, engine speed and isentropic flow rate (60). The discharge coefficient together with the knowledge on minimum geometric flow area and isentropic flow rate enables to evaluate the mass flow rate across the valve.

For present investigation, the third alternative was chosen and the nature of the variation of the boundary curves, as observed by Kastner Et Al (60) and Wallace (120), were used for computing the mass flow rate across the valves. The effect of length and shape of the manifolds on trapping efficiency may be included by considering the pressure wave actions using method of characteristics. But the increase in computational time requirement to include the wave actions does not justify in our case where the main interest is on the study of effect of engine cylinder turbulence on flame propagation.

7.8.0 Computer Simulation Program

This was written with an emphasis on the turbulent combustion stage with detail considerations of the nature of flame propagation and mass burning rate. The program can locate the flame front position at any instant during the combustion period and the flame front itself can be subjected to distortion by swirl if it exists. The measured cold level turbulence parameters were taken as the influencing parameters on turbulent flame propagation, thus it is possible to check the validity of a particular turbulent flame propagation model, which is employed in the prediction program, by comparing the predicted results on flame speeds (local flame arrival times) and cylinder pressure development with the experimentally observed ones.

The high complexity nature of the program which predicts the detail aspect of the combustion stage was achieved without excessive requirements on both computing time and computer core storage requirements by careful organisation and optimization of the program structure. The program can be run with a core requirement of 22K while the compilation time of the program is about 9 CP seconds and a typical cycle of iteration for an engine cycle takes about 10 CP seconds on a CDC 1700 series

machine.

7.8.1 Structure of the Computer Program

The overall program structure is divided into three groups according to the thermodynamic considerations involved (Section 7.3.0), these groups are designed to do the following calculations during,

(i) The Valve Opening Period

(ii) The Compression and Expansion Period

(iii) The Combustion Period

The program consists of 1 main controlling routine and 33 subroutines for the calculation of the above three stages. The variables which are constants and are necessary for successive iterative cycle are precalculated before the start of the first cycle calculation and these values are stored in the assigned arrays. These variables are cylinder volumes and total heat transfer surface areas at each engine crank angle interval and geometric flow areas of the valves at the valve opening period.

7.8.2 Input to the Program

All program input data is read by a routine called INPT before the start of the main calculation and after that there is no further input to the program. The input data consists of information on engine geometry which are bore, stroke, connecting rod length, clearance volume, inlet and exhuast valves' diameters and their lift values against engine crank angles as well as information on engine operating conditions which are engine speed, air-fuel ratio used, throttle valve opening position which specifies the mean inlet manifold pressures and temperatures and lastly the information on the measured cold level turbulence parameters for the above engine operating conditions.

7.8.3 Output from the Program

The output information consists of the detail engine performance parameters plus information on flame propagation rate, mean flame front shape on a selected horizontal section and local flame front arrival times. This information can be printed direct to a line printer or can be written onto magnetic tape or disc for processing by a plotting program for graphical output results.

7.8.4 Progam Structure for Valve Opening Period

The main routine detects this period by checking the valve opening and closing periods. During this period, the program

checks whether a back flow to the inlet port from the cylinder or back flow from the exhuast pipe into the cylinder is occuring. The upstream and downstream conditions are thus checked and the amount of flow across each valve during the quasi-time step is estimated. At the start of the quasi-time step, the main program calls to the routine GASFLOW to do all the necessary controls over the calling of the associated subroutines. The GASFLOW routine calls the following routines to do the following functions.

ISENTRO:- This routine calculates the isentropic mass flow rate across the valve for given upstream and downstream conditions. It checks whether the flow is sub-sonic or sonic and appropriate action is taken to calculate the isentropic flow rate.

VALVE:- This routine calculates the geometric flow area of the valve for each valve opening position at every engine crank angle for the valve opening periods. This routine is called only once, before the start of the first cycle of iteration. Computed geometric flow areas against crank positions are stored in dimensioned arrays.

FLOW:- This routine estimates the discharge coefficient of the valve for the existing boundary conditions and valve lift using the method of Kastner Et Al (60), and then calculates the amount of mass flow across the valve during the quasi-time step by knowing the discharge coefficient, geometric flow area and isentropic flow rate.

HTTR:- This routine calculates the amount of heat transfer to and from the gas by the surrounding metal surfaces.

With the help of the above routines, the GASFLOW routine estimates the change of properties during the quasi-time step and the computed values are returned to the MAIN routine. The steps involved in the valve opening period are shown in Table (7.2).

7.8.5 Programme Structure for Compression and Expansion Period

During this period, which corresponds to the time when all the valves are closed and combustion is absent, the routine MAIN calls to the NONFLOW routine to do all necessary controls for predicting the change in conditions of the cylinder charge which is undergoing expansion in the compression process. The cylinder charge is also subjected to heat exchange with the surrounding metal surfaces. During compression cylinder charge is taken to be composed of fresh charge and residuals and during expansion it is

Valve Opening Period Calculation

Enter the present step calculation.

Check the geometric flow area of the valves for the present crank angle position.

Calculate the isentropic flow rate across the valve for the existing upstream and downstram conditions.

Calculated the discharge coefficients of valve for existing boundary conditions.

Calculate the change of cylinder mass for the time step by knowing the effective valve area and isentropic flow rate across the valve.

Estimate the change of cylinder pressure and temperature due to change of cylinder mass.

Allow heat transfer to take place between the surrounding wall surfaces and the cylinder gases.

Calculate the new cylinder pressure and temperature after heat transfer and piston movement.

End of step calculation and return.

Table (7.2) Calculation Steps during Valve Opening Period

taken to be burnt gases at chemical equilibrium. The properties of the fresh charge and burnt gases are computed from polynomials which hold the values of properties as a function of temperature. The routines associated with calculations of this period are:-

NONFLOW:- This routine controls the calling sequence of the other associated routine in addition to calculating the change in cylinder charge conditions due to compression or expansion.

HTTR:- This is the same routine as used for calculations of heat transfer during the valve opening period and is used to estimate the amount of heat transfer to and from the gases with the surrounding metal surfaces.

PROP:- This routine holds polynomials for thermodynamic properties of fresh and burnt gases as a function of temperature for a wide range of pressures and air-fuel ratios.

The steps involved in the calculation for the compression and expansion periods are shown in Table (7.3).

7.8.6 Programme Structure for Combustion Period

This period is defined as from the start of ignition to till 99 % of the cylinder charge is burnt or 99 % of the cylinder volume is occupied by the burnt gases, whichever occurs first. During the calculation for this period the MAIN routine calls the routine 'combust' to calculate the change in cylinder pressure, temperatures in the burnt and unburnt portions of the charge and the position of the flame front. The statistically averaged value of the measured cold level turbulence intensity variations were employed as input data for the turbulence parameter of the engine cylinder flow field. At the beginning of the quasi-time step, the flame front is allowed to propagate into the unburnt region for a distance determined by the computed turbulent flame speed. During its movement to the new position it traps a certain amount of fresh charge into the reaction zone and the trapped charge is assumed to undergo an adiabatic constant volume combustion process. The newly burnt mixture thus formed is allowed to mix completely with previously burnt gases to cause pressure and temperature rises in the burnt region. The burnt region is then allowed to expand into unburnt region until pressure equilibrium is established between the two regions. After heat transfer is allowed to take palce between both burnt and unburnt gases and the surrounding metal surfaces and the two regions are subjected to the effect of piston motion. Any disturbances in pressure equilibrium thus

Compression and Expansion Period Calculation

Enter the present step calculation.

Allow the cylinder charge to expand or compress adiabatically and hence estimate the new cylinder charge pressure and temperature.

Allow heat transfer to take place and find the new cylinder pressure and temperature after heat transfer.

End of step calculation and return.

Table (7.3) Calculation Steps during Compression and Expansion Period

produced is allowed to equilibrate again by the movement of flame kernal positions. The final pressure and temperatures of the gases at the end of time -step are then returned to the calling routine MAIN.

The routines which are associated with combustion period are as follows:-

COMBUST:- This routine calls to routine FLAME to do all necessary controls over the calling of the other routines for the combustion step calculation. By using the results computed by other routines, it calculates the change in cylinder pressure, burnt gas temperature and unburnt gas temperature at the end of the step calculation.

TURINT:- This routine holds the measured statistically averaged turbulence intensity variation against crank angle period. To save in computing time, the variations of turbulence intensity against engine crank angle period were fitted in polynomial form.

TURFLME:- This routine calculates the turbulent flame speed by using the Shchelkin type equation (76), Section (6.5), and by using the measured cold level turbulence intensity values which are held in the routine TURINT.

SHAPE:- This routine estimates the volume of the burnt gases enclosed by the flame front whose position and shapes are defined by the spline curves on horizontal sections across the flame envelope. The location of flame front was done by using the co-ordinate system as mentioned under section (7.4.7). This routine is also used to find the new flame front position when the volume of the burnt gases is given, by moving the flame front radially outwards until the enclosed volume is equal to the given value of the volume of the burnt gases.

CUBIC:- This routine fits a cubic spline curve which passes through the computed locations of the flame front and the cubic spline curve is then used to find the area enclosed by the flame kernal on each horizontal cutting section across the flame envelope.

COEFF:- This routine calculates the values of the coefficient of matrix of the cubic spline fitting routine by knowing the co-ordinates of the nodel points.

SOLVE:- This routine solves the coefficients of the cubic spline curve by solving the matrix which has been defined by the routine COEFF.

TIP:- This routine locates the positions where the flame front as defined by the spline curves touches the physical cylinder

Combustion Period Calculation

Enter the present time-step calculation.

Obtain the values of turbulence intensity from measured experimental results.

Calculate the turbulent flame speed using the Shchelkin model and taking into account of measured cold level turbulence intensities.

Allow the present flame front position to move a distance as determined by the calculated flame speed while subjecting to the physical cylinder boundary conditions.

Estimate the mass of newly trapped unburnt charge and evaluate the heat release due to combustion of the newly trapped charge.

Allow the newly burnt charge to mix thoroughly with already burnt charge and calculate the pressure rise in burnt region.

Allow the burnt gas region to expand into unburnt gas region, subjecting to the cylinder physical boundary condition, until pressure equilibrium is established between the two regions.

Allow distortion of the flame kernal if swirl is present.

Allow heat transfer to take place from burnt and unburnt charges to the surrounding wall and metal surfaces.

Calculate the pressure and temperature in burnt and unburnt regions after the heat transfer process.

Allow pressure equilibrium to take place between burnt and unburnt regions for any pressure differential which exists after heat transfer and piston movement.

Calculate the final change in pressure, temperatures of burnt and unburnt regions at the end of the time-step and check for completion of the combustion.

End of the time-step calculation and return.

Table (7.4) Calculation Steps During the Combustion Period

boundary on horizontal cutting sections.

These latter four routines (CUBIC, COEFF, SOLVE, TIP) were called once for each horizontal cutting section during each time step, so that sectional areas of burnt volume of gases can be estimated and hence the enclosed volume of the burnt charge by the flame front determined.

FLAME:- This is the routine controlling the calling sequence of the above routines so as to enable the calculation of the rises in pressure and temperatures during the quasi-time step. This routine also allows heat transfer to take place from burnt and unburnt charge to surroundings. It also imposes the piston movement effect on burnt and unburnt gases.

HTTRL:- This routine estimates the exposed areas of burnt and unburnt regions to heat transfer metal surfaces.

PROP:- This routine holds polynomials for thermodynamic properties of burnt and unburnt gases. It is the same routine as used in valve opening, compression and expansion periods calculation.

The steps which are involved in combustion period calculations are shown in Table (7.4).

7.9.0 Accuracy of the Engine Cycle Simulation Model with its associated Turbulent Flame Correlation

Computer predictions for spark ignition engine performance were made and the predicted results were compared with the experimentally observed ones, which include cylinder pressure development and local flame arrival times sensed at six different ionization probe locations (Section A.4). The comparison between predicted and experimental data were made for,

(i) Engine motoring conditions and

(ii) Engine running conditions.

The predicted and measured results for an engine operating conditions at 500rpm are shown in fig (7.10) and fig (7.11), and the good agreement between them confirms the accuracy and reliability of the modelling method for heat transfer and gas exchange processes.

For engine running conditions, comparison between predicted and experimental results were made at 950 and 1020 rpm, quarter throttle. The necessary turbulence intensity data were extrapolated from the measured results based on the observed linear variation of turbulence intensity with engine speed. The error due to this extrapolation is thought to be small or negligible as the extrapolation has been done near the engine speeds employed in

in the experiment. But extrapolation of the measured turbulence intensity to far away high engine speed ranges was not done due to possible appreciable extrapolation error. Thus comparison between predicted and measured results is not made for high engine speeds due to lack of reliable turbulence intensity data. Also it is very difficult to obtain a stable engine operating point at low speed and full throttle condition, and hence comparisons are limited to low engine speeds and quarter throttle case only.

The predicted results show a very good agreement with both the measured local flame arrival times and the cylinder pressure diagram. The predictions of engine performance were made using the computer simulation model which incorporates Shchelkin's correlation (76) for turbulent flame propagation. As Shchelkin's correlation (76) allows room for adjustment of the response of the flame to suit different types of turbulent combustion situations (Section 6.0), the response of the flame to the measured cold level engine cylinder turbulence was adjusted by adjusting the value of the constant "K" in Shchelkin's formula (76) until a reasonable agreement between predicted and experimentally measured results was obtained.

$$\frac{U_T}{U_L} = \left[1 + \left(\frac{k\, u'}{U_L}\right)^2 \right]^{\frac{1}{2}} \quad - \text{Shchelkin (76)}$$

The value of 6.928 for the constant "K" in the above equation is found to give an acceptable agreement with both the measured cylinder pressure diagrams and the local flame arrival time. Shchelkin (76) suggests a value of 2.0 for the constant "K" for a steady state turbulent flame at atmospheric pressure. The higher value of the constant "K" used in our case suggests that the response of the turbulent flame front to cold level turbulence under engine combustion conditions is much higher than the response of a steady turbulent flame at atmospheric pressure. This fact is also confirmed by Lancaster (42) who suggests a value of 4 for the constant "K" in Shchelkin's Equation (76) at an engine speed of 1500 rpm.

Regarding the accuracy of the suggested value of the constant "K" in the present case, it is estimated to be within 25 % of the prescribed value. The above estimate is based on the error allow-

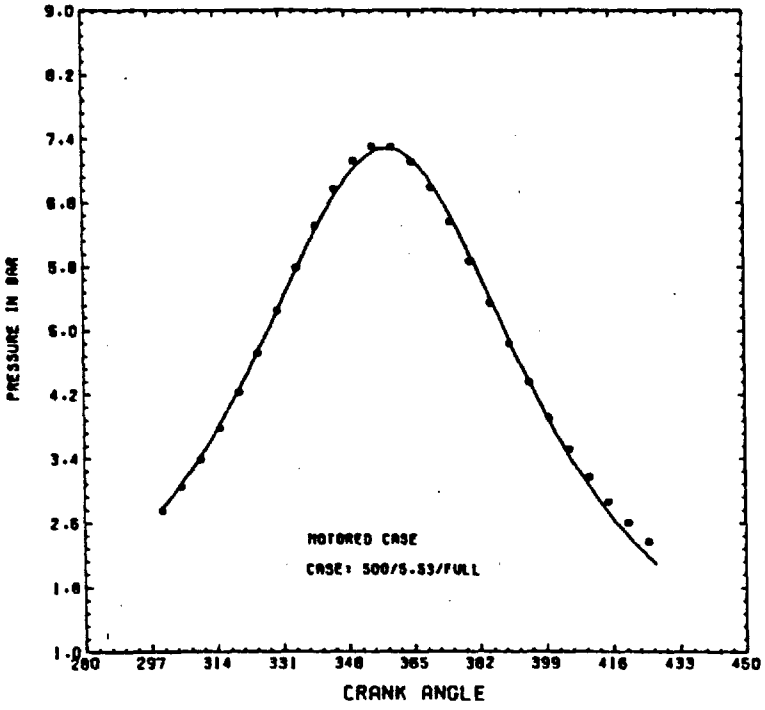


Fig (7.10) Predicted and Measured Cylinder Pressure Diagrams Speed 500rpm. Compression ratio 5.53, Throttle Full Open.

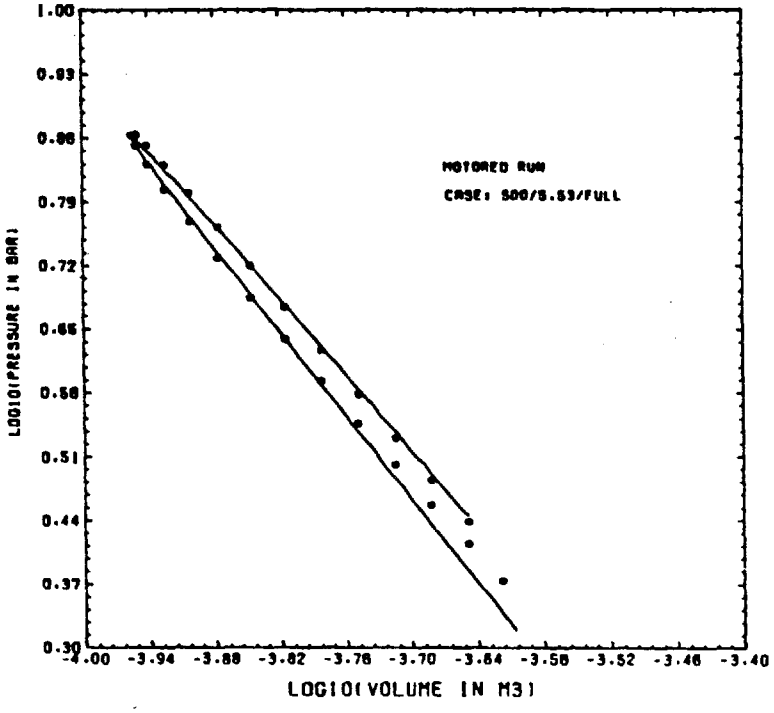
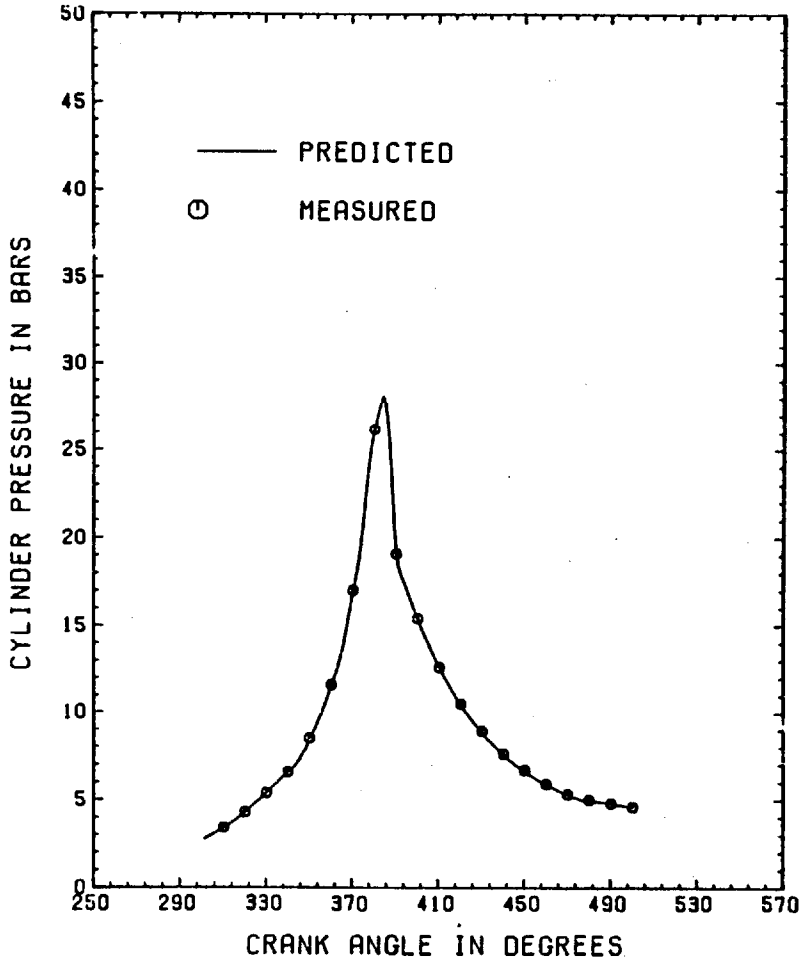


Fig (7.11) Predicted and Measured Cylinder Pressure Diagrams on log.log Scale. Speed 500rpm, compression ratio 5.53, Throttle Full Open.



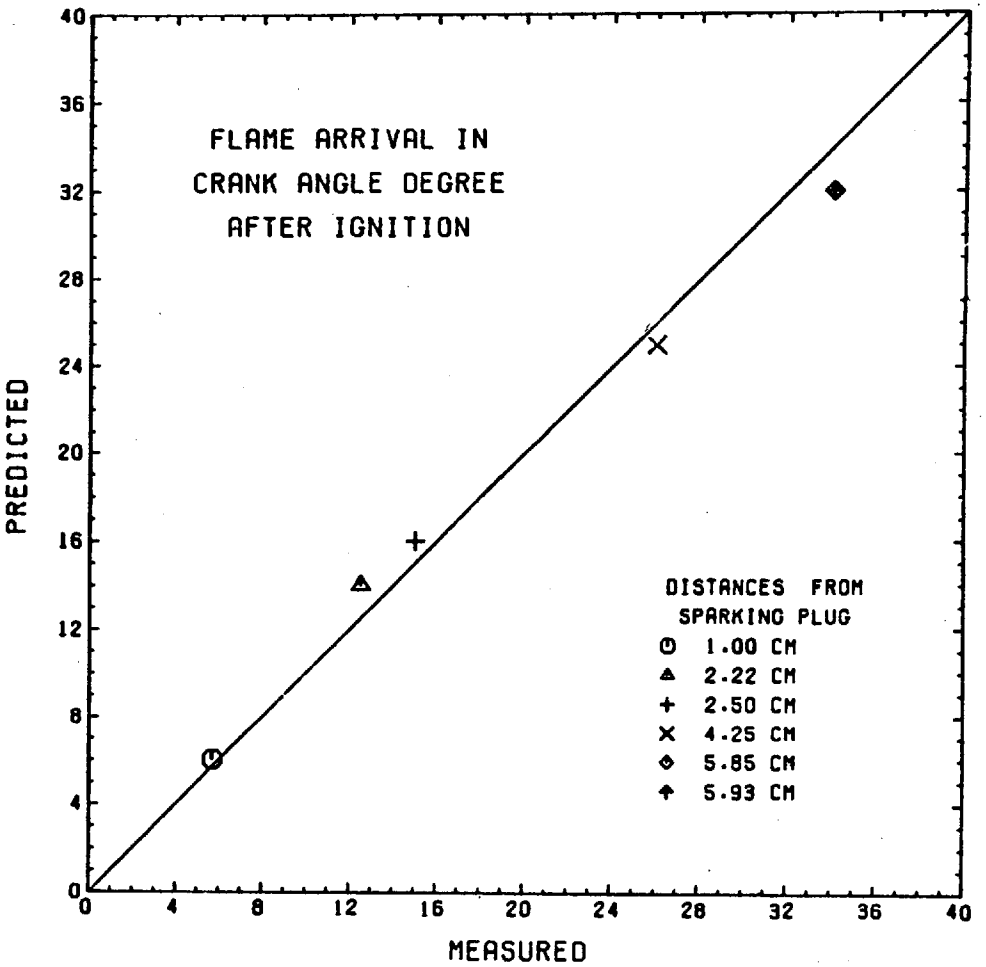


Fig (7.12) Comparison of Measured and Predicted Results on Cylinder Pressure and Flame Arrival Time (950 RPM IGN. 338 PHI 1.0 COMP. RATIO 5.53)

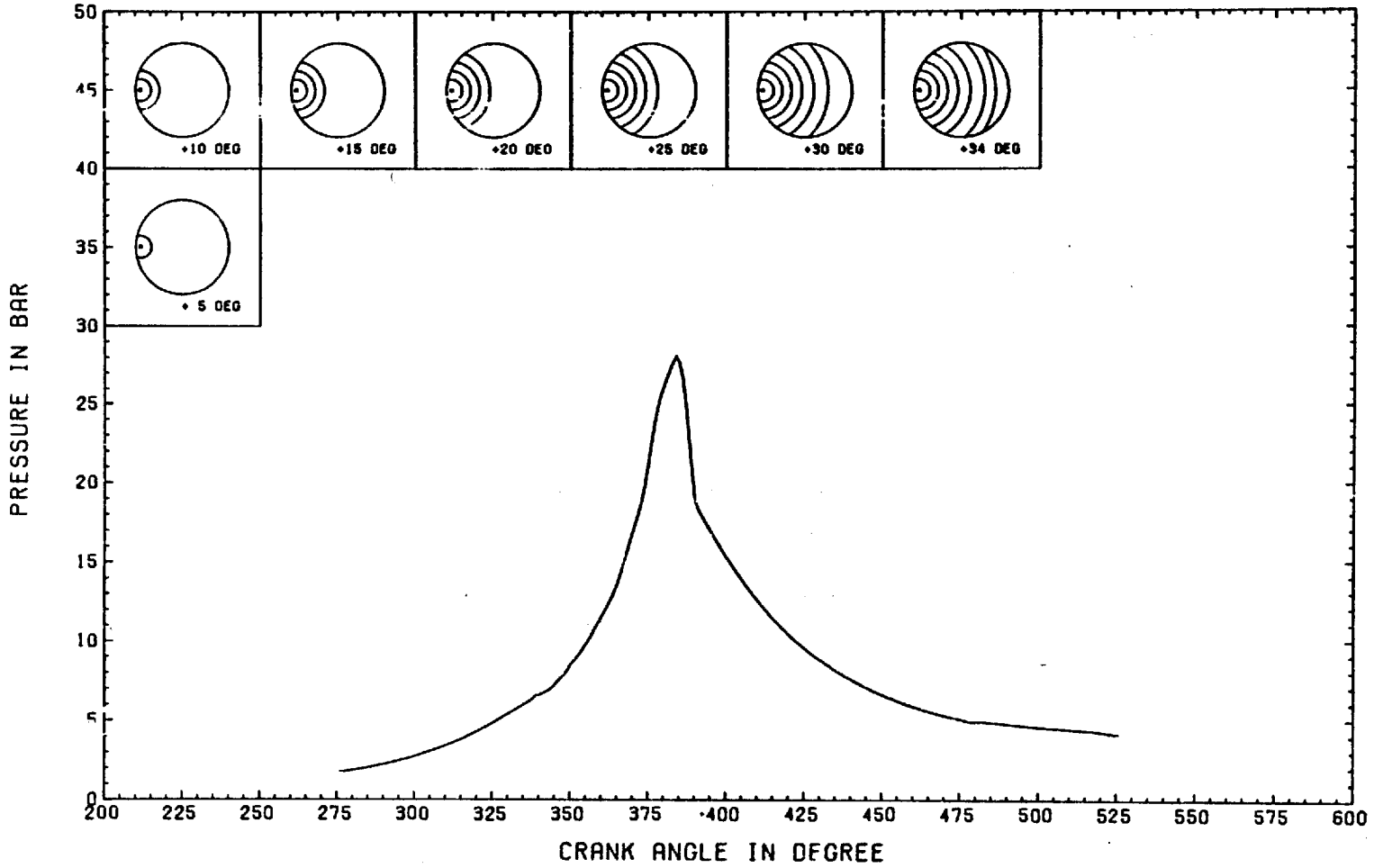


Fig (7.13) Predicted Flame Propagation Pattern and Cylinder Pressure Diagram 950 RPM

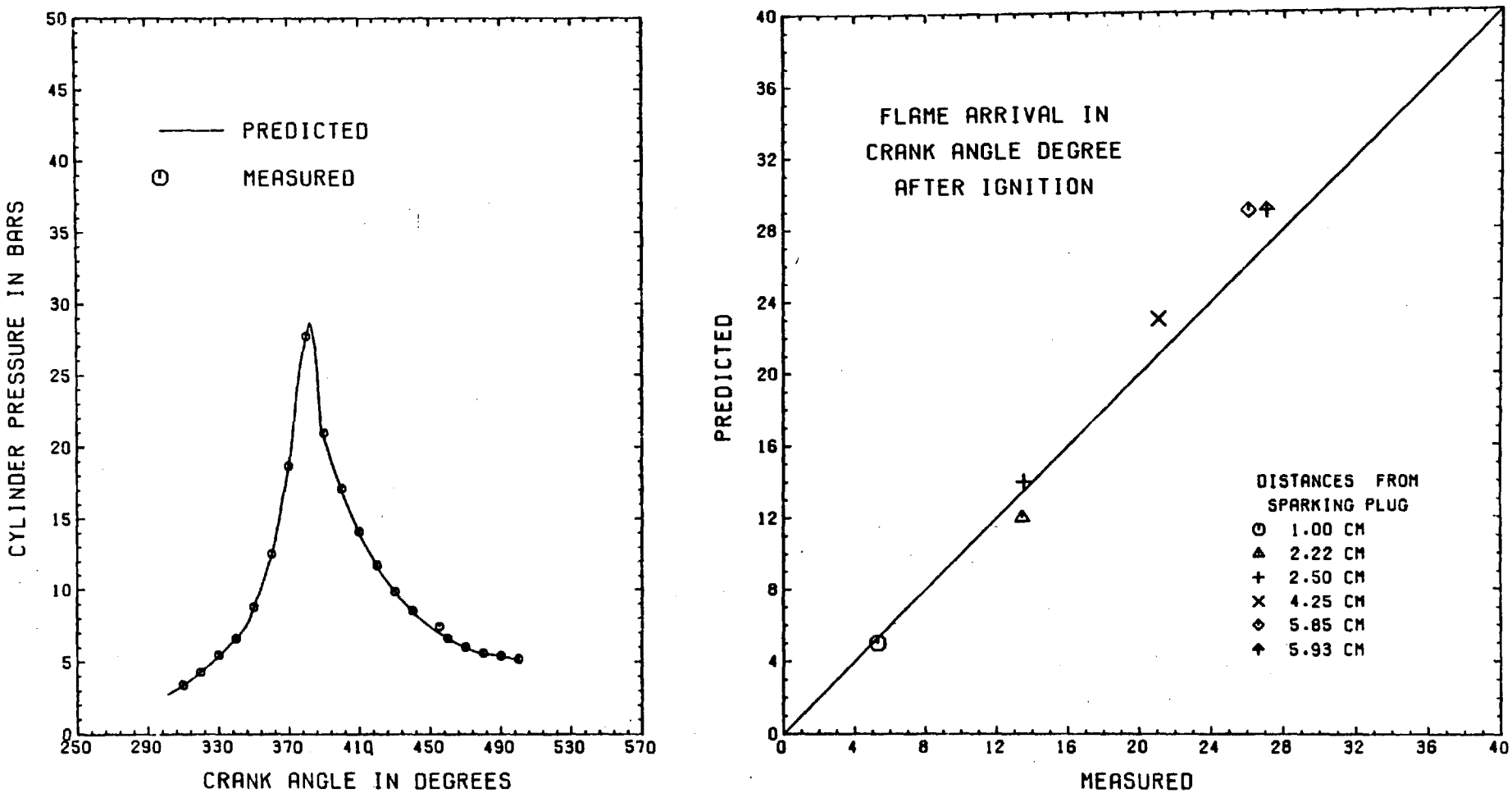


Fig (7.14) Comparison of Measured and Predicted Results on Cylinder Pressure and Flame Arrival Time
(1020 RPM IGN. 338 PHI. 1.0 COMP. RATIO 5.53)

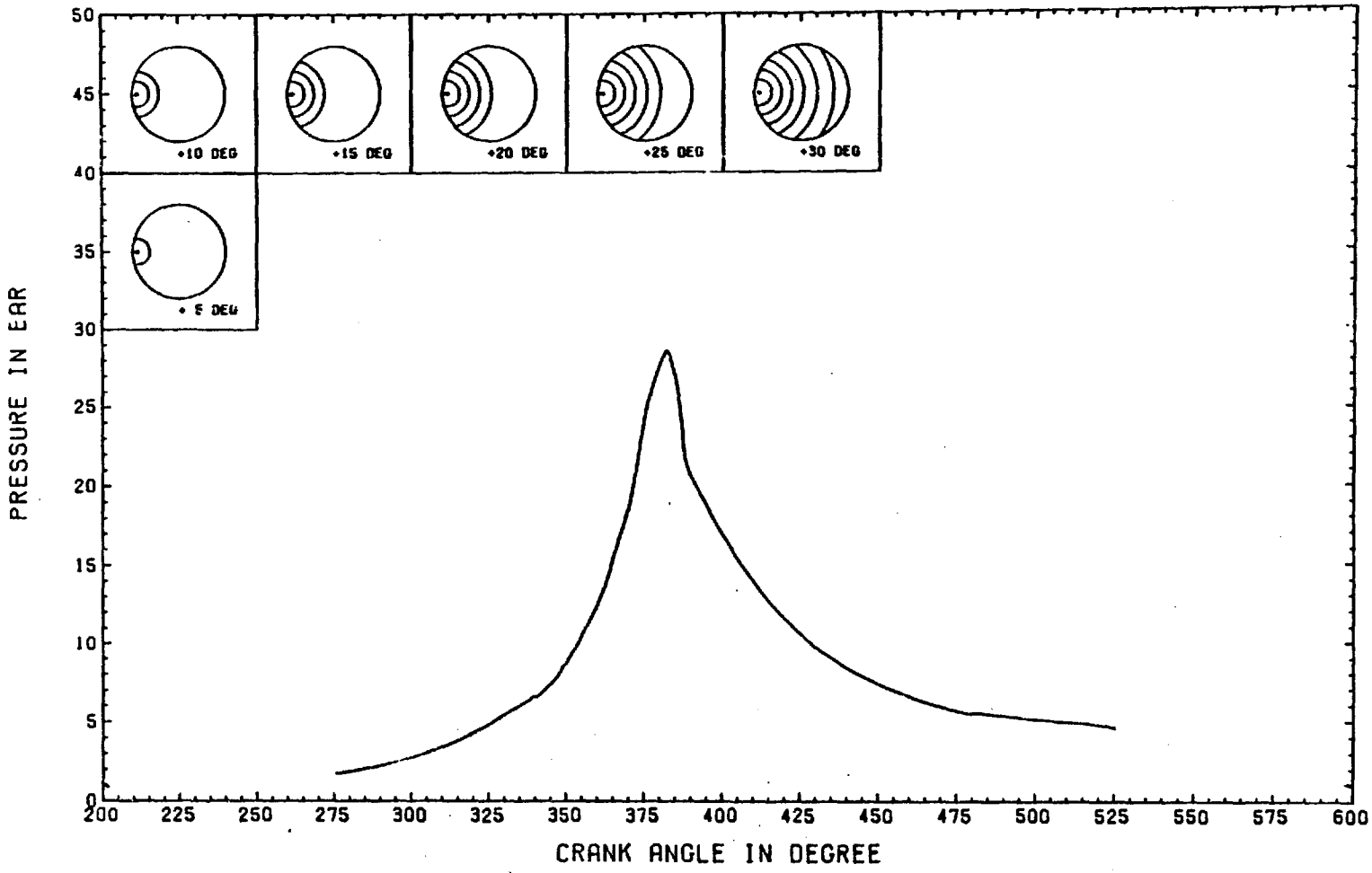


Fig (7.15) Predicted Flame Progagation Pattern and Cylinder Pressure Diagram RPM(1020)

ance of 15% for input turbulence intensity data (Section 5.0) together with the possible experimental error in measured cylinder pressure and local flame arrival times plus the allowance of accuracy for numerical and modelling methods used in constructing the engine cycle simulation programme. Though Lancaster (42) did not discuss accuracy, his turbulent flame speed data which were used for evaluating the value of the constant "K" were derived from the mass burning rate diagram which in turn was estimated from the measured cylinder pressure diagram. Thus the accuracy of Lancaster's turbulent flame data (42) seems to be less than that of the present case where local flame front arrival times were directly measured by the ionization technique. Also Lancaster's turbulence data (42) were based on the results of a single location measurement where as the turbulence intensity data in present case were based on the results of measurements made at nine different locations within the combustion chamber (Section 4). Those above factors may explain the reason for the difference in value of the constant "K" suggested by Lancaster (42) and that of the present work.

It is believed that the suggested value of the constant "k" with the specified limits in Shchelkin's Equation (76) will hold true for predicting turbulent flame propagation phenomenon in spark ignition engines.

7.10.0 Conclusions and Recommendations

The research investigation to establish the turbulence flow field and its influence on subsequent turbulent combustion field in an engine cylinder has been carried out successfully.

The research effort establishes the nature of the cold level turbulence field in the cylinder of the employed engine in very close detail and it is believed that the results provide very useful information for understanding the complex nature of the aerodynamic field within the engine combustion chamber and also serve as a useful source of experimental data for those workers in the turbulence prediction field.

The developed S.I. engine cycle simulation programme confirms the praticability of constructing a prediction model with detail consideration of the turbulent combustion stage. The developed computer model not only offers very useful detailed information of the combustion stage including flame propagation patterns, but also the modelling technique serves as a very useful guide for constructing future computer simulation

models.

The proposed laminar and turbulent flame speed models are believed to hold true for general spark ignition engine simulation applications and their use together with the above simulation technique for an S.I. engine cycle will avoid the use of arbitrary constants, given prior knowledge of the turbulence flow field parameters.

The agreement of the predicted results with the measured local flame arrival times and the cylinder pressure development confirms the accuracy and the reliability of the employed simulation technique and of the incorporated turbulent flame propagation model. It is firmly believed that the results of the present reserach effort will help in understanding the complex phenomena associated with the turbulent combustion and in developing more realistic future computer simulation models in spark ignition engine field.

It is recommended future research effort should be directed in developing a realistic prediction model for the flow pattern and the turbulence within engine cylinders of various geometries and that this prediction model be incorporated into a computer simulation program of the present type for the spark ignition engine cycle. The proposed model, together with chemical Kinetic considerations, will serve as an ideal development tool to be used during the design stage for the study of the influence of various proposed engine combustion chamber geometries on its performance and pollutant emission characteristics.

REFERENCES

1. Semenov, E.S., "Studies of Turbulent Glas Flow in Piston Engines", Combustion in Turbulent Flow, Khitrin, L.N., ed. 1959, Translated 1963.

2. Hovatin, M. and Hassman, A.W., "Measurement of Air Movements in Internal Combustion Engine Cylinders" D.I.S.A. Information, No. 8, July 1969.

3. Hassan, H. and Dent, J.C., "The Measurement of Air Velocity in a Motored Internal Combustion Engine Using a Hot Wire Anemometer", Combustion Engine Group, Proc. Inst. Mech. Engs., Vol. 185, No. 50 (1971).

4. Chen, L.L., Myers, P.S. and Uyehara, O.A., "Air Velocity Measurements in Engine by Vortex Shedding" SAE Paper 741057.

5. Arnold, M.J., Tindal, M.J., and Williams, T.J., "Measurement of Induction Gas Velocities in a Reciprocating Engine Cylinder". SAE Paper 72045.

6. Winsor, R.E. and Patterson, D.J., "Mixture Turbulence - A Key to Cyclic Combustion Variation" SAE Paper 730086.

7. Davies, P.O.A.L. and Fisher, M.J.,"Heat Transfer from Electrically Heated Cylinders" Proc. R. Society P489-526. 1964.

8. Woods, W.A. and Ghirlando, R., "Radial Flow in an Engine Cylinder near the End of Compression", Proc. I. Mech. E., Paper C82/75.

9. Ma, T.H., "Effect of Cylinder Charge Motion on Combustion" Proc. I. Mech. E. Paper C81/75.

10. Gajendra Babu, M.K. and Murthy, B.S., "Simulation and Evaluation of a 4 stroke Single Cylinder Spark Ignition Engine" SAE Paper 750687

11. Lucas, G.G. and James, E.H., "A Computer Simulation of a Spark Ignition Engine", SAE Paper 30053.

12. Hirogasu, H. and Kodata, T, "Computer Simulation for Combustion and Exhaust Emission in Spark Ignition Engine", 15th Symposium (International) on Combustion. The Combustion Institute, 1975.

13. Philips, R.A. and Orman, P.L., "Simulation of Combustion in a Gasoline Engine Using a Digital Computer". Advances in Automatic Technology Part IV, Pergamon Press, Oxford, 1966.

14. Benson, R.S., Annand, W.J.D. and Baruah,P.C., "A Simulation model for a Single Cylinder Flour Stroke Spark Ignition Engine", Inst. J. Mech. Science 17. P97-124, (1975).

15. Eichelberg, A.G., "Some New Investigations on Old Combustion Engine Problems", Engineering, Vol. 148 1939.

16. Annand, W.J.D., "Heat Transfer in the Cylinders of Reciprocating Internal Combustion Engines", Proc. I. Mech. E., Vol. 177, 1963.

17. Woschni, C.G., "A Universally Applicable Equation for the Instantaneous Heat Transfer Coefficient in the Internal Combustion Engine", SAE Paper 670931.

18. Tasaka, H. and Matsuoka, "Gas Exchange Process of Four Stroke Spark Ignition Engines Under the Condition of Partial Load, at Medium or Low Speed", Bul. of the JSME p450-458, Vol. 20, 1977.

19. Andrews, G.E., Bradley, D. and Lwakabambe, S.B., "Turbulence and Turbulent Flame Propagation - A Critical Appraisal". Combustion and Flame, Vol. 24 June 1975, p285-330.

20. Kim, Y., "Theoretical Analysis in Burning Velocities

in a Spark Ignition Engine", Trans. Japan. Soc. Mech. Engineers. No. 337.

21. Kim, Y., "Cyclic Variations Characteristics of Early Flame Propagation in a Spark Ignition Engine", Trans. Japan, Soc. Mech. Engineers. No. 343.

22. Shcetinkov, E.S., "Calculation of Flame Propagation in a Turbulent Flow". Combustion in Turbulent Flow Seminar on Combustion. Israel Program for Scientific Translations, 1963.

23. Mizutini, Y., "Amplification of Turbulence Level by a Flame and Turbulent Flame Velocity", Combustion and Flame, Vol. 19, p.203-212 (1972).

24. Edmonson, H. and Heap, M.P., "The Relation between Flame Pressure and Burning Velocity", Combustion and Flame, Vol. 13, p.323.

25. Vinckier, J. and Van-T iggeler, A., "Structure and Burning Velocity of Turbulent Premixed Flames", Combustion and Flame, Vol 12, p. 561. 1968.

26. Lefebere,A.H. and Reid, R., "The Influence of Turbulence on the Structure and Propagation of Enclosed Flames", Combustion and Flame, p355-366, Vol. 10, 1966.

27. Palm-Leis, A. and Strehlow, R.A., "On Propagation of Turbulent Flames", Combustion and Flame, p355-366 Vol. 10, 1966.

28. Markel, J.D., "FFT Pruning", Audio and Electro-Acoustics, IEEE Trans Vol. 19, p.305-311, December 1971.

29. Cochran, W.T., "What is Fast Fourior Transform", Audio and Electro-Acoustics, IEEE Trans, Bol. 15, 1967.

30. Weiver, C.S., Groeben, J.V.D., Montey, P.E., Toole, J.G., Cole, C.A., Fitzgerald, J.W., Lawrence, R.W., "Digital

Filtering with Applications to Electro Cardiogram Processing", Audio and Electro-Acoustics, IEEE Trans. Vol. 16, 1968.

31. Hempson, J.E.O., "Instrumentation Problems of Internal Combustion Engine Development", Paper ADP 3/61. The Inst. Mech. Engineers.

32. Diko, E., "Electronic Measuring Techniques for Use on Internal Combustion Engines", Bulletin IRCA Electric Traction on the Railways, 1961.

33. Heldt, P.M., "Effects of Piston Pin Off Set", Automotive Industries, 1953.

34. Steinbrenn er, H., "Measurements to Determine the Piston Ring Flutter in High Speed Reciprocating Engines", MTZ, Vol 22.

35. Furnhama, S., Tada, T., and Nakamura, T., "Some Measurements of the Piston Temperatures in a Small Type Gasoline Engine", Bul. of the Jap. Soc. Mech. Engs. Vol 7, 1964.

36. Kazachkov, R.V., "Measurement of the Piston Temperatur- of High Speed Internal Combustion Engines", Izmeritelnaya Tokhnika (Measurement Techniques), p.25-27 , English Translation, 1961.

37. Goschel, K.H., Guler H.P., and Steinbrenner, H., "Piston Temperature Measurements On a High-Speed High-Powered Diesel Engine", MTZ Vol. 22, 1961.

38. Brock, E.E. and Glasspoole, A.J., "The Thermal Loading of Cylinder Heads and Pistons on Medium Speed Oil Engines", Inst. Mech. Engs., Symposium on Thermal Loading of Diesel Engines, 1964.

39. Burgess, D.C., "Telemetery in Internal Combustion Engines" British Communications and Electronics, Vol. 19, 1963.

40. Westbrook, M.H., "A Telemetering System for Piston Engine

Research", Internal Telemetering Conference, London, Vol. 1, 1963.

41. Lancaster, D.R., "Effects of Engine Variables on Turbulence in a Spark Ignition Engine", SAE Paper 760159.

42. Lancaster, D.R., Kreger, R.B., Sorenson, S.C. and William, L.H., "Effects of Turbulence on Spark Ignition Engine Combustion", SAE Paper 760160.

43. Westbrook, M.H. and Munro, R., "The Telemetering of Information from a Working Internal Combustion Engine" Journal of Eng. for Power, p247-254, Vol.89, 1967.

44. Harrow, G.A., "Some Applications of Basic Combustion Research to Gasoline Engine Development Problems". SAE Paper 681765.

45. Arrigoni, V., Calvi, F., Cornetti , G.M. and Pozzi, U., "Turbulent Flame Structure as Determined by Pressure Development and Ionization Intensity", SAE Paper 730088

46. Croom, B.H. and Leyhe, E.W., "Thermodynamic, Transport and Flow Properties for the Products of Methane Burned in Oxygen-Enriched Air", NASA, SP3035, 1966.

47. Eyzat, P. and Guibet, J.C., "A New Look at Nitrogen Oxides Formation in Internal Combustion Engines", SAE Paper 680124.

48. Babu, M.K.G., and Murthy, B.S., "Simulation and Evaluation of a Four Stroke Single-Cylinder Spark Ignition Engine" SAE Paper 750687.

49. Samaga, B.S. and Murthy,B.S., "On the Problem of Predicting Burning Rates in a Spark Ignition Engine", SAE Paper 750688.

50. Povinelli, L.A. and Fuhs, A.E., "The Spectral Theory of Turbulent Flame Propagation", 8th Symposium on Combustion. p554-506.

51. Snyder, W.T., "Preliminary Observation of a One-Dimensional Turbulent Propane-Air Flame", 8th Symposium on Combustion, p573-581.

52. Blizard, N.C. and Keck, J.C., "Experimental and Theoretical Investigation of Turbulent Burning Model for Internal Combustion Engines", SAE Paper 740191.

53. Wersborg, B.L., Howard, J.B. and Williams G.C., "Physical Mechanism in Carbon Formation in Flames", 10th Symposium (International) on Combustion 1972.

54. N.A.C.A., "Basic Considerations on the Combustion of Hydro-carbon Fuels with Air", Report No. 1300, Propulsion Chemistry Division, Lewis Flight Propulsion Laboratory.

55. Mullins, B.P., "Studies on the Spontaneous Ignitions of Fuels Injected into a Hot Air Stream V Ignition Delay Measurement on Hydrocarbon", Fuel, Vol. 32, 1953.

56. Jost, W., "Reactions of Adiabatically Cômpressed Hydro-carbon - Air Mixtures. 3rd Symposium on Combustion, Williams and Wilkins, Baltimore.

57. Combustion Colloquim, "Transport Phenomena, Ignition, Altitude Behaviour and Sealing of Aero Engines", London Butterworths Scientific Publications, 1956.

58. Von. H. Teichmann "Reaktionskinetische Untersuchungen Zum Kiopf v organg II", Z. Elecktrochem, Vol. 47, p302-305, 1941.

59. Curry, S., "A Three Dimensional Study of Flame Propagation in a Spark Ignition Engine", SAE Trans, p628-650, Vol. 71, 1963.

60. Kastner, L.J., Williams, T.J. and White, J.B., "Poppet Inlet Valve Characteristics and their Influence on the Induction Process", Proc. I. Mech. E., Vol. 178, Pt. 1, No. 36.

61. Woods, W.A. and Khan, S.R., "An Experimental Study of Flow Through Poppet Valves", Proc. R. Mech. E., Vol. 182 Pt 3 D.

62. Woods, W.A. and Khan, S.R., "Discharge From a Cylinder Through a Poppet Valve to an Exhaust Pipe", Proc. I. Mech. E., Vol. 182 Pt 3 H.

63. Spalding, D.B., "The ESCIMO Theory of Turbulent Combustion" Heat Transfer Section Report HTS/76/13. Mechanical Engineering Department, Imperial College, London.

64. Le Feuvre, T., Myers, P.S. and Uyehara, O.A., "Experimental Instantaneous Heat Fluxes in a Diesel Engine and their Correlation", SAE Paper 690467.

65. Pflaum, W., "Heat Transfer In Diesel Engines with and without Pressure-Charging", Engineers Digest Vol. 22, No. 7, July 1961.

66. Dent, J.C. and Salama, N., "Turbulence Structure in the Spark Ignition Engine", Proc. I. Mech. E., Paper C83/75.

67. Morse, A.P., "Laser-Doppler Measurements in Reciprocating Engines", Diesel Engine Air FLow Seminar, Kings College, London, September, 1977.

68. Ricardo Consulting Engineers, "The Application of a LDV to Study Flow Rig Tests", Diesel Engine Air Flow Seminar, Kings College, London, September, 1977.

69. Newhall, H.K., "Kinetics of Engine-generated Nitrogen Oxides and Carbon Monoxide", Twelfth Int. Symposium On Combustion, 1969, p603, Combustion Institute, Pittsburgh.

70. Lee, D.W. "A Study of Air Flow in an Engine Cylinder" NACA TR No. 651, 1938.

71. Collis, D.C. and Williams, N.J., "Two Dimensional Convection form Heated Wires at Low Reynolds Numbers", J.

Fluid Mech. 1959, 6, 3, 357.

72. Willis, D.A. Meyer W.E. and Birnie, C. Jr, "Mapping of Air Flow Patterns in Engines with Induction Swirl", SAE Paper 660093.

73. Hinze, J.O., "Turbulence", Mc-Graw-Hill(Publication) 1959.

74. McAdams, W.H. "Heat Transmission", 3rd Ed., Mc-Graw-Hill, 1954.

75. Damkohler, G., "Z. Elektrochemie Angewandte Phys. Chem.", 46, 601, 1940 (English Translation NACA TM 1112, 1947).

76. Shchelkin, K.D., "Zh. Eksp. i. Teoret. Fiz", 13, 520, 1943. (English Translation NACA TM 1110, 1947).

77. Summerfield, M., Reiter, S.H., Kebely, V. and Mascolo, R.W., "Jet Propulsion", 24, 254, 1954.

78. Summerfield, M."Jet Propulsion", Vol. 20, 485, 1956.

79. Bhaduri, D., "Mechanism of Flame Propagation", J. Sci. and Industrial Research. Vol. 23, 502, 1964.

80. Wohl, K., Shore I., Rosenburg, H., and Weil, C.W., "The Burning Velocity of Turbulent Flames", 7th Symposium (Int) on Combustion, Williams and Wilkins, Baltimore, 1953.

81. Wohl, K., "Theory of Turbulent Burning Velocity", Ind. Eng. Chem. 47, 825, 1955.

82. Kalovity, B., "Open Turbulent Flames", Fourth Symposium (International) on Combustion, Williams and Wilkins, Baltimore, 1953.

83. Kalovity, B., "Selected Combustion Problems" p. 248 Butterworths, London 1954.

84. Semenov, N.N., "Progress of Phys. Sci. (USSR)", Translation NACA, TM 1026 (1942). Vol. 24, No. 4.

85. Tanford, C. and Pease R.N., "Theory of Burning Velocity - The Square Root Law for Burning Velocity", J. Chem. Phys., Vol. 15, p861-865, 1947.

86. Dugger, G.L. and Graab, D.D., "Flame Velocities of Hydrocarbon - Oxygen - Nitrogen Mixtures", Fourth Symposium (International) on Combustion, Williams and Wilkins, Baltimore, 1953.

87. Dugger, G.K. and Simon, D.M., "Prediction of Flame Velocities of Hydrocarbon Flames"., Fourth Symposium, (International) on Combustion, Williams and Wilkins, Baltimore, 1953.

88. Zeleznik, F.J., "Combustion Modelling in Internal Combustion Engines"., Combustion Science and Technology, 12, 159, 1975.

89. McBride, B.J., Heimel, S., Ehlers, J.G. and Gordon, S., "Thermodynamic Properties to 6000 K for 210 Substances Involving the First 18 Elements", NASA SP3001, 1963.

90. Taylor, C.F., "The Internal Combustion Engine in Theory and Practice", Vol II, The M.I.T. Press, 1968.

91. Thermal Laboratory, "JANF Thermochemical Data Tables", Joint Army, Navy, Air Force, Thermochemical Panel. ARPA Programmce, USAF Contract AF 33(616)-6149. Dow Chemical Corporation, Midland, Michigan, U.S.A.

92. Nyein, C., "A Study of the Effect of Value Timing on Nitric Oxide Emission", M.Sc. (Thesis), Thermal Power Station, Mech. Eng. Department, Imperial College, London. (1974).

93. Stotter, A., "Heat Transfer in Piston Cooling", SAE

Trans., Paper 660757.

94. Rouse, H. and Howe, J.W., "Basic Mechanics of Fluids" John Wiley & Sons Inc., New York.

95. Bradshaw, P., "Experimental Fluid Mechanics", Pergamon Press, Oxford, New York - Toronto.

96. Gajendra Babu, M.K., Tanakiraman, P.A. and Murthy, B.S., "Measurement of Exhaust Gas Velocity in an Internal Combustion Engine", SAE Paper, 750689.

97. Kuehl, D.K., "Laminar Burning Velocities of Propane Air Mixtures", Eighth Symposium (International) on Combustion, Baltimore, 1962.

98. Tindal, M.J. "The Use of Hot Wire and Vane Anemometer Techniques in the Measurement and Prediction of Cylinder Swirl", Diesel Engine Air Flow Seminar, King's College, London, September, 1977.

99. Benson, B.S., Annand, W.J.D. and Baruah, P.C., "A Simulation Model including Intake and Exhaust Systems for a Single Cylinder Four Stroke Cycle Spark Ignition Engine", Inst. J. Mech. Science. Vol. 17, p97-124, 1975.

100. Knight, B.E., "The Problem of Predicting Heat Transfer in Diesel Engines", Proc. R. Mech. E., Symposium on Thermal Loading of Diesel Engines, Paper 6, Vol. 179, Part 3C.

101. Shroff, H.D. and Hodgetts, D., "Simulation and Optimization of Thermodynamic Processes of Diesel Engine", SAE Paper 740194.

102. Krieger, R.B. and Borman, G.L., "The Computation of Apparent Heat Release for Internal Combustion Engines", ASME Paper 66-WA/DGP-4, 1966.

103. Kastner, L.J., Tindal , M.J. and Williams, T.J., "Velocity

and Rate of Flow Measurements in Internal Combustion Engines", Symposium on Accuracy of Electronic Measurements in Internal Combustion Engine Development. Proc. I. Mech. E., Vol. 180, Pt 3 G.

104. Von Tiggelen, A., and Decklers, J., "Chain Branching and Flame Propagation", Sixth Symposium (International) on Combustion, New York, 1957.

105. Keenan, J.H. and Kaye, J., "Thermodynamic Properties of Air, Products of Combustion and Component Gases", John Wiley & Sons, Chapman Hall, London, 1948.

106. Griffin, M.D., Anderson, J.D. and Diwakar, R., "Navier-stroke Solutions of the Flow Field in an Internal Combustion Engine", AIAA Journal, Vol. 14, No. 12, December, 1976.

107. Diwakar, R., Anderson, J.D. and Griffin, M.D., "Inviscid Solutions of the Flow Field in an Internal Combustion Engine", AIAA Journall, Vol. 14, No. 12, December, 1976.

108. Dent, J.C. and Derham, J.A. "Air Motion in A Four-Stroke Direct Injection Diesel Engine", Proc. Inst. Mech. Engs. Vol. 188, 21/74.

109. Otnes, R.K. and Enochson, L., "Digital Time Series Analysis", A Wiley - Interscience Publication.

110. Barton, R.K. Lestz, S.S. and Meyer, W.E. "An Empirical Model for Calculating Cycle-by-Cycle Cylinder Gas Motion and Combustion Variations of a Spark Ignition Engine", SAE Paper 710163.

111. Witze, P.O., "Measurments of the Spatial Distribution and Engine Speed Dependence of Turbulent Air Motion in and I.C. Engine", SAE Paper 770220.

112. Gussak, L.A. and Turkish, M.C. "Lag-Process of Combustion and its Application in Automobile Gasoline

Engines", Proc. Inst. Mech. Engs. Paper C257/76.

113. James, E.H. and Lucas, G.G., "Turbulent Flow in Spark Ignition Engine Combustion Chambers", SAE Paper 750885.

114. Heimel, S. and Weast, R.C., "Effect of Initial Mixture Temperature on the Burning Velocity of Benzene - Air, n-Heptane-Air and Isooctane-Air Mixtures", sixth Symposium (International) on Combustion. p296-302.

115. Leason, D.B., "Turbulence and Flame Propagation in Premixed Gases", Fuel, Vol. 30 p 233-239

116. Glassman, I., "Combustion", Academic Press, New York-San Francisco-London, 1977.

117. Fenn, J.B. and Calcote, H.F., "Activation Energies in High Temperature Combustion", Fourth Symposium (Internaitonal) on Combustion.

118. Golovina, E.S. and Fyodorov, G.G., "Influence of Physical and Chemical Factors on Burning Velocity", Sixth Symposium (International) on Combustion.

119. Sitkei, G. and Ramanaial, G.V., "A Rational Approach for Calculation of Heat Transfer in Diesel Engines", SAE Paper 720027.

120. Wallace, W.B., "High Output Medium Speed Diesel Engine Air and Exhaust System Flow Losses". Proc. I. Mech. Engrs. Vol 182, Pt 3D.

121. Kopa, R.D., Hollander, B.R. and Hollander, F.H., "Combustion Temperature, Pressure and Products at Chemical Equilibrium", S.A.E. Technical Progress Series, Vol 7

122. Jacob, M. and Hawkins, G.A., "Elements of Heat Transfer", John Wiley & Sons, Inc., London-New York.

123. Laws, A.M., Parker D.A. and Turner, B., "Piston Movement as a Source of Engine Noise" Paper 1/6 FISITA Congress 1972.

124. Ohigashi, S., Hamamoto, Y., and Tanabe, S., "Swirl--Its Measurement and Effect on Combustion in a Diesel Engine", Inst. Mech. Eng. Symp. on Air Pollution Control in Transport Engines, 1971.

Appendix (A.1)

Combustion Products Properties and Combustion Temperature

The properties of combustion products and the combustion temperatures as used in S.I. engine simulation programme were computed by assuming equilibrium conditions in the combustion products. During the flame propagation process, the high temperature and pressure of the cylinder charge makes the reaction rates so high that nearly all species attain equilibrium. But during the expansion process after the completion of combustion, some minor product species such as nitric oxide, hydroxide radicals etc. are known not to achieve equilibrium. This phenomenon of non-equilibrium is only important from the pollutant emission point of view (69), and does not affect the values of the properties predicted.

An equilibrium composition prediction programme was written considering 18 constituents of the combustion products, CO, CO_2, CH_4, H, H_2, OH, H_2O, C, O, O_2, O_3, NH_3, HCN, N_2, HNO_3, N, NO, NO_2. This allows a high degree of accuracy in the predicted properties of the combustion products.

A.1.1. Theoretical Considerations on Chemical Equilibrium:- If a chemical reaction involves n_R reactant species and n_p product species, the reaction can be represented as:-

$$\sum_{i=1}^{n_R} V_i A_i \underset{K_b}{\overset{K_f}{\rightleftharpoons}} \sum_{j=1}^{n_p} V_j' B_j$$

For chemical equilibrium of this reaction, the forward and reversed reaction rates are equal thus,

$$K_f \prod_{i=o}^{n_R} A_i^{V_i} = K_b \prod_{j=o}^{n_p} B_j^{V_j'}$$

The equilibrium constant of this reaction is defined as,

$$K_c = K_f / K_b = \left(\prod_{j=1}^{n_p} B_j^{V_j'} \right) / \left(\prod_{i=1}^{n_R} A_i^{V_i} \right)$$

The assumed chemical equilibrium reactions. The assumed chemcial equilibrium reactions are same as used by Kopa Et Al (121) and are shown below together with their equilibrium conditions.

Equilibrium Reaction	Equilibrium Condition
(1) $\frac{1}{2} O_2 \rightleftarrows O$	$k_1 = {}^{O}/_{O_2^{\frac{1}{2}}}$
(2) $O_2 \rightleftarrows {}^{3}/_{2}\, O_3$	$k_2 = {O_3}^{3/2}/_{O_2}$
(3) $\frac{1}{2}H_2 \rightleftarrows H$	$k_3 = H/{H_2}^{\frac{1}{2}}$
(4) $2H_2O \rightleftarrows 2H_2 + O_2$	$k_4 = {H_2}^2 . O_2/{H_2O}^2$
(5) $\frac{1}{2}O_2 + \frac{1}{2} H_2 \rightleftarrows OH$	$k_5 = OH/{O_2}^{\frac{1}{2}}.{H_2}^{\frac{1}{2}}$
(6) $CO_2 \rightleftarrows C + O_2$	$k_6 = C.O_2/CO_2$
(7) $CO \rightleftarrows C + \frac{1}{2}O_2$	$k_7 = C.{O_2}^{\frac{1}{2}}/CO$
(8) $CH_4 \rightleftarrows C + 2H_2$	$k_8 = C.{H_2}^2/CH_4$
(9) $\frac{1}{2} N_2 \rightleftarrows N$	$k_9 = N/{N_2}^{\frac{1}{2}}$
(10) $NO \rightleftarrows N + O$	$k_{10} = N.O/NO$
(11) $NO_2 \rightleftarrows \frac{1}{2}O_2 + NO$	$k_{11} = {O_2}^{\frac{1}{2}} . NO/NO_2$
(12) $NH_3 \rightleftarrows \frac{1}{2}N_2 + {}^{3}/_{2}H_2$	$k_{12} = {N_2}^{\frac{1}{2}} . {H_2}^{3/2}/ NH_3$
(13) $2HNO_3 + NO \rightleftarrows 3NO_2 + H_2O$	$k_{13} = {NO_2}^3 . H_2O/{HNO_3}^2 . NO$
(14) $HCN \rightleftarrows \frac{1}{2}H_2 + C + \frac{1}{2}N_2$	$k_{14} = {H_2}^{\frac{1}{2}} . C.{N_2}^{\frac{1}{2}}/HCN$

The above 14 chemical equilibrium conditions for the assumed reactions and the conservation of mass equations for C, H, O, N atoms (4 equations) are used to solve 18 unknown equilibrium compositions. The first three conservation of mass equations are expressed in terms of conservation of atomic ratios.

(15) Σ O atoms /Σ C atoms = Const (between reactant and product)

(16) Σ N atoms /Σ O atoms = Const

(17) Σ H atoms /Σ C atoms = Const

(18) Σ Atoms = Const

A.1.2 Solution Procedure:- This consists of initial estimates of equilibrium composition of CO_2, H_2O, N_2 and CO which are known to behave well over a wide range of equilibrium conditions (121). These estimates enable a solution to be found for the rest of the 14 components and new estimates to be made for initial four estimates. This iterative solution procedure is repeated until the error between initial estimates and corrected values lie within prescribed limits.

Equilibrium Constants:- These values of assumed 14 chemical equilibrium reactions were calculated by using Gibbs function ΔG, as defined by:-

$$\Delta G^{\circ} = -T.\Delta S + \Delta H$$

$$Ln(K_{eq}) = \frac{-\Delta G^{\circ}}{RT} = \frac{\Delta S}{R} - \frac{\Delta H}{RT}$$

The change in entropy ΔS and change in enthalpy ΔH of a reaction was calculated by knowing the specific enthalpy and entropy of reactants and products. These values were taken from NASA Tables for Thermochemical data of 210 elements (89) except for HNO_3, which is not listed in the above tables. The data for HNO_3 is taken from JANF Table (91). As the two tables employed a different datum, the data which were taken from JANF tables were transformed to the new datum as used by NASA Table (89). The datum used was that the enthalpy of formation$ of carbon (in crystal state), molecular hydrogen H_2, molecular oxygen O_2 and molecular nitrogen N_2 at 298.8 degree K were taken as zero. Computed equilibrium composition of the products for Octane + Air Mixture at several equivalent ratios (from very lean to rich), at different equilibrium pressures and temperatures are shown in fig (A.1.1) to fig (A.1.18).

A.1.3. Properties of Burnt Charges. The properties of the burnt charges were calculated by knowing the equilibrium composition of each individual component. The specific heat at constant pressure values for the components considered were taken from the above

mentioned two references.

Average Molecular Weight, M_{ave}

$$M_{ave} = \sum_{i=1}^{18} A_i \; M_i$$

Average Gas Constant, R_{ave}

$$R_{ave} = R_{universal}/M_{ave}$$

Average Specific Heat at Constant Pressure, $C_{p_{ave}}$

$$C_{p_{ave}} = \frac{1}{M_{ave}} \sum_{i=1}^{18} A_i \; C_{Pi}$$

Average Specific Heat at Constant Volume, $C_{v_{ave}}$

$$C_{v_{ave}} = C_{p_{ave}} - R_{ave}$$

The computed specific heat values at constant pressure and constant volume as a function of temperature are shown in fig (A.1.19) to fig. (A.1.21).

A.1.4 Adiabatic Combustion Temperature. The equilibrium composition predicition programme was augmented by a routine to find the adiabatic flame temperature, that is, the temperature at which the enthalpy balance (for constant pressure combustion) or internal energy balance (for constant volume combustion) occurs between the reactant and the combustion products.

Adiabatic Combustion Temperature at Constant Pressure Combustion Pressure. The condition for constant pressure combustion is the conservation of enthalpy content between reactants and combustion products. In mathematical form,

$$\left(\sum_{i=1}^{n_R} A_i \; h_i \right)_{reactant} \equiv \left(\sum_{j=1}^{n_p} B_j \; h_j \right)_{product}$$

From the specified initial conditions of the unburnt charge, that is the air-fuel ratio used, unburnt pressure and unburnt temperature values, the left hand side of the equation is fixed and can be evaluated. An initial guess for the combustion temperature is made which enables the evaluation of the right hand side of the expression. A correction of the initial estimate

of temperature is made by comparing the computed right hand side value with that of the left hand side of the expression. To attain rapid convergence, new estimate of combustion temperature is made by using the Newton-Ralphson method. Iteration stops when the error between the corrected value and estimated value lies within a prescribed limit.

Adiabetic Combustion Temperature for a Constant Volume Combustion Process:- For Const volume and combustion, the conservation of energy applies to the reactants and the products.

$$\left(\sum_{i=1}^{n_R} A_i \, u_i\right)_{\text{reactant}} \equiv \left(\sum_{j=1}^{n_p} B_j \, u_j\right)_{\text{Product}}$$

The initial conditions of the reactant enables the evaluation of the left hand side of the expression. To evaluate the right hand side, two unknowns, combustion product pressure and temperature, are involved. The classical approach is to make a guess at these two unknowns and these initial guesses are corrected again and again after evaluating the right hand side of the expression and comparing it with the value on the left hand side. This approach requires many iterative cycles before convergence in the final solution is reached. A different approach was therefore adopted which greatly reduced the number of iterations required. Instead of estimating the final pressure, a guess of the average gas constant value of the product was made. The variation of the gas constant value is small in the range of temperature of interest. The combustion pressure was evaluated by using the estimated combustion temperature and the average value of gas constant together with the knowledge of combustion product mass and combustion product volume. This enables the evaluation of the equilibrium composition and hence the right hand side of the expression. New estimates of combustion temperature and gas constant were made by using Newton-Ralphron method. Because of the small variation of the gas constant value within the temperature range of interest, only 1 or 2 iterations are required to a final estimate of the gas constant while 3 to 5 iterations are required to finalise the combustion temperature estimate. After obtaining the final values of temperature and gas constant combustion product pressure can be calculated.

Computed adiabatic combustion temperature at constant pressure and at constant volume are shown in fig (A.1.22) to fig (A.1.24).

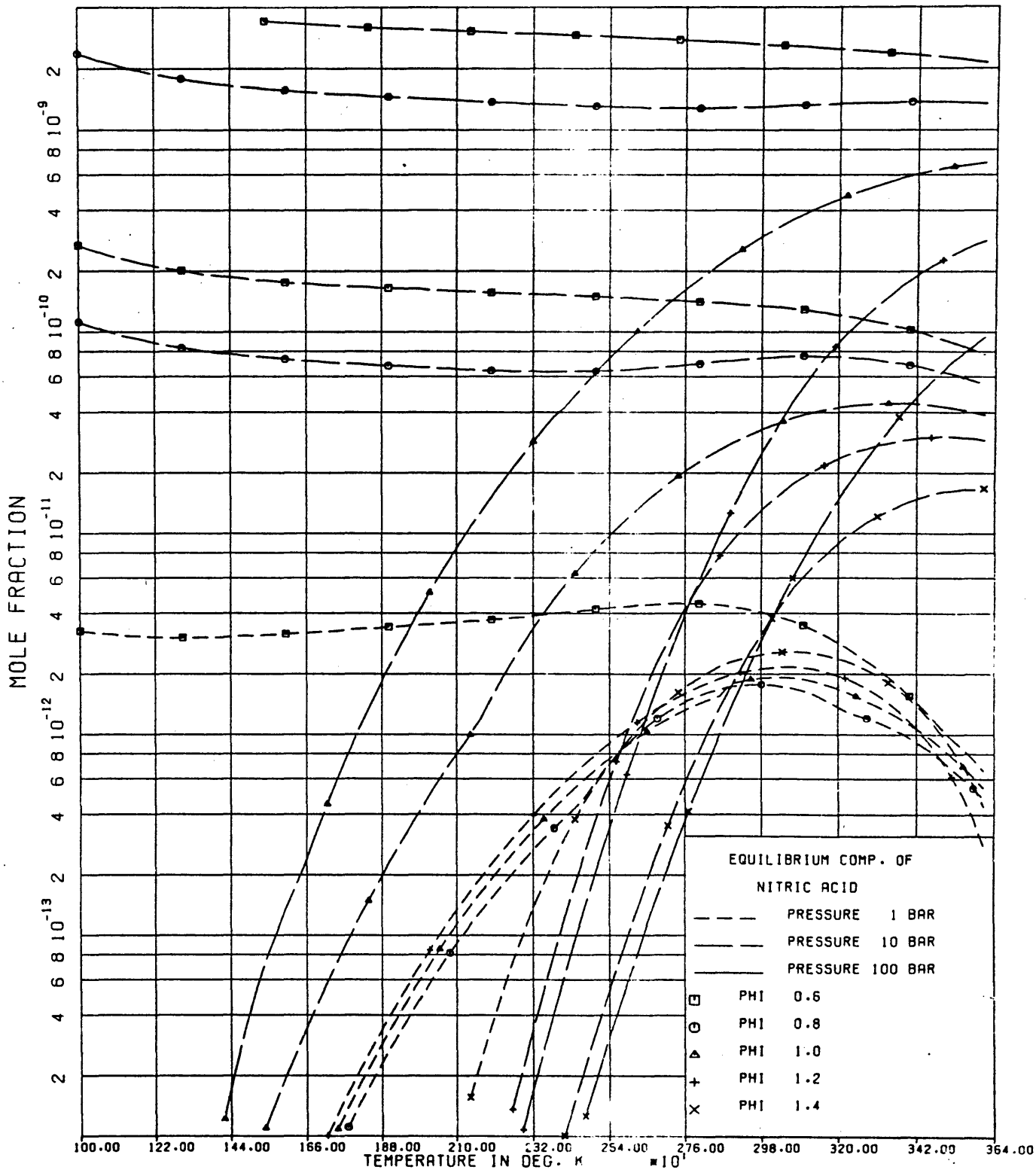


Fig (A.1.1) Equilibrium Composition of Nitric Acid.

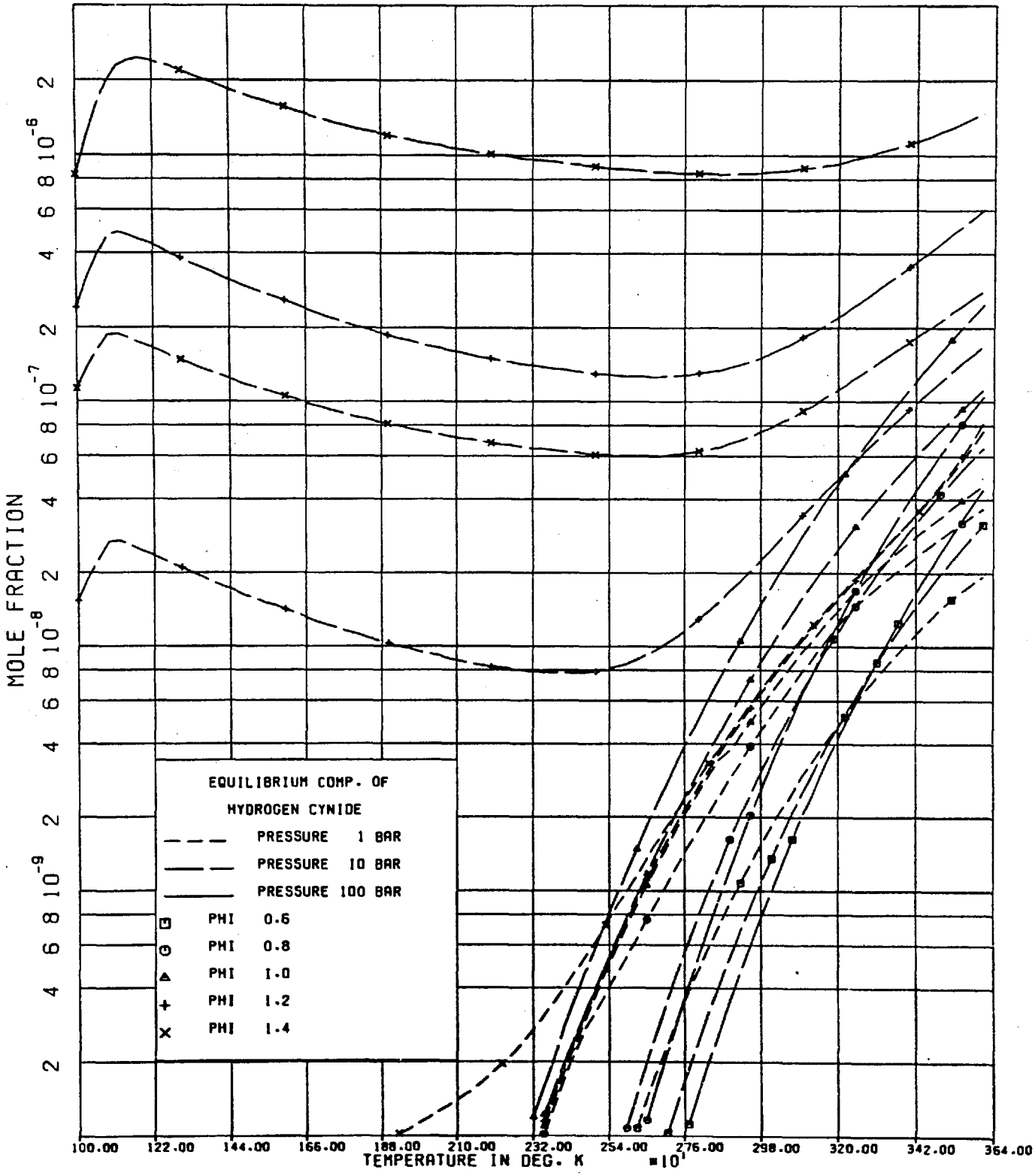


Fig (A.1.2) Equilibrium Composition of Hydrogen Cynide.

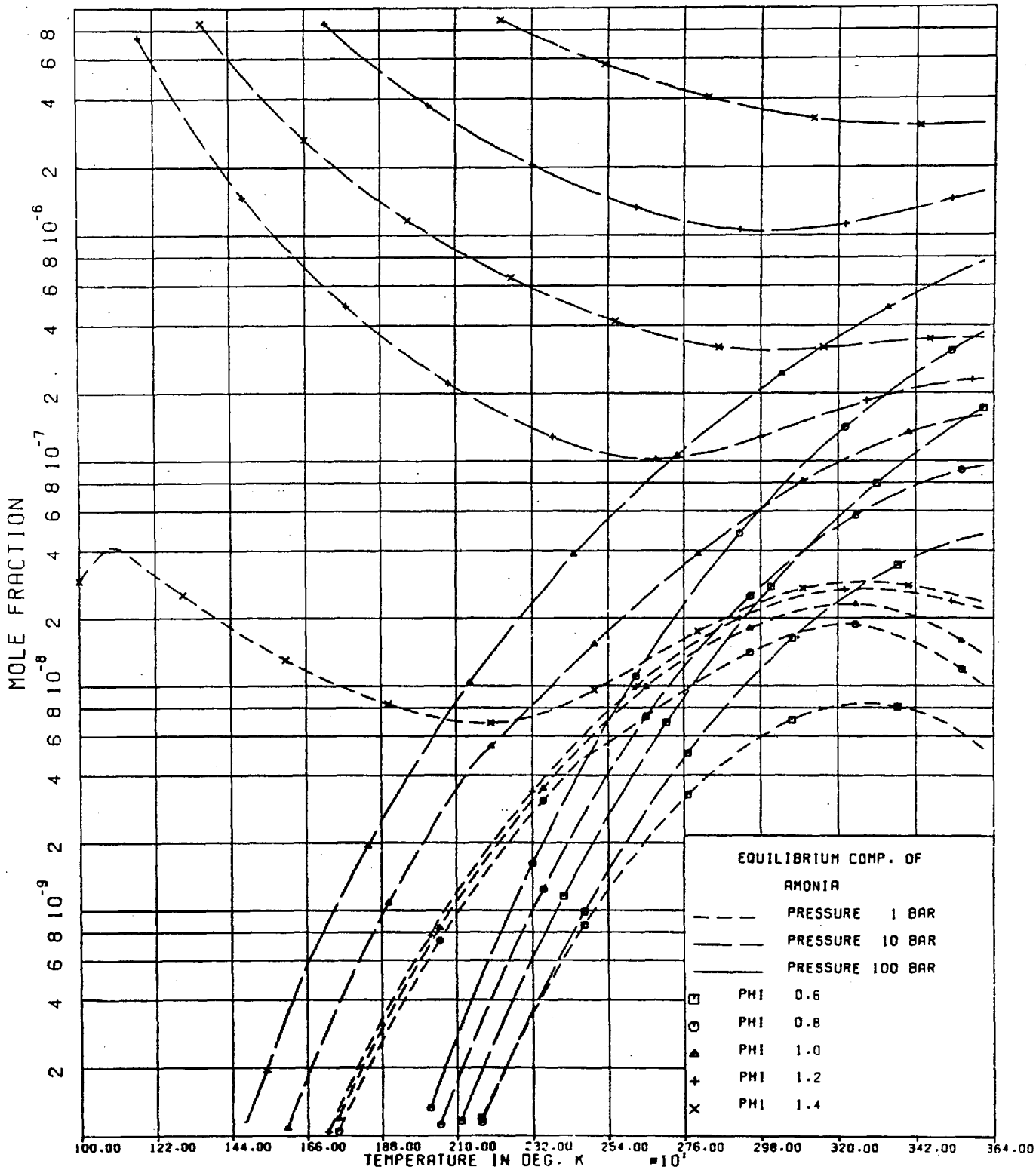


Fig (A.1.3) Equilibrium Composition of Ammonia.

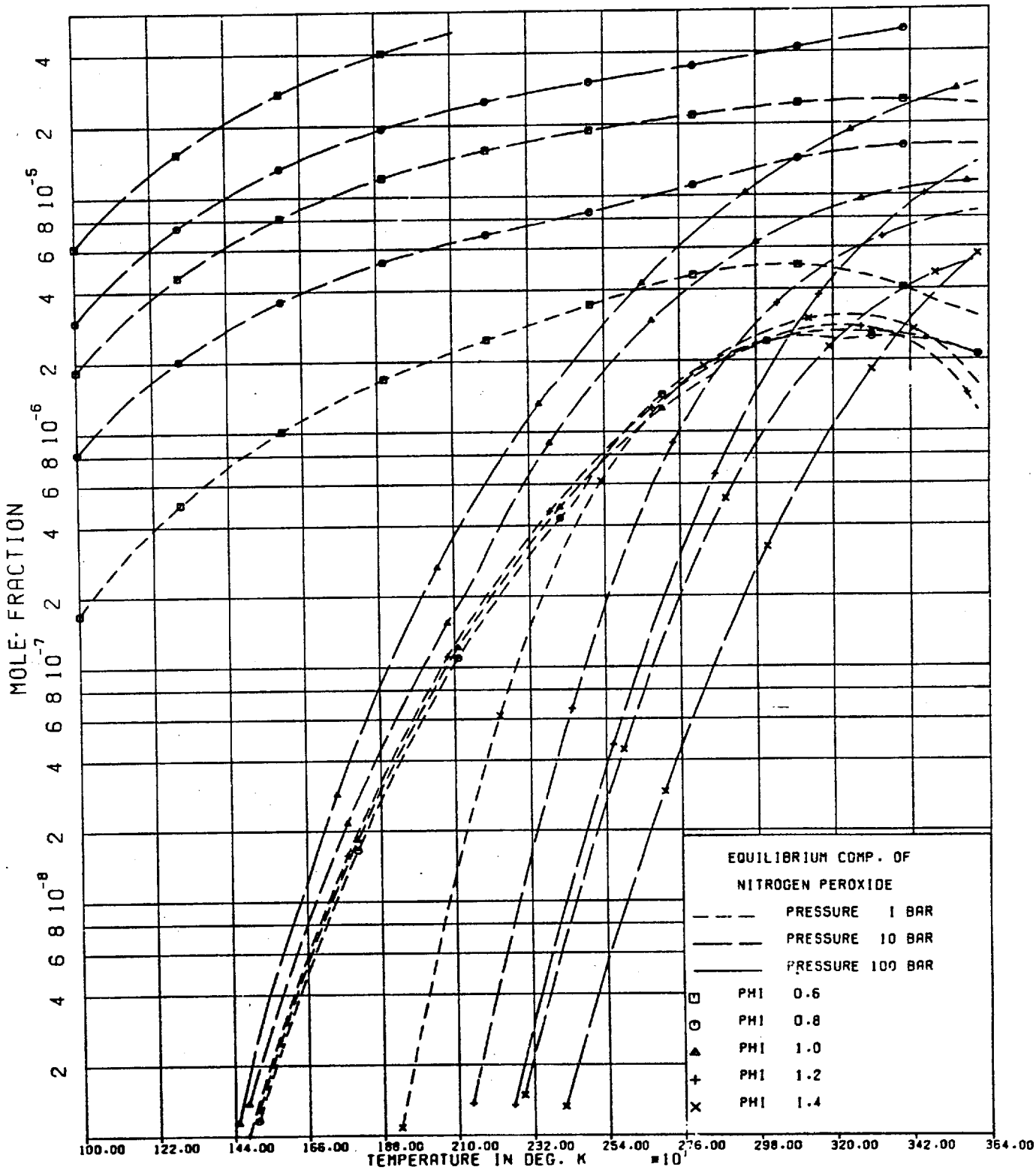


Fig (A.1.4) Equilibrium Composition of Nitrogen Peroxide.

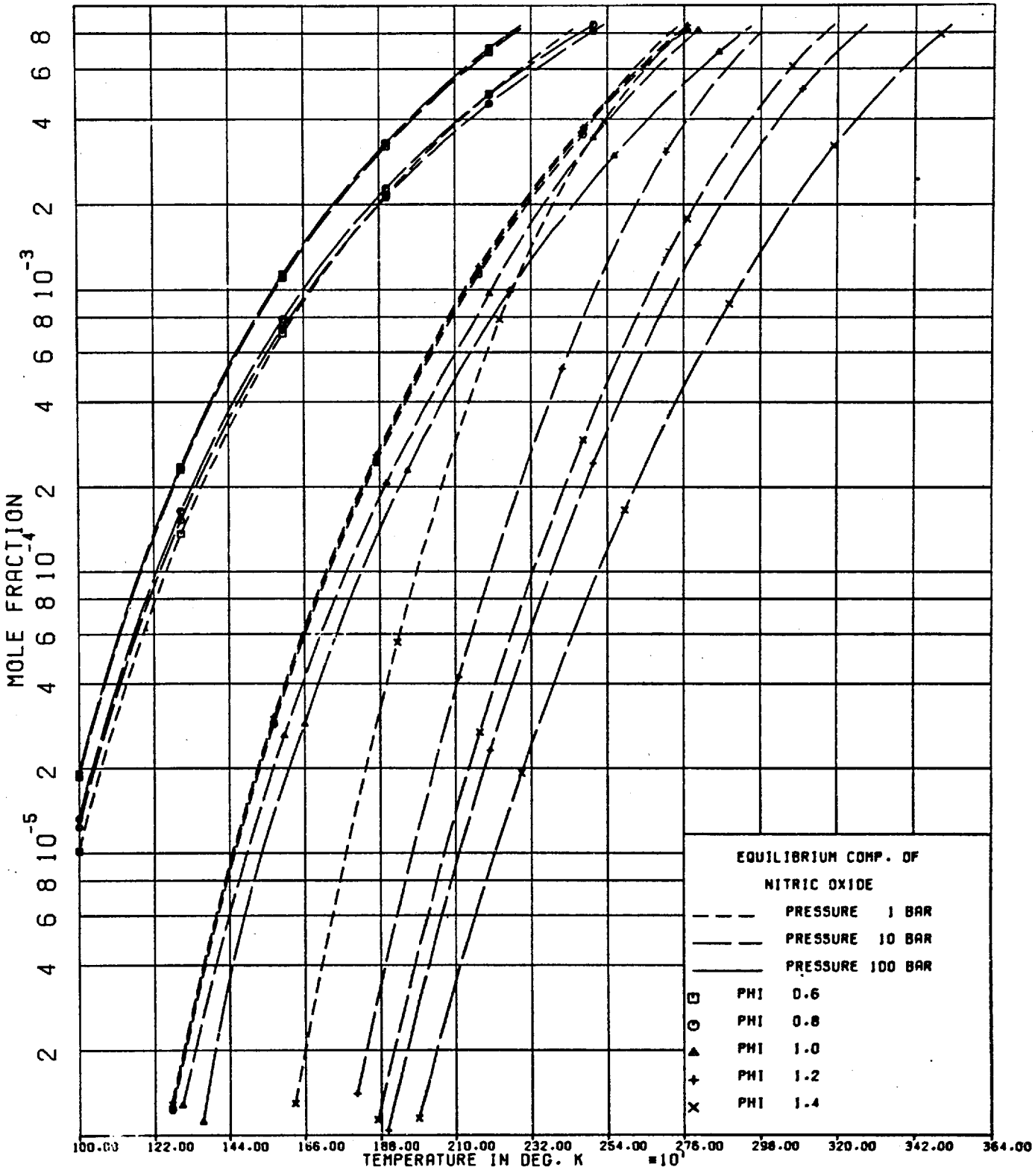


Fig (A.1.5) Equilibrium Composition of Nitric Oxide.

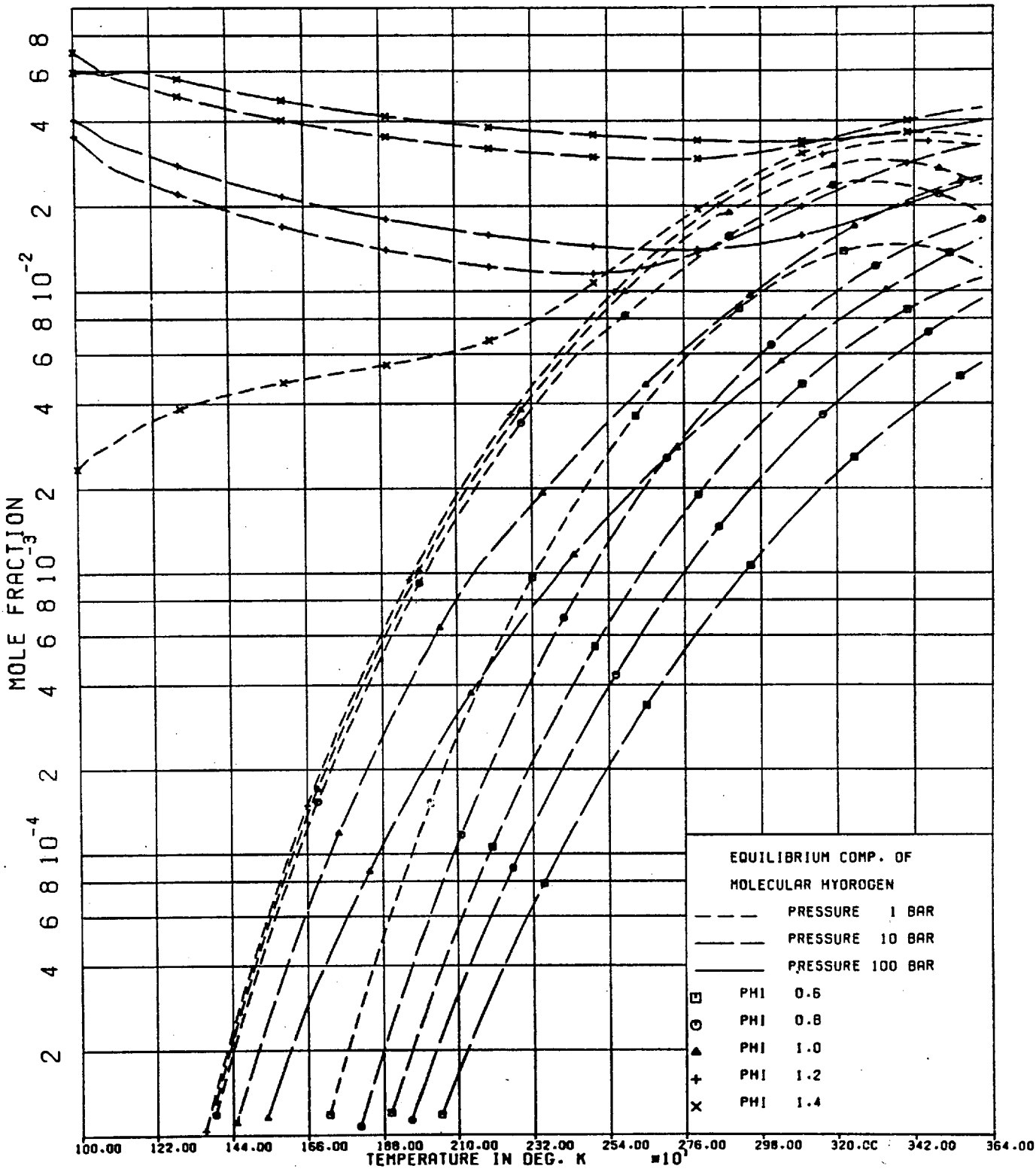


Fig (A.1.6) Equilibrium Composition of Molecular Hydrogen.

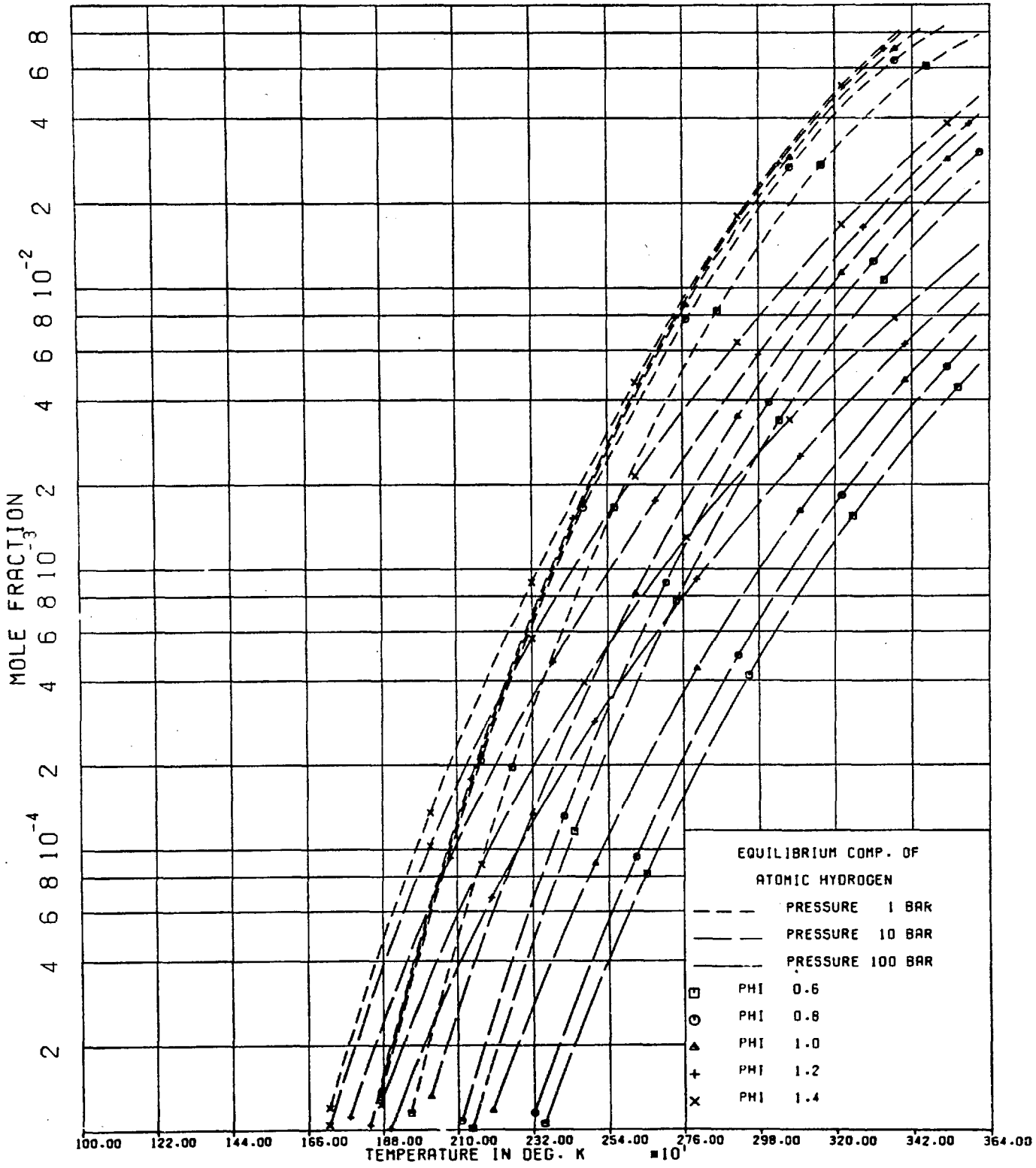


Fig (A.1.7) Equilibrium Composition of Atomic Hydrogen

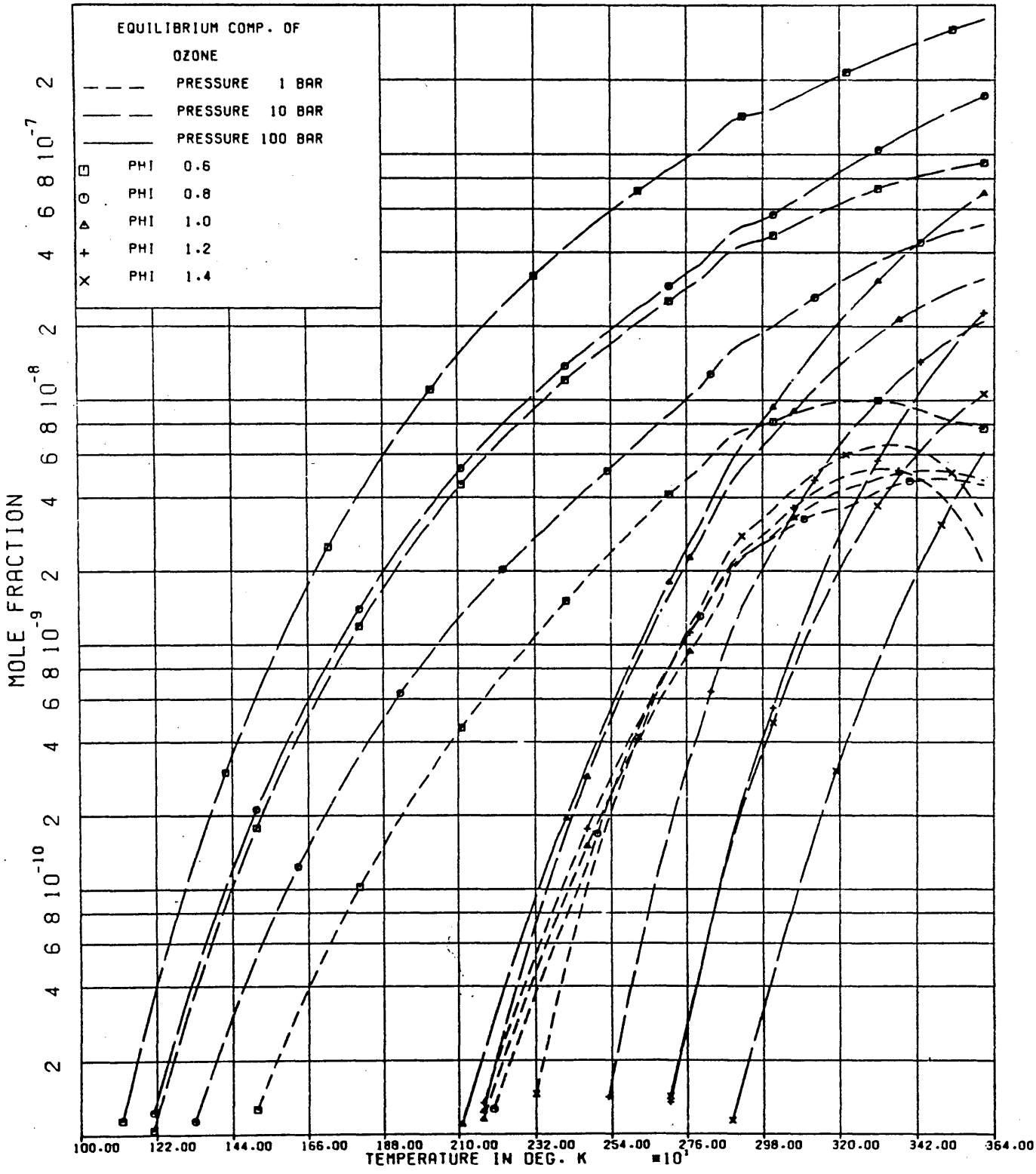


Fig (A.1.8) Equilibrium Composition of Ozone.

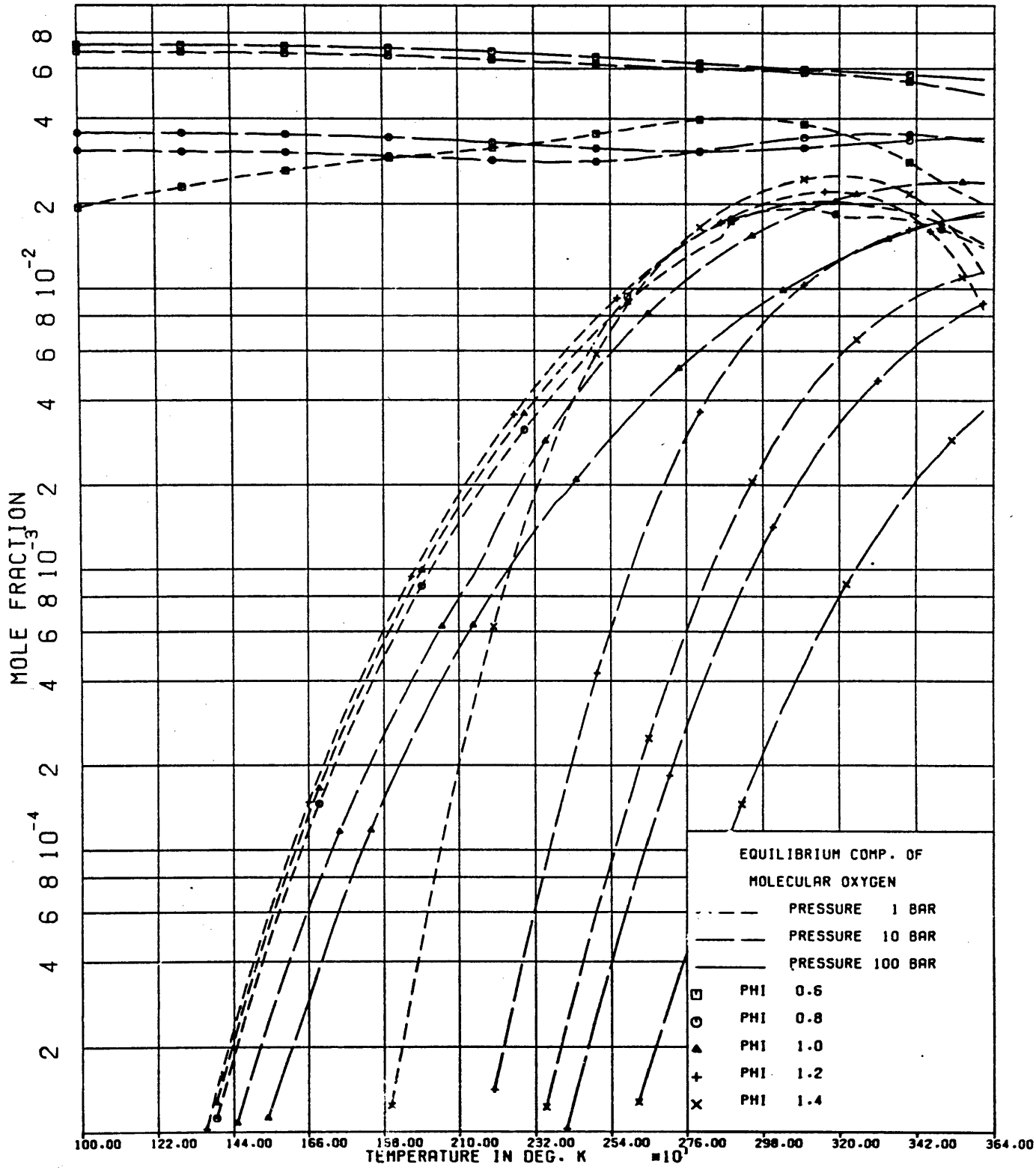


Fig (A.1.9) Equilibrium Composition of Molecular Oxygen.

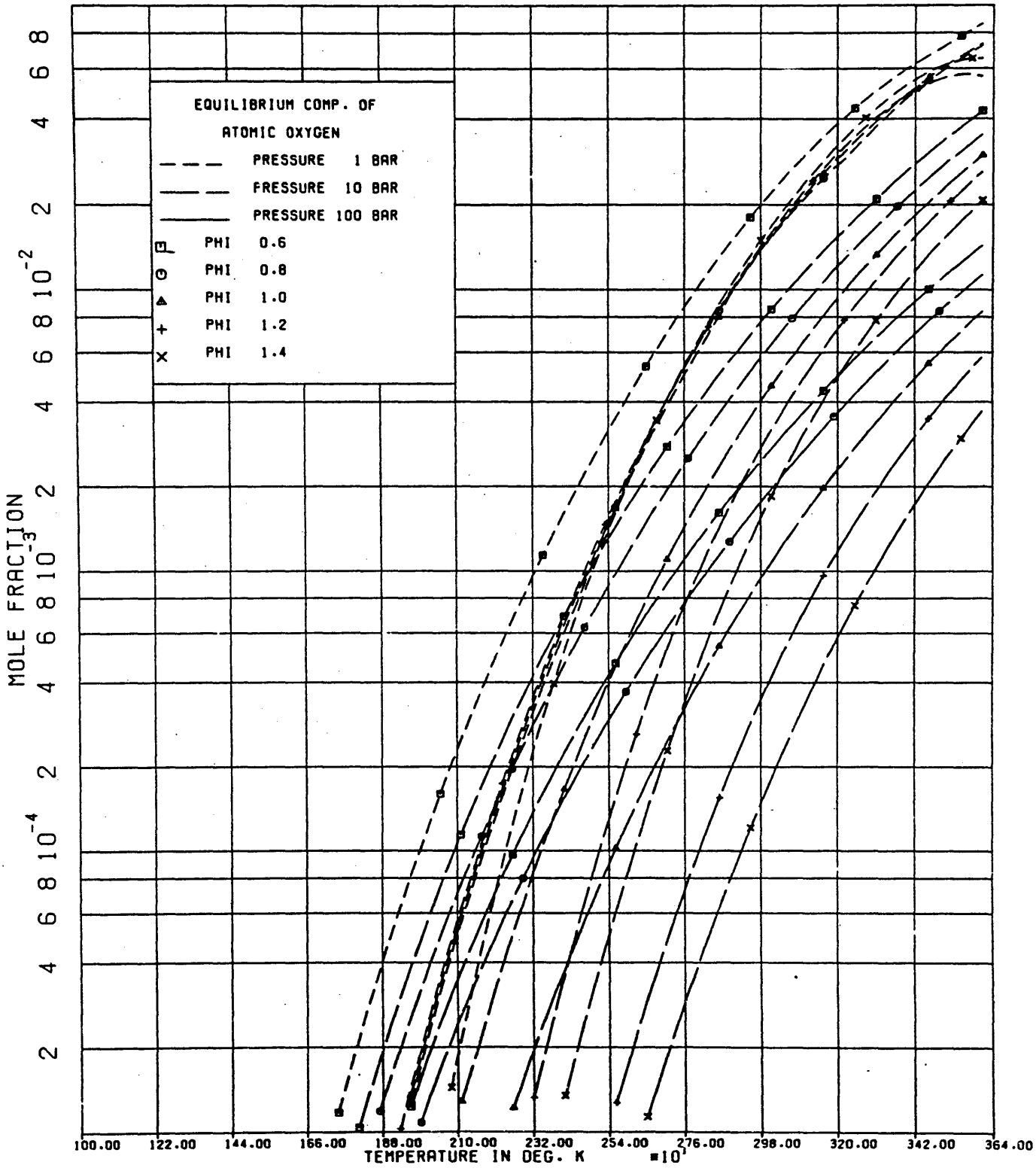


Fig (A.1.10) Equilibrium Composition of Atomic Oxygen.

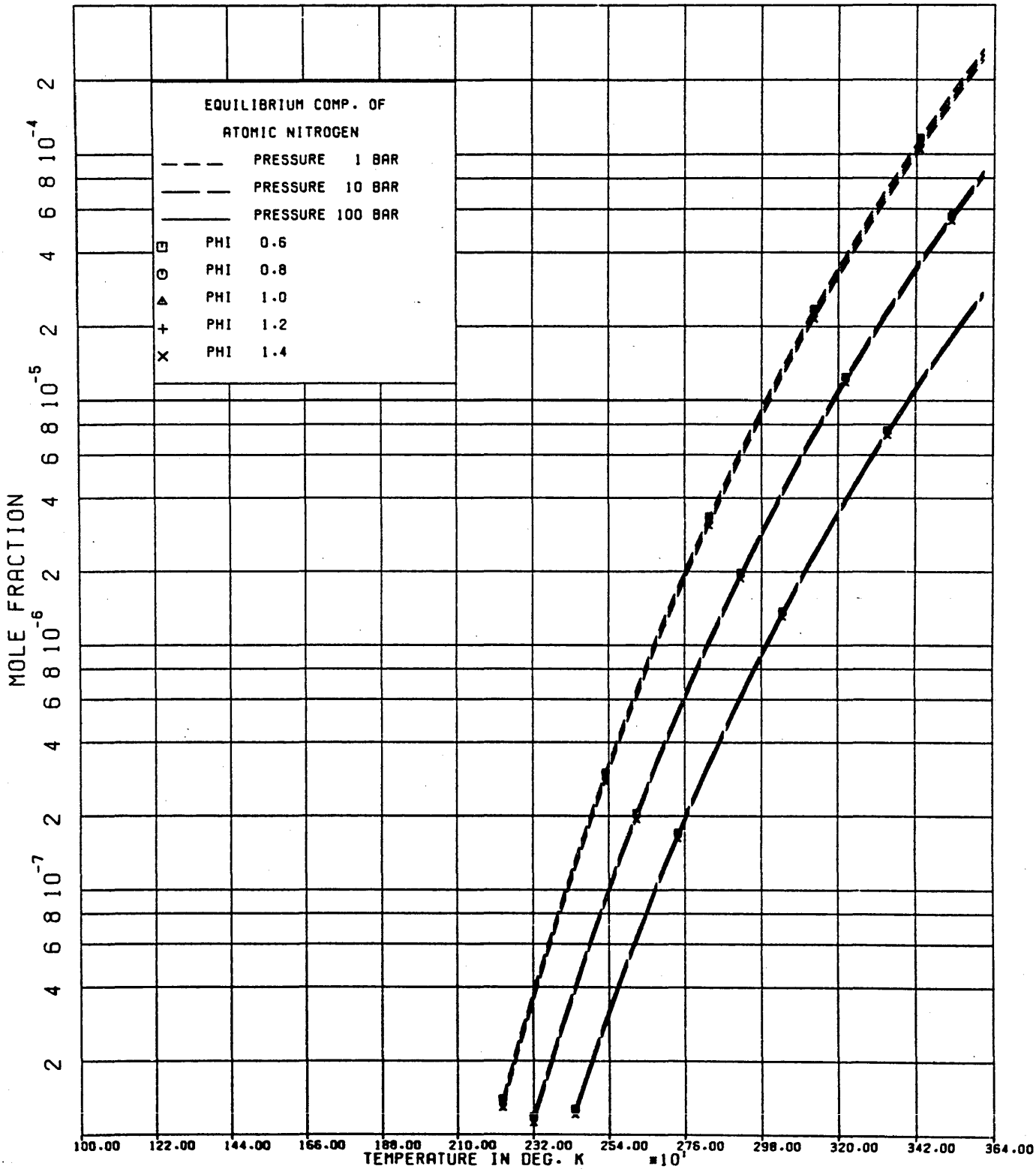


Fig (A.1.11) Equilibrium Composition of Atomic Nitrogen

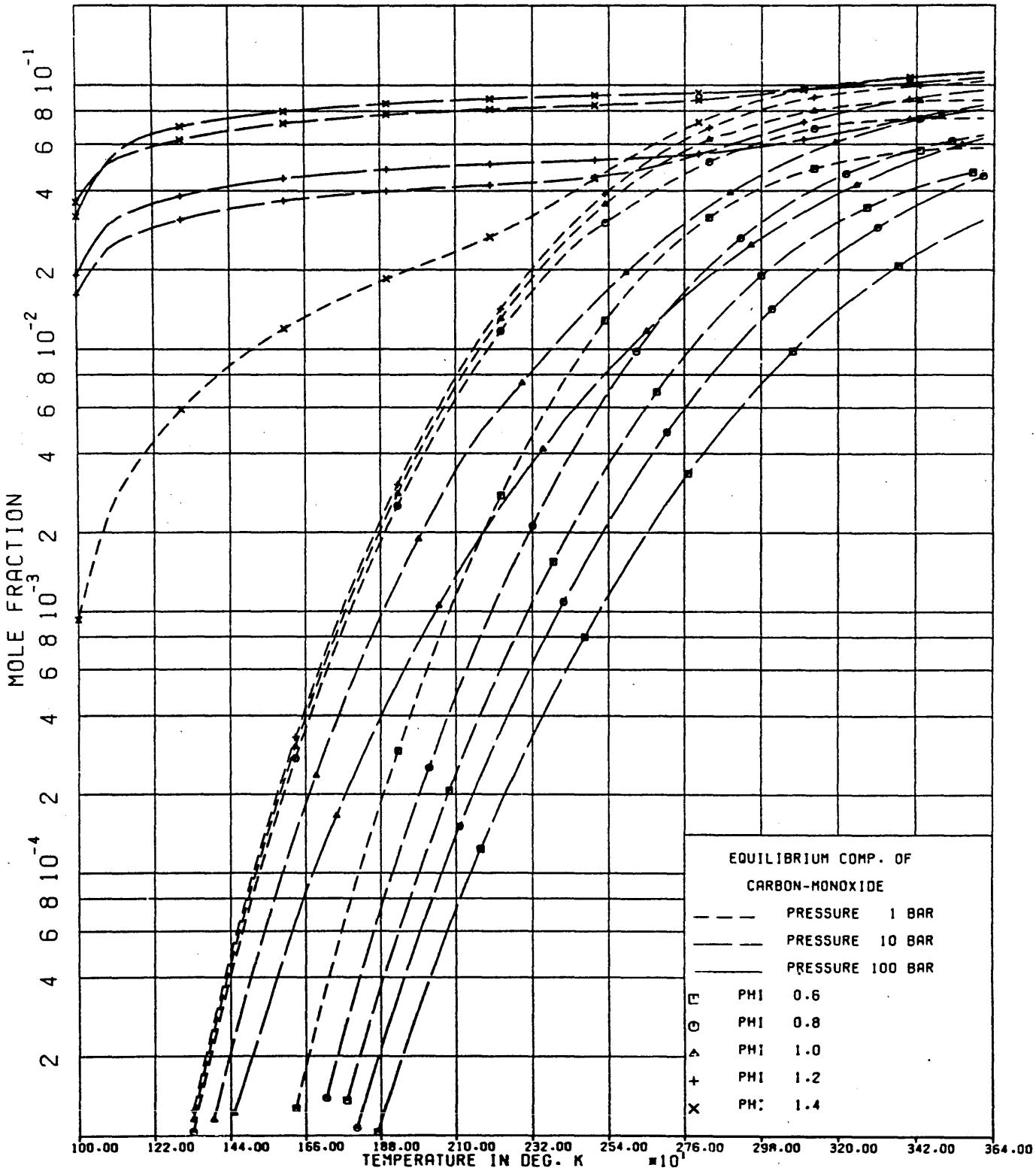


Fig (A.1.12) Equilibrium Composition of Carbon-monoxide

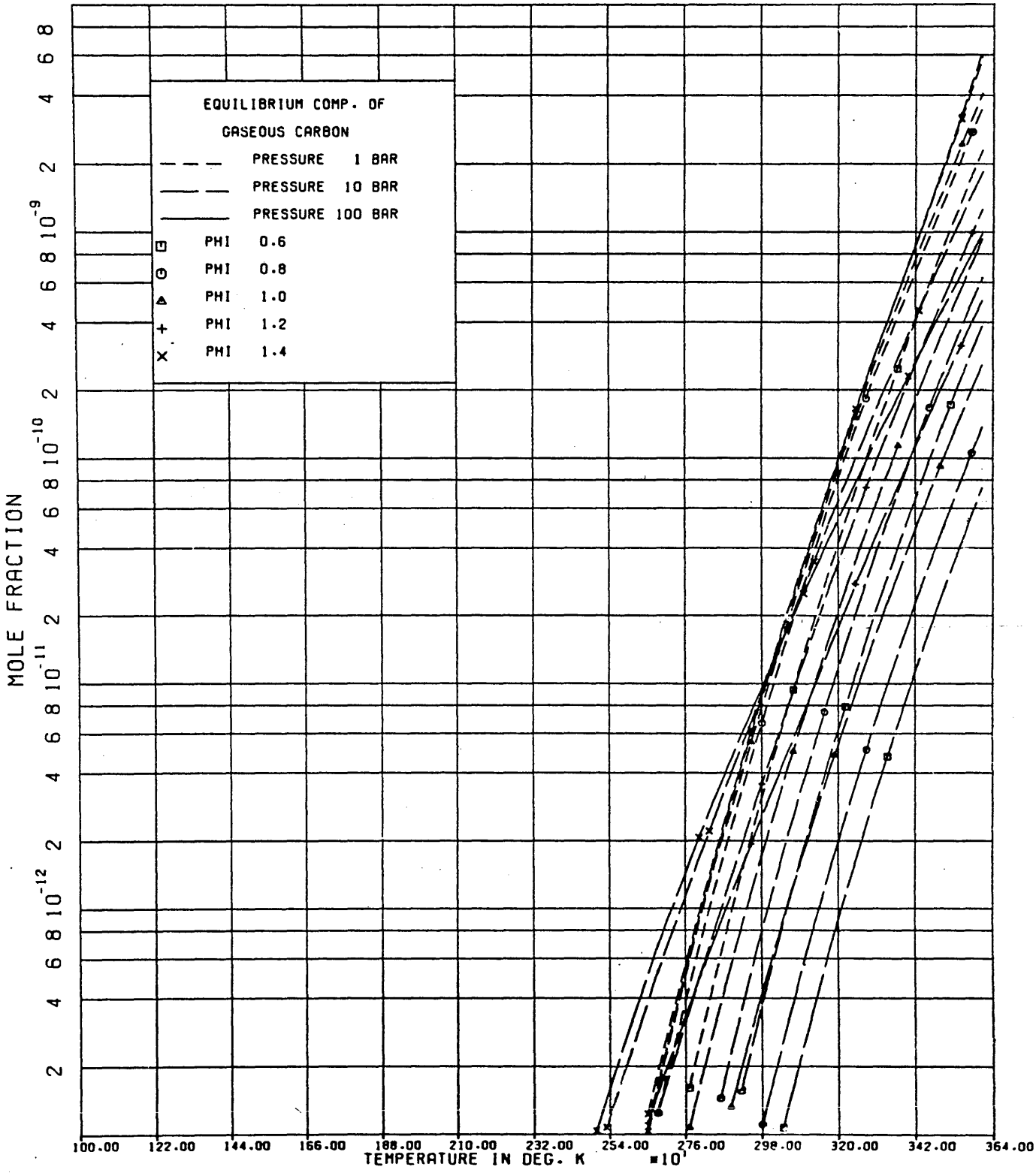


Fig (A.1.13) Equilibrium Composition of Gaseous Carbon.

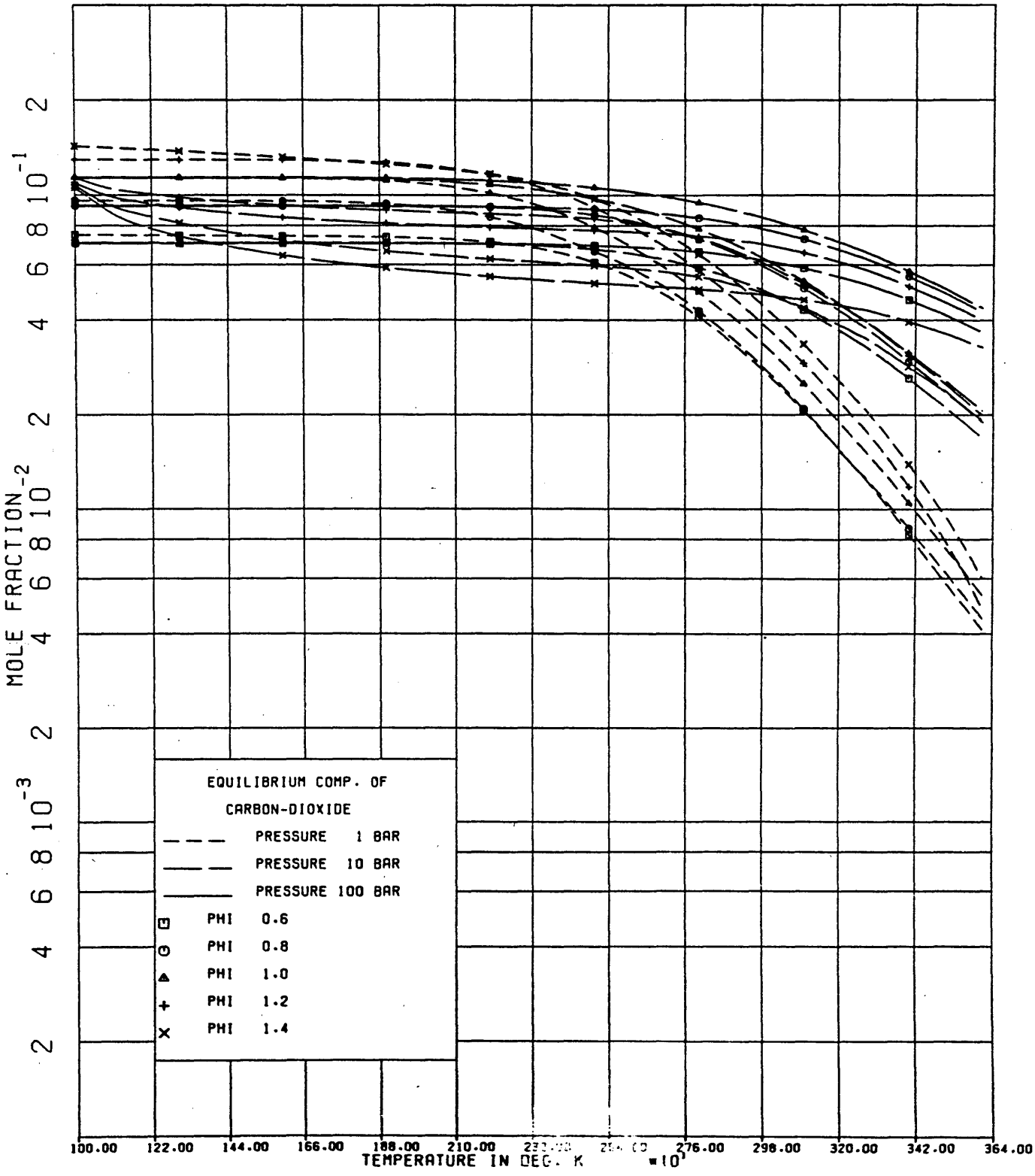


Fig (A.1.14) Equilibrium Composition of Carbon-dioxide.

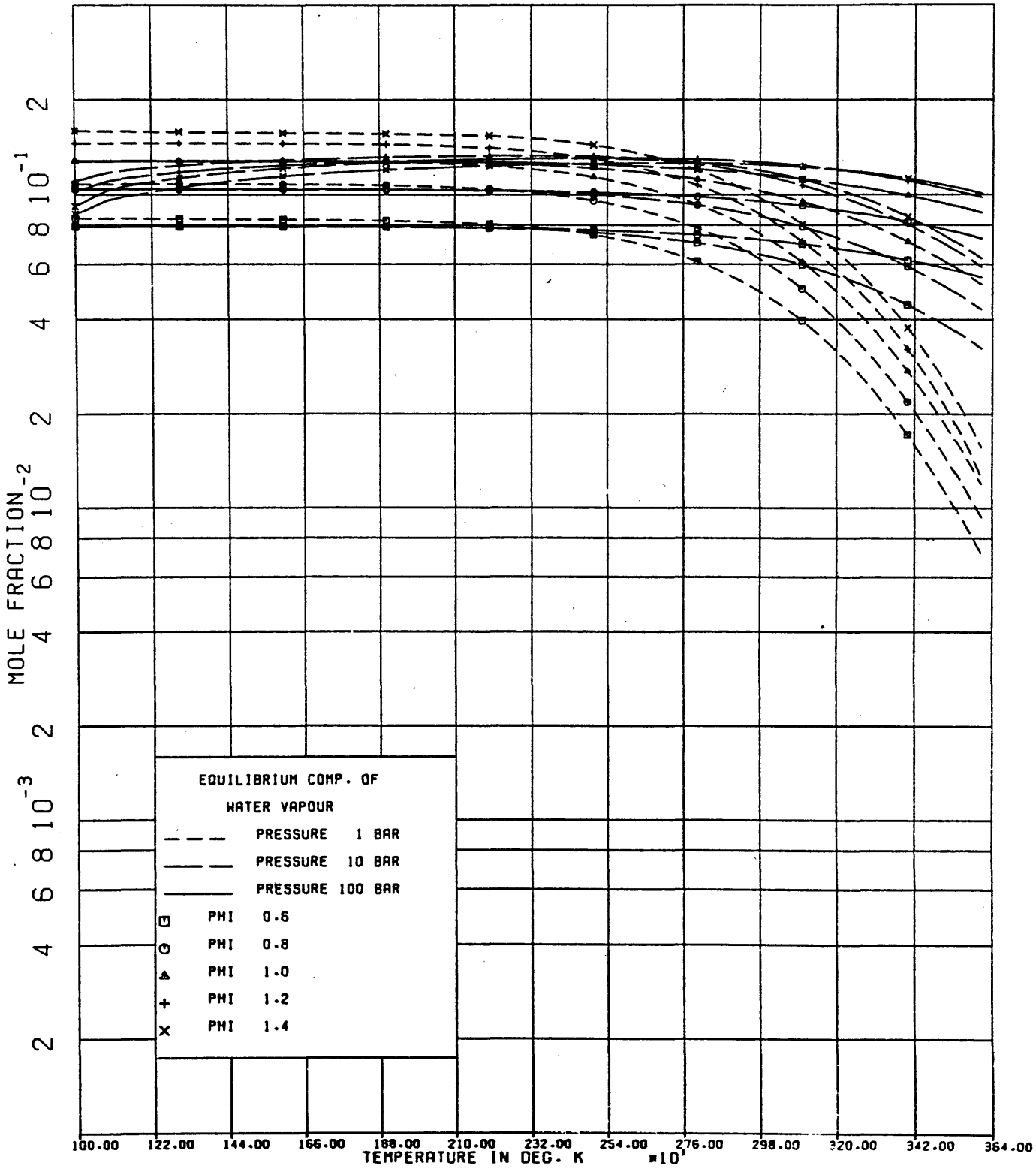


Fig (A.1.15) Equilibrium Composition of Water Vapour.

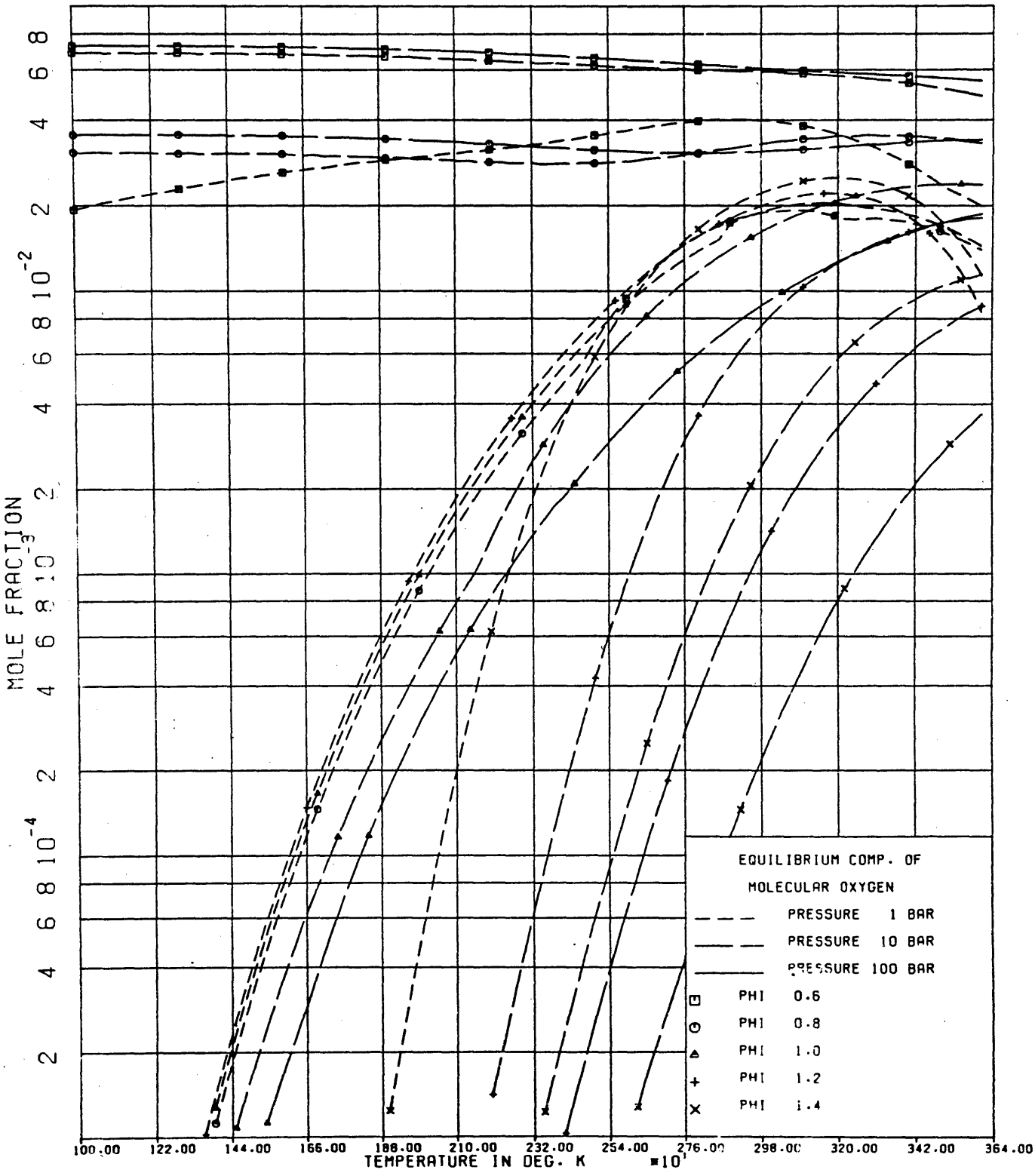


Fig (A.1.16). Equilibrium Composition of Molecular Oxygen.

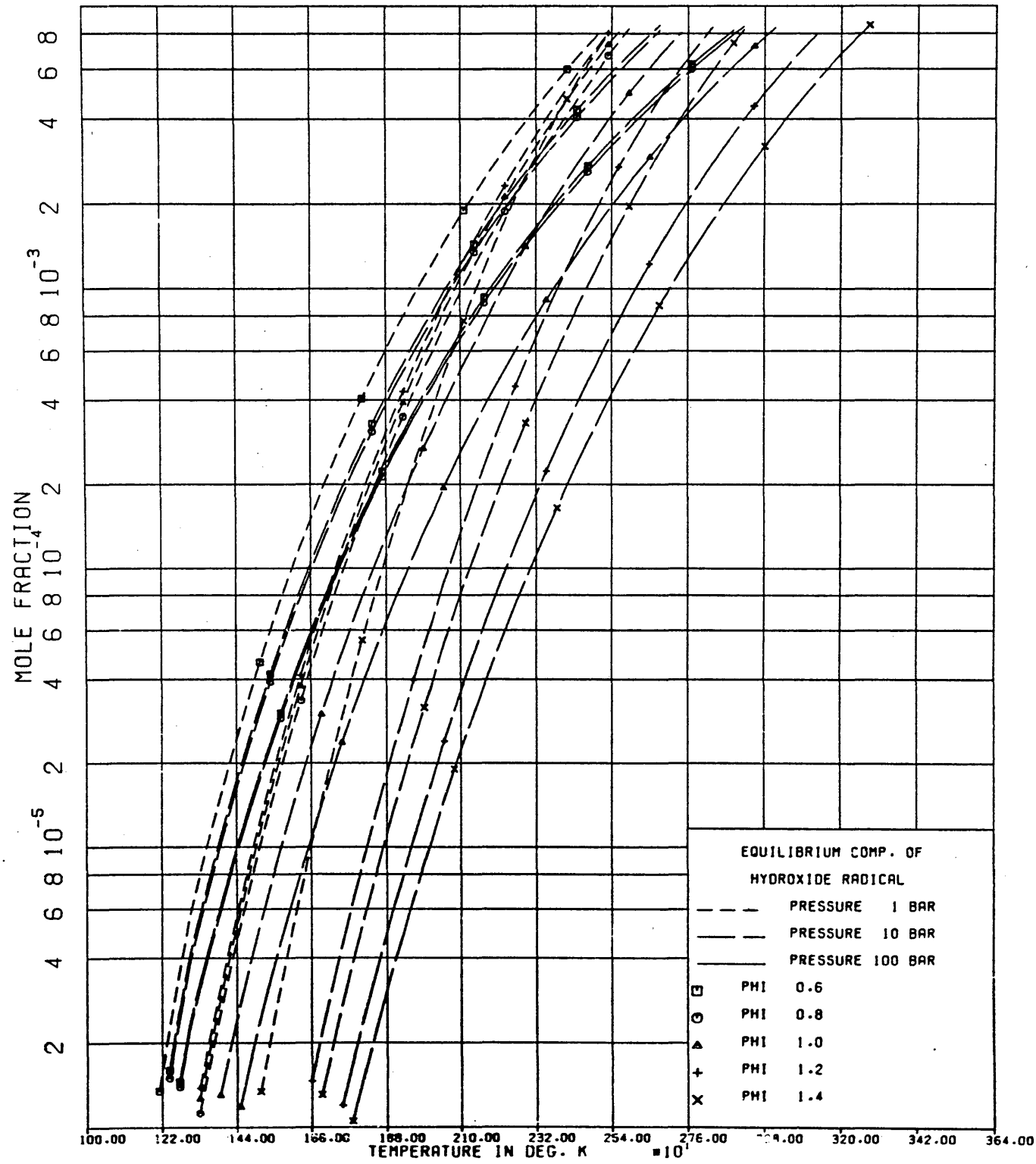


Fig (A.1.17) Equilibrium Composition of Hydroxide Radical.

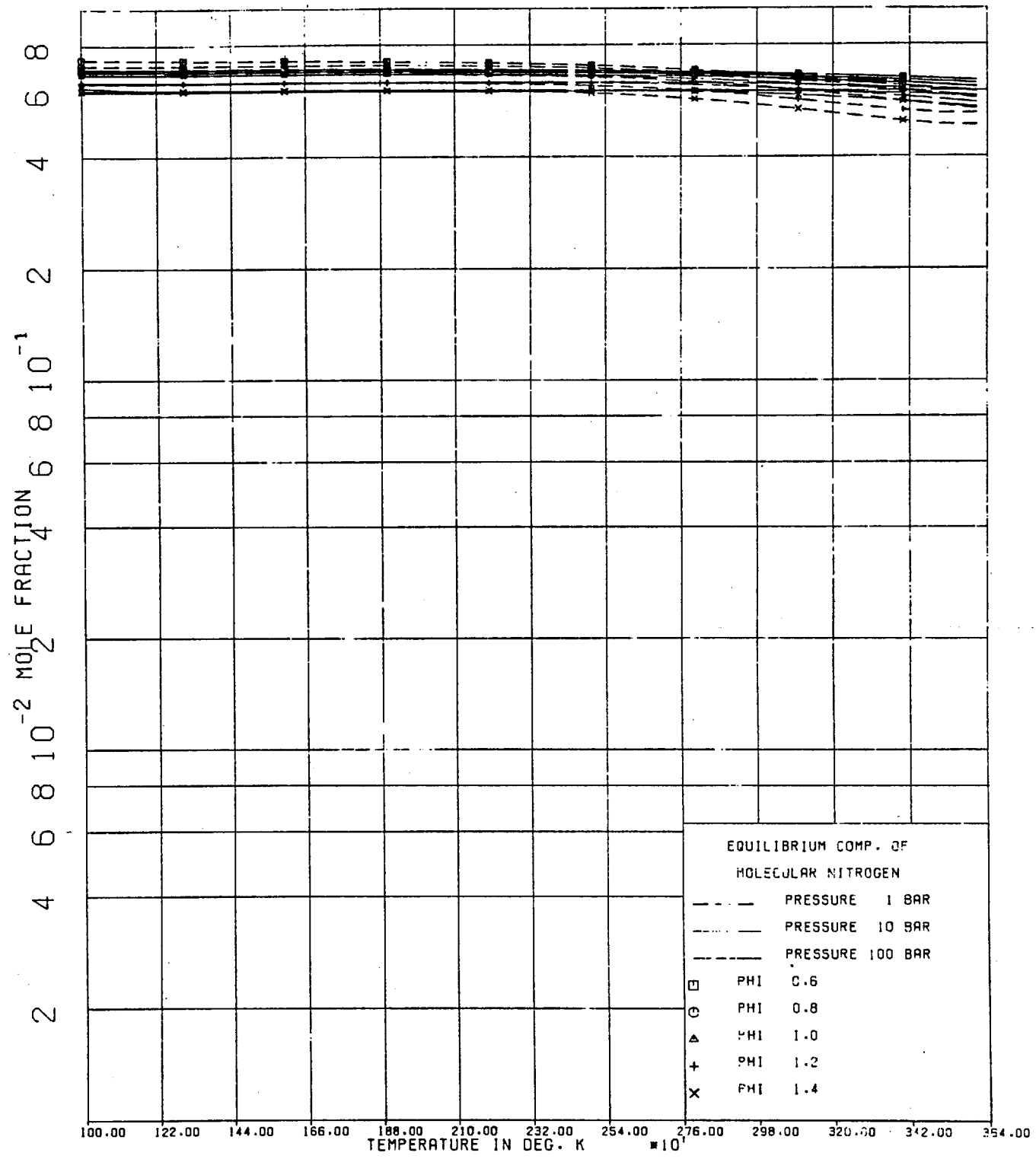


Fig (A.1.18) Equilibrium Composition of Molecular Nitrogen.

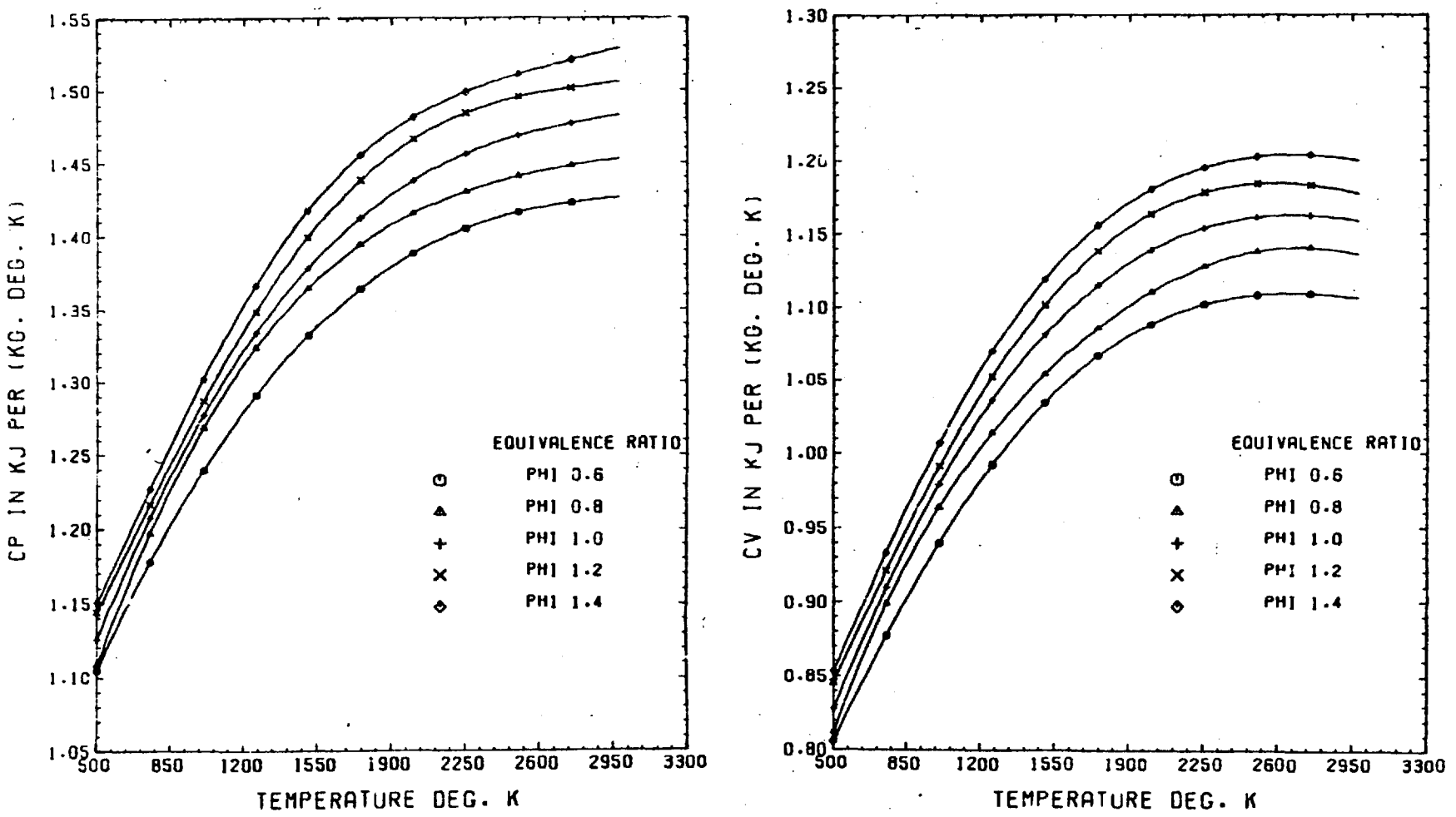


Fig (A.1.19) Specific Heat Value of Equilibrium Composition of Products at 1 Bar Pressure.

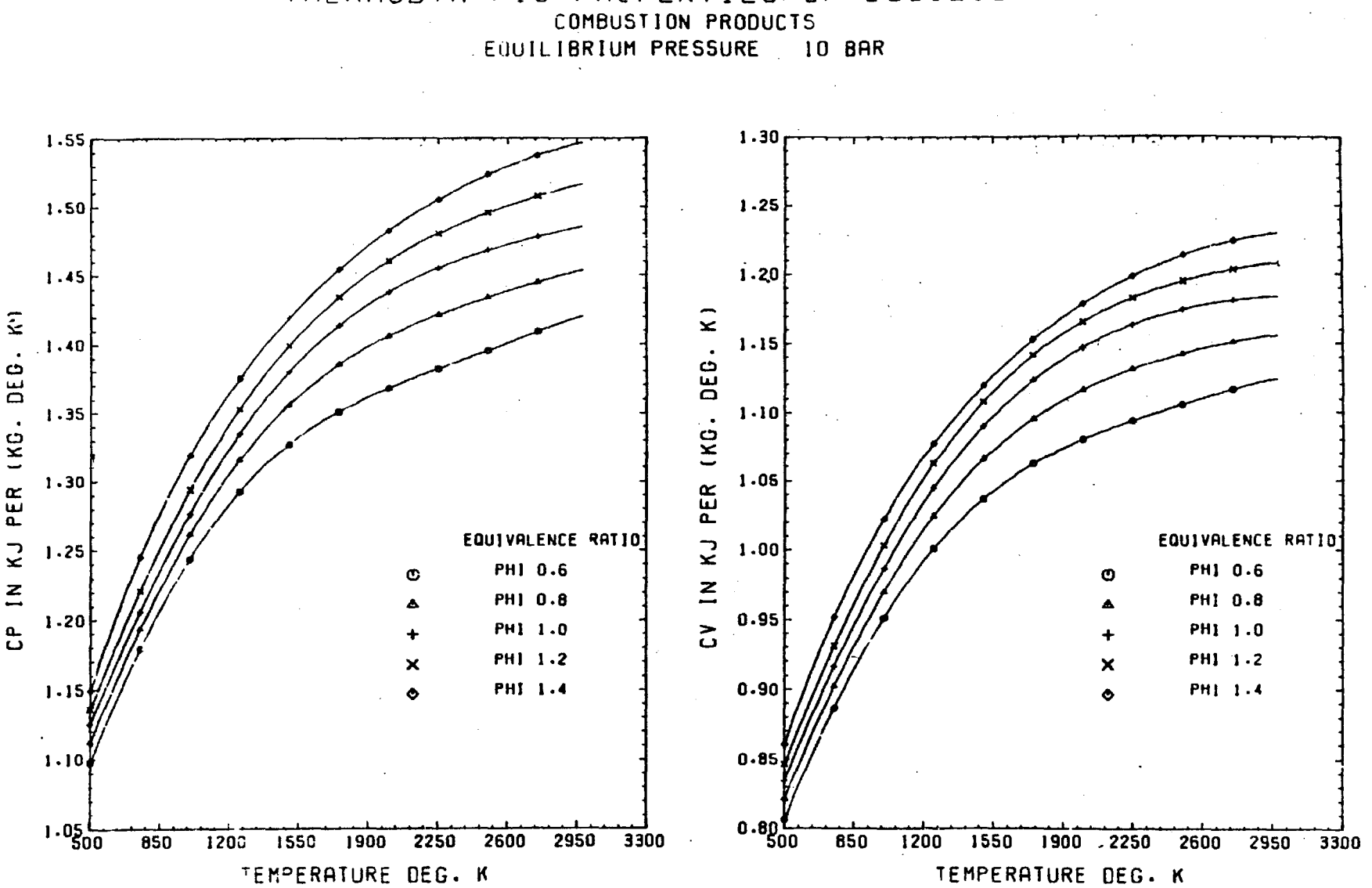


Fig (A.1.20) Specific Heat Values of Equilibrium Composition of Products at 10 Bars Pressure.

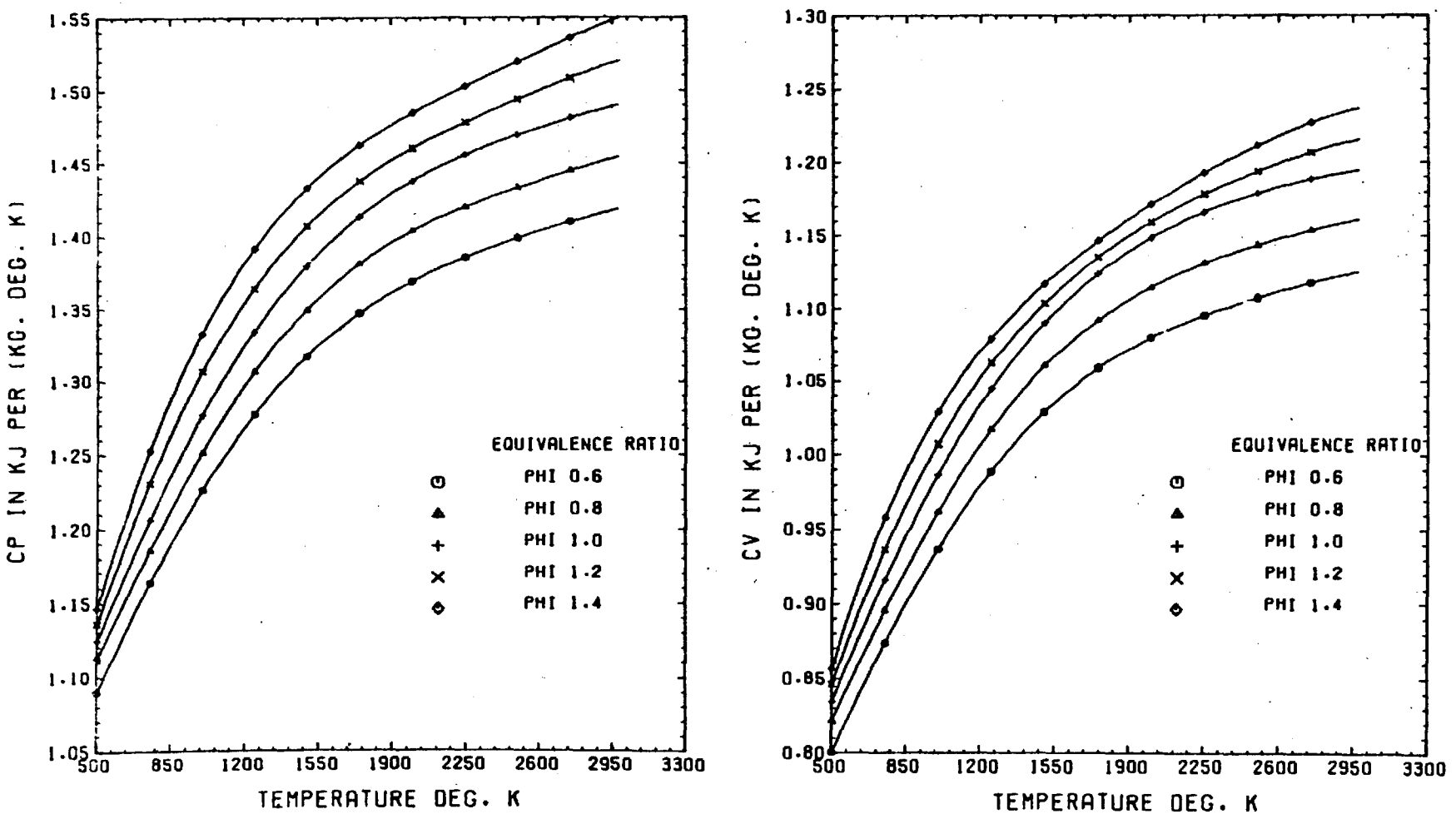


Fig (A.1.21) Specific Heat Values of Equilibrium Composition of Products at 100 Bars Pressure.

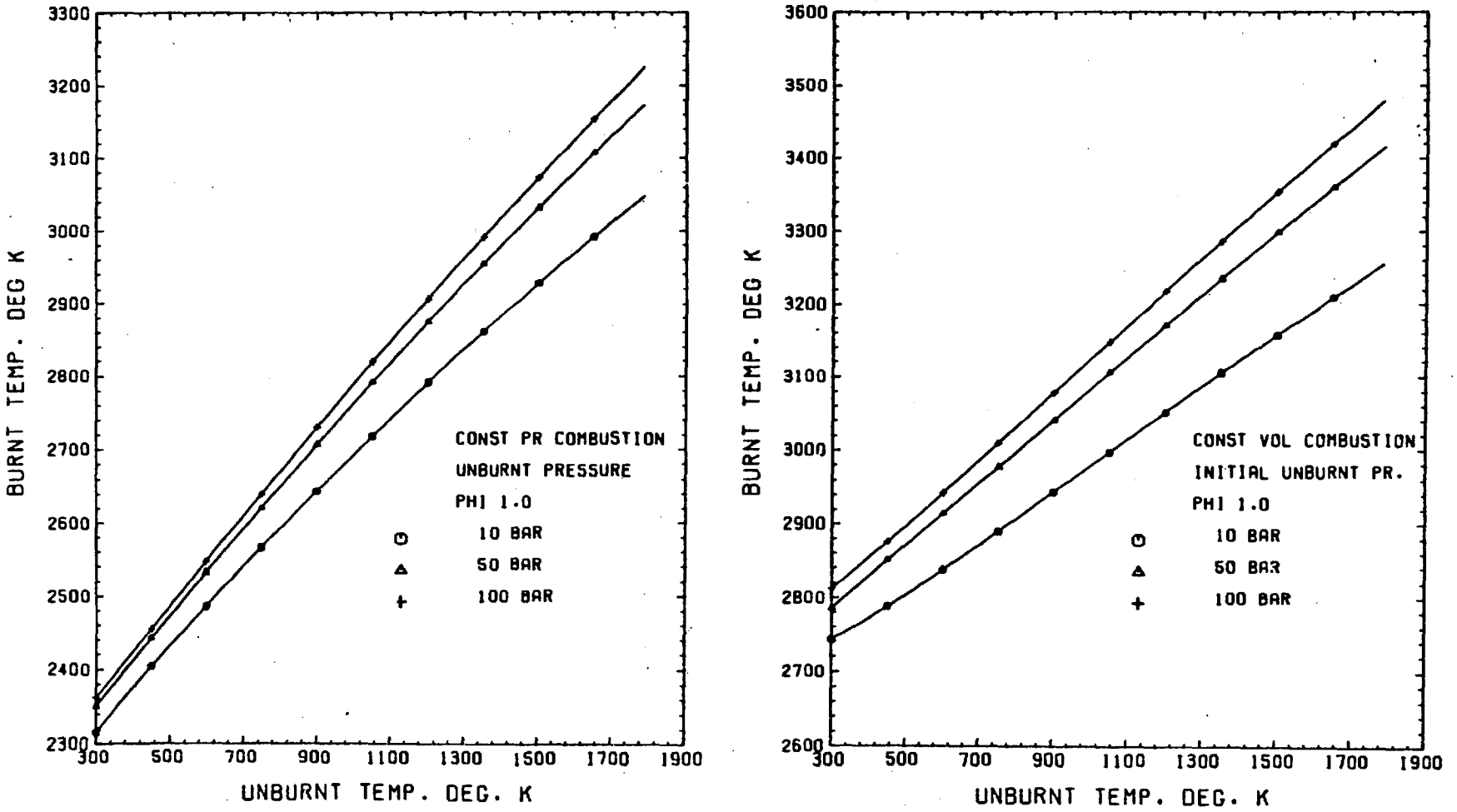


Fig (A.1.22) Adiabatic Combustion Temperature at Equivalent Ratio 1.0.

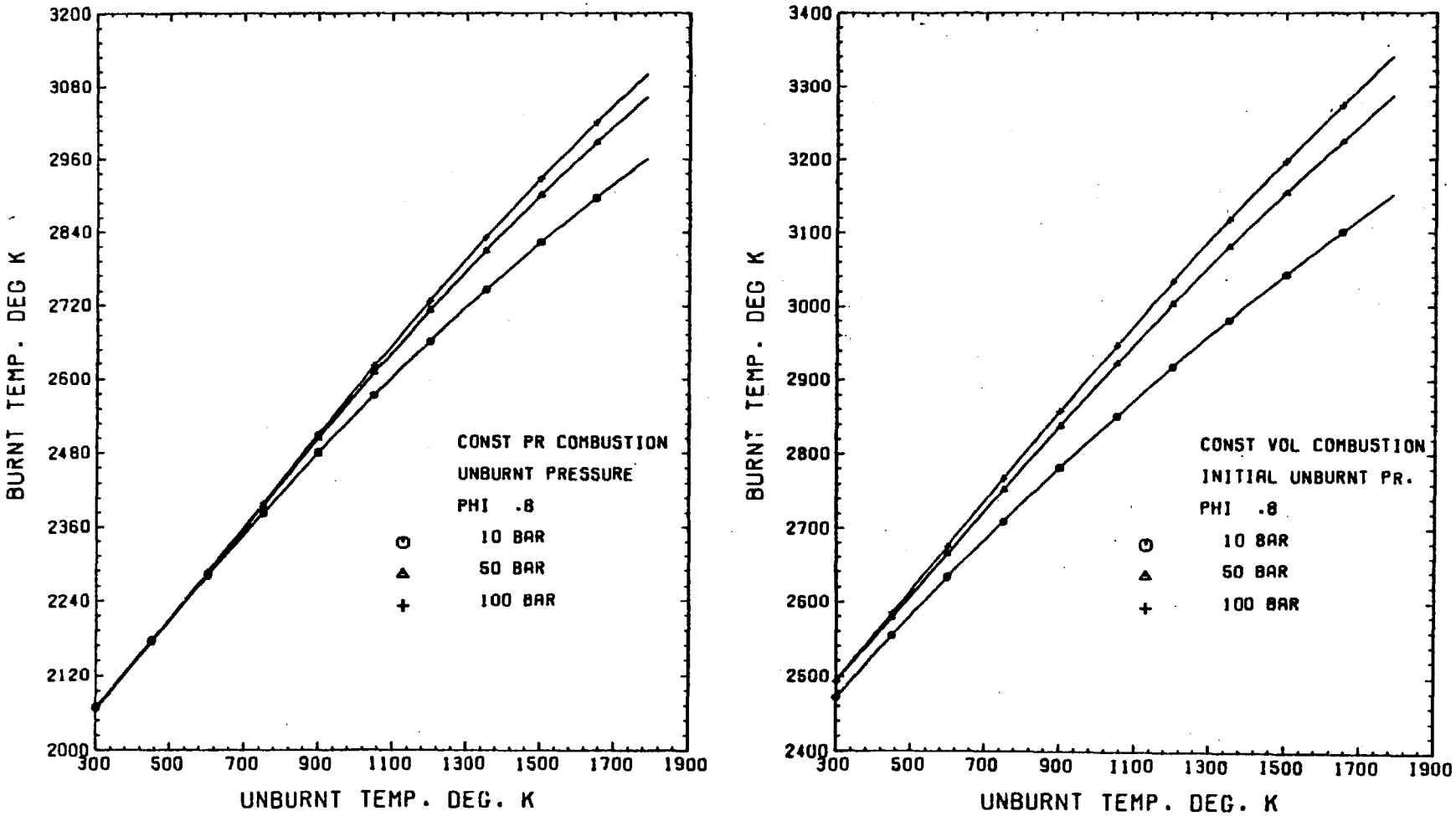


Fig (A.1.23) Adiabatic Combustion Temperatures at Equivalent Ratio 0.8.

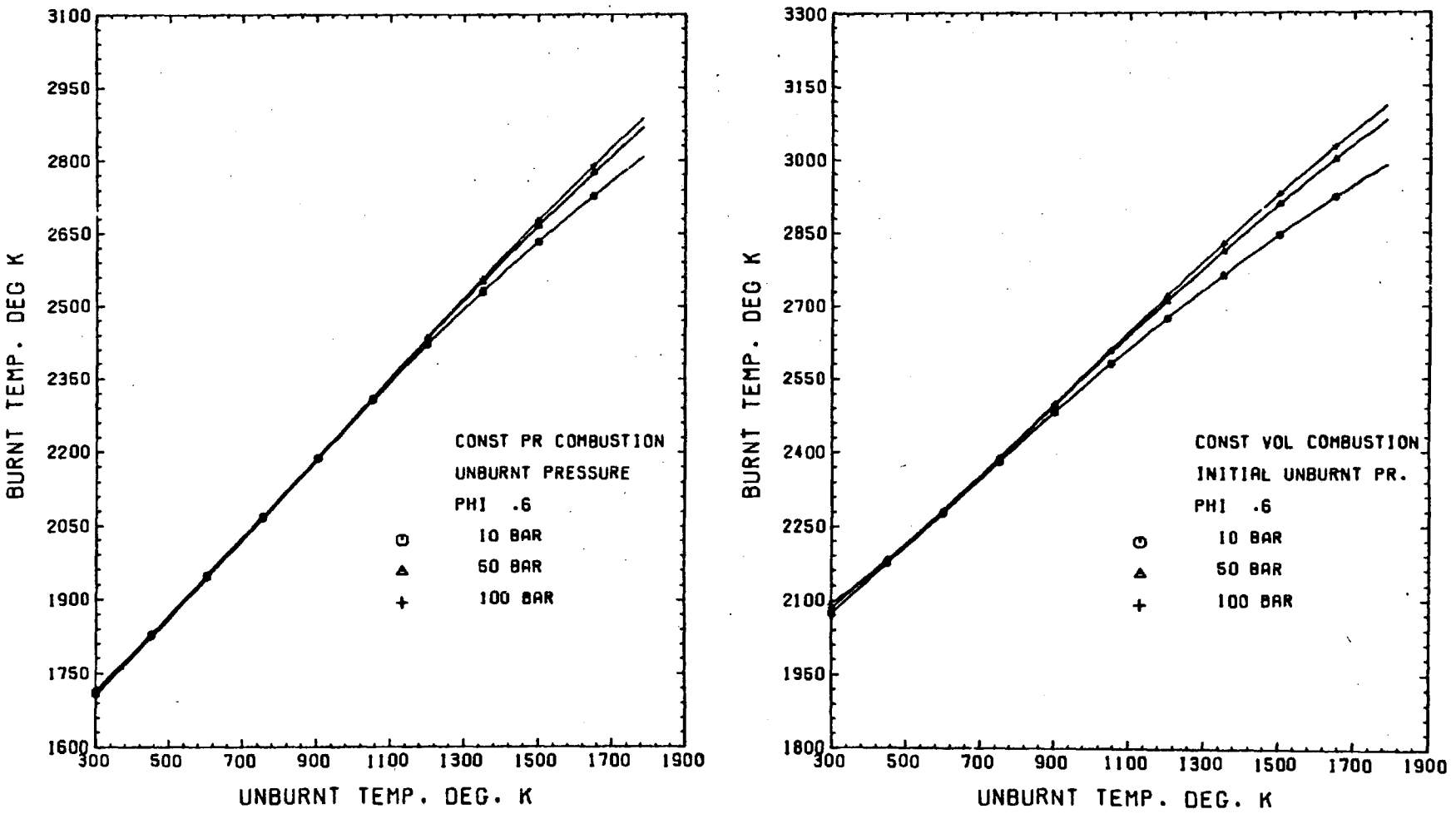


Fig (A.1.24) Adiabatic Combustion Temperature at Equivalent Ratio 0.6.

Appendix (A.2)

Digital Filtering and Design of Digital Filters:- The steps involved in digital filtering processes are:-

(i) Transformation of a digital time-sampled function into the frequency domain.

(ii) Operation on the transformed function in the frequency domain by a transfer function, (to have the required filtering effect).

(iii) Inverse transformation of the transformed function, which has been operated on by the transfer function, back into the time domain.

Each of the above steps will be briefly described.

(i) Transformation of a digital time sampled function into the frequency domain:- It is well known that the Laplace Transformation may be used to transform a continuous time domain function into the frequency domain.

$$\mathcal{L}\, x(t) = \int_0^{\infty} x(t)\, e^{-st}\, dt$$

Similar transformations can be applied to a time sampled function $X(nT)$, where T is the sampling time, $X(nT)$ can be related to the continuous time domain function $x(t)$ by:-

$$X(nT) = x(t) \sum_{n=0}^{\infty} \delta(t - nT)$$

Such that,

$$\delta(t - nT) = 1 \qquad \text{when } t = nT$$

$$\delta(t - nT) = 0 \qquad \text{when } t \neq nT$$

Thus Laplace transformation of a time sampled function $X(nT)$ can be written as,

$$\mathcal{L}\, X(nT) = \mathcal{L}\left[x(t) \sum_{n=0}^{\infty} \delta(t - nT) \right]$$

$$\mathcal{L}\, X(nT) = \mathcal{L}\left[\sum_{n=0}^{\infty} X(nT)\, \delta(t - nT) \right]$$

As $\mathcal{L}\, \delta(t-nT)$ is e^{-snT}.

$$\mathcal{L}\, X(nT) = \sum_{n=0}^{\infty} X(nT)\, e^{-snT}$$

$$= \sum_{n=0}^{\infty} X(nT)\, Z^{-n} \quad \text{where } Z = e^{sT}$$

The above transformation is usually known as Z-transformation and it transforms a time sampled digital function X(nT) into a frequency domain function and the term $\mathcal{L}$ X(nT) is denoted by X(Z). Thus,

$$X(Z) = \sum_{n=0}^{\infty} X(nT)\, Z^{-n}$$

(ii) Operation on the transformed function by a transfer function:- A transfer function, which represents the required filtering operation, is required to be used in operating on the transformed function. The transfer function is determined from a pole-zero plot of a given filter design. The Pole and Zero plot can be made by knowing the sampling time, cut-off frequency, band width and the number of poles of a chosen filter design.

(a) Transfer Function for a Low Pass Filter. The Pole and Zero plot of a four pole Low Pass filter in complex S and Z planes are shown in Fig (A.2.1). The Z-transformation of the left half of thecomplex S-plane is plotted into the region within a unit circle whereas the right half of the complex S-plane is plotted into region outside the unit circle on the Z-plane. For f_c.T (cut-off frequency x sampling time) <1, pole positions are plotted into a small circular arc on Z-plane with a radius f_c.T as shown in fig (A.2.1). Zero positions were assigned as suggested by Weiver (30) and are shown on the Z-plane. The transfer function is then determined by using the equation,

$$G(Z) = \frac{\pi Z_i}{\pi P_i}$$

where Z_i are the distances of Z from zero positions and P_i are the distances of Z from pole positions. Thus for a four pole low pass filter,

$$G(Z) = \frac{(Z-0)\quad(Z-0)}{(Z-Z_1)\ (Z-\overline{Z}_1)\ (Z-Z_2)\quad (Z-\overline{Z}_2)}$$

$$G(Z) = \frac{Z^2}{(Z-Z_1)\ (Z-\overline{Z}_1)\ (Z-Z_2)\quad (Z-\overline{Z}_2)}$$

It is to be noted that conjugate pole positions are also taken into account. A similar approach applied to the determination of the transfer function of a low pass filter having higher number of pairs of poles.

(b) Transfer Function of High Pass Filters. The Pole and Zero plot of a four pole high pass filter is shown in fig (A.2.2). By using the pole-zero plot , the transfer function G(Z) for a four pole high pass filter is:-

$$G(Z) = \frac{\pi Z_i}{\pi P_i}$$

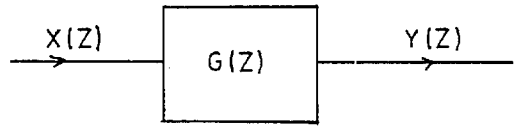
$$= \frac{(Z - 1)\quad (Z + 1)}{(Z - Z_1)\quad (Z - \overline{Z}_1)\quad (Z - Z_2)\quad (Z - \overline{Z}_2)}$$

(c) Transfer Function of a band pass filter. The Pole-Zero plot of a four pole band pass filter is shown in fig (A.2.3) and its transfer function is,

$$G(Z) = \frac{\pi Z_i}{\pi P_i}$$

$$= \frac{(Z - 1)\quad (Z + 1)}{(Z - Z_1)\quad (Z - \overline{Z}_1)\quad (Z - Z_2)\quad (Z - \overline{Z}_2)}$$

The transfer function G(Z), which is determined in the above way for a chosen filter design, is then operated on the transformed function X(Z) to give another frequency domain function Y(Z) which represents the transform of the filtered output Y(nT) in the time domain.



The function Y(Z) may then be retransformed back into time domain to give the desired time domain filtered output signal.

(iii) Retransformation of the frequency domain function Y(Z) back into the time domain. Let a time domain function Y(nT) represents the retransformation of the function Y(Z).

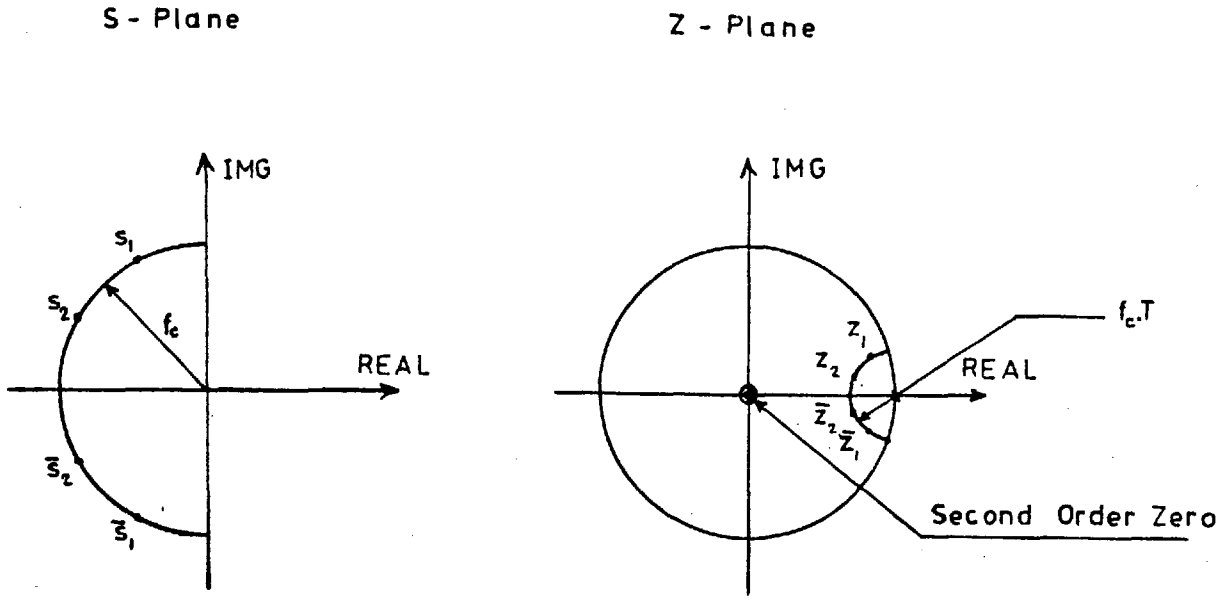


Fig (A.2.1) Pole-Zero Diagrams of a 4-Pole Low-Pass Filter.

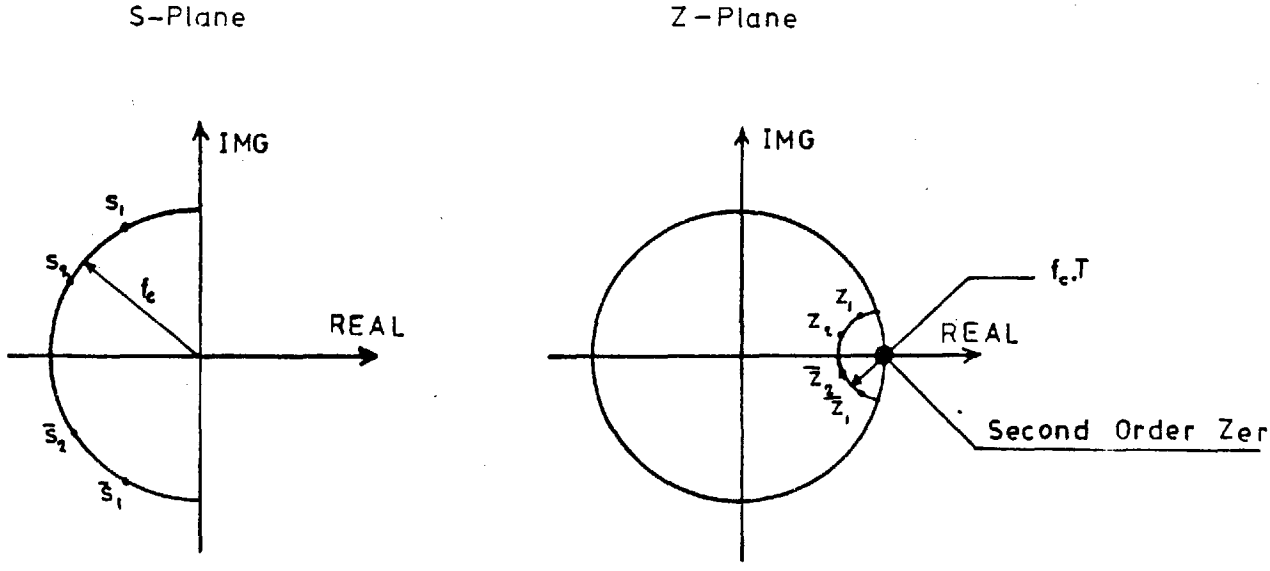


Fig (A.2.2) Pole-Zero Diagrams of a 4-Pole High-Pass Filter.

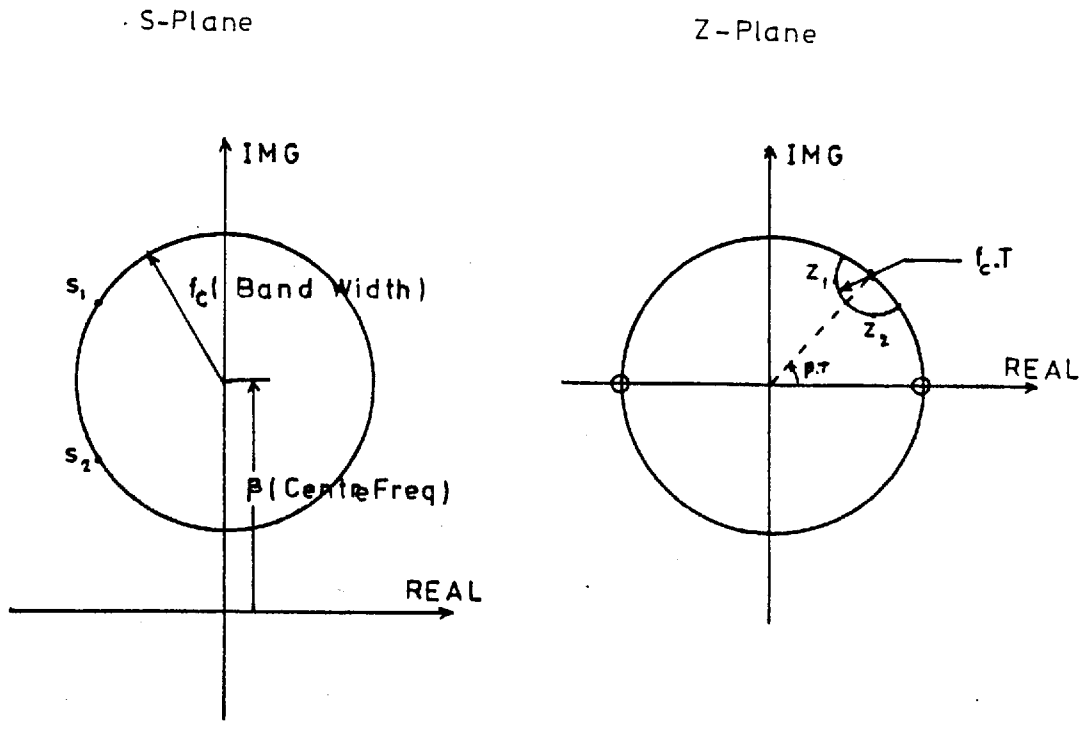


Fig (A.2.3) Pole-Zero Diagrams of a 4-Pole Band-Pass Filter.

Then by Z-tranformation,

$$Y(Z) = \sum_{n=o}^{\infty} Y(nT)\ Z^{-n}$$

But $Y(Z) = G(Z).\ X(Z)$

Thus,

$$\sum_{n=o}^{\infty} Y(nT)\ Z^{-n} = G(Z)\ .\ X(Z)$$

$$\sum_{n=o}^{\infty} Y(nT)\ Z^{-n} = G(Z).\ \sum_{n=o}^{\infty} X(nT)\ .\ Z^{-n}$$

If the transfer function G(Z) is represented in a most general form such that,

$$G(Z) = \frac{a_o + a_1\ Z^{-1} + \qquad + a_k\ Z^{-k}}{1 + b_1\ Z^{-1} + \qquad + b_m Z^{-m}}$$

the equation becomes,

$$\sum_{n=o}^{\infty} Y(nT)\ Z^{-n} = \left(\frac{a_o + a_1 Z^{-1} + \qquad + a_k Z^{-k}}{1 + b_1\ Z^{-1} + \qquad + b_m Z^{-m}} \right) \sum_{n=o}^{\infty} X(nT).Z^{-n}$$

$$\sum_{n=o}^{\infty} Y(nT)\ Z^{-n}\ .\ (\ 1 + b_1\ Z^{-1} + \qquad + b_m\ Z^{-m}) =$$

$$\sum_{n=o}^{\infty} X(nT)\ Z^{-n}.\ (\ a_o + a_1\ Z^{-1} + \qquad + a_k\ Z^{-k})$$

By equating the coefficients of Z^n $(n = -1, -2, \quad , -m)$ of the above equation, it becomes,

$$Y(nT) = a_o.x\ (nT) + a_1\ .\ X(n-1)\ T + \qquad + a_k\ .\ X(n-k)T$$

$$- b_i\ .\ Y(n-1)\ T - b_2\ .\ Y(n-2)\ T$$

$$b_m.Y\ (n-m)\ T$$

The above expression related the time sampled filter input X(nT) to the time sampled filter output Y(nT) and is the difference equation of a digital filter. The constant terms a_o, a_1,----- a_k, b_1 b_2,-----, b_m are known as filter coefficients and their values can be found by knowing the expression for the transfer function G(Z).

Arrangement of a Filter. Though it is possible to carry out the evaluation of the above filter difference equation in a single step, it is usually separated into several steps or stages to minimize the numerical truncation error. These steps can be arranged to form either,

(i) Parallel filter stages or

(ii) Cascaded filter stages.

(i) Parallel Filter Stages. In this case the transfer function G(Z) is rewritten in a partial fraction form in such a way that,

$$G(Z) = G_1(Z) + G_2(Z) + G_3(Z) + \quad + G_m(Z)$$

Then the transformation becomes,

$$Y(Z) = G(Z) \cdot X(Z)$$

$$= [\, G_1(Z)\ 1\ G_2(Z) + \quad + G_m(Z)\ ] \cdot X(Z)$$

$$= G_1(Z) \cdot X(Z) + G_2(Z) \cdot X(Z) + \quad + G_m(Z) \cdot X(Z)$$

Each G(Z) . X(Z) on the right hand side of the expression forms a parallel filter stage. If each stage is comprised of a pole and its conjucate, then the difference equation for a Mth filter stage is,

$$Ym\ (nT) = a_{2m-1} \cdot X(nT) + a_{2m} \cdot X(n-1)T - b_{2m-1} \cdot Y_m(n-1)T -$$

$$b_{2m} \cdot Ym\ (n-2)T$$

The general arrangement of a parallel filter having n stages is shown in fig (A.2.4).

(ii) Cascaded Filter Stages. For this case the transfer function G(Z) is rewritten to the following form.

$$G(Z) = G_1(Z) \cdot G_2(Z) \cdot G_3(Z) \quad \cdot G_m(Z)$$

Thus the transformation in frequency domain becomes,

$$
\begin{aligned}
Y(Z) &= G(Z) \cdot X(Z) \\
&= (G_1(Z) \cdot G_2(Z) \qquad\qquad G_m(Z) \quad) \cdot X(Z) \\
&= [\ G_2(Z) \qquad\qquad G_m(Z)\ ] \cdot G_1(Z) \cdot X(Z) \\
&= [\ G_2(Z) \qquad\qquad G_M(Z)\ ] \cdot Y_1(Z) \\
&\quad \vdots \\
&= G_m(Z) \cdot Y_{m-1}(Z)
\end{aligned}
$$

Each operation of $G_k(Z) \cdot Y_{k-1}(z)$, $k = 2, \text{-----}, m$ form a cascaded filter stage. If a stage is constructed using a pole and its conjugate, it has a difference equation of the form,

$$Y_k(nT) = Y_{k-1}(nT) - B_{2k-1} \cdot Y_k(n-1)T - B_{2k} \cdot Y_k(n-2)T$$

The general form of cascaded filter having n stages is shown in fig (A.2.5). The computed filter characteristics, their test results with a given input sinusoidal signal which is mudulated with random noise signals are shown in fig (A.2.14) to fig (A.2.16). The computed filter coefficients are given in Table (A.2.1) to Table (A.2.12).

Choice on Cascaded or Parallel Arrangement. From the difference equation of a stage of multi-stage filters, it is seen that a parallel filter stage requires more additional operations involving filter coefficients a_s than its equivalent cascaded counterpart where the coefficients a_s are either zeros or ones. Thus a cascaded filter arrangement saves about 1/3rd of the total computing time (30). Base on the saving in computing time, cascaded filter arrangments were used for separating the mean and high frequency turbulent signals from instantaneous velocity signals in the turbulence recorded data analysis.

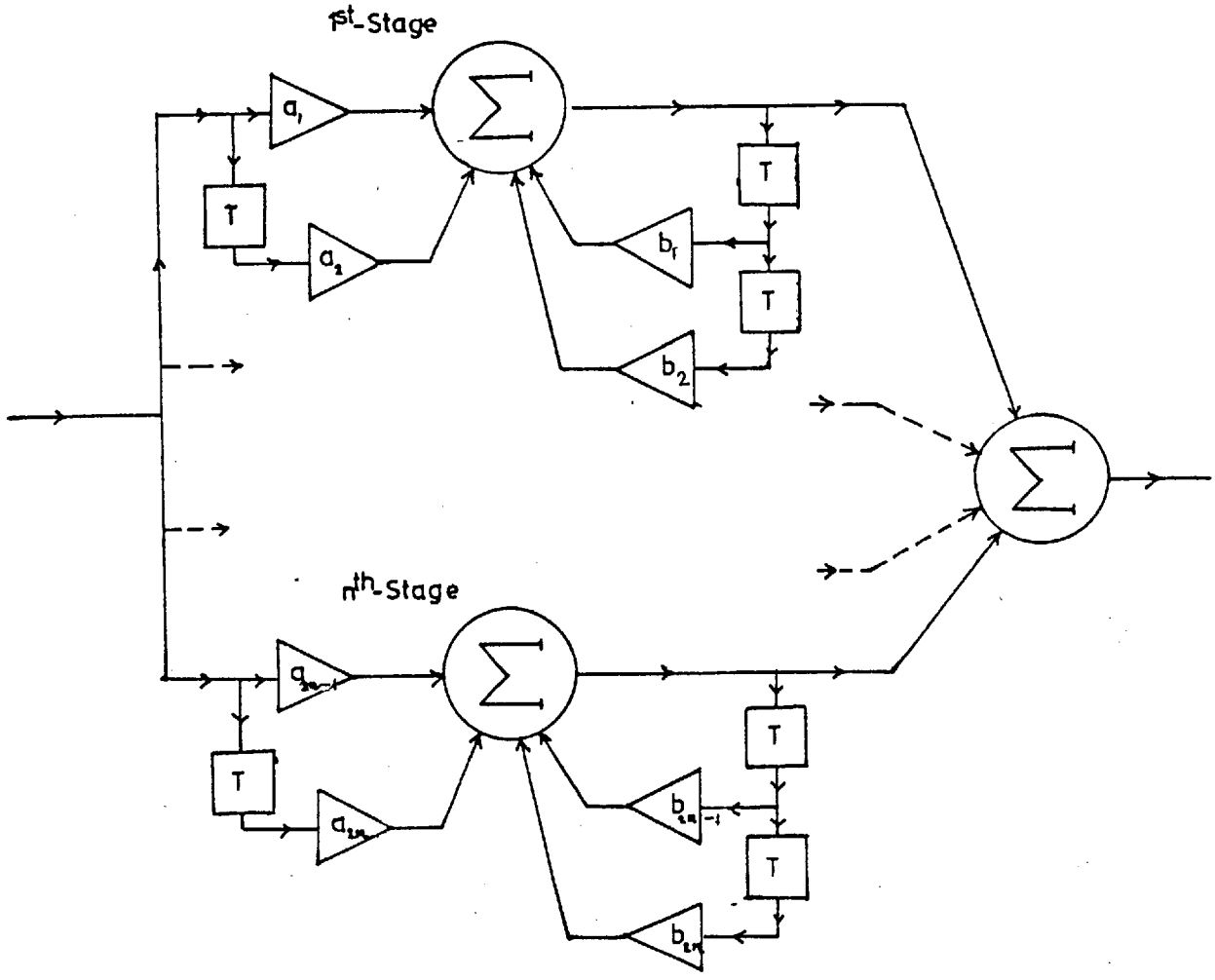


Fig (A.2.4) Arrangement of a n-stage Parallel Filter.

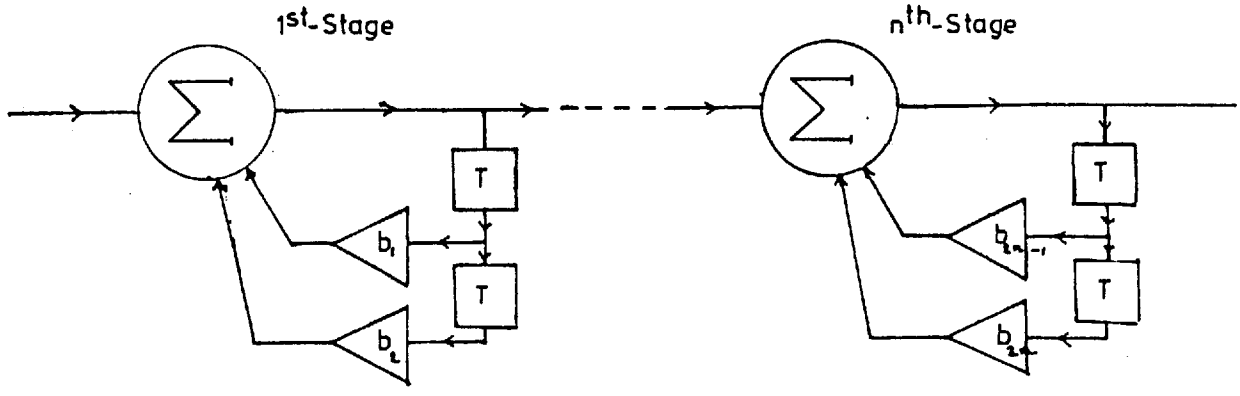


Fig (A.2.5) Arrangement of a n-stage Cascaded Filter.

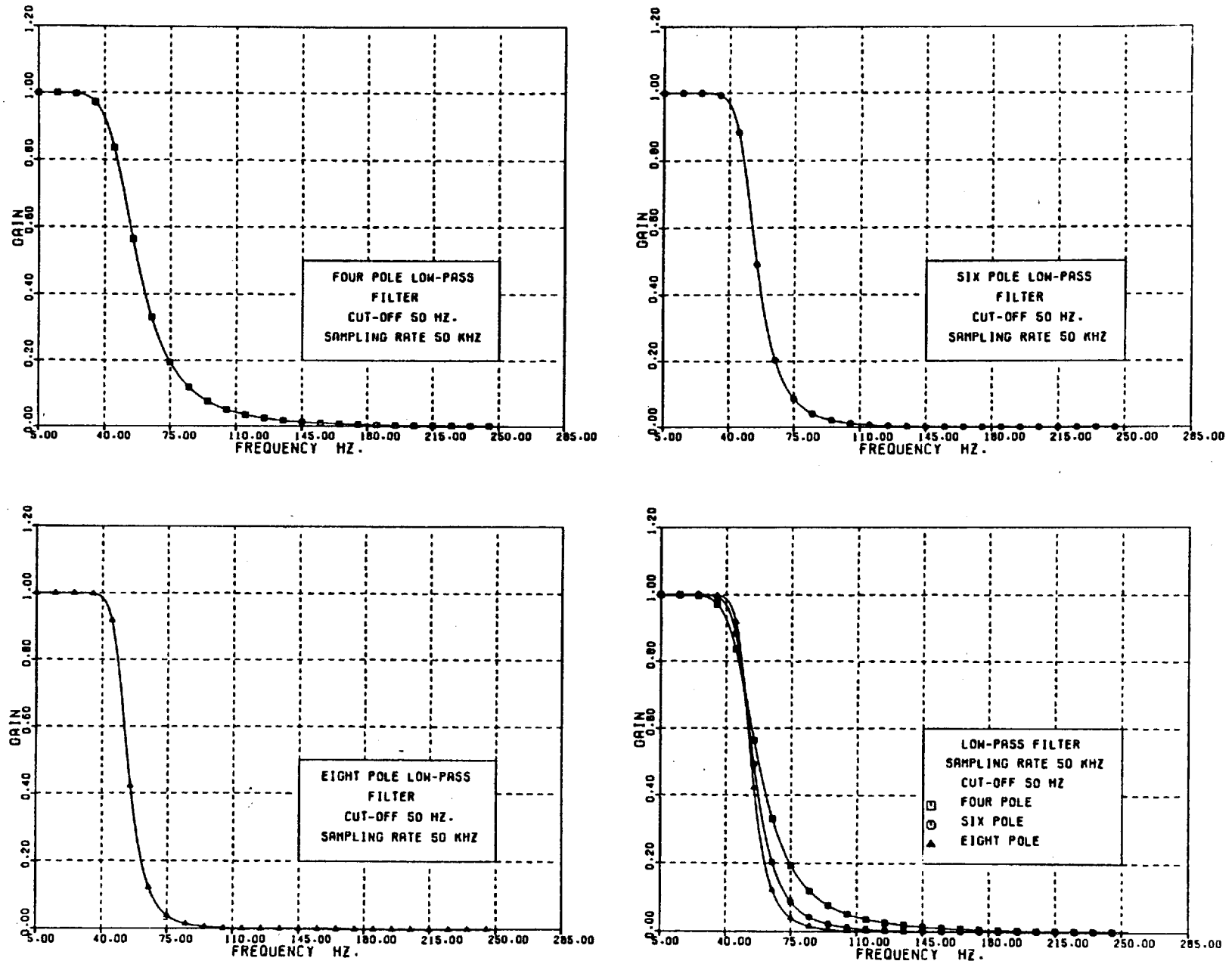


Fig (A.2.6) Characteristics of Low Pass Digital Filters having Different Number of Poles.

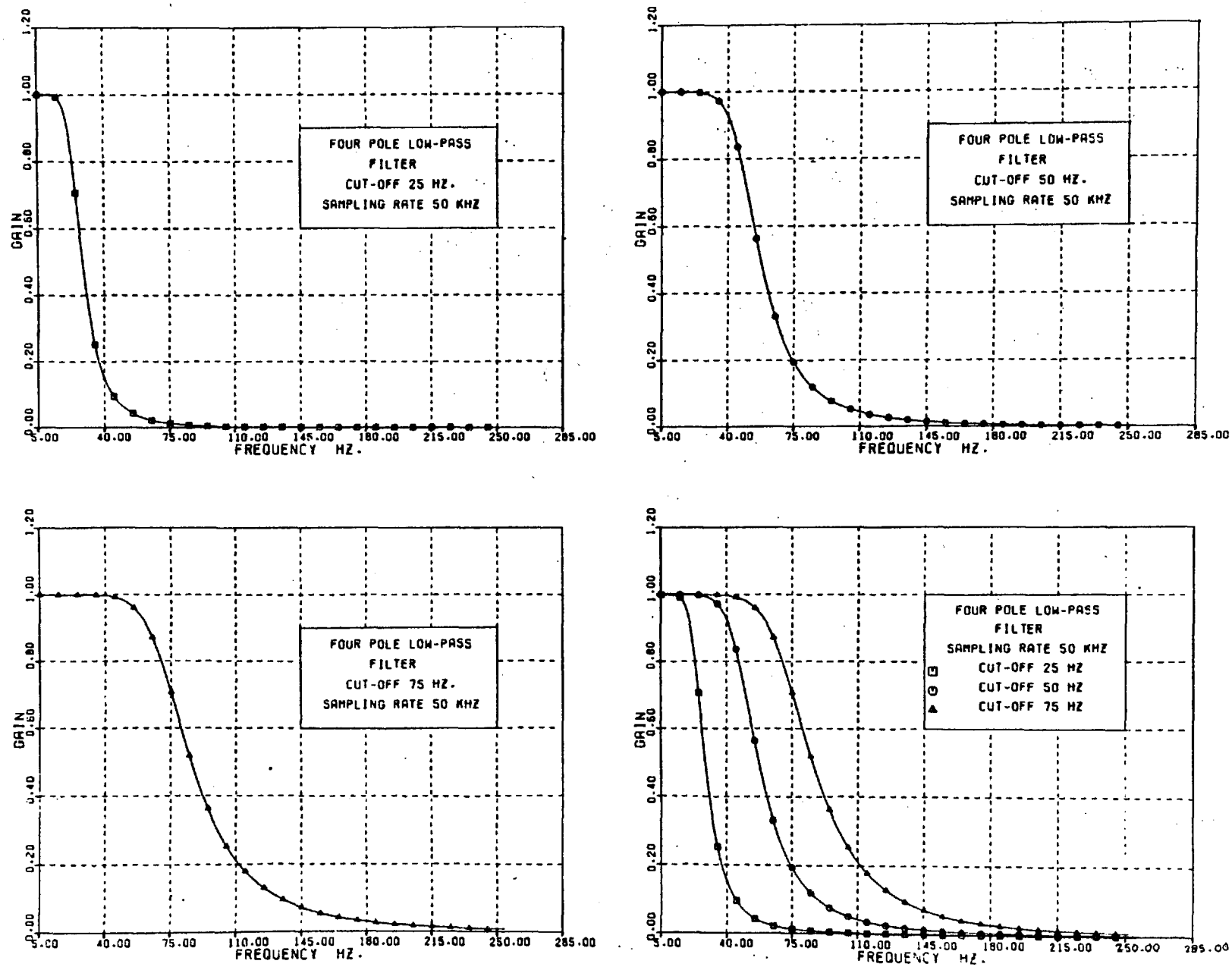


Fig (A.2.7) Effect of Cut-off Frequency on Low Pass Filter Characteristics.

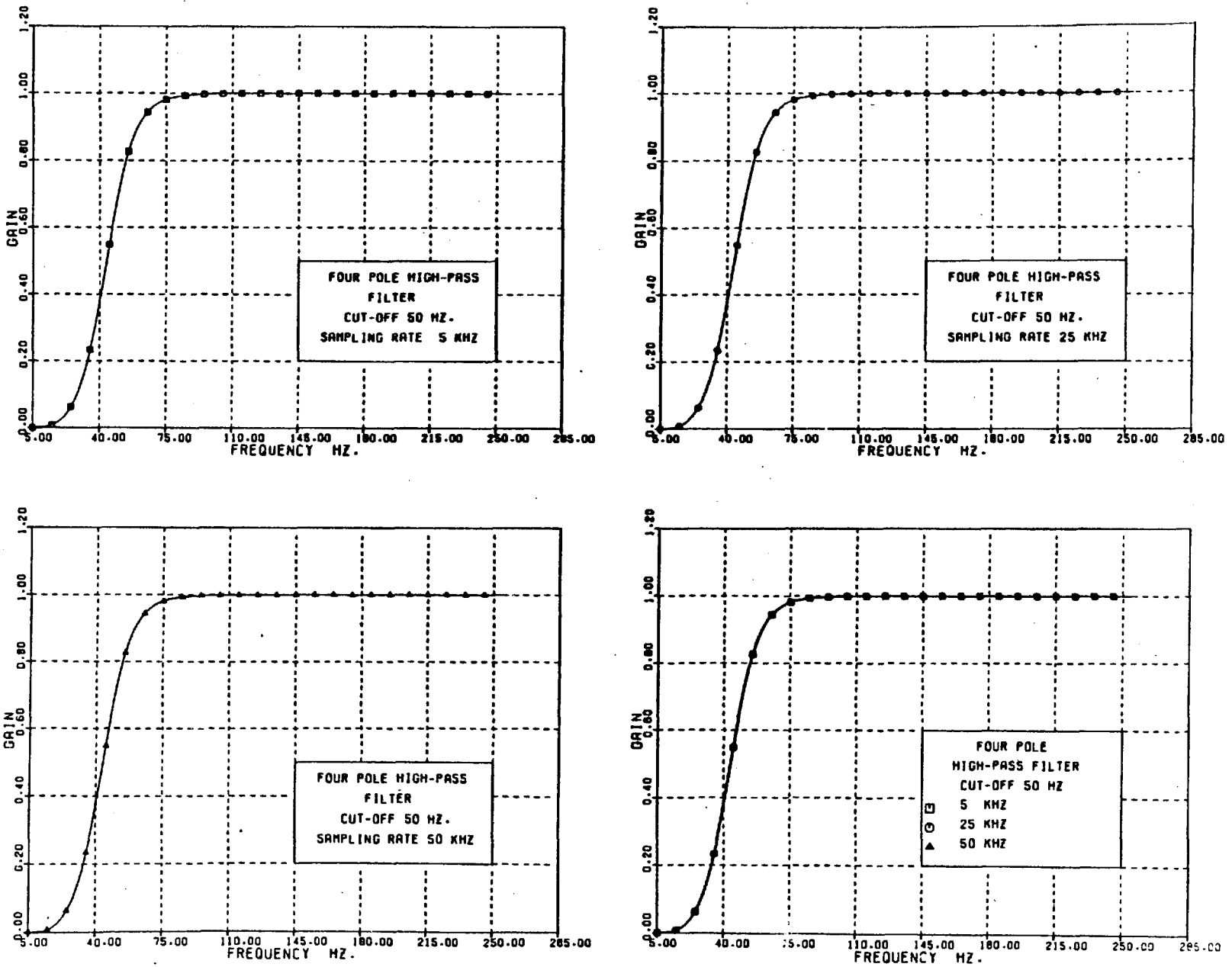


Fig (A.2.8) Effect of Sampling Rate or High-Pass Filter Characteristics.

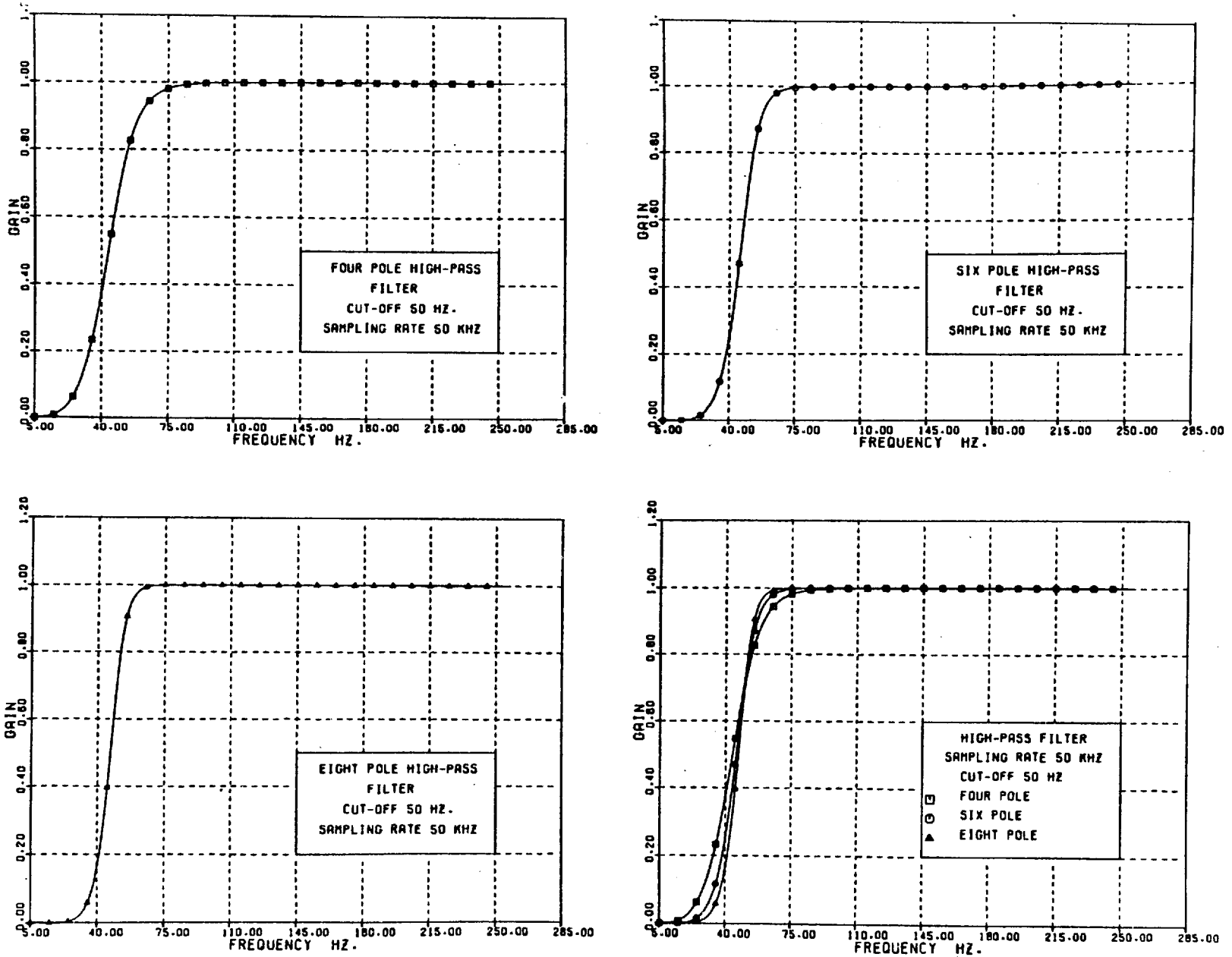


Fig (A.2.9) Effect of Number of Poles on High-Pass Filter Characteristics.

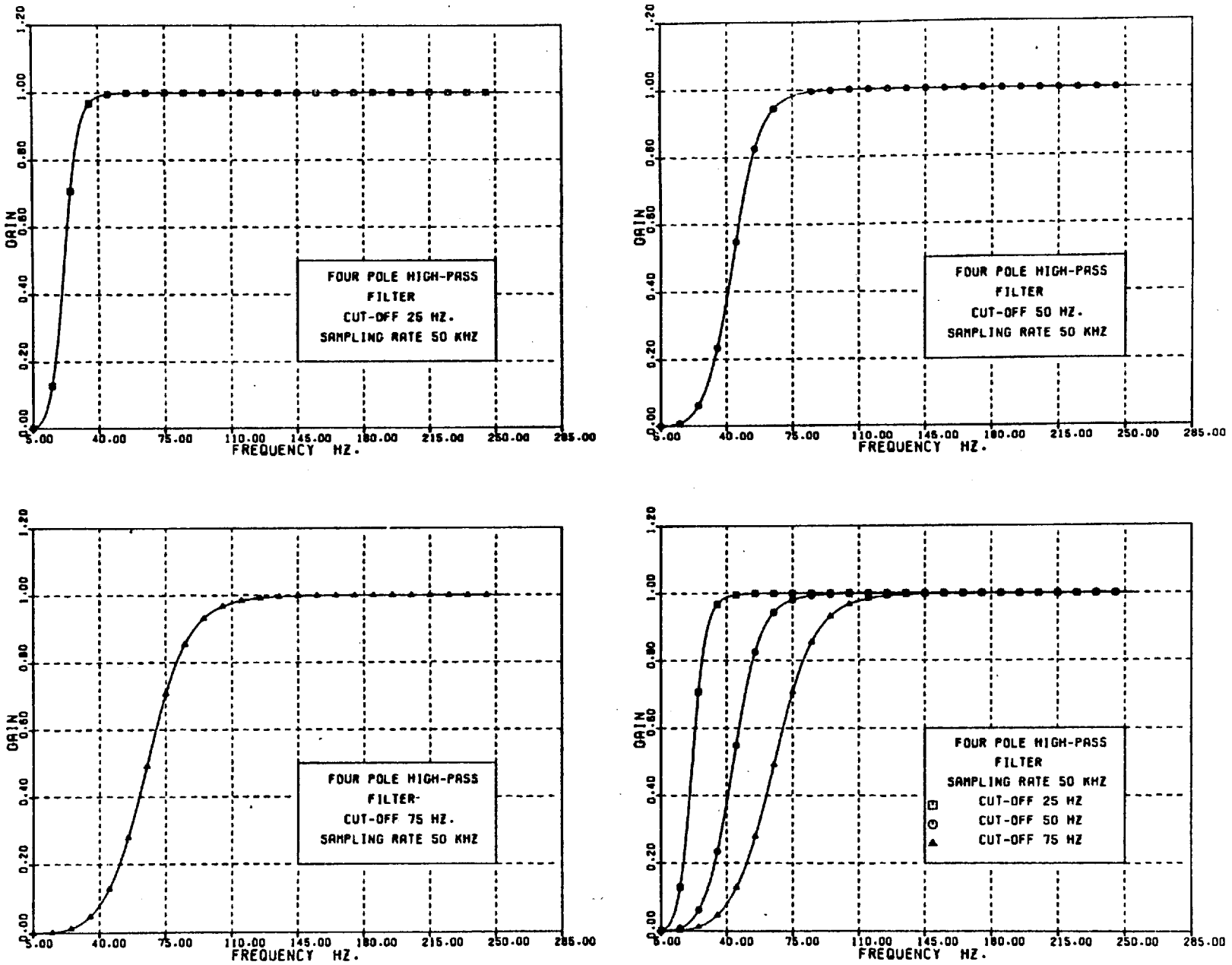


Fig (A.2.10) Effect of Cut-Off Frequency on High-Pass Filter Characteristics.

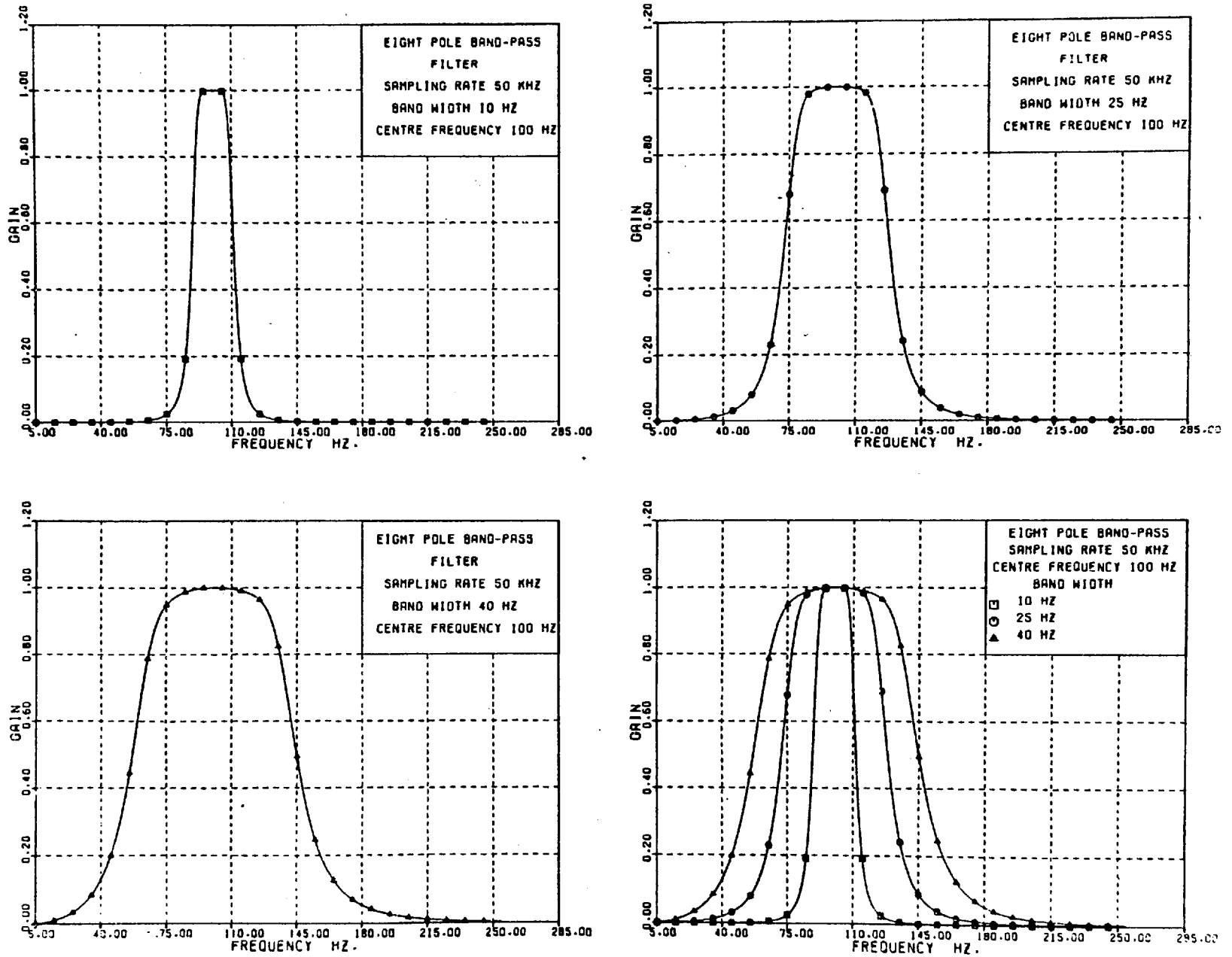


Fig (A.2.11) Effect of Band Width on Band Pass Filter Characteristics.

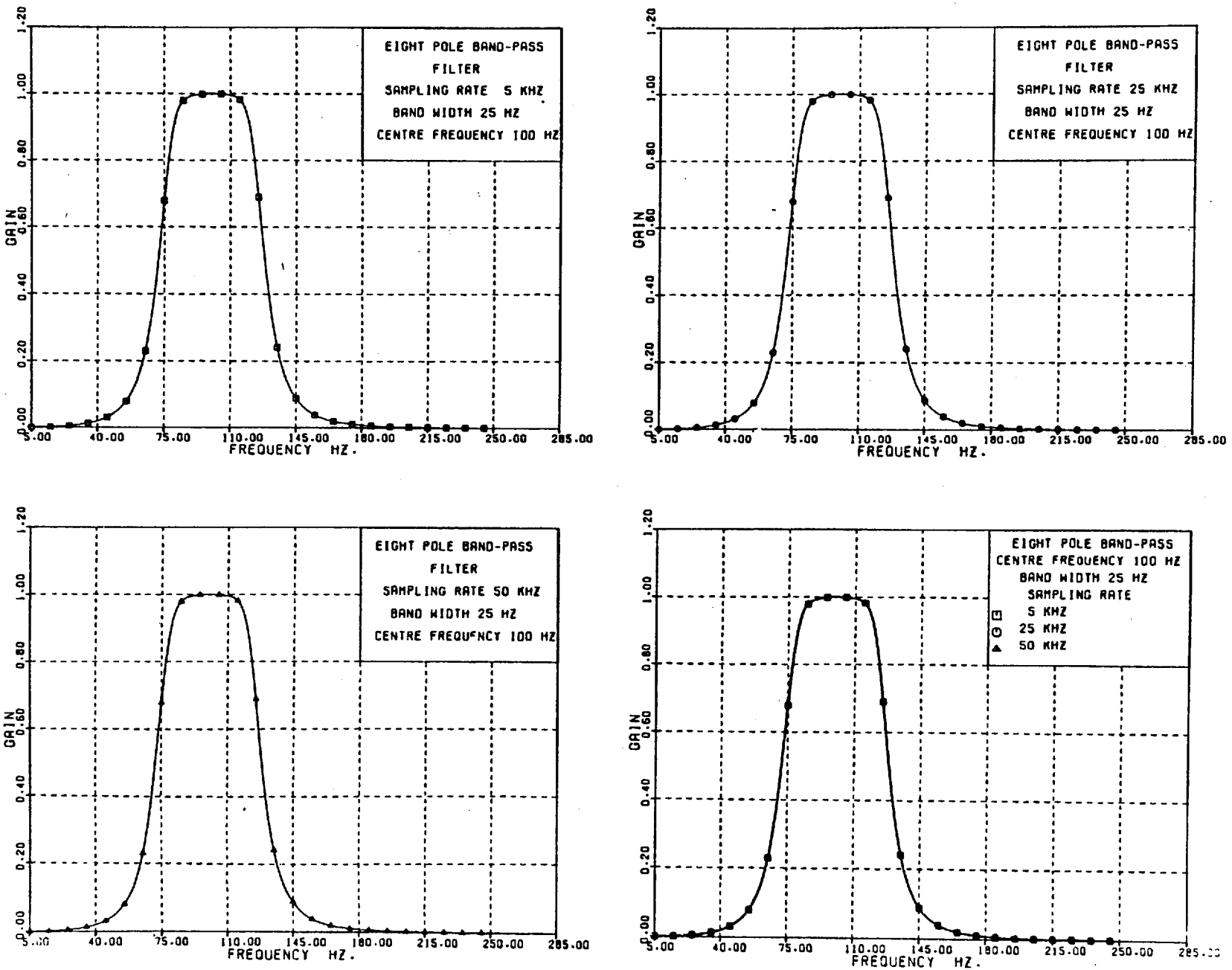


Fig (A.2.12) Effect of Sampling Rate on Band Pass Filter Characteristics.

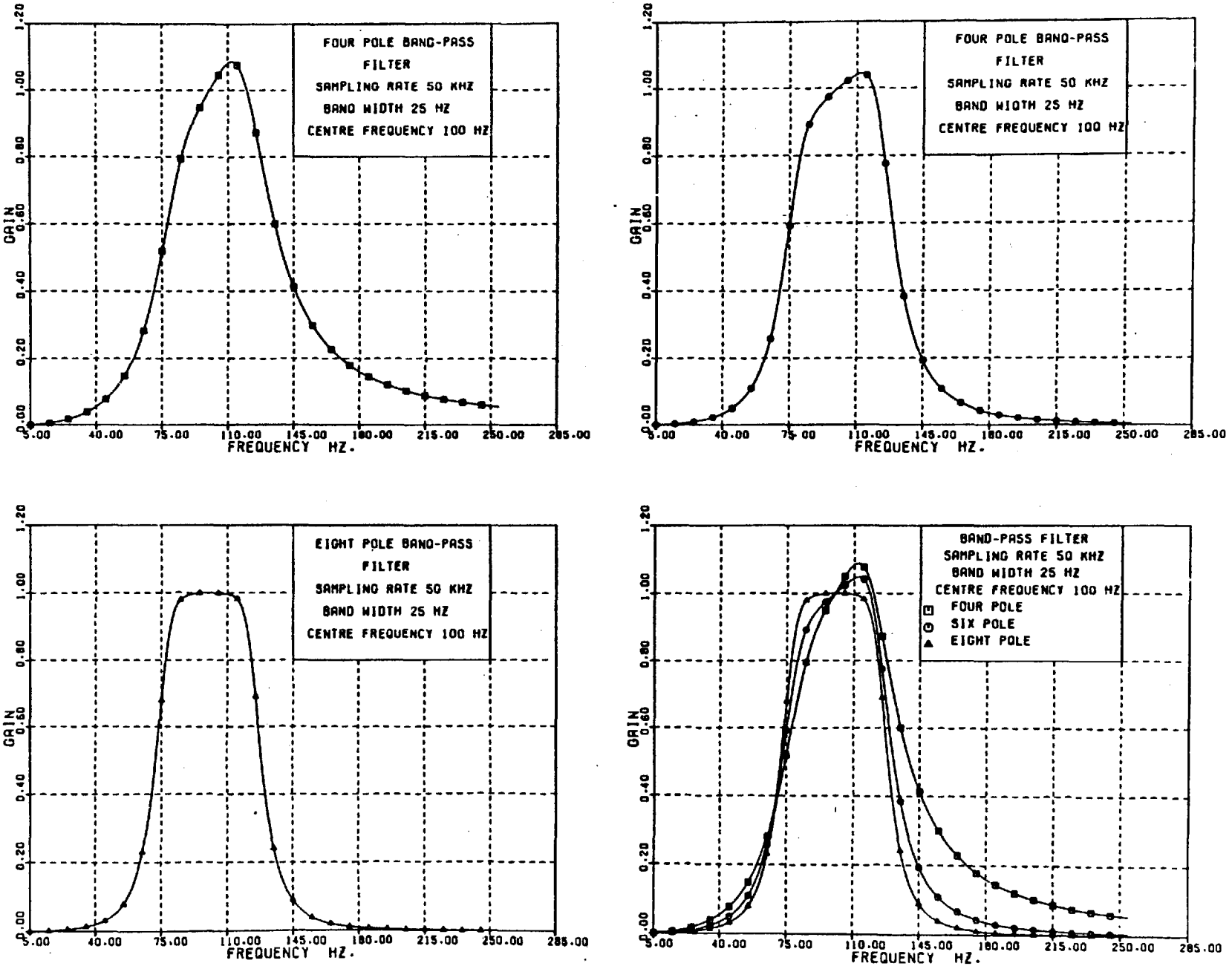


Fig (A.2.13) Effect of Number of Poles on Band Pass Filter Characteristics.

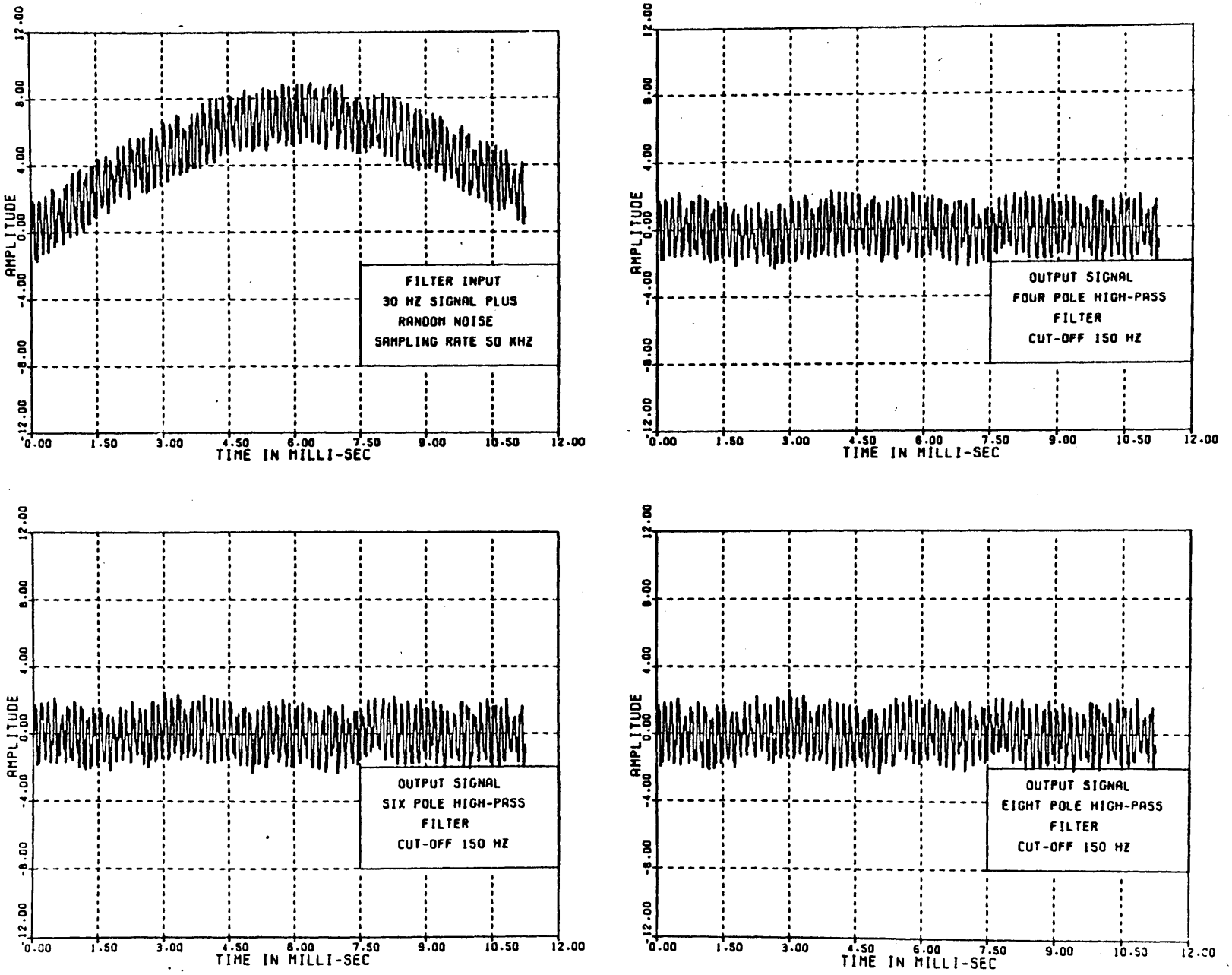


Fig (A.2.14) Test Results of a High Pass Digital Filter.

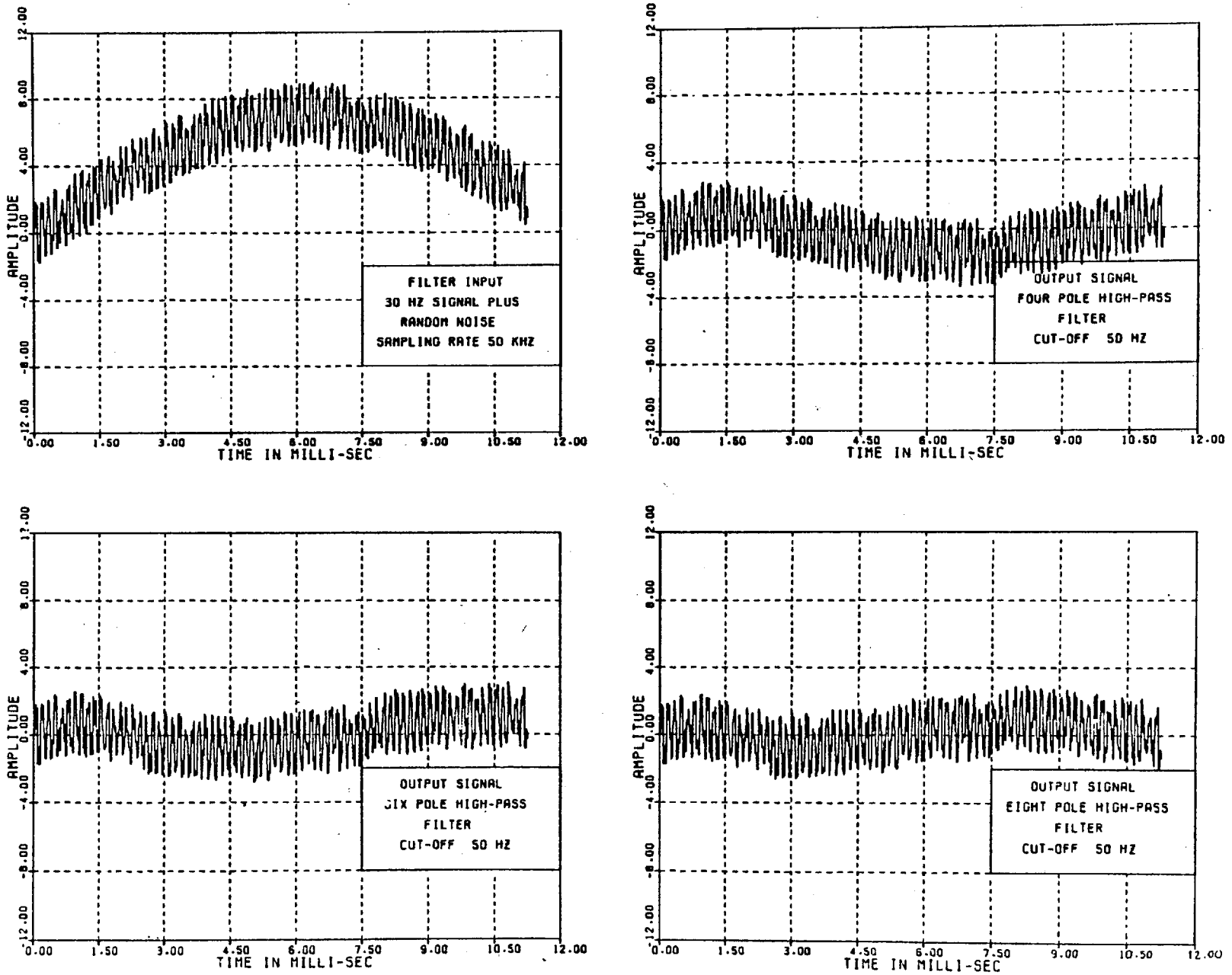


Fig (A.2.15) Test Results of a High Pass Digital Filter.

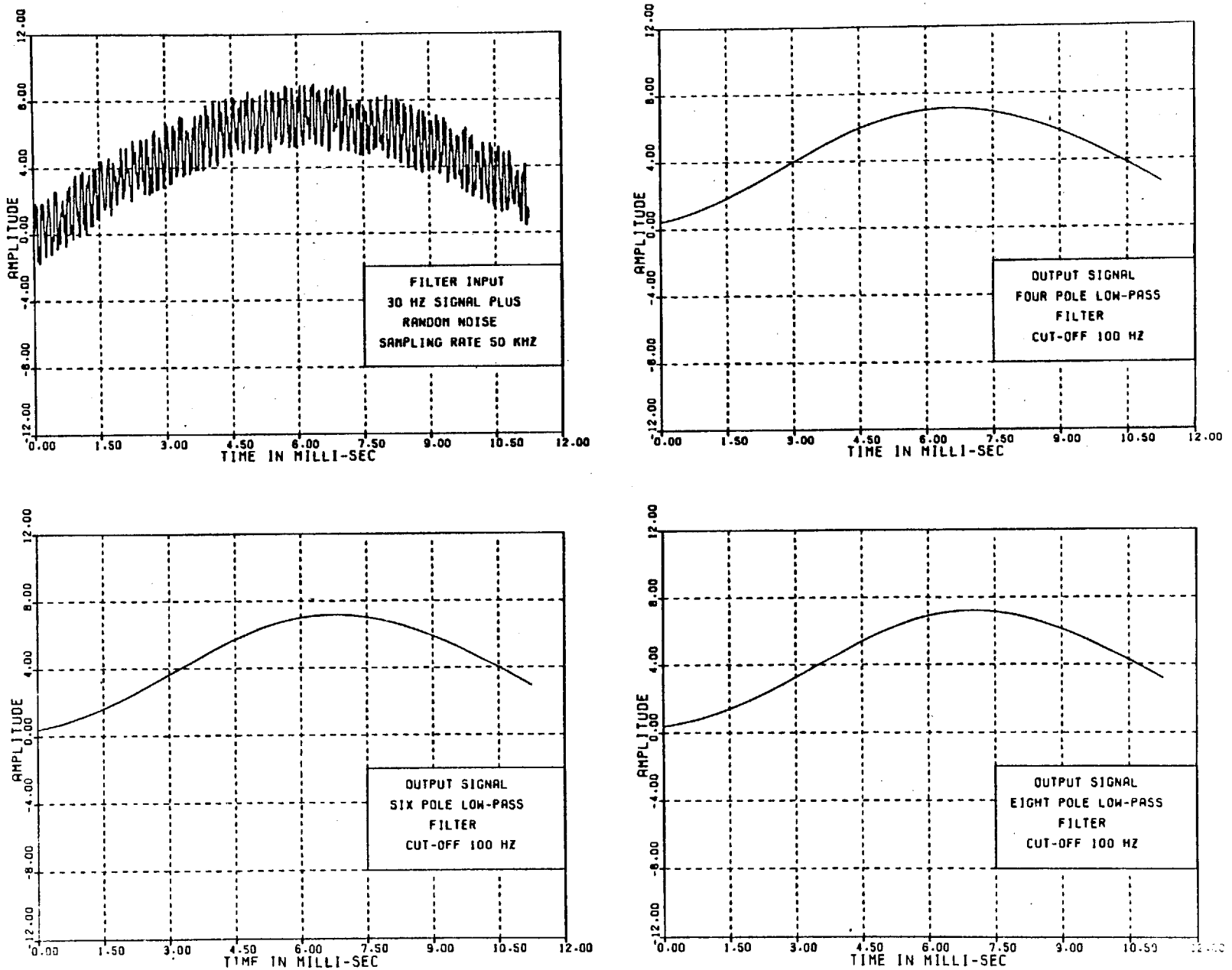


Fig (A.2.16) Test Results of a Low Pass Digital Filter.

COMPUTED FILTER COEFFICIENTS
EIGHT POLE LOW-PASS FILTER
SAMPLING RATE 5 KHZ

CUT-OFF HZ	B0	B1	B2	B3	B4	B5	B6	B7	B8
25	.87545710E-12	-1.939278678	.940235767	-1.948136842	.949098388	-1.964724893	.965694749	-1.986836154	.987817012
50	.20677928E-09	-1.880330258	.884043297	-1.897040380	.900787750	-1.928754409	.932566348	-1.971883880	.975782448
75	.48895544E-08	-1.823105203	.831209127	-1.846720719	.854936202	-1.892147289	.900574425	-1.955179632	.963894502
100	.45062093E-07	-1.767555287	.781532550	-1.797186704	.811418571	-1.854960877	.869679993	-1.936781140	.952151387
125	.24781275E-06	-1.713633562	.734824857	-1.748445972	.770116058	-1.817251109	.839845402	-1.916667352	.940551337
150	.98311835E-06	-1.661294329	.690908612	-1.700505011	.730915909	-1.779072515	.811034295	-1.894938390	.929092611
175	.31132379E-05	-1.610493105	.649616989	-1.653369210	.693711111	-1.740478204	.783211559	-1.871615487	.917773487
200	.83594955E-05	-1.561186593	.610793127	-1.607042906	.658400097	-1.701519868	.756343290	-1.846740938	.906592263
225	.19789391E-04	-1.513332653	.574299544	-1.561529440	.624886471	-1.662247780	.730396744	-1.820358046	.895547260
250	.42315495E-04	-1.466890273	.539967570	-1.516831202	.593078742	-1.622710790	.705340300	-1.792511065	.884636818
275	.83887684E-04	-1.421819544	.507696822	-1.472949673	.562890078	-1.582956333	.681143423	-1.763245145	.873859298
300	.15525260E-03	-1.378081625	.477354711	-1.429885476	.534238066	-1.543030424	.657776627	-1.732606279	.863213081
325	.27174897E-03	-1.335638723	.448825972	-1.387638418	.507044487	-1.502977666	.635211435	-1.700641246	.852696566
350	.45360471E-03	-1.294454054	.422002232	-1.346207521	.481235105	-1.462841258	.613420347	-1.667397557	.842308173
375	.72630102E-03	-1.254491868	.396781592	-1.305591086	.456739463	-1.422662995	.592376808	-1.632923395	.832046343
400	.11237702E-02	-1.215717322	.373068244	-1.265786707	.433490688	-1.382483281	.572055172	-1.597267566	.821909532
425	.16839965E-02	-1.178096559	.350772107	-1.226791323	.411425313	-1.342341132	.552430676	-1.560479440	.811896218
450	.24544944E-02	-1.141596629	.329808481	-1.188501251	.390483101	-1.302274194	.533479403	-1.522608836	.802004895
475	.34901411E-02	-1.106185480	.310097730	-1.151212221	.370606882	-1.262318744	.515178258	-1.483705265	.792234079
500	.48538497E-02	-1.071831934	.291564976	-1.114619410	.351742394	-1.222509710	.497504938	-1.443822280	.782582301
525	.66165699E-02	-1.038505664	.274139819	-1.078817474	.333838140	-1.182880677	.480437906	-1.403008018	.773048109
550	.89571127E-02	-1.006177171	.257756063	-1.043800582	.316845240	-1.143463905	.463956363	-1.361314844	.763630073
575	.11861800E-01	-.974817765	.242351469	-1.009562444	.300717307	-1.104290341	.448040224	-1.318794362	.754326777
600	.15123943E-01	-.944399543	.227867520	-.976096342	.285410311	-1.065399634	.432670091	-1.275498357	.745136823
625	.19343156E-01	-.914895369	.214249192	-.943395158	.270882466	-1.026790151	.417827235	-1.231478745	.736058829
650	.24424531E-01	-.886278854	.201444753	-.911451399	.257094112	-.988518996	.403493567	-1.186787517	.727091433
675	.30477668E-01	-.858524335	.189405562	-.880257226	.244007607	-.950602022	.389651619	-1.141476694	.718233287
700	.37615605E-01	-.831606850	.178065884	-.849804479	.231587227	-.913063853	.376284522	-1.095598265	.709483059
725	.45953645E-01	-.805502167	.167442717	-.820084701	.219799064	-.875927900	.363375987	-1.049204147	.700839435
750	.55608112E-01	-.780186663	.157435532	-.791089159	.208610937	-.839216383	.350910282	-1.002346128	.692301117
775	.66695093E-01	-.755637414	.148026512	-.762808866	.197992304	-.802950344	.338872217	-.955075821	.683866820
800	.79329065E-01	-.731832119	.139179915	-.735234612	.187914177	-.767149678	.327247120	-.907444615	.675535279
825	.93621632E-01	-.708749102	.130861934	-.708356969	.178349042	-.731833134	.316020826	-.859503625	.667305240
850	.10968019E+00	-.686367289	.123041071	-.682166325	.169270788	-.697018363	.305179652	-.811303649	.659175468
875	.12750663E+00	-.664666193	.115687516	-.656652892	.160654632	-.662721915	.294710387	-.762895119	.651144741
900	.14719633E+00	-.643625902	.108773634	-.631806732	.152477053	-.628959270	.284600273	-.714328059	.643211852
925	.16943659E+00	-.623227061	.102272861	-.607617771	.144715725	-.595744862	.274836989	-.665652036	.635375610
950	.19350596E+00	-.603450957	.096160602	-.584075814	.137349461	-.563092096	.265406637	-.616916123	.627634836
975	.21977313E+00	-.584279006	.090413637	-.561170566	.130358152	-.531013374	.256303727	-.568168052	.619988358
1000	.24829607E+00	-.565673743	.085010135	-.538891640	.123722712	-.499520114	.247511164	-.519458177	.612435057

Table (A.2.1)

COMPUTED FILTER COEFFICIENTS
EIGHT POLE LOW-PASS FILTER
SAMPLING RATE 25 KHZ

CUT-OFF HZ	B0	B1	B2	B3	B4	B5	B6	B7	B8
25	.239028176-17	-1.987711481	.987750717	-1.989566562	.989605835	-1.993003475	.993042816	-1.997512011	.997551441
50	.602137245-15	-1.975495497	.975651479	-1.979163434	.979319708	-1.985977220	.986134035	-1.994951352	.995108877
75	.151856016-13	-1.963351640	.963700447	-1.968790711	.969140497	-1.978921718	.979273319	-1.992319301	.992672294
100	.149251586-12	-1.951279502	.951895808	-1.958448434	.959067090	-1.971837449	.972460334	-1.989613141	.990241677
125	.875457106-12	-1.939278678	.940235767	-1.948136842	.949098388	-1.954724893	.965694749	-1.985326154	.987817012
150	.378417316-11	-1.927348766	.928718552	-1.937855872	.939233302	-1.957584527	.958976233	-1.983387626	.986398283
175	.125104246-10	-1.915499766	.917342416	-1.927805559	.929470756	-1.950416624	.952304459	-1.981067944	.982385477
200	.358272976-10	-1.903700078	.906105629	-1.917396286	.919809583	-1.943222258	.945679101	-1.978077097	.980578579
225	.904568836-10	-1.891900307	.895006485	-1.907197833	.910249029	-1.936001297	.939099838	-1.975015678	.978177574
250	.205770226-09	-1.880330258	.884043297	-1.897040380	.900787750	-1.928754409	.932566348	-1.971883880	.975782448
275	.436169156-09	-1.868748940	.873214400	-1.886914003	.891424613	-1.921482061	.926076312	-1.968681999	.973393187
300	.859934016-09	-1.857236162	.862518150	-1.876818777	.882159196	-1.914184715	.919535415	-1.965410333	.971009776
325	.159721196-08	-1.845791537	.851952921	-1.866754774	.872989886	-1.906562832	.913237342	-1.962069182	.968632202
350	.285125926-08	-1.834414579	.841517108	-1.856722055	.863915836	-1.899516972	.906883782	-1.958658847	.966280448
375	.489555446-08	-1.823105203	.831209127	-1.846720719	.854936202	-1.892147289	.900574425	-1.955179632	.963934502
400	.806316426-08	-1.811862730	.821027411	-1.836750803	.846049853	-1.884754540	.894308953	-1.951631844	.961594349
425	.126035756-07	-1.800686978	.810970414	-1.826812381	.837255871	-1.877339075	.888087091	-1.948015790	.959179976
450	.200326576-07	-1.789577270	.801036607	-1.816905517	.828553295	-1.869901345	.881908506	-1.944331780	.956831367
475	.303803416-07	-1.778533511	.791224483	-1.807030272	.819941175	-1.862441797	.875772908	-1.940580125	.954488508
500	.450720936-07	-1.767555287	.781532550	-1.797186704	.811418571	-1.854960877	.869679993	-1.936761140	.952151387
525	.655137096-07	-1.756642167	.771959337	-1.787374871	.802984552	-1.847459026	.863629469	-1.932875138	.949919388
550	.935331036-07	-1.745793801	.762503388	-1.777594828	.794638198	-1.839936587	.857621040	-1.928922439	.947494297
575	.131344956-06	-1.735008822	.753163268	-1.767846630	.786372597	-1.832394297	.851654413	-1.924903361	.945174201
600	.181671616-06	-1.724283883	.743937553	-1.758130328	.778204948	-1.824832294	.845729297	-1.920818224	.942859985
625	.247812756-06	-1.713633552	.734824857	-1.748445972	.770116058	-1.817251109	.839845402	-1.916667352	.940551337
650	.333731196-06	-1.703040557	.725823779	-1.738793610	.762111344	-1.809651177	.834002443	-1.912451070	.938248342
675	.444145836-06	-1.692510488	.716932958	-1.729173289	.754189833	-1.802032925	.828200135	-1.908169704	.935950985
700	.584639146-06	-1.682042997	.708151043	-1.719585054	.746350659	-1.794396781	.822438194	-1.903823581	.933659254
725	.761751496-06	-1.671637729	.699476700	-1.710028948	.738592966	-1.786743170	.816716341	-1.899413033	.931373134
750	.983118356-06	-1.661294329	.690908612	-1.700505011	.730915909	-1.779072515	.811034295	-1.894938390	.929092611
775	.125975046-05	-1.651012446	.682445477	-1.691013285	.723318648	-1.771385235	.805391780	-1.890399986	.926817673
800	.159532246-05	-1.640791730	.674086009	-1.681553806	.715800354	-1.763681750	.799788521	-1.885798156	.924548305
825	.200801336-05	-1.630631831	.665828939	-1.672126611	.708360207	-1.755962474	.794224245	-1.881133237	.922284494
850	.250805496-05	-1.620532404	.657673012	-1.662731734	.700997394	-1.748227821	.788698681	-1.876405567	.920026225
875	.311323706-05	-1.610493105	.649616989	-1.653369210	.693711111	-1.740478204	.783211559	-1.871615487	.917773487
900	.383790656-05	-1.600513691	.641659648	-1.644039058	.686500563	-1.732714029	.777762613	-1.866763337	.915526264
925	.470212936-05	-1.590593520	.633799776	-1.634741339	.679364952	-1.724935705	.772351575	-1.861849462	.913284544
950	.572798056-05	-1.580732555	.626036183	-1.625476052	.672303531	-1.717143636	.766978183	-1.856874206	.911048313
975	.693762076-05	-1.570930157	.618357858	-1.616243232	.665315436	-1.709339229	.761642175	-1.851837915	.908817557
1000	.835949556-05	-1.561186593	.610793127	-1.607042906	.658400097	-1.701519858	.756343290	-1.846740938	.906592263

Table (A.2.2)

COMPUTED FILTER COEFFICIENTS
EIGHT POLE LOW-PASS FILTER
SAMPLING RATE 50 KHZ

CUT-OFF HZ	B0	B1	B2	B3	B4	B5	B6	B7	B8
25	.94125198E-20	-1.993846646	.993856487	-1.994779498	.994789342	-1.996505484	.996515337	-1.998765106	.998774970
50	.23902817E-17	-1.987711481	.987750717	-1.989566562	.989605835	-1.993003475	.993042816	-1.997512011	.99755144
75	.6076904CE-16	-1.981504448	.981632458	-1.984361203	.984449337	-1.989494034	.989582396	-1.996240748	.996329410
100	.60218724E-15	-1.975495457	.975651479	-1.979163434	.979319708	-1.985977220	.986134035	-1.994951352	.995108877
125	.35602382E-14	-1.969414578	.969657551	-1.973973267	.974216808	-1.982453035	.982697689	-1.993643858	.993888839
150	.[illegible]5185601E-13	-1.963351640	.963760447	-1.968790711	.969140497	-1.978921718	.979273319	-1.992319301	.992672234
175	.[illegible]17022031E-12	-1.957306631	.957779941	-1.963615780	.964090637	-1.975363149	.975860881	-1.990974717	.99145624
200	.14928136E-12	-1.951279502	.951898808	-1.958448484	.959067030	-1.971637449	.972460334	-1.989613141	.990241677
225	.37480213E-12	-1.945270201	.946047824	-1.953280835	.954059719	-1.968284677	.969071637	-1.988233608	.989028601
250	.87545710E-12	-1.939278578	.940235767	-1.948136842	.949098356	-1.964724893	.965694749	-1.986836154	.987817012
275	.19815[illegible]E-11	-1.933304883	.934459416	-1.942992518	.944152961	-1.961158157	.962329628	-1.985420915	.986606906
300	.37041731[illegible]E-11	-1.927348766	.928718552	-1.937855872	.939233302	-1.957584527	.958976233	-1.983987629	.985388283
325	.69708400E-11	-1.921410277	.923012958	-1.932726916	.934339279	-1.954004063	.955634523	-1.982339523	.98419114[illegible]
350	.12310424E-10	-1.915489366	.917342416	-1.927605659	.929470756	-1.950416824	.952304459	-1.981067844	.982395477
375	.21551675E-10	-1.909585983	.911706711	-1.922492112	.924627602	-1.946822870	.948985998	-1.979871323	.981791290
400	.35827297E-10	-1.903700078	.905105929	-1.917385286	.919809583	-1.943222258	.943679101	-1.978077097	.980578579
425	.5[illegible]E-10	-1.897831603	.900538957	-1.912288190	.915016869	-1.939615047	.942383728	-1.976555203	.979377341
450	.[illegible]E-10	-1.891980507	.895006485	-1.907197833	.910249029	-1.936001297	.939099838	-1.975015678	.978177574
475	.1[illegible]E-09	-1.886146742	.889508001	-1.902113227	.905505033	-1.932381055	.935827391	-1.973458558	.976979277
500	.[illegible]77928E-09	-1.880330258	.884043297	-1.897040280	.900787750	-1.928754409	.932566348	-1.971883880	.975782448
[illegible]	.3030[illegible]722E-09	-1.874531007	.878612165	-1.891973302	.896094053	-1.925121389	.929316668	-1.970291681	.974587086
[illegible]	.436[illegible]915E-09	-1.868748940	.873214400	-1.886914003	.891424513	-1.921482051	.926078312	-1.968681509	.973393187
575	.61744660E-09	-1.862984008	.867849796	-1.881862491	.886779903	-1.917836484	.922851241	-1.967054871	.972200752
600	.[illegible]3401E-09	-1.857236152	.862518150	-1.876818777	.882159196	-1.914184715	.919635415	-1.965410333	.971009776
625	.11[illegible]678E-08	-1.851505355	.857219258	-1.871782868	.877562566	-1.910526912	.916430795	-1.963748424	.969820260
650	.16072119E-08	-1.845791537	.851952921	-1.866754774	.872989808	-1.906862832	.913237342	-1.962069182	.968632202
675	.21502523E-08	-1.840094661	.846718937	-1.861734503	.868441036	-1.903192833	.910055018	-1.960372643	.967445598
700	.28612582E-08	-1.834414679	.841517108	-1.856722065	.863915886	-1.899516872	.906883782	-1.958658647	.966260448
725	.37580210E-08	-1.828751542	.836347237	-1.851717468	.859414316	-1.895835005	.903723597	-1.956927830	.965076750
750	.48[illegible]444E-08	-1.823105203	.831209127	-1.846720719	.854936202	-1.892147289	.900574425	-1.955179632	.963894502
775	.6[illegible]51585E-08	-1.817475615	.826102583	-1.841731828	.850481421	-1.888453782	.897436226	-1.953414291	.962713703
800	.80[illegible]6425E-08	-1.811862730	.821027411	-1.836750803	.846049853	-1.884754540	.894309963	-1.951631844	.961534349
825	.10231052E-07	-1.806266500	.815983418	-1.831777651	.841641377	-1.881049619	.891192597	-1.949832331	.960356441
850	.12[illegible]7618E-07	-1.800686878	.810970414	-1.826812381	.837255871	-1.877339075	.888087091	-1.948015790	.959179975
875	.15[illegible]02E-07	-1.795123917	.805988206	-1.821855001	.832893217	-1.873622955	.884992406	-1.946182260	.958004951
900	.20832657E-07	-1.789577270	.801035607	-1.816905517	.828553295	-1.869901345	.881908506	-1.944331780	.956831367
925	.24742243E-07	-1.784047190	.796115429	-1.811965939	.824235987	-1.866174271	.878835351	-1.942464389	.955659220
950	.30[illegible]4196E-07	-1.778533531	.791224483	-1.807030272	.819941175	-1.862441797	.875772906	-1.940580125	.954488508
975	.37017[illegible]6E-07	-1.773036745	.786363585	-1.802101524	.815668742	-1.858703991	.872721132	-1.938679029	.953319231
1000	.45[illegible]20[illegible]E-07	-1.767556287	.781532550	-1.797186704	.811418571	-1.854960877	.869679993	-1.936761140	.952151387

Table (A.2.3)

COMPUTED FILTER COEFFICIENTS
EIGHT POLE HIGH-PASS FILTER
SAMPLING RATE 5 KHZ

CUT-OFF HZ	B0	B1	B2	B3	B4	B5	B6	B7	B8
25	.92263980E+00	-1.939278678	.940235767	-1.948136842	.949098388	-1.964724893	.965694749	-1.986836154	.987817012
50	.85126421E+00	-1.880330258	.884043297	-1.897040380	.900767750	-1.928754409	.932566348	-1.971883880	.975792448
75	.78541024E+00	-1.823105203	.831209127	-1.846720719	.854936202	-1.892147289	.900574425	-1.955179632	.963894502
100	.72465074E+00	-1.767555287	.781532550	-1.797186704	.811418571	-1.854960877	.869679993	-1.936761140	.952151387
125	.66859161E+00	-1.713633562	.734824857	-1.748445972	.770116058	-1.817251109	.839845402	-1.916657352	.940551337
150	.61686923E+00	-1.661294329	.690908612	-1.700505011	.730915909	-1.779072515	.811034295	-1.894938390	.929092611
175	.56914810E+00	-1.610493105	.649616989	-1.653369210	.693711111	-1.740478204	.783211559	-1.871615487	.917773487
200	.52511868E+00	-1.561186593	.610793127	-1.607042906	.658400097	-1.701519868	.756343290	-1.846740938	.906592263
225	.48449539E+00	-1.513332653	.574289544	-1.561529440	.624885471	-1.662247780	.730396744	-1.820358046	.895547260
250	.44701472E+00	-1.466890273	.539967570	-1.516831202	.593078742	-1.622710790	.705340300	-1.792511065	.884636818
275	.41243356E+00	-1.421819544	.507696822	-1.472949673	.562890078	-1.582956333	.681143423	-1.763245145	.873859298
300	.38052761E+00	-1.378081625	.477354711	-1.429885476	.534238066	-1.543030424	.657776627	-1.732606279	.863213091
325	.35109991E+00	-1.335638723	.448825972	-1.387638416	.507044487	-1.502977666	.635211435	-1.700641246	.852696566
350	.32392952E+00	-1.294454064	.422002232	-1.346207521	.481235105	-1.462841258	.613420347	-1.667397557	.842308173
375	.29887226E+00	-1.254491868	.396781592	-1.305591086	.456739463	-1.422662995	.592376808	-1.632923395	.832046343
400	.27574955E+00	-1.215717322	.373068244	-1.265786707	.433490698	-1.382483281	.572055172	-1.597267565	.821909532
425	.25441754E+00	-1.178096559	.350772107	-1.226791323	.411425313	-1.342341132	.552430676	-1.560479440	.811896218
450	.23473574E+00	-1.141596629	.329808481	-1.188601251	.390488101	-1.302274194	.533479403	-1.522608896	.802004895
475	.21657653E+00	-1.106185480	.310097730	-1.151212221	.370606882	-1.262318744	.515178258	-1.483706265	.792234079
500	.19992212E+00	-1.071831934	.291564978	-1.114619410	.351742394	-1.222509710	.497504938	-1.443822293	.782582301
525	.18468393E+00	-1.038505664	.274139819	-1.078817474	.333839140	-1.182890677	.480437906	-1.403008018	.773048109
550	.17070140E+00	-1.006177171	.257756063	-1.043800582	.316845240	-1.143463905	.463956363	-1.361314844	.763630073
575	.15794231E+00	-.974817765	.242351469	-1.009562444	.300717307	-1.104290341	.448040224	-1.318794352	.754326777
600	.14480122E+00	-.944399543	.227857520	-.976096342	.285410311	-1.065389634	.432670091	-1.275498357	.745136823
625	.13359936E+00	-.914895369	.214249192	-.943395158	.270882466	-1.026790151	.417827235	-1.231478745	.736058829
650	.12325408E+00	-.886278854	.201444753	-.911451399	.257094112	-.988518996	.403493567	-1.186787517	.727091433
675	.11372834E+00	-.858524335	.189405562	-.880257226	.244007607	-.950602022	.389651619	-1.141476694	.718233287
700	.10493029E+00	-.831606850	.178085884	-.849804479	.231587227	-.913063653	.376284522	-1.095596265	.709483059
725	.96812653E-01	-.805502167	.167442717	-.820084701	.219799064	-.875927900	.363375987	-1.049204147	.700839435
750	.89323386E-01	-.780186653	.157435632	-.791089158	.208610937	-.839216383	.350910282	-1.002346129	.692301117
775	.82413306E-01	-.755637414	.148026612	-.762809968	.197992304	-.802950344	.338872217	-.955075821	.683866820
800	.76037791E-01	-.731832119	.139179915	-.735234612	.187914177	-.767149676	.327247120	-.907444615	.675535279
825	.70155408E-01	-.708749102	.130861934	-.708356969	.178349042	-.731833134	.316020826	-.859503625	.667305240
850	.64728241E-01	-.686367289	.123041071	-.682160325	.169270788	-.697018363	.305179652	-.811303649	.659175468
875	.59720848E-01	-.664656193	.115687616	-.656652892	.160654532	-.662721915	.294710387	-.762895119	.651144741
900	.55100826E-01	-.643625902	.108773634	-.631806732	.152477053	-.628959270	.284500273	-.714328059	.643211852
925	.50838213E-01	-.623227061	.102272861	-.607617771	.144715725	-.595744862	.274836989	-.665652035	.635375610
950	.46905460E-01	-.603450867	.096169602	-.584075914	.137349461	-.563092096	.265408637	-.616916123	.627634836
975	.43276752E-01	-.584279008	.090413637	-.561170566	.130358152	-.531013374	.256303727	-.568168852	.619988368
1000	.39928856E-01	-.565693743	.085010135	-.538891640	.123722712	-.499520114	.247511164	-.519458177	.612435057

Table (A.2.4)

COMPUTED FILTER COEFFICIENTS
EIGHT POLE HIGH-PASS FILTER
SAMPLING RATE 25 KHZ

CUT-OFF HZ	B0	B1	B2	B3	B4	B5	B6	B7	B8
25	.98402559E+00	-1.987711481	.987750717	-1.989566562	.989605835	-1.993003475	.993042816	-1.99751[illegible]011	.997551441
50	.96830656E+00	-1.975495497	.975651479	-1.979163434	.979319708	-1.985977220	.986134035	-1.994951352	.995108877
75	.95283853E+00	-1.963351640	.963700447	-1.968790711	.969140497	-1.978921718	.979273319	-1.992318301	.992672294
100	.93761750E+00	-1.951279502	.951895808	-1.958448484	.959067090	-1.971837449	.972460334	-1.989613141	.990[illegible]41677
125	.92253380E+00	-1.939278678	.940235767	-1.948136842	.949098388	-1.964724893	.965694749	-1.986836154	.9876.[illegible]C12
150	.90790127E+00	-1.927348766	.928716552	-1.937855872	.939233302	-1.957584527	.958976233	-1.983987626	.985398283
175	.89359818E+00	-1.915489368	.917342416	-1.927605659	.929470756	-1.950416824	.952304459	-1.981087844	.982985477
200	.87912676E+00	-1.903700078	.906105629	-1.917386286	.919809683	-1.943222258	.945679101	-1.978077097	.980578579
225	.86528831E+00	-1.891980507	.895006485	-1.907197833	.910249029	-1.936001297	.939099838	-1.975015578	.978177574
250	.85125421E+00	-1.880330258	.884043297	-1.897040380	.900787750	-1.928754409	.932566345	-1.971883880	.975782448
275	.83756585E+00	-1.868746940	.873214400	-1.886914003	.891424813	-1.921482061	.926078312	-1.968681939	.973393187
300	.82428471E+00	-1.857235162	.862518150	-1.876818777	.882159196	-1.914184715	.919635415	-1.965410333	.971009776
325	.81111734E+00	-1.845791537	.851952921	-1.866754774	.872989888	-1.906862832	.913237342	-1.962059182	.968632202
350	.79816030E+00	-1.834414679	.841517106	-1.856722065	.863915886	-1.899516872	.906883782	-1.958658847	.966260448
375	.78541024E+00	-1.823105209	.831209127	-1.846720719	.854936202	-1.892147289	.900574425	-1.955173632	.963894502
400	.77286385E+00	-1.811862730	.821027411	-1.836750803	.846049853	-1.884754540	.894308963	-1.951631844	.961534349
[illegible]5	.76051788E+00	-1.800686878	.810970414	-1.826812381	.837255871	-1.877339075	.888087091	-1.948015790	.959179976
[illegible]	.74835914E+00	-1.789577270	.801036607	-1.816905517	.828553295	-1.869901345	.881908506	-1.944331780	.956831367
[illegible]0	.73641445E+00	-1.778533531	.791224483	-1.807030272	.819941175	-1.862441797	.875772906	-1.940580125	.954488509
500	.72465074E+00	-1.767555287	.781532550	-1.797186704	.811418571	-1.854960877	.869679993	-1.936761140	.952151387
525	.71307495E+00	-1.756642167	.771959337	-1.787374871	.802984552	-1.847459026	.863629469	-1.932875135	.949819988
550	.70168407E+00	-1.745793801	.762503388	-1.777594828	.794638198	-1.839936667	.857621040	-1.928922439	.947494297
575	.69047515E+00	-1.735009822	.753163268	-1.767846630	.786378597	-1.832394297	.851654413	-1.924903361	.945174301
600	.67944528E+00	-1.724289863	.743937558	-1.758130326	.778204846	-1.824832294	.845729297	-1.920818224	.942859986
625	.66859161E+00	-1.713633562	.734824857	-1.748445972	.770116058	-1.817251109	.839845402	-1.916667352	.940551337
650	.65791132E+00	-1.703040557	.725823779	-1.738793610	.762111344	-1.809651177	.834002443	-1.912451070	.938248342
675	.64740164E+00	-1.692510488	.716932958	-1.729173289	.754189833	-1.802032925	.828200135	-1.908169704	.935950985
700	.63705985E+00	-1.682042397	.708151043	-1.719585054	.746350659	-1.794396781	.822438194	-1.903823581	.933659254
725	.62688326E+00	-1.671637729	.699476700	-1.710029948	.738592966	-1.786743170	.816716341	-1.899413033	.931373134
750	.61686923E+00	-1.661294329	.690909612	-1.700505011	.730915909	-1.779072515	.811034295	-1.894938290	.929092611
775	.60701517E+00	-1.651012445	.682445477	-1.691013285	.723318648	-1.771385235	.805391780	-1.890399986	.926817673
800	.59731852E+00	-1.640791730	.674085009	-1.681553806	.715800354	-1.763681750	.799788521	-1.885798156	.924548205
825	.58777677E+00	-1.630631831	.665828939	-1.672126611	.708360207	-1.755962474	.794224245	-1.881133237	.922284494
850	.57838744E+00	-1.620532404	.657673012	-1.662731734	.700997394	-1.748227821	.788698681	-1.876405567	.920026226
875	.56914810E+00	-1.610493105	.649616989	-1.653369210	.693711111	-1.740478204	.783211559	-1.871615487	.917773497
900	.56005635E+00	-1.600512591	.641659646	-1.644039068	.686500563	-1.732714029	.777762613	-1.866763337	.915526[illegible]4
925	.55110993E+00	-1.590593529	.633799776	-1.634741339	.679364962	-1.724935705	.772351575	-1.861849462	.9132[illegible]44
950	.54230623E+00	-1.580736555	.626036183	-1.625476052	.672303531	-1.717143636	.766978183	-1.856874206	.911[illegible]d313
975	.53364326E+00	-1.570938357	.618367528	-1.616243232	.665315496	-1.709338223	.761642175	-1.851837915	.908817557
1000	.52511858E+00	-1.561186503	.610793127	-1.607042906	.658400097	-1.701519868	.756343290	-1.846740938	.906592263

Table (A.2.5)

COMPUTED FILTER COEFFICIENTS
EIGHT POLE HIGH-PASS FILTER
SAMPLING RATE 50 KHZ

CUT-OFF HZ	B0	B1	B2	B3	B4	B5	B6	B7	B8
25	.99198069E+00	-1.993846648	.993856487	-1.994779498	.994789342	-1.998505484	.998515337	-1.998765106	.998774970
50	.98402589E+00	-1.987711481	.987750717	-1.989566562	.989605835	-1.993003475	.993042816	-1.997512011	.997551441
75	.97613449E+00	-1.931594445	.981682458	-1.984361203	.984449337	-1.989494034	.989582296	-1.996240748	.996329410
100	.96830655E+00	-1.975495497	.975651479	-1.979163434	.979319708	-1.985977220	.986134035	-1.994951352	.995108877
125	.96054141E+00	-1.969414578	.969657551	-1.973973267	.974216808	-1.982453095	.982697669	-1.993643858	.993889839
150	.95283853E+00	-1.963351640	.963700447	-1.968790711	.969140497	-1.978921718	.979273319	-1.992318301	.992672294
175	.94519743E+00	-1.957306631	.957779941	-1.963615780	.964090637	-1.975383149	.975860881	-1.990974717	.99145624
200	.93761780E+00	-1.951279502	.951895808	-1.958446484	.959067090	-1.971837449	.972460334	-1.989613141	.990241677
225	.93008855E+00	-1.945270201	.946047824	-1.953288835	.954069719	-1.968284677	.969071637	-1.988233608	.989028601
250	.92263980E+00	-1.939278678	.940235767	-1.948136842	.949098388	-1.964724893	.965694749	-1.986836154	.987817012
275	.91524087E+00	-1.933304883	.934459416	-1.942992518	.944152961	-1.961158157	.962329628	-1.985420815	.986606906
300	.90790127E+00	-1.927348763	.928718552	-1.937855872	.939233302	-1.957584527	.958976233	-1.983987626	.985398283
325	.90062053E+00	-1.921410277	.923012958	-1.932726916	.934339279	-1.954004063	.955634523	-1.982536023	.98419114
350	.89339819E+00	-1.915489366	.917342416	-1.927605659	.929470756	-1.950416824	.952304459	-1.981067844	.982985477
375	.88623374E+00	-1.909585983	.911706711	-1.922492112	.924627602	-1.946822870	.948985998	-1.979581323	.981781290
400	.87912676E+00	-1.903700078	.906105629	-1.917386286	.919809683	-1.943222258	.945679101	-1.978077097	.980578579
425	.87207677E+00	-1.897831603	.900538957	-1.912288190	.915016969	-1.939615047	.942383728	-1.976555203	.979377341
450	.86508331E+00	-1.891980507	.895006485	-1.907197833	.910249029	-1.936001297	.939099838	-1.975015678	.978177574
475	.85814504E+00	-1.886146742	.889508001	-1.902115227	.905506033	-1.932381065	.935827391	-1.973458558	.976979277
500	.85126421E+00	-1.880330258	.884043297	-1.897040380	.900787750	-1.928754409	.932566348	-1.971883880	.975782448
525	.84443765E+00	-1.874531007	.878612165	-1.891973302	.896094053	-1.925121389	.929316668	-1.970291681	.974587096
550	.83765945E+00	-1.868748940	.873214400	-1.886914003	.891424813	-1.921482061	.926078312	-1.968681999	.973393187
575	.83094235E+00	-1.862984008	.867849795	-1.881862491	.886779903	-1.917836484	.922851241	-1.967054871	.972200752
600	.82428471E+00	-1.857236162	.862518150	-1.876818777	.882159196	-1.914184715	.919635415	-1.965410333	.971009776
625	.81767452E+00	-1.851505355	.857219258	-1.871782868	.877562566	-1.910526812	.916430795	-1.963748424	.969820260
650	.81111734E+00	-1.845791537	.851952921	-1.866754774	.872989888	-1.906862832	.913237342	-1.962069182	.968632202
675	.80461273E+00	-1.840094661	.846718937	-1.861734503	.868441036	-1.903192833	.910055018	-1.960372643	.967445598
700	.79816030E+00	-1.834414679	.841517108	-1.856722065	.863915886	-1.899516872	.906883782	-1.958658847	.966260446
725	.79175969E+00	-1.828751542	.836347237	-1.851717468	.859414316	-1.895835005	.903723597	-1.956927830	.965076750
750	.78541024E+00	-1.823105203	.831209127	-1.846720719	.854936202	-1.892147289	.900574425	-1.955179632	.963894502
775	.77911173E+00	-1.817475615	.826102583	-1.841731828	.850481421	-1.888453782	.897436226	-1.953414291	.962713703
800	.77286386E+00	-1.811862730	.821027411	-1.836750803	.846049853	-1.884754540	.894308963	-1.951631844	.961534349
825	.76666602E+00	-1.806266500	.815983418	-1.831777651	.841641377	-1.881049619	.891192597	-1.949832331	.960356441
850	.76051788E+00	-1.800686878	.810970414	-1.826812381	.837255871	-1.877339075	.888087091	-1.948015790	.959179976
875	.75441906E+00	-1.795123817	.805988206	-1.821855001	.832893217	-1.873622965	.884992406	-1.946182260	.958004951
900	.74836914E+00	-1.789577270	.801036807	-1.816905517	.828553295	-1.869901345	.881908506	-1.944331780	.956831367
925	.74236773E+00	-1.784047190	.796115429	-1.811963938	.824235987	-1.866174271	.878835351	-1.942464389	.955659220
950	.73641445E+00	-1.778533531	.791224483	-1.807030272	.819941175	-1.862441797	.875772906	-1.940580125	.954488508
975	.73050892E+00	-1.773036245	.786363585	-1.802104524	.815668742	-1.858703981	.872721132	-1.938679029	.953319231
1000	.72465074E+00	-1.767555287	.781532553	-1.797186704	.811418571	-1.854960877	.869679993	-1.936761140	.952151387

Table (A.2.6)

COMPUTED FILTER COEFFICIENTS
SIX POLE LOW-PASS FILTER
SAMPLING RATE 5 KHZ

CUT-OFF HZ	B0	B1	B2	B3	B4	B5	B6
25	.90478269E-09	-1.940156497	.941114028	-1.955578386	.956543666	-1.982890599	.983869500
50	.54496239E-07	-1.881979177	.885695613	-1.911199493	.914975785	-1.964116130	.967999193
75	.58419301E-06	-1.825425632	.833540565	-1.866904303	.875214291	-1.943721828	.952384881
100	.30890935E-05	-1.770454397	.784456719	-1.822731935	.837160686	-1.921753786	.937022437
125	.11090047E-04	-1.717024932	.738263222	-1.778719690	.800799883	-1.898258894	.921907796
150	.31164714E-04	-1.665097608	.694789874	-1.734903094	.766000055	-1.873264780	.907036962
175	.73958169E-04	-1.614633694	.653876497	-1.691315941	.732712501	-1.846879753	.892406002
200	.15508868E-03	-1.565595335	.615372344	-1.647990333	.700871501	-1.819092740	.878011047
225	.29509492E-03	-1.517945541	.579135545	-1.604956726	.670414195	-1.789973235	.863848290
250	.52399200E-03	-1.471648172	.545032585	-1.562243969	.641280452	-1.759571237	.849913985
275	.87362108E-03	-1.426667921	.512937811	-1.519879351	.613412754	-1.727937193	.836204447
300	.13857978E-02	-1.382970297	.482732969	-1.477888635	.586756085	-1.695121944	.822716051
325	.21081992E-02	-1.340521614	.454306769	-1.436296107	.561257816	-1.661176666	.809445229
350	.30950097E-02	-1.299288971	.427554473	-1.395124610	.536867609	-1.626152816	.796388473
375	.44063970E-02	-1.259240244	.402377512	-1.354395590	.513537910	-1.590102076	.783542329
400	.61079898E-02	-1.220344064	.378683121	-1.314129134	.491220861	-1.553076302	.770903399
425	.82701642E-02	-1.182569807	.356383997	-1.274344008	.469874204	-1.515127464	.758468341
450	.10967254E-01	-1.145887576	.335397979	-1.235057701	.449455193	-1.476307602	.746233868
475	.14276664E-01	-1.110268192	.315647743	-1.196286456	.429923518	-1.436668765	.734196742
500	.18277946E-01	-1.075683173	.297060519	-1.158045316	.411240818	-1.396252968	.722353781
525	.23051832E-01	-1.042104728	.279567821	-1.120346159	.393369608	-1.355142133	.710701853
550	.28679266E-01	-1.009505734	.253105198	-1.083207734	.376275207	-1.313358049	.699237877
575	.35240432E-01	-.977859732	.247611993	-1.046633696	.359923665	-1.270952317	.687958820
600	.42813915E-01	-.947140904	.233031120	-1.010642650	.344282703	-1.228006303	.676861700
625	.51475289E-01	-.917324067	.219308856	-.975238177	.329321439	-1.184541096	.665943583
650	.61297265E-01	-.888384658	.206394640	-.940430874	.315010336	-1.140617457	.655201580
675	.72347888E-01	-.860298719	.194240891	-.906228392	.301321142	-1.096265776	.644632850
700	.84690311E-01	-.833042885	.182802828	-.872637459	.288226829	-1.051596034	.634234600
725	.98382033E-01	-.806594373	.172038305	-.839663927	.275701548	-1.006597752	.624004079
750	.11347432E+00	-.780930959	.161907662	-.807312793	.263720569	-.961339956	.613938581
775	.13001172E+00	-.756031013	.152373572	-.775586239	.252260240	-.915871134	.604035444
800	.14803161E+00	-.731873393	.143400906	-.744493858	.241297935	-.870239201	.594292050
825	.16756392E+00	-.708437526	.134956604	-.714031688	.230812011	-.824491456	.584705822
850	.18863081E+00	-.685703353	.127009554	-.684204245	.220781767	-.778874550	.575274225
875	.21124657E+00	-.663551321	.119530473	-.655012544	.211187401	-.732834450	.565994764
900	.23541745E+00	-.642262379	.112491804	-.626457138	.202009971	-.687016401	.556864985
925	.26114172E+00	-.621517959	.105867615	-.598537938	.193231258	-.641264899	.547882474
950	.28840963E+00	-.601399971	.099633498	-.571254246	.184834231	-.595623858	.539044856
975	.31720359E+00	-.581890792	.093766482	-.544604788	.176802013	-.550135576	.530349793
1000	.34749828E+00	-.562973252	.088244952	-.518587719	.169116846	-.504842712	.521794985

Table (A.2.7)

COMPUTED FILTER COEFFICIENTS
SIX POLE LOW-PASS FILTER
SAMPLING RATE 25 KHZ

CUT-OFF HZ	B0	B1	B2	B3	B4	B5	B6
25	.60786962E-13	-1.987995937	.997935177	-1.991114290	.991153594	-1.996713467	.996752881
50	.38434291E-11	-1.975859903	.976015914	-1.982228930	.982385447	-1.993358906	.993516305
75	.43250873E-10	-1.963891549	.964240454	-1.973344264	.973694856	-1.989936671	.990290239
100	.24007987E-09	-1.951990529	.952607063	-1.964460636	.965081166	-1.986447117	.987074649
125	.90478269E-09	-1.940156497	.941114028	-1.955578388	.956543666	-1.982890509	.983859500
150	.26690715E-08	-1.928389109	.929759653	-1.946697851	.948081692	-1.979267476	.980674758
175	.66492002E-08	-1.916688023	.918542267	-1.937819365	.939694576	-1.975578106	.977490390
200	.14636915E-07	-1.905052898	.907460217	-1.928943259	.931381558	-1.971822851	.974316362
225	.29315213E-07	-1.893483396	.896511870	-1.920069960	.923142276	-1.968002071	.971152641
250	.54490239E-07	-1.881979177	.885695613	-1.911159493	.914975785	-1.964116130	.967999193
275	.95378633E-07	-1.870539906	.875009852	-1.902332491	.906881537	-1.960165393	.964855984
300	.15882209E-06	-1.859165249	.864453013	-1.893469141	.898858895	-1.956150226	.961722981
325	.25363655E-06	-1.847854872	.854023540	-1.884609790	.890907224	-1.952070997	.958600152
350	.39388456E-06	-1.836608443	.843719897	-1.875754741	.883025897	-1.947928074	.955487463
375	.58419301E-06	-1.825425632	.833540565	-1.866904303	.875214291	-1.943721825	.952384881
400	.85007482E-06	-1.814306111	.823484046	-1.858058784	.867471790	-1.939452629	.949292374
425	.12082568E-05	-1.803249552	.813548856	-1.849218488	.859797782	-1.935120851	.946209909
450	.16820124E-05	-1.792255629	.803733533	-1.840383716	.852191662	-1.930726868	.943137452
475	.22984985E-05	-1.781324018	.794036630	-1.831554766	.844652828	-1.926271054	.940074972
500	.30890935E-05	-1.770454397	.784456719	-1.822731935	.837180686	-1.921753786	.937022437
525	.40897362E-05	-1.759646444	.774992387	-1.813915514	.829774646	-1.917175442	.933979813
550	.53412543E-05	-1.748899838	.765642241	-1.805105793	.822434122	-1.912536400	.930947069
575	.68897498E-05	-1.738214262	.756404903	-1.796303060	.815158536	-1.907837040	.927924173
600	.87868323E-05	-1.727589398	.747279011	-1.787507598	.807947313	-1.903077744	.924911093
625	.11030047E-04	-1.717024932	.738263222	-1.778719650	.800799883	-1.898258894	.921907798
650	.13863149E-04	-1.706520548	.729356207	-1.769939613	.793715682	-1.893380873	.918914252
675	.17176427E-04	-1.696075934	.720556653	-1.761167643	.786694150	-1.888444065	.915930427
700	.21107019E-04	-1.685690780	.711863264	-1.752404053	.779734734	-1.883448855	.912956292
725	.25739206E-04	-1.675364774	.703274760	-1.743649115	.772836884	-1.878395631	.909991814
750	.31164714E-04	-1.665097608	.694789874	-1.734903094	.766000055	-1.873284790	.907036962
775	.37482990E-04	-1.654888977	.686407357	-1.726166257	.759223708	-1.868116691	.904091705
800	.44801483E-04	-1.644738573	.678125974	-1.717438864	.752507306	-1.862891752	.901156012
825	.53235902E-04	-1.634646093	.669944504	-1.708721177	.745850321	-1.857610355	.898229850
850	.62910471E-04	-1.624611234	.661861742	-1.700013451	.739252226	-1.852272891	.895313191
875	.73953169E-04	-1.614633694	.653876497	-1.691315941	.732712501	-1.846879753	.892406002
900	.86520963E-04	-1.604713174	.645987593	-1.682628897	.726230628	-1.841431333	.889508254
925	.10075002E-03	-1.594849374	.638193866	-1.673952570	.719806097	-1.835928026	.886619914
950	.11580591E-03	-1.585041998	.630494170	-1.665287205	.713438400	-1.830370227	.883740954
975	.13485882E-03	-1.575290750	.622887370	-1.656633045	.707127034	-1.824758333	.880871341
1000	.15508866E-03	-1.565595335	.615372344	-1.647990333	.700871501	-1.819092740	.878011047

Table (A.2.8)

COMPUTED FILTER COEFFICIENTS
SIX POLE LOW-PASS FILTER
SAMPLING RATE 50 KHZ

CUT-OFF HZ	B0	B1	B2	B3	B4	B5	B6
25	.955578216-15	-1.993939443	.993949283	-1.995557123	.995566971	-1.998365259	.998375120
50	.607869626-13	-1.987895937	.987935177	-1.991114290	.991153594	-1.996713467	.996752081
75	.698211976-12	-1.981869438	.981957460	-1.986671545	.986759761	-1.995044668	.995133277
100	.384342916-11	-1.975859903	.976015914	-1.982228930	.982385447	-1.993359906	.993516305
125	.145728066-10	-1.969867288	.970110317	-1.977785488	.978030503	-1.991656226	.991901361
150	.432508736-10	-1.963891549	.964240454	-1.973344264	.973694865	-1.989936671	.990290239
175	.108402946-09	-1.957932644	.958406108	-1.968902299	.969378448	-1.988200287	.988681137
200	.240079376-09	-1.951990529	.952607063	-1.964460636	.965081166	-1.986447117	.987074649
225	.483765756-09	-1.946065161	.946843107	-1.960019318	.960802933	-1.984677206	.985470771
250	.904782696-09	-1.940156497	.941114028	-1.955578386	.956543666	-1.982890599	.983865500
275	.159317926-08	-1.934264494	.935419613	-1.951137684	.952303280	-1.981087341	.982270830
300	.266907156-08	-1.928389109	.929759653	-1.946697851	.948081692	-1.979267476	.980574758
325	.428841776-08	-1.922530300	.924133940	-1.942258332	.943678818	-1.977431050	.979038290
350	.664920026-08	-1.916688023	.918542267	-1.937819365	.939694576	-1.975578106	.977490390
375	.999799646-08	-1.910862237	.912984428	-1.933380994	.935528883	-1.973708692	.975902056
400	.146369156-07	-1.905052898	.907460217	-1.928943259	.931381656	-1.971822851	.974316362
425	.209309766-07	-1.899259965	.901969432	-1.924506201	.927252815	-1.969920628	.972733216
450	.293152186-07	-1.893483396	.896511870	-1.920069860	.923142276	-1.968002071	.971152641
475	.403036096-07	-1.887723147	.891087330	-1.915634278	.919049960	-1.966067222	.969574635
500	.544962296-07	-1.881979177	.885695613	-1.911199493	.914975785	-1.964116130	.967999193
525	.725082696-07	-1.876251444	.880336519	-1.906765548	.910919670	-1.962148838	.966426310
550	.953786336-07	-1.870539906	.875009852	-1.902332481	.906881537	-1.960165393	.964855984
575	.123778906-06	-1.864844522	.869715415	-1.897900332	.902861305	-1.958165840	.963288203
600	.158822096-06	-1.859165249	.864453013	-1.893469141	.898858895	-1.956150226	.961722961
625	.201672596-06	-1.853502046	.859222452	-1.889038947	.894874227	-1.954116596	.960160297
650	.253636656-06	-1.847854872	.854023540	-1.884609790	.890907224	-1.952070997	.958600152
675	.316166866-06	-1.842223585	.848856085	-1.880181708	.886957806	-1.950007474	.957042542
700	.390884506-06	-1.836608443	.843719897	-1.875754741	.883025897	-1.947928074	.955487463
725	.479570646-06	-1.831009106	.838614786	-1.871328926	.879111417	-1.945832843	.953934911
750	.584194016-06	-1.825425632	.833540565	-1.866904303	.875214291	-1.943721828	.952384881
775	.706908526-06	-1.819857581	.828497047	-1.862480909	.871334441	-1.941595074	.950837370
800	.850074826-06	-1.814306111	.823484046	-1.858058784	.867471790	-1.939452629	.949292374
825	.101625076-05	-1.808759982	.818501377	-1.853637964	.863626262	-1.937294539	.947749888
850	.120625686-05	-1.803249552	.813548956	-1.849218486	.859797782	-1.935120851	.946209909
875	.142908596-05	-1.797744781	.808626302	-1.844800392	.856986274	-1.932931612	.944672431
900	.168701746-05	-1.792255629	.803733533	-1.840383715	.852191662	-1.930726868	.943137452
925	.197056596-05	-1.786782055	.798870369	-1.835968495	.848413871	-1.928506666	.941604967
950	.228048806-05	-1.781324019	.794036530	-1.831554765	.844652828	-1.926271054	.940074972
975	.262039706-05	-1.775881479	.789232139	-1.827142567	.840908458	-1.924020078	.938547464
1000	.298201196-05	-1.770454397	.784456719	-1.822731935	.837180686	-1.921753786	.937022437

Table (A.2.9)

COMPUTED FILTER COEFFICIENTS
SIX POLE HIGH-PASS FILTER
SAMPLING RATE 5 KHZ

CUT-OFF HZ	B0	B1	B2	B3	B4	B5	B6
25	.94111406E+00	-1.940156497	.941114028	-1.955578386	.956543666	-1.982890599	.983869500
50	.89569571E+00	-1.881979177	.885695613	-1.911199493	.914975785	-1.964116130	.967939193
75	.83354071E+00	-1.825425632	.833540565	-1.866904303	.875214291	-1.943721828	.952384881
100	.78445689E+00	-1.770454397	.784456719	-1.822731935	.837180686	-1.921753786	.937022437
125	.73826342E+00	-1.717024932	.738263222	-1.778719690	.800799883	-1.898258894	.921907796
150	.69479010E+00	-1.665097808	.694789874	-1.734903094	.765000055	-1.873284780	.907036962
175	.65397674E+00	-1.614633694	.653876497	-1.691315941	.732712501	-1.846879753	.892406002
200	.61537260E+00	-1.565595335	.615372344	-1.647990333	.700871501	-1.819092740	.878011047
225	.57912581E+00	-1.517945541	.579135545	-1.604956726	.670414195	-1.789973235	.863848290
250	.54503293E+00	-1.471848172	.545032535	-1.562243569	.641280452	-1.759571237	.849913985
275	.51293805E+00	-1.426567921	.512937811	-1.519879351	.613412754	-1.727937193	.836204447
300	.48273325E+00	-1.382970297	.482732069	-1.477888635	.586756035	-1.695121944	.822716051
325	.45430705E+00	-1.340521614	.454306769	-1.436298107	.561257816	-1.661176666	.809445229
350	.42755475E+00	-1.299268971	.427554473	-1.395124610	.536867609	-1.626152816	.796388473
375	.40237779E+00	-1.259240244	.402377512	-1.354395590	.513537310	-1.590102078	.783542329
400	.37868340E+00	-1.220344064	.378683121	-1.314129134	.491220861	-1.553076302	.770903399
425	.35638427E+00	-1.182569007	.356383997	-1.274344008	.469874204	-1.515127454	.758468341
450	.33539824E+00	-1.145887578	.335397979	-1.235057701	.449455193	-1.476307602	.746233868
475	.31564800E+00	-1.110268192	.315647743	-1.196285456	.429923518	-1.436658765	.734196742
500	.29706077E+00	-1.075683173	.297060519	-1.158045316	.411240618	-1.396262558	.722353781
525	.27956836E+00	-1.042104728	.279567821	-1.120348159	.393368608	-1.355142133	.710701853
550	.26310543E+00	-1.009505734	.263105198	-1.083207734	.376275207	-1.313358049	.699237877
575	.24761222E+00	-.977859732	.247611593	-1.046635896	.359922666	-1.270962317	.687956820
600	.23303134E+00	-.947140904	.233031120	-1.010642650	.344282703	-1.228006303	.676861700
625	.21930907E+00	-.917324067	.219308856	-.975238177	.329321439	-1.184541096	.665943583
650	.20639468E+00	-.888384658	.206394640	-.940430874	.315010336	-1.140617457	.655201530
675	.19424111E+00	-.860298719	.194240891	-.906228392	.301321142	-1.096285776	.644632030
700	.18280305E+00	-.833042885	.182802028	-.872637459	.288225829	-1.051596034	.634234600
725	.17203653E+00	-.806594373	.172038305	-.839663927	.275701548	-1.006597752	.624004079
750	.16190791E+00	-.780930960	.161907062	-.807312793	.263720569	-.961333956	.613935581
775	.15237394E+00	-.756031013	.152373572	-.775588239	.252260240	-.915871134	.604035444
800	.14340121E+00	-.731873393	.143400908	-.744493658	.241297935	-.870239201	.594292050
825	.13495596E+00	-.708437526	.134955604	-.714031688	.230812011	-.824491456	.584705822
850	.12700998E+00	-.685703353	.127009554	-.684204245	.220781757	-.778674550	.575274225
875	.11953039E+00	-.663651321	.119530473	-.655012544	.211187401	-.732834450	.565994764
900	.11249245E+00	-.642262379	.112491804	-.626457136	.202009971	-.687016401	.556864985
925	.10586841E+00	-.621517959	.105867615	-.598537936	.193231358	-.641264899	.547882474
950	.99634435E-01	-.601399971	.099633498	-.571254248	.184834231	-.595823658	.539044856
975	.93767730E-01	-.581890792	.093766432	-.544604789	.176802013	-.550135576	.530349793
1000	.88246512E-01	-.563073752	.088244052	-.518587719	.169119846	-.504842712	.521794995

Table (A.2.10)

COMPUTED FILTER COEFFICIENTS
SIX POLE HIGH-PASS FILTER
SAMPLING RATE 25 KHZ

CUT-OFF HZ	B0	B1	B2	B3	B4	B5	B6
25	.987935196+00	-1.987895937	.987935177	-1.991114290	.991153594	-1.996713467	.996752881
50	.976015946+00	-1.975859903	.976015914	-1.982228930	.982335447	-1.993358906	.993516305
75	.964240496+00	-1.963891549	.964240454	-1.973344264	.973694866	-1.989936671	.990290239
100	.952607116+00	-1.951990529	.952607063	-1.964460636	.965081166	-1.986447117	.987074649
125	.941114086+00	-1.940156497	.941114028	-1.955578386	.956543666	-1.982890599	.983869500
150	.929759726+00	-1.928389109	.929759653	-1.946697851	.948081692	-1.979267476	.980674758
175	.918542346+00	-1.916668023	.918542267	-1.937819365	.939694576	-1.975578106	.977490390
200	.907460306+00	-1.905052898	.907460217	-1.928943259	.931381856	-1.971822851	.974316362
225	.896511966+00	-1.893483396	.896511870	-1.920069860	.923142276	-1.968002071	.971152641
250	.885695716+00	-1.881979177	.885595613	-1.911199493	.914975705	-1.964116130	.967999193
275	.875009936+00	-1.870539906	.875009852	-1.902332481	.906881537	-1.960165393	.964855984
300	.864453136+00	-1.859165249	.864453013	-1.893469141	.898858895	-1.956150226	.961722981
325	.854023676+00	-1.847854872	.854023540	-1.884609790	.890907224	-1.952070937	.958600152
350	.843720036+00	-1.836608443	.843719897	-1.875754741	.883025897	-1.947928074	.955487463
375	.833540716+00	-1.825425632	.833540565	-1.866904303	.875214291	-1.943721828	.952384881
400	.823484196+00	-1.814306111	.823484046	-1.858058784	.867471790	-1.939452629	.949292374
425	.813549016+00	-1.803249552	.813548856	-1.849218488	.859797782	-1.935120851	.946209909
450	.803733696+00	-1.792255629	.803733533	-1.840383716	.852191662	-1.930726868	.943137452
475	.794036806+00	-1.781324018	.794036630	-1.831554766	.844652828	-1.926271054	.940074972
500	.784456836+00	-1.770454397	.784456719	-1.822731935	.837180686	-1.921753786	.937022437
525	.774992576+00	-1.759646444	.774992387	-1.813915514	.829774646	-1.917175442	.933979813
550	.765642436+00	-1.748899838	.765642241	-1.805105793	.822434122	-1.912535400	.930947069
575	.756405036+00	-1.738214262	.756404903	-1.796303060	.815158536	-1.907837040	.927924173
600	.747279216+00	-1.727589398	.747279011	-1.787507598	.807947313	-1.903077744	.924911093
625	.738263426+00	-1.717024432	.738263222	-1.778719690	.800799883	-1.898258894	.921907796
650	.729356416+00	-1.706520548	.729356207	-1.769939613	.793715682	-1.893380873	.918914252
675	.720556866+00	-1.696075934	.720556653	-1.761167643	.786694150	-1.888444065	.915930427
700	.711863486+00	-1.685690780	.711863264	-1.752404053	.779734734	-1.883448855	.912956292
725	.703274986+00	-1.675364774	.703274760	-1.743649115	.772836864	-1.878395631	.909991814
750	.694790106+00	-1.665097608	.694789874	-1.734903094	.766000055	-1.873284780	.907035962
775	.686407586+00	-1.654888977	.686407357	-1.726166257	.759223708	-1.868116691	.904091705
800	.678126216+00	-1.644738573	.678125974	-1.717438864	.752507308	-1.862891752	.901156012
825	.669944746+00	-1.634646093	.669944504	-1.708721177	.745850321	-1.857610355	.898229850
850	.661861986+00	-1.624611234	.661861742	-1.700013451	.739252226	-1.852272891	.895313191
875	.653876746+00	-1.614633594	.653876497	-1.691315941	.732712501	-1.846879753	.892406002
900	.645986846+00	-1.604713174	.645987593	-1.682628897	.726230626	-1.841431333	.889508254
925	.638191116+00	-1.594849374	.638193866	-1.673952570	.719806097	-1.835928026	.886619914
950	.630489426+00	-1.585041998	.630494170	-1.665287205	.713438400	-1.830370227	.883740954
975	.622880626+00	-1.575290750	.622887370	-1.656633045	.707127034	-1.824758333	.880871341
1000	.615372606+00	-1.565595335	.615372344	-1.647990333	.700871501	-1.819092740	.878011047

Table (A.2.11)

COMPUTED FILTER COEFFICIENTS
SIX POLE HIGH-PASS FILTER
SAMPLING RATE 50 KHZ

CUT-OFF HZ	B0	B1	B2	B3	B4	B5	B6
25	.99394929E+00	-1.993939443	.993949283	-1.995557123	.995566971	-1.998365259	.998375120
50	.98793519E+00	-1.987895937	.987935177	-1.991114290	.991153594	-1.996713467	.995752881
75	.98195748E+00	-1.981869438	.981957460	-1.986671545	.986759781	-1.995044568	.995133277
100	.97601594E+00	-1.975859903	.976015914	-1.982228930	.982385447	-1.993358906	.993516305
125	.97011035E+00	-1.969867288	.970110317	-1.977786486	.978030503	-1.991656226	.991901961
150	.96424049E+00	-1.963891549	.964240454	-1.973344264	.973694866	-1.989936671	.990290239
175	.95840615E+00	-1.957932644	.958406108	-1.968902299	.969378448	-1.988200297	.988681137
200	.95260711E+00	-1.951990529	.952607063	-1.964460636	.965081166	-1.986447117	.987074649
225	.94684316E+00	-1.946065151	.946843107	-1.960019318	.960802933	-1.984677206	.985470771
250	.94111400E+00	-1.940156497	.941114028	-1.955578366	.956543066	-1.982890599	.983869500
275	.93541937E+00	-1.934264494	.935419613	-1.951137684	.952303280	-1.981087341	.982270930
300	.92975972E+00	-1.928389109	.929759653	-1.946697851	.948081692	-1.979267476	.980674758
325	.92413401E+00	-1.922530300	.924133940	-1.942258332	.943878818	-1.977431050	.979081250
350	.91854234E+00	-1.916688023	.918542267	-1.937819365	.939694576	-1.975578106	.977490390
375	.91298451E+00	-1.910862237	.912984428	-1.933380994	.935528883	-1.973708692	.975902086
400	.90746030E+00	-1.905052898	.907460217	-1.928943259	.931381656	-1.971822851	.974316362
425	.90196952E+00	-1.899259965	.901969432	-1.924506201	.927252815	-1.969920628	.972733216
450	.89651190E+00	-1.893483393	.896511870	-1.920069860	.923142276	-1.968002071	.971152641
475	.89108743E+00	-1.887723147	.891087330	-1.915634278	.919049960	-1.966067222	.969574635
500	.88569571E+00	-1.881979177	.885695813	-1.911199493	.914975785	-1.964116130	.967999193
525	.88033602E+00	-1.876251444	.880336519	-1.906765548	.910919670	-1.962148838	.966426310
550	.87500803E+00	-1.870539906	.875009852	-1.902332491	.906881537	-1.960165393	.964855984
575	.86971153E+00	-1.864844522	.869715415	-1.897900332	.902861305	-1.958165840	.963288209
600	.86444613E+00	-1.859165249	.864453013	-1.893469141	.898858895	-1.956150226	.961722981
625	.85922157E+00	-1.853502046	.859222452	-1.889038947	.894874227	-1.954118596	.960160297
650	.85402367E+00	-1.847854872	.854023540	-1.884609790	.890907224	-1.952070997	.958600152
675	.84885621E+00	-1.842223685	.848856085	-1.880181708	.886957806	-1.950007474	.957042542
700	.84372003E+00	-1.836608443	.843719897	-1.875754741	.883025897	-1.947928074	.955487463
725	.83861492E+00	-1.831009106	.838614786	-1.871328926	.879111417	-1.945832843	.953934911
750	.83354071E+00	-1.825425632	.833540565	-1.866904303	.875214291	-1.943721828	.952384881
775	.82849719E+00	-1.819857981	.828497047	-1.862480909	.871334441	-1.941595074	.950837370
800	.82348419E+00	-1.814306111	.823484046	-1.858058784	.867471790	-1.939452629	.949292374
825	.81850153E+00	-1.808769982	.818501377	-1.853637964	.863626262	-1.937294539	.947749888
850	.81354901E+00	-1.803249552	.813548656	-1.849218488	.859797782	-1.935120851	.946209909
875	.80862644E+00	-1.797744781	.808626302	-1.844800392	.855986274	-1.932931612	.944672431
900	.80373369E+00	-1.792255629	.803733533	-1.840383716	.852191662	-1.930726868	.943137452
925	.79887053E+00	-1.786782055	.798870369	-1.835968495	.848413871	-1.928506656	.941604967
950	.79403680E+00	-1.781324018	.794036530	-1.831554766	.844652828	-1.926271054	.940074972
975	.78923231E+00	-1.775881479	.789232139	-1.827142567	.840908458	-1.924020078	.938547464
1000	.78445685E+00	-1.770454397	.784456719	-1.822731935	.837180686	-1.921753786	.937022437

Table (A.2.12)

Appendix (A.3)

Power - Frequency and Spectral Determination of a Turbulence Field

A knowledge of the power-frequency spectra is required to estimate the eddy size composition or eddy size distribution of the turbulent flow field. Power-frequency spectra may be obtained by using one of the three following methods.

(i) Using a Band-Pass Filtering Technique

(ii) Using a Fourier Transformation Technique and

(iii) Using a Correlation Technique

(i) The Band-Pass Filtering Technique:- The signal whose power spectra is to be determined is passed through a set of band pass filters having different center frequencies and pass band arrangements to cover the whole range of frequency of interest. The root mean square (RMS) value of the output of each band pass filter is found and represent the power in that particular band, fig (A.3.1). If the input signal is in time sampled digital form, digital filters may be used instead of analogue band filters.

(ii) Fourier Transformation Technique:- A Fourier transformation technique may be used to find the power spectra of a digital time sampled function. By Fourier transformation,

$$X(f) = \Delta t \sum_{k=o}^{k-1} x_k \, \text{Exp} \, (-j2T \, fK\Delta t)$$

where X(f) is the Fourier transformation coefficient for frequency f on a digital time sampled signal x_k, k = o, k - 1 with the sampling time Δt. X(f) may then be squared to represent the power at that particular frequency.

A Fast Fourier Transformation FFT technique may be employed instead of the above discrete Fourier Transformation technique to save computing time, but this approach gives the power spectra of a time series in a linear frequency step of $\frac{1}{2\Delta tk}$.

By Fast Fourier Transformation,

$$X_r = \sum_{k=o}^{N-1} x_k \, \text{Exp} \, (-2\pi \, jrk/N) \quad r = o \; 1, \quad , N - 1$$

OR

$$X_r = \sum_{k=o}^{N-1} x_k \, W^{rk} \quad \text{where } W = \text{Exp} \, (-2\pi j/N)$$

X_r is the rth coefficient of the Fourier Transform and x_k is the kth element of the time series under consideration. Several alternative ways to evaluate Fast Fourier Transform is presented in (109)

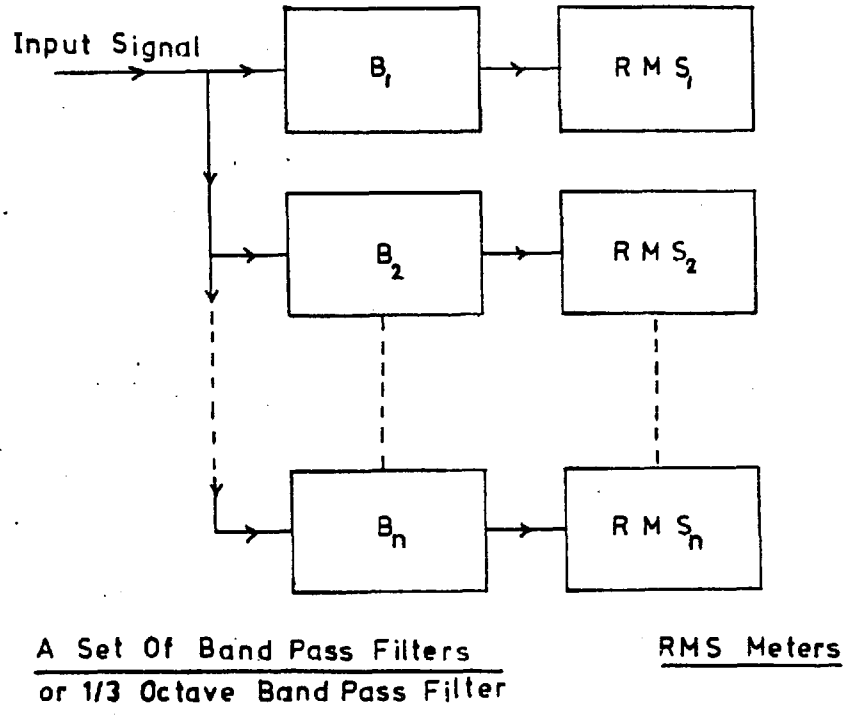


Fig (A.3.1) Arrangement of Instruments for Determining Power-Frequency Spectra Using Band-Pass Filtering Technique.

to save computing time.

(iii) Correlation Technique:- Power spectra may be evaluated by using correlation technique. For a time series x_i, i = 1, 2,---m, auto-correlation coefficients are defined as,

$$R_r = \frac{1}{N - r} \sum_{i=1}^{N-r} X_i \cdot X_{i+r} \qquad r = 0,-------,m$$

Where R_r is the rth correlation coefficient. The correlation coefficients thus defined may be used directly for estimating the sizes of eddies or may be used for estimating power spectra. For the latter case, the power spectra is related to correlation coefficients by(109),

$$G_k = 2\Delta t \left(R_o + 2 \sum_{r=1}^{m-1} R_r \cos \frac{\pi k r}{m} + R_m \cos \frac{\pi k}{m} \right) \qquad k = 0,-------,m$$

Generally, power spectra as calculated by the above three different techniques will give similar shape and trends but not identical results. In the present research effort, the discrete Fourier Transformation Technique was used to simulate a 1/3rd octave band pass filter(in frequency step $2^{1/3}$ of the previous one used) to give power spectra having good resolution at low freqency end.

Appendix (A.4)

Flame Arrival-Time Measurement by the Ionization Probe Method

An ionization probe senses the arrival of a propagating flame front by detecting the presence of ions which are carried inside the flame front. The presence of the electron ions in the flame reaction zone is mainly due to the chemi-ionization process, that is the process in which re-arrangement of the chemical species releases sufficient energy to give rise to the ionization of the product species (45). Another source of ions is the present of very fine positively charged carbon particles of size less than 100 A^{o} (53).

The ionization probe technique has been used in the past to detect the flame arrival (59, 52), and hence to give estimates of a turbulent flame propagation speed. The technique has also been applied to the study of the turbulent flame structure (45), though this type of application needs further development of technique and of data interpretation to give useful results.

When the flame front arrives at the probe position, the ions in the flame zone causes a sharp rise in induced voltage in the probe. This can be taken as the arrival time of the flame front. Normally, as the magnitude of this induced voltage is small, the probes are biased with a D-C voltage to give an increase in signal strength.

Rise Time of Probe Circuit. It is desirable to have a very short rise time or sharp response time in the probe circuit. This leads to a design involving minimum capacitance in the probe circuit as well as the use of very small sized probes. In application noises from the ignition circuit are also induced into the probe. It is thus necessary to inset a small by-pass capacitance in the circuit to by-pass these high frequency noises to the ground in order to obtain a proper ionization signal. The inclusion of additional capacitance, however, increases the rise time of the circuit. In our case a 0.0001 μF capacitor was used to by-pass these noises and the rise time of this circuit was estimated to be less than 20 micro second. This rise time value is acceptable when using ionization probes as flame arrival sensor.

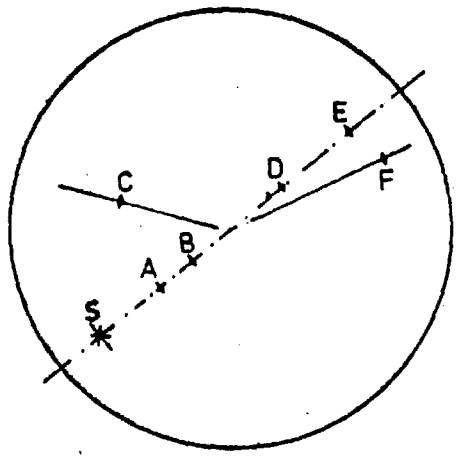
Size of Probe. It is preferable to employ probes of very small physical size to get good resolution of the ionization signal and sharp rise time though the larger probe enables

stronger ionization signals to be obtained. But very small probes do not survive long under engine combustion condition. After testing with several different sizes of the probes, steel wires of 0.024 inch diameter were employed as ionization probes as a compromise in between the requirements of good signal strength, resolution and acceptable probe service life.

Location of the Probes. The ionization probes were placed on the inside surface of the cylinder head using existing sparking plug holes. Of the four sparking plug holes, one was used for holding the sparking plug and another for the pressure transducer. Each of the remaining two sparking plug holes held a probe containing three ionization wires. Two ionization wires of each probe were bent and were insulated by ceramic clay (high temperature type) to insulate throughout its length except at the tips to make measurement away from the spark plug hole position possible. The locations of the sensor probe wire were chosen so that the probes were clear from inlet and exhaust valves opening operations. The positions employed for the probes are shown in fig (A.4.1).

Ionization Probe Circuit. The probes were biased with + 12 volts D.C. through a variable two meg. ohm resistor. This resistor was used for adjusting the biased voltage of the probe to get the maximum strength and response of the ionization signal at different engine running conditions at various air/fuel ratios. A buffer amplifier of unity gain was placed in between the recording instrument and the probe to match the high output impedance of probe to the relatively low input impedence of the recorder circuit. The employed ionization probe circuit is shown in fig (A.4.2).

Recording Method. The high speed digital data acquisition system which comprises the developed electonics and the digital tape unit, as employed in turbulence flow measurement, was used to record six channels of ionization signals, one cylinder pressure, and one dummy channel. The dummy channel was included to make a total of eight input channels so that the sequence of the multiplex recorded channels remained the same in any recorded data batch, which consists of 2048 words. (It is to be noted that for the sequence of the recording to remain the same in any recorded batch of data, the total number of multiplexed input channels must be a divisor of 2048, that is either 1 or 2 or 4 or 8 channels). A recording frequency of



	Dist From Sparking Plug (Cm)	Inclination From The Centre Line ABDE (Degree)
A	1,00	0,0
B	2,22	0,0
C	2,50	52,0
D	4,25	0,0
E	5,85	0,0
F	5,93	10,0

Fig (A.4.1) Locations of Ionization Probes.

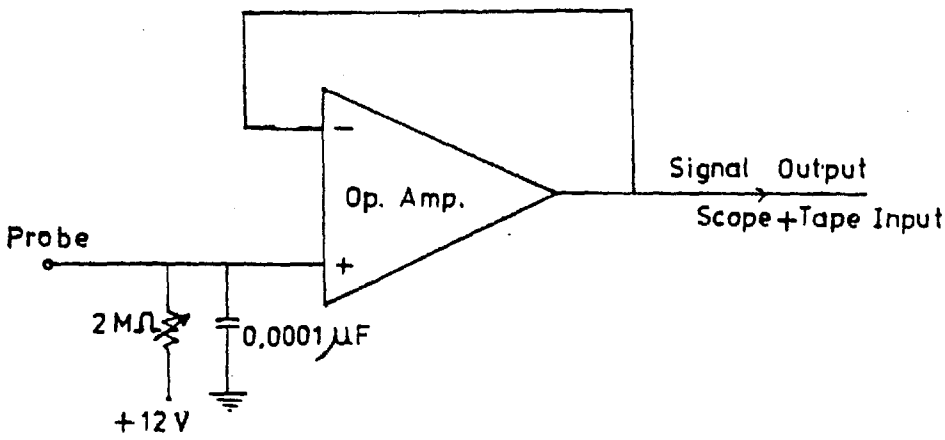


Fig (A.4.2) Employed Ionization Probe Circuit. (A total of six identical Circuits were employed for six ionization Probes).

50 KHZ was used. This corresponds to a resolution for each channel of,

$$\Delta t = \frac{8}{50 \text{ KHZ}} = 0.16 \text{ milli-second}$$

This resolution corresponds to around 1 degree engine crank angle at 1000 RPM.

Appendix (A.5)

Calibration of Hot Wire Probes

The application of hot wire anemometry to engine cylinder flow measurement requires the calibration of the hot wire probes in terms of local mass flow rate or Reynolds number, as the anemometer output voltage is affected by both velocity and fluid medium density change. For calibration purposes, the hot wire sensor element is treated as a heated metal cylinder in a flow stream. From non-dimensional considerations of heat transfer from a heated cylinder in a flow stream, the Nusselt number can be expressed as a function of Reynolds and Prandtl numbers as,

$$N_u = a\,Pr^{c_1} + b\,Pr^{c_2}\,R_e^n$$

For air, in the range of pressure and temperature of interest the Prandtl number ($\frac{C_p \mu}{k}$) remains fairly constant (it is close to 1) and can thus be treated as constant without affecting the accuracy of the calibration. Thus,

$$Nu = a + b\,R_e^n$$

This is the type of hot wire calibration equation suggested by McAdams (74) and Hinze (73). If conduction losses at the ends of the wire to the supporting prongs are to be neglected during the calibration, the calibrated values of the constants a and b contain conduction losses effects. For this type of calibration curve to be applicable, the hot wire probe must be operated in exactly the same condition as that used under calibration. Unfortunately, however, calibrations of this type cannot be used for engine flow investigations because of the fact that, the probe is not only to be operated under different operating conditions but also the amount of conduction losses are varying with time or engine compression temperature.

The effect of conduction losses on the variations in values of the constants a and b can be seen from fig (A.5.1), which is obtained by plotting the author's calibration data without taking into account the conduction losses effects. These data correspond to different wire operating temperatures and hence to different conduction loss effects. Unfortunately the amount of conduction

losses cannot be easily estimated, thus Collis and Williams (71) introduced the use of a correction factor, called the temperature loading factor, to eliminate the effect of variation in the values of the constants a and b with different wire operating temperatures. The proposed relationship is of the form,

$$N_u = (a + b\, R_e^{n}) \left({}^{Tf}/_{Tg} \right)^{0.17}$$

where Tf is the film temperature of wire and Tg is the free stream temperature. The author's calibrating data were again plotted using the above relation and is shown in fig (A.5.2). It was found that introducing the temperature loading factor or conduction loss correction factor reduces the range of variations in Nusselt-Reynolds relationship with different conduction losses, but its use does not give a unique values of a and b to satisfy all wire operating conditions.

Davies and Fisher (7) pointed out that if the amount of conduction losses could be taken into account correctly, a unique Nusselt-Reynolds relationship, that would satisfy all operating conditions and different conduction losses, would be obtained. Hovatin (2) made an arbitrary assumption that a parabolic profile temperature distribution existed along the length of the sensor wire and uses this to estimate the amount of conduction losses. For the present case, a more accurate estimate of hot wire temperature distribution and hence of the conduction losses was made by considering the energy balance of the hot wire element (Section 4.5.2). The calibration curve obtained by taking into account of conduction losses as estimated in the above way is shown in fig (A.5.3) and is the calibration curve which is used for interpreting the recorded experimental data.

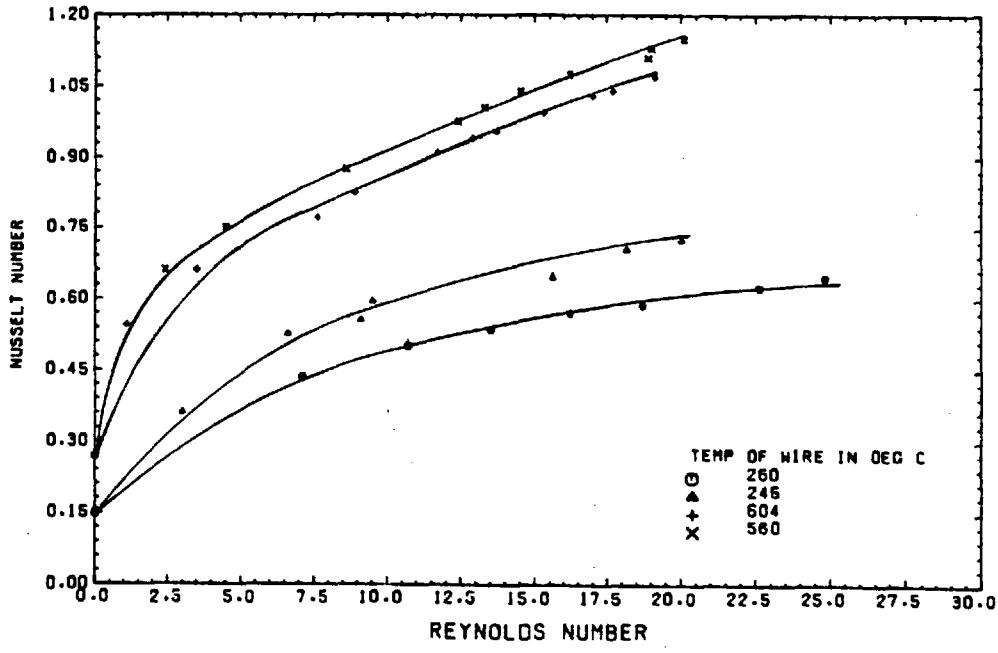


Fig (A.5.1) Nusselt-Reynolds Relationship without Consideration for conduction losses.

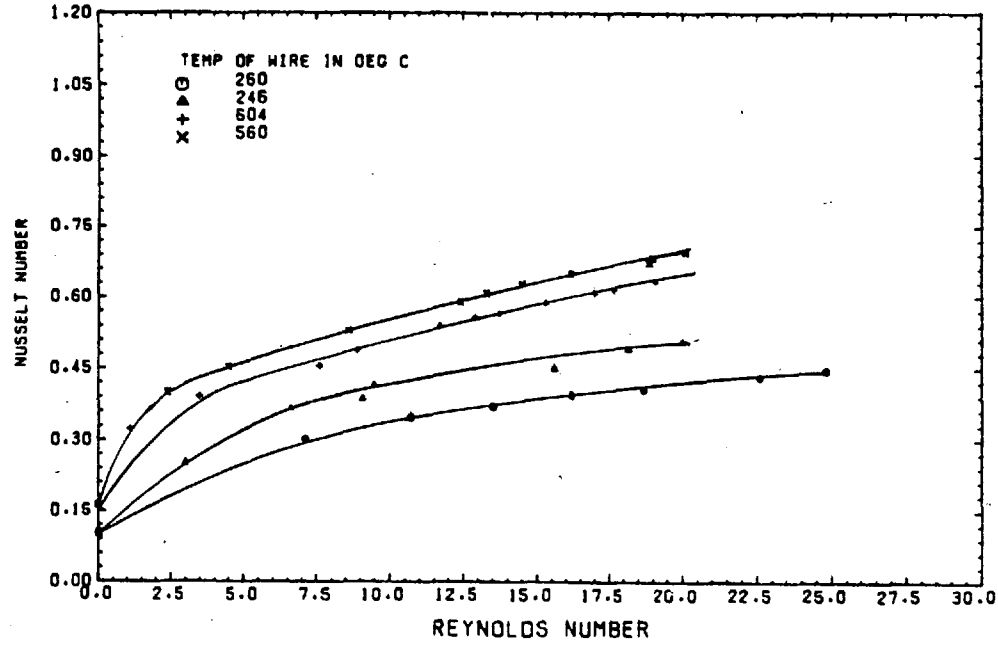


Fig (A.5.2) Nusselt-Reynolds Relationship with Temperature Loading Factor.

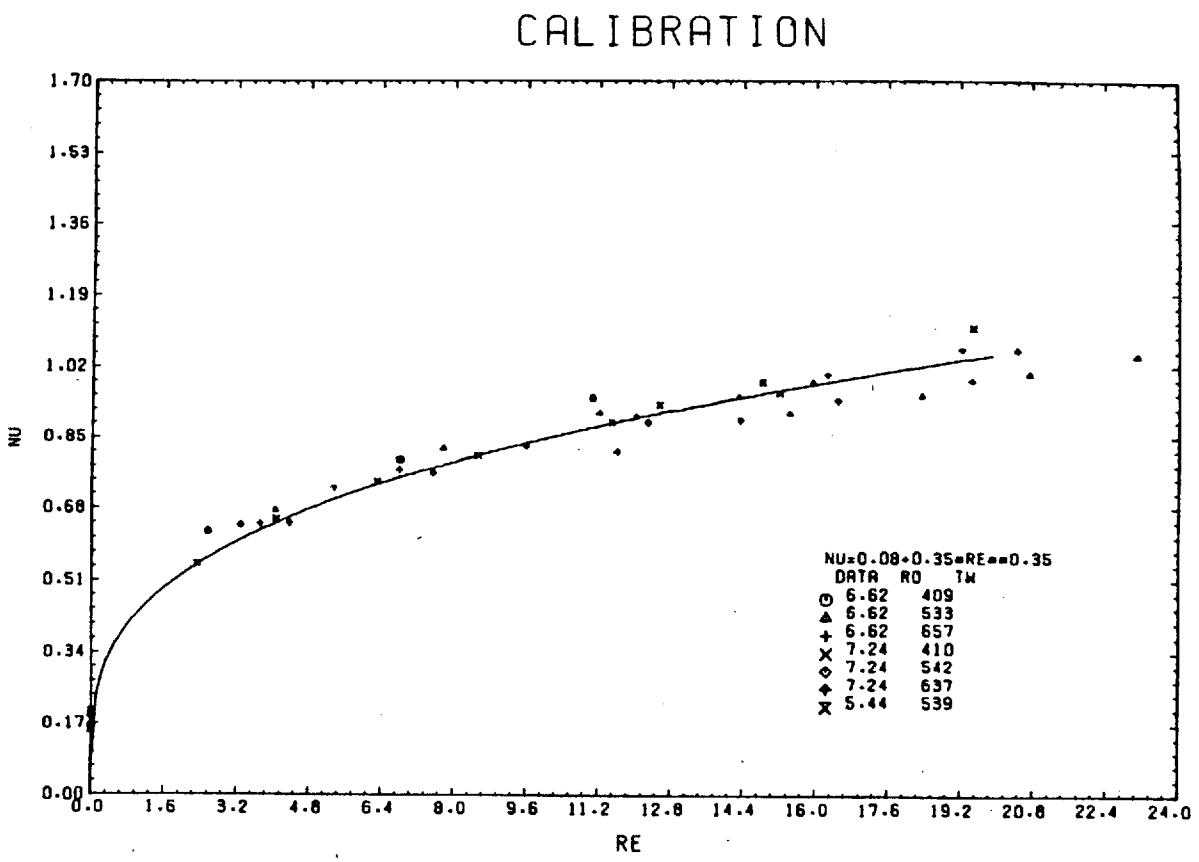


Fig (A.5.3) Nusselt-Reynolds Relationship with Consideration on Conduction Losses

Appendix (A.6)

Viscosity of Octane + Air Combustion Products

The viscosity of combustion products is estimated by evaluating the viscosity of each individual component using the formulae from Ref (46).

$$\mu_i = \frac{2.6693\ \sqrt{Mi\ T}}{\sigma^2 \Omega} \times 10^{-6} \quad N - S/M^2$$

where Mi = molecular weight of species i

T = temperature in degree K

σ = collision diameter in angstrom

(1 angstrom = 1×10^{-10} m)

Ω = collision integral

The value of Ω is calculated by use of the 'ϵ' Lennard-Jones Force constant and of the Boltzmann's Constant K whose values are taken from Ref (46) and are shown in Table (A.6.1).

For water vapour, the viscosity is evaluated by using the equation of the form, Ref (46).

$$\mu\ (H_2O) = \frac{2.5639\ \sqrt{T}}{1 + \frac{1371}{T} \times 10^{-37.4/T}} \times 10^{-6} \quad N - S/M^2 \text{ for } T \leq 1300K$$

$$\mu\ (H_2O) = \frac{1.4980\ \sqrt{T}}{1 + \frac{24.51 \times 10T}{T^2}} \times 10^{-6} \quad N - S/M^2 \text{ for } T > 1300K$$

The viscosity of each indivdual component is calculated using the above equations for a wide range of temperatures and a least square curve is fitted by using the equation of the form,

$$\hat{\mu} = aT^b \quad (T \text{ is in degrees K})$$

The values of the computed constants a and b for various component of the products are given below.

Component	a	b
CO_2	0.30441×10^{-6}	0.69638
CO	0.42224×10^{-6}	0.66226
N_2	0.42888×10^{-6}	0.65722

Component	a	b
NO	0.45192×10^{-6}	0.66528
H_2	0.21779×10^{-6}	0.64910
H	0.17132×10^{-6}	0.65915
CH_4	0.25478×10^{-6}	0.67119
NH_3	0.14052×10^{-6}	0.76257
OH	0.46463×10^{-6}	0.65772
O_2	0.48793×10^{-6}	0.66326
O	0.44987×10^{-6}	0.65987
H_2O	0.67337×10^{-7}	0.90051

The values of a and b will give viscosity in N - S/M^2 for T > 300 degrees K.

Specie	σ, angstroms (a)	ϵ/k, °K	Specie	σ, angstroms (a)	ϵ/k, °K
H_2O	-----	-----	O_2	3.433	113.0
CH_4	3.822	136.5	OH	3.110	93.8
CH	-----	-----	H_2	2.968	33.3
CO_2	3.996	190.0	H	2.497	99.8
CO	3.590	110.0	O	3.068	102.2
NH_3	3.474	312.3	N	-----	-----
NH	-----	-----	Ar	3.418	124.0
N_2	3.681	91.5	C(gas)	-----	-----
NO	3.470	119.0			

(a) 1 angstrom equals 1×10^{-10} m.

Table (A.6.1a) Collision Diameters and Lennard-Jones Force Constants

kT/ϵ	Ω	kT/ϵ	Ω	kT/ϵ	Ω	kT/ϵ	Ω	kT/ϵ	Ω
0.30	2.785	1.15	1.482	1.95	1.186	3.5	0.9999	6.0	0.8963
.35	2.628	1.20	1.452	2.0	1.175	3.6	.9932	7.0	.8727
.40	2.492	1.25	1.424	2.1	1.156	3.7	.9870	8.0	.8538
.45	2.368	1.30	1.399	2.2	1.138	3.8	.9811	9.0	.8379
.50	2.257	1.35	1.375	2.3	1.122	3.9	.9755	10.0	.8242
.55	2.156	1.40	1.353	2.4	1.107	4.0	.9700	20.0	.7432
.60	2.065	1.45	1.333	2.5	1.093	4.1	.9649	30.0	.7005
.65	1.982	1.50	1.314	2.6	1.081	4.2	.9600	40.0	.6718
.70	1.908	1.55	1.296	2.7	1.069	4.3	.9553	50.0	.6504
.75	1.841	1.60	1.279	2.8	1.058	4.4	.9507	60.0	.6335
.80	1.780	1.65	1.264	2.9	1.048	4.5	.9464	70.0	.6194
.85	1.725	1.70	1.248	3.0	1.039	4.6	.9422	80.0	.6076
.90	1.675	1.75	1.234	3.1	1.030	4.7	.9382	90.0	.5973
.95	1.629	1.80	1.221	3.2	1.022	4.8	.9343	100.0	.5882
1.00	1.587	1.85	1.209	3.3	1.014	4.9	.9305	200.0	.5320
1.05	1.549	1.90	1.197	3.4	1.007	5.0	.9269	400.0	.4811
1.10	1.514								

Table (A.6.1b) Values of kT/ϵ and Ω

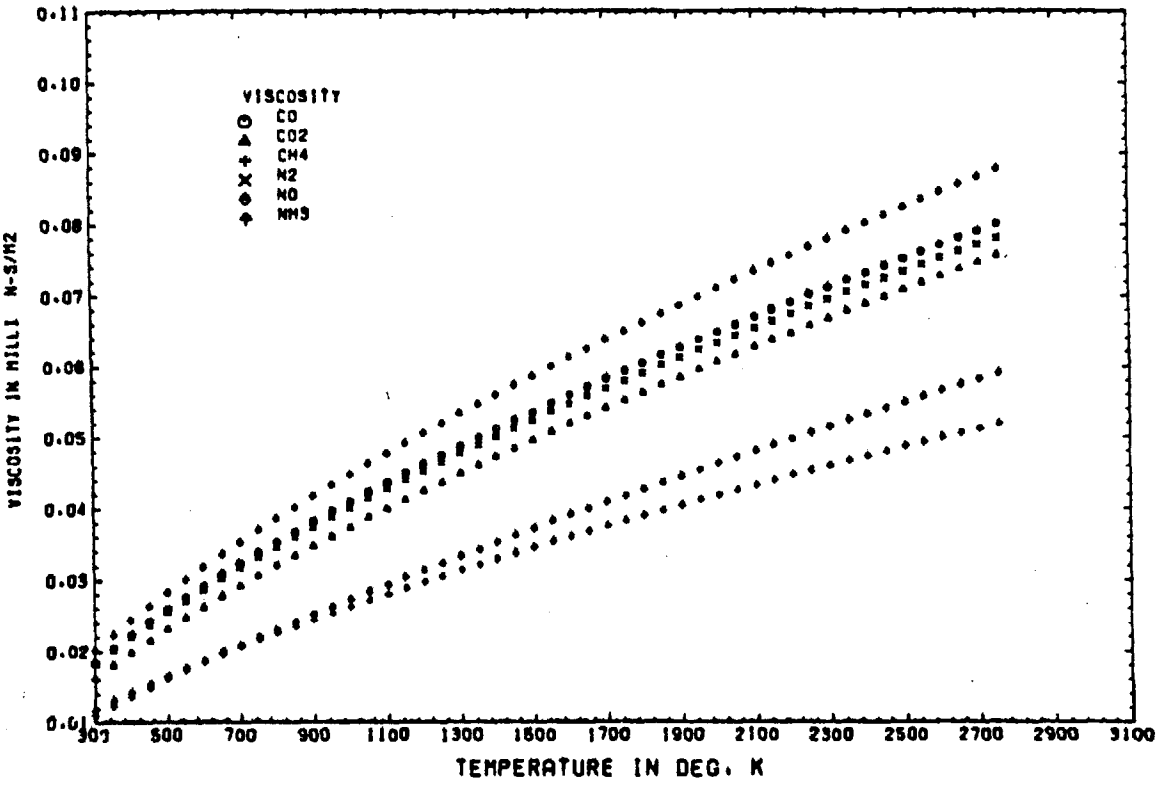


Fig (A.6.1) Computed Values of Viscosity for Components of Combustion Products.

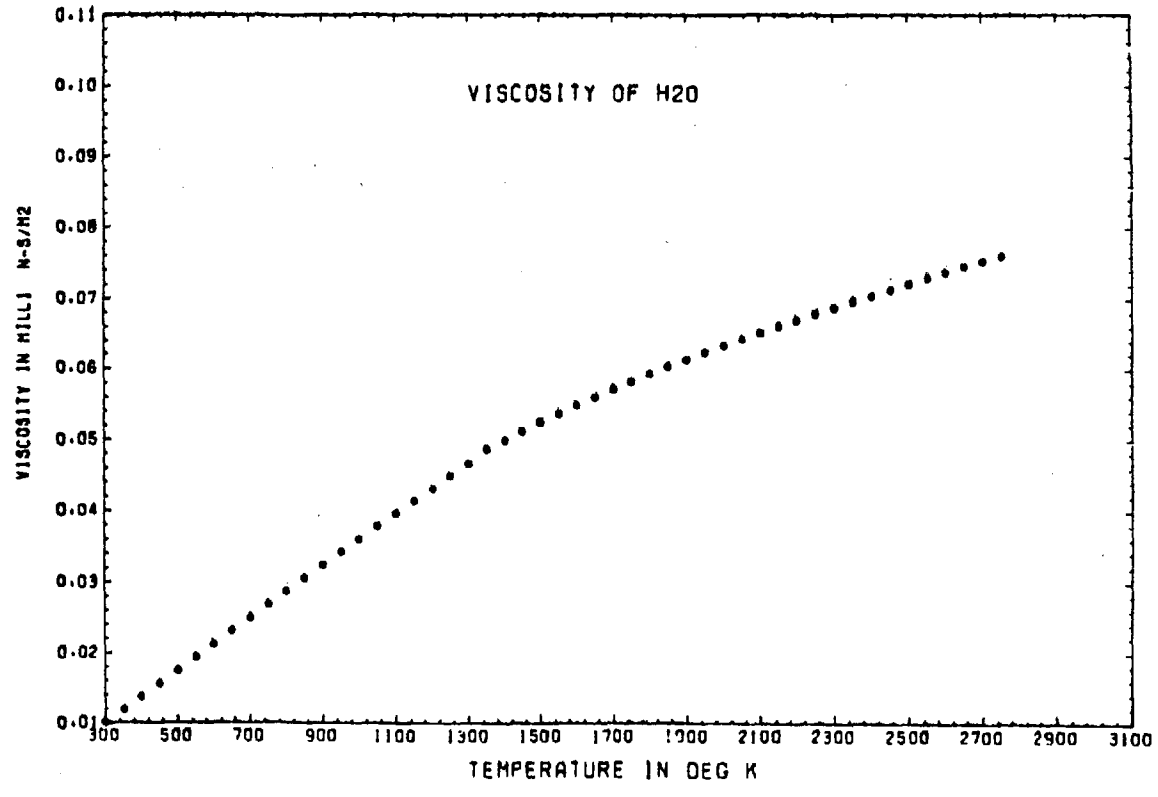


Fig (A.6.2) Computed Values of Viscosity for Water Vapour.

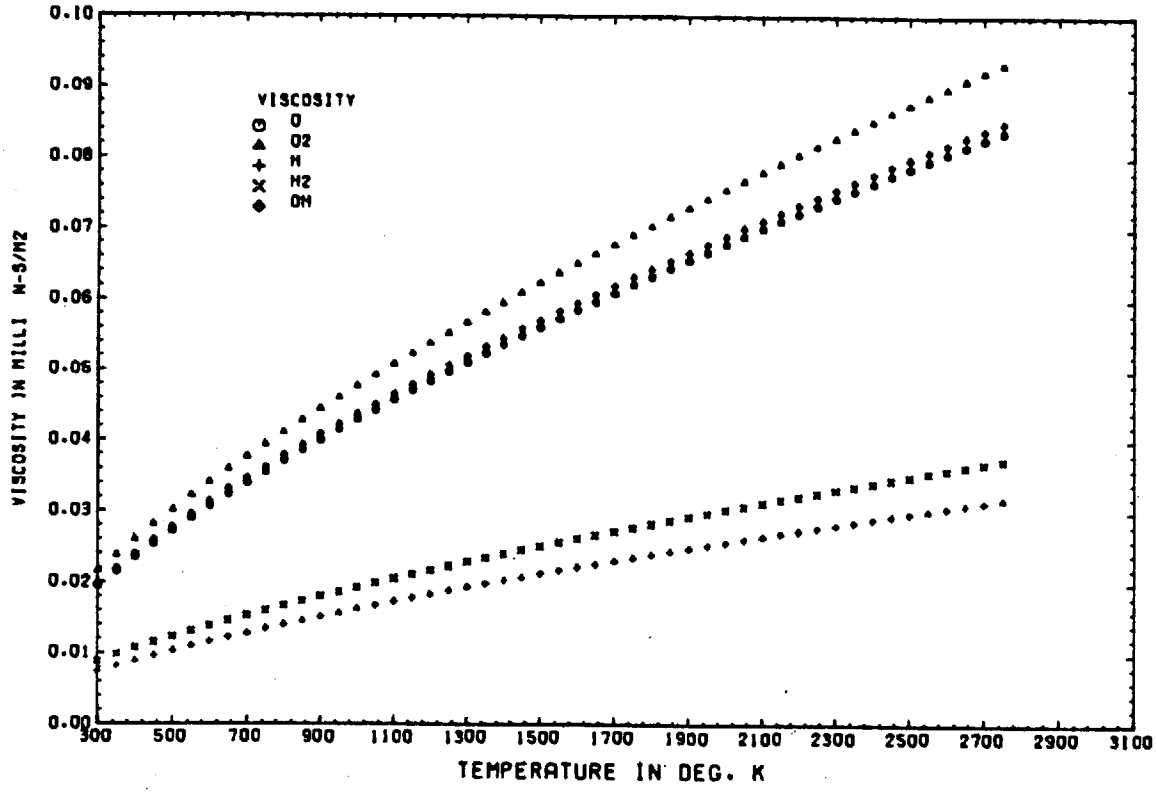


Fig (A.6.3) Computed Values of Viscosity for Compondents of Combustion Products.

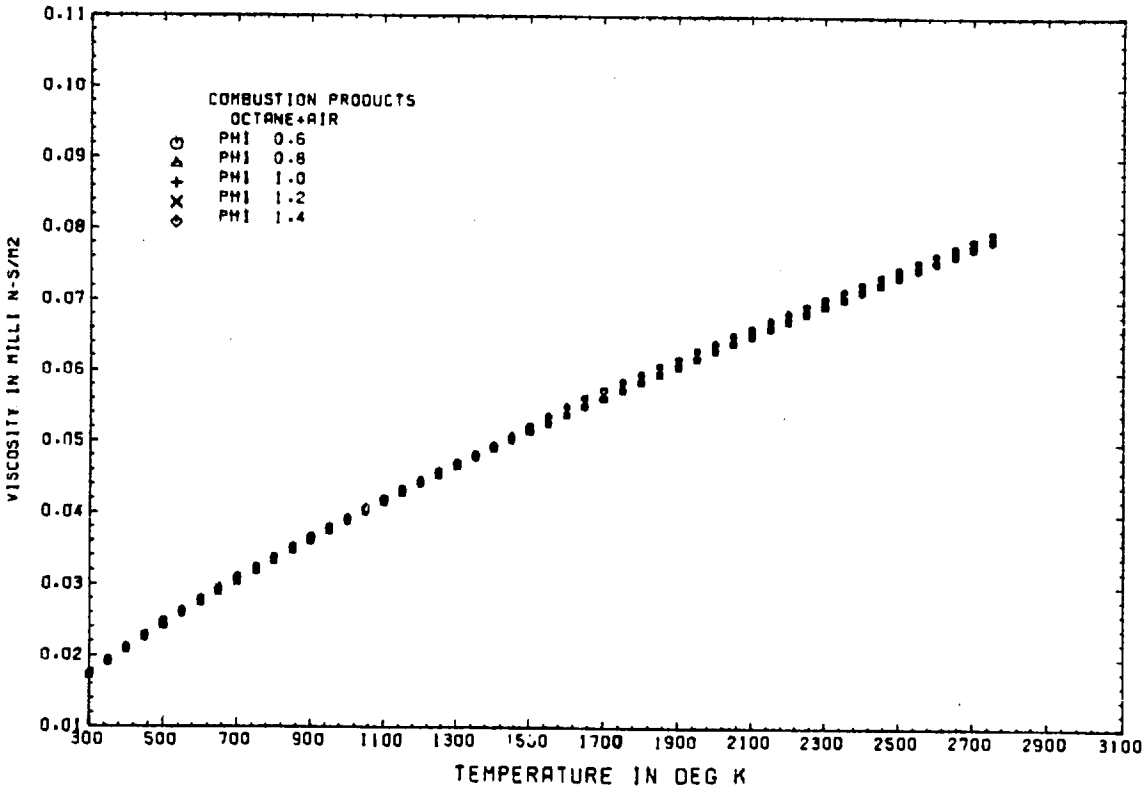


Fig (A.6.4) Computed Values of Viscosity for Octane + Air Combustion Products.

Appendix (A.7)

Data Recovery from Recorded Magnetic Tape

As explained in Section (4.51), due to the difference between the accuracy of the word length used by the computer and that of the Kennedy tape unit which is used for recording experimental data, the recorded data on magnetic tape cannot be directly read by the computer. A computer word has 60 bits word length whereas experimental data has 12 bits word length. Thus when the recorded data were read by the computer from the magnetic tape, each group of five items of experimentally recorded data was seen as a single value or recorded word, as shown below.

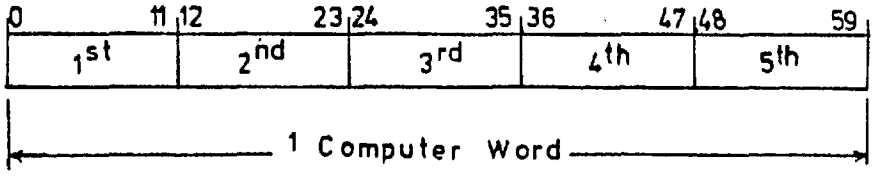
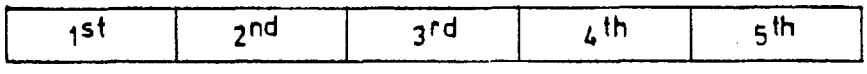


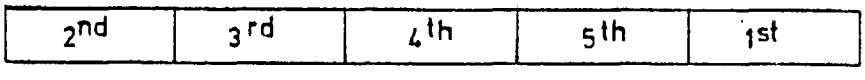
Fig (A.7.1) The structure of a computer word which consists of five items of experimentally recorded data.

The spliting of the computer data word into five equal groups is thus necessary to recover the original recorded data. This is achieved by a Shifting and Masking Operation which is done to the computer word and the steps involved are shown below.

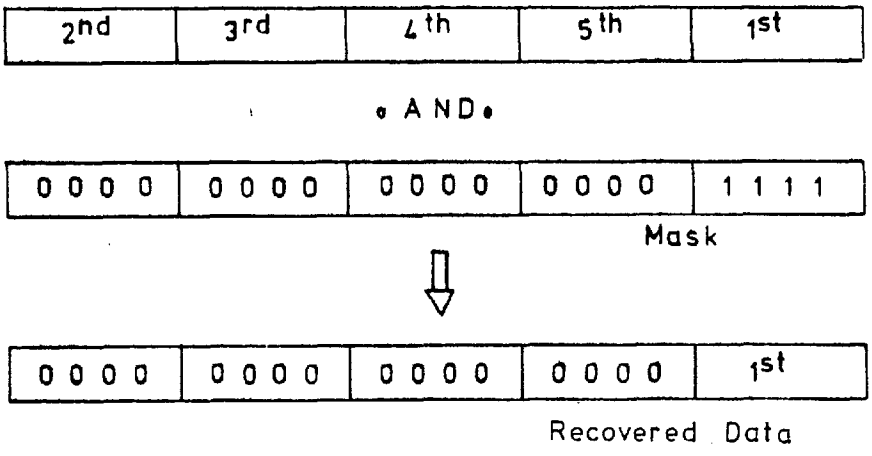
Step 1:- Reading from the magnetic tape:- Each computer data word now consists of five items of experimentally recorded data.



Step 2:- Left hand recirculating shifting of a Computer word by 12 bits:- The aim is to transfer the experimental data to be recovered to the right hand end of the computer word.



Step 3:- Masking Operation:- The aim is to mask the first four experimental values, that is to put zeros in the first 48 locations occupied by the first four experimental words. Thus the resulting masked computer word contains the right hand end outer most experimental value which has been recovered.



Step 4:- Go to Step 2 if all the five data words have not been recovered. Otherwise repeat the whole sequence with the next computer word which has been read from the magnetic tape.

Appendix (A.8)

Indexing System for Recorded Data.

As an enormours amount of data recording is involved in the analysis of the turbulence field inside engine cylinder, a reliable indexing system for recorded data is required. This was achieved by indexing of each recorded data file after each run of the experiment. Each recorded data file on the magnetic tape was transferred onto a Master Tape with appropriate indexing information, which consists of engine speed, throttle valve position, compression ratio dial reading, hot wire sensor position, hot wire sensor cold and operating resistances and its orientation. This process is shown diagrammatically in fig (A.8.1).

During the analysis of the recorded data, the analysis programme first read the information contained in the index and based on the information, the following recorded data were analysed.

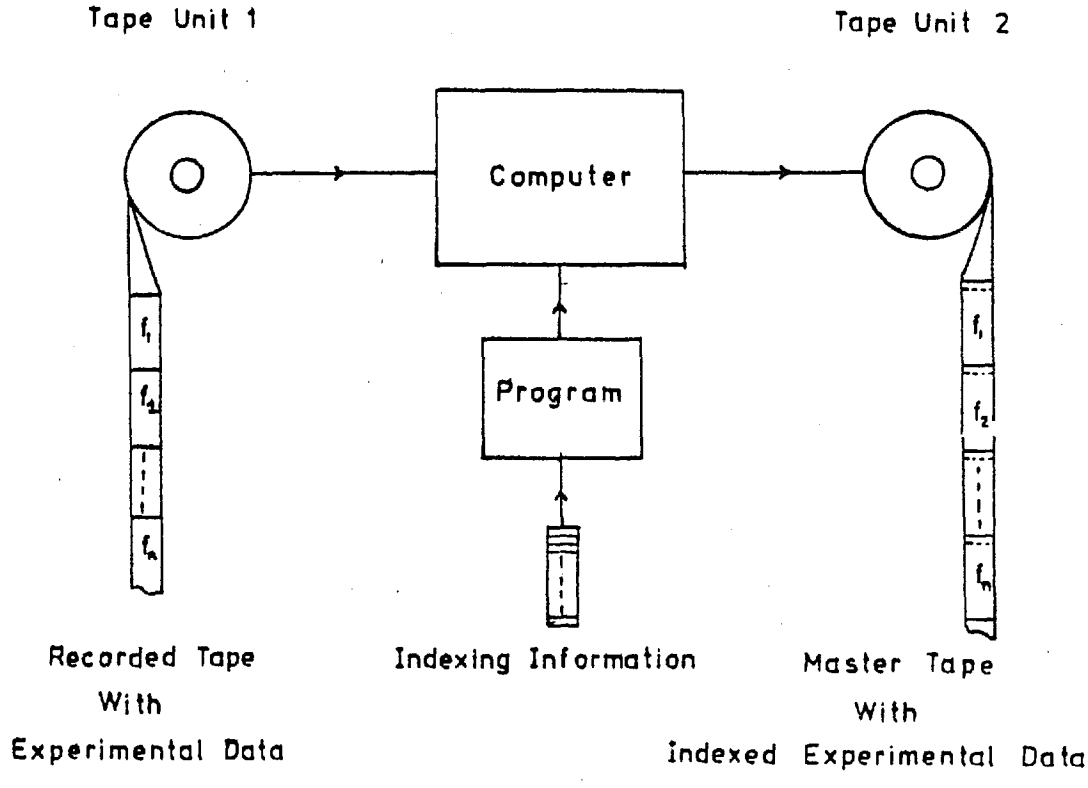


Fig (A.8.1) Indexing of Recorded Data

Appendix (A.9)

Telemetering of Information from Moving Piston.

Various forms of linkage have been employed previously to transmit information from probes which were mounted on a moving piston (34, 35, 40, 59). Each particular type of linkage employed was designed to suit a particular engine geometry and application. A similar type of telemetering linkage was required to get information from hot wire probes which were mounted on the piston crown.

Previously employed telemetering systems can be divided into two groups:-

(i) Telemetering by Using Radio Linkage and

(ii) Telemetering by Using Mechanical Linkage.

(i) Telemetering by Radio Linkage:- This type of telemetering method was used by Westbrook (40) to measure piston slap. An inductive transducer, which was mounted on the piston, was connected to a small transmitter fixed to the connecting rod. The information was transmitted to a receiver which was located outside the engine crank case.

(ii) Telemetering by Mechanical Linkage:- This type of telemetering can be subdivided into two groups, namely:-

(a) Those which give intermittent telemetering and

(b) Those which give continuous telemetering.

(a) Intermittent Telemetering Linkage:- This type was used by Stotter (93) to measure piston temperature. The contact to the probe was made only when the piston was near bottom dead centre.

(b) Continuous Telemetering Linkage:- These are of several different shapes and the previously used forms of continuous linkage are:-

Linkage having a single arm made from a flat spring, fig (A.9.2):- This type was used by Furahama Et Al (35) to measure piston temperature.

Linkage having sliding contacts, fig (A.9.3):- This form was used by Curry (59) to transmit signals from ionization probes which were fixed to the piston crown.

Linkage of Pulley and Wire type, fig (A.9.4):- This type was used by Sternbrenner (34) to measure piston temperature.

Linkage having two moving arms, fig (A.9.5):- This linkage forms a two bar linkage system where one end is connected to the big end of the connecting rod and the other end to the

crank case. The arms of the linkage were used for carrying the lead wires of the probes. This type of linkage was used by Westbrook (43) and Law Et Al (123) for telemetering of signal from probes which were mounted on piston crown.

Selection of a Linkage System:- The radio linkage type is not suitable because of its one way signal transmission with no feed back capability. Intermittent linkage is not applicable for our case. Sliding contact linkage system may introduce unwanted contact noises in turbulent flow signal. Spring arm type linkage is only suitable for low speed engines because of its inertia problem. Thus a two bar linkage system was selected for telemetering signals from hot wire probes which were mounted on the piston crown. The linkage was designed to suit the employed engine geometry and was successfully employed throughout the experimental investigation. The linkage was designed and made by the author.

Fig (A.9.1) Intermittent Linkage used by Stotter (93)

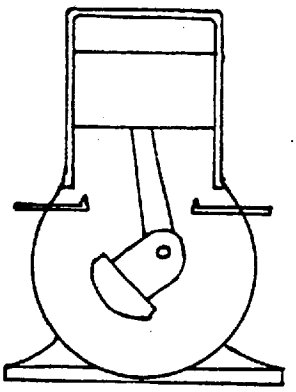


Fig (A.9.2) Continuous Linakage of the type used by Furnhama (35)

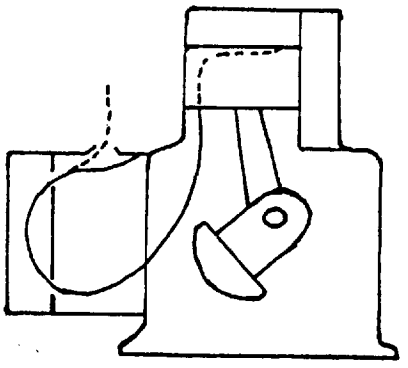


Fig (A.9.3) Sliding Contact Linkage Used by Curry (59).

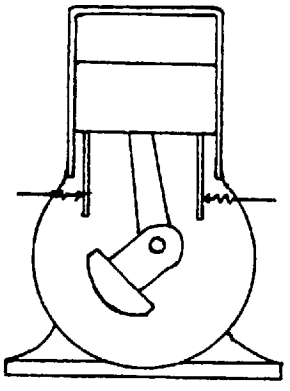


Fig (A.9.4) Wire Linkage Used by Steinbrener (34).

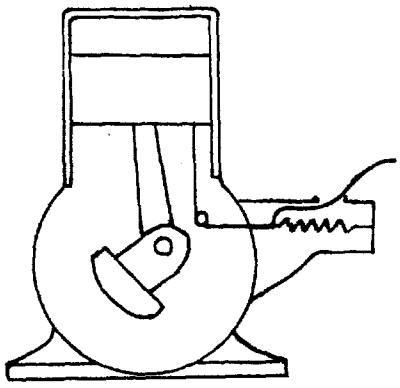
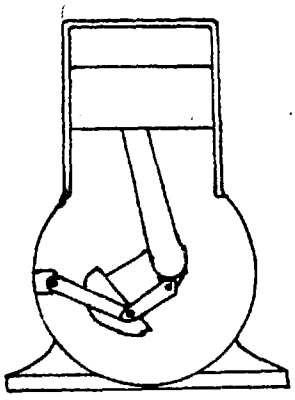


Fig (A.9.5) Continuous Bar Linkage type used by Westbrook (40) and in Present Research Work.



Appendix (A.10)

Description of the Engine Test Rig.

The engine used for the experiment is a Renauld Variable Compression Ratio Single Cylinder Engine which is coupled to an electric dynamometer.

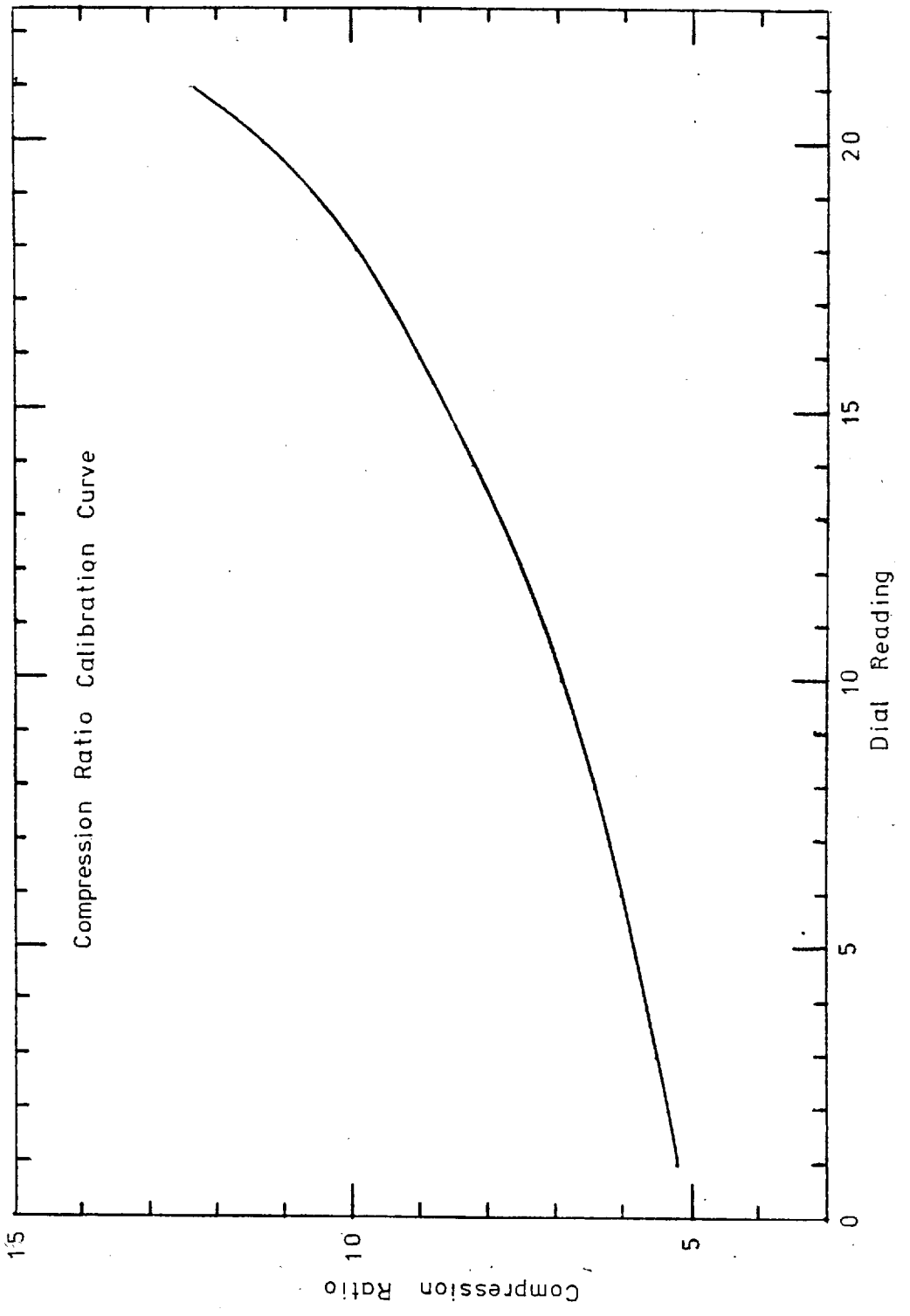
Type of Engine	Spark Ignition
Bore	80.7mm
Stroke	100.0mm
Compression Ratio	Variable

Modifications:- Engine was rebored and fitted with a new piston to reduce lubricating oil leakage. An additional telemetering crank was installed in the crank case to monitor the hot wire probes on piston crown. During turbulence measurement engine was motored under dry sump condition and a controlled amount of lubricant was fed to eliminate the lubricating oil leakage across the piston rings.

Engine Motoring Test:- Engine speed was regulated by a Ward Leonard Control Unit and was monitored by using a frequency counter counting engine revolution pulses from a magnetic pick up as well as by using the attached tachometer unit.

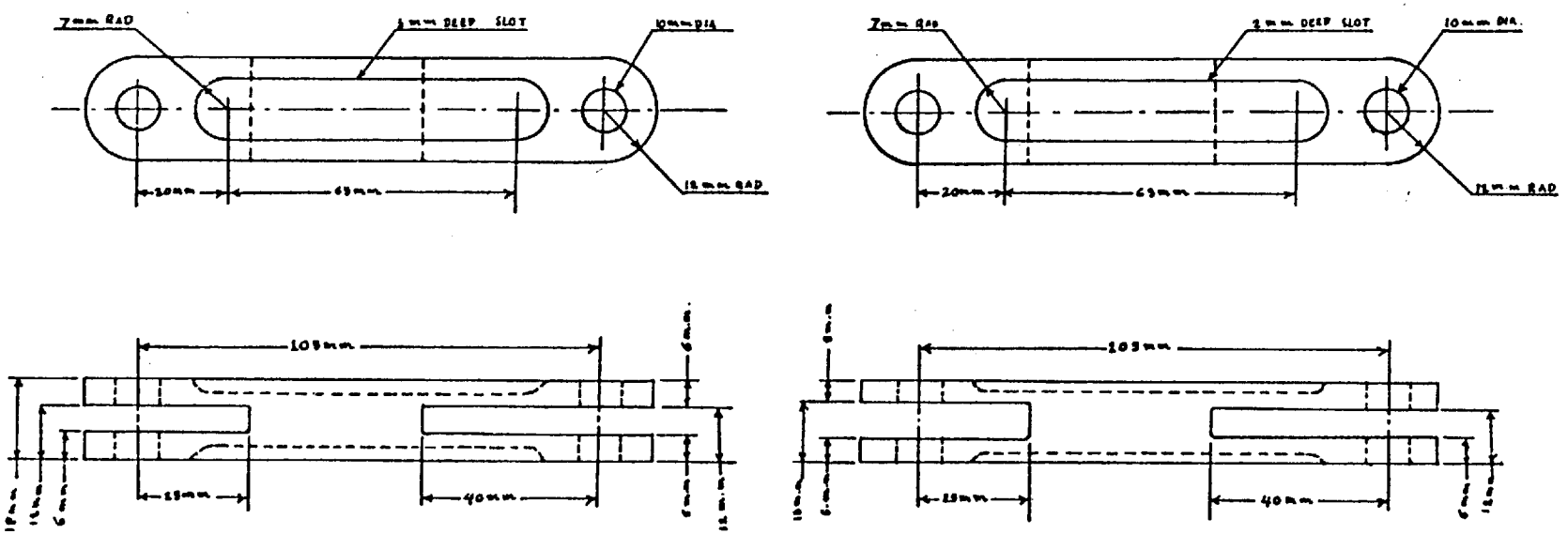
Engine Running Test:- Engine was fitted with an electronic ignition unit to improve spark energy as well as to minimize drift in ignition timing. Fuel consumption was measured by measuring the time for 100C.C. of fuel to be burnt and air consumption was measured by an attached orifice air flow meter in the inlet pipe.

Appendix (A.11)



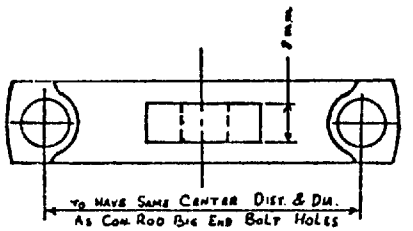
Appendix (A.12)

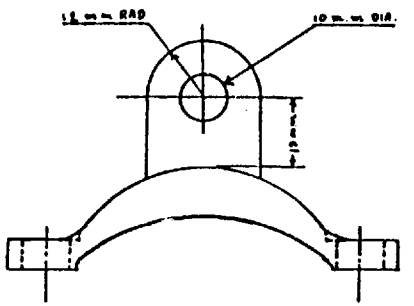
Detail Drawing Of Auxiliary Crank



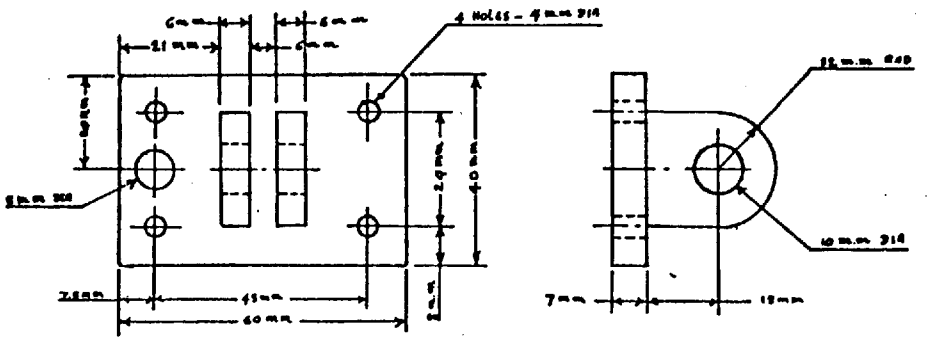
THESE TWO ARMS HAVE SAME EXTERNAL DIMENSIONS

DRAWN	CHAN NYEIN	SCALE	TITLE	AUXILIARY CRANK	1B	1	LINKAGE ARM (CON. ROD SIDE)	ALUMINIUM ALLOY	
APPROVED		1:1			1A	1	LINKAGE ARM (CRANK CASE SIDE)	ALUMINIUM ALLOY	
TRACED		DATE	AMMDTS		PART NO	NO OFF	DESCRIPTION	MATERIAL	REMARKS
CHECKED					MECHANICAL ENGINEERING DEPARTMENT IMPERIAL COLLEGE. LONDON.				

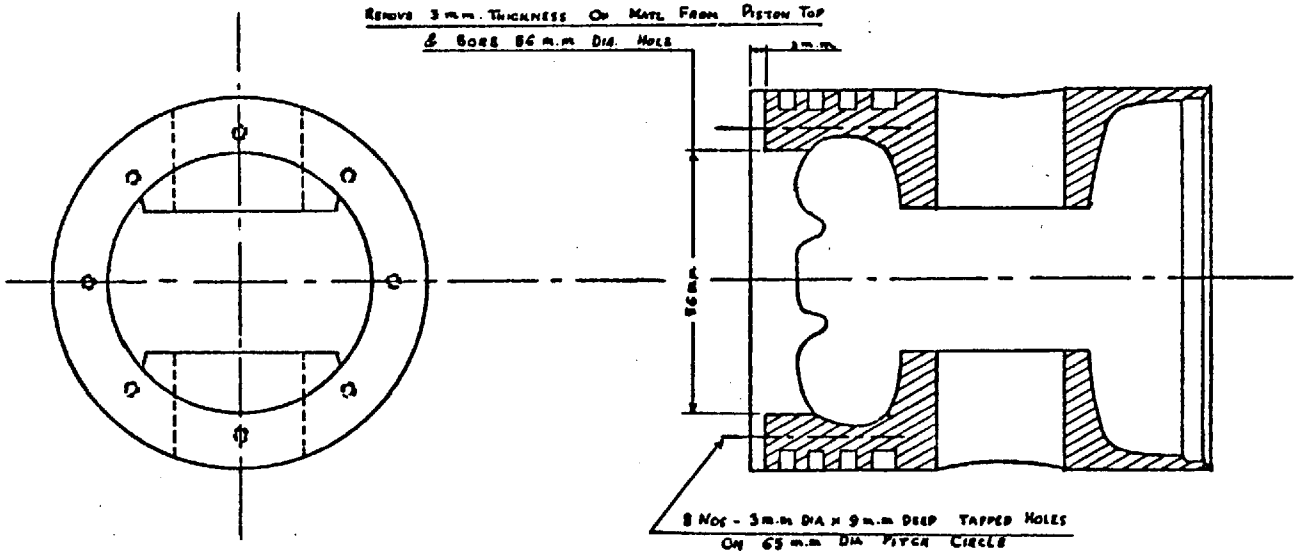




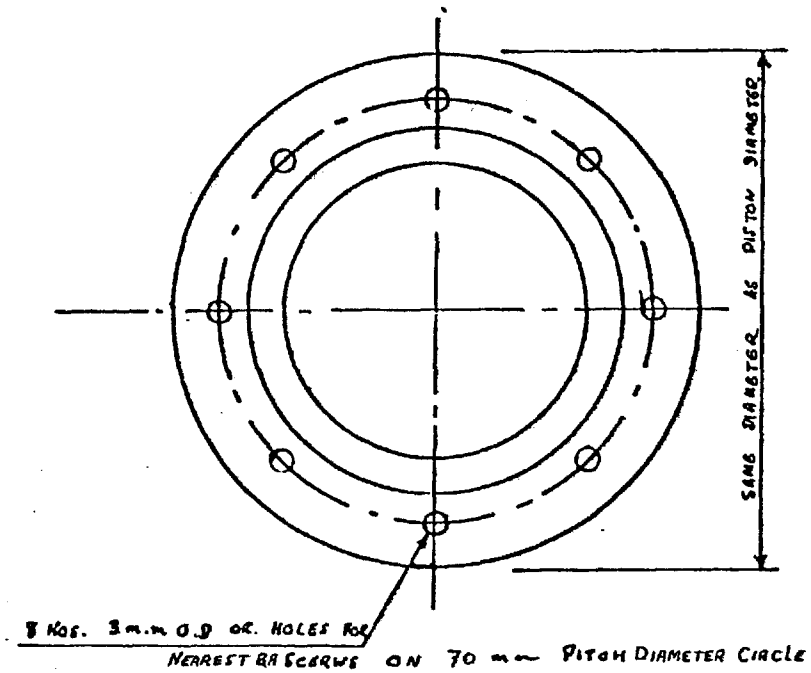
This Piece Is To Be Cut According To The Shape Of Slot In Con Rod And End Bearing Cap

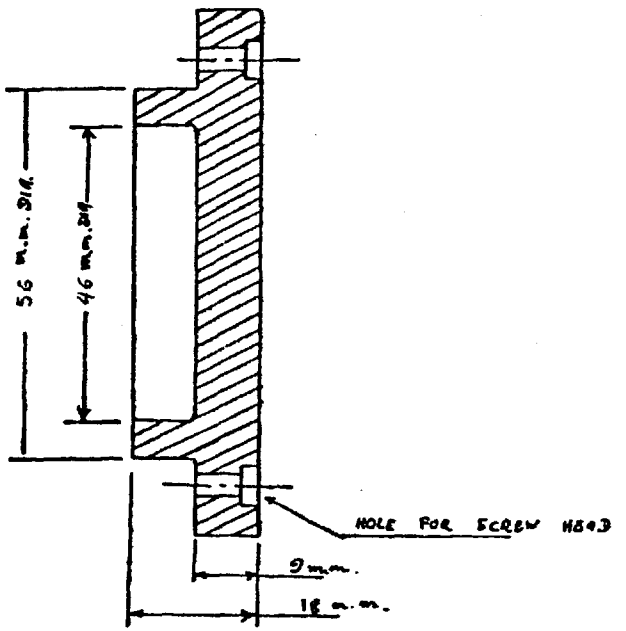


DRAWN	CHAN NYEIN	SCALE	TITLE	AUXILIARY CRANK	3	1	CRANK CASE END LINKAGE BEARING	ALUMINIUM ALLOY	
APPROVED		1:1			2	1	CONROD END LINKAGE BEARING	ALUMINIUM ALLOY	
TRACED		DATE	AMMDTS		PART NO	NO OFF	DESCRIPTION	MATERIAL	REMARKS
CHECKED					MECHANICAL ENGINEERING DEPARTMENT IMPERIAL COLLEGE. LONDON				

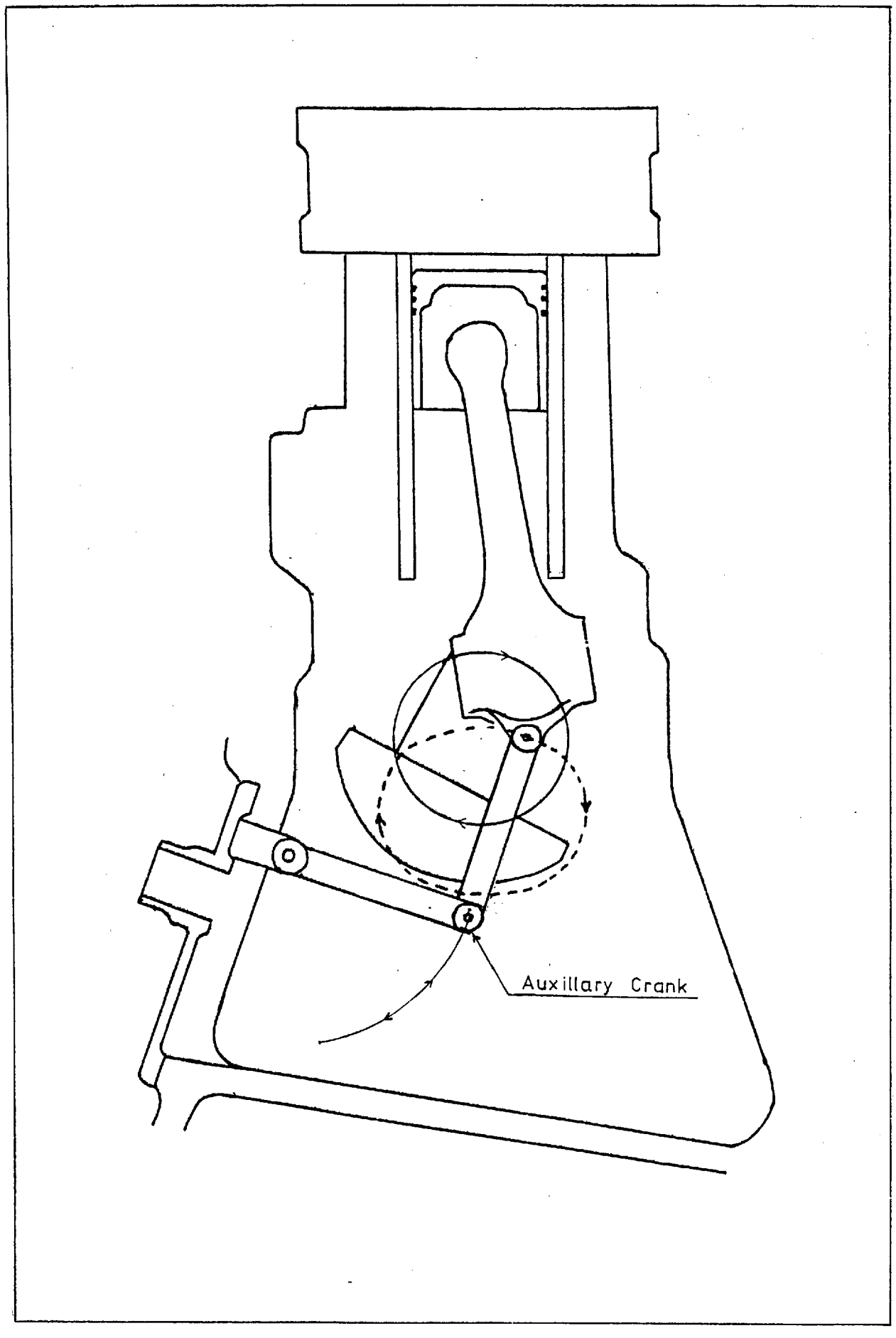


DRAWN	CHAN NYEIN	SCALE	TITLE		4	1	PISTON		
APPROVED		1:1			PART NO.	No. OFF.	DESCRIPTION	MATERIAL	REMARKS
TRACED		DATE	AMMDTS		MECHANICAL ENGINEERING DEPARTMENT IMPERIAL COLLEGE . LONDON.				
CHECKED									



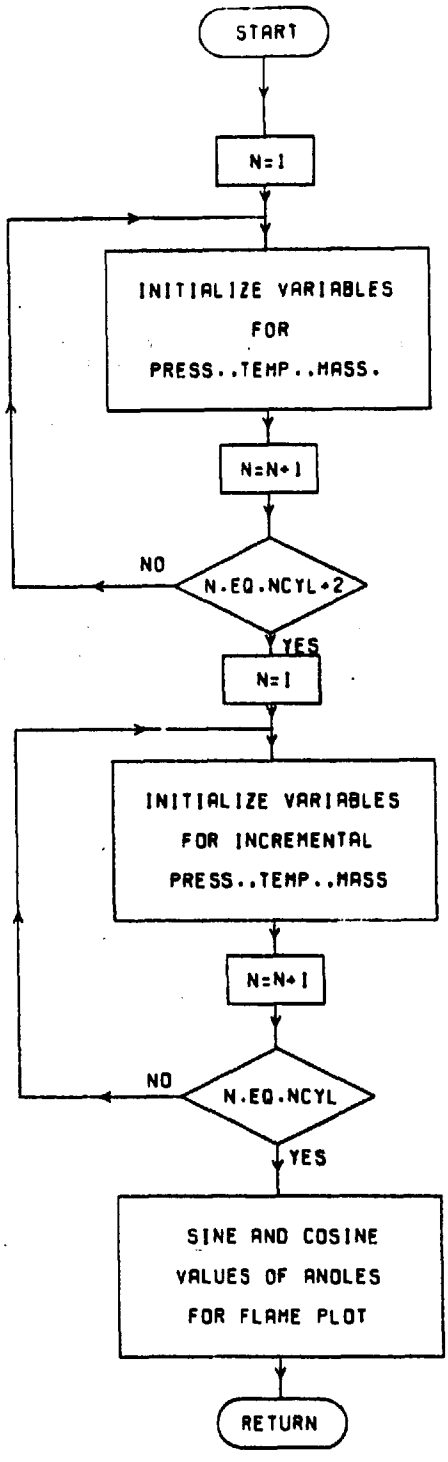


DRAWN	CHAN NYEIN	SCALE	TITLE		5	2	PISTON CROWN	ALUMINIUM	
APPROVED		1:1			PART No.	No. OFF.	DESCRIPTION	MATERIAL	REMARKS
TRACED		DATE	AMMDTS		MECHANICAL ENGINEERING DEPARTMENT				
CHECKED					IMPERIAL COLLEGE. LONDON.				

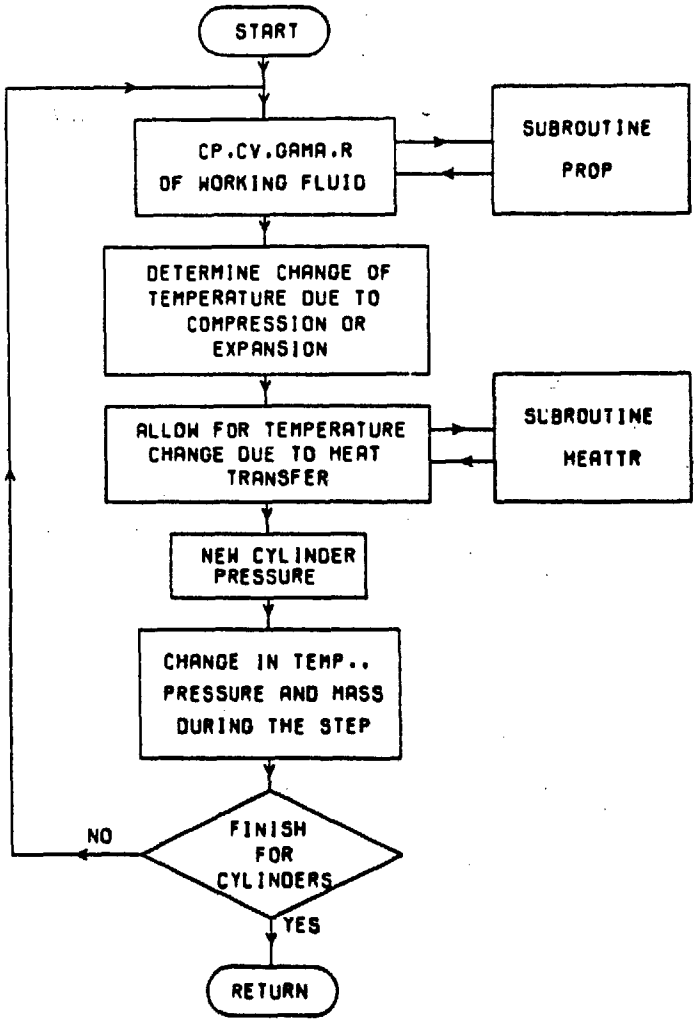

Auxillary Crank

Appendix (A.13)

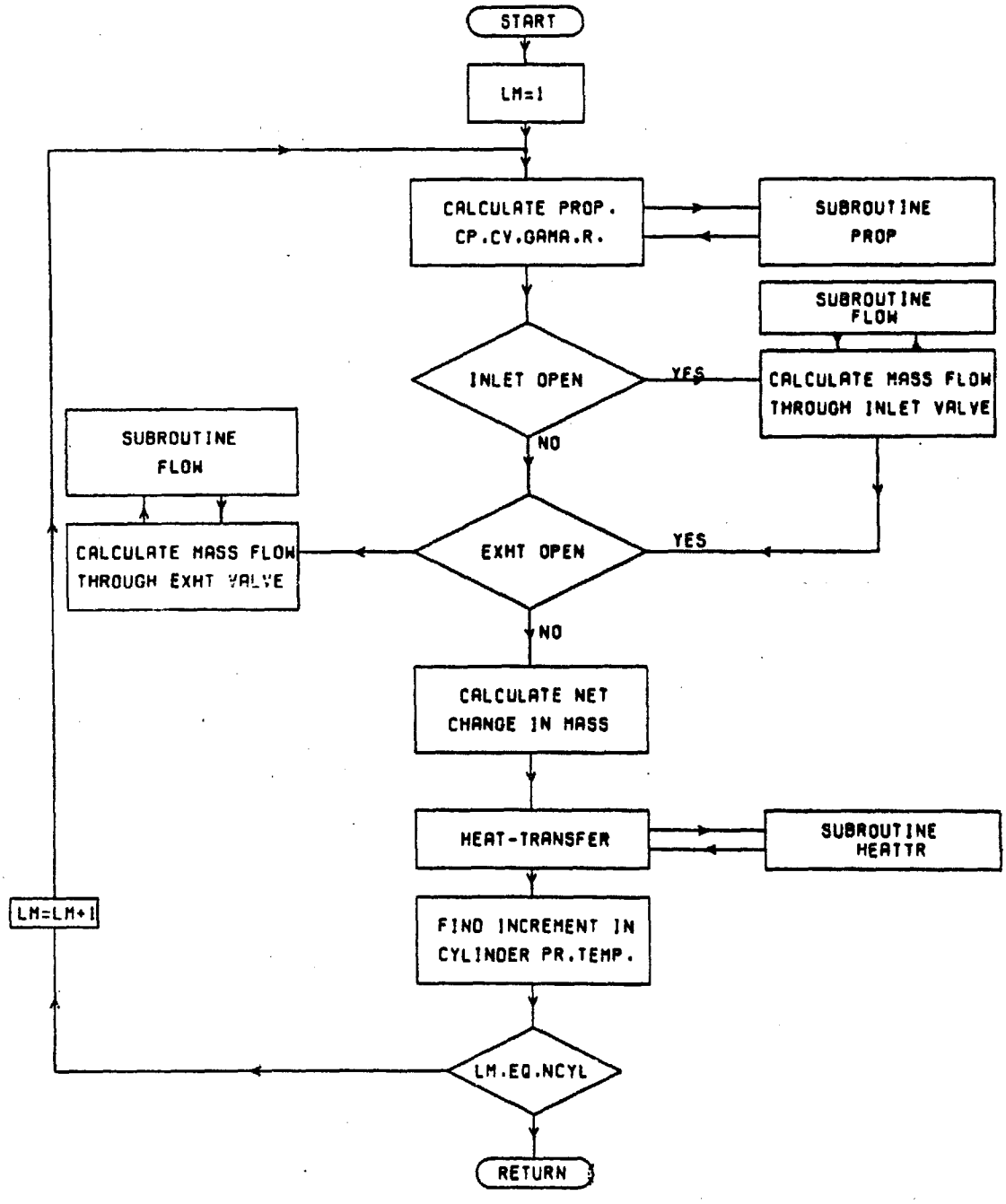
Flow Diagrams Of the Computer Programs



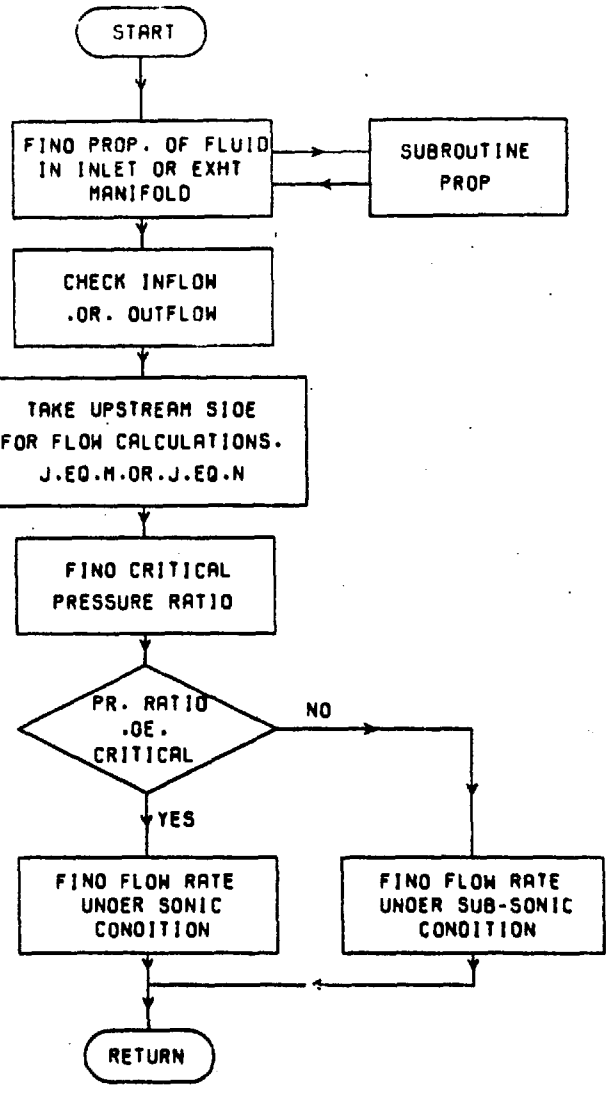
*** SUBROUTINE INITLZE ***



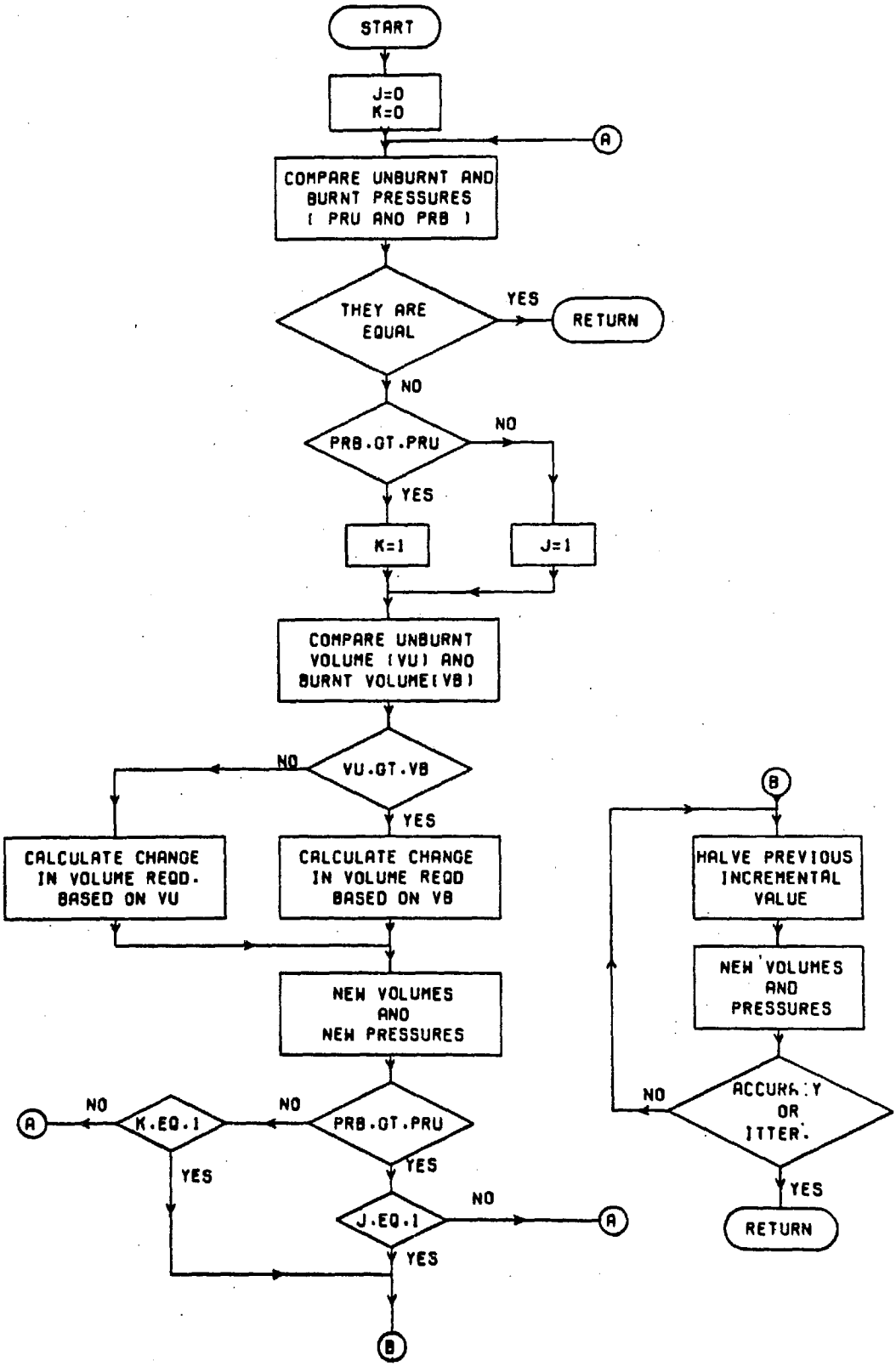
*** SUBROUTINE NONFLOW ***



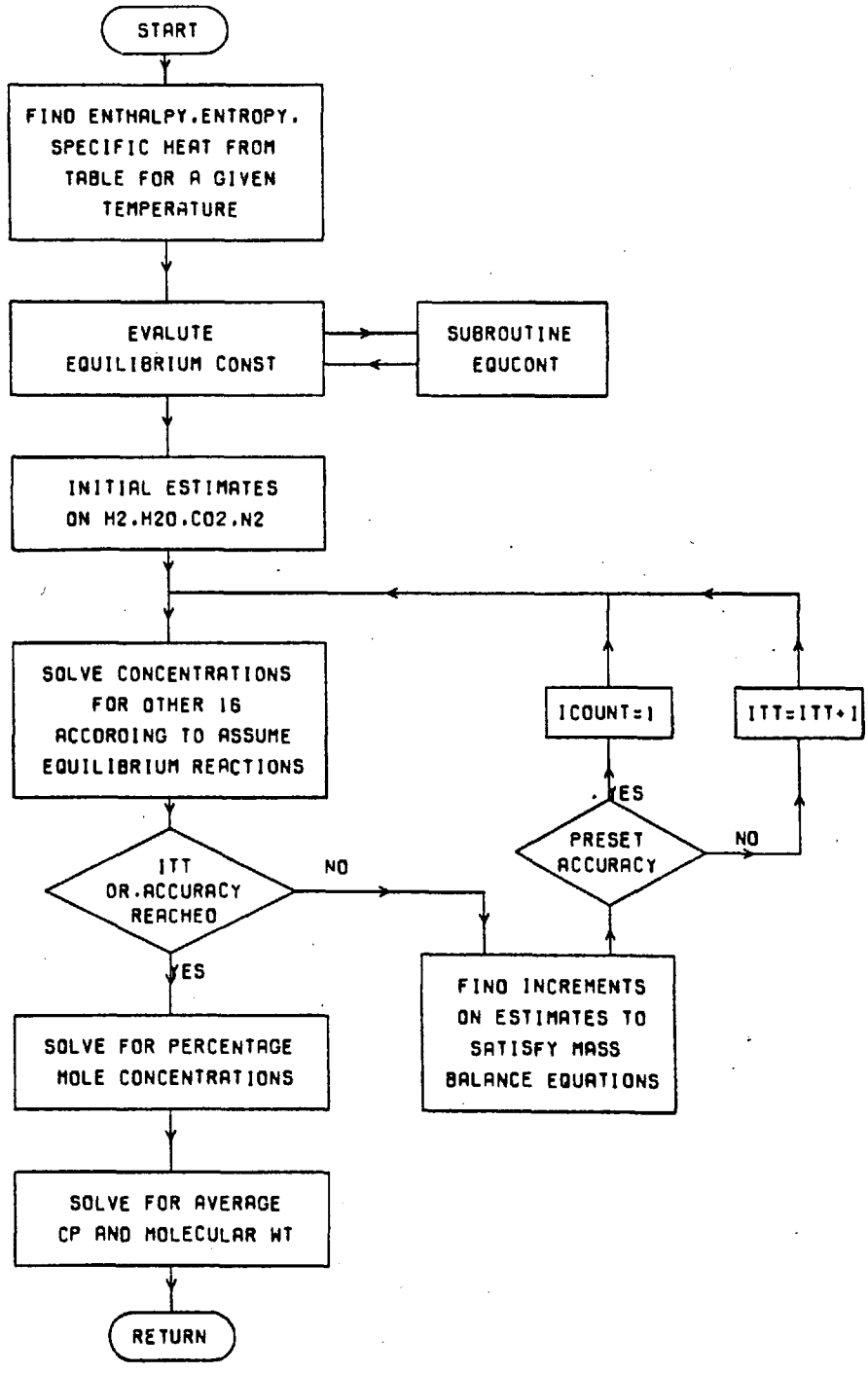
*** SUBROUTINE GASFLOW ***



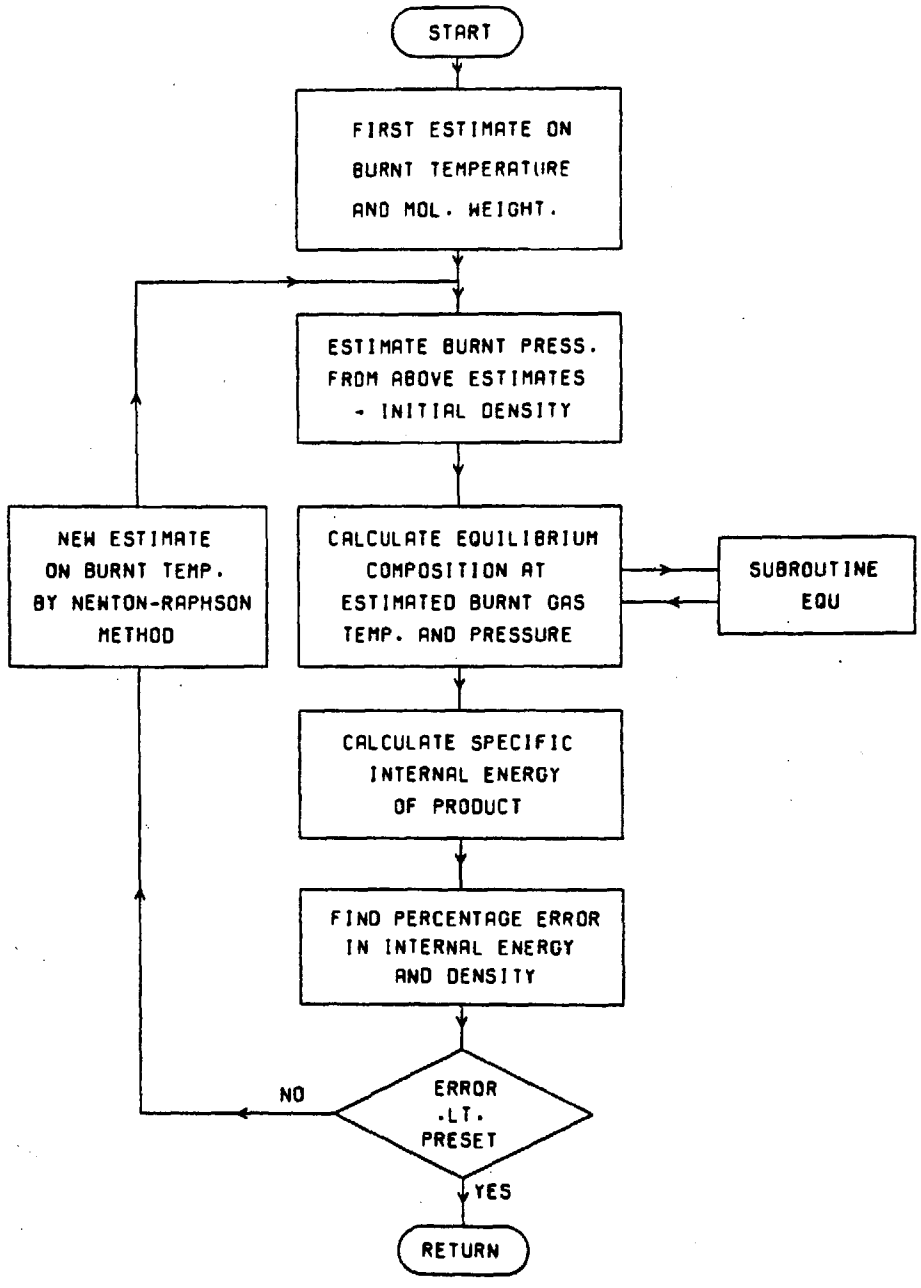
*** SUBROUTINE ISENTRO ***



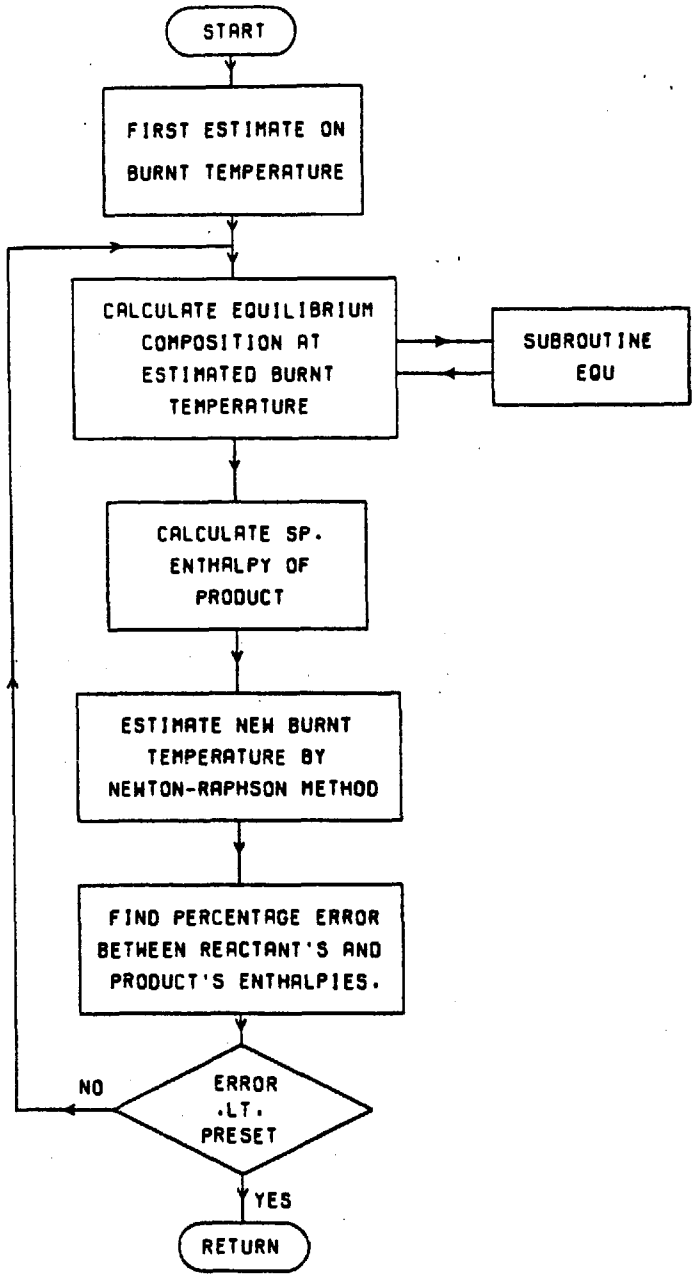
*** SUBROUTINE EQUILZR ***



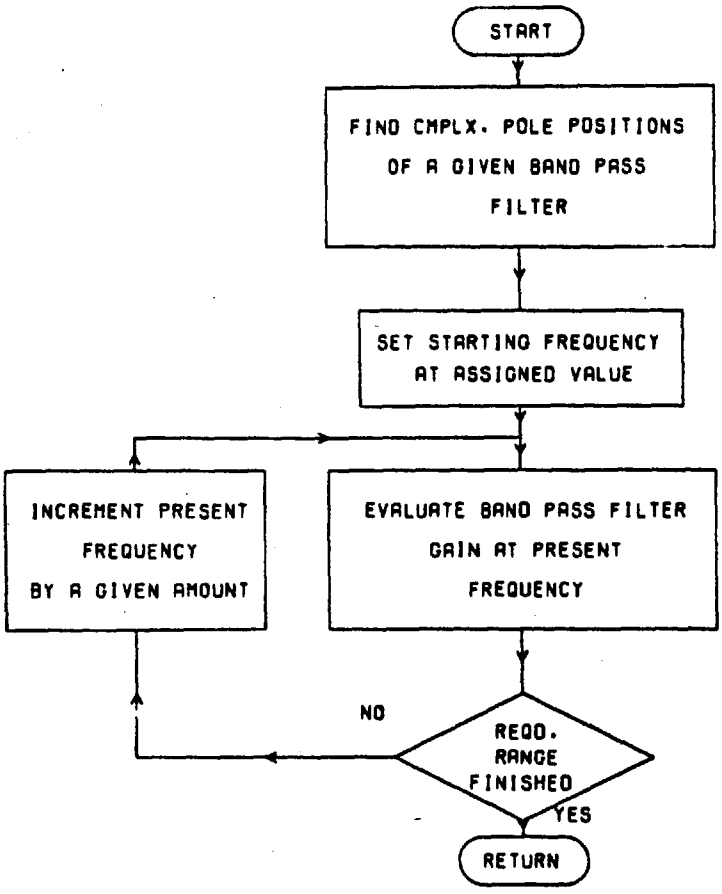
*** SUBROUTINE EQU ***



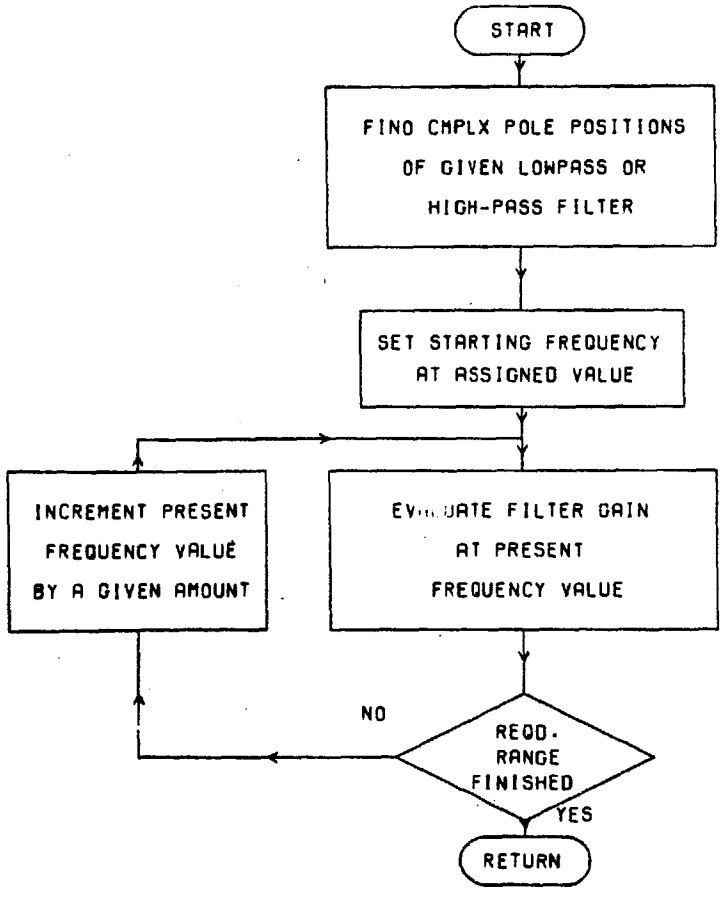
*** SUBROUTINE CONTVOL ***



*** SUBROUTINE CONSTPR ***



*** SUBROUTINE BPGAIN ***



*** SUBROUTINE LHGAIN ***

Appendix (A.14)

Tables of the Predicted Properties of Octane + Air Combustion Products

TEMP DEG. K	PR BAR	PHI	MOL WT	CP KJ/KG K	CV	R KJ/KG K	GAM
500.0	1.0	.6	28.41	1.103	.811	.292	1.360
600.0	1.0	.6	28.41	1.130	.838	.292	1.349
700.0	1.0	.6	28.41	1.159	.867	.292	1.337
800.0	1.0	.6	28.41	1.188	.896	.292	1.326
900.0	1.0	.6	28.41	1.216	.924	.292	1.316
1000.0	1.0	.6	28.41	1.242	.949	.292	1.308
1100.0	1.0	.6	28.41	1.265	.973	.292	1.301
1200.0	1.0	.6	28.41	1.286	.993	.292	1.294
1300.0	1.0	.6	28.41	1.304	1.012	.292	1.288
1400.0	1.0	.6	28.41	1.321	1.028	.292	1.284
1500.0	1.0	.6	28.41	1.335	1.043	.292	1.280
1600.0	1.0	.6	28.41	1.348	1.056	.292	1.277
1700.0	1.0	.6	28.41	1.359	1.067	.292	1.274
1800.0	1.0	.6	28.40	1.370	1.077	.292	1.271
1900.0	1.0	.6	28.39	1.379	1.086	.293	1.268
2000.0	1.0	.6	28.39	1.386	1.093	.293	1.268
2100.0	1.0	.6	28.36	1.393	1.100	.293	1.266
2200.0	1.0	.6	28.29	1.400	1.106	.294	1.265
2300.0	1.0	.6	28.29	1.403	1.110	.294	1.265
2400.0	1.0	.6	28.14	1.408	1.114	.295	1.265
2500.0	1.0	.6	28.10	1.411	1.115	.296	1.265
2600.0	1.0	.6	27.86	1.416	1.118	.298	1.267
2700.0	1.0	.6	27.67	1.418	1.118	.300	1.268
2800.0	1.0	.6	27.38	1.421	1.118	.303	1.271
2900.0	1.0	.6	27.04	1.425	1.118	.307	1.275
3000.0	1.0	.6	26.75	1.426	1.115	.310	1.278
3100.0	1.0	.6	26.20	1.433	1.116	.317	1.284
3200.0	1.0	.6	25.89	1.433	1.112	.321	1.289
3300.0	1.0	.6	25.59	1.426	1.102	.325	1.295
3400.0	1.0	.6	24.97	1.438	1.106	.333	1.301
3500.0	1.0	.6	24.58	1.432	1.094	.338	1.308

TEMP DEG. K	PR BAR	PHI	MOL WT	CP KJ/KG K	CV	R KJ/KG K	GAM
500.0	1.0	.8	28.51	1.116	.824	.291	1.353
600.0	1.0	.8	28.51	1.144	.853	.291	1.341
700.0	1.0	.8	28.51	1.175	.884	.291	1.330
800.0	1.0	.8	28.51	1.206	.914	.291	1.319
900.0	1.0	.8	28.51	1.234	.943	.291	1.309
1000.0	1.0	.8	28.51	1.261	.970	.291	1.300
1100.0	1.0	.8	28.51	1.285	.994	.291	1.293
1200.0	1.0	.8	28.51	1.307	1.015	.291	1.287
1300.0	1.0	.8	28.51	1.326	1.035	.291	1.282
1400.0	1.0	.8	28.51	1.343	1.052	.291	1.277
1500.0	1.0	.8	28.50	1.359	1.067	.291	1.273
1600.0	1.0	.8	28.50	1.372	1.081	.291	1.270
1700.0	1.0	.8	28.50	1.384	1.093	.291	1.267
1800.0	1.0	.8	28.48	1.395	1.104	.292	1.264
1900.0	1.0	.8	28.48	1.405	1.113	.292	1.262
2000.0	1.0	.8	28.44	1.413	1.121	.292	1.260
2100.0	1.0	.8	28.36	1.421	1.128	.293	1.260
2200.0	1.0	.8	28.36	1.427	1.134	.293	1.258
2300.0	1.0	.8	28.18	1.434	1.139	.295	1.259
2400.0	1.0	.8	27.91	1.440	1.142	.298	1.261
2500.0	1.0	.8	27.88	1.443	1.145	.298	1.260
2600.0	1.0	.8	27.43	1.450	1.147	.303	1.264
2700.0	1.0	.8	27.37	1.451	1.148	.303	1.264
2800.0	1.0	.8	27.30	1.449	1.145	.304	1.266
2900.0	1.0	.8	26.65	1.458	1.147	.312	1.272
3000.0	1.0	.8	26.50	1.455	1.142	.313	1.275
3100.0	1.0	.8	26.31	1.447	1.132	.316	1.279
3200.0	1.0	.8	25.50	1.463	1.138	.326	1.286
3300.0	1.0	.8	25.18	1.456	1.126	.330	1.293
3400.0	1.0	.8	24.75	1.448	1.113	.336	1.302
3500.0	1.0	.8	24.06	1.462	1.117	.345	1.309

TEMP DEG. K	PR BAR	PHI	MOL WT	CP	CV	R	GAM
				KJ/KG K		KJ/KG K	
500.0	1.0	1.0	28.60	1.126	.836	.290	1.347
600.0	1.0	1.0	28.60	1.157	.867	.290	1.335
700.0	1.0	1.0	28.60	1.189	.899	.290	1.323
800.0	1.0	1.0	28.60	1.221	.930	.290	1.312
900.0	1.0	1.0	28.60	1.251	.960	.290	1.302
1000.0	1.0	1.0	28.60	1.278	.988	.290	1.294
1100.0	1.0	1.0	28.60	1.303	1.013	.290	1.287
1200.0	1.0	1.0	28.60	1.326	1.035	.290	1.281
1300.0	1.0	1.0	28.60	1.346	1.055	.290	1.275
1400.0	1.0	1.0	28.60	1.364	1.073	.290	1.271
1500.0	1.0	1.0	28.59	1.380	1.089	.290	1.267
1600.0	1.0	1.0	28.59	1.394	1.103	.290	1.263
1700.0	1.0	1.0	28.59	1.407	1.116	.290	1.260
1800.0	1.0	1.0	28.59	1.418	1.127	.291	1.258
1900.0	1.0	1.0	28.57	1.428	1.137	.291	1.256
2000.0	1.0	1.0	28.52	1.437	1.146	.291	1.254
2100.0	1.0	1.0	28.42	1.445	1.153	.292	1.253
2200.0	1.0	1.0	28.42	1.452	1.159	.292	1.252
2300.0	1.0	1.0	28.22	1.458	1.165	.294	1.253
2400.0	1.0	1.0	28.21	1.462	1.168	.294	1.252
2500.0	1.0	1.0	27.85	1.469	1.171	.298	1.255
2600.0	1.0	1.0	27.82	1.469	1.171	.299	1.255
2700.0	1.0	1.0	27.26	1.478	1.173	.305	1.260
2800.0	1.0	1.0	27.18	1.475	1.170	.306	1.261
2900.0	1.0	1.0	26.53	1.484	1.171	.313	1.267
3000.0	1.0	1.0	26.27	1.482	1.166	.316	1.271
3100.0	1.0	1.0	25.86	1.482	1.161	.321	1.277
3200.0	1.0	1.0	25.16	1.491	1.161	.330	1.284
3300.0	1.0	1.0	24.72	1.489	1.153	.336	1.291
3400.0	1.0	1.0	24.16	1.490	1.146	.344	1.300
3500.0	1.0	1.0	23.53	1.486	1.143	.353	1.309

TEMP DEG. K	PR BAR	PHI	MOL WT	CP	CV	R	GAM
				KJ/KG K		KJ/KG K	
500.0	1.0	1.2	28.69	1.136	.847	.290	1.342
600.0	1.0	1.2	28.69	1.169	.879	.290	1.329
700.0	1.0	1.2	28.69	1.202	.912	.290	1.317
800.0	1.0	1.2	28.69	1.234	.945	.290	1.306
900.0	1.0	1.2	28.68	1.265	.976	.290	1.297
1000.0	1.0	1.2	28.68	1.294	1.004	.290	1.288
1100.0	1.0	1.2	28.68	1.319	1.030	.290	1.281
1200.0	1.0	1.2	28.68	1.342	1.053	.290	1.275
1300.0	1.0	1.2	28.68	1.363	1.074	.290	1.270
1400.0	1.0	1.2	28.68	1.382	1.092	.290	1.265
1500.0	1.0	1.2	28.67	1.398	1.108	.290	1.261
1600.0	1.0	1.2	28.67	1.413	1.123	.290	1.258
1700.0	1.0	1.2	28.67	1.426	1.137	.290	1.255
1800.0	1.0	1.2	28.67	1.438	1.148	.290	1.252
1900.0	1.0	1.2	28.64	1.449	1.159	.290	1.250
2000.0	1.0	1.2	28.59	1.458	1.168	.291	1.249
2100.0	1.0	1.2	28.48	1.467	1.175	.292	1.248
2200.0	1.0	1.2	28.47	1.474	1.182	.292	1.247
2300.0	1.0	1.2	20.25	1.481	1.187	.294	1.248
2400.0	1.0	1.2	28.23	1.485	1.190	.294	1.247
2500.0	1.0	1.2	27.83	1.492	1.194	.298	1.250
2600.0	1.0	1.2	27.79	1.492	1.193	.299	1.250
2700.0	1.0	1.2	27.16	1.502	1.196	.305	1.256
2800.0	1.0	1.2	27.07	1.499	1.192	.307	1.257
2900.0	1.0	1.2	26.25	1.511	1.195	.316	1.265
3000.0	1.0	1.2	26.08	1.507	1.188	.319	1.268
3100.0	1.0	1.2	25.81	1.499	1.177	.322	1.273
3200.0	1.0	1.2	24.86	1.517	1.183	.334	1.282
3300.0	1.0	1.2	24.54	1.507	1.168	.338	1.290
3400.0	1.0	1.2	23.92	1.507	1.160	.347	1.299
3500.0	1.0	1.2	23.22	1.515	1.157	.358	1.309

TEMP DEG. K	PR BAR	PHI	MOL WT	CP KJ/KG K	CV	R KJ/KG K	GAM
500.0	1.0	1.4	28.75	1.145	.856	.289	1.337
600.0	1.0	1.4	28.76	1.179	.890	.289	1.325
700.0	1.0	1.4	28.76	1.213	.924	.289	1.312
800.0	1.0	1.4	28.75	1.247	.958	.289	1.302
900.0	1.0	1.4	28.75	1.278	.989	.289	1.292
1000.0	1.0	1.4	28.75	1.307	1.018	.289	1.284
1100.0	1.0	1.4	28.75	1.334	1.045	.289	1.277
1200.0	1.0	1.4	28.75	1.358	1.069	.289	1.270
1300.0	1.0	1.4	28.74	1.379	1.090	.289	1.265
1400.0	1.0	1.4	28.74	1.398	1.109	.289	1.261
1500.0	1.0	1.4	28.74	1.415	1.126	.289	1.257
1600.0	1.0	1.4	28.73	1.430	1.141	.289	1.253
1700.0	1.0	1.4	28.73	1.444	1.155	.289	1.250
1800.0	1.0	1.4	28.72	1.456	1.167	.289	1.248
1900.0	1.0	1.4	28.68	1.468	1.178	.290	1.246
2000.0	1.0	1.4	28.64	1.477	1.187	.290	1.244
2100.0	1.0	1.4	28.53	1.487	1.195	.291	1.244
2200.0	1.0	1.4	28.50	1.494	1.202	.291	1.242
2300.0	1.0	1.4	28.27	1.502	1.208	.294	1.243
2400.0	1.0	1.4	28.21	1.506	1.211	.294	1.243
2500.0	1.0	1.4	27.80	1.513	1.215	.299	1.246
2600.0	1.0	1.4	27.72	1.514	1.215	.300	1.247
2700.0	1.0	1.4	27.07	1.524	1.217	.307	1.252
2800.0	1.0	1.4	26.97	1.521	1.213	.308	1.254
2900.0	1.0	1.4	26.55	1.522	1.209	.313	1.259
3000.0	1.0	1.4	25.80	1.529	1.209	.321	1.265
3100.0	1.0	1.4	25.48	1.527	1.201	.326	1.271
3200.0	1.0	1.4	24.59	1.541	1.203	.338	1.281
3300.0	1.0	1.4	24.22	1.532	1.189	.343	1.288
3400.0	1.0	1.4	23.55	1.535	1.182	.353	1.298
3500.0	1.0	1.4	22.87	1.538	1.175	.363	1.309

TEMP DEG. K	PR BAR	PHI	MOL WT	CP KJ/KG K	CV	R KJ/KG K	GAM
500.0	10.0	.6	28.41	1.103	.811	.292	1.360
600.0	10.0	.6	28.41	1.130	.838	.292	1.349
700.0	10.0	.6	28.41	1.159	.867	.292	1.337
800.0	10.0	.6	28.41	1.188	.896	.292	1.326
900.0	10.0	.6	28.41	1.216	.924	.292	1.316
1000.0	10.0	.6	28.41	1.242	.949	.292	1.308
1100.0	10.0	.6	28.41	1.265	.973	.292	1.301
1200.0	10.0	.6	28.41	1.286	.993	.292	1.294
1300.0	10.0	.6	28.41	1.304	1.012	.292	1.289
1400.0	10.0	.6	28.43	1.320	1.028	.292	1.284
1500.0	10.0	.6	28.53	1.328	1.037	.291	1.281
1600.0	10.0	.6	28.67	1.332	1.043	.290	1.278
1700.0	10.0	.6	28.68	1.343	1.053	.290	1.275
1800.0	10.0	.6	28.68	1.352	1.063	.290	1.272
1900.0	10.0	.6	28.68	1.361	1.072	.290	1.270
2000.0	10.0	.6	28.68	1.370	1.080	.290	1.268
2100.0	10.0	.6	28.67	1.377	1.087	.290	1.266
2200.0	10.0	.6	28.66	1.384	1.094	.290	1.265
2300.0	10.0	.6	28.64	1.390	1.100	.290	1.264
2400.0	10.0	.6	28.61	1.395	1.105	.290	1.263
2500.0	10.0	.6	28.57	1.400	1.110	.291	1.262
2600.0	10.0	.6	28.51	1.405	1.113	.291	1.262
2700.0	10.0	.6	28.42	1.409	1.116	.292	1.262
2800.0	10.0	.6	28.30	1.412	1.119	.293	1.262
2900.0	10.0	.6	28.16	1.415	1.120	.295	1.263
3000.0	10.0	.6	27.98	1.418	1.121	.297	1.265
3100.0	10.0	.6	27.77	1.420	1.121	.299	1.267
3200.0	10.0	.6	27.52	1.422	1.121	.302	1.269
3300.0	10.0	.6	27.25	1.424	1.120	.305	1.272
3400.0	10.0	.6	26.95	1.426	1.118	.308	1.276
3500.0	10.0	.6	26.63	1.428	1.116	.312	1.279

TEMP DEG. K	PR BAR	PHI	MOL WT	CP KJ/KG K	CV	R KJ/KG K	GAM
500.0	10.0	.8	28.52	1.115	.824	.291	1.353
600.0	10.0	.8	28.52	1.144	.853	.291	1.341
700.0	10.0	.8	28.52	1.175	.884	.291	1.330
800.0	10.0	.8	28.52	1.206	.914	.291	1.319
900.0	10.0	.8	28.52	1.234	.943	.291	1.309
1000.0	10.0	.8	28 52	1.261	.970	.291	1.300
1100.0	10.0	.8	28.52	1.285	.994	.291	1.293
1200.0	10.0	.8	28.52	1.307	1.016	.291	1.287
1300.0	10.0	.8	28.52	1.326	1.035	.291	1.281
1400.0	10.0	.8	28.52	1.343	1.052	.291	1.277
1500.0	10.0	.8	28.52	1.359	1.067	.291	1.273
1600.0	10.0	.8	28.52	1.372	1.081	.291	1.269
1700.0	10.0	.8	28.53	1.383	1.092	.291	1.267
1800.0	10.0	.8	28.58	1.390	1.100	.291	1.264
1900.0	10.0	.8	28.63	1.396	1.106	.290	1.262
2000.0	10.0	.8	28.62	1.405	1.115	.290	1.260
2100.0	10.0	.8	28.62	1.413	1.123	.290	1.259
2200.0	10.0	.8	28.60	1.420	1.130	.290	1.257
2300.0	10.0	.8	28.57	1.426	1.136	.291	1.256
2400.0	10.0	.8	28.53	1.432	1.141	.291	1.255
2500.0	10.0	.8	28.47	1.437	1.145	.292	1.255
2600.0	10.0	.8	28.39	1.442	1.149	.293	1.255
2700.0	10.0	.8	28.27	1.445	1.152	.294	1.255
2800.0	10.0	.8	28.12	1.449	1.153	.295	1.256
2900.0	10.0	.8	27.93	1.451	1.154	.297	1.258
3000.0	10.0	.8	27.72	1.454	1.154	.300	1.260
3100.0	10.0	.8	27.47	1.456	1.154	.302	1.262
3200.0	10.0	.8	27.19	1.458	1.153	.306	1.265
3300.0	10.0	.8	26.88	1.460	1.151	.309	1.268
3400.0	10.0	.8	26.55	1.462	1.149	.313	1.272
3500.0	10.0	.8	26.26	1.462	1.145	.316	1.276

TEMP DEG. K	PR BAR	PHI	MOL WT	CP KJ/KG K	CV	R KJ/KG K	GAM
500.0	10.0	1.0	28.60	1.127	.836	.290	1.347
600.0	10.0	1.0	28.60	1.157	.867	.290	1.335
700.0	10.0	1.0	28.60	1.189	.899	.290	1.323
800.0	10.0	1.0	28.60	1.221	.930	.290	1.312
900.0	10.0	1.0	28.60	1.251	.960	.290	1.302
1000.0	10.0	1.0	28.60	1.278	.988	.290	1.294
1100.0	10.0	1.0	28.60	1.303	1.013	.290	1.287
1200.0	10.0	1.0	28.60	1.326	1.035	.290	1.281
1300.0	10.0	1.0	28.60	1.346	1.055	.290	1.275
1400.0	10.0	1.0	28.60	1.364	1.073	.290	1.271
1500.0	10.0	1.0	28.59	1.380	1.089	.290	1.267
1600.0	10.0	1.0	28.59	1.394	1.103	.290	1.263
1700.0	10.0	1.0	28.59	1.407	1.116	.291	1.260
1800.0	10.0	1.0	28.59	1.418	1.127	.291	1.258
1900.0	10.0	1.0	28.59	1.428	1.138	.291	1.255
2000.0	10.0	1.0	28.56	1.437	1.147	.291	1.254
2100.0	10.0	1.0	28.53	1.446	1.154	.291	1.252
2200.0	10.0	1.0	28.51	1.453	1.161	.291	1.251
2300.0	10.0	1.0	28.44	1.459	1.167	.292	1.250
2400.0	10.0	1.0	28.40	1.465	1.172	.292	1.249
2500.0	10.0	1.0	28.28	1.470	1.176	.294	1.250
2600.0	10.0	1.0	28.18	1.474	1.179	.295	1.250
2700.0	10.0	1.0	28.01	1.478	1.182	.297	1.251
2800.0	10.0	1.0	27.83	1.482	1.183	.298	1.252
2900.0	10.0	1.0	27.65	1.484	1.183	.300	1.254
3000.0	10.0	1.0	27.38	1.487	1.183	.303	1.256
3100.0	10.0	1.0	27.14	1.488	1.182	.306	1.259
3200.0	10.0	1.0	26.84	1.491	1.181	.309	1.262
3300.0	10.0	1.0	26.48	1.493	1.180	.314	1.266
3400.0	10.0	1.0	26.16	1.495	1.177	.317	1.270
3500.0	10.0	1.0	25.78	1.497	1.175	.322	1.274

TEMP DEG. K	PR BAR	PHI	MOL WT	CP KJ/KG K	CV	R KJ/KG K	GAM
500.0	10.0	1.2	28.60	1.138	.848	.290	1.343
600.0	10.0	1.2	28.56	1.173	.882	.291	1.330
700.0	10.0	1.2	28.61	1.203	.913	.290	1.318
800.0	10.0	1.2	28.61	1.236	.946	.290	1.307
900.0	10.0	1.2	28.60	1.267	.976	.290	1.298
1000.0	10.0	1.2	28.59	1.295	1.004	.290	1.289
1100.0	10.0	1.2	28.56	1.320	1.030	.291	1.282
1200.0	10.0	1.2	28.54	1.344	1.053	.291	1.276
1300.0	10.0	1.2	28.53	1.364	1.073	.291	1.271
1400.0	10.0	1.2	28.51	1.383	1.091	.291	1.267
1500.0	10.0	1.2	28.49	1.399	1.108	.292	1.263
1600.0	10.0	1.2	28.47	1.414	1.122	.292	1.260
1700.0	10.0	1.2	28.46	1.427	1.135	.292	1.257
1800.0	10.0	1.2	28.44	1.439	1.147	.292	1.255
1900.0	10.0	1.2	28.42	1.449	1.157	.292	1.252
2000.0	10.0	1.2	28.25	1.459	1.165	.294	1.252
2100.0	10.0	1.2	28.05	1.469	1.172	.296	1.253
2200.0	10.0	1.2	28.02	1.476	1.180	.296	1.251
2300.0	10.0	1.2	27.83	1.484	1.186	.298	1.252
2400.0	10.0	1.2	27.79	1.490	1.192	.298	1.251
2500.0	10.0	1.2	27.67	1.497	1.196	.300	1.251
2600.0	10.0	1.2	27.60	1.502	1.201	.301	1.251
2700.0	10.0	1.2	27.51	1.506	1.204	.302	1.251
2800.0	10.0	1.2	27.37	1.510	1.207	.303	1.251
2900.0	10.0	1.2	27.19	1.514	1.208	.305	1.253
3000.0	10.0	1.2	26.97	1.516	1.208	.308	1.255
3100.0	10.0	1.2	26.71	1.518	1.208	.311	1.257
3200.0	10.0	1.2	26.42	1.521	1.207	.314	1.260
3300.0	10.0	1.2	26.09	1.524	1.206	.318	1.264
3400.0	10.0	1.2	25.74	1.526	1.203	.323	1.268
3500.0	10.0	1.2	25.36	1.528	1.201	.328	1.273

TEMP DEG. K	PR BAR	PHI	MOL WT	CP KJ/KG K	CV	R KJ/KG K	GAM
500.0	10.0	1.4	28.54	1.151	.860	.291	1.339
600.0	10.0	1.4	28.50	1.189	.899	.291	1.325
700.0	10.0	1.4	28.31	1.230	.937	.293	1.313
800.0	10.0	1.4	28.13	1.261	.966	.295	1.306
900.0	10.0	1.4	28.04	1.290	.994	.296	1.298
1000.0	10.0	1.4	28.03	1.318	1.022	.296	1.290
1100.0	10.0	1.4	27.80	1.343	1.045	.298	1.285
1200.0	10.0	1.4	27.82	1.366	1.067	.299	1.280
1300.0	10.0	1.4	27.76	1.386	1.087	.299	1.275
1400.0	10.0	1.4	27.71	1.405	1.105	.300	1.271
1500.0	10.0	1.4	27.66	1.421	1.121	.300	1.268
1600.0	10.0	1.4	27.63	1.436	1.135	.301	1.265
1700.0	10.0	1.4	27.59	1.448	1.148	.301	1.262
1800.0	10.0	1.4	27.57	1.461	1.160	.301	1.260
1900.0	10.0	1.4	27.54	1.472	1.170	.302	1.258
2000.0	10.0	1.4	27.26	1.483	1.178	.305	1.258
2100.0	10.0	1.4	27.24	1.492	1.187	.305	1.257
2200.0	10.0	1.4	27.03	1.501	1.193	.307	1.258
2300.0	10.0	1.4	26.86	1.509	1.200	.309	1.258
2400.0	10.0	1.4	26.83	1.516	1.206	.310	1.257
2500.0	10.0	1.4	26.72	1.522	1.211	.311	1.257
2600.0	10.0	1.4	26.68	1.528	1.217	.311	1.256
2700.0	10.0	1.4	26.64	1.533	1.221	.312	1.255
2800.0	10.0	1.4	26.56	1.538	1.225	.313	1.255
2900.0	10.0	1.4	26.45	1.542	1.228	.314	1.256
3000.0	10.0	1.4	26.29	1.546	1.230	.316	1.257
3100.0	10.0	1.4	26.08	1.549	1.231	.318	1.259
3200.0	10.0	1.4	25.84	1.552	1.231	.321	1.261
3300.0	10.0	1.4	25.54	1.555	1.230	.325	1.264
3400.0	10.0	1.4	25.21	1.558	1.228	.329	1.268
3500.0	10.0	1.4	24.84	1.561	1.226	.334	1.273

TEMP DEG. K	PR BAR	PHI	MOL WT	CP KJ/KG K	CV	R KJ/KG K	GAM
500.0	100.0	.6	28.70	1.091	.802	.289	1.361
600.0	100.0	.6	28.70	1.119	.829	.289	1.348
700.0	100.0	.6	28.70	1.148	.858	.289	1.337
800.0	100.0	.6	28.70	1.176	.887	.289	1.326
900.0	100.0	.6	28.70	1.203	.914	.289	1.317
1000.0	100.0	.6	28.70	1.228	.939	.289	1.308
1100.0	100.0	.6	28.70	1.250	.961	.289	1.301
1200.0	100.0	.6	28.70	1.270	.981	.289	1.295
1300.0	100.0	.6	28.70	1.288	.999	.289	1.290
1400.0	100.0	.6	28.70	1.304	1.014	.289	1.285
1500.0	100.0	.6	28.70	1.318	1.028	.289	1.281
1600.0	100.0	.6	28.70	1.330	1.041	.289	1.278
1700.0	100.0	.6	28.70	1.341	1.052	.289	1.275
1800.0	100.0	.6	28.70	1.351	1.062	.289	1.272
1900.0	100.0	.6	28.70	1.360	1.071	.289	1.270
2000.0	100.0	.6	28.70	1.369	1.079	.289	1.268
2100.0	100.0	.6	28.69	1.376	1.087	.289	1.266
2200.0	100.0	.6	28.69	1.383	1.093	.290	1.265
2300.0	100.0	.6	28.68	1.389	1.099	.290	1.263
2400.0	100.0	.6	28.67	1.395	1.105	.290	1.262
2500.0	100.0	.6	28.65	1.400	1.110	.290	1.261
2600.0	100.0	.6	28.63	1.404	1.114	.290	1.260
2700.0	100.0	.6	28.60	1.409	1.118	.290	1.260
2800.0	100.0	.6	28.55	1.413	1.122	.291	1.259
2900.0	100.0	.6	28.50	1.416	1.124	.291	1.259
3000.0	100.0	.6	28.42	1.419	1.127	.292	1.259
3100.0	100.0	.6	28.33	1.422	1.128	.293	1.260
3200.0	100.0	.6	28.22	1.424	1.130	.294	1.261
3300.0	100.0	.6	28.09	1.426	1.131	.296	1.262
3400.0	100.0	.6	27.94	1.428	1.131	.297	1.263
3500.0	100.0	.6	27.77	1.430	1.131	.299	1.264

TEMP DEG. K	PR BAR	PHI	MOL WT	CP KJ/KG K	CV	R KJ/KG K	GAM
500.0	100.0	.8	28.52	1.115	.824	.291	1.353
600.0	100.0	.8	28.52	1.144	.853	.291	1.341
700.0	100.0	.8	28.65	1.169	.879	.290	1.330
800.0	100.0	.8	28.65	1.199	.909	.290	1.319
900.0	100.0	.8	28.65	1.227	.937	.290	1.309
1000.0	100.0	.8	28.65	1.254	.964	.290	1.301
1100.0	100.0	.8	28.65	1.277	.987	.290	1.294
1200.0	100.0	.8	28.65	1.298	1.009	.290	1.287
1300.0	100.0	.8	28.65	1.317	1.027	.290	1.282
1400.0	100.0	.8	28.65	1.334	1.044	.290	1.278
1500.0	100.0	.8	28.65	1.349	1.059	.290	1.274
1600.0	100.0	.8	28.65	1.363	1.073	.290	1.270
1700.0	100.0	.8	28.65	1.374	1.085	.290	1.267
1800.0	100.0	.8	28.65	1.385	1.095	.290	1.265
1900.0	100.0	.8	28.65	1.395	1.105	.290	1.262
2000.0	100.0	.8	28.65	1.404	1.114	.290	1.260
2100.0	100.0	.8	28.65	1.412	1.122	.290	1.259
2200.0	100.0	.8	28.64	1.419	1.129	.290	1.257
2300.0	100.0	.8	28.63	1.425	1.135	.290	1.256
2400.0	100.0	.8	28.62	1.431	1.141	.290	1.254
2500.0	100.0	.8	28.59	1.436	1.146	.290	1.253
2600.0	100.0	.8	28.56	1.441	1.150	.291	1.253
2700.0	100.0	.8	28.52	1.445	1.154	.291	1.252
2800.0	100.0	.8	28.45	1.450	1.158	.292	1.252
2900.0	100.0	.8	28.38	1.453	1.160	.293	1.252
3000.0	100.0	.8	28.27	1.456	1.162	.294	1.253
3100.0	100.0	.8	28.15	1.458	1.164	.295	1.254
3200.0	100.0	.8	28.01	1.461	1.164	.297	1.255
3300.0	100.0	.8	27.85	1.463	1.165	.298	1.256
3400.0	100.0	.8	27.67	1.465	1.164	.300	1.258
3500.0	100.0	.8	27.47	1.466	1.164	.302	1.260

TEMP DEG. K	PR BAR	PHI	MOL WT	CP KJ/KG K	CV	R KJ/KG K	GAM
500.0	100.0	1.2	28.56	1.139	.848	.291	1.343
600.0	100.0	1.2	28.55	1.174	.883	.291	1.330
700.0	100.0	1.2	28.48	1.210	.919	.291	1.317
800.0	100.0	1.2	28.35	1.245	.953	.293	1.307
900.0	100.0	1.2	28.08	1.279	.983	.296	1.301
1000.0	100.0	1.2	27.63	1.310	1.009	.301	1.298
1100.0	100.0	1.2	27.56	1.331	1.030	.301	1.293
1200.0	100.0	1.2	27.54	1.352	1.051	.302	1.287
1300.0	100.0	1.2	27.53	1.371	1.070	.302	1.282
1400.0	100.0	1.2	27.53	1.389	1.087	.302	1.278
1500.0	100.0	1.2	27.53	1.404	1.102	.302	1.274
1600.0	100.0	1.2	27.53	1.418	1.116	.302	1.270
1700.0	100.0	1.2	27.53	1.431	1.129	.302	1.267
1800.0	100.0	1.2	27.53	1.442	1.140	.302	1.265
1900.0	100.0	1.2	27.53	1.452	1.151	.302	1.262
2000.0	100.0	1.2	27.53	1.462	1.160	.302	1.260
2100.0	100.0	1.2	27.53	1.470	1.168	.302	1.258
2200.0	100.0	1.2	27.52	1.478	1.176	.302	1.257
2300.0	100.0	1.2	27.52	1.485	1.183	.302	1.255
2400.0	100.0	1.2	27.52	1.491	1.190	.302	1.254
2500.0	100.0	1.2	27.51	1.497	1.195	.302	1.253
2600.0	100.0	1.2	27.48	1.503	1.201	.302	1.252
2700.0	100.0	1.2	27.40	1.508	1.206	.302	1.251
2800.0	100.0	1.2	27.44	1.512	1.210	.303	1.250
2900.0	100.0	1.2	27.39	1.517	1.213	.303	1.250
3000.0	100.0	1.2	27.31	1.520	1.216	.304	1.250
3100.0	100.0	1.2	27.21	1.523	1.218	.305	1.251
3200.0	100.0	1.2	27.09	1.526	1.220	.307	1.251
3300.0	100.0	1.2	26.94	1.528	1.221	.308	1.253
3400.0	100.0	1.2	26.76	1.531	1.221	.310	1.254
3500.0	100.0	1.2	26.56	1.533	1.221	.313	1.256

TEMP DEG. K	PR BAR	PHI	MOL WT	CP KJ/KG K	CV	R KJ/KG K	GAM
500.0	100.0	1.0	28.61	1.126	.836	.290	1.347
600.0	100.0	1.0	28.61	1.157	.867	.290	1.335
700.0	100.0	1.0	28.61	1.189	.899	.290	1.323
800.0	100.0	1.0	28.61	1.221	.930	.290	1.312
900.0	100.0	1.0	28.61	1.251	.960	.290	1.302
1000.0	100.0	1.0	28.61	1.278	.988	.290	1.294
1100.0	100.0	1.0	28.61	1.303	1.013	.290	1.287
1200.0	100.0	1.0	28.61	1.326	1.035	.290	1.280
1300.0	100.0	1.0	28.61	1.346	1.055	.290	1.275
1400.0	100.0	1.0	28.61	1.364	1.073	.290	1.271
1500.0	100.0	1.0	28.61	1.380	1.089	.290	1.267
1600.0	100.0	1.0	28.61	1.394	1.103	.290	1.263
1700.0	100.0	1.0	28.61	1.407	1.116	.290	1.260
1800.0	100.0	1.0	28.60	1.418	1.128	.290	1.258
1900.0	100.0	1.0	28.60	1.428	1.138	.290	1.255
2000.0	100.0	1.0	28.59	1.437	1.147	.290	1.253
2100.0	100.0	1.0	28.58	1.446	1.155	.291	1.252
2200.0	100.0	1.0	28.56	1.453	1.162	.291	1.250
2300.0	100.0	1.0	28.54	1.460	1.169	.291	1.249
2400.0	100.0	1.0	28.50	1.466	1.175	.291	1.248
2500.0	100.0	1.0	28.46	1.471	1.179	.292	1.247
2600.0	100.0	1.0	28.40	1.476	1.184	.292	1.247
2700.0	100.0	1.0	28.32	1.480	1.187	.293	1.247
2800.0	100.0	1.0	28.23	1.484	1.190	.294	1.247
2900.0	100.0	1.0	28.12	1.487	1.192	.295	1.248
3000.0	100.0	1.0	27.99	1.490	1.194	.297	1.249
3100.0	100.0	1.0	27.84	1.493	1.195	.298	1.250
3200.0	100.0	1.0	27.68	1.495	1.195	.300	1.251
3300.0	100.0	1.0	27.50	1.497	1.195	.302	1.253
3400.0	100.0	1.0	27.30	1.499	1.195	.304	1.255
3500.0	100.0	1.0	27.09	1.501	1.194	.307	1.257

TEMP DEG. K	PR BAR	PHI	MOL WT	CP KJ/KG K	CV	R KJ/KG K	GAM
500.0	100.0	1.4	28.52	1.151	.860	.291	1.339
600.0	100.0	1.4	28.51	1.189	.898	.291	1.324
700.0	100.0	1.4	28.44	1.229	.937	.292	1.312
800.0	100.0	1.4	28.27	1.269	.975	.294	1.301
900.0	100.0	1.4	27.91	1.305	1.007	.298	1.296
1000.0	100.0	1.4	27.09	1.338	1.032	.307	1.297
1100.0	100.0	1.4	26.79	1.359	1.048	.310	1.296
1200.0	100.0	1.4	26.58	1.379	1.067	.312	1.293
1300.0	100.0	1.4	26.55	1.398	1.085	.313	1.288
1400.0	100.0	1.4	26.54	1.414	1.101	.313	1.284
1500.0	100.0	1.4	26.54	1.430	1.117	.313	1.280
1600.0	100.0	1.4	26.54	1.444	1.131	.313	1.277
1700.0	100.0	1.4	26.54	1.456	1.143	.313	1.274
1800.0	100.0	1.4	26.54	1.467	1.154	.313	1.271
1900.0	100.0	1.4	26.53	1.478	1.165	.313	1.268
2000.0	100.0	1.4	26.53	1.487	1.174	.313	1.267
2100.0	100.0	1.4	26.53	1.496	1.183	.313	1.265
2200.0	100.0	1.4	26.53	1.504	1.191	.313	1.263
2300.0	100.0	1.4	26.52	1.511	1.198	.313	1.261
2400.0	100.0	1.4	26.52	1.518	1.204	.313	1.260
2500.0	100.0	1.4	26.52	1.524	1.210	.313	1.259
2600.0	100.0	1.4	26.51	1.529	1.216	.313	1.258
2700.0	100.0	1.4	26.50	1.535	1.221	.313	1.257
2800.0	100.0	1.4	26.48	1.540	1.226	.314	1.256
2900.0	100.0	1.4	26.45	1.544	1.230	.314	1.255
3000.0	100.0	1.4	26.41	1.548	1.234	.315	1.255
3100.0	100.0	1.4	26.35	1.552	1.237	.315	1.255
3200.0	100.0	1.4	26.27	1.556	1.239	.316	1.255
3300.0	100.0	1.4	26.17	1.559	1.242	.317	1.256
3400.0	100.0	1.4	26.05	1.562	1.243	.319	1.257
3500.0	100.0	1.4	25.89	1.565	1.244	.321	1.258

Appendix (A.15)

Tables of the Employed Thermochemical Data

THERMODYNAMIC PROPERTIES

ATOMIC OXYGEN MOL. WEIGHT 16.0

TEMPERATURE DEG. K	SP. HEAT CAL/MOL. K	ENTROPY CAL/MOLE. K	ENTHALPY CAL/MOLE.
100	5.6656	32.4652	58476.6
200	5.4341	36.3400	59034.0
300	5.2347	38.5010	59566.3
400	5.1347	39.9917	60084.3
500	5.0808	41.1311	60594.8
600	5.0490	42.0544	61101.1
700	5.0289	42.8311	61605.0
800	5.0154	43.5016	62107.1
900	5.0059	44.0918	62608.2
1000	4.9990	44.6188	63108.4
1100	4.9938	45.0950	63608.0
1200	4.9898	45.5294	64107.2
1300	4.9867	45.9286	64606.0
1400	4.9842	46.2981	65104.6
1500	4.9823	46.6419	65602.9
1600	4.9807	46.9634	66101.0
1700	4.9795	47.2653	66599.0
1800	4.9786	47.5499	67096.9
1900	4.9780	47.8191	67594.8
2000	4.9778	48.0744	68092.5
2100	4.9780	48.3173	68590.3
2200	4.9786	48.5489	69088.2
2300	4.9797	48.7702	69586.1
2400	4.9814	48.9822	70084.1
2500	4.9836	49.1856	70582.4
2600	4.9864	49.3811	71080.9
2700	4.9899	49.5693	71579.7
2800	4.9940	49.7509	72078.9
2900	4.9988	49.9262	72578.5
3000	5.0043	50.0956	73078.6
3100	5.0104	50.2599	73579.4
3200	5.0172	50.4191	74080.8
3300	5.0246	50.5736	74582.8
3400	5.0327	50.7237	75085.7
3500	5.0413	50.8697	75589.4
3600	5.0504	51.0119	76094.0
3700	5.0600	51.1504	76599.5
3800	5.0701	51.2855	77106.0
3900	5.0806	51.4173	77613.5
4000	5.0915	51.5461	78122.1

THERMODYNAMIC PROPERTIES

MOLECULAR OXYGEN MOL. WEIGHT. 32.0

TEMPERATURE DEG. K	SP. HEAT CAL/MOL. K	ENTROPY CAL/MOLE. K	ENTHALPY CAL/MOLE.
100	6.9567	41.3967	-1381.2
200	6.9615	46.2195	-685.4
300	7.0215	49.0504	13.0
400	7.1961	51.0923	723.2
500	7.4315	52.7228	1454.3
600	7.6704	54.0991	2209.5
700	7.8837	55.2979	2987.5
800	8.0638	56.3628	3785.2
900	8.2129	57.3214	4599.2
1000	8.3362	58.1933	5426.9
1100	8.4394	58.9928	6265.8
1200	8.5276	59.7310	7114.3
1300	8.6048	60.4167	7971.0
1400	8.6743	61.0570	8835.0
1500	8.7386	61.6577	9705.7
1600	8.7995	62.2236	10582.6
1700	8.8582	62.7588	11465.5
1800	8.9155	63.2668	12354.2
1900	8.9720	63.7503	13248.6
2000	9.0280	64.2120	14148.6
2100	9.0835	64.6538	15054.2
2200	9.1386	65.0776	15965.3
2300	9.1932	65.4851	16881.9
2400	9.2472	65.8775	17803.9
2500	9.3005	66.2560	18731.3
2600	9.3528	66.6218	19664.0
2700	9.4042	66.9758	20601.8
2800	9.4543	67.3187	21544.7
2900	9.5032	67.6513	22492.6
3000	9.5508	67.9743	23445.4
3100	9.5969	68.2883	24402.7
3200	9.6415	68.5936	25364.7
3300	9.6846	68.8910	26331.0
3400	9.7261	69.1807	27301.5
3500	9.7661	69.4632	28276.2
3600	9.8045	69.7389	29254.7
3700	9.8414	70.0080	30237.0
3800	9.8768	70.2709	31222.9
3900	9.9108	70.5279	32212.3
4000	9.9433	70.7793	33205.0

THERMODYNAMIC PROPERTIES

OZONE MOLECULAR WEIGHT. 48.0

TEMPERATURE DEG. K	SP. HEAT CAL/MOL. K	ENTROPY CAL/MOLE. K	ENTHALPY CAL/MOLE.
100	7.9570	47.9640	32096.0
200	8.3790	53.5640	33229.0
300	9.4000	57.1360	34115.0
400	10.4550	59.9920	35110.0
500	11.2960	62.4190	36199.0
600	11.9160	64.5360	37361.0
700	12.3690	66.4090	38577.0
800	12.7040	68.0630	39831.0
900	12.9560	69.5950	41115.0
1000	13.1510	70.9710	42421.0
1100	13.3030	72.2320	43744.0
1200	13.4260	73.3950	45080.0
1300	13.5260	74.4730	46426.0
1400	13.6110	75.4790	47785.0
1500	13.6820	76.4200	49150.0
1600	13.7430	77.3050	50521.0
1700	13.7960	78.1400	51898.0
1800	13.8430	78.9300	53280.0
1900	13.8850	79.6800	54665.0
2000	13.9220	80.3930	56057.0
2100	13.9570	81.0730	57451.0
2200	13.9880	81.7230	58848.0
2300	14.0170	82.3450	60248.0
2400	14.0450	82.9430	61652.0
2500	14.0700	83.5160	63057.0
2600	14.0940	84.0690	64466.0
2700	14.1170	84.6010	65876.0
2800	14.1390	85.1150	67289.0
2900	14.1600	85.6110	68104.0
3000	14.1800	86.0920	70121.0
3100	14.1990	86.5570	71540.0
3200	14.2180	87.0080	72961.0
3300	14.2360	87.4460	74383.0
3400	14.2540	87.8710	75808.0
3500	14.2720	88.2850	77234.0
3600	14.2880	88.6870	78662.0
3700	14.3050	89.0790	80092.0
3800	14.3210	89.4600	81523.0
3900	14.3370	89.8330	82956.0
4000	14.3530	90.1960	84391.0

THERMODYNAMIC PROPERTIES

ATOMIC HYDROGEN MOL. WEIGHT. 1.008

TEMPERATURE DEG. K	SP. HEAT CAL/MOL. K	ENTROPY CAL/MOLE. K	ENTHALPY CAL/MOLE.
100	4.9681	21.9650	51113.3
200	4.9681	25.4087	51610.1
300	4.9681	27.4231	52097.7
400	4.9681	28.8523	52602.8
500	4.9681	29.9609	53100.6
600	4.9681	30.8667	53597.4
700	4.9681	31.6326	54094.2
800	4.9681	32.2960	54591.0
900	4.9681	32.8812	55087.8
1000	4.9681	33.4046	55584.6
1100	4.9681	33.8781	56081.5
1200	4.9681	34.3104	56578.3
1300	4.9681	34.7081	57075.1
1400	4.9681	35.0782	57571.9
1500	4.9681	35.4190	58068.7
1600	4.9681	35.7397	58565.5
1700	4.9681	36.0408	59062.4
1800	4.9681	36.3246	59559.2
1900	4.9681	36.5934	60055.0
2000	4.9681	36.8483	60552.8
2100	4.9682	37.0907	61049.6
2200	4.9682	37.3218	61546.4
2300	4.9681	37.5426	62043.2
2400	4.9681	37.7541	62540.1
2500	4.9681	37.9569	63036.9
2600	4.9681	38.1517	63533.7
2700	4.9681	38.3392	64030.5
2800	4.9681	38.5199	64527.3
2900	4.9681	38.6942	65024.1
3000	4.9681	38.8627	65520.9
3100	4.9681	39.0256	66017.8
3200	4.9681	39.1833	66514.6
3300	4.9681	39.3362	67011.4
3400	4.9681	39.4845	67508.2
3500	4.9681	39.6285	68005.0
3600	4.9681	39.7685	68501.8
3700	4.9681	39.9046	68998.7
3800	4.9681	40.0371	69495.5
3900	4.9681	40.1661	69992.3
4000	4.9681	40.2919	70489.1

THERMODYNAMIC PROPERTIES

WATER VAPOUR MOLECULAR WEIGHT. 18.016

TEMPERATURE DEG. K	SP. HEAT CAL/MOL. K	ENTROPY CAL/MOLE. K	ENTHALPY CAL/MOLE.
100	7.9606	36.3959	-59378.5
200	7.9694	41.9157	-58582.1
300	8.0276	45.1550	-57797.9
400	8.1864	47.4839	-57783.0
500	8.4161	49.3344	-56973.1
600	8.6779	50.8917	-56143.4
700	8.9571	52.2502	-54407.3
800	9.2496	53.4652	-53497.0
900	9.5518	54.5720	-52557.0
1000	9.8577	55.5942	-51586.5
1100	10.1610	56.5480	-50585.6
1200	10.4560	57.4449	-49554.6
1300	10.7384	58.2931	-48494.8
1400	11.0056	59.0987	-47407.4
1500	11.2560	59.8667	-46294.2
1600	11.4894	60.6007	-45156.8
1700	11.7060	61.3038	-43996.9
1800	11.9065	61.9786	-42816.1
1900	12.0919	62.6274	-41616.1
2000	12.2633	63.2521	-40398.2
2100	12.4219	63.8543	-39163.9
2200	12.5689	64.4356	-37914.2
2300	12.7053	64.9973	-36650.4
2400	12.8321	65.5408	-35373.5
2500	12.9503	66.0670	-34084.3
2600	13.0607	66.5771	-32783.7
2700	13.1642	67.0720	-31472.4
2800	13.2614	67.5525	-30151.1
2900	13.3530	68.0195	-28820.3
3000	13.4395	68.4737	-27480.6
3100	13.5214	68.9157	-26132.5
3200	13.5993	69.3462	-24776.5
3300	13.6734	69.7658	-23412.8
3400	13.7442	70.1751	-22041.9
3500	13.8120	70.5745	-20664.1
3600	13.8771	70.9645	-19279.6
3700	13.9398	71.3456	-17888.7
3800	14.0002	71.7181	-16491.7
3900	14.0587	72.0826	-15088.7
4000	14.1153	72.4392	-13680.0

THERMODYNAMIC PROPERTIES

GASEOUS CARBON MOLECULAR WEIGHT. 12.011

TEMPERATURE DEG. K	SP. HEAT CAL/MOL. K	ENTROPY CAL/MOLE. K	ENTHALPY CAL/MOLE.
100	5.0847	32.2829	170308.8
200	4.9965	35.7699	170811.4
300	4.9806	37.7921	171310.1
400	4.9751	39.2241	171807.8
500	4.9726	40.3340	172305.2
600	4.9712	41.2404	172802.4
700	4.9704	42.0067	173299.5
800	4.9699	42.6703	173796.5
900	4.9695	43.2557	174293.5
1000	4.9693	43.7793	174790.4
1100	4.9694	44.2529	175287.3
1200	4.9697	44.6853	175784.3
1300	4.9706	45.0831	176281.3
1400	4.9722	45.4515	176778.4
1500	4.9748	45.7947	177275.8
1600	4.9795	46.1158	177773.4
1700	4.9835	46.4178	178271.5
1800	4.9901	46.7028	178770.2
1900	4.9981	46.9728	179269.6
2000	5.0078	47.2295	179769.9
2100	5.0190	47.4740	180271.2
2200	5.0396	47.7078	180773.7
2300	5.0456	47.9318	181277.5
2400	5.0607	48.1468	181782.9
2500	5.0769	48.3538	182289.7
2600	5.0940	48.5532	182798.3
2700	5.1118	48.7458	183308.6
2800	5.1301	48.9320	183820.7
2900	5.1488	49.1124	184334.6
3000	5.1677	49.2872	184850.4
3100	5.1867	49.4570	185368.1
3200	5.2057	49.6220	185887.8
3300	5.2245	49.7824	186409.3
3400	5.2430	49.9387	186932.6
3500	5.2612	50.0909	187457.9
3600	5.2790	50.2394	187984.9
3700	5.2963	50.3843	188513.6
3800	5.3131	50.5257	189044.1
3900	5.3294	50.6640	189576.2
4000	5.3450	50.7991	190110.0

THERMODYNAMIC PROPERTIES

NITROGEN PEROXIDE MOL. WT. 46.008

TEMPERATURE DEG. K	SP. HEAT CAL/MOL. K	ENTROPY CAL/MOLE. K	ENTHALPY CAL/MOLE.
100	7.9538	48.3828	6364.9
200	8.2302	53.9520	7169.9
300	8.8888	57.4058	8023.9
400	9.6703	60.0693	8951.6
500	10.4190	62.3091	9956.8
600	11.0632	64.2674	11031.9
700	11.5900	66.0138	12165.5
800	12.0124	67.5901	13346.4
900	12.3502	69.0252	14565.1
1000	12.6218	70.3410	15814.2
1100	12.8422	71.5547	17087.8
1200	13.0232	72.6801	18381.3
1300	13.1735	73.7286	19691.4
1400	13.2999	74.7096	21015.3
1500	13.4075	75.6310	22350.8
1600	13.5000	76.4993	23696.2
1700	13.5805	77.3202	25050.4
1800	13.6512	78.0985	26412.0
1900	13.7139	78.8383	27780.3
2000	13.7700	79.5432	29154.6
2100	13.8207	80.2163	30534.2
2200	13.8667	80.8603	31918.6
2300	13.9089	81.4776	33307.4
2400	13.9478	82.0704	34700.2
2500	13.9840	82.6405	36096.9
2600	14.0177	83.1897	37497.0
2700	14.0493	83.7193	38900.3
2800	14.0792	84.2308	40306.8
2900	14.1074	84.7253	41716.1
3000	14.1343	85.2041	43128.2
3100	14.1600	85.6679	44542.9
3200	14.1847	86.1179	45960.2
3300	14.2084	86.5548	47379.8
3400	14.2313	86.9793	48801.8
3500	14.2534	87.3921	50226.1
3600	14.2749	87.7939	51652.5
3700	14.2957	88.1853	53081.0
3800	14.3161	88.5669	54511.6
3900	14.3359	88.9390	55944.2
4000	14.3554	89.3022	57378.8

THERMODYNAMIC PROPERTIES

AMONIA MOLECULAR WT. 17.032

TEMPERATURE DEG. K	SP. HEAT CAL/MOL. K	ENTROPY CAL/MOLE. K	ENTHALPY CAL/MOLE.
100	7.9555	37.2217	-12649.1
200	8.0633	42.7546	-11850.3
300	8.5034	46.0977	-11024.3
400	9.1846	48.6346	-10140.8
500	9.9369	50.7645	-9184.9
600	10.6840	52.6426	-8153.7
700	11.4033	54.3439	-7049.1
800	12.0913	55.9119	-5874.1
900	12.7450	57.3742	-4631.9
1000	13.3599	58.7492	-3326.3
1100	13.9318	60.0697	-1961.4
1200	14.4582	61.2848	-541.5
1300	14.9389	62.4613	928.7
1400	15.3750	63.5847	2444.8
1500	15.7690	64.6591	4003.2
1600	16.1240	65.6883	5597.3
1700	16.4436	66.6756	7225.9
1800	16.7312	67.6238	8884.9
1900	16.9902	68.5355	10571.2
2000	17.2236	69.4130	12282.1
2100	17.4343	70.2585	14015.2
2200	17.6249	71.0740	15768.3
2300	17.7976	71.8614	17539.6
2400	17.9546	72.6222	19327.3
2500	18.0973	73.3581	21130.0
2600	18.2276	74.0704	22946.3
2700	18.3468	74.7606	24775.2
2800	18.4561	75.4298	26615.4
2900	18.5565	76.0793	28466.1
3000	18.6490	76.7099	30326.4
3100	18.7344	77.3228	32195.6
3200	18.8134	77.9189	34073.1
3300	18.8867	78.4990	35958.1
3400	18.9547	79.0638	37850.2
3500	19.0182	79.6142	39748.9
3600	19.0773	80.1508	41653.7
3700	19.1326	80.6742	43564.2
3800	19.1845	81.1852	45480.1
3900	19.2331	81.6841	47401.0
4000	19.2789	82.1716	49326.7

THERMODYNAMIC PROPERTIES

NITRIC ACID MOLECULAR WEIGHT. 63.016

TEMPERATURE DEG. K	SP. HEAT CAL/MOL. K	ENTROPY CAL/MOLE. K	ENTHALPY CAL/MOLE.
100	8.1070	53.0030	-34127.0
200	10.1100	59.1290	-33232.0
300	12.7950	63.7420	-32085.0
400	15.1030	67.7500	-30686.0
500	16.9300	71.3250	-29081.0
600	18.3480	74.5430	-27314.0
700	19.4510	77.4580	-25422.0
800	20.3250	80.1140	-23422.0
900	21.0310	82.5500	-21362.0
1000	21.6130	84.7970	-19229.0
1100	22.0980	86.8800	-17043.0
1200	22.5080	88.8210	-14812.0
1300	22.8580	90.6370	-12543.0
1400	23.1590	92.3420	-10242.0
1500	23.4190	93.9490	-7913.0
1600	23.6460	95.4680	-5559.0
1700	23.8430	96.9080	-3185.0
1800	24.0170	98.2760	-792.0
1900	24.1700	99.5780	1618.0
2000	24.3060	100.8220	4042.0
2100	24.4260	102.0100	6479.0
2200	24.5360	103.1400	8927.0
2300	24.6300	104.2420	11385.0
2400	24.7160	105.2920	13852.0
2500	24.7930	106.3030	16328.0
2600	24.8630	107.2760	18811.0
2700	24.9270	108.2160	21300.0
2800	24.9840	109.1240	23796.0
2900	25.0370	110.0010	26297.0
3000	25.0850	110.8510	28803.0
3100	25.1290	111.6740	31314.0
3200	25.1690	112.4730	33829.0
3300	25.2060	113.2480	36348.0
3400	25.2400	114.0010	38870.0
3500	25.2710	114.7330	41395.0
3600	25.3000	115.4450	43924.0
3700	25.3270	116.1390	46455.0
3800	25.3520	116.8140	48989.0
3900	25.3750	117.4730	51526.0
4000	25.3970	118.1160	54064.0

THERMODYNAMIC PROPERTIES

HYDROGEN CYNIDE MOLECULAR WT. 27.027

TEMPERATURE DEG. K	SP. HEAT CAL/MOL. K	ENTROPY CAL/MOLE. K	ENTHALPY CAL/MOLE.
100	6.9707	40.0328	29676.4
200	7.5808	44.9974	30396.1
300	8.5871	48.2648	31205.4
400	9.3760	50.8491	32105.6
500	9.9737	53.0080	33074.2
600	10.4699	54.8714	34097.0
700	10.9094	56.5189	35166.3
800	11.3089	58.0022	36277.5
900	11.6735	59.3555	37426.9
1000	12.0050	60.6029	38611.1
1100	12.3046	61.7614	39826.9
1200	12.5740	62.8436	41071.1
1300	12.8153	63.8600	42340.7
1400	13.0311	64.8177	43633.3
1500	13.2269	65.7235	44946.2
1600	13.3963	66.5826	46247.4
1700	13.5505	67.3994	47624.9
1800	13.6888	68.1779	48986.9
1900	13.8132	68.9214	50362.2
2000	13.9252	69.6329	51749.2
2100	14.0265	70.3148	53146.8
2200	14.1183	70.9694	54554.1
2300	14.2017	71.5989	55970.2
2400	14.2777	72.2049	57349.2
2500	14.3473	72.7892	58825.5
2600	14.4111	73.3532	60263.5
2700	14.4696	73.8982	61707.6
2800	14.5236	74.4254	63157.3
2900	14.5734	74.9359	64612.2
3000	14.6195	75.4308	66071.8
3100	14.6623	75.9108	67535.9
3200	14.7021	76.3770	69004.2
3300	14.7390	76.8300	70476.3
3400	4.7735	77.2705	7'951.9
3500	14.8056	77.6992	73430.9
3600	14.8356	78.1167	74913.0
3700	14.8636	78.5236	76397.9
3800	14.8899	78.9203	77885.6
3900	14.9144	79.3074	79375.9
4000	14.9373	79.6853	80868.5

THERMODYNAMIC PROPERTIES

CARBON-MONOXIDE MOLECULAR WT. 28.011

TEMPERATURE DEG. K	SP. HEAT CAL/MOL. K	ENTROPY CAL/MOLE. K	ENTHALPY CAL/MOLE.
100	6.9564	39.6169	-27794.5
200	6.9574	44.4340	-27098.8
300	6.9656	47.2609	-26402.8
400	7.0129	49.2699	-25704.4
500	7.1211	50.8453	-24998.2
600	7.2760	52.1568	-24278.6
700	7.4507	53.2914	-23542.3
800	7.6246	54.2978	-22788.5
900	7.7860	55.2053	-22017.8
1000	7.9305	56.0333	-21231.8
1100	8.0571	56.7952	-20432.3
1200	8.1671	57.5011	-19621.0
1300	8.2623	58.1587	-18799.4
1400	8.3447	58.7741	-17968.9
1500	8.4161	59.3523	-17130.8
1600	8.4783	59.8975	-16286.0
1700	8.5327	60.4131	-15435.4
1800	8.5805	60.9022	-14579.7
1900	8.6227	61.3673	-13719.5
2000	8.6603	61.8106	-12855.3
2100	8.6938	62.2334	-11987.6
2200	8.7238	62.6391	-11116.7
2300	8.7509	63.0275	-10242.9
2400	8.7755	63.4004	-9366.6
2500	8.7979	63.7591	-8487.9
2600	8.8184	64.1046	-7607.1
2700	8.8372	64.4378	-6724.3
2800	8.8546	64.7595	-5839.7
2900	8.8706	65.0705	-4953.4
3000	8.8856	65.3715	-4065.6
3100	8.8996	65.6630	-3176.3
3200	8.9127	65.9458	-2285.7
3300	8.9250	66.2203	-1313.8
3400	8.9366	66.4869	-500.7
3500	8.9475	66.7461	393.5
3600	8.9579	66.9983	1288.8
3700	8.9678	67.2439	2185.9
3800	8.9773	67.4831	3082.3
3900	8.9863	67.7164	3980.5
4000	8.9950	67.9441	4879.6

THERMODYNAMIC PROPERTIES

CARBON-DIOXIDE MOLECULAR WT. 44.011

TEMPERATURE DEG. K	SP. HEAT CAL/MOL. K	ENTROPY CAL/MOLE. K	ENTHALPY CAL/MOLE.
100	6.9806	42.7568	-95594.5
200	7.7331	47.7676	-94867.4
300	8.8942	51.1250	-94035.4
400	9.8762	53.8234	-93095.0
500	10.6646	56.1150	-92066.6
600	11.3098	58.1183	-90966.8
700	11.8456	59.9032	-89808.3
800	12.2929	61.5151	-88600.7
900	12.6670	62.9852	-87352.1
1000	12.9804	64.3365	-86069.1
1100	13.2438	65.5864	-84757.7
1200	13.4660	66.7486	-83421.9
1300	13.6545	67.8341	-82065.6
1400	13.8154	68.8520	-80691.9
1500	13.9536	69.8100	-79303.3
1600	14.0732	70.7145	-77901.8
1700	14.1777	71.5708	-76489.2
1800	14.2686	72.3838	-75066.8
1900	14.3491	73.1575	-73635.8
2000	14.4206	73.8954	-72197.3
2100	14.4844	74.6005	-70752.0
2200	14.5418	75.2757	-69300.6
2300	14.5937	75.9232	-67843.8
2400	14.6409	76.5454	-66383.0
2500	14.6840	77.1439	-64915.7
2600	14.7235	77.7206	-63445.3
2700	14.7600	78.2770	-61971.1
2800	14.7938	78.8144	-60493.4
2900	14.8253	79.3314	-59012.5
3000	14.8547	79.8372	-57528.4
3100	14.8823	80.3247	-56041.6
3200	14.9082	80.7976	-54552.0
3300	14.9328	81.2567	-53060.0
3400	14.9560	81.7029	-51565.5
3500	14.9781	82.1367	-50068.8
3600	14.9992	82.5590	-48569.9
3700	15.0194	82.9702	-47069.0
3800	15.0387	83.3710	-45566.1
3900	15.0573	83.7619	-44061.3
4000	15.0752	84.1434	-42554.7

THERMODYNAMIC PROPERTIES

METHANE MOLECULAR WT. 16.043

TEMPERATURE DEG. K	SP. HEAT CAL/MOL. K	ENTROPY CAL/MOLE. K	ENTHALPY CAL/MOLE.
100	7.9490	35.7221	-19490.0
200	8.0006	41.2379	-18694.1
300	8.5350	44.5590	-17873.2
400	9.6846	47.1611	-16966.0
500	11.0933	49.4716	-15927.9
600	12.5212	51.6210	-14746.8
700	13.8816	53.6544	-13426.0
800	15.1467	55.5918	-11973.7
900	16.3062	57.4438	-10400.2
1000	17.3579	59.2172	-8716.0
1100	18.3041	60.9168	-6932.1
1200	19.1508	62.5464	-5058.6
1300	19.9064	64.9017	-3105.0
1400	20.5798	65.6101	-1080.0
1500	21.1804	67.0508	1008.6
1600	21.7167	68.4352	3153.9
1700	22.1969	69.7664	5350.8
1800	22.6282	71.0478	7591.7
1900	23.0168	72.2816	9874.3
2000	23.3684	73.4713	12193.8
2100	23.6876	74.6193	14546.9
2200	23.9786	75.7281	16930.4
2300	24.2449	76.8000	19341.8
2400	24.4897	77.8370	21778.7
2500	24.7155	78.8414	24239.1
2600	24.9246	79.8149	26721.2
2700	25.1189	80.7592	29223.5
2800	25.3003	81.6761	31744.5
2900	25.4701	82.5669	34283.2
3000	25.6296	83.4331	36838.2
3100	25.7799	84.2759	39408.0
3200	25.9220	85.0967	41993.9
3300	26.0568	85.8964	44592.9
3400	26.1849	86.6762	47205.1
3500	26.3072	87.4320	49829.7
3600	26.4240	88.1798	52466.3
3700	26.5360	88.9053	55114.4
3800	26.6435	89.6144	57773.4
3900	26.7471	90.3078	60442.9
4000	26.8471	90.9863	63122.7

THERMODYNAMIC PROPERTIES

ATOMIC NYTROGEN MOLECULAR WT. 14.008

TEMPERATURE DEG. K	SP. HEAT CAL/MOL. K	ENTROPY CAL/MOLE. K	ENTHALPY CAL/MOLE.
100	4.9681	31.1872	112040.2
200	4.9681	34.6308	112537.0
300	4.9681	36.6452	113033.8
400	4.9681	38.0745	113530.6
500	4.9681	39.1831	114027.4
600	4.9681	40.0889	114524.2
700	4.9681	40.8547	115021.1
800	4.9681	41.5181	115517.9
900	4.9681	42.1033	116014.7
1000	4.9681	42.6268	116511.5
1100	4.9681	43.1003	117008.3
1200	4.9682	43.5326	117505.1
1300	4.9682	43.9302	118001.9
1400	4.9682	44.2984	118498.8
1500	4.9682	44.6412	118995.6
1600	4.9682	44.9618	119492.4
1700	4.9683	45.2630	119989.2
1800	4.9684	45.5470	120486.0
1900	4.9687	45.8156	120982.9
2000	4.9691	46.0705	121479.8
2100	4.9698	46.3129	121976.7
2200	4.9709	46.5442	122473.8
2300	4.9725	46.7652	122970.9
2400	4.9747	46.9768	123468.3
2500	4.9777	47.1800	123965.9
2600	4.9817	47.3753	124463.1
2700	4.9868	47.5634	124962.3
2800	4.9932	47.7448	125461.2
2900	5.0010	47.9202	125960.9
3000	5.0105	48.0899	126461.5
3100	5.0216	48.2544	126963.1
3200	5.0346	48.4140	127465.8
3300	5.0496	48.5691	127970.1
3400	5.0665	48.7207	128475.9
3500	5.0855	48.8673	128983.4
3600	5.1066	49.0108	129493.0
3700	5.1299	49.1510	130004.8
3800	5.1554	49.2882	130519.1
3900	5.1829	49.4224	131036.0
4000	5.2126	49.5540	131555.7

THERMODYNAMIC PROPERTIES

MOLECULAR NITROGEN MOL. WT. 28.016

TEMPERATURE DEG. K	SP. HEAT CAL/MOL. K	ENTROPY CAL/MOLE. K	ENTHALPY CAL/MOLE.
100	6.9562	38.1709	-1378.6
200	6.9571	42.9929	-683.0
300	6.9613	45.8142	12.9
400	6.9910	47.8199	710.1
500	7.0703	49.3874	1412.8
600	7.1968	50.6871	2125.8
700	7.3509	51.8079	2853.0
800	7.5131	52.8000	3596.2
900	7.6700	53.6941	4355.5
1000	7.8148	54.5098	5129.8
1100	7.9449	55.2609	5917.9
1200	8.0600	55.9572	6718.3
1300	8.1610	56.6064	7529.5
1400	8.2494	57.2145	8350.1
1500	8.3267	57.7864	9179.0
1600	8.3945	58.3260	10015.1
1700	8.4541	58.8367	10857.6
1800	8.5067	59.3215	11705.7
1900	8.5533	59.7827	12558.8
2000	8.5948	60.2225	13416.2
2100	8.6318	60.6427	14277.6
2200	8.6650	61.0451	15142.4
2300	8.6950	61.4309	16010.5
2400	8.7222	61.8016	16881.3
2500	8.7468	62.1581	17754.8
2600	8.7694	62.5016	18630.6
2700	8.7900	62.8330	19508.6
2800	8.8090	63.1530	20388.6
2900	8.8266	63.4624	21270.4
3000	8.8428	63.7619	22153.9
3100	8.8580	64.0251	23038.9
3200	8.8721	64.3336	23925.4
3300	8.8853	64.6068	24813.3
3400	8.8977	64.8722	25702.5
3500	8.9094	65.1303	26592.8
3600	8.9205	65.3815	27484.3
3700	8.9309	65.6260	28376.9
3800	8.9409	65.8643	29270.5
3900	8.9503	66.0967	30165.1
4000	8.9594	66.3234	31060.6

THERMODYNAMIC PROPERTIES

NITRIC OXIDE MOLECULAR WT. 30.008

TEMPERATURE DEG. K	SP. HEAT CAL/MOL. K	ENTROPY CAL/MOLE. K	ENTHALPY CAL/MOLE.
100	7.7205	42.2850	20148.6
200	7.7209	47.4753	20894.7
300	7.1325	50.3903	21613.2
400	7.1570	52.4424	22326.6
500	7.2867	54.0519	23048.1
600	7.4664	55.3960	23785.5
700	7.6553	56.5612	24545.7
800	7.8321	57.5951	25316.2
900	7.9887	58.5269	26107.4
1000	8.1237	59.3757	26913.2
1100	8.2389	60.1556	27731.5
1200	8.3368	60.8767	28560.4
1300	8.4201	61.5474	29398.4
1400	8.4914	62.1741	30244.0
1500	8.5528	62.7621	31096.0
1600	8.6059	63.3158	31954.3
1700	8.6521	63.8390	32817.3
1800	8.6927	64.3347	33684.0
1900	8.7286	64.8056	34555.7
2000	8.7605	65.2542	35430.1
2100	8.7891	65.6823	36307.7
2200	8.8148	66.0918	37187.9
2300	8.8382	66.4842	38070.5
2400	8.8594	66.8608	38955.4
2500	8.8789	67.2228	39842.4
2600	8.8969	67.5714	40731.2
2700	8.9135	67.9075	41621.7
2800	8.9290	68.2320	42513.8
2900	8.9434	68.5455	43407.5
3000	8.9570	68.8490	44302.5
3100	8.9698	69.1429	45198.8
3200	8.9819	69.4278	46096.4
3300	8.9933	69.7044	46995.2
3400	9.0042	69.9730	47895.1
3500	9.0146	70.2342	48796.0
3600	9.0246	70.4883	49698.0
3700	9.0342	70.7357	50600.9
3800	9.0434	70.9767	51504.8
3900	9.0523	71.2118	52409.6
4000	9.0609	71.4411	53315.3